



ANP-10263NP
Revision 0

Codes and Methods Applicability Report for
the U.S. EPR

August 2006

AREVA NP Inc.

NON-PROPRIETARY

(c) 2006 AREVA NP Inc.

Copyright © 2006

**AREVA NP Inc.
All Rights Reserved**

The design, engineering and other information contained in this document have been prepared by or on behalf of AREVA NP Inc., a jointly owned subsidiary of AREVA and Siemens, in connection with its request to the U.S. Nuclear Regulatory Commission for a pre-application review of the EPR nuclear power plant design. No use of or right to copy any of this information, other than by the NRC and its contractors in support of AREVA NP's pre-application review, is authorized.

The information provided in this document is a subset of a much larger set of know-how, technology and intellectual property pertaining to an evolutionary pressurized water reactor designed by AREVA NP and referred to as the EPR. Without access and a grant of rights to that larger set of know-how, technology and intellectual property rights, this document is not practically or rightfully usable by others, except by the NRC as set forth in the previous paragraph.

For information address: AREVA NP Inc.
An AREVA and Siemens Company
3315 Old Forest Road
Lynchburg, VA 24506

U.S. Nuclear Regulatory Commission

Disclaimer

Important Notice Concerning the Contents and Application of This Report

Please Read Carefully

This report was developed based on research and development funded and conducted by AREVA NP, Inc., and is being submitted by AREVA NP to the U.S. Nuclear Regulatory Commission (NRC) to facilitate future licensing processes that may be pursued by licensees or applicants that are customers of AREVA NP. The information contained in this report may be used by the NRC and, under the terms of applicable agreements with AREVA NP, those customers seeking licenses or license amendments to assist in demonstrating compliance with NRC regulations. The information provided in this report is true and correct to the best of AREVA NP's knowledge, information, and belief.

AREVA NP's warranties and representations concerning the content of this report are set forth in agreements between AREVA NP and individual customers. Except as otherwise expressly provided in such agreements with its customers, neither AREVA NP nor any person acting on behalf of AREVA NP:

- Makes any warranty or representation, express or implied, with respect to the accuracy, completeness, or usefulness of the information contained in this report, nor the use of any information, apparatus, method, or process disclosed in this report.
- Assumes any liability with respect to the use of or for damages resulting from the use of any information, apparatus, method, or process disclosed in this report.

Nature of Changes

Item	Section(s) or Page(s)	Description and Justification
------	--------------------------	-------------------------------

Contents

	<u>Page</u>
1.0 INTRODUCTION	1-1
1.1 References	1-3
2.0 U.S. EPR DESIGN OVERVIEW	2-1
2.1 U.S. EPR Plant Design and Features	2-2
2.1.1 Reactor Coolant System	2-2
2.1.2 Overpressure Protection	2-4
2.1.2.1 Primary Side OPP	2-4
2.1.2.2 Secondary Side OPP	2-6
2.1.3 Principal Fluid Systems	2-7
2.1.3.1 System Configuration	2-8
2.1.3.2 Safety Injection/Residual Heat Removal System	2-9
2.1.3.3 IRWST	2-12
2.1.3.4 Extra Borating System	2-13
2.1.3.5 Emergency Feedwater System	2-14
2.1.3.6 CVCS	2-16
2.1.3.7 Component Cooling Water System	2-19
2.1.3.8 Essential Service Water System	2-20
2.2 Core Design	2-21
2.2.1 General Features	2-21
2.2.2 Fuel Assemblies	2-22
2.2.3 Rod Cluster Control Assemblies and Reactivity Control	2-23
2.2.4 Core Instrumentation	2-23
2.2.4.1 Ex-Core Instrumentation	2-24
2.2.4.2 In-Core Instrumentation	2-24
3.0 VALIDATION OF FUEL ANALYSIS CODES FOR U.S. EPR	3-1
3.1 Neutronics	3-1
3.1.1 Neutronics Codes	3-1
3.1.2 Neutronic Methodologies	3-3
3.1.3 Applicability of Neutronic Codes/Methodologies to U.S. EPR	3-4
3.1.3.1 EMF-96-029(P)(A), Volumes 1 and 2, "Reactor Analysis System for PWRs," Basis for Application to U.S. EPR	3-5
3.1.3.2 BAW-10221P-A, "NEMO-K A Kinetics Solution in NEMO," Basis for Application to U.S. EPR	3-6
3.2 Thermal-Hydraulic	3-7
3.2.1 Thermal-Hydraulic Codes	3-7
3.2.2 Thermal-Hydraulic Methodology	3-9
3.2.3 Applicability of Thermal-Hydraulic Codes/Methodologies to U.S. EPR	3-11
3.3 Thermo-Mechanical	3-11
3.3.1 Thermo-Mechanical Codes	3-12

3.3.2	Thermo-Mechanical Methodology	3-13
3.3.3	Applicability of Thermo-Mechanical Codes/Methodologies to U.S. EPR	3-15
3.4	References	3-15
4.0	VALIDATION OF METHODOLOGY FOR SMALL BREAK LOCA.....	4-1
4.1	Small Break Codes and Methods	4-1
4.1.1	Event Description	4-2
4.1.2	Small Break LOCA Scenarios	4-4
4.1.3	Acceptance Criteria	4-5
4.1.4	Cases Analyzed	4-6
4.1.5	Single Failure and Preventive Maintenance	4-6
4.2	U.S. EPR Small Break LOCA Phenomena	4-7
4.2.1	Phase 1 – RCS Depressurization Following Break Initiation	4-7
4.2.2	Phase 2 – RCS Saturation and Primary Flow Coastdown	4-8
4.2.3	Phase 3 – Loop Seal Clearing Phase	4-9
4.2.4	Phase 4 – Boil-off	4-12
4.2.5	Phase 5 – Core Recovery	4-13
4.2.6	U.S. EPR Small Break LOCA Phenomena – Conclusion	4-13
4.3	S-RELAP5 Validation for U.S. EPR SBLOCA Analysis	4-13
4.3.1	S-RELAP5 Acceptance for SBLOCA Analysis	4-13
4.3.2	S-RELAP5 Acceptability for U.S. EPR SBLOCA Analysis	4-14
4.4	Conclusions	4-17
4.5	References	4-18
5.0	VALIDATION OF S-RELAP5 METHODOLOGY FOR NON-LOCA EVENTS... 5-1	
5.1	Non-LOCA Transient Codes and Methods	5-1
5.2	S-RELAP5 Validation for U.S. EPR Non-LOCA Analysis.....	5-3
5.2.1	S-RELAP5 Acceptance for Non-LOCA Analysis	5-3
5.2.2	S-RELAP5 Acceptability for U.S. EPR Non-LOCA Analysis	5-6
5.2.2.1	Increase in Heat Removal by the Secondary System	5-10
5.2.2.2	Decrease in Heat Removal by the Secondary System	5-35
5.2.2.3	Decrease in Reactor Coolant Flow Rate	5-59
5.2.2.4	Reactivity and Power Distribution Anomalies	5-67
5.2.2.5	Increase in Reactor Coolant Inventory	5-77
5.2.2.6	Decrease in Reactor Coolant Inventory	5-78
5.3	Conclusions	5-92
5.4	References	5-93
6.0	APPLICABILITY OF OTHER APPROVED METHODOLOGIES TO U.S. EPR	
	DESIGN	6-1
6.1	Use of M5 [®] Advanced Zirconium Alloy	6-1
6.2	Effects of Fuel Rod Bowing	6-2
6.3	Fuel Rod Gas Pressure Limits	6-5
6.4	Statistical Assessment of Fuel Assembly Holddown	6-7
6.5	References	6-8
7.0	SUMMARY/CONCLUSIONS.....	7-1

List of Tables

	<u>Page</u>
Table 2-1 Comparison Of Key U.S. EPR Design Parameters	2-28
Table 2-2 Preliminary Core Parameters	2-29
Table 2-3 Neutronic Core Data	2-30
Table 2-4 Thermal Hydraulic Design Data	2-31
Table 2-5 Key Fuel Assembly Characteristics	2-32
Table 2-6 Characteristics Of The RCCAs And CRDMs	2-33
Table 3-1 Neutronics Analyses Areas	3-17
Table 3-2 Typical Core Design Configurations	3-17
Table 3-3 Core Design Comparison – Typical 17x17 Versus U.S. Epr	3-18
Table 3-4 Typical Fuel Rod Design Comparison	3-19
Table 3-5 Copernic Approved Range	3-20
Table 4-1 Informal SBLOCA PIRT With Assessment/Disposition	4-19
Table 4-2 S-RELAP5 Experimental SBLOCA Benchmark Calculations	4-20
Table 5-1 Applicable SRP Chapter 15 Events	5-94
Table 5-2 Informal Non-LOCA PIRT With Assessment/Disposition	5-96

List of Figures

	<u>Page</u>
Figure 2-1 Plant Configuration	2-34
Figure 2-2 Reactor Coolant System	2-35
Figure 2-3 RCS Layout	2-36
Figure 2-4 RPV Internals	2-37
Figure 2-5 Steam Generator	2-38
Figure 2-6 Pressurizer	2-39
Figure 2-7 Reactor Coolant Pump Assembly	2-40
Figure 2-8 Pressurizer With Discharge Components	2-41
Figure 2-9 Arrangement Of The Secondary Side Overpressure Protection	2-42
Figure 2-10 Main Fluid Systems	2-43
Figure 2-11 Safety Injection System	2-44
Figure 2-12 IRWST And Related Components	2-45
Figure 2-13 Emergency Feedwater System	2-46
Figure 2-14 Chemical And Volume Control System	2-47

Figure 2-15 Component Cooling Water System	2-48
Figure 2-16 Essential Service Water System	2-49
Figure 2-17 Radial Cross Section Of A Fuel Assembly	2-50
Figure 2-18 Fuel Assembly	2-51
Figure 2-19 Fuel Assembly Top And Bottom Nozzles	2-52
Figure 2-20 Possible Rcca Pattern Covering Enveloping Requirements.....	2-53
Figure 2-21 Aeroball System.....	2-54
Figure 2-22 Arrangement Of In-Core Instrumentation Fingers	2-55
Figure 2-23 Reactor Instrumentation.....	2-56
Figure 4-1 SBLOCA Evaluation Model	4-21
Figure 5-1 U.S. EPR Reactor Coolant System Nodalization	5-102
Figure 5-2 U.S. EPR Secondary Side Nodalization.....	5-103
Figure 5-3 U.S. EPR Reactor Vessel Nodalization.....	5-104
Figure 5-4 U.S. EPR Secondary Nodalization MSLB	5-105
Figure 5-5 U.S. EPR Reactor Vessel Nodalization MSLB	5-106

Nomenclature

Acronym	Description
ADV	Atmospheric Steam Dump Valve
ATWS	Anticipated Transient Without Scram
CCFL	Counter Current Flow Limit
CCW(S)	Component Cooling Water (System)
CHF	Critical Heat Flux
COTC	Core Outlet Thermocouple
CRDM	Control Rod Drive Mechanism
CSAU	Code Scaling, Applicability, and Uncertainty
CVCS	Chemical and Volume Control System
DNB(R)	Departure from Nucleate Boiling (Ratio)
EBS	Extra Borating System
ECCS	Emergency Core Cooling System
EDG	Emergency Diesel Generator
EFW(S)	Emergency Feedwater (System)
EM	Evaluation Model
EPR	Evolutionary Power Reactor
ESW(S)	Essential Service Water (System)
FCM	Fuel Centerline Melt
FPCS	Fuel Pool Cooling System
HEPA	High Efficiency Particulate Air
HFP	Hot Full Power
HHSI	High Head Safety Injection
HL	High Load
HVAC	Heating, Ventilation, Air Conditioning
HZP	Hot Zero Power
I&C	Instrumentation and Control
IOPSRV	Inadvertent Opening of Pressurizer Safety Valve
IRWST	In-Containment Refueling Water Storage Tank
LBLOCA	Large Break LOCA
LCO	Limiting Conditions for Operation
LHSI	Low Head Safety Injection
LL	Low Load
LNEP	Loss of Non-Emergency AC Power
LNFF	Loss of Normal Feedwater Flow
LOCA	Loss-of-Coolant Accident
LOCF	Loss-of-Coolant Flow
LOCV	Loss of Condenser Vacuum
LOEL	Loss of External Load
LOOP	Loss of Offsite Power
LPD	Linear Power Density

Acronym	Description
MDNBR	Minimum Departure from Nucleate Boiling Ratio
MFP	Main Feedwater Pump
MFW(S)	Main Feedwater (System)
MFWCV	Main Feedwater Control Valve
MFWIV	Main Feedwater Isolation Valve
MHSI	Medium Head Safety Injection
MS	Main Steam
MSB	Main Steam Bypass
MSIV	Main Steam Isolation Valve
MSL	Main Steam Line
MSLB	Main Steam Line Break
MSRIV	Main Steam Relief Isolation Valve
MSRT	Main Steam Relief Train
MSRV	Main Steam Relief Valve
MSS	Main Steam System
MSSV	Main Steam Safety Valve
MTC	Moderator Temperature Coefficient
NSSS	Nuclear Steam Supply System
OPP	Overpressure Protection
PCT	Peak Clad Temperature
PDD	Power Density Detector
PDS	Pressurizer Depressurization System
PIRT	Phenomena Identification and Ranking Table
PORV	Pilot Operated Relief Valve
PRT	Pressurizer Relief Tank
PSRV	Pressurizer Safety Relief Valve
PT	Partial Trip
PWR	Pressurized Water Reactor
PZR	Pressurizer
RCCA	Rod Cluster Control Assembly
RCP	Reactor Coolant Pump
RCPB	Reactor Coolant Pressure Boundary
RCS	Reactor Coolant System
RCSL	Reactor Control, Surveillance and Limitation
RHR(S)	Residual Heat Removal (System)
RLBLOCA	Realistic Large Break LOCA
RPS	Reactor Protection System
RPV	Reactor Pressure Vessel
RT	Reactor Trip
SAFDL	Specified Acceptable Fuel Design Limit
SAHRS	Severe Accident Heat Removal System
SBLOCA	Small Break LOCA

Acronym	Description
SBO	Station Blackout
SG	Steam Generator
SGBS	Steam Generator Blowdown System
SGTR	Steam Generator Tube Rupture
SICS	Safety Information and Control System
SIS	Safety Injection System
SPND	Self-Powered Neutron Detector
SRP	Standard Review Plan
SSS	Start-Up and Shutdown System
TCV	Turbine Control Valve
TSV	Turbine Stop Valve
TT	Turbine Trip
USNRC	United States Nuclear Regulatory Commission
VCT	Volume Control Tank
WR	Wide Range

1.0 INTRODUCTION

This report presents selected codes and methods that will be used in the safety analysis of the U.S. EPR. The U.S. EPR is an evolutionary Pressurized Water Reactor (PWR) design and retains the principal features of existing four-loop plants and fuel designs. Therefore, methods currently in use (and NRC-approved) for existing plants are applicable to the U.S. EPR with minimal or no changes. Section 2 provides an overview of the U.S. EPR and presents plant design features and core/fuel design features. Additional information can be found in Reference 1-1. Design features and/or parameters are subject to modest changes up until the time of submittal of the Design Certification Application.

Section 3 of this report presents the primary fuel codes and methods used for U.S. EPR analyses. An overview of the applicable methodology is presented for core neutronics, core thermal/hydraulics, and core thermal/mechanical analyses. This material is followed by a discussion of the bases for applying these codes/methods to the U.S. EPR. Fuel analysis codes that are discussed include:

- CASMO3 and PRISM – used for core neutronics (Reference 1-2),
- NEMO-K – used for core reactivity transients (Reference 1-3),
- LYNXT – used for detailed core thermal/hydraulic analyses (Reference 1-4), and
- COPENIC – used for core thermal/mechanical analyses (Reference 1-5).

Sections 4 and 5 present the codes and methods used for Small Break LOCA (SBLOCA), and non-LOCA analyses, respectively. Large Break LOCA methodology will be addressed in a separate report. The codes and methods discussed include:

- S-RELAP5 as used for SBLOCA analyses (Reference 1-6), and
- S-RELAP5 as used for non-LOCA analyses (Reference 1-7).

Each section presents an overview of the codes/methods, a discussion of important phenomena, and the bases for applying the codes/methods to the U.S. EPR. The applicability of these methods is demonstrated in part by comparing physical characteristics of existing plants and fuel, for which the methods have been approved,

to the U.S. EPR physical characteristics. In addition, applicability is demonstrated by showing that phenomena occurring in existing plants are the same as in the U.S. EPR.

The Appendices of this report contain representative results obtained from U.S. EPR analyses using the codes/methods appearing above, as appropriate. Neutronics benchmarks are provided (Appendix A), along with application results for COPENIC (Appendix B). Analysis results for SBLOCA and non-LOCA are provided in Appendices C and D.

Section 6 identifies a number of other approved, focused methodologies that will be used for U.S. EPR analyses and provides justification for their use. These methodologies include:

- the use of M5[®] for fuel cladding and structural purposes (References 1-8 and 1-9),
- assessing the effects of fuel rod bowing (Reference 1-10),
- establishing fuel rod gas pressure limits (Reference 1-11), and
- a statistical assessment of fuel assembly hold down (Reference 1-12).

Finally, conclusions regarding the codes and methods assessments are contained in Section 7.

1.1 **References**

- 1-1. "EPR Design Description," Framatome ANP, Inc., August 2005.
- 1-2. "Reactor Analysis System for PWRs," EMF-96-029(P)(A), January 1997.
- 1-3. "NEMO-K, A Kinetics Solution in NEMO," BAW-10221P-A, September 1998.
- 1-4. "LYNXT – Core Transient Thermal-Hydraulic Program," BAW-10156-A
Revision 1, August 1993.
- 1-5. "COPERNIC Fuel Rod Design Computer Code," BAW-10231P-A, June 2002.
- 1-6. "PWR Small Break LOCA Evaluation Model, S-RELAP5 Based,"
EMF-2328(P)(A) Revision 0, March 2001.
- 1-7. "SRP Chapter 15 Non-LOCA Methodology for Pressurized Water Reactors,
"EMF-2310(P)(A) Revision 1, May 2004.
- 1-8. "Evaluation of Advanced Cladding and Structural Material (M5[®]) in PWR Reactor
Fuel," BAW-10227P-A, Revision 1, June 2003.
- 1-9. "Incorporation of M5[®] Properties in Framatome ANP Approved Methods,"
BAW-10240(P)-A, Revision 0, May 2004.
- 1-10. "Fuel Rod Bowing in Babcock & Wilcox Fuel Designs," BAW-10147P-A,
Revision 1, May 1983.
- 1-11. "Fuel Rod Gas Pressure Criterion (FRGPC)," BAW-10183P-A, July 1995.
- 1-12. "Statistical Fuel Assembly Hold Down Methodology," BAW-10243P-A,
September 2005.

2.0 U.S. EPR DESIGN OVERVIEW

The U.S. EPR is an evolutionary PWR with a rated thermal power of 4,500 MWt.* The primary system design, loop configuration, and main components are similar to those of currently operating PWRs, thus forming a proven foundation for the design.

The U.S. EPR has a four-loop Reactor Coolant System (RCS) composed of a Reactor Pressure Vessel (RPV) that contains 241 fuel assemblies, a pressurizer (PZR) including control systems to maintain system pressure, one Reactor Coolant Pump (RCP) per loop, one Steam Generator (SG) per loop, associated piping, and related control and protection systems.

The RCS is contained within a concrete containment building. The containment building is enclosed by a shield building with an annular space between the two buildings. The pre-stressed concrete shell of the containment building has a steel liner and the shield building wall is reinforced concrete. The Containment and Shield Buildings comprise the Reactor Building. The Reactor Building is surrounded by four Safeguard Buildings and a Fuel Building (see Figure 2-1). The internal structures and components within the Reactor Building, Fuel Building, and two Safeguard Buildings (including the plant Control Room) are protected against aircraft hazard and external explosions. The other two Safeguard Buildings are not protected against aircraft hazard or external explosions; however, they are separated by the Reactor Building, which restricts damage from these external events to a single safety division.

Four 100% capacity safety systems are separated into four divisions (one per Safeguard Building). This divisional separation is provided for electrical and mechanical safety systems. The four divisions of safety systems are consistent with an N+2 safety concept. With four divisions, one division can be out-of-service for maintenance and one division can fail to operate, while the remaining two divisions are available to perform the necessary safety functions even if one is ineffective due to the initiating event.

*The power level of the U.S. EPR was increased to 4590 MWt after most of the work supporting this report was performed. The AREVA NP Inc. Design Change Control procedure requires such changes to be identified and their impact assessed before being implemented. The applicability of codes and methods is part of the impact assessment. This small increase (2%) in power was judged to have no effect on report conclusions regarding code phenomena, plant transient behavior, and codes/methods applicability to the U.S. EPR.

In the event of a loss of off-site power (LOOP), each safeguard division is powered by a separate Emergency Diesel Generator (EDG). In addition to the four safety-related diesels that power various safeguards, two independent diesel generators are available to power essential equipment during a postulated Station Blackout (SBO) event—loss of offsite AC power with coincident failure of all four EDGs.

Water storage for safety injection is provided by the In-containment Refueling Water Storage Tank (IRWST). Also inside containment below the RPV, is a dedicated spreading area for molten core material following a postulated worst-case severe accident.

The fuel pool is located outside the Reactor Building in a dedicated building to simplify access for fuel handling during plant operation and handling of fuel casks. As stated previously, the Fuel Building is protected against aircraft hazard and external explosions. Fuel pool cooling is assured by two redundant, safety-related cooling trains.

Although the U.S. EPR embodies a number of improvements on existing PWR designs, these improvements are evolutionary and U.S. EPR design conditions are similar to operating PWRs. Key U.S. EPR design parameters are compared with those of a typical U.S. four-loop plant, a French N4 plant, and a German KONVOI plant in Table 2-1. Additional comparisons of core parameters between the U.S. EPR and a typical U.S. four-loop plant are provided in Tables 2-2, 2-3, and 2-4.

2.1 U.S. EPR Plant Design and Features

2.1.1 Reactor Coolant System

The RCS configuration is a conventional four-loop design. The RPV is located at the center of the reactor building and contains the core with fuel assemblies. The reactor coolant flows through the hot leg pipes to the SGs and returns to the RPV via the cold leg pipes by the RCPs. The PZR is connected to one hot leg via the surge line and to two cold legs by the spray lines.

Figure 2-2 shows a flow schematic of the RCS and Figure 2-3 shows the layout of the RCS. The RPV, PZR, and SGs are individually discussed below. Figure 2-4 shows a

cutaway view of the RPV and RPV internals. Cutaway views of the SG, PZR, and RCP are shown in Figures 2-5, 2-6, and 2-7, respectively.

For the RPV, the volume between the elevation of the RPV nozzles and the top of the active core is larger to improve the mitigation of SBLOCAs by prolonging the period until beginning of core uncover or minimizing the core uncover depth, if any. The increase in volume contributes to an improvement in the mitigation of accidents during shutdown conditions, particularly in mid-loop operation (e.g., with loss of residual heat removal (RHR)), by extending the period for operator action. Also, the increased nozzle elevation relative to the core potentially provides more driving head for reflood flow into the core.

For the PZR, a larger volume provides the following benefits:

- An increase of both water and steam volume with associated pressure and level scaling is favorable in handling many types of transients. A single countermeasure actuated at one limit can more easily become fully effective before the next limit is reached (e.g., in certain load reductions one PZR spray valve, instead of two, is sufficient to stop the pressure increase). The result is a reduction of loads on relevant systems and components (i.e., a reduced number of load cycles).
- For normal operating transients, parameter changes (e.g., pressure, and water level) are mild and thus the potential for reactor trips is minimized.
- For events such as loss of condenser, the actuation of PZR safety valves can be avoided altogether.
- For SBLOCAs, the time until the core uncovers is prolonged.

For the SG, the larger volume of the secondary side provides the following advantages:

- For normal operating transients, smooth parameter changes (e.g., pressure and water level) are obtained and thus the potential for unplanned reactor trips is further reduced.

- For mitigation of Steam Generator Tube Rupture (SGTR) scenarios, a large steam space results in a significant time delay for a mitigating response prior to filling of the SG.
- The secondary side water inventory of the SG at full load satisfies the most limiting requirement of a total loss of feedwater supply (including emergency feedwater). In this scenario, the time between reactor trip and a loss of heat removal is greater than 30 minutes and is sufficient for operating personnel to recover feedwater supply or initiate other countermeasures, such as primary side feed and bleed cooling.

The U.S. EPR design for a non-isolable Main Steam Line Break (MSLB) considers the increased water inventory in the SGs and resultant higher potential of mass and energy release into the containment. The large containment volume (approximately $2.82 \times 10^6 \text{ ft}^3$) accommodates the pressure response in combination with the design pressure.

2.1.2 *Overpressure Protection*

Overpressure Protection (OPP) protects the integrity of the Reactor Coolant Pressure Boundary (RCPB) in both hot and cold conditions. OPP is performed by the PZR safety valves in parallel with the reactor protection system and associated equipment.

The objective of OPP is to prevent the opening of non-isolable valves during all anticipated operational occurrences and accidents that have the potential for radioactive releases.

2.1.2.1 *Primary Side OPP*

Three pilot-operated safety valve discharge trains are arranged at the top of the PZR for primary side OPP. Figure 2-8 shows the PZR with its discharge components.

Automatic opening of a safety valve upon detection of RCS overpressure is ensured by pilot actuators for each of the safety valves. During normal plant operation, a spring-loaded pilot valve is used to open the safety valve.

For overpressure protection at lower RCS temperatures (e.g., cold overpressure protection), two solenoid pilot valves in series are used to open each safety valve. The setpoint is adjustable. Additionally, the pilot valves may be manually operated.

Primary side OPP is classified as safety-related and the equipment used for this function is qualified for liquid, steam, and two-phase flow operation.

The PZR discharge performs the following safety functions:

- OPP of the RCS by automatic initiation of discharge of steam, water, or two-phase fluid, depending on the specific initiating event.
- Depressurization of the RCS by discharge of steam or water for those plant conditions for which depressurization by PZR spray via the Chemical and Volume Control System (CVCS) is not available or insufficient.
- Discharge of reactor coolant to enable continued RHR in the event of complete unavailability of the secondary side heat removal, in conjunction with injection of cooled borated water by the Safety Injection System (SIS) (feed and bleed).

The PZR relief system discharges to the Pressurizer Relief Tank (PRT) which is located inside the containment. The PRT condenses the steam by mixing it with relatively cold water in the PRT. Thus, the PRT contributes to the protection of the RCS from overpressure in conjunction with the PZR relief system.

In addition to the PZR safety valves, a dedicated discharge line is provided to depressurize the RCS during a core melt condition. This guarantees depressurization to a pressure sufficiently below the level that would lead to a high pressure core melt accident. The Pressurizer Depressurization System (PDS) is manually actuated in the event of a severe accident and consists of two valves that discharge into the PRT.

PDS valves are independent of the electrical power supply units for operational considerations and for dependability during accident scenarios. These valves are supplied by the main emergency diesels, the SBO diesels, and the batteries dedicated to severe accidents.

2.1.2.2 Secondary Side OPP

On each main steam line, three discharge trains are arranged outside the containment.

The discharge trains on each line are arranged as follows:

- One discharge line is equipped with a relief valve and an isolation valve connected in series having approximately a 50% capacity of the full load flow of one SG.
- Two other discharge lines are each equipped with a dedicated safety valve having approximately a 25% capacity of the full load flow of one SG.

Figure 2-9 shows a schematic arrangement of the secondary side OPP.

Both types of discharge trains (relief and safety valves) are safety grade. The relief train designs meet ASME code requirements and will therefore be credited in OPP analyses.

In the overall concept of secondary side pressure limitation and heat removal, the following represents the hierarchy of the defense-in-depth principle:

- The first line of defense is the actuation of the turbine bypass.
- The second line of defense is the relief valve, which ensures safety grade controlled heat removal and pressure limitation.
- The third line of defense consists of the two safety valves.

Capacities of both the relief and safety valves are based on the principles discussed below.

- For anticipated operational occurrences, discharge is controlled in a way that prevents the opening of a non-isolable safety valve and applicable pressure limits are not exceeded. Protection system action (i.e., a reactor trip) is taken into account, and failure to open a discharge line is not considered for anticipated operational occurrences.
- For beyond design basis conditions, discharge capacity is sufficient to avoid exceeding applicable pressure limits, even if one of the discharge lines fails to

open. For this scenario, the protection system action (reactor trip) is taken into account.

This approach provides diversity for both valve actuation and valve type.

With the selected configuration of discharge valves, the following safety functions are performed:

- OPP and controlled heat removal at normal or upset conditions is by means of the relief valve in the event of condenser unavailability.
- OPP for emergency conditions such that 110% of design pressure is not exceeded.
- With accidents (e.g., SBLOCA), the secondary side is cooled down to approximately 870 psia at a rate of approximately 180 °F/h by means of the relief valves. This ensures adequate injection from the MHSI system. Adequate injection essentially means that the RCS inventory decrease is minimized so the respective design criteria are met.
- With a SGTR, as well as with any event involving the response of a steam dump, uncontrolled release of steam or water is prevented by closing the dedicated isolation valves if the water level increases beyond a certain limit or if a discharge valve sticks in the open position. (The safety valve response is not challenged in the event of a SGTR.)

2.1.3 *Principal Fluid Systems*

The safety functions provided by the principal fluid systems are:

- Control of reactivity
- RCS inventory and integrity
- Residual heat removal

The fluid systems that ensure or contribute to reactivity control are the Extra Borating System (EBS), the CVCS, and the SIS.

Fluid systems that ensure control of the RCS inventory are the CVCS and the SIS. Fluid systems or equipment that contribute to ensuring RCS integrity are those required for OPP and those needed for cooling and supply of injection water to the RCP seals (since damage to an RCP seal could result in loss of RCS integrity). Cooling of the RCP seals is provided by the Component Cooling Water System (CCWS), with injection water ensured by the CVCS.

RHR from the SG secondary side is ensured by the Emergency Feedwater System (EFWS) and the secondary side OPP system. The Start-Up and Shutdown System (SSS) also contributes to this function.

RHR from the primary side during shutdown conditions is ensured by the RHR System (RHRS) combined with the Low Head Safety Injection (LHSI) system.

The CCWS provides cooling to the safety systems and the Essential Service Water System (ESWS) provides the heat sink for the CCWS.

2.1.3.1 System Configuration

The following systems and their associated electrical power supply and I&C systems are arranged in a four-train configuration:

- SIS/RHRS
- EFWS
- CCWS
- ESWS

The four-train arrangement for these principal fluid systems, corresponding to the four-loop configuration of the RCS, leads to a simplified design concept for the fluid systems in that each system is connected to a single loop with no operator action required to balance flow between loops. This arrangement also allows flexibility and redundancy during plant shutdown conditions when capacity requirements for heat removal and other functions are reduced relative to the needs associated with normal power operations. The four-train configuration also offers the possibility of extending maintenance intervals on parts of the systems, which can be beneficial for preventive

maintenance or general repair requirements. For instance, preventive maintenance of one complete safety train can be performed during power operation.

The following systems are arranged in a two-train configuration:

- EBS
- Fuel Pool Cooling System (FPCS), in which two FPCS pumps operate in parallel in each of the two trains

The organization of the systems that provide injection of water into the RCS is given below.

MHSI	
Medium Head Safety Injection (MHSI) System	4 trains; cold leg injection
Accumulators	4 accumulators; cold leg injection
LHSI/RHR	
Low Head Safety Injection/ Residual Heat Removal System	4 trains; cold leg injection for short term + cold and hot leg injection for long term
EBS	
Extra Borating System	2 trains; injection of highly borated water; cold leg injection
IRWST	
In-Containment Refueling Water Storage Tank	Storage of borated water inside containment

Figure 2-10 shows a schematic of the main fluid systems. Each of the systems identified above is described in more detail below.

2.1.3.2 *Safety Injection/Residual Heat Removal System*

The SIS/RHRS performs normal shutdown cooling, as well as emergency coolant injection and recirculation functions to maintain reactor core coolant inventory and provide adequate decay heat removal following a LOCA. The SIS/RHRS can also maintain RCS inventory following a MSLB. (Figure 2-11 shows the flow schematic of the SIS/RHRS.)

The safety functions of the SIS/RHRS are:

- Rapid reflood of the RPV and the reactor core following a Large Break LOCA (LBLOCA)
- Long-term injection of water to the core for small, intermediate and LBLOCA
- Injection of water for intermediate and LBLOCA to terminate the release of steam to the containment atmosphere as early as possible
- Injection of water to the RCS for small to intermediate size LOCA or SGTR, at any pressure less than the SG safety valve or relief valve discharge pressure. Partial cooldown of the SGs by the reactor protection system ensures adequate SIS flow.
- Cooling of the IRWST in the event of a LOCA
- Mixing of water recirculated in the long term after a LOCA to ensure homogeneous boron concentration and temperature
- Injection of water, in conjunction with reducing RCS pressure through use of the PZR safety valves, to ensure RHR from the RCS and cool down to a cold shutdown condition in the event of a loss of decay heat removal via the SGs (feed and bleed mode)
- Emergency makeup to the RCS in the event of a loss of water inventory during cold shutdown or refueling

The normal operational functions of the SIS/RHRS are:

- RHR to reach and maintain cold shutdown and refueling conditions
- Transfer water from the IRWST to the reactor cavity in preparation for refueling operations
- Cooling and mixing of the IRWST contents during normal plant operating conditions.

The calculated cooling performance of the SIS/RHRS following postulated LOCAs will conform to the criteria of 10 CFR 50.46. The SIS/RHRS has sufficient capacity, diversity, and independence to perform its required safety functions following design

basis transients or accidents assuming a single failure in one train while a second train is out-of-service for preventive maintenance.

The SIS/RHRS consists of four independent trains, each providing injection capability by an accumulator pressurized with nitrogen gas, a MHSI pump, and a LHSI pump. The LHSI/RHR pumps also perform the operational functions of the RHRS. Each of the four SIS trains is provided with a separate suction connection to the IRWST. Guard pipes are provided for sump suction piping between the sump connection and the suction isolation valve. The sumps are provided with a series of screens, ensuring protection of the SIS pumps against debris entrained with IRWST fluid.

Each pump is provided with a miniflow line routed to the IRWST. The LHSI/RHR pump miniflow also provides cooling and mixing of the IRWST.

In the injection mode, the MHSI and LHSI/RHR pumps take suction from the IRWST and inject into the RCS through nozzles located in the top of the piping. These pumps are located in the Safeguard Buildings, close to the containment. The LHSI/RHR pumps and the MHSI pumps normally inject into the cold legs. In the long term following a LOCA, the LHSI discharge can be switched over to the hot legs to limit the boron concentration in the core, thus reducing the risk of crystallization in the upper part of the core.

A LHSI/RHR heat exchanger is located downstream of each LHSI/RHR pump. These heat exchangers are installed in the Safeguard Buildings and cooled by the CCWS. The accumulators are located inside the containment and inject into the RCS cold legs when the RCS pressure falls below the accumulator pressure, using the same injection nozzles as the LHSI/RHR and MHSI pumps.

During RHR operation, the LHSI/RHR pumps take suction from the RCS hot leg and discharge through the LHSI/RHR heat exchangers back to the RCS cold leg. During shutdown, the LHSI/RHR pump is used in the RHR mode, but the MHSI pump remains available for water make-up in the event of a LOCA.

All four SIS/RHRS trains are powered from separate emergency buses, each backed by an EDG. The LHSI/RHR pumps in Trains 1 and 4 are also backed-up by the SBO diesels.

One SIS/RHRS train is located in each of the Safeguard Buildings, thereby providing separation and/or physical protection from external and internal hazards.

2.1.3.3 IRWST

The function of the IRWST is to contain a large amount of borated water at a homogeneous concentration and temperature. The borated water is used to flood the refueling cavity for normal refueling. It is also the safety-related source of water for emergency core cooling in the event of a LOCA and is a source of water for containment cooling and core melt cooling in the event of a severe accident. During a LOCA, the IRWST collects the discharge from the RCS, allowing it to be recirculated by the SIS. (Figure 2-12 shows a flow diagram of the IRWST and related components.)

The IRWST is essentially an open pool within a partly immersed building structure. The walls of the IRWST are lined with an austenitic stainless steel liner to avoid interaction of the boric acid and concrete structure and to ensure water tightness. Each of the four SIS (safety-related) and two SAHRS (non safety-related) trains is provided with a separate sump suction connection to the IRWST. To prevent RCS thermal insulation and other debris from reducing the suction head of the SIS and SAHRS pumps during and following a LOCA, a series of barriers are used to minimize the amount of debris which can reach the sumps. The heavy floor beneath the RCS has strategically placed openings through which water drains to the IRWST. Each of these openings has a weir (curb) around it and a trash rack in the opening. Beneath the openings are retaining baskets which trap the larger sized debris while allowing water to flow into the tank. Each of the sumps is provided with a cage screen with reverse inclined sieves so caked debris can be backwashed to the floor of the tank. Each of the sump screens is sized such that, should all anticipated debris reach an individual screen, that screen will not be prevented from providing its function. Vortex suppressor grids under each sump screen prevent loss of suction if the IRWST water level is low. Screen backwashing

functions are accomplished via the MHSI pump miniflow lines. The LHSI miniflow lines are operated continuously to permit cooling and mixing of the IRWST water.

Except for the sump suction isolation valves, all IRWST related components are passive. The isolation valves are powered from safety-related buses. Suction lines from the IRWST are equipped with guard pipes in addition to the sump isolation valves in order to satisfy single failure criteria to prevent loss of water inventory.

2.1.3.4 *Extra Borating System*

The EBS provides high pressure boration to shut down the reactor following accidents when the CVCS is not available. The EBS is also designed to minimize fresh boron consumption and to avoid the use of active components during standby (i.e., complicated heat tracing devices to prevent crystallization). This design objective allows the RCS to be tested without first injecting fresh boron.

The EBS is a safety-related system that performs the following functions:

- Maintain the reactor in a shutdown state at any reactor temperature in the case of unavailability of the CVCS
- For Anticipated Transients Without Scram (ATWS), automatically starts to ensure the RCS boration required is provided to shut down the reactor (to a sub-critical condition)

The EBS consists of two identical primary trains. Each primary train is composed of its own boron tank, a high pressure 100% capacity pump, a test line, and injection lines to the RCS. The boron tanks and the primary train lines are filled with highly borated water and are located in a temperature controlled room that guarantees the non-crystallization of the boric acid.

The EBS does not perform any function supporting normal plant operation. During normal operation:

- The pumps are shut down except during periodic test or heating/mixing of the tanks.

- All hand-operated valves from the Extra Borating Tanks up to the RCS are normally open.
- The motorized and manual isolation valves of the test lines are normally closed.
- The motorized isolation valves of the injection lines connected to the RCS are normally closed.
- The containment isolation valves are normally open.

No active components are in service during EBS standby except the boron room heaters.

A header connecting the bottoms of the two boron tanks is normally isolated by a remotely operated, closed manual valve and can allow injection (or draining) from both tanks using only one EBS pump.

The two EBS trains are remotely operated and powered by emergency buses, each backed by an emergency diesel and further backed-up by the SBO diesels. The two trains are installed in two separate layout divisions within the Fuel Building. Each of the two trains can inject into two RCS loops via the cold legs.

2.1.3.5 Emergency Feedwater System

The EFWS supplies water to the SGs to maintain water level and remove decay heat following the loss of normal feedwater supplies due to anticipated operational transients and design basis accident conditions. This ensures the removal of heat from the RCS, which is first transferred to the secondary side via the SGs and then discharged as steam to the condenser, or via the SG MSRVs. (Figure 2-13 shows the flow schematic of the EFWS.)

During normal power operation, the feedwater supply to the SGs is provided by the Main Feedwater System (MFWS). For start-up and shutdown operation of the plant, a dedicated system, the Start-up and Shutdown System (SSS), is provided. The SSS is actuated automatically in the event of a low level in the SGs following a reactor trip with the loss of the MFWS. The SSS actuation reduces the frequency of the EFWS actuation and increases the reliability of the entire feedwater system.

The EFWS is a safety-related system that performs the following functions:

- Provide sufficient flow to the SGs to recover and maintain SG water inventory and remove residual heat from the RCS via the SGs and MSRVs to assist in the cooldown and depressurization of the RCS to RHR conditions under design basis transient and accident conditions
- Isolation of EFWS flow to the affected SG following a MSLB to prevent overcooling the RCS and the associated insertion of positive reactivity
- Isolation of EFW pump flow to the SG with a tube rupture upon SG high level to mitigate the potential radiological consequences of a SGTR event
- Provide sufficient volume in the storage pools to maintain hot shutdown conditions for 24 hours following beyond design basis events (SBO and loss of ultimate heat sink)

The EFWS has sufficient capacity and independence to perform its required safety functions following design basis transients or accidents assuming a single failure in one EFW pump train and a second train being out-of-service for preventive maintenance.

The EFWS does not perform any functions supporting normal plant operation.

The EFWS has four separate and independent trains, each consisting of a water storage pool, pump, control valves, isolation valves, piping, and instrumentation. A supply header is provided that allows cross-connecting the storage pools to the pump suction, and another header that allows cross-connecting the discharge of the pumps to the SGs. These headers are normally isolated and require local operator action to change storage pool or pump discharge alignment. The non-safety Demineralized Water Distribution System can be used to provide make-up to the EFWS storage pools.

Each of four emergency feedwater pumps is powered by a separate electrical division supplied by its own EDG. In case of common mode failure of all EDGs, two of the motor-driven EFW pumps are powered by two diverse SBO diesels.

One EFWS train is located in each of the Safeguard Buildings, providing separation and/or physical protection from external and internal hazards. The storage pools are internally lined concrete and are structurally part of each Safeguard Building.

2.1.3.6 CVCS

The Chemical and Volume Control System (CVCS) is the interface system between the high pressure RCS and the low pressure systems in the Nuclear Auxiliary Building and Fuel Building. The CVCS provides a flow path for the continuous letdown and charging of RCS water. The CVCS maintains the RCS water inventory at the desired level via the PZR level control system and provides RCP seal water injection and auxiliary spray for PZR cooldown.

The CVCS is an operational system and is not required for the mitigation of design basis accidents. However, the CVCS may be utilized to preclude the use of safety systems during minor transients (e.g., boron dilution events). The system is normally in continuous operation during all modes of plant operation from normal power operation to cold shutdown.

The system performs the following operational functions:

- Continuous control of the RCS water inventory during all normal plant operating conditions utilizing the charging and letdown flow path
- Provide make-up to the RCS in the event of a loss of inventory due to limited leakage
- Adjust the RCS boron concentration as required for power variation control, plant start-up or shutdown, or core burnup compensation through the addition of boron and/or demineralized water
- Reduce PZR pressure by diverting charging flow to the PZR auxiliary spray nozzle and condensing the steam bubble in the PZR to reach RHRS conditions
- Inject cooled and purified water into the RCP seals to ensure cooling and leak tightness and return any seal leakage to the CVCS

- Provide primary coolant chemical control by interfacing with the coolant purification, treatment, degasification, and storage systems
- Control the concentration and the nature of dissolved gases in the RCS by maintaining the required hydrogen concentration in the charging flow and degasifying the reactor coolant, when required
- Filling and draining the RCS during shutdown conditions

The major components of the CVCS are two redundant centrifugal Charging Pumps, a Volume Control Tank (VCT), a Regenerative Heat Exchanger, two high pressure coolers in parallel (cooled by CCW), two parallel high pressure Reducing Stations, a low pressure Reducing Station, and associated valves and piping. (Figure 2-14 shows a flow schematic of the CVCS.)

The letdown portion of the system receives water from the RCS Loop 1 crossover leg and exits the RCS through two motor-operated isolation valves connected in series. The flow then passes through the shell side of a regenerative heat exchanger transferring heat to the charging flow returning to the RCS on the tube side. The letdown flow is further cooled in the high pressure coolers and depressurized by the pressure reduction valves. Downstream of the pressure reduction valves, a safety valve provides overpressure protection of the letdown piping inside the Reactor Building. A bypass connection is provided to allow discharging letdown flow to the Reactor Coolant Drain Tank. This connection permits letdown from the RCS if a portion of the CVCS system or equipment outside containment is not available. Also, a connection to the discharge of the RHRS is arranged to allow letdown flow when the RCS is depressurized. The letdown flow then passes through the Reactor Building into the Fuel Building. In the Fuel Building, the letdown flow is sampled and purified. During power operation, the purification flow rate is sufficient to treat at least one RCS volume in one-half day under normal conditions.

Letdown flow is degasified in the Coolant Degasification System if required. Letdown flow is then directed to the VCT and to the Hydrogenation Station where hydrogen gas is mixed into the flow stream to provide oxygen scavenging which results from the

radiolysis of reactor coolant. The VCT acts as a surge tank to permit smooth control of variations in charging and letdown flow rates. Provisions also allow for the diversion of any excess letdown flow to the Coolant Storage and Supply System due to the volume expansion of RCS resulting from system heatup or any boration or dilution. Connections are provided to the CVCS to allow for chemical additions and for boric acid and demineralized water makeup.

The Charging Pumps take suction from the VCT/letdown line and increase the pressure to allow the purified coolant to be returned to the RCS. The charging pumps can also take suction from the IRWST in the event of low level in the VCT or if a dilution accident is detected. If either condition is detected, the motor-operated valves from the IRWST automatically open and the motor-operated valves from the VCT/letdown line automatically close.

The main charging pump discharge flow passes through the tube side of the regenerative heat exchanger where the temperature is increased prior to injection into the cold legs of RCS Loops 2 and 4. The charging flow rate is constant during power operation and letdown flow is controlled to maintain the PZR level.

A portion of the charging flow is delivered to the RCPs for shaft seal water. The seal water is automatically controlled by motor-operated control valves to each RCP during plant conditions when seal injection is required for RCP operation. Leakage through the RCP seals is returned to the VCT to maintain CVCS inventory.

A three-way motor-operated valve downstream of the regenerative heat exchanger is provided for aligning CVCS injection flow to the pressurizer auxiliary spray nozzle to allow for reducing RCS pressure in order to reach RHR conditions.

A low-pressure reducing station is provided to allow the RHRS to utilize the letdown flow path and the coolant purification system during shutdown conditions when the RHRS is in operation.

Even though the CVCS is not required to perform any design basis accident mitigation functions and is only an operational system, the CVCS charging pumps and

motor-operated valves are powered from emergency buses which are further backed-up by EDGs.

Major components of the CVCS are located in the Reactor Building and the Fuel Building. These components are protected from external hazards by the building design and are physically separated or provided with protection from internal hazards.

2.1.3.7 Component Cooling Water System

The CCWS ensures the capability to transfer heat from safety-related systems and operational cooling loads to the heat sink via the ESWS under all normal operating conditions. (Figure 2-15 shows a flow schematic of the CCWS.)

The CCWS performs the following safety functions:

- Heat removal from the SIS/RHRS to the ESWS
- Heat removal from the FPCS to the ESWS as long as any fuel assemblies are located in the spent fuel storage pool outside containment
- Cooling of the thermal barriers of the RCP seals
- Heat removal from the Heating, Ventilation, Air Conditioning (HVAC) chillers of Divisions 2 and 3
- Cooling of the SAHRS by two separated trains that are part of a dedicated cooling chain (this function is used for prevention of core melt and severe accident mitigation)

The CCWS consists of four separate safety classified trains (1, 2, 3 and 4) corresponding to the four layout divisions (1, 2, 3 and 4) and two separate common loop sets. One of the common loops (common 1) is connected normally either to safety train 1 or to safety train 2. The other common loop (common 2) is connected either to safety train 3 or to safety train 4.

Each safety classified train consists of the following equipment:

- One pump, equipped with the necessary minimum flow line and cooling line.
Each train is capable of providing 100% of the train needs.

- One heat exchanger located downstream of the CCWS pump. This heat exchanger is cooled by the ESWS. Its bypass line is connected to the CCWS side and equipped with a control valve to control the CCWS temperature when the ESWS temperature is low.
- One surge tank (concrete tank with a steel liner) which is connected to the pump suction line and located above the highest CCW load. The surge tank is connected to a demineralized water make-up to compensate for CCWS normal leaks or component draining water.
- One sampling line, which is connected permanently to a radiation monitor.
- One chemical additive supply line.
- A set of isolation valves that separate the train from the common load set.

Two separate dedicated trains cool the SAHRS when it is used during a severe accident scenario involving core melt. Each train consists of the following equipment:

- One pump with power supplied by the SBO diesel
- One heat exchanger located downstream of the pump
- One surge tank
- One demineralized water supply line with pressurizing pump

2.1.3.8 Essential Service Water System

The ESWS consists of four separated safety-classified trains that provide cooling of the CCWS heat exchangers with water from the heat sink during all normal plant operating conditions, transients, and accidents. The ESWS also includes two additional trains of dedicated cooling for severe accident mitigation. (Figure 2-16 shows a flow schematic of the ESWS.)

The safety function of the ESWS is to cool the CCWS. It also provides cooling of the SAHRS (via the dedicated SAHRS cooling chain).

The ESWS provides cooling water to the four CCWS/ESWS heat exchangers which, in turn, cool components of the safety systems. Each train consists primarily of the suction

pipe from the heat sink, the pump, the discharge pipe from the pump to the ESWS/CCWS heat exchanger, and the outlet pipe from the heat exchanger to the heat sink.

The divisions of the ESWS trains are grouped two-by-two into separate rooms belonging to the same civil structures in such a way that an internal hazard affecting one train does not affect the other train.

Electrical power is supplied by independent power trains, which are backed-up by the main EDGs.

The ESWS pumps are installed in the Service Water Buildings.

2.2 Core Design

2.2.1 General Features

The U.S. EPR has a rated core thermal power of approximately 4,500 MWt. The reactor core consists of an array of 241 fuel assemblies with the following characteristics:

- A 17 x 17 lattice composed of 265 fuel rods mechanically joined in a square array
- Optimized and proven fuel rod design parameters
- Enrichment of up to 5 wt% ^{235}U
- Gd_2O_3 integral burnable poison with Gd concentration of 2 wt% to 8 wt%
- Highly corrosion-resistant and low-growth M5[®] cladding and tubing
- Monobloc[™] guide thimbles to increase structural strength
- Low growth M5[®] intermediate spacers
- Alloy 718 end spacers providing improved fuel rod support and flow-induced fretting resistance
- Debris-resistant robust FUELGUARD[™] bottom nozzle

- Removable top nozzle for ease of assembly repair

Preliminary values of the key core parameters are given in Table 2-2. Additional data for neutronic and thermal-hydraulic design are provided in Tables 2-3 and 2-4. In addition to the U.S. EPR values, values for a current U.S. four-loop plant are also provided for comparison purposes.

2.2.2 Fuel Assemblies

The fuel rods are mechanically restrained axially and radially in the fuel assembly structure by eight M5[®] intermediate HTP grids and two Alloy 718 end HMP spacer grids. The grids have integrated curved flow channels for promoting the mixing of the coolant and improving the heat transfer between the cladding and the coolant. The intermediate grids are axially constrained with welds to the guide thimbles. The end grids are axially constrained by sleeves that are welded to the guide thimbles above and below the grids.

Twenty-four positions in the 17 x 17 array are equipped with M5[®] Monobloc™ guide thimbles, which are joined to the grids and the top and bottom nozzles. The guide thimbles are used as locations for Rod Cluster Control Assemblies (RCCAs) and stationary core component assemblies such as thimble plug assemblies and neutron source assemblies. The guide thimbles are also used as locations for the movable or fixed in-core instrumentation. Each guide thimble also utilizes a quick-disconnect connection for efficient removal and replacement of the top nozzle.

The top nozzle of the fuel assembly is the structural element that interfaces with the upper core plate. The top nozzle also supports the holddown springs of the fuel assembly, which are used to prevent hydraulic lift-off of the fuel assembly during operation. The holddown springs are Alloy 718 leaf springs that are bolted in two diagonal corners of the top nozzle. The top nozzle also incorporates an appropriate interface for the fuel handling equipment, RCCA, and stationary core components. The 180° rotational symmetry of the fuel assembly provides additional flexibility for fuel management.

The bottom nozzle of the fuel assembly serves as the structural element that interfaces with the lower core plate. The bottom nozzle shape directs and equalizes the flow distribution and also filters out small debris.

Illustrations of the fuel assembly are provided as follows:

- Figure 2-17: Radial cross section of a fuel assembly
- Figure 2-18: Fuel assembly in axial view
- Figure 2-19: Photographs of the top nozzle and bottom nozzle of the fuel assembly

Key fuel assembly characteristics are given in Table 2-5.

2.2.3 *Rod Cluster Control Assemblies and Reactivity Control*

The core has a fast shutdown system consisting of eighty-nine RCCAs. All RCCAs are of the same type, consisting of twenty-four individual and identical absorber rods fastened to a common spider assembly. These rods are constructed of stainless steel tubing that contains neutron absorbing materials. When fully inserted, they cover nearly the complete active fuel assembly length. The rod absorber material is typically Ag-In-Cd (AIC) alloy. Typical characteristics of the RCCAs and control rod drive mechanisms are given in Table 2-6. A RCCA pattern is shown in Figure 2-20.

The core is cooled and moderated by light water at a pressure of 2250 psia. The coolant contains boron (^{10}B enriched) as a neutron absorber. The boron concentration in the coolant is varied to control slow reactivity changes necessary for compensating xenon poisoning or burn-up effects during power operation and for compensating large reactivity changes associated with large temperature variations during cooldown or heatup phases.

2.2.4 *Core Instrumentation*

The safety approach for the protection of the core relies partly on the capacity to predict and measure the nuclear power level (or level of neutron flux) as well as the three-dimensional power distribution. The measurement of the nuclear power level (or neutron flux level) is performed by loop temperature instrumentation and wide range ex-

core flux (power) instrumentation, as is classically done on PWRs. The capacity to predict and measure the three-dimensional power distribution relies on two types of in-core instrumentation.

2.2.4.1 Ex-Core Instrumentation

During power operation, the nuclear power level is measured principally by a four-fold redundant primary heat balance that relies on temperature measurements in the cold and hot legs of the RCS loops. The primary heat balance is periodically updated (once a month) against the secondary heat balance.

The core is also monitored and protected when operated at very low power levels or in subcritical conditions. The appropriate surveillance and protective functions rely on redundant ex-core neutron flux channels covering approximately 9 to 10 decades of the total neutron flux range below the nominal power.

2.2.4.2 In-Core Instrumentation

In-core instrumentation is top-mounted and consists of:

- An aeroball measurement system as the movable reference core instrumentation
- A quantity of fixed in-core detector fingers containing axially distributed Self-Powered Neutron Detectors (SPNDs), used in four-fold redundant channels for core surveillance and core protection purposes during power operation
- A quantity of Core Outlet Thermocouples (COTCs) having the same radial locations as the SPNDs, used mainly for measuring the margin-to-saturation in post-accident or degraded thermal hydraulic conditions

2.2.4.2.1 Aeroball System

The system for power distribution assessment is an aeroball system. Stacks of vanadium alloy steel balls, inserted from the top of the reactor vessel, are pneumatically transported into the reactor core inside guide thimbles of the fuel assemblies. This system is simple and reliable. The guide tubes for the balls have a small inner diameter

(0.079 in); their bend radii are small (only a few inches); and there are no major constraints for locating the measurement room and routing the tubing. The time periods necessary for a flux measurement are 3 minutes for activation followed by 5 minutes for activity measurements. This system therefore allows flux-mapping measurements in time intervals of 10 to 15 minutes. Figure 2-21 shows a schematic of the aeroball system.

The aeroball probes are carried and distributed over the core by 12 in-core lances. Each in-core lance bears four aeroball fingers and one SPND finger. Aeroball probes are distributed radially throughout the core. Figure 2-22 shows the radial distribution arrangement of in-core instrumentation fingers. Figure 2-23 shows the in-core instrumentation inside a longitudinal cross section of the RPV.

After activation, the activity of the ball-columns is measured in a measuring table by means of thirty-six surface-barrier semi-conductors per column. These detectors are equally distributed over the active length and integrate the activity over a length of ~2.4 in.

The electronic part of the measuring system consists of pulse counters. This technique, combined with the short half-life of the V^{52} isotope (3.7 min.) that serves as the indicator, restricts the range of power over which accurate three-dimensional flux mapping is possible. In practice, acceptable three-dimensional flux maps can be obtained at approximately 30% reactor power.

2.2.4.2.2 Fixed In-Core Instrumentation

The fixed in-core instrumentation consists of SPNDs and COTCs. The SPNDs have a fast response time. At twelve radial locations, six SPNDs are placed in a Power Density Detector (PDD)-finger to cover the core. Each of the yokes of the aeroball system contains one PDD-finger that is replaceable should a detector become defective. The number and the distribution of the SPNDs within the core allow the system to detect and assess local power density increases caused by flux and power redistributions that occur under non-steady-state conditions. The in-core detector system design also makes allowance for a proper “functional” signal redundancy. As core burnup

progresses, the power-to-signal ratio and the reference power distribution change.

Therefore, calibration of the SPNDs to reference conditions is performed at regular intervals.

For the U.S. EPR there are six axial planes in the core and twelve detectors distributed radially in a plane. The calibration of the SPNDs is performed using measured data constructed from aeroball measurements. For High Level Power Density (HLPD), the SPNDs in an axial plane are calibrated to a single measured peak parameter within that plane. For Departure from Nuclear Boiling Ratio (DNBR), each of the SPND strings (six detectors over the six axial regions) are calibrated against the hot pin axial power in the core. SPND calibration factors are generated for both local and hot channel power densities. SPND calibration factors are also generated for axial flux difference (axial-offset) and azimuthal imbalance signals.

Under perturbed conditions, SPNDs change in line with the neutron flux at the detector location. Consequently, the calibrated SPND signals are able to accurately follow or track the highest linear heat generation rates distributed over the core. These signals are used for core control, limitation, and protection purposes. They are processed together with other selected process variables to yield continuous monitoring signals representative of core conditions. Specific core surveillance and core protection systems are based upon digital equipment that measures and/or calculates the safety-relevant parameters of the core, such as peak power, DNBR, Linear Heat Generation Rate (LHGR) margin, axial offset, and core power tilt. These systems operate properly for relatively slow core-related Condition I events and are introduced in order not to overly penalize the operation of the plant. As a consequence, they are able to operate without significant loss of accuracy under conditions such as dropped control rods, RCCA misalignments, and single failure.

Core surveillance and core protection systems are also equipped with sufficient redundant and diverse information including:

- RCCA positions
- Temperature, flow rates, power level

- Axial power distributions
- Radial power distributions

This allows these systems to monitor Condition I events, even if there is a partial unavailability of sensors.

The available information necessary for characterizing the power distribution and thermal-hydraulic conditions is distributed to all the surveillance and protective channels simultaneously. This is possible due to the intrinsic system redundancy; the overlapping of information; the diversity of sensors; and the independence of their calibration procedures. This allows the detection of degraded operating conditions and failed sensors and differentiates between the two.

The COTCs are located in the top nozzle of the instrumented fuel assemblies and are radially distributed over the core in the same way as the SPND fingers. At every location, there is space for three thermocouples. These sensors are primarily used for post-accident measurement purposes, but they may also be used for obtaining additional information relative to radial power distribution and local thermal hydraulic conditions.

Table 2-1 Comparison of Key U.S. EPR Design Parameters

Parameter	U.S. EPR	Current U.S. 4-Loop	French N4	German KONVOI
Design life (yrs)	60	40	40	40
Thermal power (MWt)	4,500	3,411	4,250	3,850
Hot leg temp (°F)	624	610	626	619
Cold leg temp (°F)	564	547	558	558
RCS flow per loop (gpm)	125,000	90,000	109,420	100,450
Primary system pressure (psia)	2,250	2,250	2,250	2,290
Steam pressure (psia)	1,118	870	1,030	935
Steam flow per loop (Mlb/h)	5.1	3.8	4.9	4.2
Total RCS volume (ft ³)	16,245	12,600	14,830	14,210
PZR volume (ft ³)	2,650	1,800	2,120	2,300
SG secondary inventory (lb _m)	182,000	106,000	134,500	101,000
Number of fuel assemblies	241	193	205	193
Fuel lattice	17 x 17	17 x 17	17 x 17	18 x 18
Active fuel length (ft)	13.78	12.00	14.01	12.80
Rods per assembly	265	264	264	300
Average linear heat rate (kW/ft)	4.98	5.44	5.46	5.09
Best estimate peak operating linear heat rate (kW/ft)	12.95 ⁽¹⁾	13.06 ⁽²⁾	13.65 ⁽³⁾	12.73 ⁽³⁾
Number of RCCAs	89	53	73	61
Primary volume/power (ft ³ /MWt)	3.61	3.69	3.49	3.69
Secondary mass/power (lb _m /MWt/SG)	40.4	31.1	31.6	26.2
PZR steam-to-RCS liquid volume	0.070	0.061	0.061	0.065
LOCA break area/system volume (1/ft)	3.17 x 10 ⁻⁴	3.27 x 10 ⁻⁴	2.78 x 10 ⁻⁴	3.35 x 10 ⁻⁴
Accumulator volume/RCS volume	0.35	0.30	0.30	0.68
Containment free volume (ft ³)	2.82 x 10 ⁶	2.62 x 10 ⁶	2.58 x 10 ⁶	2.50 x 10 ⁶

⁽¹⁾Based on a total peaking factor (F_q) of 2.6⁽²⁾Based on a total peaking factor (F_q) of 2.4⁽³⁾Based on a total peaking factor (F_q) of 2.5

Table 2-2 Preliminary Core Parameters

	U.S. EPR	Current U.S. 4-Loop
Nuclear power	4,500 MWt	3,411 MWt
Number of fuel assemblies	241	193
Fuel assembly pitch in core (cold)	8.466 in	8.466 in
Number of fuel rods/fuel assembly	265	264
Fuel assembly length (cold, without springs)	15.76 ft	13.24 ft
Active length (cold)	13.78 ft	12 ft
Average linear power (at rated power)	4.98 kW/ft	5.44 kW/ft
Diameter of fuel rods	0.374 in	0.374 in
Number of guide tubes per assembly	24	25
Guide tube outer diameter	0.490 in	0.482 in
Number of spacer grids per assembly	10	8
Fuel rod pitch	0.496 in	0.496 in
Total fuel rod length (cold)	14.93 ft	12.65 ft
Total fuel assembly mass	1,731 lb _m	1426 lb _m
Assembly UO ₂ mass	1,338 lb _m	1153 lb _m

Table 2-3 Neutronic Core Data

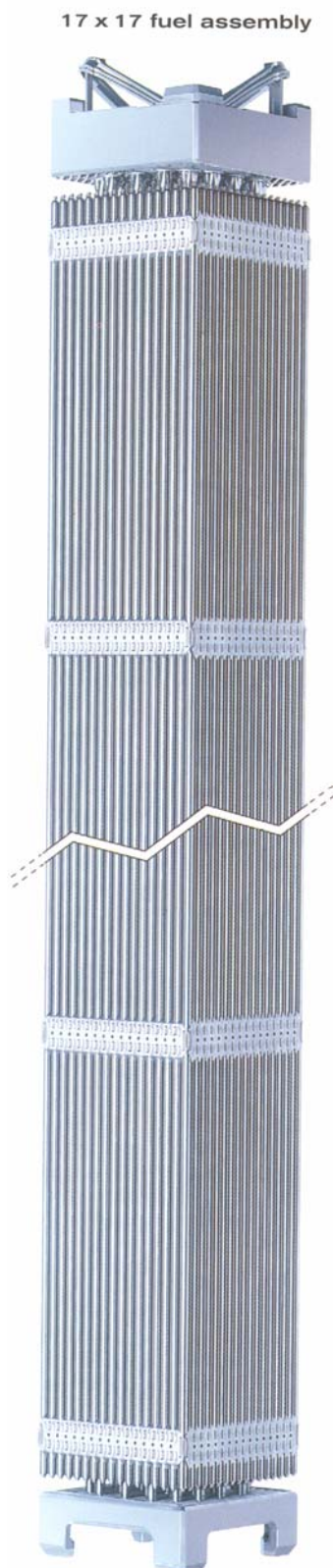
Active Core	U.S. EPR	Current U.S. 4-Loop
• Equivalent diameter	12.35 ft	11.06 ft
• Core average active fuel height, first core (cold dimensions)	13.78 ft	12 ft
• Height-to-diameter ratio	1.115	1.09
• Total cross-section area	119.96 ft ²	96.04 ft ²
Fuel Rods		
• Number	63,865	51,145
• Outside diameter	0.374 in	0.374 in
• Diametral gap	.0065 in	.0065 in
• Clad thickness	.0225 in	.0225 in
• Clad material	M5 [®]	Zircaloy-4
Co-Mixed Burnable Poison (Typical)Gd₂O₃		
• Material	Gd ₂ O ₃	Gd ₂ O ₃
• Gadolinium concentration (wt%)	2 – 8	2 - 8
• UO ₂ carrier enrichment (wt% ²³⁵ U)	~0.7 (host enrichment*)	~0.7 (host enrichment*)

*Host enrichment is the non-gadolinium fuel pin enrichment.

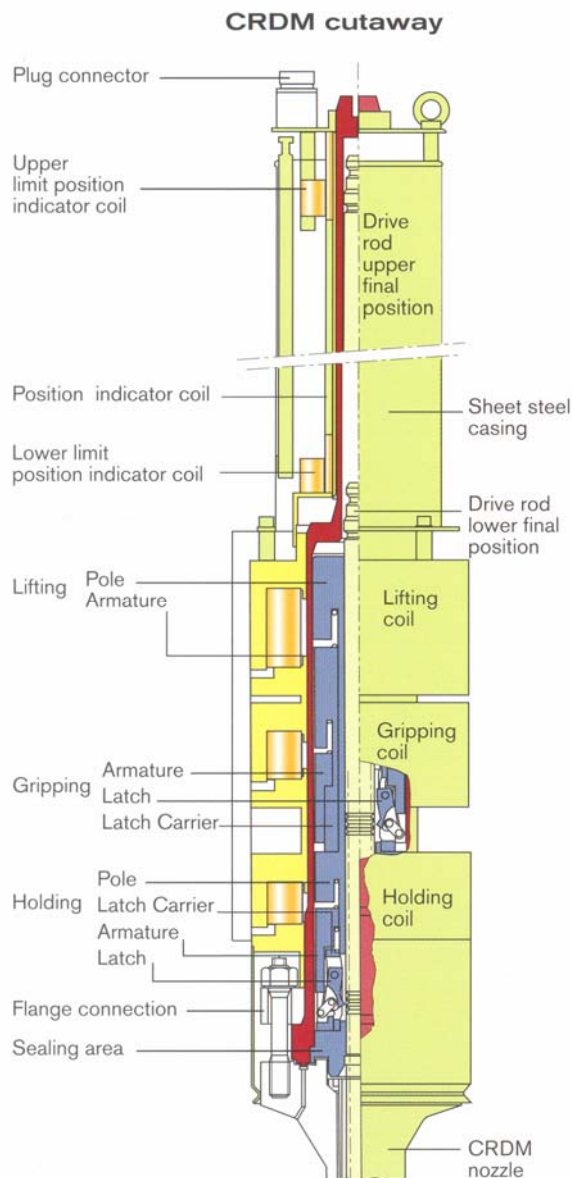
Table 2-4 Thermal Hydraulic Design Data

	U.S. EPR	Current U.S. 4-Loop
Total core heat output	4500 MWt	3411 MWt
Number of loops	4	4
Nominal system pressure	2250 psia	2250 psia
Coolant flow: <ul style="list-style-type: none"> Core flow area Core average coolant velocity Core average mass velocity Vessel flow rate (Best Estimate) Thermal design flow Best estimate flow Mechanical design flow 	63.6 ft ² 15.8 ft/s 2.8 Mlb _m /h-ft ² 184 Mlb _m /h ~479,000 gpm ~499,000 gpm ~539,000 gpm	51.1 ft ² 15.6 ft/s 2.5 Mlb _m /h-ft ² 138 Mlb _m /h ~348,000 gpm ~360,000
Coolant temperature (°F): <ul style="list-style-type: none"> Nominal inlet Average rise in vessel Average rise in core Average in core Average in vessel 	564 61 65 597 595	547 63 68 582 578
Heat transfer: <ul style="list-style-type: none"> Heat transfer surface area Average core heat flux Maximum core heat flux (nominal operation) Average linear power density Peak linear power for normal operating conditions w/uncertainty 	86,170 ft ² 178,200 Btu/h-ft ² ~463,300 Btu/h-ft ² ⁽¹⁾ 4.98 kW/ft ~12.9 kW/ft ⁽¹⁾	59,700 ft ² 189,800 Btu/h-ft ² ~455,500 Btu/h-ft ² ⁽²⁾ 5.44 kW/ft ~13 kW/ft ⁽²⁾
Fuel assembly: <ul style="list-style-type: none"> Number of fuel assemblies Fuel assembly pitch Active fuel height Lattice pitch Number of fuel rods per assembly Number of control rod assembly or instrumentation guide thimbles per assembly Fuel rod diameter Guide thimble outside diameter 	241 8.466 in 165.35 in 0.496 in 265 24 0.374 in 0.490 in	193 8.466 in 144 in 0.496 in 264 25 0.374 in 0.482 in

⁽¹⁾ Based on total peaking factor (F_q) of 2.6⁽²⁾ Based on total peaking factor (F_q) of 2.4

Table 2-5 Key Fuel Assembly Characteristics

Characteristics	Data
Fuel Assemblies	
Fuel rod array	17 x 17
Lattice pitch	0.496 in
Number of fuel rods per assembly	265
Number of guide thimbles per assembly	24
Materials	
Mixing spacer grids	M5 [®]
Top & bottom spacer grids	Inconel 718
Guide thimbles	M5 [®]
Nozzles	Stainless steel
Holddown springs	Inconel 718
Fuel Rods	
Outside diameter	0.374 in
Active length	13.78 ft
Cladding thickness	0.0225 in
Cladding material	M5 [®]

Table 2-6 Characteristics of the RCCAs and CRDMs

Characteristics	Data
RCCAs	
Quantity	89
Number of rods per assembly	24
Absorber	
Material	AIC
- Weight composition (%): Ag, In, Cd	80, 15, 5
- Density	634.89 lb/ft ³
- Outer diameter	[]
Cladding	
Material	AISI 316 stainless steel
Surface treatment (externally)	Ion-nitriding
Outer diameter	0.381 in
Inner diameter	[]
Fill Gas	
Control Rod Drive Mechanisms (CRDMs)	
Quantity	89
Stepping speed	14.76 in/min or 29.53 in/min
Maximum scram time allowed	3.5 s
Materials	Forged 304 stainless steel Magnetic 410 stainless steel Non-magnetic stainless steel

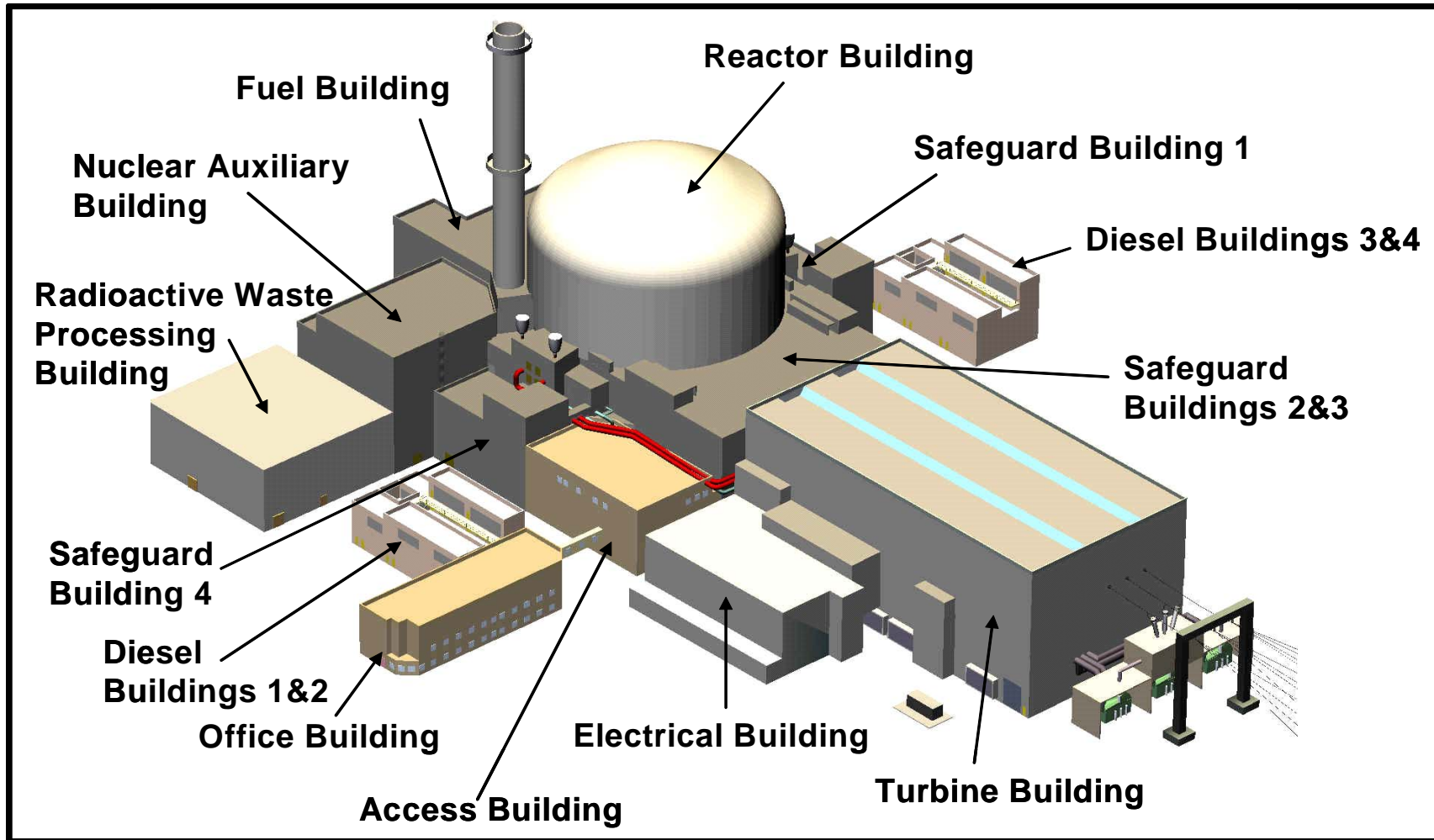
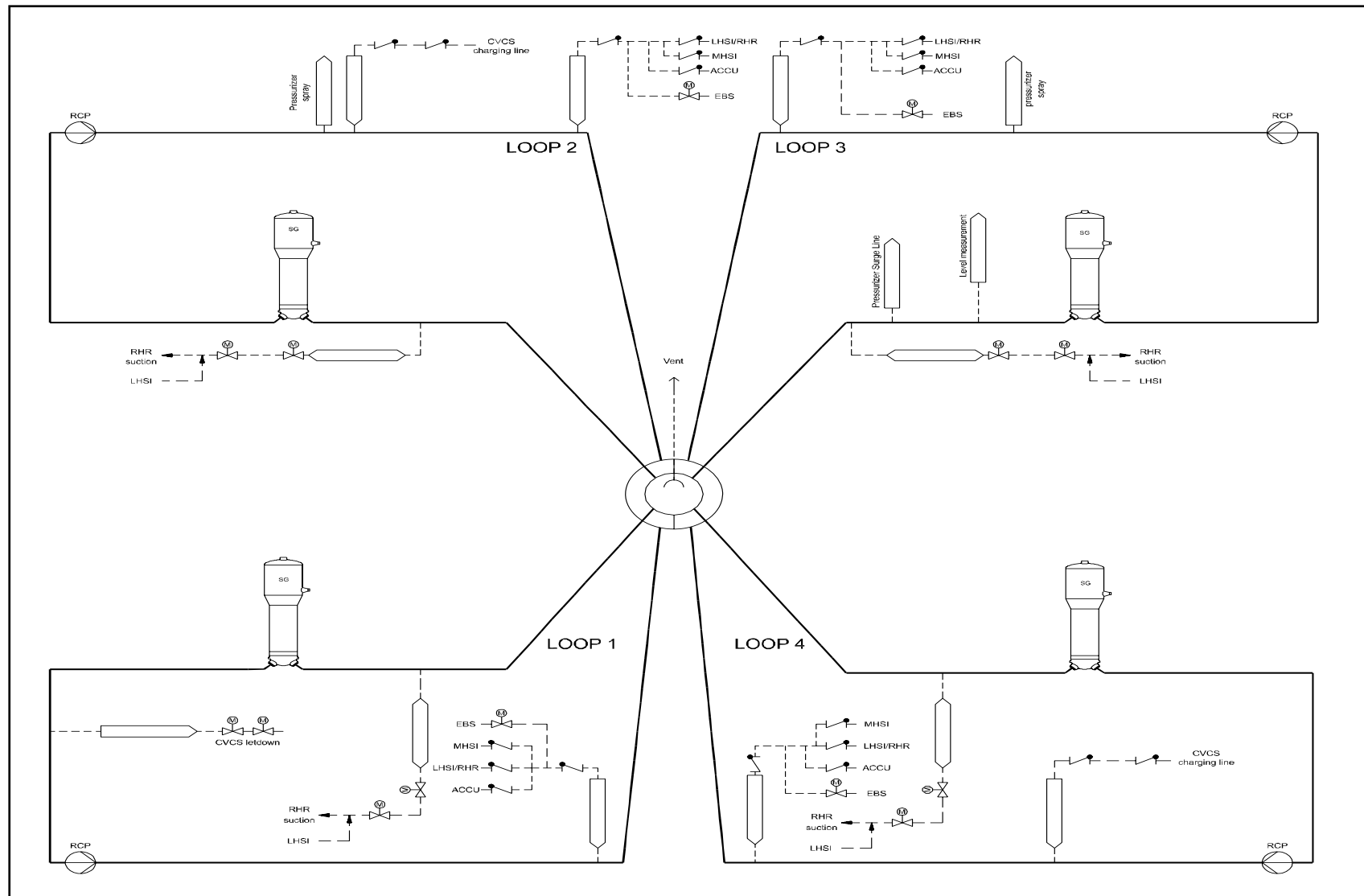


Figure 2-1 Plant Configuration

**Figure 2-2 Reactor Coolant System**

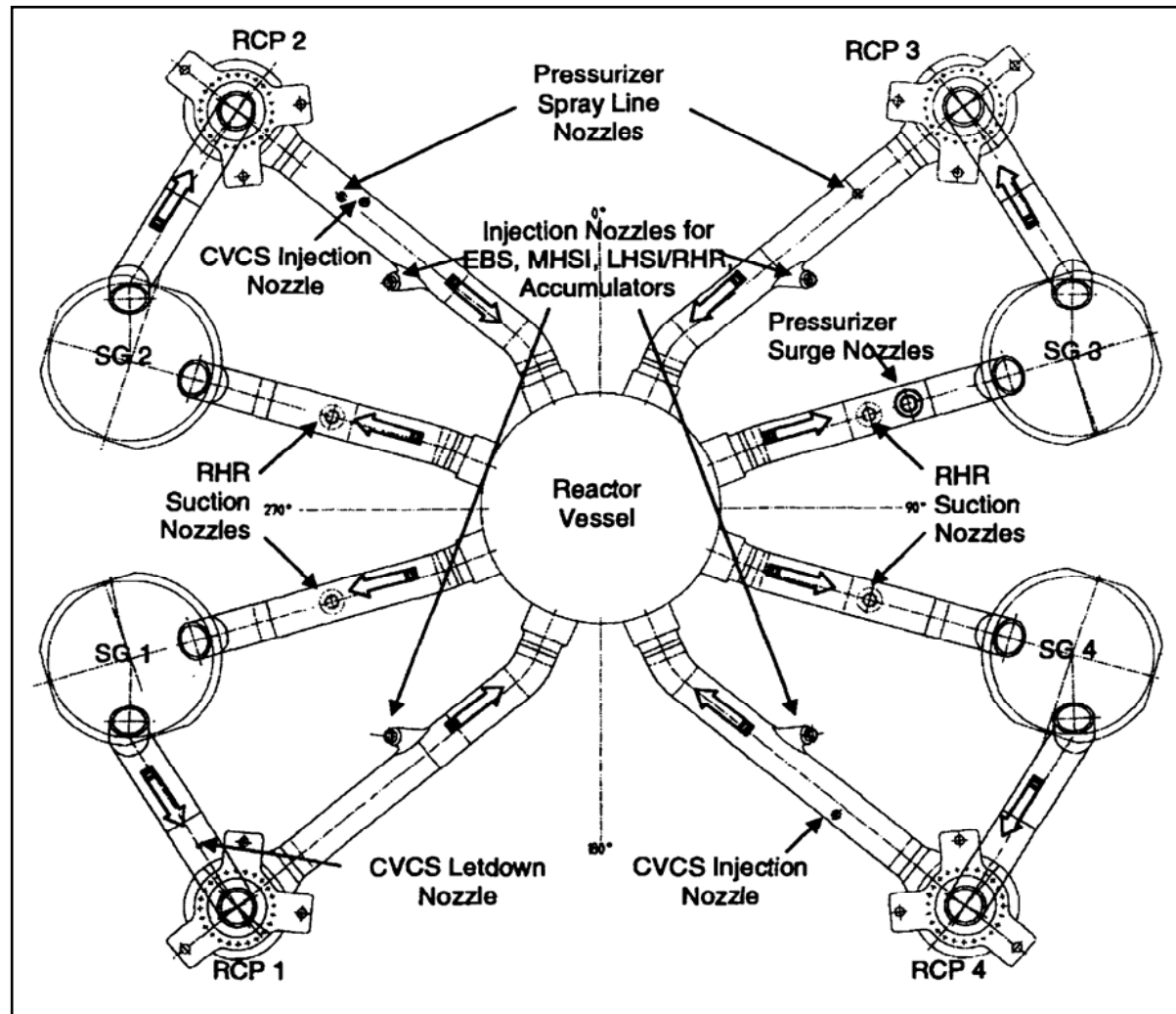
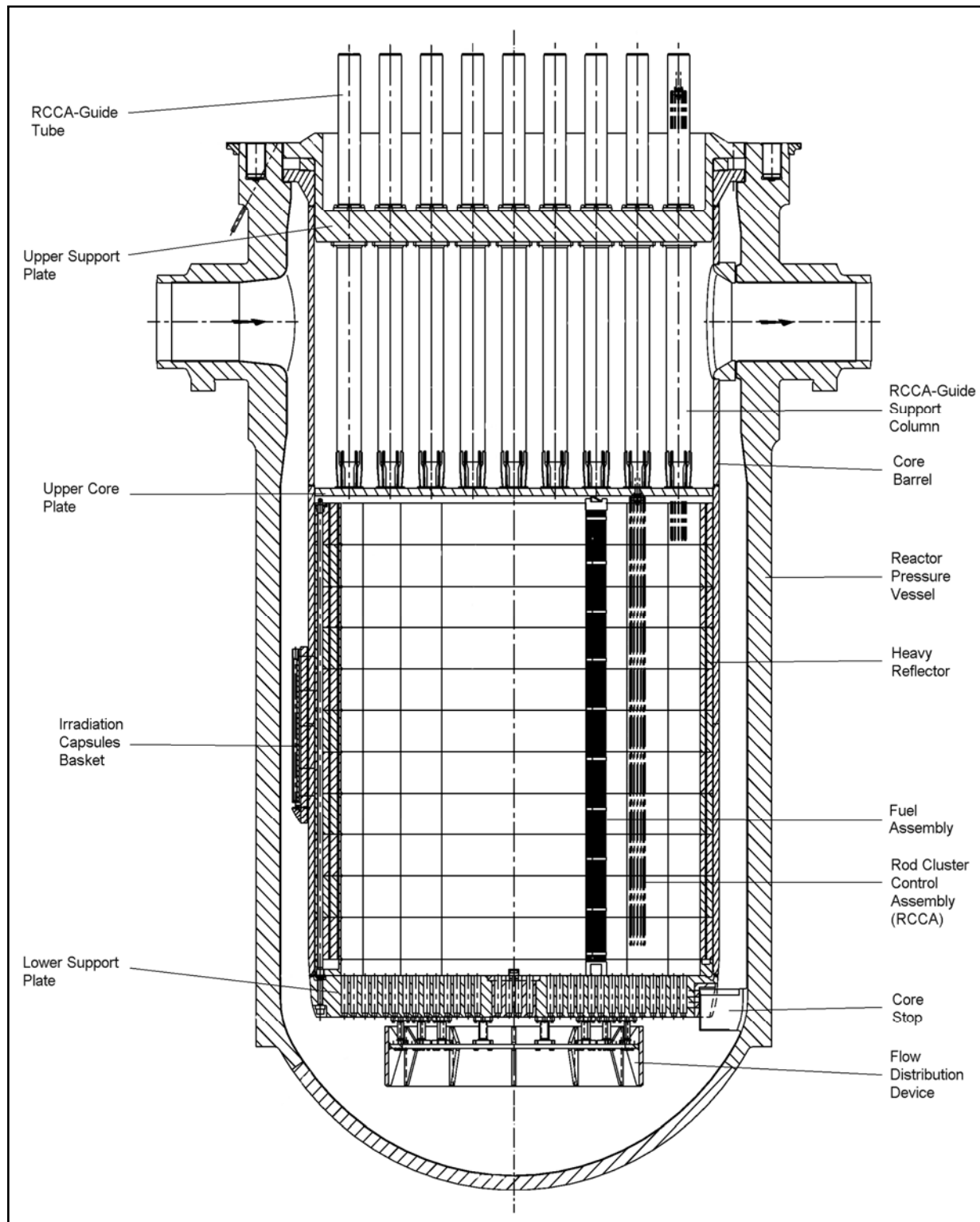
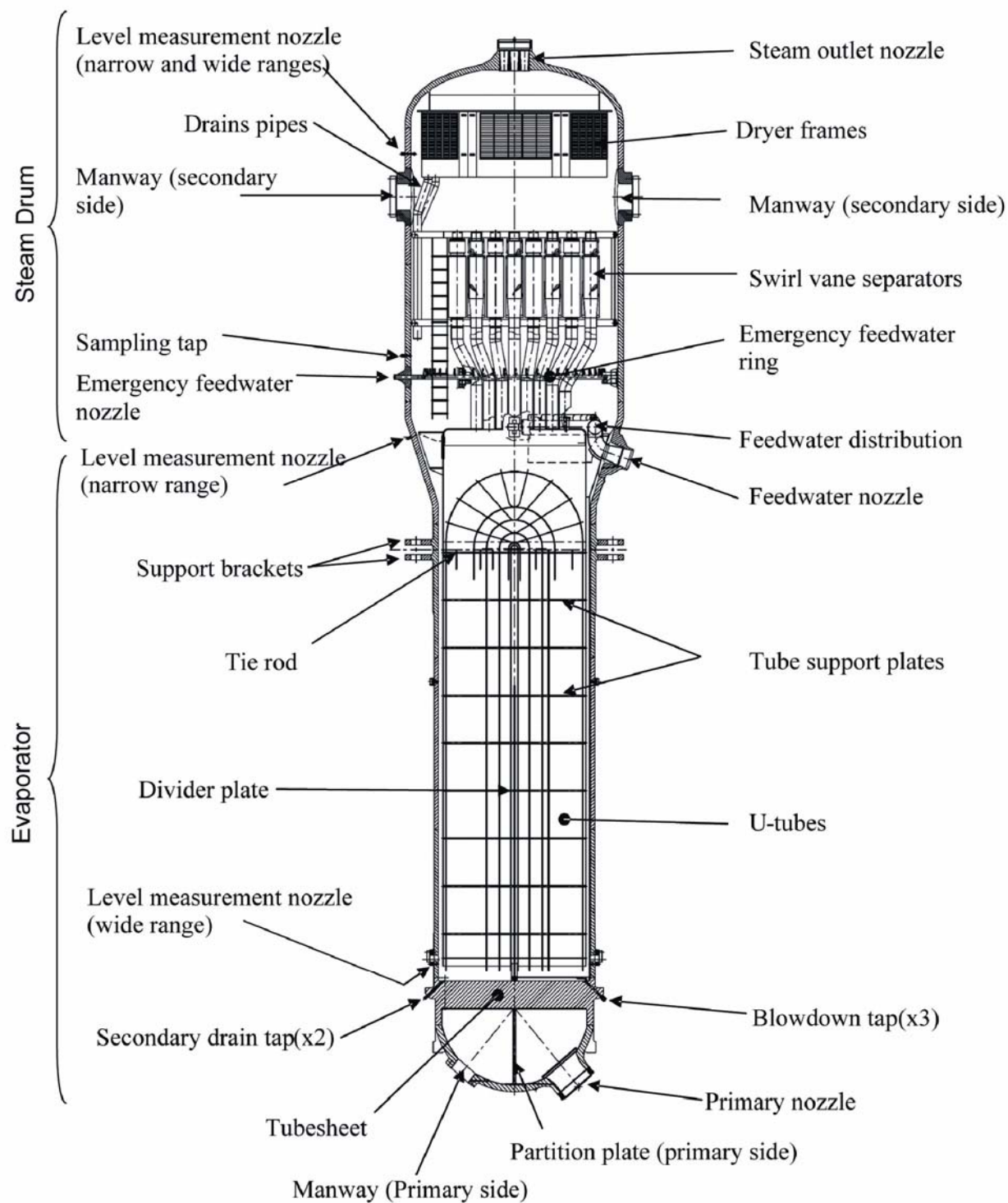
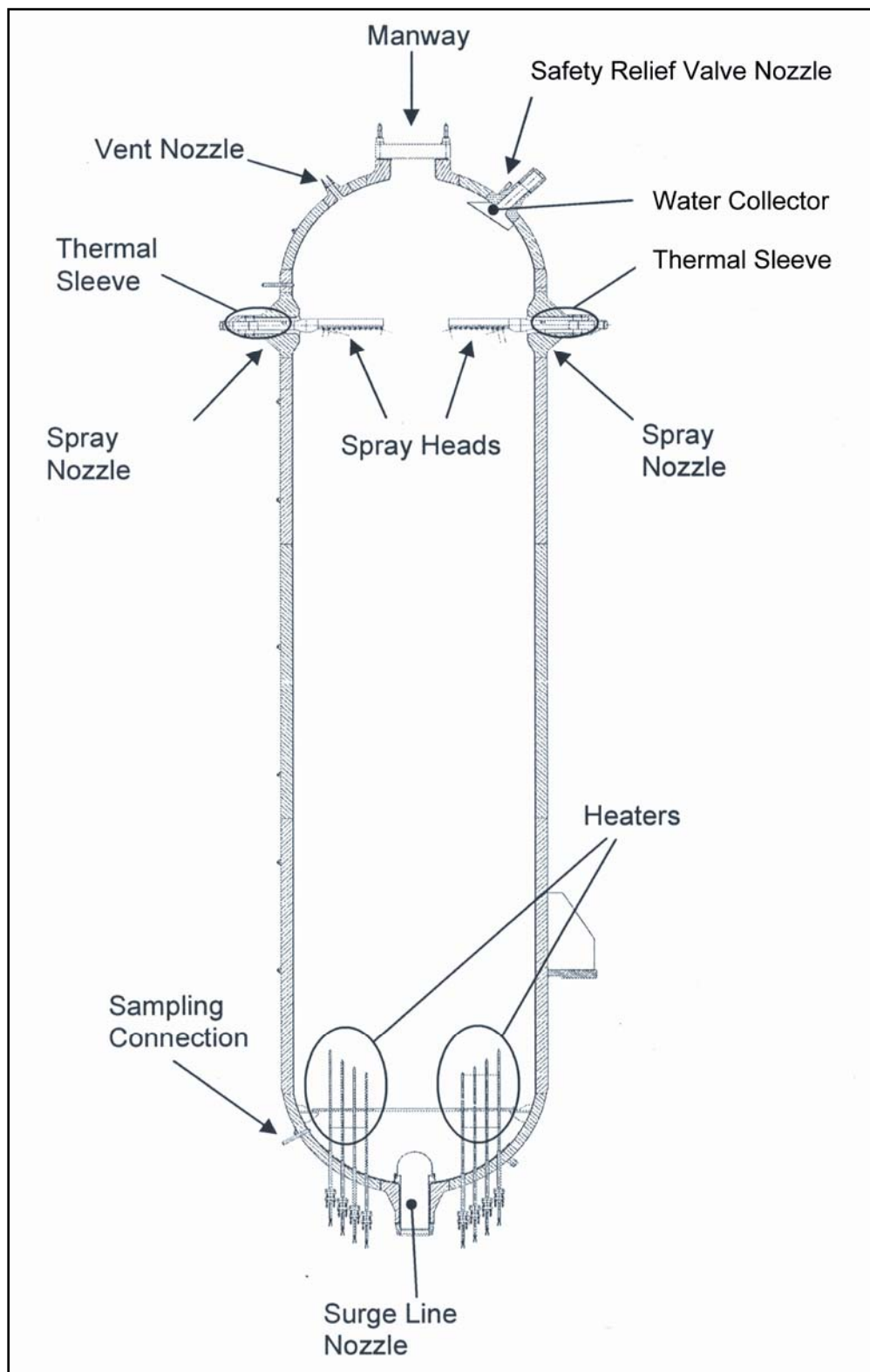
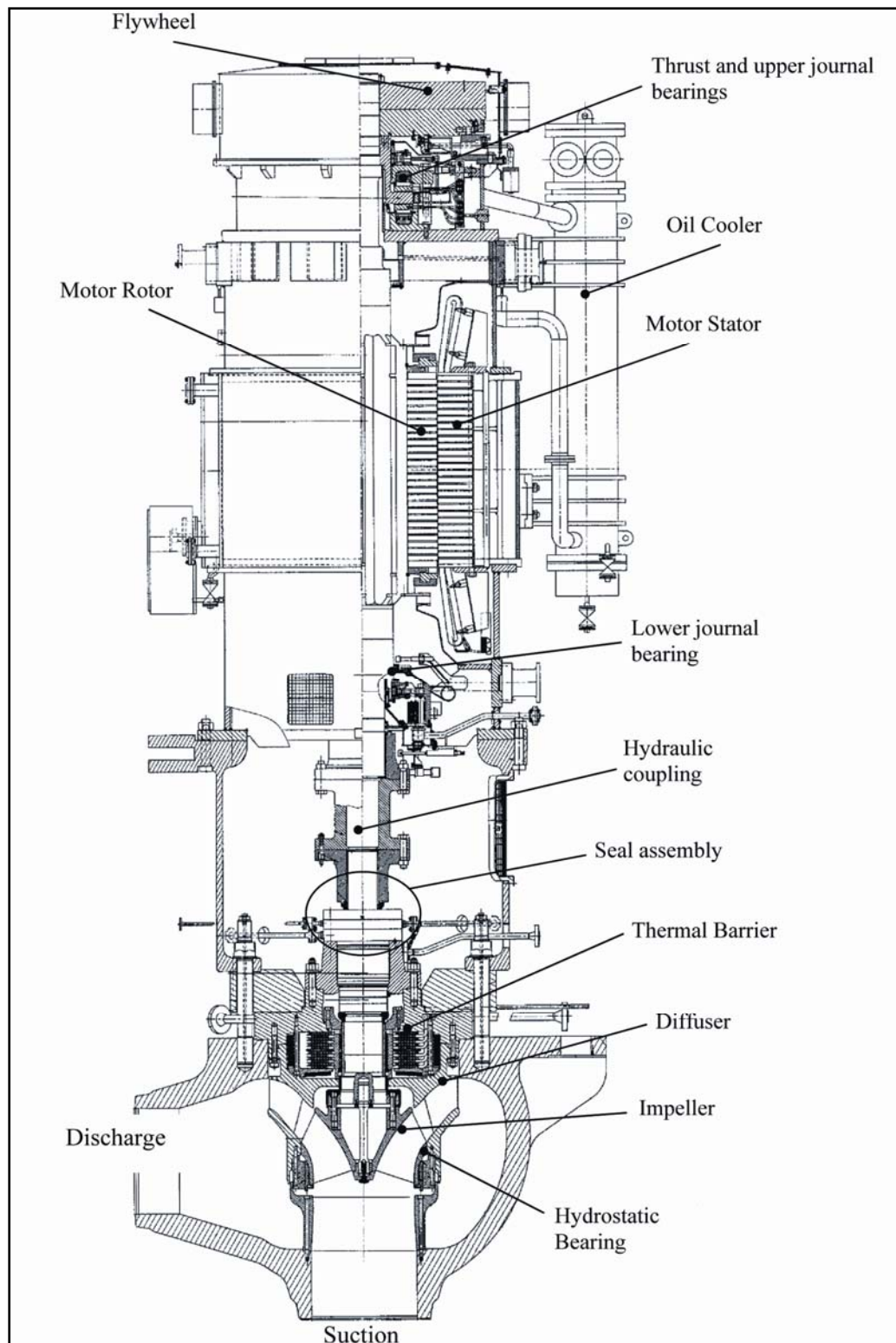


Figure 2-3 RCS Layout

**Figure 2-4 RPV Internals**

**Figure 2-5 Steam Generator**

**Figure 2-6 Pressurizer**

**Figure 2-7 Reactor Coolant Pump Assembly**

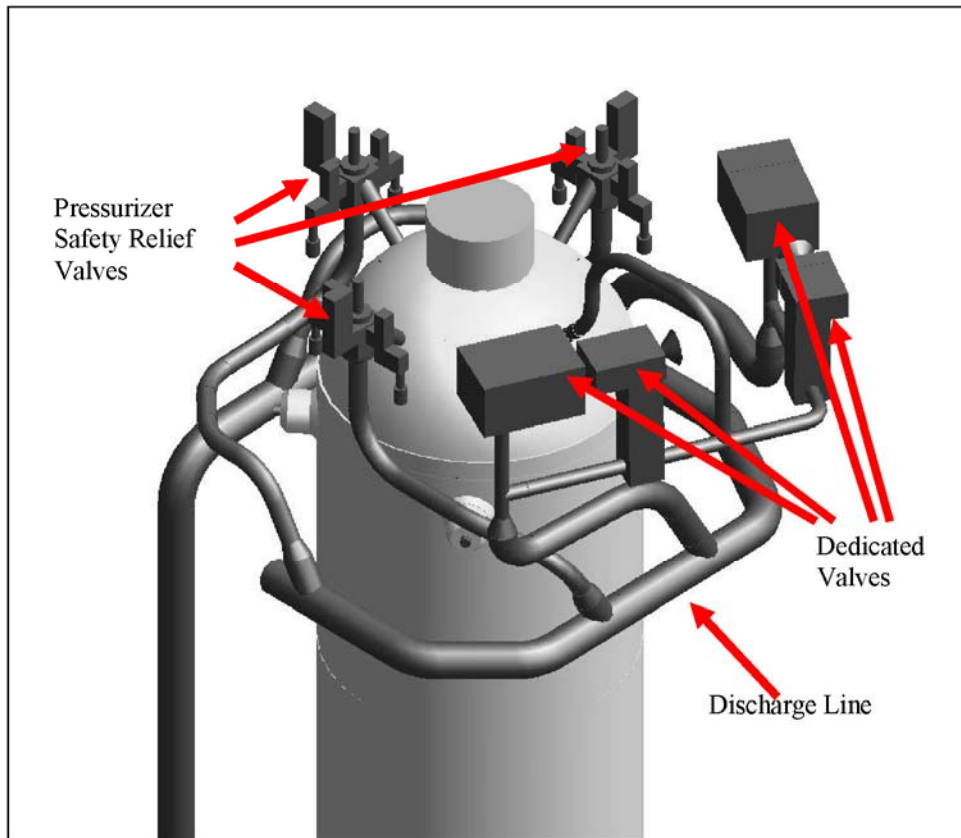


Figure 2-8 Pressurizer With Discharge Components

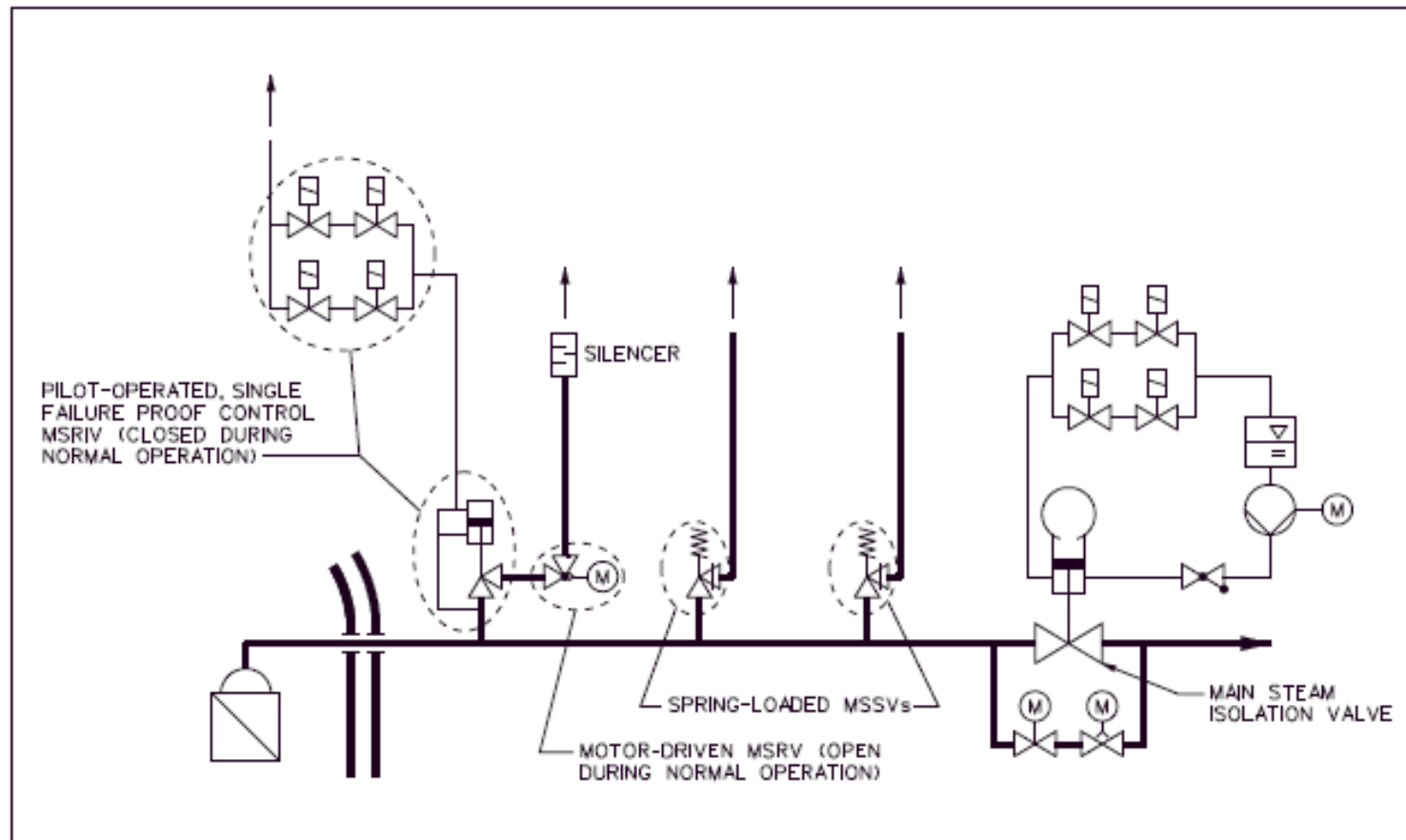


Figure 2-9 Arrangement of the Secondary Side Overpressure Protection

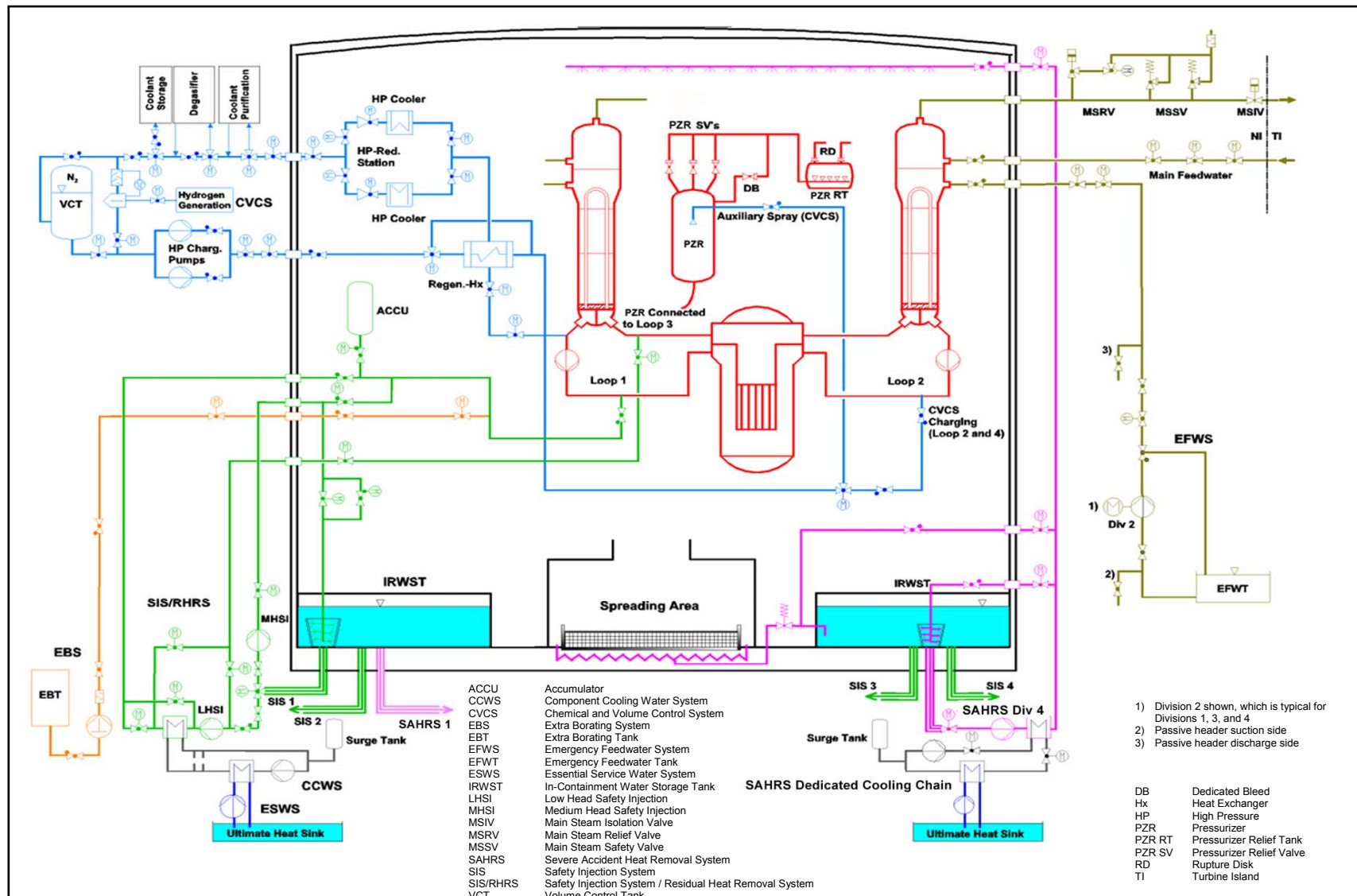


Figure 2-10 Main Fluid Systems

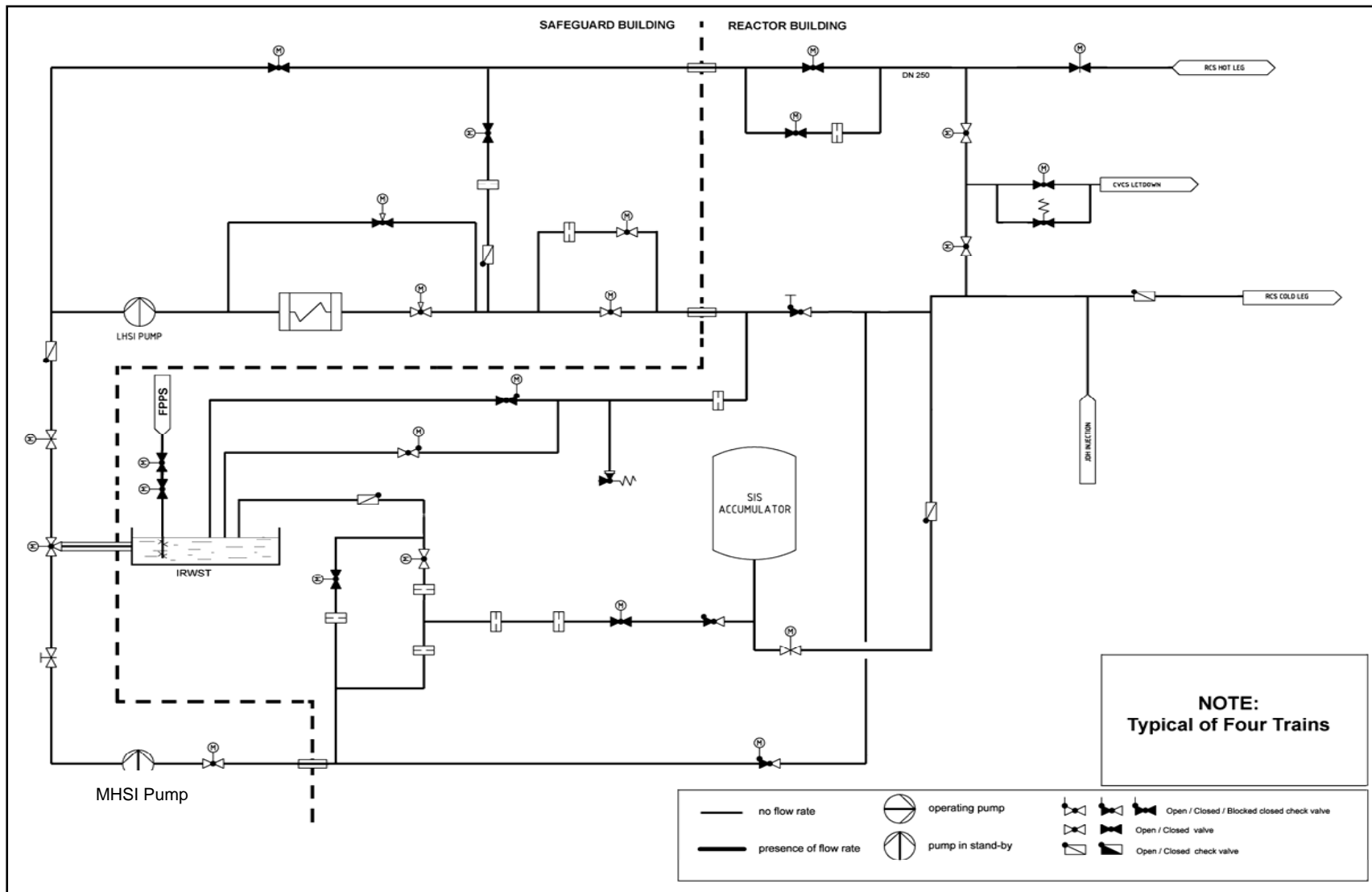


Figure 2-11 Safety Injection System

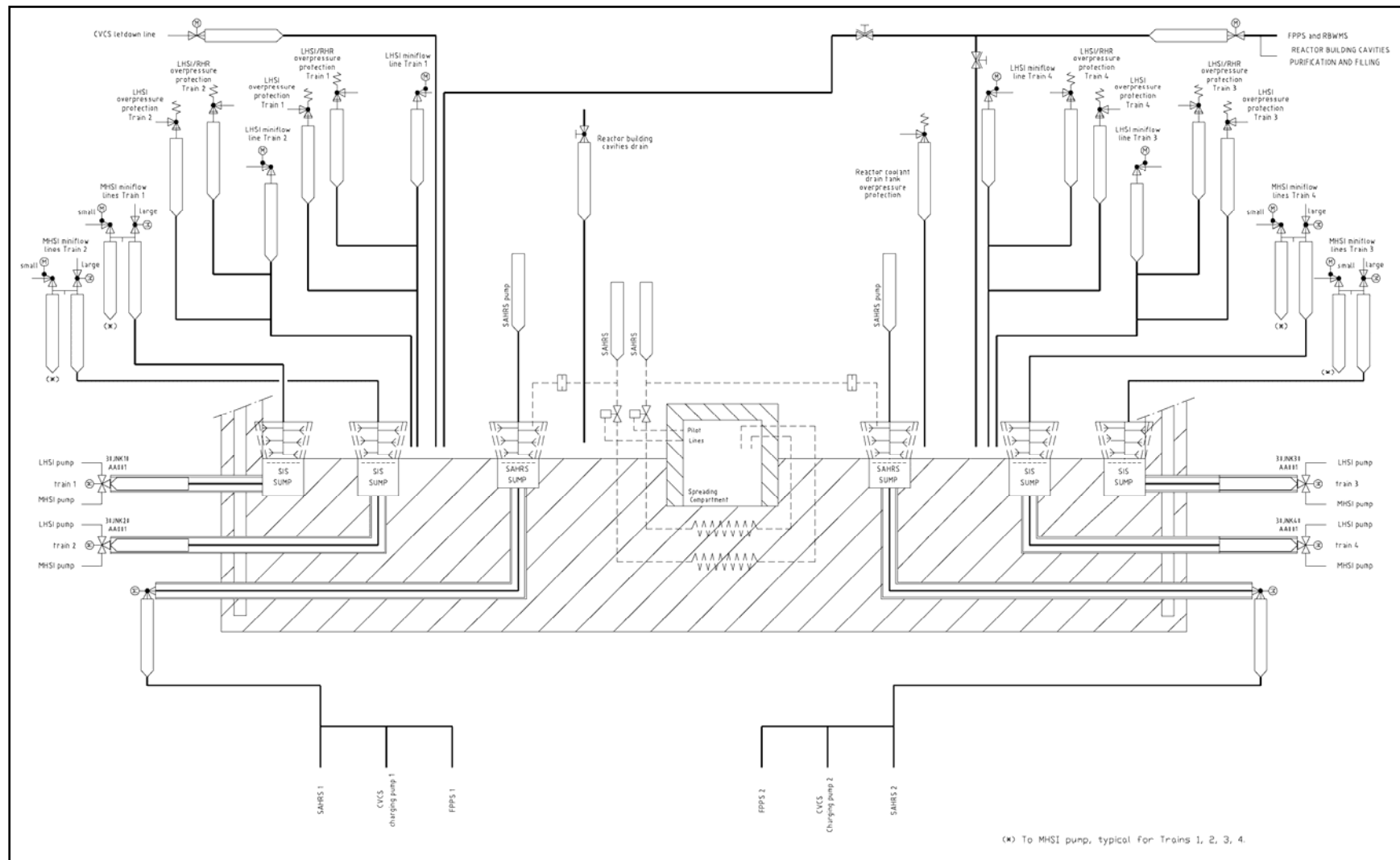


Figure 2-12 IRWST and Related Components

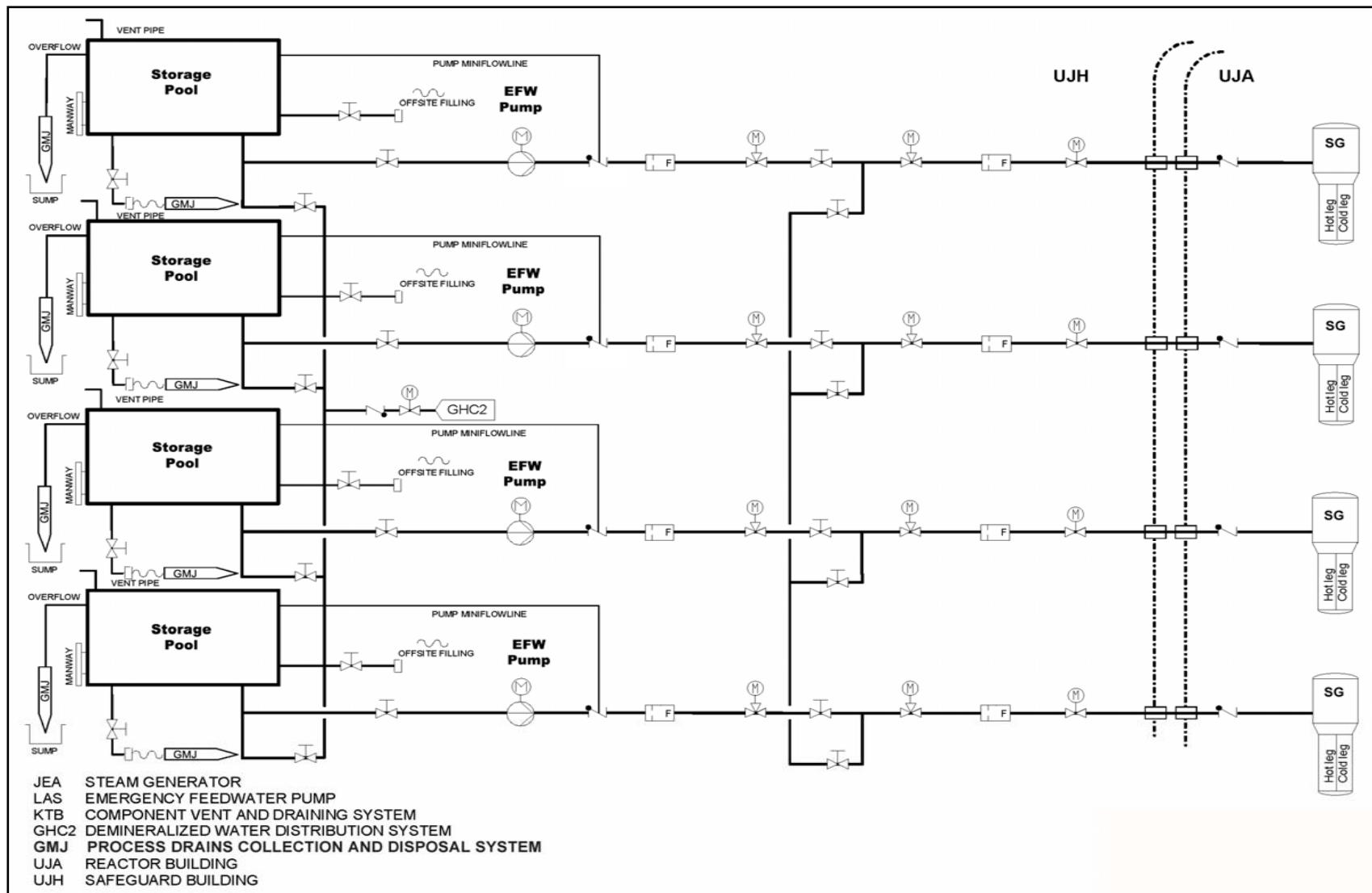
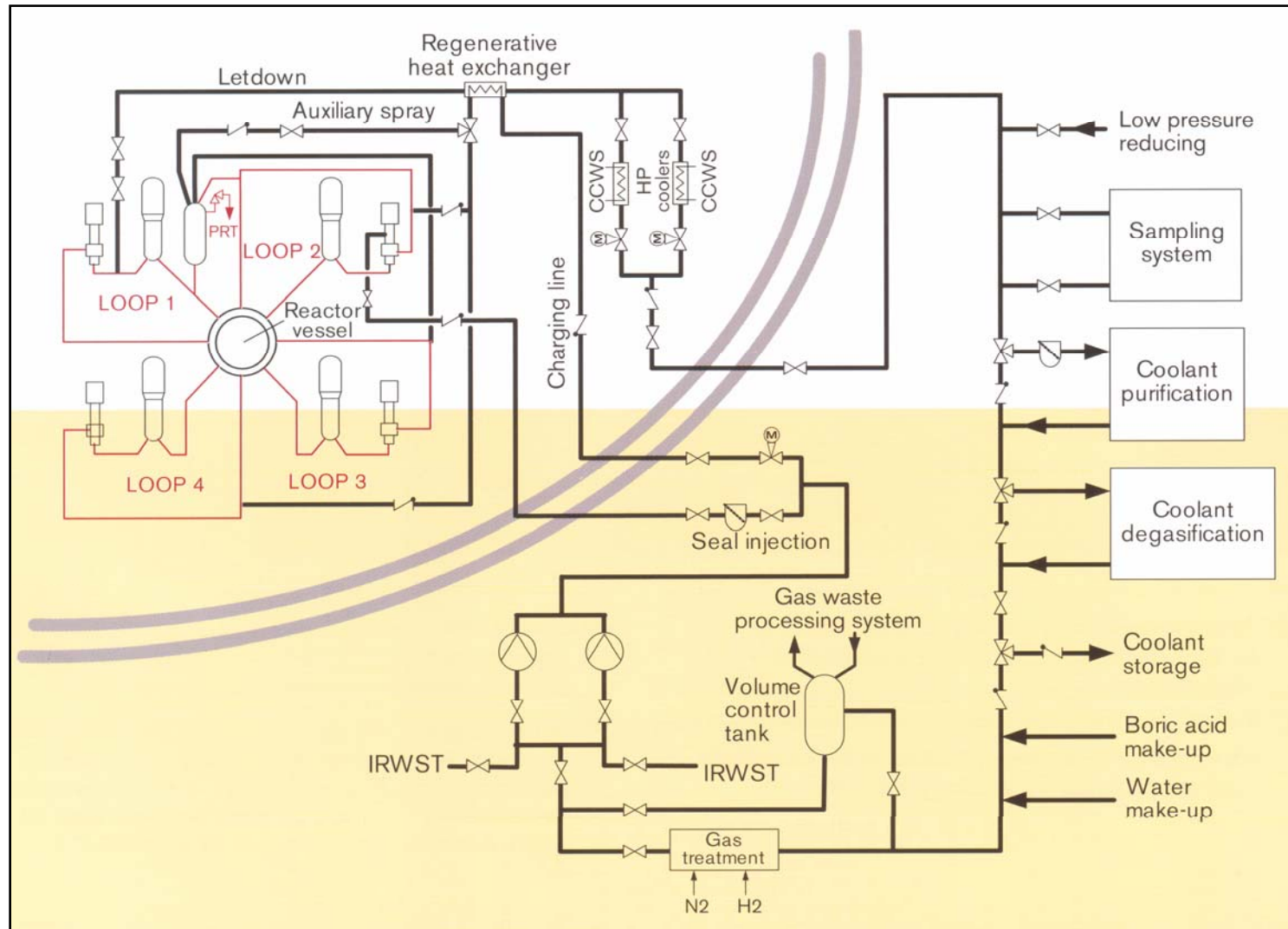


Figure 2-13 Emergency Feedwater System

**Figure 2-14 Chemical and Volume Control System**

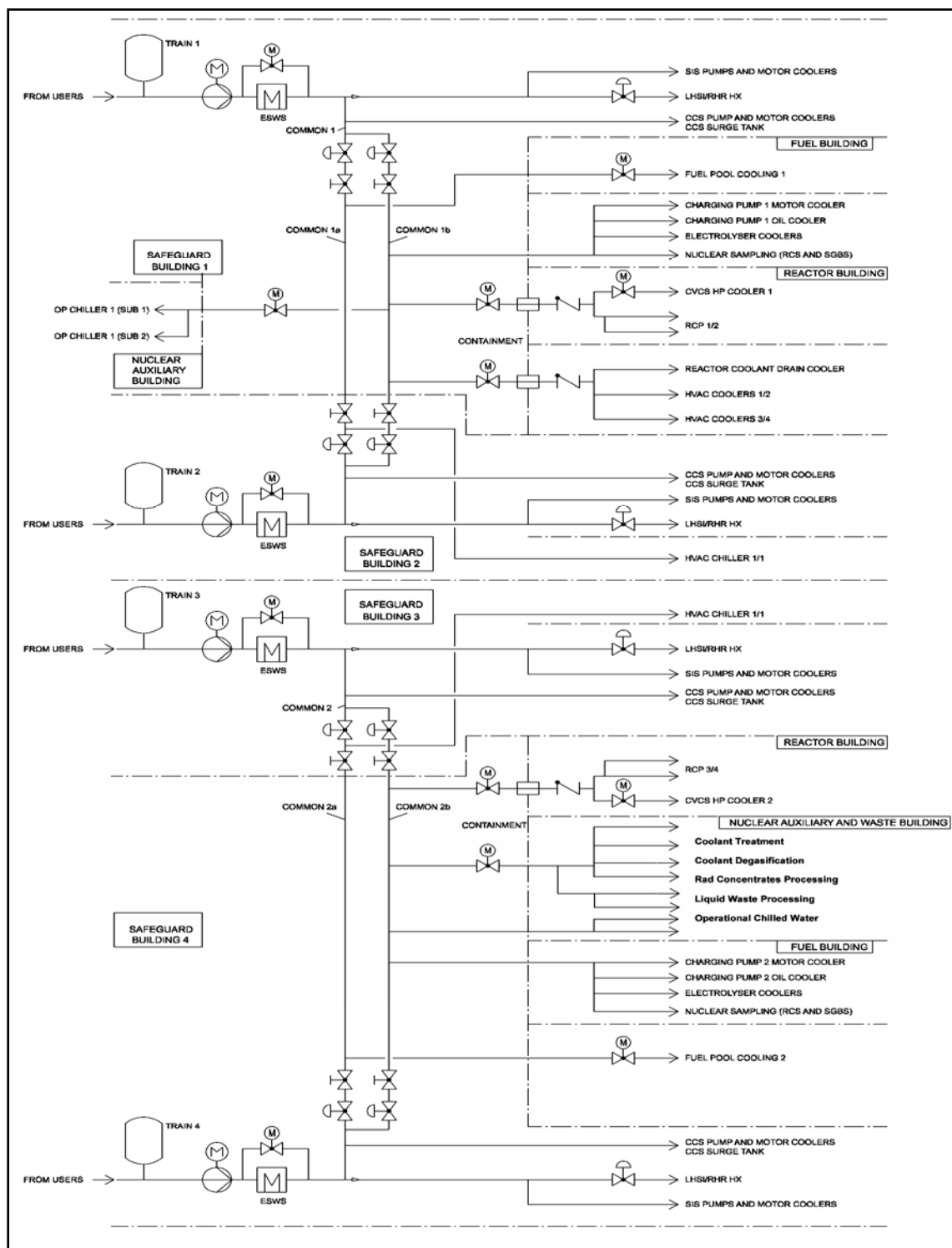


Figure 2-15 Component Cooling Water System

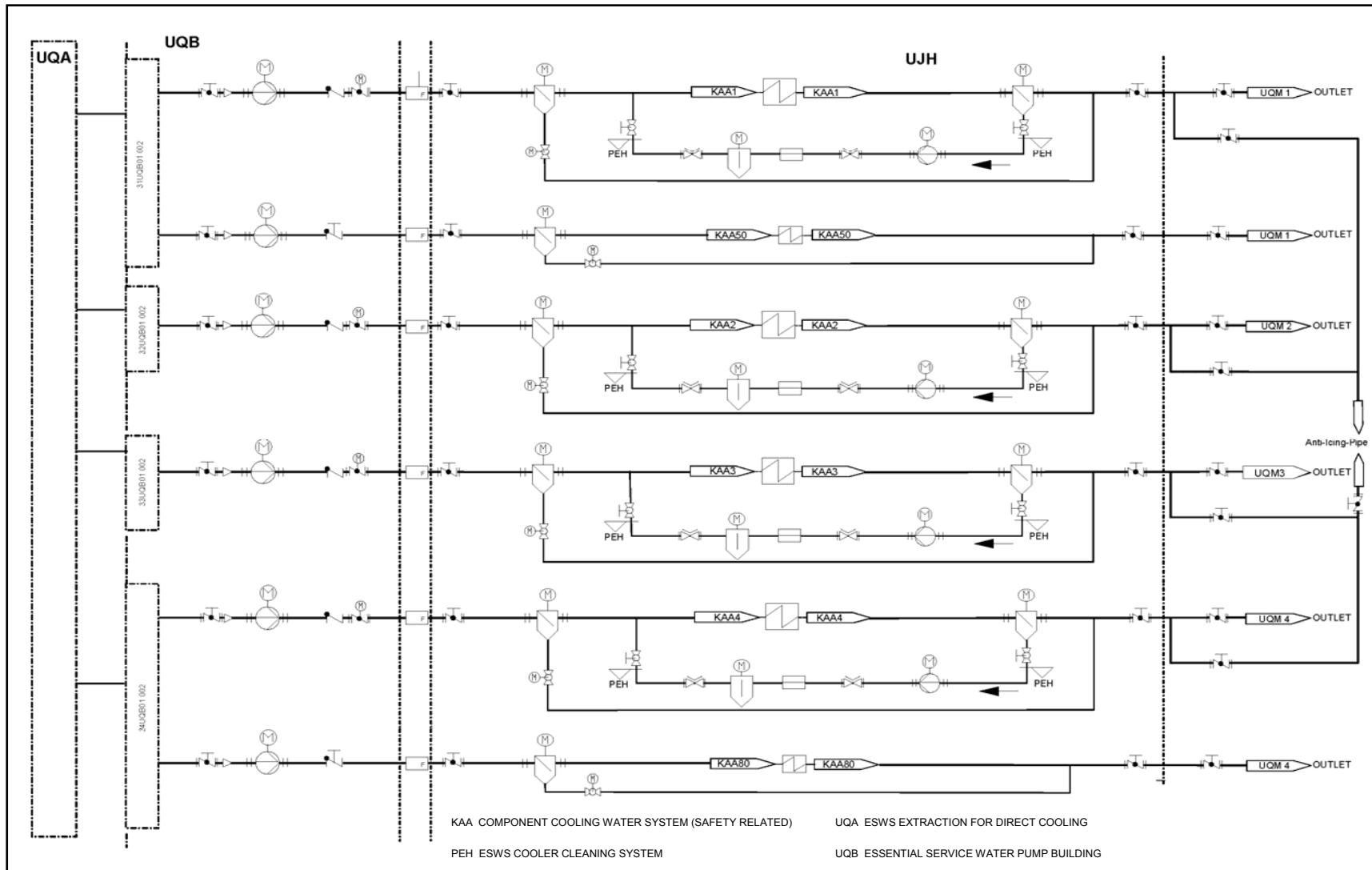


Figure 2-16 Essential Service Water System

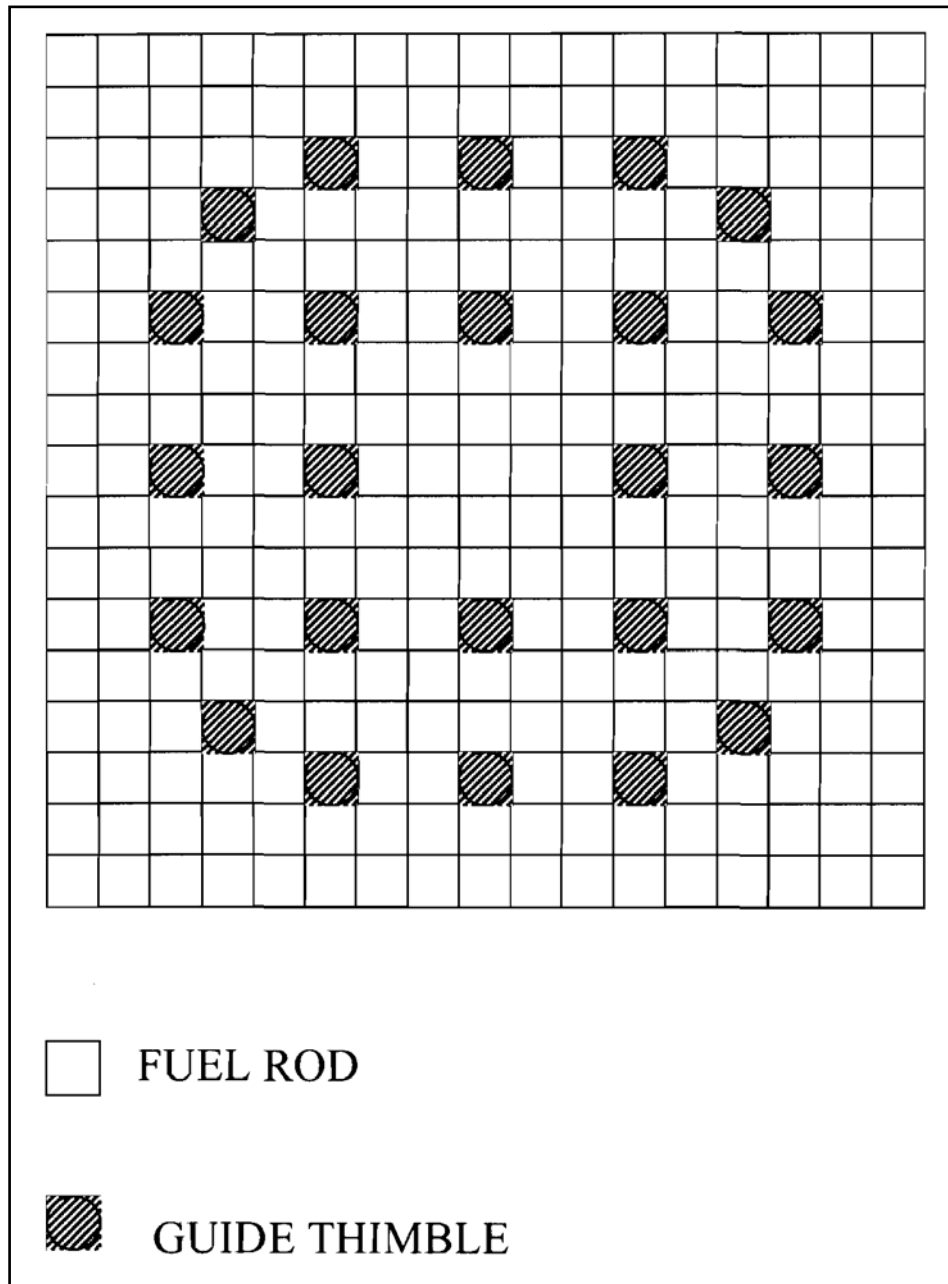
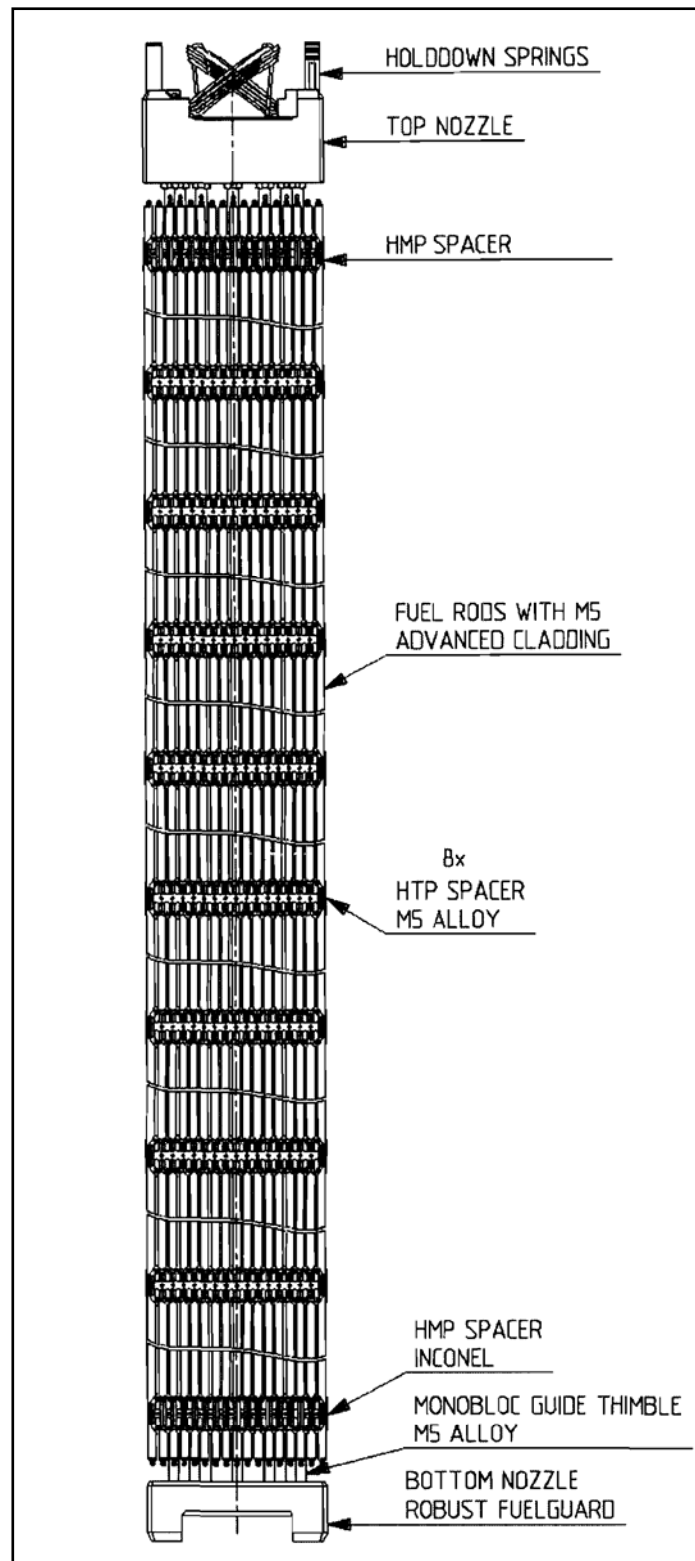


Figure 2-17 Radial Cross Section of a Fuel Assembly

**Figure 2-18 Fuel Assembly**

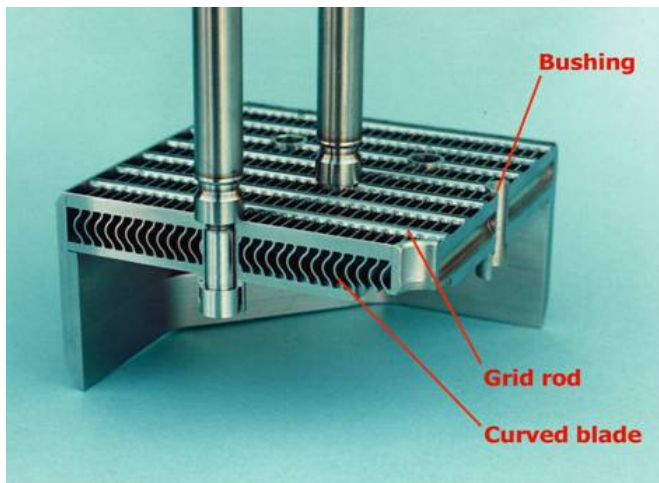
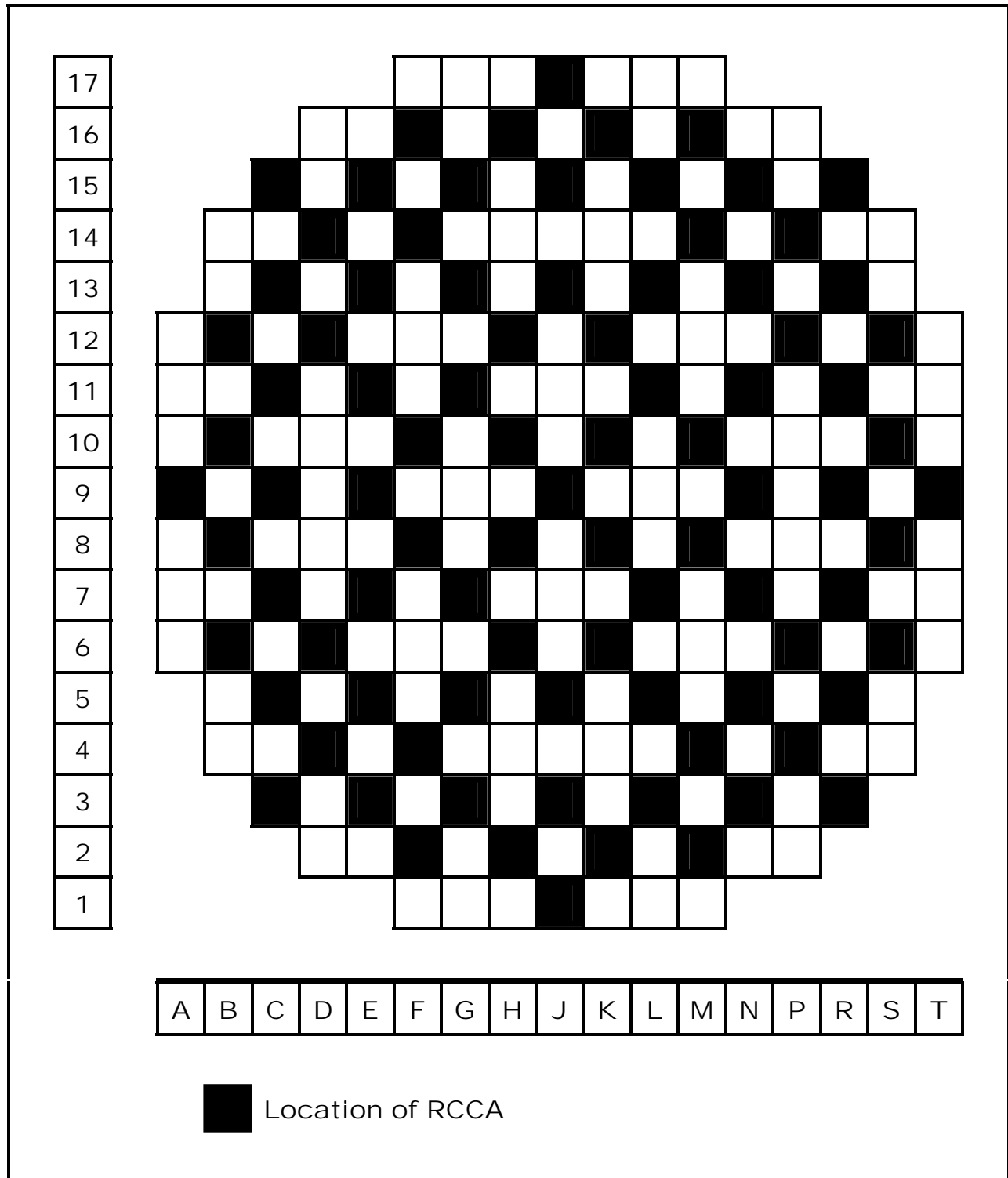
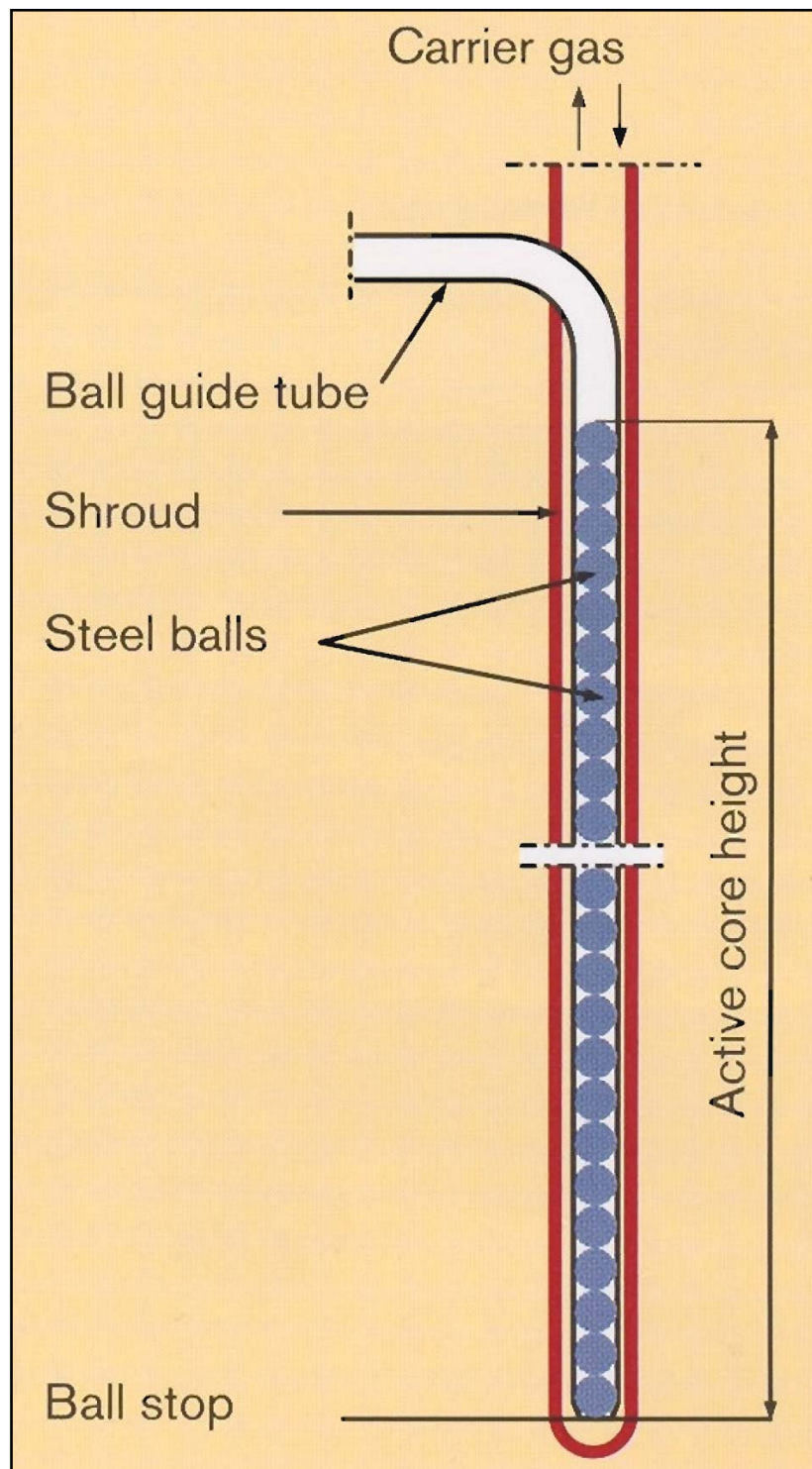


Figure 2-19 Fuel Assembly Top and Bottom Nozzles

**Figure 2-20 Possible RCCA Pattern Covering Enveloping Requirements**

**Figure 2-21 Aeroball System**

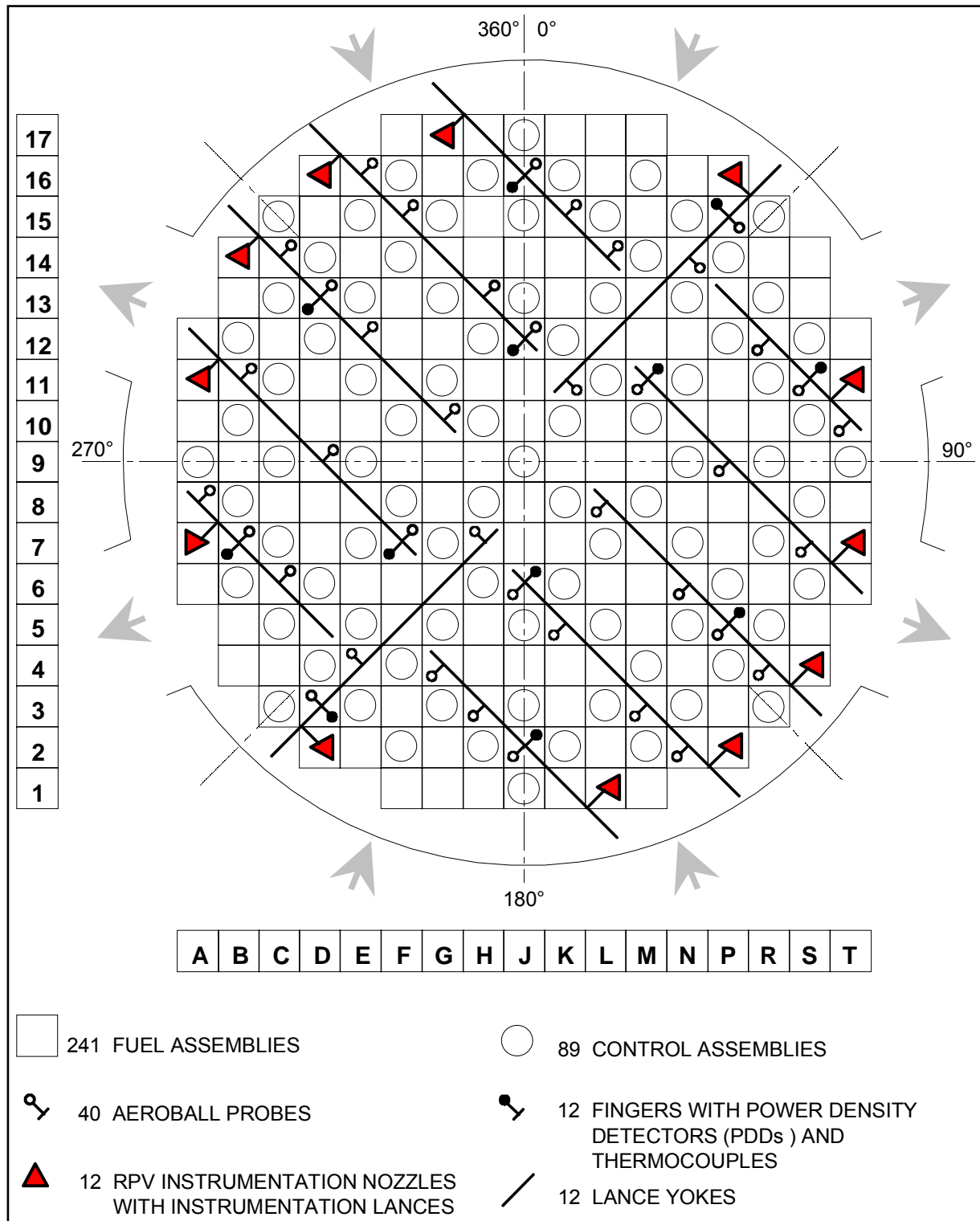
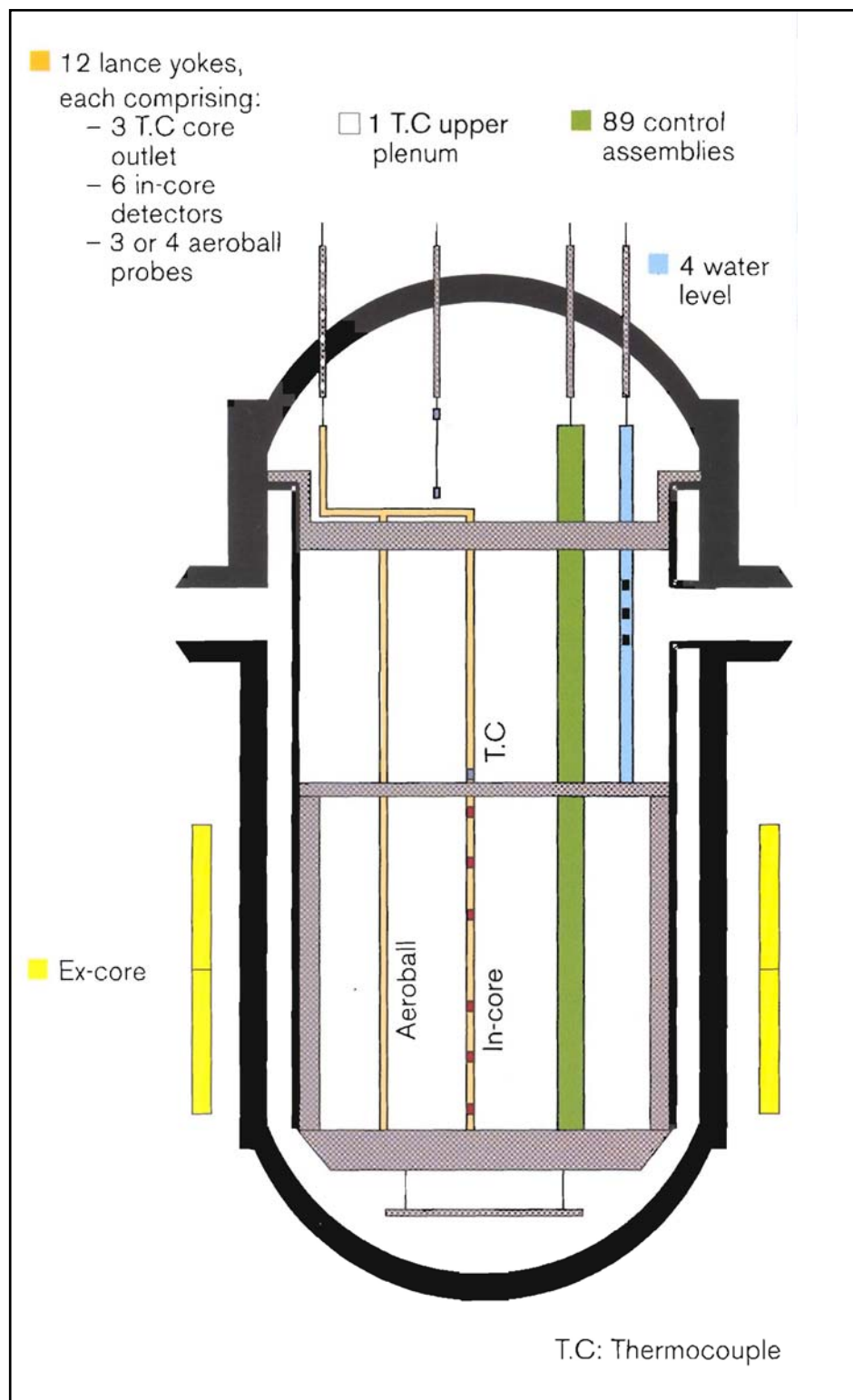


Figure 2-22 Arrangement of In-core Instrumentation Fingers

**Figure 2-23 Reactor Instrumentation**

3.0 VALIDATION OF FUEL ANALYSIS CODES FOR U.S. EPR

PWR fuel analyses consist of three distinct engineering disciplines: (1) Neutronic; (2) Thermal-Hydraulic (T-H); and (3) Thermo-Mechanical. Each discipline is governed by several methodology topicals each of which employ one or more major codes/code systems to perform the design calculations. Each methodology topical has been reviewed and approved for use by the NRC. They have also been applied to a variety of commercial reactor designs for which AREVA NP is currently providing or has recently provided fuel. These designs encompass a wide variety of fuel and core configurations and operating parameters. The U.S. EPR design is geometrically, functionally, and phenomenologically similar to these designs, thereby lending justification for extending currently approved methodologies to the U.S. EPR. The following three sections will discuss each engineering discipline and its applicable codes/methods in more detail.

3.1 *Neutronics*

PWR fuel neutronics analyses fall within three general analytical areas:

- (1) Core Design/Follow;
- (2) Power Distribution Monitoring; and
- (3) Safety Analyses/T-H/Thermo-Mechanical Support.

Several neutronics methodology topicals have been developed and approved by the NRC to support analyses in each of the areas. Table 3-1 displays the correlation between the various neutronic design topicals intended for use in the U.S. EPR and the analysis area(s) in which they are used.

3.1.1 *Neutronics Codes*

Each of the neutronic methodologies employs one or more computer codes to perform the analyses. The codes themselves have also been approved by the NRC for use within the topical reports noted above. The major codes employed are:

- CASMO-3G/MICBURN-3

- PRISM
- NEMO-K

CASMO-3G is an industry standard multi-group, two-dimensional transport theory code used for burnup calculations on PWR and BWR fuel assemblies and/or simple pin cells. It is used in conjunction with the MICBURN-3 code which is a multi-group, one-dimensional transmission probability code that is used to calculate microscopic burnup in rods containing absorber (poison) material that is initially homogeneously distributed. The code system is designed to handle a geometry consisting of cylindrical fuel rods of varying compositions in a square pitch array with allowance for fuel rods loaded with a burnable absorber, burnable absorber rods, cluster control rods, in-core instrument channels, water gaps, boron steel curtains, and cruciform control rods in the regions separating fuel assemblies. The code system is used to generate assembly lattice cross section data as a function of burnup, discontinuity factors, and heterogeneous form factors which are then passed to the core simulator code (PRISM). Several branch calculations are generally run off the base depletion branch. This allows modeling of dependencies on coolant/fuel temperatures, coolant density, boron concentration, presence of control elements, etc. The code system was extensively benchmarked against a variety of critical experiments which encompass multiple fuel assembly designs.

PRISM is a three-dimensional core simulator code used to calculate core power distributions and perform reactivity analyses using assembly data from the CASMO-3G code. The code uses a nodal expansion method to solve the two-group neutron diffusion theory representation of the reactor core. It provides for thermal-hydraulic feedback, modeling of equilibrium or time-dependent xenon and samarium, and isotopic depletion. In addition, it allows for the generation of pin-by-pin power distributions using a pin power reconstruction technique. A continuous cross section representation was developed covering all combinations of thermal hydraulic parameters possible in stationary reactor states. The code has been thoroughly benchmarked against startup

physics test results and core follow data obtained from several domestic and foreign commercial power reactors.

NEMO-K is a three-dimensional, reactor kinetics code incorporating time-dependent solutions for neutronics, fuel temperature, and coolant properties into the steady-state NEMO computer code. NEMO-K solves the nodal balance equations in three dimensions to determine the neutron flux, source, relative power density (including pin power reconstruction), and reactor core reactivity. The code tracks both the power generated within the fuel and that deposited directly in the water. The fuel pin temperature model assumes a circular rod with azimuthally symmetric heat generation and no axial conduction. The transient thermal-hydraulic model assumes no mixing between channels and a constant pressure throughout the core. The three time-dependent models have each been individually benchmarked against experimental data and RELAP5 evaluations. The overall total core model was benchmarked in accordance with the Nuclear Energy Agency Committee for Reactor Physics (NEACRP) reference benchmarking specification document (Reference 3-3). The results demonstrated the adequacy of the code to model three-dimensional time-dependent transients and accurately predict reactivity, power distribution, and differential and integral rod worths during fast (rod ejection type) as well as slower (rod drop type) core transients.

3.1.2 *Neutronic Methodologies*

Neutronics analysis falls within three basic design areas as noted in Section 3.1. The neutronics methodologies though are not developed specifically for a given analysis area; rather there is significant crossover and support for each of the areas.

The first design area is core reload/follow analyses for which the predominant methodology is EMF-96-029(P)(A) (Reference 3-1). This methodology describes the use of the MICBURN/CASMO/PRISM code system when developing core models to evaluate steady-state core behavior with burnup at hot zero power (HZP) or hot full power (HFP). The code system has been benchmarked to criteria based on those suggested in ANSI/ANS-19.6.1-1985 (Reference 3-4). In addition, the code system has

been reviewed and approved for use by the NRC for analysis of numerous core configurations (see Table 3-2).

The next design area is power distribution monitoring. The methodology for reconstructing the measured power distributions for comparison to calculated power distributions for plants that use the Aeroball Measurement System is presented in Appendix A, Section A.3. A discussion on how these measured power distributions are used in subsequent in-core monitoring will be provided in a topical to be submitted at the time of U.S. EPR design certification application.

The final analysis area is safety analysis/T-H/thermo-mechanical support. As in the previous two cases, Reference 3-1 provides the primary methodology for performing the calculations. In this case, branch calculations are typically performed from various points off the base core depletion. These generally consist of the calculation of core power distributions, reactivity parameters, rod/bank worths, critical boron concentrations, etc. at beginning-, middle-, and end-of-cycle (BOC, MOC, and EOC). These parameters also allow for varying power levels, moderator temperatures, and xenon conditions. In order to support analyses of certain types of rapidly evolving transients (i.e. control rod ejection, main steam line break, uncontrolled rod/bank drop/withdrawal), without imposing the excessive conservatism inherent in a static reactor approximation, it is often necessary to employ three-dimensional transient techniques. For these cases, the topical report BAW-10221P-A, "NEMO-K A Kinetics Solution in NEMO" (Reference 3-2) is applied. This methodology provides for modeling of neutron kinetics with transient modeling of the fuel rod and coolant temperatures to provide a more accurate prediction of core reactivity, power distributions, and rod/bank integral and differential worths.

3.1.3 *Applicability of Neutronic Codes/Methodologies to U.S. EPR*

The foundation for almost all PWR neutronic calculations is found in EMF-96-029(P)(A) (Reference 3-1). It provides the basis for the calculations from which the other neutronics methodologies are then derived. The BAW-10221P-A topical (Reference 3-2) discussed later serves to augment Reference 3-1 capabilities.

3.1.3.1 EMF-96-029(P)(A), Volumes 1 and 2, "Reactor Analysis System for PWRs," Basis for Application to U.S. EPR

This methodology was developed with the concept of simplifying future computer code upgrades. As such it was developed with an emphasis on the methodology for performing validation of the code system. A standard set of validation criteria based on industry standards (Reference 3-4) was applied within it. The initial validation report served to demonstrate the applicability of the methodology to current core configurations. This included both Westinghouse and Combustion Engineering core designs with their differing fuel rod/assembly designs, core sizes, control rod designs, and in-core detectors (both moveable U²³⁵ fission chambers and fixed Rhodium detectors). The methodology has also been satisfactorily implemented on the Palisades reactor core configuration which incorporates BWR-style wide and narrow water gaps and cruciform control blades. Many of these cores include unique design characteristics which have been successfully modeled with the methodology. Examples include the part-length shield bundles used in the H.B. Robinson reactor as well as full-length shield bundles and hafnium rod inserts used in the Palisades reactor. Finally, a number of different fuel management schemes have been evaluated from 12-month to 24-month cycles using various burnable poison absorbers/configurations.

The U.S. EPR represents a minor change from these core configurations. The U.S. EPR fuel will consist of 17x17 bundles very similar to the standard 17x17 fuel used in U.S. PWRs except that the instrument tube has been replaced with a fuel rod. The main difference is the fuel height, which is 13.78 ft for an active zone, as opposed to the standard 12 ft designs in most U.S. plants, other than the South Texas Plant, which uses 14 ft fuel assemblies. The U.S. EPR also incorporates a heavy reflector around the core periphery to reduce vessel fluence rather than using shield bundles as other U.S. reactors have done.

The U.S. EPR core features the Aeroball in-core Measurement System (AMS) and fixed Co⁵⁹ Self-Powered Neutron Detectors (SPNDs), which allow for continuous in-core power distribution monitoring. Since the U.S. EPR fuel assembly does not have an instrument tube, both the Aeroball thimbles and fixed SPNDs will be loaded into corner

guide tube cells. This particular style of in-core monitoring has been modeled successfully and used for many years in European reactors and will be used to provide protection-grade input to the U.S. EPR reactor protection system.

Lastly, the fuel management schemes will be similar to current designs (i.e., 18 to 24 months) and will use gadolinia to control initial core reactivity. Control rod designs are similar to standard U.S. designs.

A neutronic methodology change with regard to the U.S. EPR design is the thermal energy cutoff used to develop the two-group cross sections for the core simulator code. The U.S. EPR will use a 0.625 eV cutoff energy rather than the originally benchmarked 1.855 eV cutoff. This change was made in part to facilitate global convergence with the European methodology.

Given the nature of these changes, there are no significant differences that cannot be handled by performing appropriate validation calculations in accordance with the methodology as approved in EMF-96-029(P)(A) (Reference 3-1). Appendix A provides new benchmarks based on the revised CASMO/MICBURN/PRISM methodology. These benchmarks duplicate the scope of calculations performed in EMF-96-029(P)(A) but were done for reactor geometries which more closely match those expected for the U.S. EPR design (in particular, 193 assembly, 4-loop designs using an aeroball power monitoring system with SPND incore detectors).

3.1.3.2 BAW-10221P-A, "NEMO-K A Kinetics Solution in NEMO," Basis for Application to U.S. EPR

The NEMO-K methodology comprises a straightforward implementation of time-dependent solutions for neutron flux, fuel temperature, and coolant properties into the previously NRC-approved steady-state neutronics methodology NEMO (Reference 3-8). It uses cross section data for both fuel and reflector compiled from CASMO-3 calculations. Nodal history data (e.g. nuclide densities and moderator history) are provided from base core depletions such as those from NEMO and PRISM. The code can then basically restart from an appropriate point during the cycle depletion using cross sections applicable for those conditions and model the three-dimensional core kinetics response to the reactivity transient being modeled. Typical transients

which may require this type of modeling include control rod ejection, uncontrolled bank withdrawal, and dropped rod(s). NEMO-K is directly applicable to the U.S. EPR for many of the same reasons stated for the PRISM methodology (Section 3.1.3.1). Specifically, the U.S. EPR fuel and core designs are substantially bounded by designs currently licensed in the U.S. using AREVA developed and NRC approved methodologies including NEMO-K. In addition, NEMO-K's main difference with core simulator codes is the implementation of the time-dependent solutions noted above. These equations are generic in nature and therefore applicable to the U.S. EPR. Cross section input to NEMO-K will come from CASMO-3 which was discussed earlier. Also, NEMO-K has been benchmarked against several industry standard benchmarks and code systems including PANTHER and RELAP5. These benchmarks validate NEMO-K's general applicability across a wide range of potential PWR reactor configurations. Therefore, the NEMO-K code remains directly applicable to the U.S. EPR for the purpose of evaluating 3D transient core response.

3.2 *Thermal-Hydraulic*

PWR fuel T-H analyses fall within three general analyses areas:

- (1) Non-LOCA DNB/Fuel Temperature Analyses,
- (2) Reactor Coolant Flow/Temperature/Pressure Distributions, and
- (3) Setpoint Evaluation.

The setpoint methodology for the U.S. EPR will be addressed in a separate topical report. This section will focus on the LYNXT topical report, BAW-10156A, Rev. 1, "LYNXT Core Thermal-Hydraulic Program – Revision 1" (Reference 3-5) and the application of LYNXT to DNB and reactor flow analyses in general.

3.2.1 *Thermal-Hydraulic Codes*

LYNXT is a versatile thermal-hydraulics cross-flow code capable of predicting flow and temperature (enthalpy) distributions in confined geometries where wall shear forces are more dominant than intra-fluid shear forces. LYNXT is an improved version of the COBRAIV-1 code developed at Battelle Pacific Northwest Laboratories under the

sponsorship of the Energy Research and Development Administration and the NRC. It contains the following features not found in COBRAIV-1:

- 1) a direct solution of the cross-flow equation,
- 2) convergence enhancements to the cross-flow equation,
- 3) a more extensive critical heat flux library,
- 4) an option for code-generated water thermal properties,
- 5) a dynamic gap conductance fuel model, and
- 6) an implicit pressure-velocity (PV) algorithm.

The PV algorithm was incorporated specifically to improve convergence in main steam line break type problems (especially with accompanying loss of offsite power) where cross-flow terms can become significant relative to the axial flow term. The PV solution models cross-flow parameters with either the donor-cell or transverse scaling methods and the axial flow parameters are modeled only with the donor-cell method.

The code can handle a variety of reactor flow problems from inter-assembly to inter-subchannel using one-pass analyses. The single-pass analysis involves modeling the subchannel being analyzed (i.e., hot channel) with communicating neighboring subchannels in one simulation. The reactor core is modeled as a collection of quasi-one-dimensional flow channels which may represent an actual subchannel, fuel bundle, or combination of subchannels/bundles. The end result is a code which permits the analysis of a wide range of reactor transients, from relatively slow loss of coolant flow accidents to rapid, asymmetric, control rod assembly ejection accidents.

The code has been benchmarked against experimental data (IBDCF Test Facility results), other approved thermal-hydraulic codes (LYNX1/LYNX2, COBRA3C, RADAR), other approved fuel performance codes (TACO/TACO2/TAFY), and analytical solutions. In addition, the CHF correlations contained within the code are independently validated and approved over their applicable operating ranges. These results demonstrated the code's ability to:

- Perform analysis over a broad range of reactor flow problems ranging from bundle to subchannel.
- Perform accurate analysis using one-pass rather than more elaborate two-pass techniques.
- Model transient fuel performance in a manner that accurately represents more sophisticated fuel performance codes.
- Analyze a wide range of transients from relatively slow four-pump coast downs to fast rod ejections.
- Handle both axial upflow and low or reverse flow situations.

3.2.2 *Thermal-Hydraulic Methodology*

LYNX is the primary code used to perform thermal-hydraulic licensing calculations. In addition to its main role in determining transient DNBRs, it can be used to:

- Analyze baffle gap jetting (including experimental benchmarks).
- Perform steaming rate calculations.
- Calculate pressure drops.
- Calculate crossflow velocities and general flow distributions.
- Assess thermal mixing.
- Reduce CHF data.
- Evaluate guide tube boiling.
- Provide void fraction data to neutronics for steam line break analyses.

The code has been approved and used to support Chapter 15 licensing analyses for a variety of B&W and Westinghouse reactors using both 15x15 and 17x17 fuel along with several styles of spacer grids.

The following NRC restrictions are imposed on the code's use for licensing applications:

- The CHF correlation used in LYNXT must be demonstrated to be applicable and its use will then be restricted to the range of applicability demonstrated for that correlation.
- One-pass modeling in LYNXT is acceptable, provided the correct hot subchannel is chosen. Sensitivity studies should be performed to ensure that the one-pass model layout provides sufficient detail to provide the correct boundary conditions for the hot channel.
- LYNXT shall not be used for reflood transients unless separately justified since the rod-to-coolant heat transfer package is based on RELAP4/COBRAIV-1.
- The multipliers on the transition and stable film boiling regimes, XTRANS and XSTABLE, should not be set greater than 1.0 unless otherwise justified.
- The applicability of the LYNXT PV algorithm is restricted to the following ranges:
 - Mass Flux (absolute value) – 0.0 to 3.0 $\text{Mlb}_m/(\text{hr-ft}^2)$
 - System Pressure – 500 to 3000 psia
 - Local Heat Flux – 0.0 to 0.8 $\text{MBTU}/(\text{hr-ft}^2)$
- When using the PV algorithm, the licensee is responsible for verifying the adequacy of the cross-flow resistance chosen whenever reverse and recirculating flows are observed in the analyses.

In general licensing applications the code is supplied initial conditions from other NRC approved neutronic (such as CASMO/PRISM), systems (such as RELAP5), and fuel performance (such as COPENIC) codes including radial power distributions, inlet and outlet fluid conditions, and heat transfer coefficients. The code then solves for core-wide fluid conditions and DNBRs.

3.2.3 *Applicability of Thermal-Hydraulic Codes/Methodologies to U.S. EPR*

LYNXT will provide the basis for DNB and core flow distribution modeling calculations performed in support of U.S. EPR licensing activities. The code and the methodology for using it are described in topical report BAW-10156A (Reference 3-5).

This methodology has been used extensively to provide Chapter 15 licensing support for current B&W and Westinghouse style PWRs. This support has consisted of steady-state and transient analyses of DNBRs, core flow distributions, and fuel temperatures over a wide range of thermal-hydraulic conditions and core/fuel designs. In addition, all CHF correlations contained within the code and intended for use in licensing calculations are validated against a database of test results which include fuel geometries for which the code is intended to be used.

The U.S. EPR will to operate within the same range of thermal-hydraulic conditions for which the code has been previously validated. Table 3-3 compares typical U.S. EPR T-H parameters with those of current reactor designs. In general, the U.S. EPR will operate in the same thermal-hydraulic regime as current U.S. reactors which are being licensed with the LYNXT methodology. The major difference is in active core height. This will be accounted for in the development of the U.S. EPR CHF correlation which will contain data from U.S. EPR representative fuel designs and will be correlated using the LYNXT code.

LYNXT currently has a dynamic gap conductance model based on TACO/TACO2 fuel performance methodology. This dynamic gap conductance model available in LYNXT will not be used for U.S. EPR analysis. Rather, the constant gap conductance model will be used with conservatively generated gap values. Therefore, the LYNXT methodology is directly applicable to U.S. EPR thermal-hydraulic analysis applications.

3.3 *Thermo-Mechanical*

PWR fuel thermo-mechanical analyses encompass a broad range of calculations including thermal modeling (fuel temperatures), mechanical analyses (creep & strain), cladding corrosion/hydriding, and material related calculations such as fission gas release and swelling and densification of fuel. The COPENIC code topical,

BAW-10231PA-00, "COPERNIC Fuel Rod Design Computer Code," (Reference 3-6) discusses the methodology used to perform these types of analyses.

3.3.1 *Thermo-Mechanical Codes*

COPERNIC is a general-purpose fuel rod design and licensing code. It is used to calculate parameters such as fuel temperature distributions, fuel rod internal pressure, and cladding creep and strains that directly impact plant safety licensing. The code consists of several individual phenomenological models, each simulating the various mechanisms at work in a fuel rod. Typically, each model is empirically or semi-empirically fit to various databases comprising the various fuel and cladding materials. Some of the main models include:

- Thermal Model
 - Fuel Rod-to-Coolant Heat Transfer
 - Pellet-Cladding Gap Conductance
 - Fuel Thermal Conductivity
 - Heat Transfer Gap Closure
 - Fuel Pellet Radial Power Profile
- Fission Gas Release
- Pellet Strain
 - Fractured Fuel Relocation
 - Fuel Densification-Solid Swelling
 - Gaseous Swelling
- Cladding Strain
 - Irradiation Creep
 - High Stress Creep and Relaxation
 - Irradiation Growth

- Cladding Corrosion/Hydriding
- Internal Rod Pressure
- Material Properties

The individual models are tied together within COPENIC by a master program which divides the fuel rod geometry up at each elevation into a series of concentric rings (macro-zones). These macro-zones are further divided into micro-zones. Material properties are held constant within each micro-zone during a given time-step. Time steps are divided into macro-time steps and micro-time steps. User defined transient quantities (e.g., linear power, fast flux, T-H data, etc.) are input at the macro-time steps. Micro-time steps are defined within the code based on variation of certain quantities that relate to heat transfer, mechanical behavior, and fission gas release. An axisymmetric cylindrical geometry is assumed along with a generalized plane-strain hypothesis (i.e., the stress solution is actually a one-dimensional radial solution combined with uniform axial strain). The applicable mechanisms at work in each ring are then evaluated individually within the constraints (boundary conditions) imposed by adjacent concentric rings. This quasi-two-dimensional solution at a given elevation and time step is basically independent of the solution at elevations above or below the plane being evaluated. Similarly, axial conduction in the fuel and cladding is neglected. These independent planar solutions are then summed using a bookkeeping approach to yield certain overall fuel rod properties such as internal void volume, total fission gas release, and rod internal pressure. This approach is then repeated for additional time-steps to simulate time-dependent behavior.

3.3.2 *Thermo-Mechanical Methodology*

COPENIC is the primary design tool for light water reactor fuel rods using UO₂, Gd₂O₃-UO₂, and MOX fuels in conjunction with M5[®] cladding. It can be run in a best-estimate manner or, when used for certain licensing calculations, several models also have the capability of performing bounding analyses (fission gas release, LOCA initialization, fuel melting point, and creep collapse initialization). The code is approved for steady-state (or slowly changing) fuel rod performance and evaluation of rapid

transients. Although the code is not a true dynamics code (e.g., the spatial and temporal piece-wise solution assumes static equilibrium even during rapid transients and inertial effects are explicitly ignored), the overall output has been benchmarked to sufficient test reactor ramp data to demonstrate conservatism over the range of time scales and transient types relevant to commercial PWR safety analyses applications.

The following criteria are applied when using COPENIC to verify fuel rod designs:

- Fuel rod internal pressure shall be limited so that (1) there is no outward cladding creep during steady-state operation and (2) extensive DNB propagation will not occur.
- During a hypothesized LOCA event; (1) fuel rod fragmentation shall not occur, and (2) 10CFR50 temperature and oxidation limits shall not be exceeded.
- Fuel melting during normal operation and anticipated operating occurrences shall be precluded.
- The maximum uniform hoop strain in the cladding (elastic plus plastic) shall not exceed 1%.
- Cladding creep collapse shall be precluded throughout the life of the fuel rod.
- Cladding peak oxide thickness shall not exceed a best-estimate predicted value of 100 microns.

COPENIC is used either to directly evaluate compliance with these criteria or to provide initialization input to other computer codes that evaluate compliance with these criteria. These analyses include:

- Fuel rod internal pressure analyses
- Fuel melt analyses
- Cladding strain analyses
- Creep collapse initialization analyses
- Cladding peak oxide thickness analyses

COPERNIC has been reviewed and approved for use on current PWR fuel rod designs (typical designs noted in Table 3-4 below). The code and its individual models have been benchmarked over a range of design parameters to provide allowance for anticipated future design changes. Table 3-5 includes a list of approved ranges for the major design parameters.

3.3.3 *Applicability of Thermo-Mechanical Codes/Methodologies to U.S. EPR*

COPERNIC will provide the basis for fuel performance calculations performed in support of U.S. EPR licensing activities. The code and the methodology for using it are described in topical report BAW-10231P-A (Reference 3-6).

This methodology is approved for use on Chapter 15 licensing basis transients within the limitations placed on it either internally by AREVA NP or in the SER. Review and approval of the methodology are mainly a function of the adequacy of the data used to benchmark the various models within the code.

U.S. EPR fuel rod design data are generally bounded by the data used to benchmark COPERNIC (see Table 3-4). The main difference again is the active length. Since the spatial discretization model in COPERNIC largely neglects axial effects, the code results are relatively insensitive to fuel rod lengths. Therefore, the methodology is directly applicable to U.S. EPR calculations providing that the remainder of the fuel parameters intended for the U.S. EPR are maintained within the qualified range of the code's models.

Appendix B contains sample calculations using the COPERNIC methodology.

These calculations duplicate in part those performed in Section 12 of the original topical report (Reference 3-6) and demonstrate the ability of the code to evaluate U.S. EPR fuel designs and obtain reasonable results.

3.4 *References*

- 3-1. "Reactor Analysis System for PWRs," EMF-96-029(P)(A), Volumes 1 and 2, January 1997.
- 3-2. "NEMO-K A Kinetics Solution in NEMO," BAW-10221P-A, September 1998.

-
- 3-3. H. Finnemann and A.G. Galati, "NEACRP 3-D LWR Core Transient Benchmark," Final Specifications, NEACRP-L-335, (Revision 1), October 1991, (January 1992).
 - 3-4. "Reload Startup Physics Tests for Pressurized Water Reactors," ANSI/ANS-19.6.1-1985, American Nuclear Society, 1985.
 - 3-5. "LYNXT Core Transient Thermal-Hydraulic Program – Revision 1," BAW-10156A, Revision 1, August 1993.
 - 3-6. "COPERNIC Fuel Rod Design Computer Code," BAW-10231P-A, Revision 1, January 2004.
 - 3-7. "Evaluation of Advanced Cladding and Structural Material (M5[®]) in PWR Reactor Fuel," BAW-10227P-A, Revision 1, June 2003.
 - 3-8. "NEMO-Nodal Expansion Method Optimized," BAW-10180A, Revision 1, March 1993.

Table 3-1 Neutronics Analyses Areas

Topical Report	Core Design/ Follow	Power Distribution Monitoring	Safety Analyses Support
EMF-96-029(P)(A), Volumes 1 and 2, "Reactor Analysis System for PWRs" (Reference 3-1)	X	X	X
BAW-10221P-A, "NEMO-K A Kinetics Solution in NEMO" (Reference 3-2)			X

Table 3-2 Typical Core Design Configurations

Design Parameter	Range of Conditions Previously Evaluated/Licensed
Assembly Lattice Size	Westinghouse – 15x15 and 17x17 Combustion Engineering – 14x14 and 15x15 (Palisades)
Assembly/Rod Designs	Standard Fuel Assemblies Shield Assemblies (Part length/Robinson and Full length/Palisades) Palisades (high burnup with Hafnium Inserts) Axial blankets Gadolinia and IFBA Rods
Cladding	Zr-4 and M5 [®]
Core Size (# of Assemblies)	Westinghouse –157 and 193 Combustion Engineering– 204 and 217
Control Rod Design	Westinghouse - AIC Combustion Engineering – Al ₂ O ₃ -B ₄ C Palisades – AIC (Cruciform shape)
Spacer Grid Design	Bimetallic Spacers HTP Spacers HMP Spacers IFM Spacers
In-core Detectors	Moveable U ²³⁵ Fission Chambers and Fixed Rhodium Detectors

Table 3-3 Core Design Comparison – Typical 17x17 versus U.S. EPR

Parameters	U.S. 4-Loop¹	U.S. EPR¹
Reactor Thermal power (MW _t)	3411	4500
Primary System Average in Vessel Coolant Temperature (°F)	578	595
Pressure (psia)	2250	2250
RCS Flow Rate per Loop (gpm)	90,000	125,000
Number of Fuel Assemblies	193 FA	241 FA
Fuel Types	UO ₂ , Gd ₂ O ₃ in 17x17 Array	
Active Fuel Length (ft)	12	13.78
Number of Fuel Rods per Assembly	264	265
Number of Guide Tubes per Assembly	25	24
Number of Grids per Assembly	8	10
Average LHGR (kW/ft)	5.44	4.98

¹ Section 2.

Table 3-4 Typical Fuel Rod Design Comparison

Parameters	Mark-B¹	Advanced Mark-BW¹	U.S. EPR
PWR Type	B&W 177 FA	Westinghouse 157/193 FA	AREVA 241 FA
Fuel Types	UO ₂ , Gd ₂ O ₃		
Cladding Material	Zr-4, M5 [®]		
Fuel Rod Length (in)	154.16	152.16	179.13
Fuel Stack Length (in)	140.60	144.00	165.354
Plenum Length (in)	9.87	7.01	7.969
Plenum Volume (in ³)	0.94	0.48	0.604
Cladding OD (in)	0.430	0.374	0.374
Cladding ID (in)	0.377	0.329	0.329
Pellet Diameter (in)	0.3700	0.3225	0.3225
Pellet-Clad Gap (in)	0.0070	0.0065	0.0065
Pellet Density (%TD)	96.0	95.0/96.0	96.0
Fill Gas Pressure (psia)	[]

¹ Reference 3-7

Table 3-5 COPENIC Approved Ranges

Parameter	Range of Validity¹
Fuel ²	UO ₂ , MOX & UO ₂ -Gd ₂ O ₃
Cladding	M5 [®]
Enrichment	UO ₂ ≤ 5 wt% U ²³⁵
	MOX ≤ 6% Pu
	UO ₂ -Gd ₂ O ₃ ≤ 8% Gd
Initial Pellet Density	≥ 92.5% TD
Max. Rod Power	80 kW/m
Rod Avg. Burnup	UO ₂ ≤ 62 GWd/MTU
	MOX ≤ 50 GWd/MTU
	UO ₂ -Gd ₂ O ₃ ≤ 55 GWd/MTU

¹ Reference 3-6.² COPENIC analyses are only applicable to fuel produced using the IDR or ADU processes.

4.0 VALIDATION OF METHODOLOGY FOR SMALL BREAK LOCA

The purpose of this section is to briefly describe and then to demonstrate the applicability of AREVA NP's NRC-approved, SBLOCA EM (Reference 4-1) to U.S. EPR plants. Based on design, geometric, functional, and phenomenological similarities to current Westinghouse 4-loop plants, the applicability of the SBLOCA EM without modification to the U.S. EPR plant will be justified.

4.1 *Small Break Codes and Methods*

The SBLOCA transient response is calculated using the S-RELAP5 code, which in addition to calculating the overall system response, also calculates the hot rod temperature transient using the RODEX2 fuel models and the NUREG-0630 swelling and rupture models. The approach used is deterministic; and complies with 10CFR50 Appendix K requirements. The methodology was approved by the U.S. NRC for Westinghouse and Combustion plants. The U.S. EPR resembles the Westinghouse 4-loop plant design in basic RCS and secondary side design and falls within the same typical range of operating and accident conditions. Therefore, the methodology approved for the analysis of SBLOCAs for Westinghouse 4-loop designs is appropriate for the U.S. EPR. Differences in design can be accommodated within the basic simulation capability and range of applicability of S-RELAP5 through minor changes in modeling.

The methodology (Reference 4-1) uses the S-RELAP5 computer code to simulate the responses of the primary and secondary coolant systems. The methodology was approved for fuel designs with Zircaloy-4 cladding. Extension to fuel designs with M5[®] cladding was approved via Reference 4-2. The S-RELAP5 code is a PWR system transient analysis code that was approved for use in SBLOCA events for Westinghouse and Combustion Engineering two-, three- and four-loop reactor designs. The methodology is approved for SBLOCA evaluation with the following limitation:

S-RELAP5 is acceptable for modeling transients where the break flow area is less than or equal to 10% of the cold leg area.

The fuel rod conditions are calculated by RODEX2 where the fuel conditions are taken to be at the desired burnup (Reference 4-3). The resulting fuel parameters are input to the S-RELAP5 code. This is illustrated by the flowchart in Figure 4-1.

[

]

4.1.1 *Event Description*

LOCAs are defined as postulated accidents that would result from the loss of reactor coolant from piping breaks in the reactor coolant pressure boundary at a rate exceeding the capacity of the normal reactor coolant makeup system. The breaks are postulated to occur at various locations and include a spectrum of break sizes. The loss of a significant quantity of reactor coolant inventory would degrade heat removal from the reactor core unless the water is replenished. The NRC's General Design Criterion 35 requires each PWR to be equipped with an ECCS that refills the vessel in a timely manner to satisfy the requirements of the regulations for ECCS given in 10 CFR Part 50 (Section 50.46 and Appendix K).

SBLOCA transients are defined as any break in the primary system with a flow area of up to 10% of a cold leg pipe area. A break in the cold leg of a reactor system is considered to be most limiting because it causes the greatest direct loss of ECCS fluid through the break and restricts core venting by placing the “loop seals” between the core outlet and break.

The analysis described in this report covers only the period from break initiation up to the time a controlled state is reached. The controlled state is reached when the following conditions are met:

- The core is subcritical.
- The decay heat is removed.

Calculations should be carried out to the point when the core mixture level is fully recovered or until the cladding surface temperature for all axial nodes is less than 1600 °F, whichever occurs sooner.

In the case of the U.S. EPR, SBLOCAs cover a range of sizes up to about 0.5 ft² in area. Only breaks in the cold leg at the pump discharge between the SIS injection location and the reactor vessel need be considered because they are most limiting. This location causes the greatest loss of SIS water and has the greatest tendency for break plugging. The result is less venting at the break and greater core uncovering with subsequently higher peak cladding temperatures.

Three major categories of SBLOCAs are readily identified:

- (1) Breaks that are small enough to be offset by MHSI before there is a major loss of inventory,
- (2) Intermediate size breaks that are too small to rapidly depressurize the RCS, yet are too large to be immediately offset by MHSI – thereby leading to a quasi-steady pressure plateau for a period of time before steam release through the break accelerates the depressurization; moderate repressurization may occur as the primary system refills

- (3) Breaks that are large enough to depressurize the RCS to the discharge pressure of the accumulators.

The exact type of SBLOCA break size in each category is determined by:

- Physical design of the NSSS
- Core power
- SIS pump capacity and availability assumptions
- Accumulator injection setpoint

4.1.2 Small Break LOCA Scenarios

A SBLOCA break results in a loss of reactor coolant inventory that cannot be compensated for by the CVCS. The loss of primary coolant causes a decrease in primary system pressure and pressurizer level. A reactor trip occurs on low PZR pressure. The RT signal automatically trips the turbine and closes the MFW high-load lines. Because of the unavailability of the steam dump to condenser due to the assumed LOOP, as secondary side pressure increases, the Main Steam Relief Trains (MSRTs) open to dump steam to the atmosphere and enable the programmed partial cooldown. The SGs are fed (in case of LOOP) by the EFWS, which is actuated on low SG level or SIS actuation in combination with LOOP.

The SIS is actuated on very low (low-low) PZR pressure. The SI signal automatically starts the MHSI and LHSI pumps (the U.S. EPR does not have HHSI pumps) and initiates a partial cooldown of the secondary system. The partial cooldown cools the primary system and lowers RCS pressure sufficiently to enable the injection of MHSI water into the cold legs. The partial cooldown is performed by all SGs via the steam dump to the atmosphere. It automatically decreases the respective relief valve setpoints corresponding to a cooling rate of 180 °F/h down to nominally 870 psia, a pressure that is low enough to permit the needed MHSI injection while still high enough to prevent core re-criticality.

- For Category 1 and 2 small breaks, the break is too small to depressurize the RCS independent of heat removal in the SGs. In this case, RCS pressure

(saturation pressure) remains slightly above the SG pressure. As the secondary side is depressurized to produce a programmed 180 °F/h, primary system pressure follows. If the size of the break is small enough, the MHSI will be able to offset the break flow and refill the primary system. If not, the primary system will continue to deplete until steam is vented through the break, thereby augmenting the depressurization process. If the break is in the cold leg discharge piping, this does not occur until the loop seal in the cold leg pump suction piping clears and steam can be vented to the break directly or via the downcomer. The subsequent repressurization, if the system refills and reforms the loop seal, is limited by the shut-off head of the MHSI, nominally 1407 psia. The steam generators provide a mechanism to remove decay heat should the combination of MHSI and break flow be inadequate alone.

- For Category 3 small breaks, the break is large enough to relieve sufficient steam to depressurize the RCS to the accumulator discharge pressure without need for heat removal in the SG. In fact, heat transfer eventually reverses and the secondary side becomes a heat source to the primary system.

Evolution of the RCS water inventory depends on the balance between ECCS flow rates (MHSI and accumulators) and break flow rate. The core may uncover before SI flow is able to compensate for the break flow. If it does, fuel cladding temperature increases above saturation in the uncovered portion of the core. The larger the depth of core uncover, the more cladding temperature increases. For the outcome to be acceptable, it must satisfy the U.S. regulatory criteria specified in 10CFR Part 50, Section 50.46 and Appendix K. A more detailed, phase-by-phase description of the SBLOCA scenario is provided in Section 4.2, U.S. EPR Small Break LOCA Phenomena.

4.1.3 *Acceptance Criteria*

The SBLOCA is designated event number 15.6.5 in the Standard Review Plan (SRP) of the Nuclear Regulatory Commission (NRC). The following are the regulatory requirements set forth in 10CFR50.46 (1)-(5) of the Code of Federal Regulations that govern the analysis of a SBLOCA:

1. The calculated maximum fuel element cladding temperature shall not exceed 2200°F.
2. The calculated total oxidation of the cladding shall nowhere exceed 0.17 times the total cladding thickness before oxidation.
3. The calculated total amount of hydrogen generated from the chemical reaction of the cladding with water or steam shall not exceed 0.01 times the hypothetical amount that would be generated if all of the metal in the cladding cylinders surrounding the fuel, excluding the cladding surrounding the plenum volume, were to react.
4. Calculated changes in core geometry shall be such that the core remains amenable to cooling.
5. Long-term coolability should be demonstrated.

These criteria were established to provide a significant margin in ECCS performance following a LOCA.

4.1.4 Cases Analyzed

A spectrum of break sizes in the cold leg pump discharge piping will be analyzed to determine the limiting break size for the U.S. EPR design and show that it is adequately mitigated. Because of the U.S. EPR's similarity to Westinghouse 4-loop plants, sensitivity studies presented in Reference 4-1 on break location, S-RELAP5 model nodalization, and computational timestep remain applicable.

The break spectrum analyzed will span a wide enough range of break sizes to identify the limiting break size and establish a clear trend in the PCT.

4.1.5 Single Failure and Preventive Maintenance

As with current PWR design, the assumption of LOOP following reactor scram is penalizing for U.S. EPR SBLOCA analysis because it causes the loss of main feedwater and the main condenser as well as the dependency on emergency diesel generators to power the safety systems. This delays the delivery of ECCS injection and establishes the most limiting active failure, the loss of one emergency diesel in combination with

LOOP. This causes one complete SIS train of MHSI and LHSI/RHR and one EFWS train to be unavailable.

In addition to the single failure of one SIS diesel, an additional SIS string is assumed to be unavailable due to preventive maintenance. This removes another train of MHSI and LHSI/RHR and another EFWS train.

It is further assumed that one of the two SIS trains that function is associated with the RCS loop affected by the break. This maximizes the opportunity for injection to be diverted directly to the break. Refer to Section 2.1.3, Principal Fluid Systems, for a description of the U.S. EPR ECCS.

4.2 U.S. EPR Small Break LOCA Phenomena

4.2.1 Phase 1 – RCS Depressurization Following Break Initiation

This phase is characterized by rapid primary system depressurization and the approach to saturation in the hot legs. A reactor trip is generated on low pressurizer pressure, the turbine is tripped and the SG pressure rises to the MSRT setpoint. SBLOCA analyses assume a LOOP in conjunction with the reactor trip as a conservative assumption.

Phase 1 is influenced most by:

- Core / Fuel Rod Behavior
- Break Flow Characteristics – Moody Model per 10 CFR 50.46, Appendix K

The fuel rod model in S-RELAP5 is prescribed by NUREG-0630 (swelling and rupture models, Reference 4-3). These models are applicable for SBLOCA events in a variety of PWR designs. Since the U.S. EPR has a core design similar to Westinghouse 4-loop plant, these models are applicable to the U.S. EPR. The fuel rod behavior during a SBLOCA event is not different for the U.S. EPR.

The Moody model is used to determine break flow as for any U.S. PWR. Hence, the break flow characteristics are the same for the U.S. EPR as for any PWR. The main phenomena during this phase of a SBLOCA for the U.S. EPR are the same as those for

other PWRs. Therefore, since S-RELAP5 can simulate this phase of a SBLOCA event for current U.S. PWR plants, it can simulate it for the U.S. EPR plant.

4.2.2 Phase 2 – RCS Saturation and Primary Flow Coastdown

Core cooling is minimized as the result of LOOP and subsequent reactor coolant pump coastdown. Natural circulation of the RCS fluid is established and is sufficient to remove fuel stored energy. Saturation of the RCS and its depressurization occur during this phase due to the combination of programmed SG cooldown and low quality break flow. Cladding temperatures approach saturation during this phase.

The main phenomena affecting Phase 2 are discussed below:

- Core: The RCS loop hydraulic and thermal-hydraulic design of the U.S. EPR does not differ appreciably from current U.S. PWR designs. Like them, the U.S. EPR RV and SGs are situated in the same relative geometrical relationships important for flow to be induced by gravitational head. The design of the U.S. EPR therefore has no effect on the ability of S-RELAP5 to model this aspect of a SBLOCA event.

Counter Current Flow Limit (CCFL) at the core exit as well as the CCFL at the SG inlet plenum may not occur in all PWR designs. S-RELAP5 has the capability to track the occurrence of CCFL in the U.S. EPR at these locations and to apply the appropriate correlation if the phenomenon is encountered during the event.

Fuel rod behavior is the same as during Phase 1.

- Downcomer Bypass: The U.S. EPR vessel design includes upper head to downcomer bypass to enhance venting. This is provided in other PWRs, and comparison with experimental tests confirm the ability of S-RELAP5 to model these phenomena. The SBLOCA methodology accounts for flow leakage between the downcomer and hot leg nozzle penetrations.
- Steam Generator: SG heat transfer is an important phenomenon during this phase of the event. Its importance is increased for the U.S. EPR because it

relies on SG depressurization to reduce the primary pressure to the MHSI injection pressure.

The only significant differences between the U.S. EPR SG design and current PWR SG designs are the increased size and volume of the unit and the incorporation of an axial economizer that utilizes a split downcomer and lower tube bundle region. The difference in size of the unit does not affect the ability of S-RELAP5 to simulate the related hydrodynamic and thermodynamic phenomena. The U.S. EPR SG economizer is modeled explicitly for SBLOCA analyses.

The ability of the S-RELAP5 code using standard U-tube SG modeling techniques to depressurize the primary by SG depressurization was demonstrated by the assessment of BETHSY Test 9.1b (Reference 4-1). The event was initiated by opening a 2-inch break located at the centerline on the discharge side of the pump. HHSI was assumed to be unavailable, which ensured core uncover and fuel rod heat-up. When the cladding temperature reached 723 °K (842 °F), a steam generator dump to the atmosphere was opened to depressurize the primary system below the accumulator pressure and the shut-off head of the LHSI. The test was adequately predicted by S-RELAP5. This comparison to data provides confidence that the SG/primary system heat transfer package implemented in S-RELAP5 can simulate the programmed depressurization of the U.S. EPR SGs.

- Break Flow Characteristics:

Same as for Phase 1.

4.2.3 Phase 3 – Loop Seal Clearing Phase

For small breaks large enough to experience this phase, it is characterized by a loss of natural circulation and the establishment of reflux mode cooling. During this phase, SIS injection is insufficient to balance the break flow and the RCS continues to drain. Steam fills the upper region of the SG U-bends and natural circulation is interrupted. RCS

pressure reaches a plateau (the duration of the plateau depends on break size) at a value near the secondary pressure and a quasi-steady primary-to-secondary temperature differential is established. Some of the decay heat is removed through the break. The remainder is removed by the condensation of primary system steam in the SG tubes.

U.S. EPR features and phenomena affecting Phase 3:

- Core: The core mixture level depends on the reactor power and the S-RELAP5 heat transfer correlations and phase separation model. These models and associated phenomena are consistent with current PWR designs using S-RELAP5 for SBLOCA analysis. S-RELAP5 has the capability to exercise the decay heat model consistent with 10CFR50 Appendix K requirements with 20% uncertainty added. The fuel model uses the S-RELAP5 heat transfer correlations to calculate the cladding temperature and the NUREG-0630 clad ballooning and rupture model to calculate the fuel response to a SBLOCA event. The Baker-Just (Reference 5-5) metal-water reaction is used for calculating the oxidation rate during the transient. These models are independent of the size of the plant and are appropriate to be used in all PWR deterministic SBLOCA analyses. The U.S. EPR is similar to a Westinghouse plant; hence, the S-RELAP5 treatment of fuel phenomena is applicable to this plant design.
- Downcomer Bypass: The S-RELAP5 methodology models two downcomer bypass paths. The amount of flow between the upper downcomer region to the vessel upper head through the RV spray nozzles or leakage between the downcomer and hot leg nozzle penetration is plant specific. The bypass is modeled based on geometric data. This type of approach is consistent with SBLOCA analyses for other PWRs and is applicable to the U.S. EPR.
- Steam Generator: The phenomena occurring in the SG are the same as described in Phase 2.

- Loop Seal: Loop seal behavior is important for this third phase of a SBLOCA transient. The liquid level is depressed to the level of the top of the horizontal loop seal piping. Once the loop seal clears, steam previously trapped in the upper parts of the RCS can be vented to the break. The break flow transitions from a low quality mixture to primarily steam. For some break sizes, the inner vessel mixture level can fall prior to loop seal venting, causing a short period of core uncover. Following loop seal clearing, the core mixture level recovers to the cold leg elevation, as steam pressure is relieved.

Details of the loop seals vary between plant designs. The design of the U.S. EPR loop seal is consistent with a large 3- or 4-loop Westinghouse type plant design. For the U.S. EPR, the elevation from the bottom of the loop seal center line (the horizontal segment) to the cold leg centerline is about 8.5 ft. For Westinghouse plants this elevation is about 10.3 ft. Moreover, the distance from the top of the core for U.S. EPR to the cold leg centerline is about 7.2 ft, which is similar to the Westinghouse design. Hence, there will be a smaller core depression to clear the loop seal for the U.S. EPR relative to other PWRs. S-RELAP5 is capable of predicting loop seal clearing.

[

]

- Pump: The RCP and the RCS loop hydraulic designs do not differ appreciably from current PWR designs, so the design of the U.S. EPR has no effect on the ability of S-RELAP5 to simulate pump performance.

- Cold Leg: Phenomena occurring in the broken and in the intact cold leg loops of the U.S. EPR plant during this phase of an SBLOCA are similar to those predicted for a 4- or 3-loop Westinghouse plant. The main phenomena are horizontal stratification and ECCS condensation. The cold legs of the U.S. EPR are modeled using the same approach used for Westinghouse plants.
- Downcomer: The reactor vessel downcomer is modeled using a two-dimensional (θ , z) component. The use of the two-dimensional component is needed given the multidimensional flow patterns found in the vessel downcomer during SBLOCA events. This representation allows S-RELAP5 to accurately calculate the amount of SIS flow bypassing the core to be discharged out the break and the amount of SIS flow that penetrates into the vessel. The U.S. EPR downcomer has a variable cross-sectional area, which is different than other PWRs; however, this difference does not change the phenomena which occur in the downcomer. Therefore, the modeling of the downcomer is adequate to represent the phenomena in the U.S. EPR downcomer.
- Break Flow Characteristics: The discussion of break flow presented for Phase 1 is valid for this phase as well.

4.2.4 Phase 4 – Boil-off

Following loop seal venting, the vessel mixture level decreases. In this period, the decrease is due to the boil-off of the liquid inventory in the reactor vessel. The mixture level will reach a minimum. In some cases, this causes a deep core uncover. The boil-off period ends when the core liquid level reaches this minimum. By this time, the RCS has depressurized to the point, usually the accumulator setpoint, where SIS flow into the vessel matches or exceeds the rate of core boil-off.

The main phenomena occurring in this phase are:

- Core: The phenomena in the core during boil-off for the U.S. EPR are similar to those for a 4-loop U.S. PWR design. The only difference is that the additional SIS capacity of the U.S. EPR design reduces the extent and

duration of core uncover. Therefore, the S-RELAP5 SBLOCA methodology is adequate to model the U.S. EPR core during this period without modification.

- Pump: Same as transient Phase 3.
- Downcomer: Same as transient Phase 3.
- Break Flow Characteristics: Same as transient Phase 3.

4.2.5 Phase 5 – Core Recovery

The core recovery period extends from the time at which the inner vessel mixture reaches a minimum in the boil-off period, until all parts of the core are covered by a low quality mixture. The SBLOCA is considered to be mitigated when the SIS injection exceeds the break flow and long-term heat removal is assured. The calculation is terminated when the fuel temperature transient in the core has been reversed.

The main phenomena in this phase are core heat transfer, rewet and quench, and break flow which S-RELAP5 predicts.

4.2.6 U.S. EPR Small Break LOCA Phenomena – Conclusion

The phenomena identified in the preceding sections as being important to simulating a SBLOCA for the U.S. EPR plant are the same as those for current U.S. PWRs. Conditions are similar as well and so are within the range of applicability of the S-RELAP5 code. It is concluded, therefore, that since the AREVA S-RELAP5 based methodology has been approved by the NRC for small break analysis of current U.S. PWR designs, it is equally applicable to the U.S. EPR.

4.3 S-RELAP5 Validation for U.S. EPR SBLOCA Analysis

4.3.1 S-RELAP5 Acceptance for SBLOCA Analysis

Table 4-1, reproduced from Reference 4-1, presents the results of an informal PIRT and provides the basis for assuring that S-RELAP5 adequately simulates the important SBLOCA phenomena identified in Section 4.2. It also identifies how the adequacy of the code to predict the phenomena was assessed.

As described more fully in Reference 4-1, the PIRT utilized a group of experts in thermal-hydraulics and safety analysis who initially identified and ranked the phenomena individually. A consensus was then reached on which phenomena were significant and their relative ranking. The ability of S-RELAP5 to simulate the important phenomena was then assessed through benchmarks to test data. The informal PIRT and associated assessments, therefore, provide assurance that the system code S-RELAP5 is adequately qualified for thermal-hydraulic safety analysis of SBLOCA transients.

Table 4-2 summarizes the two separate-effects tests and three integral tests used to validate S-RELAP5 performance under SBLOCA conditions. The tests were chosen specifically to test the two-dimensional core model, loop seal clearing and core heat transfer. Their applicability range covers the relevant break sizes, loop seal clearing and core heatup conditions of interest. These benchmarks analyses are described in Reference 4-1.

The sensitivity studies described in Reference 4-1 were performed to assess the impact of the variation of certain aspects of the S-RELAP5 model on peak clad temperature. The results reflect a stable, converged methodology.

Based on the phase-by-phase identification of important SBLOCA phenomena for the U.S. EPR described in Section 4.2, these benchmarks and sensitivity studies are equally applicable to the U.S. EPR. Additional studies are not required.

4.3.2 *S-RELAP5 Acceptability for U.S. EPR SBLOCA Analysis*

This section describes how the S-RELAP5 model used to analyze SBLOCA events was adjusted to accommodate differences in the U.S. EPR design relative to those plants for which the SBLOCA methodology was developed and approved.

- Larger RCS Component Volumes: The S-RELAP5 model of the U.S. EPR will inherently reflect the effect of increased coolant mass, stored energy and coolant heat capacity. Ratios of coolant volume to nominal reactor power level and pressurizer steam volume to total RCS volume (Table 2-1) show that the dynamics of thermal-hydraulic transients for the U.S. EPR should be

similar to those of current PWRs. The standard treatment of this phenomenon in S-RELAP5 is applicable to the U.S. EPR. The Reference 4-1 methodology is suitable for modeling U.S. EPR RCS component volumes.

- Larger RCS Coolant Flow Rate and Component Flow Areas: The S-RELAP5 model of the U.S. EPR inherently reflects these parameters. The RCS flow rate of the U.S. EPR is comparable to that of other PWRs on a per MWt basis. Similarly, the ratios of RPV and RCS loop flow rates to associated component flow areas result in comparable coolant flow velocities between current PWR models and the U.S. EPR. The standard treatment of this phenomenon in S-RELAP5 is applicable to the U.S. EPR. The Reference 4-1 methodology is suitable for modeling U.S. EPR RCS coolant flow and component flow areas.
- Heavy Reflector Replacing the Core Barrel Thermal Shield Pads: The S-RELAP5 model of the U.S. EPR inherently reflects this design. Relative to current conventional PWRs, the U.S. EPR reflector region consists of a larger proportion of metal than of coolant. The effect of the metal in the reflector will be represented by standard heat conductors, and the bypass flow through coolant flow channels present in the reflector metal structure will be simulated by suitable standard flow paths. Modeling of specific plant design differences is considered an acceptable plant-specific application of the currently approved methodology. The Reference 4-1 methodology is suitable for modeling the U.S. EPR heavy reflector.
- Long Core with HTP Grids and No Intermediate Grids: The S-RELAP5 model of the U.S. EPR inherently reflects these parameters. Modeling of specific plant design differences is considered an acceptable plant-specific application of the currently approved methodology. The Reference 4-1 methodology is suitable for modeling the U.S. EPR core design. The modeling of HTP grids and the long core complies with the present methodology and guidelines.

- U-tube SG with Axial Economizer: The S-RELAP5 model of the U.S. EPR SG inherently reflects the physical design and functionality of the integral axial economizer.
- Redundancy and Diversity of Safety Systems and Emergency Power Supply: The U.S. EPR design philosophy (four physically separated, isolated trains) results in significant additional redundancy and diversity of systems and power supply trains relative to current PWR designs. The additional capability is beneficial and is reflected in individual analysis assumptions for system performance with equipment out-of-service and single-failure. These features have no direct impact on the ability to model safety system performance with S-RELAP5. Modeling of specific plant design differences is considered an acceptable plant-specific application of the currently approved methodology. The Reference 4-1 methodology is suitable for modeling the U.S. EPR safety system design and the S-RELAP5 model of the U.S. EPR inherently reflects its design and functionality.
- Main Steam Relief Train: The steam line from each SG has a single MSRT, which consists of a normally open motor-driven angled control valve (MSRV) and an upstream, normally closed, fast-opening angled globe valve (MSRIV) with automatically resettable setpoints. S-RELAP5 has the capability of simulating the performance and control behavior of these valves. The Reference 4-1 methodology is suitable for modeling the U.S. EPR MSRT design and the S-RELAP5 model of the U.S. EPR inherently reflects its design and functionality.
- Digital I&C Systems: The functionality of the U.S. EPR -specific algorithms for the systems credited in the analyses of these events are modeled using standard S-RELAP5 control components. Modeling of specific plant design differences is an acceptable plant-specific application of the currently approved methodology. The Reference 4-1 methodology is suitable for modeling the U.S. EPR I&C system functions and the S-RELAP5 model of the U.S. EPR inherently reflects its design and functionality.

- Low Core Average Power Density: The S-RELAP5 model of the U.S. EPR inherently reflects this parameter. The standard treatment of this parameter in S-RELAP5 is applicable to the U.S. EPR. This modeling is an acceptable plant-specific application of the approved Reference 4-1 methodology.
- Higher Total Core Peaking (F_Q): The S-RELAP5 model of the U.S. EPR inherently reflects this parameter. The standard treatment of this parameter in S-RELAP5 is applicable to the U.S. EPR. This modeling is an acceptable plant-specific application of the approved Reference 4-1 methodology.
- Higher RCS Operating Temperature at Full Load: The S-RELAP5 model of the U.S. EPR inherently reflects this parameter, as allowed by the Reference 4-1 methodology. The standard treatment of this parameter in S-RELAP5 is applicable to the U.S. EPR. This modeling is an acceptable plant-specific application of the approved Reference 4-1 methodology.
- Higher SG Operating Pressure: The S-RELAP5 model of the U.S. EPR inherently reflects this parameter in the SG modeling and steady-state initialization. The standard treatment of this parameter in S-RELAP5 is applicable to the U.S. EPR. This modeling is an acceptable plant-specific application of the approved Reference 4-1 methodology.
- Preventive Maintenance During Operation: The Technical Specifications for the U.S. EPR allow full-power operation of the plant with one train of certain four-train systems out-of-service for on-line preventive maintenance. This has no direct influence on the Reference 4-1 analysis methodology other than it must be considered in the determination of operable system capacities, with one train out-of-service for maintenance and another out-of-service due to single failure.

4.4 **Conclusions**

The NRC-approved methodology described in Reference 4-1 for analyzing small break LOCA events in current Westinghouse and Combustion Engineering plants is appropriate for analysis of these events in the U.S. EPR design. The hardware

differences between these designs are accommodated within the basic capability of S-RELAP5 to model PWR fluid systems and simulate the associated thermal-hydraulic phenomena. Because of the similarity of the U.S. EPR design and its range of operational and accident conditions to those of current U.S. PWR plants, no new phenomena need to be considered and the S-RELAP5 based SBLOCA methodology can be applied to the U.S. EPR without modification.

4.5 *References*

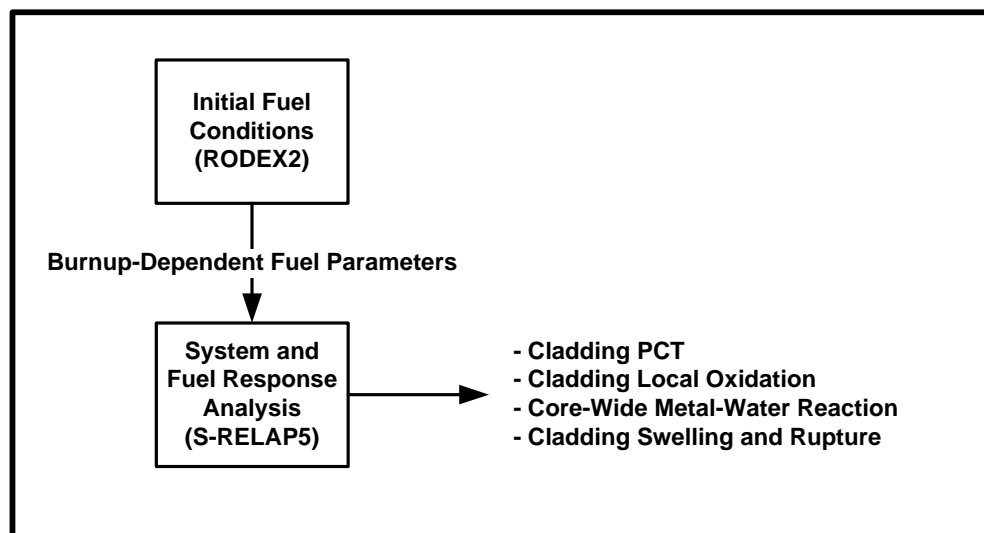
- 4-1. "PWR Small Break LOCA Evaluation Model, S-RELAP5 Based," Revision 0, EMF-2328 (P)(A), March 2001.
- 4-2. "Incorporation of M5[®] Properties in Framatome ANP Approved Methods," BAW-10240(P)(A), May 2004.
- 4-3. Powers, D. A., and R. O. Meyers, "Cladding Swelling and Rupture Models for LOCA Analysis," NUREG-0630, April 1980.
- 4-4. ANS Standard "Decay Energy Release Rates Following Shutdown of Uranium-Fueled Thermal Reactors," October 1971, Revised October 1973.
- 4-5. L. Baker and L.C. Just, "Studies of Metal-Water Reactions at High Temperature: III. Experimental and Theoretical Studies of Zirconium-Water Reaction," ANL-6548, 1962.

Table 4-1 Informal SBLOCA PIRT with Assessment/Disposition

--

Table 4-2 S-RELAP5 Experimental SBLOCA Benchmark Calculations

Experiment	Description	SBLOCA Relevancy
2-D Flow Tests	Separate effects test with parallel 14x14 bundles, full width, partial height, with one bundle blocked and various flows in the other.	Two-dimensional core model
Semiscale S-UT-8	Scaled PWR integral facility, test series designed to investigate effects of ECCS on SBLOCA.	Core heat-up before loop seal clearing
LOFT LP-SB-3	Scaled PWR integral test facility, test series designed to study core heat transfer during slow boil-off SBLOCA (1.84 inch equivalent).	Core heat transfer during boil-off phase
UPTF-A5RUN11E	Full-scale PWR test facility, test series designed to study loop seal clearing behavior with vapor super heat.	Loop seal clearing
BETHSY Test 9.1b	Scaled PWR integral test facility, test series designed to study SBLOCA without HHSI.	Integral effects: 2-inch equivalent small break, three-loop facility, loop seal clearing

Figure 4-1 – SBLOCA Evaluation Model

5.0 VALIDATION OF S-RELAP5 METHODOLOGY FOR NON-LOCA EVENTS

This section presents the AREVA NP non-LOCA transient methodology that will be used to analyze non-LOCA events for the U.S. EPR design. The selected codes and methods are first described, followed by a validation of their applicability to U.S. EPR non-LOCA analysis. The validation includes a review of the key phenomena associated with each of the non-LOCA event categories.

5.1 *Non-LOCA Transient Codes and Methods*

The methodology to be used to perform the non-LOCA safety analysis for the U.S. EPR uses of the S-RELAP5 computer code to simulate the responses of the primary and secondary coolant systems. S-RELAP5 is capable of simulating a wide range of upset conditions and modeling the response of the NSSS, reactor protection, engineered safeguards, safety/relief valves, and the impact of automatic controllers on the event sequence. The methodology for the application of S-RELAP5 to non-LOCA events is described in Reference 5-1. This methodology was approved by the NRC and has been applied to perform the safety analyses supporting a wide range of CE and Westinghouse designed PWR plants.

The S-RELAP5 code includes many generic component models from which general systems can be simulated. These components include pumps, valves, pipes, heat releasing or absorbing structures, reactor point kinetics, electric heaters, jet pumps, turbines, separators, accumulators, and control and trip system components. In addition, special process models are included for effects such as form loss, flow at an abrupt area change, branching, choked flow, counter-current flow limit (CCFL), boron tracking, and non-condensable gas transport. The reactor fuel is represented as a heat releasing or absorbing structure. The fuel is modeled in S-RELAP5 as described in Section 3.2 of Reference 5-1. For the U.S. EPR, input for fuel characteristics is obtained from the approved fuel thermal mechanical computer code COPENIC (see Section 3.3.2) in lieu of RODEX2.

S-RELAP5 evolved from the AREVA NP ANF-RELAP code, a modified RELAP5/MOD2 version used for pressurized water reactor (PWR) plant licensing analyses that included

steam line break analysis and PWR non-LOCA Chapter 15 event analyses. The evolution of the S-RELAP5 code has resulted in a code structure similar to RELAP5/MOD3 including RELAP5/MOD3 reactor kinetics and control systems and trip system models. S-RELAP5 was benchmarked against a series of LOFT experiments, and against ANF-RELAP simulations. The results of these comparisons are presented in Reference 5-1.

The S-RELAP5 non-LOCA methodology is applicable to the SRP Chapter 15 events given in Table 5-1.

The methodology is applicable to Condition I, II, III, and IV events, classified on the basis of frequency:

CONDITION I: events expected to occur frequently in the course of power operation, refueling, maintenance or plant maneuvering.

CONDITION II: events expected to occur on a frequency of once per year during plant operation.

CONDITION III: events expected to occur once in the lifetime of the plant.

CONDITION IV: events not expected to occur that are evaluated to demonstrate design adequacy.

The acceptance criteria associated with the Chapter 15 non-LOCA events follow the SRP (Reference 5-2) and are summarized below:

1. Specified Acceptable Fuel Design Limits (SAFDLs); DNB and Fuel Centerline Melt (FCM)
2. Pressure in the reactor coolant and main steam systems < 110% of design
3. An incident of moderate frequency does not result in a more serious plant condition without other faults occurring independently
4. Offsite dose consequences (plant Condition III or IV)
5. Energy deposition limits
6. Loss of shutdown margin

In addition to identifying the events, Table 5-1 also identifies the corresponding plant condition and acceptance criteria for each event from those defined above.

As can be seen from the description presented in Section 2 of this report, the U.S. EPR design is very similar to the PWR designs for which the S-RELAP5 methodology has been approved. Section 5.2 of this report will present information validating the Reference 5-1 methodology for U.S. EPR non-LOCA analyses for events in the above categories. It will be shown that the Reference 5-1 methodology for analyzing the NSSS response is directly applicable to the U.S. EPR, requiring only input changes to accommodate particular design features.

5.2 *S-RELAP5 Validation for U.S. EPR Non-LOCA Analysis*

This section provides the validation of the applicability of the S-RELAP5 code methodology for analyzing non-LOCA transients for the U.S. EPR. The validation is presented in three parts. First, a review of the S-RELAP5 methodology and the basis for acceptance is presented. Next, the U.S. EPR design features are presented and compared to current PWRs. Finally, based on these design differences, it will be shown that the phenomena expected during the response of the various Chapter 15 non-LOCA events for the U.S. EPR will not change from that identified for the Reference 5-1 methodology. This will be demonstrated for each event category defined in the Standard Review Plan (Reference 5-2).

5.2.1 *S-RELAP5 Acceptance for Non-LOCA Analysis*

As discussed in Section 5.1 of this report the S-RELAP5 methodology (Reference 5-1), for the analysis of SRP Chapter 15 Non-LOCA events, has been reviewed and approved by the NRC. The methodology was designed for PWRs with specific application to Combustion Engineering and Westinghouse plants.

The assessment of S-RELAP5 for application to Chapter 15 non-LOCA transient events consisted of the simulation of four Loss-of-Fluid-Test (LOFT) program transient tests and comparison with ANF-RELAP calculations of various transients. The four LOFT tests that were simulated are:

-
- LOFT L6-1 Loss of Load
 - LOFT L6-2 Loss of Primary Flow
 - LOFT L6-3 Excessive Steam Load
 - LOFT L6-5 Loss of Feedwater

The four LOFT tests represent the key phenomena in SRP Categories

- 15.1 - Increase in Heat Removal by the Secondary System,
- 15.2 - Decrease in Heat Removal by the Secondary System, and
- 15.3 - Decrease in Reactor Coolant Flow Rate.

Overall, the predictions of the LOFT transient tests show good agreement with the measured results and good agreement with the calculated results of ANF-RELAP. The simulations performed by the code included modeling of automatic control components and systems such as pressurizer sprays and heaters, feedwater control, pressure control, steam generator level control, and reactor power.

Sample problems provided to demonstrate the methodology include:

- Pre-scrum Main Steam Line Break (MSLB)
- Post-scrum MSLB
- Loss of External Load
- Loss of Normal Feedwater Flow
- Loss of Forced Reactor Coolant Flow
- Uncontrolled Bank Withdrawal
- Steam Generator Tube Rupture

The sample problems included typical NSSS model nodalization to handle the spectrum of non-LOCA events. The MSLB nodalization was defined differently, particularly in the reactor vessel to conservatively treat the effects of the cooldown in the broken loop. It was noted that the nodalization was considered typical and that the nodalization may

vary from plant-to-plant to handle specific design features. Typical nodalization diagrams associated with the S-RELAP5 methodology were presented in Figures 6.1 through 6.5 of Reference 5-1.

For DNBR evaluations, output from S-RELAP5 is used as input to LYNXT or the alternate DNBR evaluation method described in Section 5.4.7.2 of Reference 5-1. In both cases a suitable, approved CHF correlation is applied. The LYNXT application is described in Section 3.2 of this report.

The methodology also considers certain assumptions when analyses of the various events are performed. These include:

- Timing of Loss-of-Offsite Power
- Mitigating Systems
- Operator Actions
- Single Failures
- Number of Loops Operating
- Axial and Radial Power Distributions

In performing the analysis, values and equipment are selected for the above in accordance with the guidelines provided in the appropriate Regulatory Guides, Standard Review Plan, and computer code user guides to ensure conservative calculations are performed. In addition, the analyst must ascertain where it is appropriate to use nominal or technical specification values for the initial core power level, initial reactor coolant flow rate, initial reactor coolant temperature, initial reactor pressure and pressurizer level, moderator temperature reactivity coefficient, Doppler reactivity coefficient, reactor protection system trip and equipment setpoints and time delays, and scram characteristics.

Based on Reference 5-1, the NRC staff concluded that the S-RELAP5 code, with conservative input modeling assumptions, is capable of addressing the thermal-hydraulic responses of the target non-LOCA events in a conservative manner in

keeping with the SRP guidance and is therefore an acceptable replacement for the ANF-RELAP code.

In addition, it was noted that for individual applications justification would still be required which is expected to include: nodalization, defense of the chosen parameters, any needed sensitivities, justification of the conservative nature of the input parameters, and calculated results.

5.2.2 S-RELAP5 Acceptability for U.S. EPR Non-LOCA Analysis

The acceptability of S-RELAP5 non-LOCA methodology for U.S. EPR Chapter 15 analyses is based on the similarity of the U.S. EPR design to the design of current operating CE and Westinghouse PWRs. Furthermore, as described below, the design features of the U.S. EPR as compared to PWRs in general do not change the important phenomena expected to occur during non-LOCA events. Therefore, since the S-RELAP5 methodology for non-LOCA analysis was based on standard PWR designs, it is directly applicable to the U.S. EPR. These arguments will be further expanded in the sections below.

The process used to determine the acceptability of the S-RELAP5 non-LOCA methodology for the U.S. EPR Chapter 15 analyses is outlined below.

- Examine the design differences between the U.S. EPR and PWRs for which the methodology was approved (CE and Westinghouse plants).
- Examine the expected response of the U.S. EPR for the various classes of non-LOCA events where S-RELAP5 would be applied.
- Determine the key phenomena associated with the U.S. EPR response and compare to the key phenomena identified as part of the review of Reference 5-1.
- Determine the applicability of the S-RELAP5 methodology based on the above.

These elements will be further discussed in the following paragraphs.

Section 2 of this report presented a design overview of the U.S. EPR. It can be seen from this description that the U.S. EPR is fundamentally similar to the standard PWRs

on which the S-RELAP5 methodology was based. Outside of a limited number of design improvement features, the U.S. EPR mirrors a standard 4-loop PWR. Some of the key design improvement features include:

- MSRT valves
- Primary and secondary system component sizing
- Redundancy and diversity of safety systems (4 trains)
- Preventive maintenance during operation
- MHSI with no HHSI
- SG with axial economizer
- Non-linear T_{avg} program as a function of power
- Heavy reflector is used between the core and core barrel
- No lower penetration in the reactor vessel
- Pressurizer safety valves are pilot operated (spring-driven)
- Digital I&C RPS includes some unique trips, e.g., low DNBR, high core power based on enthalpy balance, and lack of a high flux trip in the power mode (includes a rate trip)
- RCCA control program (three control modes at power and a fourth control mode at low power)
- Non-safety grade partial trip function

These features have been considered in assessing the applicability of the S-RELAP5 methodology to the U.S. EPR. The sections below report the results of that assessment for each event category.

Typical nodalization diagrams used in the non-LOCA sample problems were illustrated in Figures 6.1 through 6.5 of Reference 5-1 as noted above. To model the U.S. EPR slight changes were necessary to model specific design features. These included:

[

]

Nodalization diagrams developed for the U.S. EPR (sample problems) are illustrated in Figures 5-1 through 5-5 of this report. The changes in nodalization resulted from

implementing the U.S. EPR design features noted above and are not changes in the methodology. These changes are considered an acceptable plant specific application of the approved methodology. Sample problems, using the modified model nodalizations, are presented in Appendix D to illustrate results for the U.S. EPR using the Reference 5-1 methodology. The same analysis approach taken in Reference 5-1 regarding the biasing of initial conditions to ensure a conservative result was used in the sample problems presented. The sample problems selected are cases presented in Reference 5-1. These cases are intended to illustrate the response of the U.S. EPR using the S-RELAP5 methodology as compared to a standard PWR to further demonstrate the applicability of the methods. For the U.S. EPR design certification it is expected that a spectrum of cases (sensitivities) for each category will be necessary to characterize potentially limiting cases.

For DNBR evaluations, output from S-RELAP is used as input to LYNXT or the alternate DNBR evaluation method described in Section 5.4.7.2 of Reference 5-1. In both cases a suitable, approved CHF correlation is applied. The LYNXT application is described in Section 3.2 of this report.

Part of the correspondence submitted in support of the approval of the S-RELAP5 methodology for non-LOCA analysis included the results of an informally constructed PIRT that applied to non-LOCA transients for PWRs of the Westinghouse and CE design. Table 5-2 presents the material submitted. Part of the process, as described above, for determining the acceptability of the Reference 5-1 methodology to the U.S. EPR was to determine the key phenomena for the U.S. EPR from the expected response and compare that against the key phenomena used in the Reference 5-1 methodology development. Table 5-2 was used as a reference to identify any potential new phenomena that may result for the U.S. EPR. The results of that review are also presented in the sections below for each event category. Each section contains a description of the expected response of the U.S. EPR for the given event, a discussion of the key phenomena related to the given event, and a discussion of the potential impact of key design differences and operating characteristics between the U.S. EPR and a standard PWR.

5.2.2.1 Increase in Heat Removal by the Secondary System

Events in this category include:

- decrease in feedwater temperature
- increase in feedwater flow
- increase in steam flow
- inadvertent opening of a SG relief/safety valve
- steam system piping failures

Since the first four events above involve similar phenomena, they will be discussed as part of the same group and placed in a category of moderate overcooling events. The steam system piping failures will be discussed separately.

5.2.2.1.1 Moderate Overcooling Events**5.2.2.1.1.1 Event Description**

A number of transient events involve an unplanned increase in heat removal by the secondary system. The design of the U.S. EPR secondary systems (MSS and MFW) is very similar to those of current operating PWR plants. The MSS consists of an individual steam line from each SG, with a number of relief valves meeting in a common header with flow from the header to the turbine or condenser via MSB. The MFW and condensate system consists of a dual train of multiple stages of feedwater heating, electrically operated condensate and MFW pumps, and MFW control and isolation valves.

Excessive heat removal by the secondary system, i.e., a heat removal rate in excess of the heat generation rate in the core, may be initiated by malfunctions or failures resulting in a decrease in feedwater temperature, an increase in feedwater flow rate, or an increase in steam flow resulting from failure of a pressure regulating valve (turbine governor or steam bypass) or steam generator relief or safety valve. The excess heat removal causes a decrease in moderator temperature. With a negative moderator temperature coefficient, the decrease in moderator temperature increases core

reactivity and can lead to a power level increase and a decrease in shutdown margin.

The U.S. EPR rod control is designed to maintain a constant moderator average temperature. The rod control system could therefore pull control rods out of the core to increase core power in response to the decreasing moderator temperature or insert control rods to constrain the increasing core power. In either case, the power level increase may lead to a new quasi-steady-state operating condition or a reactor trip.

Decrease in Feedwater Temperature

A reduction in feedwater temperature may be caused by the accidental opening of a feedwater bypass valve which diverts flow around a portion of the feedwater heaters. In the event of an accidental opening of a bypass valve, there is a sudden reduction in feedwater inlet temperature to the steam generators. At power, this increased subcooling will create a greater load demand on the RCS. With the plant at no-load conditions, the addition of cold feedwater may cause a decrease in RCS temperature and thus a reactivity insertion due to the effects of the negative moderator temperature coefficient of reactivity. However, the rate of energy change is reduced as load and feedwater flow decrease; thus, the no-load transient is typically less severe than the full power case. The net effect on the RCS due to a reduction in feedwater temperature is similar to the effect of increasing secondary steam flow.

During power operation, a reduction in feedwater temperature leads to either a new steady-state condition at an increased power level or to a reactor trip, e.g., High Core Power Level or Low DNBR.

At shutdown conditions, a reduction in feedwater temperature leads to a reduction of the core shutdown margin whose amplitude depends on the uncontrolled insertion of reactivity from the resultant cooldown. The high shutdown margin of the U.S. EPR provides an intrinsic efficient mitigation means against such an event.

Increase in Feedwater Flow

The increase in feedwater flow event is initiated by a failure or misoperation of the feedwater control system and results in an increase in feedwater flow to one or more of the steam generators. The typical limiting event is full opening of a main feedwater

control valve. The course of the transient is determined by the thermal-hydraulic response of the secondary side, which in turn depends upon the design of the steam generator. In the subsequent discussion of the event progression it is assumed that the turbine steam demand remains constant, i.e., the turbine valves move so as to keep the steam flow to the turbine constant.

The thermal-hydraulic response of a steam generator with internal feedwater preheating differs from one without this feature. The axial economizer section of the U.S. EPR SG design acts in part as a preheater. In this SG design 100% of the feedwater flows into the inlet portion of the axial economizer at the top of an enclosed section of the cold side of the downcomer region. The heat transfer mode in this isolated portion of the downcomer, as well as a portion of the isolated section of the lower tube bundle associated with the axial economizer region, is convective heat transfer to subcooled liquid. The heat transfer within the axial economizer is therefore sensitive to changes in feedwater flow rate. A rapid increase in feedwater flow may cause a rapid decrease in primary system temperature due to enhanced heat transfer in the axial economizer downcomer and tube bundle regions. This decrease in primary side temperature may cause a rapid increase in core power (assuming that the Moderator Temperature Coefficient (MTC) is large and negative) which, in turn increases steam production over that which is being demanded by the turbine. Consequently, the secondary side pressure increases and the turbine valves begin closing to keep demand constant.

The rising secondary pressure limits the increase in nucleate boiling heat transfer along the tubes (saturation temperature increases along with the pressure) and the decrease in the primary system's temperature may be arrested. If the reactor does not trip on High Core Power Level or High SG Pressure a quasi-steady-state persists until the High Steam Generator Level Reactor Trip (RT)/Turbine Trip (TT) signal is reached.

An increase in feedwater flow potentially presents two challenges to reactor safety. First, the increased power may challenge core SAFDLs. Second, the excessive feedwater flow may result in a significant reduction in the affected SG operating void fraction and fluid temperature, and a consequent increase in SG liquid inventory prior to and after reactor trip. The increased inventory could potentially result in a liquid

overflow of the affected SG once the cold water inventory heats up and expands from residual core decay heat, RCP heat addition and continued steam void formation. Overfilling the SG could result in the introduction of water into the steam lines and subsequent damage with the potential for violating the SRP acceptance criterion that “an incident of moderate frequency should not generate a more serious plant condition without other faults occurring independently.”

To prevent these criteria from being violated the plant is designed to automatically terminate the event by closing the dedicated MFW isolation valves (both the MFW-HL and MFW-LL control and isolation valves) on the safety-classified High SG level RT signal in the affected SG.

The event is analyzed to validate the high level protection function setpoint. During power operation, should a reactor trip be activated by a signal other than High SG level (e.g., by core protection signals High Core Power Level, High LPD or Low DNBR) the severity of the initiating event would automatically be reduced by the automatic safety-classified isolation of all main feedwater high-load lines, which is associated with any RT signal. Single failure of the associated isolation valve would result in continued excess feedwater addition until the High SG Water Level MFW/SSS isolation signal was generated, closing the downstream MFWIV.

Increase in Steam Flow

An increase in steam flow event may be initiated by a failure or misoperation of the main steam system that results in an increase in steam flow from the steam generators. The event could be caused by rapid opening of the turbine valves, the steam dump (MSRT) or MSB valves. Whatever the cause, the increase in steam flow creates a mismatch between the energy being generated in the reactor core and the energy being removed by the secondary system and results in a cooldown of the primary system. A power increase will occur if the moderator temperature reactivity feedback coefficient is negative or if the rod control system is in an automatic mode and begins to pull control rods from the reactor core in response to the increased steam flow. If the power increase is sufficiently large either an overpower (High Core Power Level) or thermal

margin (High LPD or Low DNBR) limit will be reached and the event will be terminated by a reactor trip. If the power increase is less than these limits the reactor will stabilize at an increased power level.

The predominant factor in the increase in steam flow analysis is the initiating event. The range of initiating events determines how large a steam flow increase must be considered. In the U.S. EPR design, the MSS is able to discharge steam by the following means:

- The turbine inlet control valves to the turbine
- 1 Main Steam By-pass system consisting of 6 valves with a combined capacity of 50/55% (min/max) of full load steam generation
- 4 Main Steam Relief Trains, one per steam generator, with a capacity 50/55% of the steam generator full load steam generation
- 8 Main Steam Safety Valves, two per steam generator, each with a capacity 25/27.5% of full load steam generation

Excessive increase in steam flow can be due to a inadvertent opening of a MSRT or MSSV, the spurious actuation of the “partial cooldown” I&C function (which dumps steam through the MSB or MSRTs to decrease RCS temperature at a 180 °F/h cooldown rate), or the spurious opening of the MSB or turbine inlet valves.

Inadvertent Opening of SG Relief/Safety Valve

The inadvertent opening of a SG relief/safety valve event is a subset of the increase in steam flow as discussed above.

5.2.2.1.1.2 Specific Event Phenomena

Table 5-2 illustrates the phenomena associated with each of the Chapter 15 non-LOCA event categories. Based on the expected response of the U.S. EPR, as described above, the key phenomena associated with moderate overcooling events are discussed below. An evaluation of the ability of the Reference 5-1 methodology to appropriately treat the phenomena is also included in the discussion.

- Fuel Rod Heat Transfer: The U.S. EPR uses fuel assembly and fuel rod designs essentially identical except for length to current PWR fuel. Heat transfer from the clad is to circulating coolant water as in current PWR designs. Therefore, the standard treatment of this phenomenon in S-RELAP5 is applicable to the U.S. EPR. The Reference 5-1 methodology is suitable for analyzing U.S. EPR fuel rod heat transfer phenomena during moderate overcooling events.
- Kinetics feedback, Reactivity Control: The core designs for the U.S. EPR are expected to be similar except for length (active fuel height) and reflector composition to current PWR core designs, with comparable fuel enrichments and RCS boron concentrations. Similarly, the control element design used in the U.S. EPR is essentially identical to current PWR designs (multi-fingered steel clad Ag-In-Cd absorber control elements stepwise inserted/withdrawn from the top of the fuel assembly, released upon RT). The standard treatment of this phenomenon in S-RELAP5 is applicable to the U.S. EPR. The Reference 5-1 methodology is suitable for analyzing U.S. EPR kinetics feedback and reactivity control phenomena during moderate overcooling events.
- Pressurizer phenomena (vertical fluid thermal stratification, wall condensation, spray (subcooled droplet interaction with steam), interfacial heat and mass transfer, convective heat transfer to walls):

The only significant difference between the U.S. EPR pressurizer design and current PWR pressurizer designs is the increased volume of steam and liquid. This has no effect on the ability of S-RELAP5 to simulate the expected pressurizer phenomena listed above. The standard treatment of this phenomenon in S-RELAP5 is applicable to the U.S. EPR. The Reference 5-1 methodology is suitable for analyzing U.S. EPR pressurizer phenomena during moderate overcooling events.

- SG primary/secondary heat transfer (U-tube SG phenomena, primary side single-phase convective heat transfer, tube wall heat conduction, secondary side single- and two-phase heat transfer pre- and post-CHF, feedwater injection, recirculation, carryover, steam separation, thermal stratification in the downcomer, and level indication and control):

The significant differences between the U.S. EPR U-tube SG design and current PWR U-tube SG designs are the increased size/volume of the unit and the incorporation of an axial economizer with a split downcomer and lower tube bundle region. The difference in size of the unit has no effect on the ability of S-RELAP5 to simulate the related hydrodynamic and thermodynamic phenomena. The fluid flow and heat transfer phenomena within the axial economizer region (single- and two-phase fluid flow, convection and nucleate boiling heat transfer) are similar to those in other regions of current PWR U-tube SG designs modeled using the Reference 5-1 methodology. Explicit modeling of the axial economizer geometry in the U.S. EPR S-RELAP5 SG model is allowed by the Reference 5-1 methodology (page 3-1) and would be considered an acceptable plant-specific application of the currently approved methodology. The Reference 5-1 methodology is suitable for analyzing U.S. EPR SG primary/secondary heat transfer phenomena during moderate overcooling events.

- Critical flow of steam (through primary and secondary relief valves): The fluid media in the U.S. EPR pressurizer, RCS and MSS are the same as those used in current PWR designs. The relief valve internal designs are also similar to standard relief valve designs and thus do not introduce any new hydraulic phenomena. The standard treatment of this phenomenon in S-RELAP5 is applicable to the U.S. EPR. The Reference 5-1 methodology is suitable for analyzing U.S. EPR relief valve flow phenomena during moderate overcooling events.
- Asymmetric RCS cooldown: The Increase in Feedwater Flow event, failure open of a single MFWCV, results in an asymmetric heat load on a single SG

and primary coolant loop. The increased feedwater flow through the axial economizer section of the affected SG may result in the primary side fluid exiting the SG at significantly colder temperatures than other loops. Only a relatively small portion of the flow entering an U.S. EPR RV inlet nozzle mixes with flow from other loops, resulting in most of the inlet nozzle flow exiting the vessel through the outlet nozzle feeding the same loop. Therefore, the fluid in the affected loop will cool progressively until RT. This will likely require application of the sectorized core and RV modeling described in Reference 5-1 for the pre-scrum MSLB event to the analysis of the Increase in Feedwater Flow event for the U.S. EPR.

Based on this review of expected phenomena, no changes are required to the Reference 5-1 methodology for overcooling event analyses of the U.S. EPR.

5.2.2.1.1.3 Disposition of Event-Specific U.S. EPR Design Differences

U.S. EPR design differences (relative to conventional U.S. PWR designs) that could potentially impact the applicability of the methodology to analyze this event for the U.S. EPR are listed below, along with disposition arguments that justify the applicability.

Component Design Differences:

- Larger RCS Component Volumes: The S-RELAP5 model of the U.S. EPR will inherently reflect the effect of increased coolant mass, stored energy, and coolant heat capacity. Ratios of coolant volume to nominal NSSS power level and pressurizer steam volume to total RCS volume show that the dynamics of thermal-hydraulic transients for the U.S. EPR should be similar to those of current PWRs. The standard treatment of this phenomenon in S-RELAP5 is applicable to the U.S. EPR. The Reference 5-1 methodology is suitable for modeling U.S. EPR RCS component volumes.
- U-tube SG with Axial Economizer: The S-RELAP5 model of the U.S. EPR SG will inherently reflect this design. The model nodalization will be modified as needed to accurately reflect the design and performance of the economizer. Modeling of specific plant design differences is allowed by the Reference 5-1

methodology (page 3-1) and is considered an acceptable plant-specific application of the currently approved methodology. The Reference 5-1 methodology is suitable for modeling the U.S. EPR SG design.

- Digital I&C Systems: The functionality of the U.S. EPR -specific algorithms for the systems credited in the analyses of these events may be modeled using standard S-RELAP5 control components. Modeling of specific plant design differences is allowed by the Reference 5-1 methodology (page 3-1, Reference 5-1) and is considered an acceptable plant-specific application of the currently approved methodology. The Reference 5-1 methodology is suitable for modeling the U.S. EPR I&C system functions.
- Low DNB and High LPD Reactor Trips: The Low DNBR and High LPD RT functions utilize in-core based measurements of local core power distributions at several locations in each core quadrant. While modeling of specific plant design differences is allowed by the Reference 5-1 methodology (page 3-1, Reference 5-1) and is considered an acceptable plant-specific application of the currently approved methodology, the determination of the timing of a Low DNBR or High LPD trip is expected to be treated in a “de-coupled” manner, external to S-RELAP5. When it is necessary to credit these RT functions, thermal-hydraulic conditions from the S-RELAP5 run will be used as boundary conditions to the external determination of trip functional response. Except for the possible activation of the reactivity addition from scrammed control rods, the trip functions will not be explicitly simulated in the S-RELAP5 model. This approach results in no new or unexpected phenomena in the S-RELAP5 simulation of the event. The Reference 5-1 methodology is suitable for modeling the effects of an U.S. EPR Low DNBR or High LPD RT.

Differences in Operating Conditions:

- Higher RCS Operating Temperature at Full Load: The S-RELAP5 model of the U.S. EPR will inherently reflect this parameter, as allowed by the Reference 5-1 methodology (page 3-1, Reference 5-1). The standard treatment of this

parameter in S-RELAP5 is applicable to the U.S. EPR. This modeling would be considered an acceptable plant-specific application of the approved Reference 5-1 methodology.

- Higher SG Operating Pressure: The S-RELAP5 model of the U.S. EPR will inherently reflect this parameter. The standard treatment of this parameter in S-RELAP5 is applicable to the U.S. EPR. This modeling is considered an acceptable plant-specific application of the approved Reference 5-1 methodology.
- Higher No-Load RCS Temperature: The S-RELAP5 model of the U.S. EPR will inherently reflect this parameter. The standard treatment of this parameter in S-RELAP5 is applicable to the U.S. EPR. This modeling is considered an acceptable plant-specific application of the approved Reference 5-1 methodology.
- Higher No-Load SG Pressure: The S-RELAP5 model of the U.S. EPR will inherently reflect this parameter. The standard treatment of this parameter in S-RELAP5 is applicable to the U.S. EPR. This modeling is considered an acceptable plant-specific application of the approved Reference 5-1 methodology.
- Part Power RCS Average Temperature Program: S-RELAP5 models of the U.S. EPR at part power operating conditions will inherently reflect the applicable conditions from the average temperature control program (including associated SG pressure). The standard treatment of these parameters in S-RELAP5 is applicable to the U.S. EPR. This modeling is considered an acceptable plant-specific application of the approved Reference 5-1 methodology.

5.2.2.1.1.4 Conclusion Regarding Methodology Applicability

Based on the results of the reviews above, it is concluded that the methodology described in Reference 5-1 is applicable to analyzing the moderate overcooling events for the U.S. EPR without modification.

5.2.2.1.2 Main Steam System Piping Failures

The Reference 5-1 methodology breaks down this event into two phases; the pre-scrum MSLB and the post-scrum MSLB. As a result, the discussion below is broken into the same two phases.

5.2.2.1.2.1 Pre-Scrum MSLB Event Description

The Main Steam Line Break event, as defined in Section 15.1.5 of the U.S. Nuclear Regulatory Commission's Standard Review Plan (SRP) (Reference 5-2), is initiated by a postulated break in a main steam line. Break sizes ranging up to a double-ended guillotine break in a main steam line are evaluated in the pre-scrum MSLB analysis. Since the U.S. EPR design does not include reverse flow check valves in the steam lines, steam released through a break will flow to the break from all of the steam generators prior to MSIV closure.

The system responses for the pre-scrum phase of the MSLB event are similar to those for the Increase in Steam Flow event (Section 5.2.2.1.1.1). The resultant RCS cooldown, in conjunction with a negative moderator temperature coefficient (MTC), inserts positive reactivity. If the plant is operating at power, this causes the reactor power to increase.

If the break is large enough, the reactor will trip on a Low Steam Generator Pressure, High Steam Generator Pressure Decrease, Low Pressurizer Pressure, or possibly a High Ex-core Neutron Flux Rate RT signal. Smaller breaks will prolong the cooldown until the reactor trips on an overpower (High Core (Thermal) Power Level, Low DNBR or High LPD) signal or a High Containment Pressure signal (for breaks inside the reactor containment) or until the reactor reaches a new steady-state condition at an elevated power level.

When the reactor and turbine are tripped, isolation of the high-load feedwater lines is initiated. Also, if, as postulated for an at-power loss-of-offsite-power case, offsite power is lost when the turbine is tripped, the reactor coolant pumps and main feedwater pumps begin to coast down at that time. The achievement of a new steady-state condition or reactor trip terminates the pre-scrum phase of the MSLB event.

When the Low Steam Generator Pressure or High Steam Generator Pressure Decrease setpoint is reached (either in connection with the reactor trip or at a later time during the transient), closure of the MSIVs is initiated. This isolates the three unaffected steam generators from the break, but steam release through the break and the resultant RCS cooldown (via the affected steam generator and its RCS loop) continue.

The increase in reactor power during the pre-scrum phase of an MSLB event can challenge the MDNBR and FCM SAFDL acceptance criteria. The focus of the pre-scrum analysis is to determine the degree of any resulting fuel damage for input to the radiological evaluation of the MSLB event. From the standpoint of the challenge to the SAFDLs during the pre-scrum portion of the event, the event is over a few seconds after RT, i.e., once the control rods have inserted and core power has been reduced (evaluation of possible fuel failure during a post-scrum return to power is a focus of the post-scrum MSLB evaluation, addressed in Section 5.2.2.1.2.5).

The pre-scrum challenge to SAFDLs for a typical currently operating conventional PWR is exacerbated by the effects of ex-core neutron power indication decalibration and harsh containment conditions. Ex-core power decalibration is caused by reactor vessel downcomer fluid density changes which result in power-range ex-core detector shadowing during heatup or cooldown transients. The nuclear power level indicated by the ex-core detectors is lower than the actual reactor power level when the coolant entering the reactor vessel is cooler than the normal full-power temperature (and higher when the inlet coolant is warmer than the normal full-power temperature). This effect is taken into account in the modeling of any ex-core power-dependent reactor trips credited in the pre-scrum MSLB analysis. The design of the U.S. EPR includes the following RT functions and trip function inputs which would be impacted by ex-core power decalibration:

- High neutron flux rate of change
- High neutron flux (intermediate range), applicable only for initial power level < 10%
- Insertion limit power level input to the Low DNBR and High LPD RTs

The High Core Power Level RT is based on a thermal power measurement not affected by decalibration. The Low DNBR and High LPD RTs are based on local in-core flux measurements by SPNDs which are not affected directly by downcomer water density but may be mildly decalibrated by the effect on detector response of reductions in local core fluid temperature and increased fluid density and boron concentration. These effects are considered in the determination of the required trip thresholds.

Harsh containment conditions can be caused by the release of steam within the reactor containment if the break is postulated to occur within the containment building. Under such conditions, only those trips which have been qualified for harsh environments may be credited (unless the trip action can be shown to be accomplished prior to the achievement of harsh conditions) and increased uncertainties are included in all affected environmentally qualified trip setpoints.

5.2.2.1.2.2 *Pre-Scram MSLB Event Specific Phenomena*

Table 5-2 illustrates the phenomena associated with each of the Chapter 15 non-LOCA event categories. Based on the expected response of the U.S. EPR, as described above, the key phenomena associated with the pre-scram MSLB event are discussed below. An evaluation of the ability of the Reference 5-1 methodology to appropriately treat the phenomena is also included in the discussion.

- Fuel Rod heat transfer: The U.S. EPR is expected to use fuel assembly and fuel rod designs essentially identical except for length to current PWR fuel. Therefore, the standard treatment of this phenomenon in S-RELAP5 is applicable to the U.S. EPR. The Reference 5-1 methodology is suitable for analyzing U.S. EPR fuel rod heat transfer phenomena during the pre-scram period of MSLB events.

- Kinetics feedback, Reactivity Control: The core designs for the U.S. EPR are expected to be similar except for length (active fuel height) and reflector composition to current PWR core designs, with comparable fuel enrichments and RCS boron concentrations. Similarly, the control element design used in the U.S. EPR is essentially identical to current PWR designs (multi-fingered steel clad Ag-In-Cd absorber control elements stepwise inserted/withdrawn from the top of the fuel assembly, released upon RT). The standard treatment of this phenomenon in S-RELAP5 is applicable to the U.S. EPR. The Reference 5-1 methodology is suitable for analyzing U.S. EPR kinetics feedback and reactivity control phenomena during the pre-scam period of MSLB events.
- Primary system heat and mass transfer: During these events, the thermal-hydraulic conditions within the U.S. EPR RCS loops remain essentially similar to those at normal operating conditions (i.e., forced circulation of subcooled liquid), as in current PWR designs. The standard treatment of this phenomenon in S-RELAP5 is applicable to the U.S. EPR. The Reference 5-1 methodology is suitable for analyzing U.S. EPR primary system heat and mass transfer phenomena during the pre-scam period of MSLB events.
- Pressurizer phenomena (vertical fluid thermal stratification, wall condensation, spray (subcooled droplet interaction with steam), interfacial heat and mass transfer, and convective heat transfer to walls):

The only significant difference between the U.S. EPR pressurizer design and current PWR pressurizer designs is the increased volume of steam and liquid. This has no effect on the ability of S-RELAP5 to simulate the expected pressurizer phenomena listed above. The standard treatment of this phenomenon in S-RELAP5 is applicable to the U.S. EPR. The Reference 5-1 methodology is suitable for analyzing U.S. EPR pressurizer phenomena during the pre-scam period of MSLB events.

- SG primary/secondary heat transfer (U-tube SG phenomena, primary side single phase convective heat transfer, tube wall heat conduction, secondary side single and two-phase heat transfer pre- and post-CHF, feedwater injection, recirculation, carryover, steam separation, thermal stratification in the downcomer, level indication and control):

The only significant differences between the U.S. EPR U-tube SG design and current PWR U-tube SG designs are the increased size/volume of the unit and the incorporation of an axial economizer with a split downcomer and lower tube bundle region. The difference in size of the unit has no effect on the ability of S-RELAP5 to simulate the related hydrodynamic and thermodynamic phenomena.

The fluid flow and heat transfer phenomena within the axial economizer region (single and two-phase fluid flow, convection and nucleate boiling heat transfer) are similar to those in other regions of current PWR U-tube SG designs modeled using the Reference 5-1 methodology. The MSLB SG model outlined in Reference 5-1 (a single SG boiler node with “steam-only” connecting junction to the steam dome) is expected to remain a conservative approach for calculating SG heat removal for the U.S. EPR SG since it forces all energy to be removed by conversion of the SG liquid inventory to steam, with no liquid release or carryover. Therefore, the Reference 5-1 methodology is suitable for analyzing U.S. EPR SG primary/secondary heat transfer phenomena during the pre-scrum period of MSLB events.

- Critical flow of steam through the break: The fluid media in the U.S. EPR SG and MSS are the same as those used in current PWR designs. The standard treatment of this phenomenon in S-RELAP5 is applicable to the U.S. EPR. The Reference 5-1 methodology is suitable for analyzing flow through a break in the U.S. EPR steam line during the pre-scrum period of MSLB events.
- Containment Pressurization: As outlined in Reference 5-1, the Pre-Scram MSLB analysis uses a simple containment model in order to simulate the

containment high pressure trip. Sensitivity studies have shown that a single volume S-RELAP5 representation can be used to conservatively underpredict the containment pressure response during the pre-scrum phase of the event for conventional U.S. PWR containment designs. The underprediction of pressure conservatively delays the containment high pressure reactor trip. If the containment high pressure reactor trip is credited a sensitivity analysis will be performed for the U.S. EPR to confirm that this approach is still conservative.

- Primary Coolant Flow coastdown (pump coastdown, pump inertia, cumulative primary system loop flow resistance):

Loss of power to RCPs is expected to be modeled at RT for some pre-scrum MSLB event scenarios. The U.S. EPR RCP and RCS loop hydraulic designs do not differ appreciably from current PWR designs, so the design of the U.S. EPR has no effect on the ability of S-RELAP5 to simulate the related phenomena. The Reference 5-1 methodology is suitable for analyzing U.S. EPR RCP flow coastdown during the pre-scrum period of MSLB events.

Based on these considerations, it can be seen that the Reference 5-1 methodology is suitable for simulating the various phenomena that occur during this event for the U.S. EPR.

5.2.2.1.2.3 Disposition of Pre-Scrum MSLB Event Specific U.S. EPR Design Differences

U.S. EPR design differences—relative to conventional U.S. PWR designs—that could potentially impact the applicability of the methodology to analyzing this event for the U.S. EPR are listed below, along with disposition arguments that justify the applicability:

Component Design Differences:

- Larger RCS Component Volumes: The S-RELAP5 model of the U.S. EPR will inherently reflect the effect of increased coolant mass, stored energy, and coolant heat capacity. Ratios of coolant volume to nominal NSSS power level and pressurizer steam volume to total RCS volume show that the dynamics of

thermal-hydraulic transients for the U.S. EPR should be similar to those of current PWRs. The standard treatment of this phenomenon in S-RELAP5 is applicable to the U.S. EPR. The Reference 5-1 methodology is suitable for modeling U.S. EPR RCS component volumes.

- Larger RCS Coolant Flow Rate & Component Flow Areas: The S-RELAP5 model of the U.S. EPR will inherently reflect these parameters. The RCS flow rate of the U.S. EPR is comparable to that of other PWRs on a per MWt basis. Similarly, the ratios of RV and RCS loop flow rates to associated component flow areas result in comparable coolant flow velocities between current PWR models and the U.S. EPR. The standard treatment of this phenomenon in S-RELAP5 is applicable to the U.S. EPR. The Reference 5-1 methodology is suitable for modeling U.S. EPR RCS coolant flow and component flow areas.
- U-tube SG with Axial Economizer: The MSLB SG model nodalization outlined in Reference 5-1 (a single SG boiler node with “steam-only” connecting junction to the steam dome) is expected to remain a conservative approach for calculating SG heat removal for the U.S. EPR SG since it forces all energy to be removed by conversion of the SG liquid inventory to steam, with no liquid release or carryover. The Reference 5-1 methodology is suitable for modeling the U.S. EPR SG heat transfer during a MSLB event.
- Digital I&C Systems: The functionality of the U.S. EPR -specific algorithms for the systems credited in the analyses of these events may be modeled using standard S-RELAP5 control components. Modeling of specific plant design differences is allowed by the Reference 5-1 methodology (page 3-1, Reference 5-1) and is considered an acceptable plant-specific application of the currently approved methodology. The Reference 5-1 methodology is suitable for modeling the U.S. EPR I&C system functions.
- Low DNB Reactor Trip: If necessary, the functionality of this reactor trip function will be considered in a de-coupled manner using thermal-hydraulic inputs derived from the S-RELAP5 transient response to determine the timing

of the reactor trip. The reactivity addition from the tripped rods may be modeled using standard S-RELAP5 trip and control components. Modeling of specific plant design differences is allowed by the Reference 5-1 methodology (page 3-1, Reference 5-1) and is considered an acceptable plant-specific application of the currently approved methodology. The Reference 5-1 methodology is suitable for modeling the effects of the U.S. EPR Low DNBR RT.

- High Linear Power Density Reactor Trip: If necessary, the functionality of this reactor trip function will be considered in a de-coupled manner using thermal-hydraulic inputs derived from the S-RELAP5 transient response to determine the timing of the reactor trip. The reactivity addition from the tripped rods may be modeled using standard S-RELAP5 trip and control components. Modeling of specific plant design differences is allowed by the Reference 5-1 methodology (page 3-1, Reference 5-1) and is considered an acceptable plant-specific application of the currently approved methodology. The Reference 5-1 methodology is suitable for modeling the effects of the U.S. EPR High LPD RT.
- Partial Trip Capability: The effects of this non-safety-grade U.S. EPR feature would only be modeled if it were to produce an adverse impact on the analysis. This is not expected to be the case, unless the resulting core power distributions are determined to be possibly more limiting than those which result assuming it does not function. Therefore, it is assumed that the PT does not have an adverse impact on the transient and need not be considered in the analysis.

If it is determined to be otherwise, the effects of the PT function on the thermal-hydraulic transient response may be represented using standard S-RELAP5 control and reactivity components. Modeling of specific plant design differences is allowed by the Reference 5-1 methodology (page 3-1, Reference 5-1) and is considered an acceptable plant-specific application of the currently approved methodology. The Reference 5-1 methodology is suitable for modeling the effects of the U.S. EPR partial trip function (if needed).

Differences in Operating Conditions:

- Higher RCS Operating Temperature at Full Load: The S-RELAP5 model of the U.S. EPR will inherently reflect this parameter, as allowed by the Reference 5-1 methodology (page 3-1, Reference 5-1). The standard treatment of this parameter in S-RELAP5 is applicable to the U.S. EPR. This modeling is considered an acceptable plant-specific application of the approved Reference 5-1 methodology.
- Higher SG Operating Pressure: The S-RELAP5 model of the U.S. EPR will inherently reflect this parameter, as allowed by the Reference 5-1 methodology (page 3-1, Reference 5-1). The standard treatment of this parameter in S-RELAP5 is applicable to the U.S. EPR. This modeling is considered an acceptable plant-specific application of the approved Reference 5-1 methodology.
- Part Power RCS Average Temperature Program: S-RELAP5 models of the U.S. EPR at part power operating conditions will inherently reflect the applicable conditions from the average temperature control program (including associated SG pressure). The standard treatment of these parameters in S-RELAP5 is applicable to the U.S. EPR. This modeling is considered an acceptable plant-specific application of the approved Reference 5-1 methodology.

5.2.2.1.2.4 Conclusion Regarding Pre-Scram MSLB Methodology Applicability

Based on the results of the reviews above, it is concluded that the methodology described in Reference 5-1 is applicable to analyzing the pre-scrum MSLB event for the U.S. EPR without modification.

5.2.2.1.2.5 Post-Scram MSLB Event Description

The MSLB event consists of a postulated break in a main steam line. Break sizes ranging up to a double-ended guillotine break in a main steam line are evaluated in the post-scrum MSLB analysis. Since the U.S. EPR design does not include reverse flow

check valves in the steam lines, steam released through a break will flow to the break from all of the steam generators prior to MSIV closure. For the post-scrum MSLB the potential exists for a return to critical if the continued cooldown is sufficient to erode the shutdown margin attributed to inserted control rods.

The system responses for the pre-scrum phase of the MSLB event were discussed in Section 5.2.2.1.2.1. Following reactor trip (the post-scrum phase), blowdown through the break and cooldown of the RCS continue. With a strongly negative MTC, positive reactivity is inserted and the potential for a return to critical is possible. If a return to power occurs the potential exists to challenge SAFDLs, particularly, if a control rod is assumed stuck out of the core. A stuck control rod results in high local peaking once the reactor returns to power. The post-scrum response of the MSLB is further described below.

When the Low Steam Generator Pressure or High Steam Generator Pressure Decrease setpoint is reached (either in connection with the reactor trip or at a later time during the transient), closure of the MSIVs is initiated. If the break is located upstream of an MSIV, the effect of the MSIV closure signal is to isolate three out of the four steam generators from the break.

Steam release through the break and the resultant RCS cooldown (via the affected steam generator¹ and its RCS loop) continue. The ongoing insertions of positive moderator and Doppler reactivity (both of which are due to the RCS cooldown) continue to erode the shutdown margin. When the Low-Low Steam Generator Pressure or High-High Steam Generator Pressure Decrease setpoint is subsequently reached, isolation of the low-load feedwater line for the affected steam generator is initiated.

When the Low-Low Steam Generator Level setpoint is reached in the affected steam generator, emergency feedwater to that steam generator is actuated. This prolongs the

¹ The steam generator that continues to blow down through the break after the MSIV closure signal has been issued is termed the affected steam generator.

release of steam through the break, the RCS cooldown, and the associated erosion of the shutdown margin.

If the shutdown margin is eroded sufficiently for the reactor to return to power—in conjunction with augmented radial power peaking near the stuck-out scram RCCA—fuel design limits (DNB and/or fuel centerline melt) may be challenged. If fuel design limits are exceeded the fuel is assumed to fail. The resulting fuel failure fractions are used to predict off-site dose consequences.

From the standpoint of challenge to the fuel design limits, the event is over when an operator takes control and terminates emergency feedwater delivery to the affected steam generator, resulting in a sustained period of RCS reheat and reactor shutdown margin recovery.

5.2.2.1.2.6 Post-Scram MSLB Event Specific Phenomena

Table 5-2 illustrates the phenomena associated with each of the Chapter 15 non-LOCA event categories. Based on the expected response of the U.S. EPR, as described above, the key phenomena associated with the post-scram MSLB event are discussed below. An evaluation of the ability of the Reference 5-1 methodology to appropriately treat the phenomena is also included in the discussion.

- Critical steam flows from steam generator(s) to break: The U.S. EPR's normal-operation steam generator fluid conditions and steam outlet flow restrictor throat areas are similar to those of conventional U.S. PWR designs. Therefore, the methodology is suitable for simulating critical flows from the steam generator(s) to the break.
- Steam generator depressurizations and inventory depletions: The U.S. EPR's steam generator secondary-side operating conditions are similar to those of conventional U.S. PWR designs. Also, except for the axial economizer that occupies a 180-degree sector of the downcomer and the lower boiler region, the U.S. EPR's steam generator secondary-side design is similar to that of conventional U.S. PWR designs. Since the axial economizer has no significant

effect on secondary-side pressure and inventory changes, the methodology is suitable for simulating steam generator depressurizations and inventory depletions.

- Asymmetric RCS cooldowns: The U.S. EPR's RCS loops arrangement and operating conditions are similar to those of conventional U.S. 4-loop PWR designs. Therefore, the methodology is suitable for simulating asymmetric RCS cooldowns.
- Primary-to-secondary heat transfer: The U.S. EPR's primary and secondary coolant system operating conditions are similar to those of conventional U.S. PWR designs. Also, except for the axial economizer, the U.S. EPR's steam generator design is similar to that of conventional U.S. PWR designs. Since the axial economizer results in no change in the heat transfer regime, the methodology is suitable for simulating primary-to-secondary heat transfer.
- Steam generator tube pressure drops: The U.S. EPR's RCS operating conditions and steam generator tube design are similar to those of conventional U.S. PWR designs. Therefore, the methodology is suitable for simulating the steam generator tube primary-side pressure drops.
- Reactor coolant pump coastdowns and RCS natural convection flows (for reactor coolant pump trip transients): The U.S. EPR's RCS loop arrangements, elevations, and operating conditions are similar to those of conventional U.S. PWR designs. Furthermore, except for having a slower coastdown, the U.S. EPR's reactor coolant pump design is similar to that of conventional PWRs. Since the slower pump coastdown affects the relative timing but not the fundamental phenomena of the transient, the methodology is suitable for simulating reactor coolant pump coastdowns and RCS natural convection flows (for transient cases during which the reactor coolant pumps are tripped).
- Core heat generation before and after reactor trip: The U.S. EPR's fuel and core designs are similar to those of conventional U.S. PWR designs.

Therefore, the methodology is suitable for simulating heat generation in the U.S. EPR core.

- Moderator, Doppler, scram, and boron reactivity feedbacks: The U.S. EPR's reactivity coefficients and RCCA design/operation are similar to those of conventional U.S. PWR designs. Furthermore, the U.S. EPR's pumped safety injection system boron concentrations are similar to those of conventional PWRs. Therefore, the methodology is suitable for simulating the U.S. EPR's moderator, Doppler, scram, and boron reactivity feedbacks.
- Reactor coolant contractions and expansions: As mentioned above, the U.S. EPR's RCS operating conditions are similar to those of conventional U.S. PWR designs. Furthermore, except for having a larger volume, the U.S. EPR's RCS design is similar to that of conventional U.S. 4-loop PWRs. Since the larger volume affects the relative magnitudes of contractions and expansions but not the fundamental phenomena, the methodology is suitable for simulating reactor coolant contractions and expansions.
- Pressurizer out-surges and in-surges: In addition to the information on reactor coolant contractions and expansions mentioned above, it should be noted that—except for having a larger pressurizer volume—the U.S. EPR's pressurizer design and its surge line design are similar to those of conventional U.S. PWRs. Since the larger pressurizer and total RCS volumes affect the magnitudes and durations of pressurizer out-surges and in-surges but not the fundamental phenomena, the methodology is suitable for simulating pressurizer out-surges and in-surges.
- Vertical stratification and flashing of fluids in pressurizer and vessel upper head: The U.S. EPR's pressurizer and vessel upper head operating conditions are similar to those of conventional U.S. PWR designs. Also, except for the larger volumes, the U.S. EPR's pressurizer and vessel upper head designs are similar to those of conventional U.S. PWR designs. Since the larger volumes do not significantly affect vertical stratification and flashing of fluids in those

volumes, the methodology is suitable for simulating pressurizer and vessel upper head fluid vertical stratification and flashing.

- Injection of borated water into RCS cold legs: ECCS fluid is injected into the U.S. EPR's RCS cold legs in a similar fashion to how such is done for conventional U.S. PWR designs. Therefore, the methodology is suitable for simulating injection of borated water into the U.S. EPR's RCS cold legs.
- Critical steam flows through main steam safety relief valves. The U.S. EPR's main steam conditions and main steam safety relief valve internal designs are similar to those of conventional U.S. PWR designs. Therefore, the methodology is suitable for simulating critical steam flows through the main steam safety relief valves.

Based on these considerations, it can be concluded that the Reference 5-1 methodology is suitable for simulating the various phenomena that occur during the post-scrum MSLB event for the U.S. EPR.

5.2.2.1.2.7 Disposition of Post-Scram MSLB Event Specific U.S. EPR Design Differences

U.S. EPR design differences—relative to conventional U.S. PWR designs—that could potentially impact the applicability of the methodology to analyzing this event for the U.S. EPR are listed below, along with disposition arguments that justify the applicability:

- Steam generators with axial economizers: The U.S. EPR steam generator design features an axial economizer which channels the feedwater through the 180° sector of the downcomer and lower boiler regions that corresponds to the cooler, downflow legs of the U-tubes. However, modeling this feature is not warranted for a Main Steam Line Break analysis, in which all of a steam generator's downcomer and boiler regions are lumped together into a single volume and the feedwater is injected into the bottom of that volume.
- Main steam relief trains: The U.S. EPR features safety-grade main steam relief trains with adjustable setpoints that automatically actuate steam generator

partial depressurization on a Safety Injection signal. To be present, this feature is well within the code's control system capabilities and the previously analyzed ranges of thermal-hydraulic conditions. Thus, it is considered an acceptable plant-specific application of the currently approved methodology (as may be seen from page 3-1 of Reference 5-1).

- Emergency Feedwater System: The U.S. EPR features a dedicated Emergency Feedwater System that is not normally used to deliver feedwater at low-power operating conditions but is in other respects very similar to conventional auxiliary feedwater systems. Because of such similarities, modeling the Emergency Feedwater System is considered an acceptable plant-specific application of the currently approved methodology.
- Protection System trip differences: The U.S. EPR includes a safety-grade High Steam Generator Pressure Decrease reactor trip/MSIV closure trip that is not included in conventional Reactor Protection Systems. Furthermore, unlike conventional Reactor Protection Systems, the U.S. EPR's High Core Power reactor trip has only a ΔT power component and lacks an ex-core nuclear instrumentation detector power component. However, modeling these differences is well within S-RELAP5's control system capabilities, and doing so is considered an acceptable plant-specific application of the currently approved methodology.
- Constant vessel average temperature for power levels above 60%: Unlike conventional U.S. PWRs, which operate with vessel average temperatures that increase with power level, the U.S. EPR maintains the vessel average temperature constant for power levels above 60%. Although this makes it necessary to disposition or analyze additional cases beyond the zero-power and full-power cases that are mentioned on page 5-17 of Reference 5-1, this is considered an acceptable application of the currently approved methodology.

5.2.2.1.2.8 Conclusion Regarding Post-Scram MSLB Methodology Applicability

Based on the material presented above, it is concluded that the methodology described in Reference 5-1 is applicable to analyze the post-scrum MSLB event for the U.S. EPR without modification.

5.2.2.2 Decrease in Heat Removal by the Secondary System

Events in this category include:

- Loss of External Load (LOEL)
- Turbine Trip (TT)
- Loss of Condenser Vacuum (LOCV)
- Closure of MSIVs
- Loss of Non-emergency AC Power
- Loss of Normal Feedwater Flow
- Feedwater System Pipe Breaks Inside and Outside Containment

For discussion purposes this category will be broken into three parts. The first involves abrupt changes in steam flow to the turbine and includes the top four items above. The second category involves a loss of secondary heat sink from a loss of AC power or loss of normal feedwater. Feedwater System pipe breaks are discussed separately as a third category.

5.2.2.2.1 LOEL/TT/LOCV/MSIV Closure Events

5.2.2.2.1.1 Event Description

A number of transient events involve an unplanned decrease in heat removal by the secondary system. In the case of the U.S. EPR design, the LOEL and TT events are characterized by a decrease in heat removal by the secondary system caused by the abrupt closure of the turbine stop valves, due to a direct TT or as a result of a fast closure of the turbine control valves due to a LOEL on the generator. The cessation of flow to the turbine results in a mismatch between the primary side power generation

rate and secondary side heat removal rate. The major differences between the two initiating events are a temporary increase in RCP speed and flow, following a LOEL due to the temporary increase in turbo-generator speed following the LOEL; and the rapid closure of the Turbine Stop Valves (TSVs) after a TT versus the closure of the slower Turbine Control Valves (TCVs) following a LOEL.

For both events, the decreased heat removal from the RCS following the TSV or TCV closure causes an eventual increase in moderator temperature. The increase in moderator temperature results in an expansion of the coolant inventory leading to a pressurizer surge and an increase in RCS pressure. The cessation of steam flow to the turbine results in an accumulation of steam in the MSS with continued heat transfer from the RCS to the SG secondary side. This results in an increase in SG and MSS temperature and pressure.

In the U.S. EPR design, reactor power would be quickly reduced by a control grade “partial trip” function which inserts a limited number of control rods in an effort to avoid a RT. The control-grade MSB system would operate to control SG pressure and the control-grade pressurizer spray would operate to control RCS pressure. The non-safety-grade partial trip function, MSB system and pressurizer spray are not credited in the safety analysis for overpressure protection. As a result, in the safety analysis of these events, the MSRTs and/or MSSVs operate to control SG pressure and the safety-grade PSRVs open to control RCS pressure.

Loss of Condenser Vacuum (LOCV) is an independent cause of initiation of a turbine trip. The major additional consequence of losing condenser vacuum is the deactivation of the MSB system to prevent overpressurizing the condenser. Since the MSB system is not credited in the safety analysis, the LOCV event is typically bounded by the TT event.

The MS line from each of the four U.S. EPR SGs contains a MSIV downstream of the MSRT and MSSV branch line tee which isolates flow to the turbine and MSB header when the valve is fully closed. The U.S. EPR MSIVs are pilot operated gate valves with a stroke time around 5 seconds. Closure of all MSIVs may result from a spurious I&C

signal. The closure of all MSIVs results in isolation of steam flow from all SGs, with consequences similar to those described earlier for the LOEL/TT events. One difference for this event arises from the fact that the MSIVs are located upstream of the MSB header. Closure of all 4 MSIVs may result in the occurrence of a TT due to a non safety-grade low MSB header pressure TT signal prior to complete closure of the MSIVs. The valve location also results in a smaller isolated MSS volume than the LOEL/TT events where the MSIVs remain open.

Following the TSV, TCV or MSIV closure, steam pressure and temperature increase significantly as the kinetic energy of flowing steam is changed to pressure and internal energy, and as thermal energy from the RCS continues to be transferred to the steam generators. The higher secondary side temperature causes a decrease in primary-to-secondary heat transfer and RCS temperature begins to increase. The resulting increase in primary pressure, secondary pressure and primary coolant temperature during LOEL, TT and MSIV closure events challenge three safety criteria: the primary side RCS overpressurization limit, the secondary side overpressurization limit, and the MDNBR SAFDL.

It is assumed that the electrical disturbances which initiated the load rejection do not cause a premature reactor trip by affecting RPS sensed equipment or instrumentation (RCP speed, Engineered Safeguards, etc.). The RCS temperature increase continues until a RPS setpoint is reached and a reactor trip occurs. Coolant thermal expansion causes a rapid surge into the pressurizer, increasing pressurizer pressure and level. A reactor trip on High-High Pressurizer Pressure will usually be the "first-out" trip signal, particularly if the operation of pressurizer spray, MSB and partial trip are not credited. The first-out reactor trip signal when pressurizer spray is enabled may be High SG pressure, or Low DNBR (unique U.S. EPR RT functions not typical of current PWR designs).

The main feedwater pumps for the U.S. EPR design are electrically powered. Since LOOP is not postulated until RT, main feedwater operation would continue as normal until that time. All but one (e.g., two of the three Main Feedwater Pumps (MFPs) at HFP) are tripped (non-safety-grade) upon RT with one remaining in operation. The

MFV-HL feedlines also normally isolate (safety-grade) upon RT with the MFV-LL line remaining open. The EFWS would be activated on low SG level to maintain SG levels and the secondary heat sink.

A controlled stable state is reached following the RT, with the plant in a hot shutdown condition with residual heat removed by either forced (no LOOP) or natural (LOOP at RT/TT) circulation of primary coolant from the core to the SGs and secondary side heat removal via the MSRTs and MFV or EFV.

5.2.2.2.1.2 *Event Specific Phenomena*

Table 5-2 illustrates the phenomena associated with each of the Chapter 15 non-LOCA event categories. Based on the expected response of the U.S. EPR, as described above, the key phenomena associated with LOEL/TT/MSIV Closure events are discussed below. An evaluation of the ability of the Reference 5-1 methodology to appropriately treat the phenomena is also included in the discussion.

- Fuel Rod heat transfer: The U.S. EPR is expected to use fuel assembly and fuel rod designs essentially identical except for length to current PWR fuel. Therefore, the standard treatment of this phenomenon in S-RELAP5 is applicable to the U.S. EPR. The Reference 5-1 methodology is suitable for analyzing U.S. EPR fuel rod heat transfer phenomena during LOEL, TT or MSIV closure events.
- Kinetics feedback, Reactivity Control: The core designs for the U.S. EPR are expected to be similar except for length (active fuel height) and reflector composition to current PWR core designs, with comparable fuel enrichments and RCS boron concentrations. Similarly, the control element design used in the U.S. EPR is essentially identical to current PWR designs (multi-fingered steel clad Ag-In-Cd absorber control elements stepwise inserted/withdrawn from the top of the fuel assembly, released upon RT). The standard treatment of this phenomenon in S-RELAP5 is applicable to the U.S. EPR. The Reference 5-1 methodology is suitable for analyzing U.S. EPR kinetics

feedback and reactivity control phenomena during LOEL, TT or MSIV closure events.

- Primary system heat and mass transfer: During these events, the thermal-hydraulic conditions within the U.S. EPR RCS loops remain essentially similar to those at normal operating conditions (i.e. forced circulation of subcooled liquid), as in current PWR designs. The standard treatment of this phenomenon in S-RELAP5 is applicable to the U.S. EPR. The Reference 5-1 methodology is suitable for analyzing U.S. EPR primary system heat and mass transfer phenomena during LOEL, TT or MSIV closure events.
- Pressurizer phenomena (vertical fluid thermal stratification, wall condensation, spray (subcooled droplet interaction with steam), interfacial heat and mass transfer, and convective heat transfer to walls):

The only significant difference between the U.S. EPR pressurizer design and current PWR pressurizer designs is the increased volume of steam and liquid. This has no effect on the ability of S-RELAP5 to simulate the expected pressurizer phenomena listed above. The standard treatment of this phenomenon in S-RELAP5 is applicable to the U.S. EPR. The Reference 5-1 methodology is suitable for analyzing U.S. EPR pressurizer phenomena during LOEL, TT or MSIV closure events.

- Primary Coolant Flow coastdown (pump coastdown, pump inertia, cumulative primary system loop flow resistance):

Loss of power to RCPs is expected to be modeled at RT for the RCS overpressurization and SAFDL margin event scenarios. The U.S. EPR RCP and RCS loop hydraulic designs do not differ appreciably from current PWR designs, so the design of the U.S. EPR has no effect on the ability of S-RELAP5 to simulate the related phenomena. The standard treatment of this phenomenon in S-RELAP5 is applicable to the U.S. EPR. The Reference 5-1 methodology is suitable for analyzing U.S. EPR primary coolant flow

phenomena during LOEL, TT or MSIV closure events where LOOP is considered.

- SG primary/secondary heat transfer (U-tube SG phenomena, primary side single phase convective heat transfer, tube wall heat conduction, secondary side single- and two-phase heat transfer pre- and post-CHF, feedwater injection, recirculation, carryover, steam separation, thermal stratification in the downcomer, level indication and control):

The only significant differences between the U.S. EPR U-tube SG design and current PWR U-tube SG designs are the increased size/volume of the unit and the incorporation of an axial economizer with a split downcomer and lower tube bundle region. The difference in size of the unit has no effect on the ability of S-RELAP5 to simulate the related hydrodynamic and thermodynamic phenomena. The fluid flow and heat transfer phenomena within the axial economizer region (single- and two-phase fluid flow, convection and nucleate boiling heat transfer) are similar to those in other regions of current PWR U-tube SG designs modeled using the Reference 5-1 methodology. Explicit modeling of the axial economizer geometry in the U.S. EPR S-RELAP5 SG model is allowed by the Reference 5-1 methodology (page 3-1, Reference 5-1) and would be considered an acceptable plant-specific application of the currently approved methodology. The Reference 5-1 methodology is suitable for analyzing U.S. EPR SG primary/secondary heat transfer phenomena during LOEL, TT or MSIV closure events.

- Critical flow of steam through primary and secondary relief valves: The fluid media in the U.S. EPR pressurizer, RCS and MS are the same as those used in current PWR designs. The relief valve internal designs are also similar to standard relief valve designs and thus do not introduce any new hydraulic phenomena. The standard treatment of this phenomenon in S-RELAP5 is applicable to the U.S. EPR. The Reference 5-1 methodology is suitable for analyzing U.S. EPR relief valve flow phenomena during LOEL, TT or MSIV closure events.

Based on this review of expected phenomena, no changes are required to the Reference 5-1 methodology for LOEL/TT/MSIV Closure analyses of the U.S. EPR.

5.2.2.2.1.3 Disposition of Event Specific U.S. EPR Design Differences

U.S. EPR design differences (relative to conventional U.S. PWR designs) that could potentially impact the applicability of the methodology to analyzing these events are listed below, along with disposition arguments that justify the applicability:

Component Design Differences:

- Larger RCS Component Volumes: The S-RELAP5 model of the U.S. EPR will inherently reflect the effect of increased coolant mass, stored energy, and coolant heat capacity. Ratios of coolant volume to nominal NSSS power level and pressurizer steam volume to total RCS volume show that the dynamics of thermal-hydraulic transients for the U.S. EPR should be similar to those of current PWRs. The standard treatment of this phenomenon in S-RELAP5 is applicable to the U.S. EPR. The Reference 5-1 methodology is suitable for modeling U.S. EPR RCS component volumes.
- U-tube SG with Axial Economizer: The S-RELAP5 model of the U.S. EPR SG will inherently reflect this design. The model nodalization will be modified as needed to accurately reflect the design and performance of the economizer. Modeling of specific plant design differences is allowed by the Reference 5-1 methodology (page 3-1, Reference 5-1) and is considered an acceptable plant-specific application of the currently approved methodology. The Reference 5-1 methodology is suitable for modeling the U.S. EPR SG design.
- MSRT/Variable MSRT relief capacity: The steam line from each SG has a single MSRT, consisting of a normally open motor-driven angled control valve (MSRV) and an upstream, normally closed, fast-opening angled globe valve (MSRIV) with automatically re-settable setpoints. With appropriate input, the S-RELAP5 model has the capability of simulating the performance and control behavior of these valves. The S-RELAP5 model of the U.S. EPR MSS will inherently reflect the design. Modeling of specific plant design differences is

allowed by the Reference 5-1 methodology (page 3-1, Reference 5-1) and is considered an acceptable plant-specific application of the currently approved methodology. The Reference 5-1 methodology is suitable for modeling the U.S. EPR MSRT design.

- Digital I&C Systems: The functionality of the U.S. EPR-specific algorithms for the systems credited in the analyses of these events may be modeled using standard S-RELAP5 control components. Modeling of specific plant design differences is allowed by the Reference 5-1 methodology (page 3-1, Reference 5-1) and is considered an acceptable plant-specific application of the currently approved methodology. The Reference 5-1 methodology is suitable for modeling the U.S. EPR I&C system functions.
- Low DNB and High LPD Reactor Trips: The Low DNBR and High LPD RT functions utilize in-core based measurements of local core power distributions at several locations in each core quadrant. While modeling of specific plant design differences is allowed by the Reference 5-1 methodology (page 3-1, Reference 5-1) and is considered an acceptable plant-specific application of the currently approved methodology, the determination of the timing of a Low DNBR or High LPD trip is expected to be treated in a “de-coupled” manner, external to S-RELAP5. When it is necessary to credit these RT functions, thermal-hydraulic conditions from the S-RELAP5 run will be used as boundary conditions to the external determination of trip functional response. Except for the possible activation of the reactivity addition from scrambled control rods, the trip functions will not be explicitly simulated in the S-RELAP5 model. This approach results in no new or unexpected phenomena in the S-RELAP5 simulation of the event. The Reference 5-1 methodology is suitable for modeling the effects of an U.S. EPR Low DNBR or High LPD RT.

Differences in Operating Conditions:

- Low Core Average Power Density: The S-RELAP5 model of the U.S. EPR will inherently reflect this parameter. The standard treatment of this parameter in S-RELAP5 is applicable to the U.S. EPR. This modeling is considered an acceptable plant-specific application of the approved Reference 5-1 methodology.
- Higher RCS Operating Temperature at Full Load: The S-RELAP5 model of the U.S. EPR will inherently reflect this parameter, as allowed by the Reference 5-1 methodology (page 3-1, Reference 5-1). The standard treatment of this parameter in S-RELAP5 is applicable to the U.S. EPR. This modeling is considered an acceptable plant-specific application of the approved Reference 5-1 methodology.
- Higher SG Operating Pressure: The S-RELAP5 model of the U.S. EPR will inherently reflect this parameter, as allowed by the Reference 5-1 methodology (page 3-1, Reference 5-1). The standard treatment of this parameter in S-RELAP5 is applicable to the U.S. EPR. This modeling is considered an acceptable plant-specific application of the approved Reference 5-1 methodology.
- Part Power RCS Average Temperature Program: S-RELAP5 models of the U.S. EPR at part power operating conditions will inherently reflect the applicable conditions from the average temperature control program (including associated SG pressure). The standard treatment of these parameters in S-RELAP5 is applicable to the U.S. EPR. This modeling is considered an acceptable plant-specific application of the approved Reference 5-1 methodology.

5.2.2.2.1.4 Conclusion Regarding Methodology Applicability:

Based on the results of the reviews above, it is concluded that the methodology described in Reference 5-1 is applicable to analyzing LOEL, TT and closure of all MSIV events for the U.S. EPR without modification.

5.2.2.2.2 Loss of Non-Emergency AC Power (LNEP) / Loss of Normal Feedwater Flow (LNFF)**5.2.2.2.2.1 Event Description****LNEP**

The LNEP event (SRP 15.2.6) is initiated by a complete loss of either offsite or onsite power, coincident with a turbine trip. The loss of power results in immediate reactor coolant pump coastdown and MFW termination. Consequently, the event causes an overheating on the primary and secondary sides with a risk of DNB, filling of the pressurizer, and overpressure. The loss of power may be caused by a complete loss of the offsite grid or by a loss of the onsite AC distribution system.

The normal response of the U.S. EPR design to a loss of offsite power leading to immediate reactor and turbine trip is as follows:

- The reactor trip signal “low-reactor coolant pump speed in 2 of 4 loops” provides DNB protection for the complete loss of flow due to LOOP. If this signal is not credited, the reactor will trip a short time later on Low SG Level.
- As the steam system pressure rises following the trip, the MSRTs automatically open to the atmosphere. The condenser is not available for steam dump.
- The steam generator MSRTs and MSSVs, limit the secondary system pressure.
- The standby diesel generators start on loss of voltage on the plant emergency busses and begin to supply plant vital loads.
- The emergency feedwater system (EFWS) supplied by the diesel generators begins operation automatically ensuring long-term heat removal of reactor coolant system heat. EFWS is actuated on Low-Low SG level.
- Auxiliary spray provides a limitation of the primary pressure.
- Three PSRVs are available for RCS pressure limitation.

If the reactor is at power when the event occurs, the decaying reactor coolant flow causes an immediate increase in core coolant temperatures. Also, the sudden loss of

subcooled MFW flow, decaying reactor coolant flow, and termination of steam flow to the turbine all cause steam generator heat removal rates to decrease. This, in turn, augments the increase in reactor coolant temperatures. The reactor coolant expands, due to the increase in coolant temperatures, and surges into the pressurizer. The resulting increase in pressure actuates the pressurizer spray system until the short-term heatup phase of the event is terminated by a reactor scram.

The termination of steam flow to the turbine and the continuing primary-to-secondary transfer of the decaying core power cause the steam generator pressures to rapidly increase. When steam generator pressures and coolant temperatures have increased to the appropriate values, the MSRTs (since the steam dump system is inoperable shortly following a LOOP) and/or the MSSVs serve to limit the increase in steam generator pressures.

Steam generator liquid levels, which have been steadily dropping since the termination of MFW flow, soon reach the Low-Low steam generator level EFW actuation setpoint. This initiates the starting sequence for the EFW pumps.

When the delivery of EFW begins, the rate of level decrease in the steam generators receiving the EFW slows. If an EFW pump fails to start, EFW would not be delivered to the affected steam generator.

Eventually, a long-term heatup phase of the event may begin if primary-to-secondary heat transfer degrades as a result of steam generator tube uncover. If EFW is not being delivered to one of the steam generators, that steam generator will completely dry out.

As the decay heat level drops, liquid levels in the fed steam generators stabilize and then begin to rise. Also, reactor coolant temperatures stabilize and then begin to decrease. These conditions mark the end of the challenge to the event acceptance criteria.

Between the LNEP and the LNFF events, the LNEP event will typically be more limiting regarding pressurizer overfill since the RCS will experience natural circulation which will

result in a larger primary-to-secondary temperature difference, a higher primary coolant temperature, and therefore more surge into the pressurizer.

LNFF

A LNFF could result from MFW pump failure or control valve malfunction. The bounding event with respect to flow reduction and reduction in the capability of the secondary side to remove the heat generated in the reactor core is the failure of the pumps. For the U.S. EPR design, tripping of all the MFW pumps and the SSS pump represents the enveloping and most unfavorable case because it is equivalent to the total loss of all operational FW supply.

The normal response of the U.S. EPR plant design to a complete loss of normal feedwater event is as follows:

- Start-up of the standby MFW pump.
- Reactor power reduction by partial trip (PT), dropping of some control rods, to a power level of about 50% on the following signal: “difference between reactor power (and) normalized FW flow.” Parallel to this reactor power reduction, the generator/turbine output is reduced.
- Actuation of the MS bypass.
- Normal PZR spray.

The non-safety grade counter-measures provide for rapid adaptation of the reactor power to the available FW flow after loss of all MFW and start-up of the MFW pump which is in standby.

If the standby pump is assumed not to start, RT is initiated by the same signal as PT after a short delay.

The analysis of the LNFF event takes no credit for the non-safety-grade PT or RT on “difference between reactor power and FW flow.” The sudden loss of subcooled MFW flow, while the plant continues to operate at power, causes steam generator heat removal rates to decrease. This, in turn, causes reactor coolant temperatures to

increase. The reactor coolant expands, surging into the pressurizer. The resulting increase in pressure actuates the pressurizer spray system and may cause the pressurizer PSRVs to open.

Steam generator liquid levels, which have been steadily dropping since the termination of MFW flow, soon reach the low steam generator level reactor trip setpoint. This initiates a reactor scram—which ends the short-term heatup phase of the event.

The automatic turbine trip at reactor scram and the continuing primary-to-secondary transfer of the decaying core power and the reactor coolant pump heat cause steam generator pressures to rapidly increase. When steam generator pressures and coolant temperatures have increased to the appropriate values, the steam dump system, MSRTs and/or the MSSVs serve to limit the increase in steam generator pressures. However, credit is typically not taken for the steam dump system since it is not safety grade.

Steam generator levels continue to drop and soon reach the Low-Low steam generator level EFW actuation setpoint. This initiates the starting sequence for the EFW pumps. When the delivery of EFW begins, the rate of level decrease in the fed steam generators slows.

Eventually, a long-term heatup phase of the event may begin if primary-to-secondary heat transfer degrades as a result of steam generator tube uncover. If EFW is not being delivered to one of the steam generators that steam generator will dry out.

As the decay heat level drops, liquid levels in the fed steam generators stabilize and then begin to rise. Also, reactor coolant temperatures stabilize and then begin to decrease. These conditions mark the end of the challenge to the event acceptance criteria.

Between the LNEP and the LNFF events, the LNFF event will typically be more limiting regarding minimum steam generator inventory due to increased pump heat since the RCPs continue to operate in the LNFF event, but not in the LNEP event.

5.2.2.2.2.2 *Event Specific Phenomena*

Table 5-2 illustrates the phenomena associated with each of the Chapter 15 non-LOCA event categories. Based on the expected response of the U.S. EPR, as described above, the key phenomena associated with LNEP/LNFF events are discussed below. An evaluation of the ability of the Reference 5-1 methodology to appropriately treat the phenomena is also included in the discussion.

- Primary system heat and mass transfer: During these events, the thermal-hydraulic conditions within the U.S. EPR RCS loops remain essentially similar to those at normal operating conditions (i.e., forced circulation of subcooled liquid), as in current PWR designs. The standard treatment of this phenomenon in S-RELAP5 is applicable to the U.S. EPR. The Reference 5-1 methodology is suitable for analyzing U.S. EPR primary system heat and mass transfer phenomena during LNEP/LNFF events.
- Pressurizer phenomena (vertical fluid thermal stratification, wall condensation, spray (subcooled droplet interaction with steam), interfacial heat and mass transfer, and convective heat transfer to walls):

The only significant difference between the U.S. EPR pressurizer design and current PWR pressurizer designs is the increased volume of steam and liquid. This has no effect on the ability of S-RELAP5 to simulate the expected pressurizer phenomena listed above. The standard treatment of this phenomenon in S-RELAP5 is applicable to the U.S. EPR. The Reference 5-1 methodology is suitable for analyzing U.S. EPR pressurizer phenomena during LNEP/LNFF events.

- SG primary/secondary heat transfer (U-tube SG phenomena, primary side single-phase convective heat transfer, tube wall heat conduction, secondary side single- and two-phase heat transfer pre- and post-CHF, feedwater injection, recirculation, carryover, steam separation, thermal stratification in the downcomer, level indication and control):

The only significant differences between the U.S. EPR U-tube SG design and current PWR U-tube SG designs are the increased size/volume of the unit and the incorporation of an axial economizer with a split downcomer and lower tube bundle region.

The difference in size of the unit has no effect on the ability of S-RELAP5 to simulate the related hydrodynamic and thermodynamic phenomena.

The economizer design affects the initial mass of water in the split downcomer and the initial mass and heat transfer in the lower tube bundle region, where the void distribution on the cold side of the split tube bundle will be lower than on the hot side of the bundle. These differences are expected to become negligible after RT when SG heat removal is provided by EFW flow, which is distributed to both sides of the SG.

The fluid flow and heat transfer phenomena within the axial economizer region (single- and two-phase fluid flow, convection and nucleate boiling heat transfer) are similar to those in other regions of current PWR U-tube SG designs modeled using the Reference 5-1 methodology. Explicit modeling of the axial economizer geometry in the U.S. EPR S-RELAP5 SG model is allowed by the Reference 5-1 methodology (page 3-1, Reference 5-1) and is considered an acceptable plant-specific application of the currently approved methodology.

The Reference 5-1 methodology is suitable for analyzing U.S. EPR SG primary/secondary heat transfer phenomena during LNEP/LNFF events.

- Natural Circulation (hydrodynamics and thermodynamics): The RCS loop hydraulic and thermal-hydraulic design of the U.S. EPR does not differ appreciably from current PWR designs. The RV and SGs are situated in the same relative geometrical relationships important for flow induced by gravitational head as in several currently analyzed RCS designs; so the design of the U.S. EPR has no effect on the ability of S-RELAP5 to simulate the related phenomena, which has been demonstrated in Reference 5-1. The

Reference 5-1 methodology is suitable for analyzing U.S. EPR natural circulation flow phenomena during the LNEP/LNFF events.

- Core Heat Generation Before and After Reactor Trip: The U.S. EPR's fuel and core designs are similar to those of conventional U.S. PWR designs. Therefore, the methodology is suitable for simulating heat generation in the U.S. EPR core.

Based on these considerations, it is concluded that the Reference 5-1 methodology is suitable for simulating the various phenomena that occur during these events for the U.S. EPR.

5.2.2.2.2.3 Disposition of Event Specific U.S. EPR Design Differences

U.S. EPR design differences (relative to conventional U.S. PWR designs) that could potentially impact the applicability of the methodology to analyzing these events are listed below, along with disposition arguments that justify the applicability.

Component Design Differences:

- Larger RCS Component Volumes: The S-RELAP5 model of the U.S. EPR will inherently reflect the effect of increased coolant mass, stored energy, and coolant heat capacity. Ratios of coolant volume to nominal NSSS power level and pressurizer steam volume to total RCS volume show that the dynamics of thermal-hydraulic transients for the U.S. EPR should be similar to those of current PWRs. The standard treatment of this phenomenon in S-RELAP5 is applicable to the U.S. EPR. The Reference 5-1 methodology is suitable for modeling U.S. EPR RCS component volumes.
- Higher RCP Heat Addition to RCS: The S-RELAP5 model of the U.S. EPR will inherently reflect this parameter. The standard treatment of this phenomenon in S-RELAP5 is applicable to the U.S. EPR. The Reference 5-1 methodology is suitable for modeling U.S. EPR RCP heat addition to the RCS.
- Heavy Reflector in Place of Core Barrel Thermal Shield Pads: The S-RELAP5 model of the U.S. EPR will inherently reflect this design. Relative to current

conventional PWRs, the U.S. EPR reflector region consists of a larger proportion of metal than of coolant. The effect of the metal in the reflector will be represented by standard heat conductors, and the bypass flow through coolant flow channels present in the reflector metal structure will be simulated by suitable standard flow paths. Modeling of specific plant design differences is allowed by the Reference 5-1 methodology (page 3-1, Reference 5-1) and is considered an acceptable plant-specific application of the currently approved methodology. The Reference 5-1 methodology is suitable for modeling the U.S. EPR heavy reflector.

- U-tube SG with Axial Economizer: The S-RELAP5 model of the U.S. EPR SG will inherently reflect this design. The model nodalization will be modified as needed to accurately reflect the design and performance of the economizer. Modeling of specific plant design differences is allowed by the Reference 5-1 methodology (page 3-1, Reference 5-1) and is considered an acceptable plant-specific application of the currently approved methodology. The Reference 5-1 methodology is suitable for modeling the U.S. EPR SG design.
- Redundancy and Diversity of Safety Systems and Emergency Power Supply: The U.S. EPR design philosophy (typically four physically separated, isolated trains) results in significant additional redundancy and diversity of systems and power supply trains relative to current PWR designs. The additional capability is beneficial and is reflected in individual analysis assumptions for system performance with equipment out-of-service and single failure. These features have no direct impact on the ability to model safety system performance with S-RELAP5. Modeling of specific plant design differences is allowed by the Reference 5-1 methodology (page 3-1, Reference 5-1) and is considered an acceptable plant-specific application of the currently approved methodology. The Reference 5-1 methodology is suitable for modeling the U.S. EPR safety system design.
- Main Steam Relief Train: The steam line from each SG has a single MSRT, consisting of a normally open motor-driven angled control valve (MSRV) and an

upstream, normally closed, fast-opening angled globe valve (MSRIV) with automatically resettable setpoints. With appropriate input, the S-RELAP5 model has the capability of simulating the performance and control behavior of these valves. The S-RELAP5 model of the U.S. EPR MSS will inherently reflect the design. Modeling of specific plant design differences is allowed by the Reference 5-1 methodology (page 3-1, Reference 5-1) and is considered an acceptable plant-specific application of the currently approved methodology. The Reference 5-1 methodology is suitable for modeling the U.S. EPR MSRT design.

Differences in Operating Conditions:

- Higher RCS Operating Temperature at Full Load: The S-RELAP5 model of the U.S. EPR will inherently reflect this parameter, as allowed by the Reference 5-1 methodology (page 3-1, Reference 5-1). The standard treatment of this parameter in S-RELAP5 is applicable to the U.S. EPR. This modeling is considered an acceptable plant-specific application of the approved Reference 5-1 methodology.
- Higher SG Operating Pressure: The S-RELAP5 model of the U.S. EPR will inherently reflect this parameter, as allowed by the Reference 5-1 methodology (page 3-1, Reference 5-1). The standard treatment of this parameter in S-RELAP5 is applicable to the U.S. EPR. This modeling is considered an acceptable plant-specific application of the approved Reference 5-1 methodology.
- Preventive Maintenance During Operation: It is expected, due to the additional redundancy and separation of many U.S. EPR systems, that the Technical Specifications for the U.S. EPR will allow operation with one train of many systems out-of-service for on-line preventive maintenance. This has no direct influence on the Reference 5-1 analysis methodology other than that this fact must be considered in the determination of operable system capacities, with

one train out-of-service for maintenance and another out-of-service due to single failure.

5.2.2.2.2.4 Conclusion Regarding Methodology Applicability

Based on the results of the reviews above, it is concluded that the methodology described in Reference 5-1 is applicable to analyzing the LNEP and LNFF events for the U.S. EPR.

5.2.2.2.3 Feedwater System Piping Failures

5.2.2.2.3.1 Event Description

The Feedwater Line Break event, as defined in Section 15.2.8 of the U.S. Nuclear Regulatory Commission's SRP (Reference 5-2), is initiated by a postulated break in a feedwater line.

Break sizes ranging up to a double-ended guillotine break in the main feedwater line are evaluated. Typically, the larger breaks located near the steam generator, while the plant is operating at full power, present the most challenge to RCS heatup and overpressure limits. The FWLB event establishes the design requirements for the EFW system.

A FWLB located near the steam generator results in termination of main feedwater delivery to all of the steam generators (while they continue to steam at full load) and liquid/steam blowdown from the affected steam generator. This results in significant decreases in secondary-side inventories of both the affected and unaffected steam generators. The reactor trips when the low steam generator level setpoint is reached. EFW flow is also initiated on a low steam generator level signal. Out of four trains, one train is out for preventive maintenance, one train is the single failure, one train is associated with the broken loop, and one train feeds one unaffected steam generator.

Following reactor trip and turbine trip the blowdown of the affected steam generator continues to reduce steam generator pressures and secondary side inventories. When the Low-Low Steam Generator Pressure or High-High Steam Generator Pressure Decrease setpoint is reached (in the affected steam generator), the Main Feedwater System is isolated from the break. This would normally restore main feedwater delivery

to the unaffected steam generators (assuming that no failures in the Main Feedwater System and no LOOP has occurred). However, in the analysis, restoration of non-safety-grade main feedwater delivery to the unaffected steam generators for offsite-power-available cases is not credited.

Ongoing depletion of the affected steam generator's inventory eventually causes it to dry out. This, along with depleted inventories in the unaffected steam generators, contributes to heatup of the RCS.

The unaffected steam generator pressures increase up to the main steam relief train setpoint and then are maintained there as steam is released to remove core decay heat and (for cases with offsite power remaining available) reactor coolant pump heat.

As the reactor coolant heats up, it expands and begins surging into the pressurizer, and its pressure begins to increase. The pressurizer pressure reaches the setpoints of the PSRVs and they open to maintain RCS pressure.

At one hour after reactor trip the operator redirects the affected steam generator's emergency feedwater to one of the unfed unaffected steam generators. This configuration is sufficient to restore the inventories of the fed steam generators and effectively remove heat from the RCS.

5.2.2.2.3.2 *Event Specific Phenomena*

Table 5-2 illustrates the phenomena associated with each of the Chapter 15 non-LOCA event categories. Based on the expected response of the U.S. EPR, as described above, the key phenomena associated with feedwater line break events are discussed below. An evaluation of the ability of the Reference 5-1 methodology to appropriately treat the phenomena is also included in the discussion.

- Critical flows from affected steam generator to break: The U.S. EPR's normal-operation steam generator fluid conditions and minimum cross-section within the main feedwater inlet nozzle and distribution ring are similar to those of conventional U.S. PWR designs. Therefore, the methodology is suitable for simulating critical flows from the affected steam generator to the break.

- Steam generator depressurizations, inventory depletions, and repressurizations: The U.S. EPR's steam generator secondary-side operating conditions are similar to those of conventional U.S. PWR designs. Also, except for the axial economizer that occupies a 180° sector of the downcomer and the lower boiler region, the U.S. EPR's steam generator secondary-side design is similar to that of conventional U.S. PWR designs. Since the steam generator secondary-side pressure and inventory changes during this event are governed by the secondary-side fluid conditions and the choked flow area, the axial economizer has no significant effect on this event. Thus, the methodology is suitable for simulating steam generator depressurizations, inventory depletions, and repressurizations during this event.
- Asymmetric RCS cooldowns and heatups: The U.S. EPR's RCS loops arrangement and operating conditions are similar to those of conventional U.S. 4-loop PWR designs. Therefore, the methodology is suitable for simulating asymmetric RCS cooldowns and heatups.
- Primary-to-secondary heat transfer: The U.S. EPR's primary and secondary coolant system operating conditions are similar to those of conventional U.S. PWR designs. Also, except for the axial economizer, the U.S. EPR's steam generator design is similar to that of conventional U.S. PWR designs. Since the axial economizer results in no change in the heat transfer regime, the methodology is suitable for simulating primary-to-secondary heat transfer.
- Steam generator tube pressure drops: The U.S. EPR's RCS operating conditions and steam generator tube design are similar to those of conventional U.S. PWR designs. Therefore, the methodology is suitable for simulating the steam generator tube primary-side pressure drops.
- Reactor coolant pump coastdowns and RCS natural convection flows (for reactor coolant pump trip transients): The U.S. EPR's RCS loop arrangements, elevations, and operating conditions are similar to those of conventional U.S. PWR designs. Furthermore, except for having a slower coastdown, the U.S.

EPR's reactor coolant pump design is similar to that of conventional PWRs.

Since the slower pump coastdown affects the relative timing but not the fundamental phenomena of the transient, the methodology is suitable for simulating reactor coolant pump coastdowns and RCS natural convection flows (for transient cases during which the reactor coolant pumps are tripped).

- Core heat generation before and after reactor trip: The U.S. EPR's fuel and core designs are similar to those of conventional U.S. PWR designs. Therefore, the methodology is suitable for simulating heat generation in the U.S. EPR core.
- Moderator, Doppler, and scram reactivity feedbacks: The U.S. EPR's reactivity coefficients and RCCA design/operation are similar to those of conventional U.S. PWR designs. Therefore, the methodology is suitable for simulating the U.S. EPR 's moderator, Doppler, and scram reactivity feedbacks.
- Reactor coolant contractions and expansions: As mentioned above, the U.S. EPR's RCS operating conditions are similar to those of conventional U.S. PWR designs. Furthermore, except for having a larger volume, the U.S. EPR's RCS design is similar to that of conventional U.S. 4-loop PWRs. Since the larger volume affects the relative magnitudes of contractions and expansions but not the fundamental phenomena, the methodology is suitable for simulating reactor coolant contractions and expansions.
- Pressurizer out-surges and in-surges: In addition to the information on reactor coolant contractions and expansions mentioned above, it should be noted that—except for having a larger pressurizer volume—the U.S. EPR's pressurizer design and its surge line design are similar to those of conventional U.S. PWRs. Since the larger pressurizer and total RCS volumes affect the magnitudes and durations of pressurizer out-surges and in-surges but not the fundamental phenomena, the methodology is suitable for simulating pressurizer out-surges and in-surges.

- Vertical stratification and flashing of fluid in pressurizer: The U.S. EPR's pressurizer operating conditions are similar to those of conventional U.S. PWR designs. Also, except for the larger volume, the U.S. EPR's pressurizer design is similar to that of conventional U.S. PWR designs. Since the larger volume does not significantly affect vertical stratification and flashing of fluid in the pressurizer, the methodology is suitable for simulating pressurizer fluid vertical stratification and flashing.
- Pressurizer spray: The U.S. EPR's pressurizer operating conditions and spray design are similar to those of conventional U.S. PWR designs. Therefore, the methodology is suitable for simulating pressurizer spray.
- Critical steam flows through main steam safety relief valves: The U.S. EPR's main steam conditions and main steam safety relief valve internal designs are similar to those of conventional U.S. PWR designs. Therefore, the methodology is suitable for simulating critical steam flows through the main steam safety relief valves.

Based on these considerations, it can be seen that the Reference 5-1 methodology is suitable for simulating the various phenomena that occur during the event for the U.S. EPR.

5.2.2.2.3.3 Disposition of Event Specific U.S. EPR Design Differences

U.S. EPR design differences—relative to conventional U.S. PWR designs—that could potentially impact the applicability of the methodology to analyzing this event for the U.S. EPR are listed below, along with disposition arguments that justify the applicability:

- Steam generators with axial economizers: The U.S. EPR steam generator design features an axial economizer which channels the feedwater through the 180° sector of the downcomer and lower boiler regions that corresponds to the cooler, downflow legs of the U-tubes. This design feature is considered an acceptable plant-specific application of the currently approved methodology.

- Main steam relief trains: The U.S. EPR features safety-grade main steam relief trains with fluid-driven and motor-driven valves and with setpoints that are lower than those of its conventional spring-loaded main steam safety valves. This design feature is considered an acceptable plant-specific application of the currently approved methodology.
- Emergency Feedwater System: The U.S. EPR features a dedicated Emergency Feedwater System that is not normally used to deliver feedwater at low-power operating conditions but is in other respects very similar to conventional auxiliary feedwater systems. Because of such similarities, modeling the Emergency Feedwater System is considered an acceptable plant-specific application of the currently approved methodology.
- Protection System trip differences: The U.S. EPR includes a safety-grade High Steam Generator Pressure Decrease reactor trip/MSIV closure trip and a safety-grade Low-Low Steam Generator Level steam generator normal blowdown isolation trip that are not included in conventional Reactor Protection Systems. However, modeling these differences is well within S-RELAP5's control system capabilities, and is considered an acceptable plant-specific application of the currently approved methodology.
- Pressurizer auxiliary spray: Unlike conventional U.S. PWR designs, the U.S. EPR features a dedicated automatically controlled pressurizer auxiliary spray system that uses RCS charging pumps to counteract pressurizer overpressure when the reactor coolant pumps are not operating. However, because of similarities to conventional pressurizer spray systems, modeling this design feature is an acceptable plant-specific application of the currently approved methodology.

5.2.2.2.3.4 Conclusion Regarding Methodology Applicability

Based on the material presented above, it is concluded that the methodology described in Reference 5-1 is applicable to analyzing Feedwater Line Break events for the U.S. EPR without modification.

5.2.2.3 Decrease in Reactor Coolant Flow Rate

Events in this category include:

- Loss of Forced Reactor Coolant Flow
- Reactor Coolant Pump Rotor Seizure
- Reactor Coolant Pump Shaft Break

5.2.2.3.1 Loss of Forced Reactor Coolant Flow**5.2.2.3.1.1 Event Description**

The Loss of Forced Reactor Coolant Flow event, as defined in Sections 15.3.1 and 15.3.2 of the U.S. Nuclear Regulatory Commission's Standard Review Plan (SRP) (Reference 5-2), is characterized by a decrease in forced RCS flow. A decrease in reactor coolant flow (occurring while a plant is at power) results in degradation of core heat transfer, reduction in DNB margin, and a challenge to the DNB SAFDL. The primary concern with this event is the challenge to the DNB SAFDL. The fuel centerline melt SAFDL is not challenged since there is no significant increase in core power for this event. The reduction in primary system flow and associated increase in core coolant temperatures result in a reduction in DNBR margin. The increasing primary system coolant temperatures also result in expansion of the primary coolant volume, causing an in-surge into the pressurizer and an increase in the pressure of the primary system. However, pressure limits are not challenged by this event. The purpose for analyzing this event for the U.S. EPR is to protect the DNB SAFDL.

There may be either a partial or a total loss of RCS flow. A partial loss of coolant flow may be caused by a mechanical or electrical failure in a pump motor, a fault in the power supply to the pump motor, or a pump motor trip caused by such anomalies as over-current or phase imbalance. A complete loss of forced coolant flow may result from the simultaneous loss of electrical power to all pump motors or decay in the frequency of their electrical power supply system.

In general, a reactor trip on a low flow signal or low RCP speed provides protection for the reactor core during these flow decreases. A reactor trip on low flow in the affected loop provides protection for the core for a single pump loss of flow event. The partial trip will not be credited.

The MDNBR is controlled by the interaction of the primary coolant flow decay, the trip signal, the trip signal generation delay time, the scram delay time, and the core power decrease following reactor trip. The power-to-flow ratio initially increases, peaks, and then declines as the challenge to the DNB SAFDL is mitigated by the decline in core power due to the reactor trip.

A complete loss of forced reactor coolant flow may result from a simultaneous fault in the electrical supplies of all reactor coolant pumps due to LOOP or a fast decay of frequency in the external grid. The enveloping case corresponds to a rapid decrease in frequency.

The frequency decay leads to a stronger reduction of RCP speed and coolant flow than in the case of free coastdown resulting from LOOP. If the reactor is at power, the heat flux transferred from the fuel to the coolant is at first nearly unchanged. Thus, DNBR decreases, and this can result in DNB with subsequent fuel or cladding damage if the reactor is not tripped in due time. But reactor (and turbine) trip is initiated promptly by the signal "low-reactor coolant pump speed in 2 of 4 loops" (RCP Speed <91%). Before reactor and turbine trip, the average reactor coolant temperature and consequently PZR water level and primary pressure increase strongly because of a rapid primary flow reduction.

A partial loss of coolant flow can result from a mechanical or electrical failure in a reactor coolant pump or from a fault in the power supply or I&C to the pump or pumps supplied by a reactor coolant pump bus. If the reactor is at power at the time of the event, the immediate effect of loss of coolant flow is an increase in the coolant temperature. This increase could result in DNB with subsequent fuel rod damage if the reactor were not tripped.

The enveloping event coming into question for partial loss of reactor coolant flow is the loss of one RCP and it is classified as a Condition II event (an incident of moderate frequency). The necessary protection for a partial loss of coolant flow event is provided by (assuming no availability of the partial trip) a low reactor coolant flow signal.

After RT due to LOOP, the event will be similar to a Loss of Coolant Flow (LOCF) event. Following RT, a stable plant condition is reached. Normal plant shutdown may then proceed. If offsite power is available after RT and TT, the event remains asymmetric in nature.

5.2.2.3.1.2 *Event Specific Phenomena*

Table 5-2 illustrates the phenomena associated with each of the Chapter 15 non-LOCA event categories. Based on the expected response of the U.S. EPR, as described above, the key phenomena associated with loss of coolant flow events are discussed below. An evaluation of the ability of the Reference 5-1 methodology to appropriately treat the phenomena is also included in the discussion.

- Fuel Rod heat transfer: The U.S. EPR is expected to use fuel assembly and fuel rod designs essentially identical except for length to current PWR fuel. Therefore, the standard treatment of this phenomenon in S-RELAP5 is applicable to the U.S. EPR. The Reference 5-1 methodology is suitable for analyzing U.S. EPR fuel rod heat transfer phenomena during LOCF events.
- Kinetics feedback, Reactivity Control: The core designs for the U.S. EPR are expected to be similar except for length (active fuel height) and reflector composition to current PWR core designs, with comparable fuel enrichments and RCS boron concentrations. Similarly, the control element design used in the U.S. EPR is essentially identical to current PWR designs (multi-fingered steel clad Ag-In-Cd absorber control elements stepwise inserted/withdrawn from the top of the fuel assembly, released upon RT). The standard treatment of this phenomenon in S-RELAP5 is applicable to the U.S. EPR. The Reference 5-1 methodology is suitable for analyzing U.S. EPR kinetics

feedback and reactivity control phenomena during LOCF events for predicting the overall NSSS response.

- Primary Coolant Flow Coastdown (pump coastdown, pump inertia, cumulative primary-system loop flow resistance):

The U.S. EPR RCP and RCS loop hydraulic designs do not differ appreciably from current PWR designs, so the design of the U.S. EPR has no effect on the ability of S-RELAP5 to simulate the related phenomena. The standard treatment of this phenomenon in S-RELAP5 is applicable to the U.S. EPR. The Reference 5-1 methodology is suitable for analyzing U.S. EPR primary coolant flow phenomena during LOCF events.

- Pressurizer Phenomena (vertical fluid thermal stratification, wall condensation, spray (subcooled droplet interaction with steam), interfacial heat and mass transfer, and convective heat transfer to walls):

The only significant difference between the U.S. EPR pressurizer design and current PWR pressurizer designs is the increased volume of steam and liquid. This has no effect on the ability of S-RELAP5 to simulate the expected pressurizer phenomena listed above. The standard treatment of this phenomenon in S-RELAP5 is applicable to the U.S. EPR. The Reference 5-1 methodology is suitable for analyzing U.S. EPR pressurizer phenomena during LOCF events.

Based on this review of expected phenomena, no changes are required to the Reference 5-1 methodology for LOCF analyses of the U.S. EPR. The S-RELAP5 code is able to predict all major phenomena which control the evolution of a LOCF event and as such will adequately predict a LOCF event in the U.S. EPR plant.

5.2.2.3.1.3 Disposition of Event Specific U.S. EPR Design Differences

This section identifies U.S. EPR design differences (relative to conventional U.S. PWR designs) that are relevant to the LOCF analyses. The U.S. EPR design differences that

could potentially impact the applicability of the methodology to analyzing this event are listed below, along with disposition arguments that justify the applicability:

- Constant vessel average temperature for power levels above 60%: Unlike most conventional U.S. PWRs, which operate with vessel average temperatures that increase with power level, the U.S. EPR maintains the vessel average temperature constant for power levels above 60%. This makes it necessary to disposition or analyze additional cases beyond the full-power cases. However, this is considered an acceptable application of the currently approved methodology.

5.2.2.3.1.4 Conclusion regarding methodology Applicability

Based on the material presented above, it is concluded that the methodology described in Reference 5-1 is applicable to analyzing loss of coolant flow events for the U.S. EPR.

5.2.2.3.2 Reactor Coolant Pump Rotor Seizure/Shaft Break

5.2.2.3.2.1 Event Description

The Reactor Coolant Pump Rotor Seizure event as defined in Section 15.3.3 and Reactor Coolant Pump Shaft Break as defined in Section 15.3.4 of the U.S. Nuclear Regulatory Commission's Standard Review Plan (SRP) (Reference 5-2), are characterized by a decrease in forced RCS flow.

Reactor Coolant Pump Rotor Seizure (Locked Rotor-SRP 15.3.3)

The Reactor Coolant Pump Rotor Seizure event is postulated to be caused by the instantaneous seizure of a reactor coolant pump rotor. Flow through the faulted RCS loop rapidly decreases, causing a reactor trip on a Low RCS Loop Flow signal within 1 to 4 seconds and a turbine trip on the reactor trip. Furthermore, a LOOP assumed to occur coincident with the turbine trip, causes the remaining reactor coolant pumps to begin coasting down.

Following the reactor trip, heat stored in the fuel rods continues to be transferred to the reactor coolant causing the coolant to expand. The combination of the relatively high

fuel rod surface heat fluxes, decreasing core flow, and increasing coolant temperatures just after the reactor trip challenges the DNBR safety limit. At the same time, the heat transfer to the secondary side of the steam generators is reduced, first because the reduced flow results in a decreased tube side heat transfer and then because the shell side temperature increases (turbine steam flow is reduced to zero upon reactor/turbine trip). The rapid expansion of the coolant in the reactor core, combined with reduced heat transfer in the steam generators, causes an insurge into the pressurizer and a pressure increase in the reactor coolant system. The in-surge into the pressurizer compresses the steam volume, actuates the automatic spray system which mitigates the overpressurization and prevents the opening of the pressurizer safety valves.

Reactor Coolant Pump Shaft Break

The Reactor Coolant Pump Shaft Break event is initiated by a failure of a reactor coolant pump shaft that results in a free-wheeling impeller. The impact of a pump shaft break is a loss of pumping power from the faulted pump and a reduction of the RCS flow rate.

The Reactor Coolant Pump Shaft Break event is terminated by a Low RCS Loop Flow reactor trip. The plant response to this event is similar to that described above for the Reactor Coolant Pump Rotor Seizure event but occurs in a slower fashion with possibility of backflow.

5.2.2.3.2.2 Event Specific Phenomena

Table 5-2 illustrates the phenomena associated with each of the Chapter 15 non-LOCA event categories. Based on the expected response of the U.S. EPR, as described above, the key phenomena associated with RCP Rotor Seizure/Break events are discussed below. An evaluation of the ability of the Reference 5-1 methodology to appropriately treat the phenomena is also included in the discussion.

- Fuel rod heat transfer: The U.S. EPR is expected to use fuel assembly and fuel rod designs essentially identical except for length to current PWR fuel. Therefore, the standard treatment of this phenomenon in S-RELAP5 is

applicable to the U.S. EPR. The Reference 5-1 methodology is suitable for analyzing U.S. EPR fuel rod heat transfer phenomena during the RCP Rotor Seizure and Shaft Break events.

- Kinetics feedback, Reactivity Control: The core designs for the U.S. EPR are expected to be similar except for length (active fuel height) and reflector composition to current PWR core designs, with comparable fuel enrichments and RCS boron concentrations. Similarly, the control element design used in the U.S. EPR is essentially identical to current PWR designs (multi-fingered steel clad Ag-In-Cd absorber control elements stepwise inserted/withdrawn from the top of the fuel assembly, released upon RT). The standard treatment of this phenomenon in S-RELAP5 is applicable to the U.S. EPR. The Reference 5-1 methodology is suitable for analyzing U.S. EPR kinetics feedback and reactivity control phenomena during the RCP Rotor Seizure and Shaft Break events.

- Primary Coolant Flow Coastdown (pump coastdown, pump inertia, cumulative primary-system loop flow resistance):

The U.S. EPR RCP and RCS loop hydraulic designs do not differ appreciably from current PWR designs, so the design of the U.S. EPR has no effect on the ability of S-RELAP5 to simulate the related phenomena. The standard treatment of this phenomenon in S-RELAP5 is applicable to the U.S. EPR. The Reference 5-1 methodology is suitable for analyzing U.S. EPR primary coolant flow phenomena during RCP Rotor Seizure and Shaft Break events.

- Pressurizer Phenomena (vertical fluid thermal stratification, wall condensation, spray (subcooled droplet interaction with steam), interfacial heat and mass transfer, and convective heat transfer to walls):

The only significant difference between the U.S. EPR pressurizer design and current PWR pressurizer designs is the increased volume of steam and liquid. This has no effect on the ability of S-RELAP5 to simulate the expected pressurizer phenomena listed above. The standard treatment of this

phenomenon in S-RELAP5 is applicable to the U.S. EPR. The Reference 5-1 methodology is suitable for analyzing U.S. EPR pressurizer phenomena during RCP Rotor Seizure and Shaft Break events.

- SG primary/secondary heat transfer (U-tube SG phenomena, primary side single-phase convective heat transfer, tube wall heat conduction, secondary side single- and two-phase heat transfer pre- and post-CHF, feedwater injection, recirculation, carryover, steam separation, thermal stratification in the downcomer, level indication and control):

The only significant differences between the U.S. EPR U-tube SG design and current PWR U-tube SG designs are the increased size/volume of the unit and the incorporation of an axial economizer with a split downcomer and lower tube bundle region. The difference in size of the unit has no effect on the ability of S-RELAP5 to simulate the related hydrodynamic and thermodynamic phenomena. The fluid flow and heat transfer phenomena within the axial economizer region (single- and two-phase fluid flow, convection and nucleate boiling heat transfer) are similar to those in other regions of current PWR U-tube SG designs modeled using the Reference 5-1 methodology. Explicit modeling of the axial economizer geometry in the U.S. EPR S-RELAP5 SG model is allowed by the Reference 5-1 methodology (page 3-1, Reference 5-1) and would be considered an acceptable plant-specific application of the currently approved methodology. The Reference 5-1 methodology is suitable for analyzing U.S. EPR SG primary/secondary heat transfer phenomena during RCP Rotor Seizure and RCP Shaft Break events.

5.2.2.3.2.3 Disposition of Event Specific U.S. EPR Design Differences

This section identifies U.S. EPR design differences (relative to conventional U.S. PWR designs) that are relevant to RCP rotor seizure/shaft break safety analyses. The U.S. EPR design differences that could potentially impact the applicability of the methodology to analyzing these events are listed below, along with disposition arguments that justify the applicability:

- Constant vessel average temperature for power levels above 60%: Unlike most conventional U.S. PWRs, which operate with vessel average temperatures that increase with power level, the U.S. EPR maintains the vessel average temperature constant for power levels above 60%. This may make it necessary to disposition or analyze additional cases other than the full-power cases. However, this is considered an acceptable application of the currently approved methodology.
- Partial Trip Capability: The effects of this non-safety-grade U.S. EPR feature may be modeled using standard S-RELAP5 control and reactivity components if by doing so it would exacerbate the event consequences. Modeling of specific plant design differences is allowed by the Reference 5-1 methodology (page 3-1, Reference 5-1) and is considered an acceptable plant-specific application of the currently approved methodology. The Reference 5-1 methodology is suitable for modeling the effects of the U.S. EPR Partial Trip function. The partial reactor trip will not be used to analyze the RCP Rotor seizure and RCP Shaft Break if it provides a mitigating effect. However, its effect on the results of these events (DNBR and system pressure) will need to be addressed.

5.2.2.3.2.4 Conclusion Regarding Methodology Applicability

Based on the material presented above, it is concluded that the methodology described in Reference 5-1 is applicable to analyzing RCP Rotor Seizure and RCP Shaft Break events for the U.S. EPR.

5.2.2.4 Reactivity and Power Distribution Anomalies

Events in this category include:

- Uncontrolled Bank Withdrawal from a Subcritical or Low Power Condition
- Uncontrolled Bank Withdrawal at Power
- RCCA Misoperation (Rod Drop, Single Rod Withdrawal)
- Spectrum of Rod Ejection Accidents

Each of these is discussed separately below.

5.2.2.4.1 Uncontrolled Bank Withdrawal from a Subcritical or Low Power Condition

5.2.2.4.1.1 Event Description

The Uncontrolled RCCA Bank Withdrawal from a Subcritical/Low-Power Condition event, which is defined in Section 15.4.1 of the U.S. Nuclear Regulatory Commission's SRP (Reference 5-2), is initiated from a subcritical or low-power (e.g., startup-range) condition by a failure in the RCCA position control system or an operator error that results in an uncontrolled withdrawal of a group of RCCA banks.

Withdrawal of the affected RCCAs inserts positive reactivity. If (as will be assumed in the analysis) the event is initiated with the reactor at the lowest power level possible following an extended shutdown, the extremely low neutron population under such a condition delays a power increase as the affected RCCAs are withdrawn until a significant amount of positive reactivity has been inserted. This delay, in conjunction with the high withdrawal rate and combined worth of the affected RCCAs that will be assumed in the analysis, results in a prompt-critical power spike.

The power spike is quickly countered by Doppler reactivity feedback, as the fuel temperatures begin to increase, and is shortly thereafter terminated by reactor trip on a High Positive Neutron Flux Rate, Low Neutron Flux Doubling Time (Intermediate Range), or High Neutron Flux (Intermediate Range) signal. Although the power peaks at a high level during the power spike, the duration is short enough to preclude significant energy deposition.

Due to thermal inertia of the fuel, the fuel temperature and fuel rod heat flux excursions lag behind and are less pronounced than the power spike. The margin to fuel melt during the event is minimized at the high point of the fuel centerline temperature excursion.

The core coolant temperature response, in turn, lags behind and is less pronounced than the fuel temperature and fuel rod heat flux excursions. The margin to DNB is

eroded by the fuel rod heat flux excursion and the core coolant temperature response. Furthermore, if (as will be assumed in the analysis) offsite power is lost when the reactor is tripped, the reactor coolant pumps will begin to coast down, further eroding the margin to DNB for a brief period of time until the scram RCCAs begin to drop into the core.

5.2.2.4.1.2 *Event Specific Phenomena*

Table 5-2 illustrates the phenomena associated with each of the Chapter 15 non-LOCA event categories. Based on the expected response of the U.S. EPR, as described above, the key phenomena associated with RCCA withdrawal from subcritical or low power level are discussed below. An evaluation of the ability of the Reference 5-1 methodology to appropriately treat the phenomena is also included in the discussion.

- Core heat generation: The U.S. EPR's fuel and core designs are similar to those of conventional U.S. PWR designs. Therefore, the methodology is suitable for simulating heat generation in the U.S. EPR core.
- Doppler, moderator, and RCCA withdrawal/insertion reactivity feedbacks: The U.S. EPR's reactivity coefficients and RCCA design/operation are similar to those of conventional U.S. PWR designs. Therefore, the methodology is suitable for simulating the U.S. EPR's Doppler, moderator, and RCCA withdrawal/insertion reactivity feedbacks.
- Fuel-to-cladding gap heat transfer: The operating conditions and mechanical design of the U.S. EPR's fuel are similar to those of conventional U.S. PWR designs. Therefore, the methodology is suitable for simulating the U.S. EPR's fuel-to-cladding gap heat transfer.
- Peak-power fuel pellet centerline temperature responses to power spikes: The operating conditions, power peaking, and mechanical design of the U.S. EPR's fuel are similar to those of conventional U.S. PWR designs. Therefore, the methodology is suitable for simulating the U.S. EPR's peak-power fuel pellet centerline temperature responses to power spikes.

Based on these considerations, it is concluded that the Reference 5-1 methodology is suitable for simulating the various phenomena that occur during a RCCA withdrawal from a subcritical or low power level for the U.S. EPR.

5.2.2.4.1.3 Disposition of Event Specific U.S. EPR Design Differences

There are no U.S. EPR design differences (relative to conventional U.S. PWR designs) that could potentially impact the applicability of the Reference 5-1 methodology for analyzing this event for the U.S. EPR.

5.2.2.4.1.4 Conclusion Regarding Methodology Applicability

Based on the material presented above, it is concluded that the methodology described in Reference 5-1 is applicable to analyzing a RCCA Withdrawal from Subcritical or Low Power Level for the U.S. EPR without modification.

5.2.2.4.2 Uncontrolled Bank Withdrawal at Power

5.2.2.4.2.1 Event Description

The Uncontrolled RCCA Bank Withdrawal at Power event, which is defined in Section 15.4.2 of the U.S. Nuclear Regulatory Commission's SRP (Reference 5-2), is initiated from a power-operation state by a failure in the RCCA position control system or an operator error that results in an uncontrolled withdrawal of a group of RCCA banks.

Withdrawal of the RCCAs causes the reactor power to increase. The rate of the reactor power increase is determined by the withdrawal rate and combined worth of the RCCAs. If the resultant reactor power increase is relatively slow, the fuel rod heat fluxes and core coolant temperatures will closely track the increasing reactor power, and the margin to DNB will be eroded. The pressurizer spray function acts to minimize the pressure increase and provides the minimum margin to DNB. Offsite power is assumed lost at reactor trip resulting in a coastdown of RCPs and a reduction in RCS flow. The Low DNBR and High LPD reactor trips provide protection against exceeding the fuel design limits for these events.

If, on the other hand, the reactor power increase is relatively rapid, the increase in the core coolant temperatures will significantly lag behind the increases in the fuel rod heat fluxes and the reactor power, and the margin to fuel centerline melt will be eroded more than the margin to DNB. Core protection is provided by the reactor trips on High In-core LPD or High Positive Ex-core Neutron Flux Rate signals.

5.2.2.4.2.2 *Event Specific Phenomena*

Table 5-2 illustrates the phenomena associated with each of the Chapter 15 non-LOCA event categories. Based on the expected response of the U.S. EPR, as described above, the key phenomena associated with RCCA Bank Withdrawal at Power event are discussed below. An evaluation of the ability of the Reference 5-1 methodology to appropriately treat the phenomena is also included in the discussion.

- Core heat generation: The U.S. EPR's fuel and core designs are similar to those of conventional U.S. PWR designs. Therefore, the methodology is suitable for simulating heat generation in the U.S. EPR core.
- Moderator, Doppler, and RCCA withdrawal/insertion reactivity feedbacks: The U.S. EPR's reactivity coefficients and RCCA design/operation are similar to those of conventional U.S. PWR designs. Therefore, the methodology is suitable for simulating the U.S. EPR's moderator, Doppler, and RCCA withdrawal/insertion reactivity feedbacks.
- Reactor coolant expansions and contractions: The U.S. EPR's RCS operating conditions are similar to those of conventional U.S. PWR designs. Furthermore, except for having a larger volume, the U.S. EPR's RCS design is similar to that of conventional U.S. 4-loop PWRs. Since the larger volume affects the relative magnitudes of expansions and contractions but not the fundamental phenomena, the methodology is suitable for simulating reactor coolant expansions and contractions.
- Pressurizer in-surges and out-surges: In addition to the information on reactor coolant expansions and contractions mentioned above, it should be noted

that—except for having a larger pressurizer volume—the U.S. EPR's pressurizer design and its surge line design are similar to those of conventional U.S. PWRs. Since the larger pressurizer and total RCS volumes affect the magnitudes and durations of pressurizer in-surges and out-surges but not the fundamental phenomena, the methodology is suitable for simulating pressurizer in-surges and out-surges.

- Vertical stratification and flashing of fluid in pressurizer: The U.S. EPR's pressurizer operating conditions are similar to those of conventional U.S. PWR designs. Also, except for the larger volume, the U.S. EPR's pressurizer design is similar to that of conventional U.S. PWR designs. Since the larger volume does not significantly affect vertical stratification and flashing of fluid in the pressurizer, the methodology is suitable for simulating pressurizer fluid vertical stratification and flashing.
- Pressurizer spray: The U.S. EPR's pressurizer operating conditions and spray design are similar to those of conventional U.S. PWR designs. Therefore, the methodology is suitable for simulating pressurizer spray.
- Primary-to-secondary heat transfer: The U.S. EPR 's primary and secondary coolant system operating conditions are similar to those of conventional U.S. PWR designs. Also, except for the axial economizer, the U.S. EPR's steam generator design is similar to that of conventional U.S. PWR designs. Since the axial economizer results in no change in the heat transfer regime, the methodology is suitable for simulating primary-to-secondary heat transfer.

Based on these considerations, it is concluded that the Reference 5-1 methodology is suitable for simulating the various phenomena that occur during the event for the U.S. EPR.

5.2.2.4.2.3 *Disposition of Event Specific U.S. EPR Design Differences*

U.S. EPR design differences—relative to conventional U.S. PWR designs—that could potentially impact the applicability of the methodology to analyzing this event for the U.S. EPR are listed below, along with disposition arguments that justify the applicability:

- Low DNBR reactor trip: The U.S. EPR features a Low DNBR reactor trip that is actuated when the measured in-core LPDs, core inlet temperature, pressurizer pressure, and core flow rate are such that the MDNBR calculated using (1) the DNBR correlation for the limiting fuel design in the core and (2) the measured conditions mentioned above reaches the Low DNBR reactor trip setpoint. This design feature has not previously been modeled in a U.S. licensing analysis. Its application will be addressed in a setpoint methodology topical report (separate from the safety analysis methodology topical report) and falls outside the scope of this document.
- High LPD reactor trip: The U.S. EPR similarly features a High LPD reactor trip that is actuated when the maximum measured in-core LPD reaches the High LPD reactor trip setpoint. This design feature has not previously been modeled in a U.S. licensing analysis. Its application will be addressed in a setpoint methodology topical report (separate from the safety analysis methodology topical report) and falls outside the scope of this document.
- Constant vessel average temperature for power levels above 60%: Unlike conventional U.S. PWRs, which operate with vessel average temperatures that increase with power level, the U.S. EPR maintains the vessel average temperature constant for power levels above 60%. Although this makes it necessary to disposition or analyze additional cases beyond those typically dispositioned or analyzed, doing so is considered an acceptable application of the currently approved methodology.

5.2.2.4.2.4 Conclusion regarding methodology Applicability

Based on the material presented above, it is concluded that the methodology described in Reference 5-1 is applicable to analyzing this event for the U.S. EPR without modification.

5.2.2.4.3 RCCA Misoperation

Events in this category include the dropped control rod/bank and single rod withdrawal. The single rod withdrawal, except for local peaking, is similar to the bank withdrawal discussed in the previous two sections. Therefore, the event discussed below is the dropped control rod/bank event.

5.2.2.4.3.1 Event Description

The Dropped Control Rod / Bank event, which is addressed by Section 15.4.3 of the U.S. Nuclear Regulatory Commission's SRP (Reference 5-2), is initiated by either (1) a failure in the drive mechanism of a single RCCA or in its power supply that causes the affected RCCA to drop into the fully inserted position or (2) a failure in the power supply of a single RCCA bank or sub-bank that causes the affected RCCA bank or sub-bank to drop into the fully inserted position.

Full insertion of the affected RCCA(s) (1) initially decreases the reactor power (commensurate with the worth[s] of the affected RCCA(s)) but (2) increases radial power peaking (commensurate with the worth(s) and location(s) of the affected RCCA(s)). In response to the initial decrease in reactor power, the RCS temperatures also initially decrease.

The non-safety-grade Rod Drop limitation function would normally reduce the turbine/generator load setpoint to match the decreased reactor power level and block automatic withdrawal of control RCCAs that would be commanded in an attempt to maintain the initial reactor power level and average coolant temperature; but these actions will not be credited in the analysis.

In response to a RCCA(s) drop, the turbine control valves automatically open (attempting to maintain the initial turbine/generator load), and the RCSL System commands withdrawal of control RCCAs (attempting to maintain the initial reactor power level and average coolant temperature). These actions cause the reactor power to increase (with possible power overshoot—depending on the dropped RCCA worth, and the overall interaction of the RCSL System with the moderator and Doppler reactivity feedbacks) until a new equilibrium condition with augmented radial power peaking is reached—or until the indicated MDNBR or LPD reaches the Low DNBR or High LPD reactor trip setpoint (respectively) and the reactor is tripped.

5.2.2.4.3.2 *Event Specific Phenomena*

Table 5-2 illustrates the phenomena associated with each of the Chapter 15 non-LOCA event categories. Based on the expected response of the U.S. EPR, as described above, the key phenomena associated with Dropped RCCA/Bank events are discussed below. An evaluation of the ability of the Reference 5-1 methodology to appropriately treat the phenomena is also included in the discussion.

- Core heat generation: The U.S. EPR's fuel and core designs are similar to those of conventional U.S. PWR designs. Therefore, the methodology is suitable for simulating heat generation in the U.S. EPR core.
- Moderator, Doppler, and RCCA withdrawal/insertion reactivity feedbacks: The U.S. EPR's reactivity coefficients and RCCA design/operation are similar to those of conventional U.S. PWR designs. Therefore, the methodology is suitable for simulating the U.S. EPR's moderator, Doppler, and RCCA withdrawal/insertion reactivity feedbacks.
- Reactor coolant contractions and expansions: The U.S. EPR's RCS operating conditions are similar to those of conventional U.S. PWR designs. Furthermore, except for having a larger volume, the U.S. EPR's RCS design is similar to that of conventional U.S. 4-loop PWRs. Since the larger volume affects the relative magnitudes of contractions and expansions but not the

fundamental phenomena, the methodology is suitable for simulating reactor coolant contractions and expansions.

- Pressurizer out-surges and in-surges: In addition to the information on reactor coolant contractions and expansions mentioned above, it should be noted that, except for having a larger pressurizer volume, the U.S. EPR's pressurizer design and its surge line design are similar to those of conventional U.S. PWRs. Since the larger pressurizer and total RCS volumes affect the magnitudes and durations of pressurizer out-surges and in-surges but not the fundamental phenomena, the methodology is suitable for simulating pressurizer out-surges and in-surges.
- Vertical stratification and flashing of fluid in pressurizer: The U.S. EPR's pressurizer operating conditions are similar to those of conventional U.S. PWR designs. Also, except for the larger volume, the U.S. EPR's pressurizer design is similar to that of conventional U.S. PWR designs. Since the larger volume does not significantly affect vertical stratification and flashing of fluid in the pressurizer, the methodology is suitable for simulating pressurizer fluid vertical stratification and flashing.
- Primary-to-secondary heat transfer: The U.S. EPR's primary and secondary coolant system operating conditions are similar to those of conventional U.S. PWR designs. Also, except for the axial economizer, the U.S. EPR's steam generator design is similar to that of conventional U.S. PWR designs. Since the axial economizer results in no change in the heat transfer regime, the methodology is suitable for simulating primary-to-secondary heat transfer.

Based on these considerations, it is concluded that the Reference 5-1 methodology is suitable for simulating the various phenomena that occur during the event for the U.S. EPR.

5.2.2.4.3.3 Disposition of Event Specific U.S. EPR Design Differences

U.S. EPR design differences (relative to conventional U.S. PWR designs) that could potentially impact the applicability of the methodology to analyzing this event are listed below, along with disposition arguments that justify the applicability:

- Low DNBR and High LPD reactor trips: The U.S. EPR features a Low DNBR reactor trip that is actuated when the measured in-core LPDs, core inlet temperature, pressurizer pressure, and core flow rate are such that the second-lowest (or lowest, for certain events) DNBR calculated using (1) the DNBR correlation for the limiting fuel design in the core and (2) the measured conditions mentioned above reaches the Low DNBR reactor trip setpoint. Similarly, the U.S. EPR features a High LPD reactor trip that is actuated when the second-highest measured in-core LPD reaches the High LPD reactor trip setpoint. These design features have not previously been modeled in a U.S. licensing analysis. Their application will be addressed in a setpoint methodology topical report (separate from the safety analysis methodology topical report) and falls outside the scope of this document.

5.2.2.4.3.4 Conclusion Regarding Methodology Applicability

Based on the material presented above, it is concluded that the methodology described in Reference 5-1 is applicable to analyzing the dropped control rod/bank event for the U.S. EPR without modification.

5.2.2.4.4 Spectrum of Rod Ejection Accidents

The current methodology for evaluating these events is being revised. A separate report will be submitted for NRC review and approval.

5.2.2.5 Increase in Reactor Coolant Inventory

Events in this category include:

- Inadvertent Operation of the ECCS at Power

- Chemical and Volume Control System (CVCS) malfunction that Increases Reactor Coolant Inventory

As presented in Section 2 of this report, the U.S. EPR design does not include High Head Safety Injection pumps and the CVCS is not part of the Safety Injection System. Therefore, inadvertent operation of the ECCS at power is a non-event for the U.S. EPR. At normal operating pressure an inadvertent signal to start ECCS will result in the ECCS pumps operating dead headed. No water will be injected to the RCS.

In the case of a CVCS malfunction the plant is designed to normally control pressurizer level by running one of two charging pumps and controlling letdown by adjusting the letdown control valve. If the letdown control valve fails closed, the pressurizer will slowly fill, and the plant will trip on high pressurizer level. This event is similar to an inadvertent ECCS operation at power event for a current PWR and no new phenomena are introduced for the U.S. EPR. The Reference 5-1 methodology is directly applicable for the analysis of this event for the U.S. EPR.

5.2.2.6 Decrease in Reactor Coolant Inventory

Events in this category include:

- Inadvertent Opening of a Pressurizer Pressure Relief Valve
- Steam Generator Tube Rupture

5.2.2.6.1 Inadvertent Opening of a Pressurizer Safety Relief Valve

5.2.2.6.1.1 Event Description

The Inadvertent Opening of a Pressurizer Safety Relief Valve (IOPSRV) (SRP 15.6.1) event is initiated by a spurious opening of a Pressurizer Safety Relief Valve (PSRV) which is normally closed during plant operation, and such permanent PSRV opening represents a LOCA on the hot side of the primary system. In normal power operation the opening or closing demand of the three PSRVs is hydraulic and valve-specific so that a failure can only impact a single PSRV.

The IOPSRV results in a loss of reactor coolant inventory which can not be compensated for by the CVCS (the CVCS is a non-safety system and no credit is taken for CVCS injection since this will improve the outcome of this event.) The loss of primary coolant results in a decrease in primary system pressure whereas the pressurizer level decreases for a short time followed by a level increase due to PSRV outflow and voiding.

A reactor trip occurs on low PZR pressure. The RT signal automatically trips the turbine, and closes the MFW high-load lines. LOOP is assumed coincident with the RT. The MFW system is lost due to LOOP; the Emergency Feedwater System is actuated on low SG level. In the short term the fuel design limits on DNB could be challenged as a result of the decreasing RCS pressure.

A SI signal is actuated on low PZR pressure. It automatically starts the MHSI and LHSI pumps and initiates a partial cooldown of the secondary system. The partial cooldown cools the primary system and lowers the RCS pressure. During the partial cooldown, the RCS pressure decreases sufficiently to allow MHSI injection into the cold legs. The partial cooldown is performed by all SGs via the steam dump to condenser or to the atmosphere, by automatically decreasing the respective relief valve setpoints at the constant cooling rate of 180 °F/h down to a fixed pressure value, low enough to permit the needed MHSI injection and high enough to prevent core recriticality.

5.2.2.6.1.2 Event Specific Phenomena

Table 5-2 illustrates the phenomena associated with each of the Chapter 15 non-LOCA event categories. Based on the expected response of the U.S. EPR, as described above, the key phenomena associated with an inadvertent opening of a safety relief valve are discussed below. An evaluation of the ability of the Reference 5-1 methodology to appropriately treat the phenomena is also included in the discussion.

- Fuel Rod heat transfer: The U.S. EPR is expected to use fuel assembly and fuel rod designs essentially identical except for length to current PWR fuel. Therefore, the standard treatment of this phenomenon in S-RELAP5 is

applicable to the U.S. EPR. The Reference 5-1 methodology is suitable for analyzing U.S. EPR fuel rod heat transfer phenomena during IOPSRV event.

- Kinetics feedback, Reactivity Control: The core designs for the U.S. EPR are expected to be similar except for length (active fuel height) and reflector composition to current PWR core designs, with comparable fuel enrichments and RCS boron concentrations. Similarly, the control element design used in the U.S. EPR is essentially identical to current PWR designs (multi-fingered steel clad Ag-In-Cd absorber control elements stepwise inserted/withdrawn from the top of the fuel assembly, released upon RT). The standard treatment of this phenomenon in S-RELAP5 is applicable to the U.S. EPR. The Reference 5-1 methodology is suitable for analyzing U.S. EPR kinetics feedback and reactivity control phenomena during the IOPSRV event.
- Primary system heat and mass transfer: During these events, the thermal-hydraulic conditions within the U.S. EPR RCS loops remain essentially similar to those at normal operating conditions (i.e., forced circulation of subcooled liquid), as in current PWR designs. The standard treatment of this phenomenon in S-RELAP5 is applicable to the U.S. EPR. The Reference 5-1 methodology is suitable for analyzing U.S. EPR primary system heat and mass transfer phenomena during the IOPSRV event.
- Pressurizer phenomena (vertical fluid thermal stratification, wall condensation, spray (subcooled droplet interaction with steam), interfacial heat and mass transfer, convective heat transfer to walls, loss of inventory through the open PSRV):

The only significant difference between the U.S. EPR pressurizer design and current PWR pressurizer designs is the increased volume of steam and liquid. This has no effect on the ability of S-RELAP5 to simulate the expected pressurizer phenomena listed above. The standard treatment of this phenomenon in S-RELAP5 is applicable to the U.S. EPR. The Reference 5-1

methodology is suitable for analyzing U.S. EPR pressurizer phenomena during the IOPSRV event.

- SG primary/secondary heat transfer (U-tube SG phenomena, primary side single phase convective heat transfer, tube wall heat conduction, secondary side single- and two-phase heat transfer pre- and post-CHF, feedwater injection, recirculation, carryover, steam separation, thermal stratification in the downcomer, level indication and control):

The only significant differences between the U.S. EPR U-tube SG design and current PWR U-tube SG designs are the increased size/volume of the unit and the incorporation of an axial economizer with a split downcomer and lower tube bundle region. The difference in size of the unit has no effect on the ability of S-RELAP5 to simulate the related hydrodynamic and thermodynamic phenomena. The fluid flow and heat transfer phenomena within the axial economizer region (single- and two-phase fluid flow, convection and nucleate boiling heat transfer) are similar to those in other regions of current PWR U-tube SG designs modeled using the Reference 5-1 methodology. Explicit modeling of the axial economizer geometry in the U.S. EPR S-RELAP5 SG model is allowed by the Reference 5-1 methodology (page 3-1, Reference 5-1) and is considered an acceptable plant-specific application of the currently approved methodology. The Reference 5-1 methodology is suitable for analyzing U.S. EPR SG primary/secondary heat transfer phenomena during the IOPSRV event.

- Critical flow through the open PSRV including two-phase flow through a steam safety valve: The fluid media in the U.S. EPR pressurizer, are the same as those used in current PWR designs. The PSRV internal design is similar to standard relief valve designs and, thus, does not introduce any new hydraulic phenomena. The standard treatment of this phenomenon in S-RELAP5 is applicable to the U.S. EPR. The Reference 5-1 methodology is suitable for analyzing U.S. EPR relief valve flow phenomena during an IOPSRV event.

The S-RELAP5 code is approved to predict all these phenomena for Westinghouse and Combustion Engineering PWRs; hence for the U.S. EPR plant, it will adequately predict these phenomena.

5.2.2.6.1.3 Disposition of Event Specific U.S. EPR Design Differences

U.S. EPR design differences—relative to conventional U.S. PWR designs—that could potentially impact the applicability of the methodology to analyze this event for the U.S. EPR are listed below, along with disposition arguments that justify the applicability:

Component Design Differences:

- Larger RCS Component Volumes: The S-RELAP5 model of the U.S. EPR will inherently reflect the effect of increased coolant mass, stored energy, and coolant heat capacity. Ratios of coolant volume to nominal NSSS power level and pressurizer steam volume to total RCS volume show that the dynamics of thermal-hydraulic transients for the U.S. EPR should be similar to those of current PWRs. The standard treatment of this phenomenon in S-RELAP5 is applicable to the U.S. EPR. The Reference 5-1 methodology is suitable for modeling U.S. EPR RCS component volumes.
- Greater Capacity PSRVs: The greater capacity of the opened PSRV, compared to the PORV capacity for U.S. PWRs, coupled with MSRT I actuation, leads to larger and longer primary depressurization. For conventional PWRs the event results in a rapidly decreasing RCS pressure until this pressure reaches a value corresponding to the hot leg saturation pressure. At this time the pressure decrease is slowed considerably. For U.S. EPR, the depressurization continues due to MSRT actuation (first on high secondary pressure and then as a result of partial cooldown on SI). The RCS pressure plateaus at a pressure almost equal to the SG pressure at the end of the partial cooldown. However, this feature does not affect the DNB calculation for this event nor does it require changes to the S-RELAP5 methodology.
- Pilot Operated PSRVs versus Spring Operated PSRVs: The S-RELAP5 model of the U.S. EPR pressurizer will inherently reflect the design. Modeling of

specific plant design differences is allowed by the Reference 5-1 methodology (page 3-1, Reference 5-1) and is considered an acceptable plant-specific application of the currently approved methodology. The Reference 5-1 methodology is suitable for modeling the U.S. EPR PSRV design.

- Digital I&C Systems: The functionality of the U.S. EPR -specific algorithms for the systems credited in the analyses of this event may be modeled using standard S-RELAP5 control components. Modeling of specific plant design differences is allowed by the Reference 5-1 methodology (page 3-1, Reference 5-1) and is considered an acceptable plant-specific application of the currently approved methodology. The Reference 5-1 methodology is suitable for modeling the U.S. EPR I&C system functions.
- Low DNB Reactor Trips: The Low DNBR RT functions utilize in-core based measurements of local core power distributions at several locations in each core quadrant. While modeling of specific plant design differences is allowed by the Reference 5-1 methodology (page 3-1, Reference 5-1) and is considered an acceptable plant-specific application of the currently approved methodology, the determination of the timing of a Low DNBR trip is expected to be treated in a “de-coupled” manner, external to S-RELAP5. When it is necessary to credit these RT functions, thermal-hydraulic conditions from the S-RELAP5 run will be used as boundary conditions to the external determination of trip functional response. Except for the possible activation of the reactivity addition from scrammed control rods, the trip functions will not be explicitly simulated in the S-RELAP5 model. This approach results in no new or unexpected phenomena in the S-RELAP5 simulation of the event. The Reference 5-1 methodology is suitable for modeling the effects of an U.S. EPR Low DNBR RT.

Differences in Operating Conditions:

- Low Core Average Power Density: The S-RELAP5 model of the U.S. EPR will inherently reflect this parameter. The standard treatment of this parameter in S-RELAP5 is applicable to the U.S. EPR. This modeling is considered an

acceptable plant-specific application of the approved Reference 5-1 methodology.

- Higher RCS Operating Temperature at Full Load: The S-RELAP5 model of the U.S. EPR will inherently reflect this parameter, as allowed by the Reference 5-1 methodology (page 3-1, Reference 5-1). The standard treatment of this parameter in S-RELAP5 is applicable to the U.S. EPR. This modeling is considered an acceptable plant-specific application of the approved Reference 5-1 methodology.
- Higher SG Operating Pressure: The S-RELAP5 model of the U.S. EPR will inherently reflect this parameter, as allowed by the Reference 5-1 methodology (page 3-1, Reference 5-1). The standard treatment of this parameter in S-RELAP5 is applicable to the U.S. EPR. This modeling is considered an acceptable plant-specific application of the approved Reference 5-1 methodology.

5.2.2.6.1.4 Conclusion Regarding Methodology Applicability

Based on the material presented above, it is concluded that the methodology described in Reference 5-1 is applicable to analyzing the IOPSRV event for the U.S. EPR.

5.2.2.6.2 Steam Generator Tube Rupture

5.2.2.6.2.1 Event Description

The typical sequence of events in case of a single tube SGTR is as follows:

From Initiation to Leak Cancellation (Short Term)

The SGTR event is initiated by a double-ended break of a single steam generator tube (shortest tube) on the top side of the tube sheet. Coolant from the RCS begins to escape through the break, driven by the pressure differential between the RCS and the SG secondary side, increasing the inventory and pressure in the affected SG.

The SGTR event proceeds differently, depending on the response of the CVCS.

a) With response of the CVCS:

As the break flow begins to depressurize the RCS, the charging pumps activate in order to make-up the lost inventory. For the U.S. EPR, the CVCS system is not safety classified; hence the assumption of the CVCS availability will depend if it creates a more conservative outcome for the transient. For U.S. EPR, the CVCS is able to compensate for one tube rupture break. A reactor trip will not occur unless and until one is initiated by the operator.

If LOOP occurs at the time of reactor trip, the heat removal is performed by means of the MSRTs of the unaffected SGs operating at a lower pressure. At the time of LOOP, the RCPs are lost, together with the main feedwater, the SSS and, the main steam bypass is unavailable.

Some time after tripping the reactor, when the ruptured SG has been identified, the operator will isolate the affected SG on its steam side (by closing the MSIV) and initiate a partial cooldown. At the completion of the cooldown, the charging pumps are throttled to reduce the leak flow. Thereafter, charging flow is restored as necessary to maintain core exit subcooling.

As the primary pressure decreases, the signal to start the SI pumps is reached and the MHSI pumps are ready to inject when the pressure in the primary drops below the MHSI pump shutoff head. The leak is stopped when the pressure in the affected SG reaches the pressure in the primary.

The level in the unaffected SGs drops to the level of EFW actuation and EFW starts injecting.

The control state is reached when the leak is stopped.

b) Without response of the CVCS:

Without the injection from the charging system, the RCS pressure and inventory will continue to decrease resulting in a reactor trip on a low RCS

pressure signal, high SG level in the affected SG, or manual operator action. Following the reactor trip, the turbine will trip and, in the case of LOOP, the reactor coolant pumps will coast down and make-up flow will terminate until emergency diesel generator power is available. As the RCS pressure continues to decrease due to the leak, a low pressurizer pressure signal activates the SI. On SI signal (or manual operator action), the partial cooldown is automatically initiated in all four SGs. The controlled state is reached during the partial cooldown, when MHSI flowrate matches the SGTR leak flow. The MSIVs are not closed at this point in time.

At the end of partial cooldown, primary pressure is given by MHSI shut off head, and a contaminated SGTR direct flow still enters the affected SG, leading to its level increase. At this stage, the SI and SGTR mass flow balance is reached.

On high-high SG level (provided that partial cooldown via all SG's has been performed), the affected SG is automatically isolated on its steam side (closure of its MSIV, the MSIV of the three unaffected SGs remaining open).

In case of manual actuation of partial cooldown, the operator could manually isolate the affected SG (at the latest after end of partial cooldown) without waiting for high-high SG level. Then, the pressure balance between primary side and affected SG is reached and the leak is finally cancelled. This is the end of the short-term phase.

From Control State to Safe Shutdown State

The safe shutdown state is defined as a state where the LHSI is connected in RHR mode and the affected SG is isolated. One out of four LHSI trains operating in RHR mode is sufficient to ensure the heat removal. The sequence of actions to be performed by the operator to reach the safe shutdown state (RHR operation) can proceed in

several directions and is highly dependent on the plant's Emergency Operating Procedures. The sequence of events differs if RCPs are available or not.

a) With the RCPs available:

If the RCPs are available they are restarted sequentially. After the RCPs restart, the plant reaches a stable condition, 20 to 30 minutes later. The MSRTs in the unaffected SGs are opened at a reduced cooldown rate 90 °F/h. When the RHR temperature is reached the cooldown is stopped. The primary cooldown is performed via pressurizer spray or a safety valve. When the desired primary side temperature is reached, the MHSI pumps which kept the primary at ~1406 psia are stopped and the accumulators are disconnected. One PZR safety valve is opened to reduce the primary pressure to RHR level. Following the RCS depressurization, the pressure in the affected SG also drops because of leak backflow to the primary side.

b) Without the RCPs available:

If the RCPs are not available, the affected SG is depressurized via the MSRT such that there is no backflow to the RCS. If the MSRT fails for any reason, the depressurization can also be done via the bypass valve of the MS isolation valve without risk of leak backflow. If the water level in the affected SG is too high, some inventory reduction can be performed by opening the SG blowdown line between the affected SG and an unaffected one before depressurization.

5.2.2.6.2.2 *Event Specific Phenomena*

Table 5-2 illustrates the phenomena associated with each of the Chapter 15 non-LOCA event categories. Based on the expected response of the U.S. EPR, as described above, the key phenomena associated with SGTR events are discussed below. An evaluation of the ability of the Reference 5-1 methodology to appropriately treat the phenomena is also included in the discussion.

- Pressurizer phenomena (vertical fluid thermal stratification, wall condensation, spray (subcooled droplet interaction with steam), interfacial heat and mass transfer, convective heat transfer to walls, loss of inventory through the ruptured steam generator tube):

The only significant difference between the U.S. EPR pressurizer design and current PWR pressurizer designs is the increased volume of steam and liquid. This has no effect on the ability of S-RELAP5 to simulate the expected pressurizer phenomena listed above. The standard treatment of this phenomenon in S-RELAP5 is applicable to the U.S. EPR. The Reference 5-1 methodology is suitable for analyzing U.S. EPR pressurizer phenomena during the SGTR event.

- Vertical stratification and flashing of fluids in pressurizer and vessel upper head: The U.S. EPR's pressurizer and vessel upper head operating conditions are similar to those of conventional U.S. PWR designs. Also, except for the larger volumes, the U.S. EPR's pressurizer and vessel upper head designs are similar to those of conventional U.S. PWR designs. Since the larger volumes do not significantly affect vertical stratification and flashing of fluids in those volumes, the methodology will be suitable for simulating pressurizer and vessel upper head fluid vertical stratification and flashing.
- SG primary/secondary heat transfer and level response (U-tube SG phenomena, primary side single phase convective heat transfer, tube wall heat conduction, secondary side single- and two-phase heat transfer pre- and post-CHF, feedwater injection, recirculation, carryover, steam separation, thermal stratification in the downcomer, level indication and control):

The only significant differences between the U.S. EPR U-tube SG design and current PWR U-tube SG designs are the increased size/volume of the unit and the incorporation of an axial economizer with a split downcomer and lower tube bundle region. The difference in size of the unit has no effect on the ability of S-RELAP5 to simulate the related hydrodynamic and thermodynamic

phenomena. The fluid flow and heat transfer phenomena within the axial economizer region (single- and two-phase fluid flow, convection and nucleate boiling heat transfer) are similar to those in other regions of current PWR U-tube SG designs modeled using the Reference 5-1 methodology. Explicit modeling of the axial economizer geometry in the U.S. EPR S-RELAP5 SG model is allowed by the Reference 5-1 methodology (page 3-1, Reference 5-1) and is considered an acceptable plant-specific application of the currently approved methodology. The Reference 5-1 methodology is suitable for analyzing U.S. EPR SG primary/secondary heat transfer phenomena and level response during the SGTR event.

- Critical flow through the break: The fluid media in the U.S. EPR SG, RCS and MSS are the same as those used in current PWR designs. The standard treatment of this phenomenon in S-RELAP5 is applicable to the U.S. EPR. The Reference 5-1 methodology is suitable for analyzing flow through a break in the U.S. EPR SGTR event.
- Natural Circulation (hydrodynamics and thermodynamics): The RCS loop hydraulic and thermal-hydraulic design of the U.S. EPR does not differ appreciably from current PWR designs. The RV and SG are situated in the same relative geometrical relationships important for flow induced by gravitational head as in several currently analyzed RCS designs. So the design of the U.S. EPR has no effect on the ability of S-RELAP5 to simulate the related phenomena, which has been demonstrated in Reference 5-1. The Reference 5-1 methodology is suitable for analyzing U.S. EPR natural circulation flow phenomena during the SGTR event.
- Core heat generation before and after trip: The U.S. EPR's fuel and core designs are similar to those of conventional U.S. PWR designs. Therefore, the methodology is suitable for simulating heat generation in the U.S. EPR core.

The methodology of Reference 5-1 has the ability to predict the important phenomena which control a SGTR event. In particular S-RELAP5 adequately models the effects of

pressurizer in-surges, out-surges, condensation due to pressurizer spray, expansion and contraction of the reactor coolant, primary to secondary heat transfer, SG pressure and core heat generation and natural circulation. It has models to calculate the flow through the broken tube as well as the MHSI injection flow. The Reference 5-1 methodology is able to predict all major phenomena which control the evolution of a SGTR event in the U.S. EPR plant.

5.2.2.6.2.3 Disposition of Event Specific U.S. EPR Design Differences

U.S. EPR design differences—relative to conventional U.S. PWR designs—that could potentially impact the applicability of the methodology to analyzing this event for the U.S. EPR are listed below, along with disposition arguments that justify the applicability:

Component Design Differences:

- Larger RCS Component Volumes: The S-RELAP5 model of the U.S. EPR will inherently reflect the effect of increased coolant mass, stored energy, and coolant heat capacity without modifications to the code. Ratios of coolant volume to nominal NSSS power level and pressurizer steam volume to total RCS volume show that the dynamics of thermal-hydraulic transients for the U.S. EPR should be similar to those of current PWRs. The ability of S-RELAP5 to model a SGTR event is not affected by the larger RCS component volumes.
- U-tube SG with Axial Economizer: The S-RELAP5 model of the U.S. EPR SG will inherently reflect this design without code modifications. The model will be modified as needed to accurately reflect the design and performance of the economizer. It is expected that the modeling of the economizer will have no effect on the SGTR event; however, the economizer will be modeled.
- Redundancy and Diversity of Safety Systems and Emergency Power Supply: The U.S. EPR design philosophy (typically four physically separated, isolated trains) results in significant additional redundancy and diversity of systems and power supply trains relative to current PWR designs. The additional capability is beneficial and is reflected in individual analysis assumptions for system performance with equipment out-of-service and single-failure. These features

have no direct impact on the ability to model safety system performance with S-RELAP5, so no modifications to models or methods are required to reflect the available performance. The code has the ability to model all the safety systems that mitigate a SGTR event.

- No High Head Safety Injection Pumps: The S-RELAP5 model of the U.S. EPR safety injection systems will inherently reflect this design without code modifications. This feature may be beneficial for a SGTR event.
- Medium Head Safety Injection Pump Head: The S-RELAP5 model of the U.S. EPR safety injection systems will inherently reflect this design without code modifications. The existence of only MHSI will not affect the ability of S-RELAP5 to model the SGTR transient.
- Main Steam Relief Train: The steam line from each SG has a single MSRT, consisting of a normally open motor-driven angled control valve (MSRV) and an upstream, normally closed, fast-opening spring-loaded angled globe valve (MSRIV) with automatically resettable setpoints. With appropriate input, the S-RELAP5 model has the capability of simulating the performance and control behavior of these valves. The S-RELAP5 model of the U.S. EPR MSS will inherently reflect this design without code modifications. The MSRT system is used to mitigate a SGTR event. Its actions are similar to the ADV and MSRV in a Westinghouse Steam Generator. The ability of the MSRT system to change setpoints is unique to the U.S. EPR and can be modeled with the S-RELAP5 control system. The SGTR evolution is similar to a Westinghouse U-tube SG, albeit milder. Since S-RELAP5 can be used to analyze a SGTR event for a Westinghouse plant, the code is capable of modeling a SGTR event for the U.S. EPR without code modifications.
- Pilot Operated versus Spring Operated PSRVs: The S-RELAP5 model of the U.S. EPR pressurizer will inherently reflect this design without code modifications.

Differences in Operating Conditions:

- Higher RCS Operating Temperature at Full Load: The S-RELAP5 model of the U.S. EPR will inherently reflect these parameters without code or significant model modifications. The higher RCS operating temperature may have an effect on the timing of the main events for the SGTR event, however the methodology does not need model changes to reflect this feature.
- Higher SG Operating Pressure: The S-RELAP5 model of the U.S. EPR will inherently reflect these parameters without code or significant model modifications. The effect of higher SG operating pressure is beneficial for the SGTR event since it results in earlier equilibration between primary and secondary, without SG overfill.
- Higher No-Load RCS Temperature: The S-RELAP5 model of the U.S. EPR will inherently reflect these parameters without code or significant model modifications.
- Higher No-Load SG Pressure: The S-RELAP5 model of the U.S. EPR will inherently reflect these parameters without code or significant model modifications. If the SGTR event at HZP needs to be analyzed, higher SG pressure coupled with the increased MSRT setpoint is beneficial for a SGTR event.

5.2.2.6.2.4 Conclusion Regarding Methodology Applicability

Based on the results of the reviews above, it is concluded that the methodology described in Reference 5-1 is applicable to analyze the SGTR event for the U.S. EPR.

5.3 Conclusions

This section has presented the basis for concluding that the S-RELAP5 SRP Chapter 15 Non-LOCA Methodology for Pressurized Water Reactors is directly applicable to the U.S. EPR. In short, this conclusion has been reached based on the following points.

- The design of the U.S. EPR is similar to current CE and Westinghouse PWRs for which the methodology is approved.
- The design differences between the U.S. EPR and current PWRs do not result in the introduction of any new thermal-hydraulic phenomena. U.S. EPR unique features can be accommodated by an acceptable plant specific application of the methodology.
- The expected response of the U.S. EPR to the various classes of non-LOCA events where S-RELAP5 would be applied does not introduce any new thermal-hydraulic phenomena beyond those phenomena considered in the approved S-RELAP5 methodology. Fluid conditions encountered during the expected responses are similar to the conditions encountered in existing plants and, therefore, within the range of applicability of S-RELAP5.

5.4 *References*

- 5-1. “SRP Chapter 15 Non-LOCA Methodology for Pressurized Water Reactors,” EMF-2310(P)(A), Revision 1, June 16, 2004.
- 5-2. *USNRC Standard Review Plan*, NUREG-0800, Revision 2, June 1987.

Table 5-1 Applicable SRP Chapter 15 Events

Event	SRP No.	Plant Condition	Applicable Criteria
15.1 Increase in heat Removal by the Secondary System			
Decrease in Feedwater Temperature	15.1.1	II	1
Increase in Feedwater Flow	15.1.2	II	1,3
Increase in Steam Flow	15.1.3	II	1
Inadvertent Opening of Steam Generator Relief/Safety Valve	15.1.4	II	1
Steam System Piping Failures Inside and Outside Containment	15.1.5	IV	4
15.2 Decrease in heat removal by Secondary System			
Loss of Outside Electrical Load	15.2.1	II	1,2
Turbine Trip (TT)	15.2.2	II	1,2
Loss of Condenser Vacuum	15.2.3	II	1,2
Closure of Main Steam Isolation Valve (MSIV)	15.2.4	II	1,2
Steam Pressure Regulator Failure	15.2.5	II	1,2
Loss of Non-Emergency Power to Station Auxiliaries	15.2.6	II	1,2
Loss of Normal Feedwater	15.2.7	II	1,2,3
Feedwater System Pipe Breaks Inside and Outside Containment	15.2.8	IV	1,2
15.3 Decrease in Reactor Coolant Flow Rate			
Loss of Forced Reactor Coolant Flow	15.3.1	II	1,2
Flow Controller Malfunctions	15.3.2	II	1,2
Reactor Coolant Pump (RCP) Rotor Seizure	15.3.3	IV	2,4
RCP Shaft Break	15.3.4	IV	2,4
15.4 Reactivity and Power Distribution Anomalies			
Uncontrolled Rod Cluster Control Assembly (RCCA) Bank Withdrawal from a Subcritical or Low Power Startup Condition	15.4.1	II	1,2
Uncontrolled RCCA Bank Withdrawal at Power	15.4.2	II	1,2
RCCA Misoperation	15.4.3		
Dropped Rod/Bank	15.4.3.1	II	1
Single Rod Withdrawal	15.4.3.2	III	1
Statically Misaligned RCCA	15.4.3.3	II	1
Startup of an Inactive Loop at an Incorrect Temperature	15.4.4	II	1
Chemical and Volume Control System (CVCS) malfunction that Results in a Decrease of Boron Concentration (Boron Dilution)	15.4.6	II	1,6
Inadvertent Loading and Operation of a Fuel Assembly in an Improper Position (Misloaded Assembly)	15.4.7	III	1

Event	SRP No.	Plant Condition	Applicable Criteria
Spectrum of Rod Ejection Accidents	15.4.8	IV	5
15.5 Increase in Reactor Coolant Inventory			
Inadvertent Operation of the Emergency Core Cooling System (ECCS) that Increases Reactor Coolant Inventory	15.5.1	II	1,2,3
CVCS Malfunction that Increases Reactor Coolant Inventory	15.5.2	II	1,2,3
15.6 Decrease in Reactor Coolant Inventory			
Inadvertent Opening of a pressurizer Pressure Relief/Safety Valve	15.6.1	II	1
Radiological Consequences of the Failure of Small Lines Carrying Primary Coolant Outside Containment	15.6.2	II	4
Radiological Consequences of Steam Generator Tube Rupture	15.6.3	IV	4

Table 5-2. Informal Non-LOCA PIRT with Assessment/Disposition

--	--

Table 5-2. Informal Non-LOCA PIRT with Assessment/Disposition (Cont.)

--	--

Table 5-2. Informal Non-LOCA PIRT with Assessment/Disposition (Cont.)

--	--

Table 5-2. Informal Non-LOCA PIRT with Assessment/Disposition (Cont.)

--	--

Table 5-2. Informal Non-LOCA PIRT with Assessment/Disposition (Cont.)

--	--

Table 5-2. Informal Non-LOCA PIRT with Assessment/Disposition (Cont.)

--	--

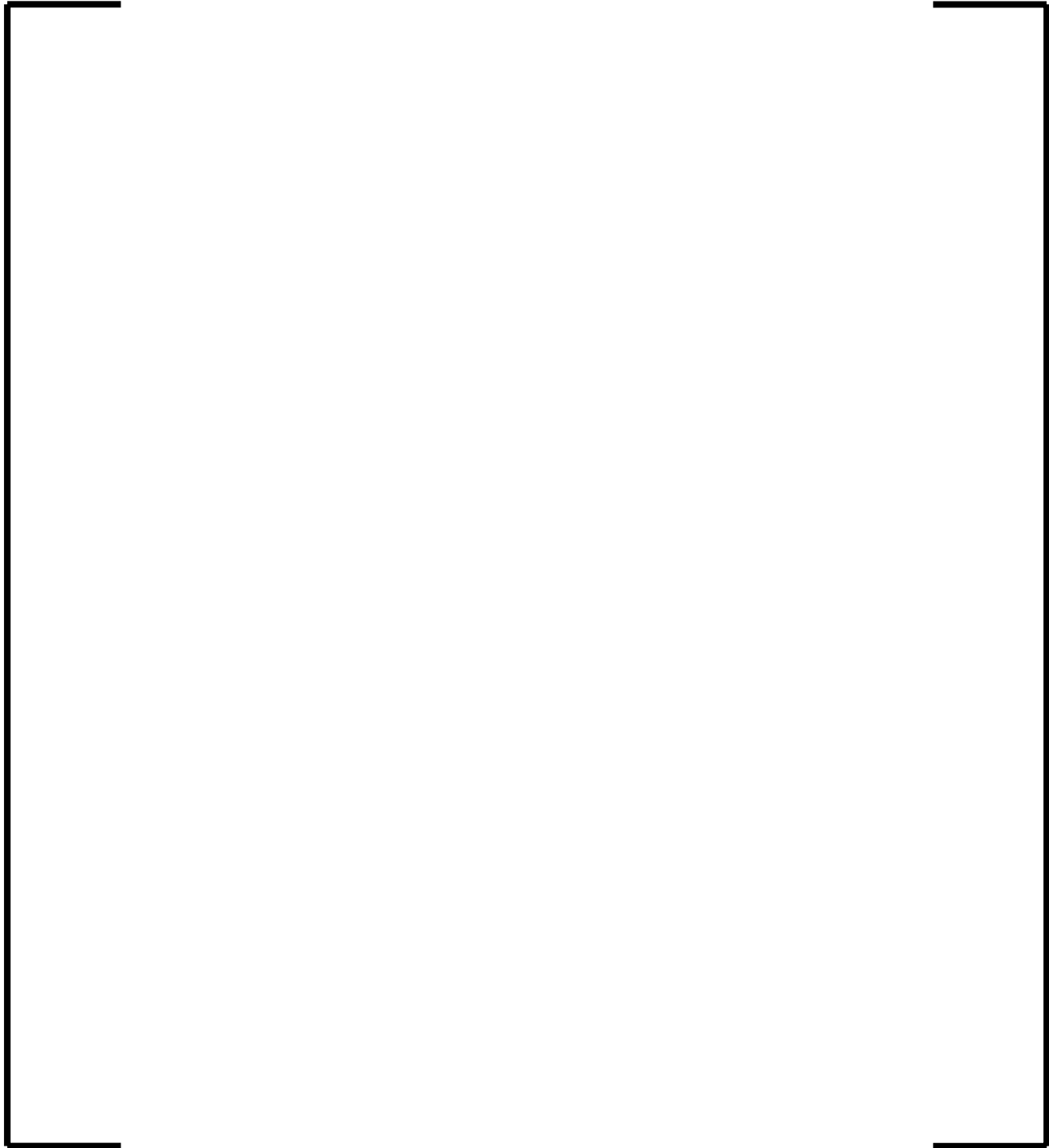


Figure 5-1 U.S. EPR Reactor Coolant System Nodalization

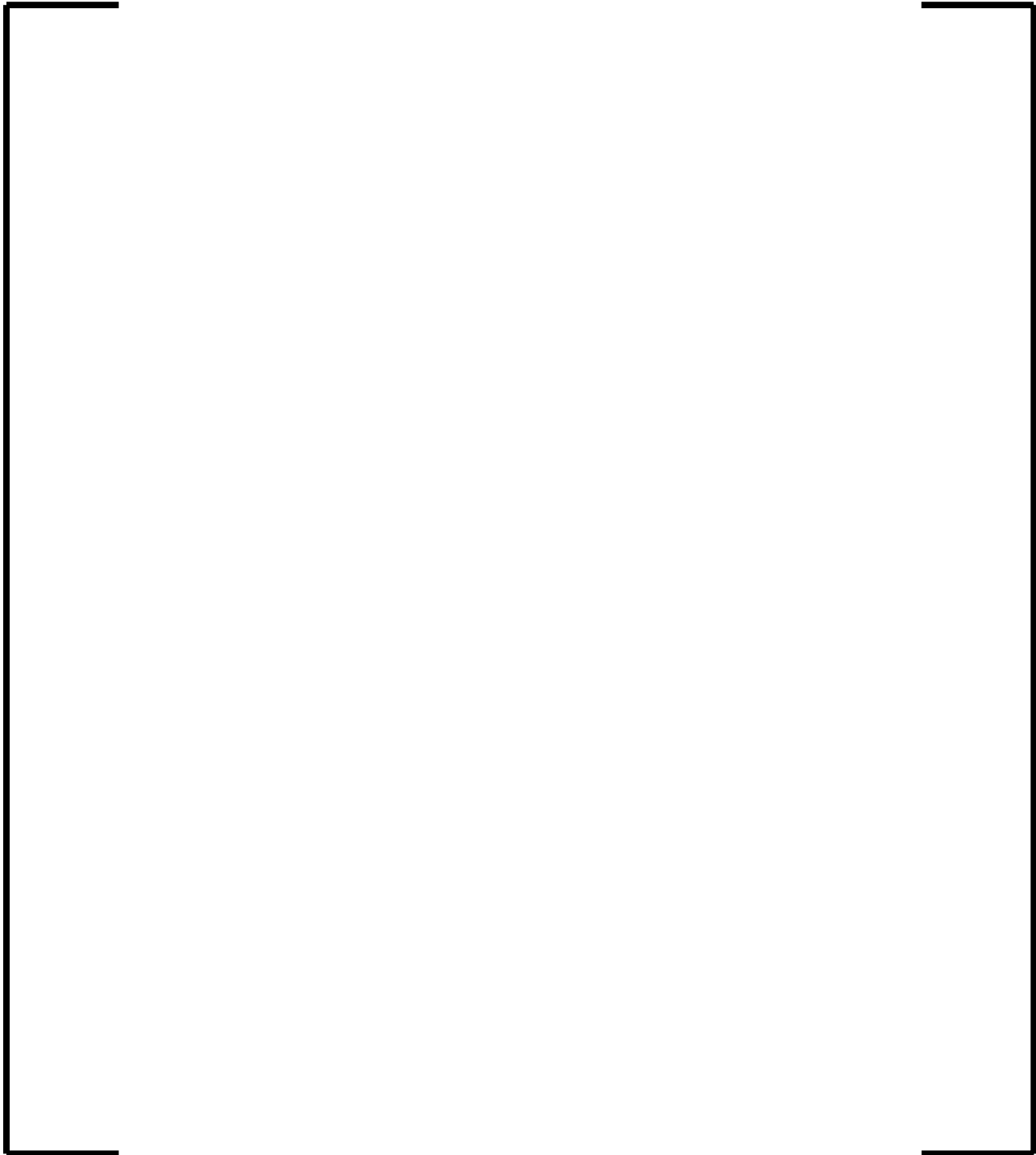


Figure 5-2 U.S. EPR Secondary Side Nodalization

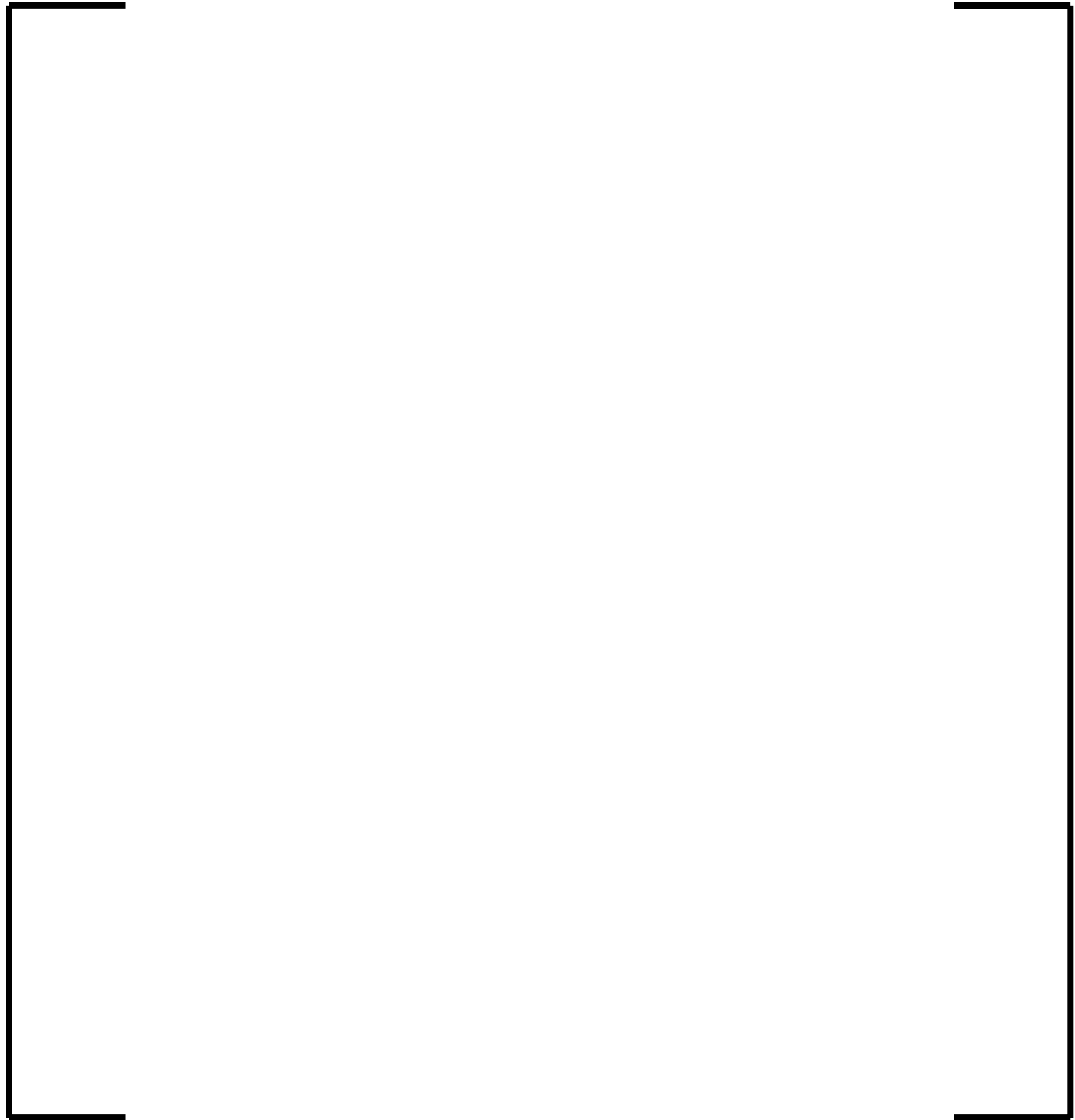


Figure 5-3 U.S. EPR Reactor Vessel Nodalization

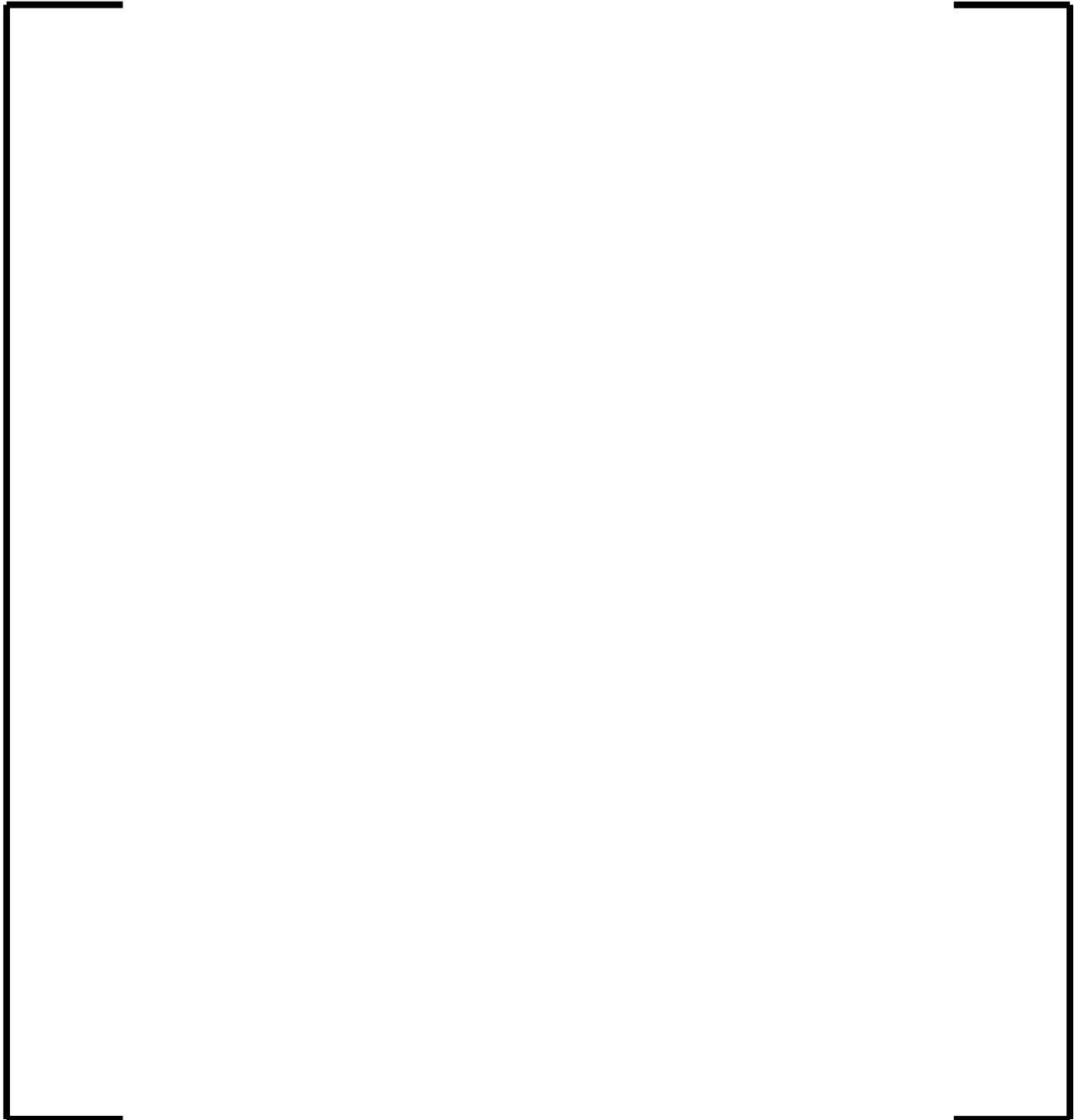


Figure 5-4 U.S. EPR Secondary Nodalization MSLB

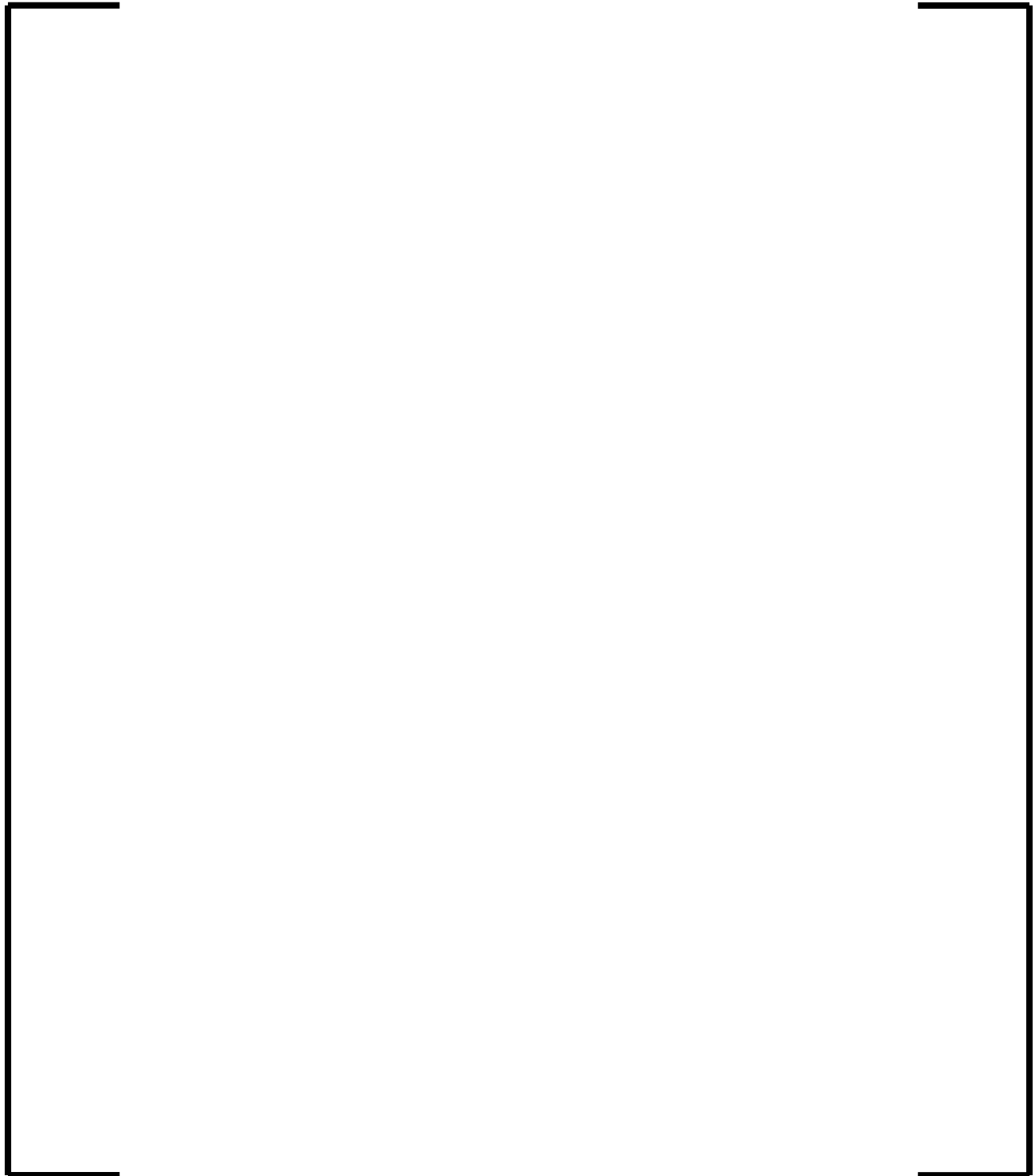


Figure 5-5 U.S. EPR Reactor Vessel Nodalization MSLB

6.0 APPLICABILITY OF OTHER APPROVED METHODOLOGIES TO U.S. EPR DESIGN

6.1 *Use of M5[®] Advanced Zirconium Alloy*

The U.S. EPR fuel design will use AREVA NP's M5[®] advanced zirconium alloy for fuel rod cladding and end plugs, guide thimbles, and intermediate spacer grids. M5[®] is a proprietary alloy with a nominal composition of 1.0 weight percent niobium, 0.125 weight percent oxygen, and the balance zirconium (References 6-1 and 6-2). Detailed information on the composition limits and thermomechanical treatment of M5[®] has been provided (Reference 6-3). The alloy provides superior performance in terms of corrosion, hydrogen pickup, axial growth, and diametral creep.

The analysis of a plant using M5[®] requires analytical models that reflect its performance. Such models have been approved through the topical report that describes the behavior of M5[®] (Reference 6-3) and through topical reports that describe the use of the models with COPENIC (Reference 6-4) and RODEX2-2A and S-RELAP5 (Reference 6-5). These codes and their applicability to U.S. EPR fuel are discussed in detail in Sections 3.3, 4, and 5.

Various mechanisms will affect M5[®] during irradiation. These include the following

- Water-side corrosion
- Fuel-side corrosion
- Hydrogen pickup
- Irradiation hardening
- Irradiation growth
- Elastic deformation
- Creep
- Heat conduction

For each mechanism, the environment seen by M5[®] in a U.S. EPR will be very similar to that in existing PWRs. Tables 2-1, 2-2, and 3-4 also show the similarity of the core, fuel assembly, and fuel rod designs for current PWRs and the U.S. EPR. Therefore, it is appropriate to use existing models for M5[®] in designing fuel assemblies for the U.S. EPR, provided that the models are used within the ranges for which they have been approved.

The safety evaluation report (SER) for Reference 6-3 concludes that the M5[®] properties and mechanical design methodology are acceptable for fuel reload licensing applications for Mark-B and Mark-BW fuel designs, respectively. In spite of the references to specific fuel designs, however, the focus of the report is primarily on the M5[®] material, that is, its suitability for purpose, its properties, and its incorporation into licensing analysis models. Most approvals of individual acceptance criteria and analytical models are general with no reference to a particular fuel design, only to the maximum currently approved burnup. Applicability is not restricted to a specific fuel design or fuel design feature. Such reasoning again leads to the conclusion that it is appropriate to use existing models for M5[®] in designing fuel assemblies for the U.S. EPR, provided that the models are used within the ranges for which they have been approved.

6.2 *Effects of Fuel Rod Bowing*

This section discusses fuel rod bowing, its effect on fuel performance, and the basis for using existing treatments of bowing for U.S. EPR fuel. The approach described here follows that in References 6-6 and 6-7. These topical reports and their SERs describe methods of analysis for the effects of fuel rod bowing. The methods will be applied, without change, to U.S. EPR fuel. The analysis of U.S. EPR fuel will thus use the same methods that AREVA currently uses for PWR fuel. Compliance of U.S. EPR fuel with appropriate acceptance criteria will be demonstrated in a later report submittal.

Under irradiation, fuel rods have a tendency to develop a bow out of their original vertical axis of alignment. This bowing can reduce the safety margin to the onset of departure from nucleate boiling (DNB) and can also create local increases in fuel rod

linear heat rates. Two effects can contribute to a decrease in margin to DNB. When bowed, the fuel rod moves closer to fuel rods in one direction, while moving farther away from fuel rods in the other direction. When the fuel rods move closer together, a narrowing of the coolant channel occurs. This decreases the coolant mass flow rate in the channel, locally causing an enthalpy rise that is greater than normal. When the fuel rods move farther apart, the larger coolant channel provides additional water moderation for neutrons, resulting in a higher capture rate by fissile species and hence a local increase in fuel rod linear heat rate. Both of these phenomena reduce the safety margin to the onset of DNB. The effect of bowing on fuel rod performance is ultimately reflected in reactor operating limits and setpoints.

The determination of the effects of rod bow on operating limits and setpoints is made in four steps. The first step quantifies rod bow as a function of operating and manufacturing parameters. The second step involves using physics codes to determine peaking changes in fuel rods due to bow, and the determination of a power peaking penalty. The third step is a thermal hydraulic analysis to determine the impact of the change in flow channel areas and subsequent peaking changes to fuel performance limits. The fourth step takes the thermal hydraulic analysis and applies the derived limits to determine the operating limits and setpoints.

AREVA NP quantifies rod bow by measuring the water channels, that is, the space between two adjacent fuel rods (or a fuel rod and an adjacent guide tube) in the same row. The space is measured by means of a probe that is passed through the water channels of a fuel assembly. If the geometry of a fuel assembly were perfect, all of the fuel-rod-to-fuel-rod water channels would be the same size. Rod bow and, to a lesser extent, manufacturing variations result in a distribution of water channel widths. The standard deviation of this distribution has been approved as a measure of rod bow, and the amount of rod bow has been correlated with the assembly average burnup.

Methods similar to those used in References 6-6 and 6-7 can be used to develop a correlation for rod bow that is applicable to U.S. EPR fuel. As defined in Reference 6-6, fuel rod bow is a characteristic of a single span of a fuel rod, that is, of a section of fuel

rod that extends from one spacer grid to the next. This definition is appropriate because fuel rods are constrained against transverse motion by the spacer grids. Table 3-4 shows the similarity of the fuel rods between the Advanced Mark-BW design and the U.S. EPR design. The overall fuel rod length is greater in the U.S. EPR design, but a U.S. EPR fuel assembly has two more spacer grids than an Advanced Mark-BW assembly, so the span length is slightly reduced. In light of these similarities, it is expected that a correlation for rod bow as a function of burnup can also be developed for U.S. EPR fuel. Such a correlation will be provided in a later report submittal.

The second step in understanding the effects of rod bow involves using physics codes to determine peaking changes and determining a power peaking penalty. The peaking analysis used to determine the penalty for rod bowing is not affected by fuel length, it being a two dimensional (x-y) analysis, and would be the same regardless of the actual length of the fuel. As is described in the preceding paragraph and Table 2-2, the geometry of the fuel rod array in a U.S. EPR is similar to that in existing reactors. Therefore, the same neutronic codes and methods are applicable to the analysis of rod bow in the U.S. EPR as well.

Parallelism between Advanced Mark-BW and U.S. EPR fuel also applies for the third step, thermal hydraulic analysis. As is described in the preceding paragraph, the geometry of the fuel rod array in a U.S. EPR is similar to that in existing reactors. Therefore, the thermal hydraulic methods described in section 6 of Reference 6-6 are applicable to the U.S. EPR as well.

The fourth step, derivation of reactor operating limits and setpoints, requires an analysis that is specific to the U.S. EPR. That analysis is deferred to a later report submittal.

It is noted that Reference 6-6 includes a discussion and analysis of fuel assembly bow. An analysis of fuel assembly bow will be developed for the U.S. EPR, but that analysis is deferred to a later report submittal.

6.3 *Fuel Rod Gas Pressure Limits*

Fuel rod internal gas pressures tend to increase as irradiation progresses, and a gas pressure limit is necessary to ensure that the fuel rods remain in an analyzed state. This section describes the method for establishing a fuel rod gas pressure limit that will be used for U.S. EPR fuel rod design. The approach described here follows that in Reference 6-8. This topical report and its SER will be applied, without change, to U.S. EPR fuel. The acceptance criteria for fuel rod gas pressure will thus be the same as those that AREVA currently uses for analysis of PWR fuel.

Reference 6-8 describes a pin pressure criterion and associated implementation methodology that permit a small number of fuel rods to operate at internal gas pressures above nominal reactor coolant system pressure. The criterion and methodology allow greater fuel cycle design flexibility while maintaining cladding integrity. The criterion is as follows: The internal pressure of the peak fuel rod in the reactor is limited to a value below that which would cause (1) the fuel-cladding gap to increase due to outward cladding creep during steady-state operation and (2) extensive departure from nucleate boiling propagation to occur. The report gives a proprietary limit on the difference between the maximum fuel rod internal gas pressure and the nominal reactor coolant system pressure.

The purpose of the first limit is to prevent the opening of the fuel-cladding gap, which could degrade heat transfer and thereby lead to excessive fuel temperatures, excessive internal rod gas pressures due to fission gas release, and excessive cladding stresses and strains. Compliance with this limit is determined by using a fuel rod performance code. The criterion has been approved (Reference 6-4) for use with COPENIC. When pin pressure exceeds system pressure, the code evaluates whether the rate of outward cladding creep exceeds the rate of fuel pellet swelling.

The purpose of the second limit is to prevent cladding ballooning during normal operation. The concern is that power peaking can cause DNB on fuel rods with pin pressures that are above nominal system pressure. Since a balloon would affect coolant flow, ballooning could cause DNB to propagate to surrounding fuel rods.

Reference 6-8 addresses this concern by performing a statistical core analysis to determine failure rates for bounding distributions of burnup and power peaking.

Two other potential effects of increased fuel rod pressures are also discussed in Reference 6-8: hydride reorientation and effects on LOCA. Hydride reorientation was considered by laboratory tests on Zircaloy-4 cladding. The tests showed that rod pressure for Zircaloy-4 cladding is not limited by hydride reorientation. Results for M5[®] cladding are at least as good as those for Zircaloy-4 because, for a given burnup, the hydrogen content of M5[®] is much lower than that of Zircaloy-4.

During a postulated loss-of-coolant accident (LOCA), the reactor coolant system pressure drops below the fuel rod internal pressure, and the cladding may swell and rupture. LOCA calculations were performed for rod internal pressures that were set to 1) the nominal system pressure and 2) the maximum allowable pressure described above. The latter case allowed a larger linear heat generation rate at extended burnups, but both cases provided acceptable LOCA performance. Therefore, use of the fuel rod gas pressure criterion does not lead to unacceptable LOCA performance.

The fuel rod gas pressure criterion is applicable to the U.S. EPR fuel design because of the similarity between U.S. EPR fuel and existing fuel and because the criterion is stated in terms that are independent of small changes in the design. Similarity of the fuel rod dimensions, fuel rod spacing, and fuel rod materials may be seen from Tables 2-1 and 3-4. That the criterion is independent of small changes in the design can be seen because it is stated in terms that are independent of the design. Designs are determined to be acceptable by analyses that take the design into account. For example, an analysis for opening of the fuel-cladding gap will reflect the details of the fuel rod design and the properties of the fuel and cladding materials. This is equally true for analyses of DNB propagation, hydride reorientation, and LOCA performance. Therefore, although the applications presented in Reference 6-8 are for specific fuel designs, the criterion and methodology are generic and can be applied to any PWR fuel design. Reference 6-8 is applicable to the U.S. EPR fuel design without modification.

6.4 Statistical Assessment of Fuel Assembly Holddown

This section describes the use of a statistical approach in designing holddown springs for fuel assemblies. This approach will be used for U.S. EPR fuel assemblies. The approach described here follows that in Reference 6-10. This topical report and its SER will be applied, without change, to U.S. EPR fuel. The acceptance criteria for fuel assembly holddown will thus be the same as those that AREVA currently uses for analysis of PWR fuel.

The net force on a fuel assembly consists of the downward force due to the holddown spring and the weight of the components, minus the upward forces due to buoyancy and drag of the upward fluid flow. If the net holddown force is negative, the fuel assembly could lift off its lower support grid and cause damage. If the net holddown force is too great, excessive compression forces could cause bowing or twisting of the fuel assembly. Ideally, the holddown spring force is just sufficient to assure that the fuel assembly remains seated during normal operation and anticipated operational occurrences. Regulatory guidance supports the criterion that the net holddown force must be positive; the *Standard Review Plan* (Reference 6-9) states that the worst-case hydraulic loads for normal operation should not exceed the holddown capability of the fuel assembly (either gravity or holddown springs).

A number of variables, including the core volumetric flow rate, the holddown spring constant, the hydraulic lift resistance, and the spring compression, affect the net holddown force. In a deterministic calculation, each of these is set to the limiting value that produces the smallest holddown force. In a statistical calculation, each of the variables is assigned a distribution of values, and the distributions are combined to calculate a distribution for the net holddown force. A tolerance limit is then imposed to achieve the desired levels of protection and confidence.

Reference 6-10 presents an approved statistical methodology for calculating the required holddown force. The methodology entails five steps:

1. Identify the independent variables affecting the dependent variable, i.e., net holddown force on the fuel assembly.

2. Develop a model to determine the value of the dependent variable as a function of the values of the independent variables.
3. Quantify the uncertainties in the independent variables, including those that will be treated probabilistically as well as those that will be treated deterministically.
4. Perform a Monte-Carlo analysis to propagate the uncertainties in the independent variables through to the dependent variable.
5. Establish the tolerance limit of the dependent variable, i.e., net holddown force, to achieve the desired protection level and confidence.

Each of the variables has an uncertainty about its nominal value for a given core configuration, operating condition, and time in life condition. Such a condition is referred to as a statepoint. It may not be evident in advance which of these statepoints yields the smallest net holddown force. Therefore, a series of statepoints is examined across the range of plant operating conditions to assure that the most limiting cases are considered.

The methodology described in Reference 6-10 has been approved by the NRC for all PWR fuel designs. Such approval is appropriate because the same processes, such as buoyancy, hydraulic lift, and spring compression, apply to all PWR fuel assemblies. In addition, the design of the U.S. EPR fuel is similar to that of existing fuel assemblies, as may be seen from Tables 2-1 and 3-4. Therefore, this methodology is applicable to U.S. EPR fuel.

6.5 *References*

- 6-1. Didier Gilbon, Annie Soniak, Sylvie Doriot, and Jean-Paul Mardon, "Irradiation Creep and Growth Behavior, and Microstructural Evolution of Advanced Zr-Base Alloys," *Zirconium in the Nuclear Industry: Twelfth International Symposium, ASTM STP 1354*, G. P. Sabol and G. D. Moan, Eds., American Society for Testing and Materials, West Conshohocken, PA, 2000, pp. 51-73.
- 6-2. Jean-Paul Mardon, Daniel Charquet, and Jean Senevat, "Influence of Composition and Fabrication Process on Out-of-Pile and In-Pile Properties of

-
- M5[®] Alloy,” *Zirconium in the Nuclear Industry: Twelfth International Symposium, ASTM STP 1354*, G. P. Sabol and G. D. Moan, Eds., American Society for Testing and Materials, West Conshohocken, PA, 2000, pp. 505-524.
- 6-3. “Evaluation of Advanced Cladding and Structural Material (M5[®]) in PWR Reactor Fuel,” BAW-10227P-A, Revision 1, June 2003.
- 6-4. “COPERNIC Fuel Rod Design Computer Code,” BAW-10231P-A, Revision 1, January 2004.
- 6-5. “Incorporation of M5[®] Properties in Framatome ANP Approved Methods,” BAW-10240(P)-A, Revision 0, May 2004.
- 6-6. “Fuel Rod Bowing in Babcock & Wilcox Fuel Designs,” BAW-10147P-A, Revision 1, May 1983.
- 6-7. “Extended Burnup Evaluation,” BAW-10186P-A, Revision 2, June 2003.
- 6-8. “Fuel Rod Gas Pressure Criterion (FRGPC),” BAW-10183P-A, Revision 0, July 1995.
- 6-9. “Standard Review Plan,” NUREG-0800
- 6-10. “Statistical Fuel Assembly Hold Down Methodology”, BAW-10243P-A, September 2005.

7.0 SUMMARY/CONCLUSIONS

The U.S. EPR is an evolutionary PWR design that is geometrically, functionally, and phenomenologically similar to existing plants and fuel designs. AREVA NP codes and methodology in use (and NRC-approved) for analyses of existing plants and fuel were reviewed to confirm their applicability to the U.S. EPR.

The codes and methodologies examined were:

- CASMO3 and PRISM – used for core neutronics,
- NEMO-K – used for core reactivity transients,
- LYNXT – used for detailed core thermal/hydraulic analyses,
- COPENIC – used for core thermal/mechanical analyses,
- S-RELAP5 as used for SBLOCA analyses,
- S-RELAP5 as used for non-LOCA transient analyses, and
- focused methodologies addressing:
 - the use of M5[®],
 - the assessment of fuel rod bow,
 - the establishment of fuel rod gas pressure limits,
 - a statistical assessment of fuel assembly hold down,

In general, the reviews:

- confirmed the physical similarities between the U.S. EPR and existing designs,
- confirmed that the U.S. EPR responses to various initiating events or conditions are similar to the responses of existing designs and within the range of applicability of S-RELAP5, and
- confirmed that the phenomena governing the U.S. EPR responses were the same as those phenomena governing the responses of existing plants.

On the basis of these reviews, it was concluded that the existing codes and methodologies (References 1-2 through 1-12) are appropriate for U.S. EPR analyses, in most cases without change. Any necessary changes have been identified and justified within this report.

APPENDIX A

CORE NEUTRONICS

APPENDIX A TABLE OF CONTENTS

A.1.0	Treatment of U.S. EPR Heavy Reflector	A-1
A.1.1	Introduction.....	A-1
A.1.2	Generalization of the Equivalent Reflector Model	A-2
A.1.3	Translation of the heavy Reflector Geometry into Slab Geometries	A-4
A.1.4	Generation of the Equivalent Heavy Reflector Cross Sections for the EPR	A-5
A.1.5	Qualification of PRISM Reflector Model	A-8
A.1.6	Conclusion.....	A-11
A.2.0	SAV95 Benchmarking Results	A-12
A.2.1	Introduction.....	A-12
A.2.2	Summary	A-13
A.2.3	Methodology Description	A-14
A.2.4	Validation.....	A-14
A.3.0	Power Distribution Uncertainties for POWERTRAX/S.....	A-26
A.3.1	Introduction.....	A-26
A.3.2	Inferred Relative Power Distribution Calculation	A-26
A.3.3	Inferred Relative Power Distribution Uncertainties	A-32
A.4.0	References	A-35

List of Tables

Table A-2.1:	Summary of SAV95 Validation Criteria and Results.....	A-36
Table A-2.2:	Results of SAV95 Calculations with Startup Physics Test Measurements.....	A-37
Table A-2.3:	Results of SAV95 Calculations with Core Follow Measurements	A-38
Table A-2.4:	Hot Zero Power All Rods Out Critical Boron Concentrations	A-39
Table A-2.5:	Plant A Cycle 1 Hot Zero Power Rod Bank Worth	A-40
Table A-2.6:	Plant A Cycle 2 Hot Zero Power Rod Bank Worth	A-40
Table A-2.7:	Plant A Cycle 3 Hot Zero Power Rod Bank Worth	A-40
Table A-2.8:	Plant A Cycle 4 Hot Zero Power Rod Bank Worth	A-41
Table A-2.9:	Plant A Cycle 5 Hot Zero Power Rod Bank Worth	A-41
Table A-2.10:	Plant A Cycle 6 Hot Zero Power Rod Bank Worth	A-41
Table A-2.11:	Plant A Cycle 7 Hot Zero Power Rod Bank Worth	A-42
Table A-2.12:	Plant A Cycle 8 Hot Zero Power Rod Bank Worth	A-42
Table A-2.13:	Plant A Cycle 9 Hot Zero Power Rod Bank Worth	A-42
Table A-2.14:	Plant A Cycle 10 Hot Zero Power Rod Bank Worth	A-43
Table A-2.15:	Plant A Cycle 11 Hot Zero Power Rod Bank Worth	A-43
Table A-2.16:	Plant A Cycle 12 Hot Zero Power Rod Bank Worth	A-43
Table A-2.17:	Plant A Cycle 13 Hot Zero Power Rod Bank Worth	A-44
Table A-2.18:	Plant B Cycle 1 Hot Zero Power Rod Bank Worth	A-44
Table A-2.19:	Summary of Total Bank Worths.....	A-45
Table A-2.20:	Hot Zero Power All Rods Out Isothermal Temperature Coefficient.....	A-46
Table A-2.21	Power Distribution Summary for Plants G1 and G2	A-47
Table A-3.1:	Derivation of Inferred Power Distribution Uncertainties.....	A-51

List of Figures

Figure A-1.1 Typical Layout of the Reflector in a Standard PWR	52
Figure A-1.2 Typical Layout of the Reflector in the EPR.....	52
Figure A-1.3 1-D Reflector Model	53
Figure A-1.4 2-D Reflector Model	53
Figure A-1.5 U.S. EPR Reflector Geometry	54
Figure A-1.6 Reflector Coolant Channel in Re-entrant Corner	55
Figure A-1.7: Comparisons of the Differences between MCNP and PRISM Radial Powers for the Standard and Heavy Reflectors with the Standard Core Design	56
Figure A-1.8: Comparisons of the Differences between MCNP and PRISM Radial Powers for the Heavy Reflectors with the Different Core Designs	57
Figure A-1.9: Comparisons of the Differences between MCNP and PRISM Radial Powers for the Standard and Heavy Reflectors with the Standard Core Design at High Boron	58
Figure A-1.10 Comparisons of the Differences between MCNP and PRISM Radial Powers for the Standard and Heavy Reflectors with the Standard Core Design at Low Fuel and Moderator Temperatures	59
Figure A-2.1: SAV95 Calculation Flowchart.....	60
Figure A-2.2(a) Plant G2 Assembly Guide Tube Configuration	61
Figure A-2.2(b) Plant G1 Assembly Guide Tube Configuration	62
Figure A-2.3: Plant A Cycle 1 Critical Boron Concentration	63
Figure A-2.4: Plant A Cycle 2 Critical Boron Concentration	63
Figure A-2.5: Plant A Cycle 3 Critical Boron Concentration	64
Figure A-2.6: Plant A Cycle 4 Critical Boron Concentration	64
Figure A-2.7: Plant A Cycle 5 Critical Boron Concentration	65
Figure A-2.8: Plant A Cycle 6 Critical Boron Concentration	65
Figure A-2.9: Plant A Cycle 7 Critical Boron Concentration	66
Figure A-2.10: Plant A Cycle 8 Critical Boron Concentration	66
Figure A-2.11: Plant A Cycle 9 Critical Boron Concentration	67
Figure A-2.12: Plant A Cycle 10 Critical Boron Concentration	67
Figure A-2.13: Plant A Cycle 11 Critical Boron Concentration	68
Figure A-2.14: Plant A Cycle 12 Critical Boron Concentration	68
Figure A-2.15: Plant B Cycle 1 Critical Boron Concentration	69
Figure A-2.16: Plant G2 Cycle 1 Critical Boron Concentration	69
Figure A-2.17: Plant G2 Cycle 2 Critical Boron Concentration	70
Figure A-2.18: Plant G2 Cycle 3 Critical Boron Concentration	70
Figure A-2.19: Plant G2 Cycle 4 Critical Boron Concentration	71
Figure A-2.20: Plant G2 Cycle 5 Critical Boron Concentration	71
Figure A-2.21: Plant G1 Cycle 26 Critical Boron Concentration	72
Figure A-2.22: Plant G1 Cycle 27 Critical Boron Concentration	72
Figure A-2.23: Plant G1 Cycle 28 Critical Boron Concentration	73
Figure A-2.24: Plant G1 Cycle 29 Critical Boron Concentration	73
Figure A-2.25: Plant G1 Cycle 30 Critical Boron Concentration	74
Figure A-2.26: Plant A BOC 1 Assembly Power Distribution	75
Figure A-2.27: Plant A MOC 1 Assembly Power Distribution.....	76
Figure A-2.28: Plant A EOC 1 Assembly Power Distribution	77
Figure A-2.29: Plant A BOC 2 Assembly Power Distribution	78
Figure A-2.30: Plant A MOC 2 Assembly Power Distribution.....	79

Codes and Methods Applicability Report
for the U.S. EPR

Page A-iii

Figure A-2.31: Plant A EOC 2 Assembly Power Distribution	80
Figure A-2.32: Plant A BOC 3 Assembly Power Distribution	81
Figure A-2.33: Plant A MOC 3 Assembly Power Distribution.....	82
Figure A-2.34: Plant A EOC 3 Assembly Power Distribution	83
Figure A-2.35: Plant A BOC 4 Assembly Power Distribution	84
Figure A-2.36: Plant A MOC 4 Assembly Power Distribution.....	85
Figure A-4.37: Plant A EOC 4 Assembly Power Distribution	86
Figure A-2.38: Plant A BOC 5 Assembly Power Distribution	87
Figure A-2.39: Plant A MOC 5 Assembly Power Distribution.....	88
Figure A-2.40: Plant A EOC 5 Assembly Power Distribution	89
Figure A-2.41: Plant A BOC 6 Assembly Power Distribution	90
Figure A-2.42: Plant A MOC 6 Assembly Power Distribution.....	91
Figure A-2.43: Plant A EOC 6 Assembly Power Distribution	92
Figure A-2.44: Plant A BOC 7 Assembly Power Distribution	93
Figure A-2.45: Plant A MOC 7 Assembly Power Distribution.....	94
Figure A-2.46: Plant A EOC 7 Assembly Power Distribution	95
Figure A-2.47: Plant A BOC 8 Assembly Power Distribution	96
Figure A-2.48: Plant A MOC 8 Assembly Power Distribution.....	97
Figure A-2.49: Plant A EOC 8 Assembly Power Distribution	98
Figure A-2.50: Plant A BOC 9 Assembly Power Distribution	99
Figure A-2.51: Plant A MOC 9 Assembly Power Distribution.....	100
Figure A-2.52: Plant A EOC 9 Assembly Power Distribution	101
Figure A-2.53: Plant A BOC 10 Assembly Power Distribution	102
Figure A-2.54: Plant A MOC 10 Assembly Power Distribution.....	103
Figure A-2.55: Plant A EOC 10 Assembly Power Distribution	104
Figure A-2.56: Plant A BOC 11 Assembly Power Distribution	105
Figure A-2.57: Plant A MOC 11 Assembly Power Distribution.....	106
Figure A-2.58: Plant A EOC 11 Assembly Power Distribution	107
Figure A-2.59: Plant A BOC 12 Assembly Power Distribution	108
Figure A-2.60: Plant A MOC 12 Assembly Power Distribution.....	109
Figure A-2.61: Plant A EOC 12 Assembly Power Distribution	110
Figure A-2.62: Plant B BOC 1 Assembly Power Distribution	111
Figure A-2.63: Plant B MOC 1 Assembly Power Distribution.....	112
Figure A-2.64: Plant B EOC 1 Assembly Power Distribution	113
Figure A-2.65: Plant G2 BOC 1 Assembly Power Distribution.....	114
Figure A-2.66: Plant G2 MOC 1 Assembly Power Distribution	115
Figure A-2.67: Plant G2 EOC 1 Assembly Power Distribution.....	116
Figure A-2.68: Plant G2 BOC 2 Assembly Power Distribution.....	117
Figure A-2.69: Plant G2 MOC 2 Assembly Power Distribution	118
Figure A-2.70: Plant G2 EOC 2 Assembly Power Distribution.....	119
Figure A-2.71: Plant G2 BOC 3 Assembly Power Distribution.....	120
Figure A-2.72: Plant G2 MOC 3 Assembly Power Distribution	121
Figure A-2.73: Plant G2 EOC 3 Assembly Power Distribution.....	122
Figure A-2.74: Plant G2 BOC 4 Assembly Power Distribution.....	123
Figure A-2.75: Plant G2 MOC 4 Assembly Power Distribution	124
Figure A-2.76: Plant G2 EOC 4 Assembly Power Distribution.....	125
Figure A-2.77: Plant G2 BOC 5 Assembly Power Distribution.....	126
Figure A-2.78: Plant G2 MOC 5 Assembly Power Distribution	127
Figure A-2.79: Plant G2 EOC 5 Assembly Power Distribution.....	128

Codes and Methods Applicability Report
for the U.S. EPR

Page A-iv

Figure A-2.80: Plant G1 BOC 26 Assembly Power Distribution	129
Figure A-2.81: Plant G1 MOC 26 Assembly Power Distribution	130
Figure A-2.82: Plant G1 EOC 26 Assembly Power Distribution	131
Figure A-2.83: Plant G1 BOC 27 Assembly Power Distribution	132
Figure A-2.84: Plant G1 MOC 27 Assembly Power Distribution	133
Figure A-2.85: Plant G1 EOC 27 Assembly Power Distribution	134
Figure A-2.86: Plant G1 BOC 28 Assembly Power Distribution	135
Figure A-2.87: Plant G1 MOC 28 Assembly Power Distribution	136
Figure A-2.88: Plant G1 EOC 28 Assembly Power Distribution	137
Figure A-2.89: Plant G1 BOC 29 Assembly Power Distribution	138
Figure A-2.90: Plant G1 MOC 29 Assembly Power Distribution	139
Figure A-2.91: Plant G1 EOC 29 Assembly Power Distribution	140
Figure A-2.92: Plant G1 BOC 30 Assembly Power Distribution	141
Figure A-2.93: Plant G1 MOC 30 Assembly Power Distribution	142
Figure A-2.94: Plant G1 EOC 30 Assembly Power Distribution	143
Figure A-2.95: Plant A BOC 1 Axial Power Distribution	144
Figure A-2.96: Plant A MOC 1 Axial Power Distribution	145
Figure A-2.97: Plant A EOC 1 Axial Power Distribution	146
Figure A-2.98: Plant A BOC 2 Axial Power Distribution	147
Figure A-2.99: Plant A MOC 2 Axial Power Distribution	148
Figure A-2.100: Plant A EOC 2 Axial Power Distribution	149
Figure A-2.101: Plant A BOC 3 Axial Power Distribution	150
Figure A-2.102: Plant A MOC 3 Axial Power Distribution	151
Figure A-2.103: Plant A EOC 3 Axial Power Distribution	152
Figure A-2.104: Plant A BOC 4 Axial Power Distribution	153
Figure A-2.105: Plant A MOC 4 Axial Power Distribution	154
Figure A-2.106: Plant A EOC 4 Axial Power Distribution	155
Figure A-2.107: Plant A BOC 5 Axial Power Distribution	156
Figure A-2.108: Plant A MOC 5 Axial Power Distribution	157
Figure A-2.109: Plant A EOC 5 Axial Power Distribution	158
Figure A-2.110: Plant A BOC 6 Axial Power Distribution	159
Figure A-2.111: Plant A MOC 6 Axial Power Distribution	160
Figure A-2.112: Plant A EOC 6 Axial Power Distribution	161
Figure A-2.113: Plant A BOC 7 Axial Power Distribution	162
Figure A-2.114: Plant A MOC 7 Axial Power Distribution	163
Figure A-2.115: Plant A EOC 7 Axial Power Distribution	164
Figure A-2.116: Plant A BOC 8 Axial Power Distribution	165
Figure A-2.117: Plant A MOC 8 Axial Power Distribution	166
Figure A-2.118: Plant A EOC 8 Axial Power Distribution	167
Figure A-2.119: Plant A BOC 9 Axial Power Distribution	168
Figure A-2.120: Plant A MOC 9 Axial Power Distribution	169
Figure A-2.121: Plant A EOC 9 Axial Power Distribution	170
Figure A-2.122: Plant A BOC 10 Axial Power Distribution	171
Figure A-2.123: Plant A MOC 10 Axial Power Distribution	172
Figure A-2.124: Plant A EOC 10 Axial Power Distribution	173
Figure A-2.125: Plant A BOC 11 Axial Power Distribution	174
Figure A-2.126: Plant A MOC 11 Axial Power Distribution	175
Figure A-2.127: Plant A EOC 11 Axial Power Distribution	176
Figure A-2.128: Plant A BOC 12 Axial Power Distribution	177

Codes and Methods Applicability Report
for the U.S. EPR

Page A-v

Figure A-2.129: Plant A MOC 12 Axial Power Distribution	178
Figure A-2.130: Plant A EOC 12 Axial Power Distribution	179
Figure A-2.131: Plant B BOC 1 Axial Power Distribution	180
Figure A-2.132: Plant B MOC 1 Axial Power Distribution	181
Figure A-2.133: Plant B EOC 1 Axial Power Distribution	182
Figure A-2.134: Plant G2 BOC 1 Axial Power Distribution.....	183
Figure A-2.135: Plant G2 MOC 1 Axial Power Distribution	184
Figure A-2.136 Plant G2 EOC 1 Axial Power Distribution.....	185
Figure A-2.137 Plant G2 BOC 2 Axial Power Distribution.....	186
Figure A-2.138 Plant G2 MOC 2 Axial Power Distribution	187
Figure A-2.139: Plant G2 EOC 2 Axial Power Distribution.....	188
Figure A-2.140: Plant G2 BOC 3 Axial Power Distribution.....	189
Figure A-2.141: Plant G2 MOC 3 Axial Power Distribution	190
Figure A-2.142: Plant G2 EOC 3 Axial Power Distribution.....	191
Figure A-2.143: Plant G2 BOC 4 Axial Power Distribution.....	192
Figure A-2.144: Plant G2 MOC 4 Axial Power Distribution	193
Figure A-2.145: Plant G2 EOC 4 Axial Power Distribution.....	194
Figure A-2.146: Plant G2 BOC 5 Axial Power Distribution.....	195
Figure A-2.147: Plant G2 MOC 5 Axial Power Distribution	196
Figure A-2.148: Plant G2 EOC 5 Axial Power Distribution.....	197
Figure A-2.149: Plant G1 BOC 26 Axial Power Distribution.....	198
Figure A-2.150: Plant G1 MOC 26 Axial Power Distribution	199
Figure A-2.151: Plant G1 EOC 26 Axial Power Distribution.....	200
Figure A-2.152: Plant G1 BOC 27 Axial Power Distribution.....	201
Figure A-2.153: Plant G1 MOC 27 Axial Power Distribution	202
Figure A-2.154: Plant G1 EOC 27 Axial Power Distribution.....	203
Figure A-2.155: Plant G1 BOC 28 Axial Power Distribution.....	204
Figure A-2.156: Plant G1 MOC 28 Axial Power Distribution	205
Figure A-2.157: Plant G1 EOC 28 Axial Power Distribution.....	206
Figure A-2.158: Plant G1 BOC 29 Axial Power Distribution.....	207
Figure A-2.159: Plant G1 MOC 29 Axial Power Distribution	208
Figure A-2.160: Plant G1 EOC 29 Axial Power Distribution.....	209
Figure A-2.161: Plant G1 BOC 30 Axial Power Distribution.....	210
Figure A-2.162: Plant G1 MOC 30 Axial Power Distribution	211
Figure A-2.163: Plant G1 EOC 30 Axial Power Distribution.....	212

A.1.0 *Treatment of U.S. EPR Heavy Reflector*

A.1.1 Introduction

The reflector for a standard PWR consists of a thin steel shroud followed by a large water reflector as shown in Figure A-1.1. In the U.S. EPR the reflector consists of large steel reflector that contains flow channels for cooling in the steel reflector. This is followed by a thin water region as shown in Figure A-1.2. The approach to generate the reflector cross sections for these two reflector designs is similar.

The reflector geometry of the U.S. EPR replaces the shroud with a heavy steel reflector. This geometry will minimize the thermalization of neutrons leaving the core while reflecting more fast neutrons back into the core than is possible with the standard reflector geometries. This then reduces core leakage, and improves the overall core neutron economy. As with the standard reflector designs, the U.S. EPR reflector cross sections can be affected by core leakage, assembly lattice design, and the design of the heavy reflector.

An equivalent reflector model is used to produce reflector cross sections for the PRISM 3D core simulator nodal code. This method models a heterogeneous reflector using a response function at the fuel reflector boundary. Generation of the reflector cross sections accounts for the core leakage (e.g., low-leakage), the assembly lattice design, (e.g., 14X14 or 17X17), the shroud thickness or heavy reflector, the water region, and the presence of a thermal shield. With these considerations, the reflector cross sections generated using this equivalent reflector model are specific to the core configuration, and assembly lattice design (e.g., 15x15, 17x17 or 18x18).

For the standard reflector, the process used to generate the radial reflector cross sections treats the problem using slab geometries of the fuel, water gaps, shroud, thermal shield and barrel. The re-entrant corners use a 2-D geometry to account for neutrons that leak from one corner assembly and then reenter the adjacent corner assembly. In the case of the heavy reflector, the 1-D process of

the equivalent reflector model is used to translate the fuel and reflector geometries into slabs that are then used to generate the reflector cross sections. The 2-D model for re-entrant corners is not used to generate the heavy reflector cross sections. The top and bottom reflectors are also generated in this manner and the technique is consistent for both the conventional reactors and the U.S. EPR.

A.1.2 Generalization of the Equivalent Reflector Model

For a conventional PWR, two geometries are considered in the radial direction. The first geometry considered is the simple case where the fuel assemblies in the core have a single face adjacent to the reflector, and the second case considers a corner where the assemblies have two faces adjacent to the reflector. In the case of the corner reflector model, the re-entrant condition where a neutron leaves one assembly passes through the reflector and enters another assembly must be considered. The axial reflector is treated similar to the case where the assembly has one face adjacent to the shroud.

Both the radial and axial reflectors in a PWR are strongly heterogeneous. This is demonstrated in Figure A-1.1 which provides a representation of the interface between the core and reflector for a conventional PWR design. From Figure A-1.1, it can be seen that two geometries can be defined to model the reflector. These include a 1-D slab geometry to model the reflector edges as shown in Figure A-1.3, and a 2-D model which consider the re-entrant corners as shown in Figure A-1.4.

Axially the reflector model will be defined using a 1-D slab similar to the geometry shown in Figure A-1.3.

The equivalent reflector model conserves the 1-D nodal response as well as the 2-D nodal response. The model used for conventional PWR cores has the following features:

1. The modeling of the reflectors is based on a heterogeneous treatment of the reflector.
2. Reflector cross sections for the re-entrant corners are generated using a 2-D spectral calculation in order to capture the effect of the neutrons leaving one fuel assembly traveling through the reflector (hatched areas in Figure A-1.4) and entering another fuel assembly.
3. The equivalent cross sections generated with the equivalent reflector model use the same nodal flux solver as in the PRISM code. Therefore, the reflector cross sections are generated to be consistent with the reactor calculation. The reflector cross sections conform to the nodalization of the reactor calculation and include a consistent transverse leakage formulation for the 2-D case.

With all the water present, the standard PWR reflector is efficient at reflecting thermal neutrons. The U.S. EPR uses a heavy steel reflector which varies from 10 to 20 cm in thickness and contains several relatively small coolant channels and a moderator zone spaced far from the fuel (see FigureA-1.5). Because of this design, the heavy reflector is better than the standard PWR reflector at reflecting fast neutrons back into the core.

Since the heavy steel reflector is better at reflecting fast neutrons directly back into the core, the 2-D method for re-entrant corners is not required. Therefore, seven 1-D slab geometries are defined to represent the seven unique geometries of the heavy reflector. Fuel nodes are then added to the left boundary of the reflector nodes and reflective symmetry is applied to the north, south and west boundaries. A vacuum boundary condition is applied to the east boundary of the reflector. The flux solutions from the corresponding eigenvalue problems for these spectral geometries provide the heterogeneous reflector response matrix at the fuel/reflector interface. The corresponding homogeneous (diffusion theory based) reflector response matrix at this interface can be determined by solving for a number of consistent boundary value problems so that the matrix elements

depend analytically on the cross sections of the homogeneous reflector node.

The requirement that the heterogeneous and homogeneous response functions be equal sets up a series of non-linear equations for the equivalent cross sections. Solving this set of equations will produce cross section libraries for the seven radial reflector node geometries shown in Figure A-1.5.

The generation of the equivalent reflector cross sections for the standard reflector and the U.S. EPR heavy reflector are equivalent. For the standard reflector, a 1-D slab geometry is used for all locations except the re-entrant corners, and for the heavy reflector, the seven reflector geometries are modeled using slab geometries.

A.1.3 Translation of the Heavy Reflector Geometry into Slab Geometries

The U.S. EPR heavy reflector is subdivided into seven geometries as shown in Figure A-1.5. The reflector is modeled using two nodes each equivalent in size to a fuel assembly (FA). This treatment is necessary to be consistent with the nodal treatment in PRISM with 1-node per FA. Using Figure A-1.6 as an illustration for the homogenization process each of the seven reflector geometries are transformed into specific 1-D slab geometries.

These homogenizations are performed using the following rules:

1. The steel and water regions should not be spatially homogenized in the reflector spectral geometry.
2. The thickness of a reflector spectral geometry should be at least two FA sides ($=2 \cdot L_{FA}$).
3. A coolant channel of area A can be turned into a water slab of thickness $b = A/L_{FA}$.
4. If the distance of the water channel is located in the re-entrant corner of the reflector with distances L_x and L_y (Figure A-4) from the fuel in the x-

and y-directions respectively, then the distance d of the corresponding water slab in a 1-D slab geometry is calculated according to

$$\frac{1}{d} = \frac{1}{2} \left(\frac{1}{L_x} + \frac{1}{L_y} \right).$$

5. Neighboring water slabs (Area A_i and distance d_i , $i=1, \dots, n$) can be condensed into a single water slab (Area A and distance d) using the relationship $\frac{A}{d} = \sum_{i=1}^n \frac{A_i}{d_i}$ and $A = \sum_{i=1}^n A_i$. By applying this rule, water slabs with a thickness < 0.2 cm are eliminated. The exception is the additional water gap between the fuel assemblies and the start of the heavy reflector.
6. Water areas in the reflector other than coolant channels are converted to water slabs by means of Rule #4, where the distance d is the center of mass distance in the x-direction.

The water channels inside the heavy reflector along with the water outside the reflector are treated explicitly when defining the heterogeneous slab geometries.

A.1.4 Generation of the Equivalent Heavy Reflector Cross Sections for the U.S. EPR

Including fuel nodes on the left edge of the reflector slab geometries and assigning the appropriate boundary conditions (reflective symmetry to north, south, and west boundaries, and vacuum to the east boundary) defines a set of reflector geometries. The corresponding eigenvalue problems are solved using the 2-D multi-group nodal transport theory model.

The transport theory solutions at the reflector/fuel interface are used to determine the heterogeneous response function matrices. Additionally, from the heterogeneous calculations, a consistent set of homogeneous diffusion theory boundary value problems can be defined with consistent boundary values derived from the heterogeneous cases. The homogeneous cases have a

reflector node with an area equivalent to a single FA. This configuration is consistent with the PRISM calculation. The homogeneous diffusion theory boundary value cases are used to develop the homogeneous response surface functions.

In general, the elements for the homogeneous reflector response matrices are known functions of the coefficients of the diffusion equation and the discontinuity factors in the reflector node. Determining the equivalent cross sections for the homogeneous reflector node means that the set of non-linear equations can be solved that satisfy the requirement that the homogeneous response function be equal to the heterogeneous response function can be solved.

At a thermal cutoff of 0.625 eV, the homogeneous response function for the fast group ranges from 12.2 to 14.1 for the U.S. EPR heavy reflector, and from 5 to 6 for a standard water-shroud reflector. This illustrates the difference in how these two reflector types reflect fast neutrons.

The reflector model in PRISM is not purely macroscopic. The cross section for the PRISM reflector model consists of a macroscopic structural material cross section Σ^{STRM} , a water microscopic cross section σ_{H2O} , and a microscopic boron cross section σ_{B10} with the respective particle number densities N_{H2O} and N_{B10} . Therefore, the equivalent reflector cross sections for the reflector in PRISM is defined as

$$\Sigma^{Equiv.} = \Sigma^{STRM} + N_{H2O}\sigma_{H2O} + N_{B10}\sigma_{B10}$$

The water and boron particle number densities and microscopic cross sections are generated in the spectral calculation using conventional homogenization and condensation. The PRISM reflector library also contains the consistent moderator volume fraction of the reflector node. This water volume fraction is then used by PRISM instead of N_{H2O} and N_{B10} during the rebuilding of the macroscopic cross sections at the node state point conditions.

In addition to the mass affects on the cross sections, the heavy reflector cross sections also have a dependency on boron concentration C_B and moderator temperature T_M . To investigate the importance of these dependencies, heavy reflector cross section libraries were generated for the reflector geometries using the following conditions:

$C_B = 500$ ppm and $T_M = 20, 100, 150, 200, 250, 290, 310$ and 340 °C

$T_m = 310$ °C and $C_B = 0, 500, 750, 1000, 1250, 1500, 1750$ and 2000 ppm

To compensate for only using a 1-D calculation in the generation of the U.S. EPR heavy reflector cross sections, an adjustment to the moderator volume fraction in the reflector is made. The adjustment factor is necessary to compensate for the small inconsistencies seen in the y-direction caused by performing the linearization of the reflector in the x-direction from slab geometry. The correction factor was generated at BOC xenon free conditions for a fresh core at the following conditions:

$C_B = 500$ ppm, $T_m = 312.2$ °C and $T_f = 500$ °C

The adjustment factor was calculated using a representative first core loading pattern, and are determined by comparing the normalized FA fission rate distributions from a reference MCNP calculation to the normalized power distribution from a consistent PRISM calculation using the unadjusted reflector cross sections. The power distribution from PRISM can be used instead of the fission rate distribution because in a UO_2 core, κ_g (Ws/fission) is approximately constant for different FA types. The adjustment factors obtained for the U.S. EPR heavy reflector are applied to the base set of reflector cross sections, and the final cross section libraries with dependencies on boron and moderator temperature are created for each reflector node.

A.1.4.1 MCNP Model

The MCNP5 model used in the calculations presented in this document uses the JEF-2.2 continuous energy library validated for 300K, 600K and 900K with U-235 cross sections taken from the ENDF-B6 library. Typically, 450 million neutron

histories were used to assure that no significant trends exist in the fission rates and that the statistical error of the pin fission rate is less than 1%. The MCNP core inputs are derived from the CASMO inputs used to develop the PRISM cross sections. This is done to provide consistency in the engineering inputs between PRISM and MCNP.

A.1.4.2 PRISM Model

The PRISM model is based on the CASMO-3 K40 cross section library and is developed consistent with the requirements imposed by model development required for reactor design calculations. The PRISM model treats the heavy reflector as a single node of FA size. This approximation was treated in the homogenization of the reflector for the generation of the heavy reflector cross sections. The only restriction imposed on the PRISM calculations are that the feedback model not be used. This requirement is necessary for the PRISM calculations to be consistent with MCNP.

A.1.5 Qualification of PRISM Reflector Model

Since no measured data exists for a core with a heavy reflector, calculational comparisons are required for verification of the performance of the PRISM reflector cross sections obtained from the equivalent reflector model. Therefore, reflector cross sections generated according to the method described in Section A-1.4 were qualified for the U.S. EPR heavy reflector geometry by comparing 2-D fresh core MCNP results to equivalent 2-group 2-D PRISM reactor calculations. These comparisons include different first core loadings with moderator temperature variations over the range $20 \leq T_m \leq 340$ °C and over a range of boron concentrations from $0 \leq C_B \leq 1500$ ppm.

Two core loading patterns were used for these comparisons. These loading patterns consider scenarios that place different enrichments and poison loadings out on the core periphery. For each core design, two sets of MCNP and PRISM calculations were performed. The first set of calculations was performed modeling a standard PWR reflector with a thin shroud. The second set of

calculations was performed using the heavy reflector. By performing these two sets of calculations the impact of the heavy reflector on the process used in generating reflector cross sections with the equivalent reflector model can be shown.

The comparisons between MCNP and PRISM are presented below. The maps presented on the following pages show the difference $(\text{PRISM} - \text{MCNP}) * 100$ for the standard reflector and then the heavy reflector using a specific core design and reactor conditions.

In Figure A-1.7 a comparison is made for the first core design with standard operating conditions ($C_B=500$ ppm, $T_M=312.2$ °C, $T_F=500$ °C), the standard deviation for the standard reflector cases is 0.7% and the standard deviation for the heavy reflector case is 0.9%. The observed differences are small and the standard deviation between the two cases indicates that the use of the homogeneous radial heavy reflector cross sections in PRISM only has a small impact on the comparisons to MCNP at average conditions. The accuracy between PRISM and MCNP remains the same for the heavy reflector and standard PWR reflector cases.

The comparison in Figure A-1.8 examines the effect of different loading patterns using the cross sections generated for the heavy reflector. This comparison is also made using standard operating conditions ($C_B=500$ ppm, $T_M=312.2$ °C, $T_F=500$ °C). The standard deviation of the first loading pattern is 0.9% while the standard deviation when using the second loading pattern is 0.7%. Therefore, the derivation of the heavy reflector cross section libraries is not significantly dependent on the core loading pattern used to generate the libraries.

The comparison in Figure A-1.9 is for the first loading pattern with the boron concentration increased to 1300 ppm ($C_B=1300$ ppm, $T_M=312.2$ °C, $T_F=500$ °C). The PRISM to MCNP comparisons are for both the standard PWR reflector and the heavy reflector. The results from this comparison show that the standard deviation based on the standard PWR reflector is 1.0% and the standard

deviation for the heavy reflector case is 1.0%. This shows good agreement between the standard PWR reflector model and the heavy reflector model with a change in boron concentration.

The final comparison is provided in Figure A-1.10 for the first core loading pattern and considers a change in both the fuel temperature and the moderator temperature. In this case these temperatures have both been set to 100 °C ($C_B=500$ ppm, $T_M=100$ °C, $T_F=100$ °C). The PRISM and MCNP comparisons in this figure consider both the standard PWR reflector and the heavy reflector. The standard deviation for the case with a standard PWR reflector is 2.2% and the standard deviation for the heavy reflector case is 1.4%. As expected the results are worse for the standard PWR reflector due to the amount of water in the reflector region as compared to the U.S. EPR heavy reflector. The change in moderator temperature changes the moderation characteristics of the water in the reflector region and with all the water present in the standard PWR reflector, the solution is going to be more sensitive to the moderation characteristics. The heavy reflector case shows a much smaller change relative to the base case. For the heavy reflector cases, the observed standard deviation is 0.9% for the base case with a change to 1.4% in the temperature branch case.

Additionally power distributions have been made between PRISM and measured plant data for the standard PWR reflector model. These comparisons include Plant A (Westinghouse 157 assembly core), Plant B (Westinghouse 157 assembly core), Plant G1 (Siemens-KONVOI 177 assembly core) and Plant G2 (Siemens-KONVOI 193 assembly core). These plants represent different core and assembly geometries and have shrouds of different thicknesses. All of these benchmarks were performed using reflector cross sections generated using the equivalent reflector model. These cores also provide a range of assembly lattices. The Plant G1 lattice is 15X15, the Plant A and Plant B lattices are 17X17 and the Plant G2 lattice is 18X18. The comparisons of the radial power distributions show good agreement between PRISM and measurement. In all

cases the 0.05 RMS error criterion is met. And all the maps show no tendency toward an in-out tilt.

A.1.6 Conclusion

The reflector homogenization used in the equivalent reflector model is generic for nodal codes as it conserves the nodal response. Homogenization errors are practically eliminated by selecting a set of cross sections that forces the homogeneous response to match the heterogeneous response. The equivalent reflector cross sections therefore depend only on the inherent reflector properties. The equivalent reflector model cross sections can therefore be tabulated as functions of moderator temperature and boron concentration.

The equivalent reflector cross section method was extended to the heavy reflector. In this case, the 2-D calculation was not performed for the re-entrant corners. Rather adjustment factors were generated through comparisons to MCNP. These adjustment factors compensate for the size, number, and position of the reflector water channels. In the PRISM to MCNP comparisons made for both the standard and heavy reflector models, it was shown that PRISM is able to predict the MCNP results. These comparisons also show that the heavy reflector is less sensitive to changes in boron concentration and moderator temperature. This was expected as the heavy reflector is mostly steel with little moderator.

The equivalent reflector model is applicable in the generation of cross sections for the heavy reflector. The method of matching the homogeneous response function to the heterogeneous response function is valid for whatever type of reflector geometry exists. The 2-D calculation used in the equivalent reflector model for the standard PWR reflector design to treat the transverse leakage in the re-entrant nodes was not used for the heavy reflector.

Comparisons between MCNP and PRISM data generated based on 2-D standard reflector model with 0.625 eV thermal energy cutoff for the Siemens - KONVOI plant, which is a 193 assembly plant with a 1/2 inch shroud, showed

good agreement. Good agreement was also obtained between the measured power distributions and the PRISM power distributions for Plant A and B, which are both 157 assembly cores with a 9/8 inch shroud. Therefore, the above described methodology used to generate the heavy reflector cross sections, which rely on matching MCNP results with PRISM results, is appropriate and is expected to yield good agreement with future measured power distributions in the EPR.

A.2.0 SAV95 Benchmarking Results

A.2.1 Introduction

AREVA NP Inc. currently uses the SAV95 (MICBURN/CASMO/PRISM) code system, an NRC approved methodology (Reference A-1), for reload core design. It is the intention of AREVA NP to use this same code system for first core and reload core designs for the U.S. EPR. Reference A-1 requires a new set of benchmarking and validation in case of core designs that are not contained within the specific restrictions set forth by the above document. These restrictions are stated below:

- 1) SAV95 application will be supported by additional code validation to ensure that the methodology and uncertainties are applicable:
 - a) For designs differing from the Westinghouse reactors with 157 fuel assemblies with either 15x15 or 17x17 fuel rod arrays, and CE reactors with 217 fuel assemblies with 14x14 fuel rod arrays,
 - b) When using incore monitoring systems differing from the INPAX-W and INPAX-2 systems contained in this safety evaluation when Siemens Power Corporation (SPC) [AREVA NP] provides input from SAV95.
- 2) Modifications to the code and methodology will be validated using the criteria approved in EMF-96-029(P).

- 3) The validation will be maintained by SPC [AREVA NP] and be available for NRC audit.

The purpose of this document is to provide further validation of the SAV95 system, required by Reference A-1, for U.S. EPR core design calculations based on the following points which fall outside of the above restrictions:

- 1) The U.S. EPR has 241 fuel assemblies with 17x17 fuel rod arrays which have a 13.78 ft. active fuel length; this design is not included in the above restrictions.
- 2) The U.S. EPR will use, as its incore monitoring system, POWERTRAX/S, which is not included in the above restrictions.
- 3) Calculations for U.S. EPR designs will use a 0.625 e.V. cutoff for thermal neutrons, rather than the currently approved 1.855 e.V. thermal cutoff.
- 4) The methodology used for U.S. EPR calculations of the reflector cross-sections is different from the previously approved methodology. (See Section A.1 for reflector cross-section generation methodology)

A.2.2 Summary

The AREVA NP U.S. EPR neutronics design methodology consists of a cross-section generator computer code system and a reactor core simulator computer code system. A flowchart which summarizes these code systems is shown in Figure A-2.1.

The cross-section generator is used to calculate basic nuclear parameters that are required by the reactor core simulator. Input to the cross-section generator includes a nuclear data library (e.g. ENDF/B files), as well as the user input describing the assembly lattice.

The reactor core simulator is used to model the reactor core and perform the basic core calculations required for fuel cycle design, safety analyses, and core

operation follow. This includes input, such as pin-by-pin power distributions, required for an incore monitoring code. Input to the reactor core simulator includes the basic nuclear parameters calculated by the cross-section generator, as well as the user input describing the core.

The demonstration of the adequacy of the design methodology consists of verification that the methodology performs satisfactorily. The neutronics design methodology must produce accurate predictions, as exemplified by comparison with measured results. Additionally, if the methodology is used to produce input for an incore monitoring system, then the associated power distribution measurement uncertainties must be within the previously approved measurement uncertainties for that incore monitoring system.

These considerations are used to establish requirements which, when satisfied, demonstrate that the AREVA NP U.S. EPR neutronic design methodology is acceptable for use in first core and reload core design, licensing, and calculation of startup and core follow data. These requirements include methodology requirements, validation requirements, and verification of previously approved measurement uncertainties for incore monitoring.

A summary of the key validation results for the SAV95 code system is presented in Table A-2.1. The results demonstrate the adequacy of the SAV95 code system to perform neutronic design analyses for the U.S. EPR.

A.2.3 Methodology Description

The methodology description presented in Reference A-1 remains unchanged.

A.2.4 Validation

The AREVA NP neutronics design package, SAV95, consists of a cross-section generator code system and a reactor core simulator computer code system.

Data calculated with SAV95 are compared to measured data in order to demonstrate the accuracy and capability of the code system. Following are comparisons of data calculated with the SAV95 code system to measured data obtained from critical experiments, startup physics tests, and core follow data

obtained from commercial reactors. The validation criteria chosen for the SAV95 model is based on ANSI/ANS-19.6.1 standard Reference A-2.

A.2.4.1 Critical Experiment Reactivity Measurements

The results of the comparison of the SAV95 code system to critical experiments, presented in Reference A-1 for the validation of MICBURN-3/CASMO-3, are still applicable because the U.S. EPR will use the same codes with changes in methodology that do not affect the validity of these experiments.

A.2.4.2 Validation with Commercial Reactor Measurements

A.2.4.2.1 Description of Reactor Cores

The validation calculations originally performed in Reference A-1 involve comparisons with measurements obtained at commercial reactors. Each sample plant has an associated plant type specification and fuel type specification.

The 'plant type' specification refers to the NSSS vendor and the total number of fuel assemblies in the core, examples of 'plant types' in Reference A-1 include:

- Westinghouse reactor containing 157 assemblies
- Combustion Engineering reactor containing 217 assemblies

The 'fuel type' specification refers to the size of the rod array and the guide tube configuration in an assembly, examples of 'fuel types' in Reference A-1 include:

- 14x14 array with Combustion Engineering guide tube configuration
- 15x15 array with Westinghouse guide tube configuration
- 17x17 array with Westinghouse guide tube configuration

A unique combination of a plant type and a fuel type will be referred to as a 'plant/fuel type'. Additional validation in this section shows that the SAV95 code system is capable of adequately modeling PWR cores, such as the U.S. EPR.

This validation used the following plant/fuel types:

- Westinghouse 157 assembly, 17x17 array
- Siemens KONVOI 193 assembly, 18x18 array

- Siemens KONVOI 177 assembly, 15x15 array

For each sample plant, measured data from one or more cycles is used in comparisons with predictions. A description of each plant and cycle used in the validation calculations is provided in order to illustrate the range of parameters used in the benchmarking. This description includes:

- Description of the fresh and burnt fuel assemblies, including:
 - Initial enrichments
 - Burnable poison loading
- Cycle length
- Any unique features of this plant/cycle

Four plants, each with a unique plant/fuel type combination, are used in this validation against commercial reactor measurements. The sample plants and corresponding cycle descriptions are:

Plant A

Plant Type: Westinghouse reactor containing 157 assemblies

Fuel Type: 17x17 array with Westinghouse guide tube configuration

Plant A Cycle 1

This cycle was loaded with 157 fresh fuel assemblies, including 53 at 2.1 w/o U-235, 52 at 2.6 w/o U-235, and 52 at 3.1 w/o U-235. The fresh fuel contained 1040 discrete burnable absorber rods utilizing boron, which were loaded in guide tube locations. The cycle operated to approximately 15,285 MWd/MTU.

Plant A Cycle 2

This cycle design loaded 52 fresh assemblies, including 36 at 3.60 w/o U-235 and 16 at 4.00 w/o U-235. The burned fuel assemblies included 105 once-burnt assemblies at 3.10, 2.60, and 2.10 w/o U-235. The fresh fuel contained 576 discrete burnable absorber rods utilizing boron, which were loaded in guide tube locations. The cycle operated to approximately 12,593 MWd/MTU.

Plant A Cycle 3

This cycle design loaded 52 fresh assemblies, including 24 at 4.00 w/o U-235 and 28 at 4.40 w/o U-235. The burned fuel assemblies included 53 once-burnt assemblies at 4.00, 3.60, and 2.10 w/o U-235, and 52 twice-burnt assemblies at 3.10 and 2.60 w/o U-235. The fresh fuel included 4144 fuel rods with boron-coated pellets. The cycle operated to approximately 15,117 MWd/MTU.

Plant A Cycle 4

This cycle design loaded 60 fresh assemblies, including 32 at 4.40 w/o U-235 and 28 at 4.80 w/o U-235. The burned fuel assemblies included 52 once-burnt assemblies at 4.40 and 4.00 w/o U-235, and 45 twice-burnt assemblies at 4.00, 3.60, and 3.10 w/o U-235. The fresh fuel contained 176 discrete burnable absorber rods utilizing boron, which were loaded in guide tube locations, and 5,504 fuel rods with boron-coated pellets. The cycle operated to approximately 18,035 MWd/MTU.

Plant A Cycle 5

This cycle design loaded 60 fresh assemblies, including 32 at 4.40 w/o U-235 and 28 at 4.80 w/o U-235. The burned fuel assemblies included 64 once-burnt assemblies at 4.80, 4.40, and 2.10 w/o U-235, and 33 twice-burnt assemblies at 4.40 and 4.00 w/o U-235. The fresh fuel contained 96 discrete burnable absorber rods utilizing boron (loaded in guide tube positions) and 4,096 fuel rods with boron-coated pellets. The cycle operated to approximately 19,198 MWd/MTU.

Plant A Cycle 6

This cycle design loaded 52 fresh assemblies at 4.95 w/o U-235. The burned fuel assemblies included 69 once-burnt assemblies at 4.80, 4.40, and 2.10 w/o U-235, and 36 twice-burnt assemblies at 4.80 and 4.40 w/o U-235. The fresh

fuel contained 832 gadolinia-bearing fuel rods in concentrations of 2, 6, and 8 w/o Gd_2O_3 . The cycle operated to approximately 18,367 MWd/MTU.

Plant A Cycle 7

This cycle design loaded 60 fresh fuel assemblies at 4.81 w/o U-235. The burned fuel assemblies included 77 once-burnt assemblies at 4.95 and 2.10 w/o U-235, and 20 twice-burnt assemblies at 4.80 w/o U-235. The fresh fuel contained 944 gadolinia-bearing fuel rods in concentrations of 2, 4, 6, and 8 w/o Gd_2O_3 . The cycle operated to approximately 19,051 MWd/MTU.

Plant A Cycle 8

This cycle design loaded 60 fresh fuel assemblies, including 24 at 4.47 w/o U-235 and 36 at 4.90 w/o U-235. The burned fuel assemblies included 60 once-burnt assemblies at 4.81 w/o U-235, and 37 twice-burnt assemblies at 4.95 and 3.10 w/o U-235. The fresh fuel contained 1168 gadolinia-bearing fuel rods in concentrations of 2, 6, and 8 w/o Gd_2O_3 . The cycle operated to approximately 18,815 MWd/MTU.

Plant A Cycle 9

This cycle design loaded 56 fresh fuel assemblies, including 20 at 4.35 w/o U-235 and 36 at 4.85 w/o U-235. The burned fuel assemblies included 60 once-burnt assemblies at 4.90 and 4.47 w/o U-235, and 41 twice-burnt assemblies at 4.81 and 3.10 w/o U-235. The fresh fuel contained 1088 gadolinia-bearing fuel rods in concentrations of 2, 4, 6, and 8 w/o Gd_2O_3 . The cycle operated to approximately 18,731 MWd/MTU.

Plant A Cycle 10

This cycle design loaded 60 fresh fuel assemblies, including 32 at 4.25 w/o U-235 and 28 at 4.75 w/o U-235. The burned fuel assemblies included 61 once-burnt assemblies at 4.85, 4.35, and 2.10 w/o U-235, and 36 twice-burnt

assemblies at 4.90 w/o U-235. The fresh fuel contained 1136 gadolinia-bearing fuel rods in concentrations of 2, 4, 6, and 8 w/o Gd_2O_3 . The cycle operated to approximately 18,910 MWd/MTU.

Plant A Cycle 11

This cycle design loaded 65 fresh fuel assemblies at 4.95 w/o U-235. The burned fuel assemblies included 64 once-burnt assemblies at 4.75 and 4.25 w/o U-235, and 28 twice-burnt assemblies at 4.85 w/o U-235. The fresh fuel contained 1208 gadolinia-bearing fuel rods in concentrations of 2, 4, 6, and 8 w/o Gd_2O_3 . The cycle operated to approximately 19,003 MWd/MTU.

Plant A Cycle 12

This cycle design loaded 64 fresh fuel assemblies, including 36 at 4.35 w/o U-235 and 28 at 4.85 w/o U-235. The burned fuel assemblies included 65 once-burnt assemblies at 4.95 w/o U-235 and 28 twice-burnt assemblies at 4.75 w/o U-235. The fresh fuel contained 1568 gadolinia-bearing fuel rods in concentrations of 2, 4, 6, and 8 w/o Gd_2O_3 . The cycle operated to approximately 19,742 MWd/MTU.

Plant A Cycle 13

This cycle design loaded 65 fresh fuel assemblies at 4.95 w/o U-235. The burned fuel assemblies included 64 once-burnt assemblies at 4.85 and 4.35 w/o U-235, and 28 twice-burnt assemblies at 4.95 w/o U-235. The fresh fuel contained 1588 gadolinia-bearing fuel rods in concentrations of 2, 4, 6, and 8 w/o Gd_2O_3 . The cycle was incomplete at the time of this document being released but will operate nominally to 20,246.

Plant B

Plant Type: Westinghouse reactor containing 157 assemblies

Fuel Type: 17x17 array with Westinghouse guide tube configuration

Plant B Cycle 1

This cycle was loaded with 157 fresh fuel assemblies, including 53 at 1.8 w/o U-235, 52 at 2.4 w/o U-235, and 52 at 3.1 w/o U-235. The fresh fuel contained 448 discrete burnable absorber rods utilizing boron, which were loaded in guide tube locations, and 352 gadolinia-bearing fuel rods in a concentration 8 w/o Gd_2O_3 . The cycle operated to approximately 14,808 MWd/MTU.

Plant G2

Plant Type: Siemens - KONVOI reactor containing 193 assemblies

Fuel Type: 18x18 array (guide tube configuration shown in Figure 4.1(a))

Only limited startup physics data is available for this plant.

Plant G2 Cycle 1

This cycle was loaded with 193 fresh fuel assemblies, including 69 at 1.9 w/o U-235, 68 at 2.5 w/o U-235, and 56 at 3.2 w/o U-235. The fresh fuel contained 1152 gadolinia-bearing fuel rods with concentrations of 3, 5, and 7 w/o Gd_2O_3 . The cycle operated to approximately 16,695 MWd/MTU.

Plant G2 Cycle 2

This cycle design loaded 72 fresh fuel assemblies, including 4 at 3.2 w/o U-235, 52 at 3.45 w/o U-235, and 16 at 3.5 w/o U-235. The burned fuel assemblies included 121 once-burnt assemblies at 3.2, 2.5, and 1.9 w/o U-235. The fresh fuel contained 624 gadolinia-bearing fuel rods in a concentration of 7 w/o Gd_2O_3 . The cycle operated to approximately 13,207 MWd/MTU.

Plant G2 Cycle 3

This cycle design loaded 64 fresh fuel assemblies, including 48 at 3.45 w/o U-235 and 16 at 3.5 w/o U-235. The burned fuel assemblies included 100 once-burnt assemblies at 3.5, 3.45, 3.2, and 2.5 w/o U-235, and 29 twice-burnt assemblies at 3.1 and 1.9 w/o U-235. The fresh fuel contained 576 gadolinia-

bearing fuel rods in a concentration of 7 w/o Gd_2O_3 . The cycle operated to approximately 13,108 MWd/MTU.

Plant G2 Cycle 4

This cycle design loaded 64 fresh fuel assemblies, including 44 at 3.45 w/o U-235 and 20 at 3.5 w/o U-235. The burned fuel assemblies included 80 once-burnt assemblies at 3.5, 3.45, 2.5, and 1.9 w/o U-235, 37 twice-burnt assemblies at 3.5, 3.45, 3.2, and 2.5 w/o U-235, and 12 thrice-burnt assemblies at 1.9 w/o U-235. The fresh fuel contained 528 gadolinia-bearing fuel rods in a concentration of 7 w/o Gd_2O_3 . The cycle operated to approximately 11,560 MWd/MTU.

Plant G2 Cycle 5

This cycle design loaded 44 fresh fuel assemblies, including 32 at 3.8 w/o U-235, 4 at 3.5 w/o U-235, and 8 at 3.45 w/o U-235. The burned fuel assemblies included 72 once-burnt assemblies at 3.5 and 3.45 w/o U-235, and 77 twice-burnt assemblies at 3.5, 3.45, and 3.2 w/o U-235. The fresh fuel contained 336 gadolinia-bearing fuel rods in a concentration of 7 w/o Gd_2O_3 . The cycle operated to approximately 11,612 MWd/MTU.

Plant G1

Plant Type: Siemens - KONVOI reactor containing 177 assemblies

Fuel Type: 15x15 array (guide tube configuration shown in Figure 4.1(b))

Only limited startup physics data is available for this plant.

Plant G1 Cycle 26

This cycle contained 44 fresh fuel assemblies, including 20 at 3.50 w/o U-235, 16 at 4.00 w/o U-235, and 8 at 3.75 w/o U-235. The burned fuel assemblies included 32 once-burnt assemblies at 3.75 w/o U-235, 24 twice-burnt assemblies at 3.75 and 3.50 w/o U-235, 49 thrice-burnt assemblies at 3.75 and 3.50 w/o U-235, and 28 fourth-burnt assemblies at 3.50 w/o U-235. The fresh fuel contained

128 gadolinia-bearing fuel rods in a concentration of 2 w/o Gd_2O_3 . The cycle operated to approximately 12,796 MWd/MTU.

Plant G1 Cycle 27

This cycle contained 48 fresh fuel assemblies, including 28 at 4.00 w/o U-235 and 20 at 3.50 w/o U-235. The burned fuel assemblies included 44 once-burnt assemblies at 4.00, 3.75, and 3.50 w/o U-235, 33 twice-burnt assemblies at 3.75 and 3.50 w/o U-235, 24 thrice-burnt assemblies at 3.75 and 3.50 w/o U-235, 8 fourth-burnt assemblies at 3.50 w/o U-235, and 20 fifth-burnt assemblies at 3.50 w/o U-235. The cycle operated to approximately 13,014 MWd/MTU.

Plant G1 Cycle 28

This cycle contained 48 fresh fuel assemblies at 4.00 w/o U-235. The burned fuel assemblies included 44 once-burnt assemblies at 4.00 and 3.50 w/o U-235, 44 twice-burnt assemblies at 4.00, 3.75 and 3.50 w/o U-235, 33 thrice-burnt assemblies at 3.75 and 3.50 w/o U-235, and 8 fourth-burnt assemblies at 3.75 w/o U-235. The fresh fuel contained 128 gadolinia-bearing fuel rods in a concentration of 5 w/o Gd_2O_3 . The cycle operated to approximately 13,053 MWd/MTU.

Plant G1 Cycle 29

This cycle contained 48 fresh fuel assemblies, including 40 at 4.00 w/o U-235, 4 at 3.75 w/o U-235, and 4 at 3.50 w/o U-235. The burned fuel assemblies included 52 once-burnt assemblies at 4.00 w/o U-235, 44 twice-burnt assemblies at 4.00 and 3.50 w/o U-235, 25 thrice-burnt assemblies at 4.00, 3.75 and 3.50 w/o U-235, and 8 fifth-burnt assemblies at 3.50 w/o U-235. The fresh fuel contained 192 gadolinia-bearing fuel rods in a concentration of 5 w/o Gd_2O_3 . The cycle operated to approximately 13,057 MWd/MTU.

Plant G1 Cycle 30

This cycle contained 44 fresh fuel assemblies, including 40 at 4.40 w/o U-235, and 4 at 4.00 w/o U-235. The burned fuel assemblies included 48 once-burnt assemblies at 4.00, 3.75 and 3.50 w/o U-235, 52 twice-burnt assemblies at 4.00 w/o U-235, 25 thrice-burnt assemblies at 4.00, 3.75 and 3.50 w/o U-235, and 8 fourth-burnt assemblies at 3.50 w/o U-235. The fresh fuel contained 192 gadolinia-bearing fuel rods in a concentration of 5 w/o Gd₂O₃. The cycle operated to approximately 12,922 MWd/MTU.

A.2.4.2.2 Startup Physics Test Measurements

Comparisons include two different plant/fuel types with additional data, as available from Siemens - KONVOI type reactors. Additionally, 14 cycles of operation are evaluated. Startup physics test predictions are compared to the available measured data at beginning-of-cycle for each cycle of each plant/fuel type. The parameters and criteria compared are:

- 1) All rods out critical boron concentration
Criteria: Calculated within ± 50 ppm of measured
- 2) Individual control bank worths
Criteria: Individual bank worths calculated within $\pm 15\%$ or ± 100 pcm of measured, whichever is larger
- 3) Total control bank worth
Criteria: Total bank worth calculated within $\pm 10\%$ of measured
- 4) All rods out isothermal temperature coefficient
Criteria: Calculated within ± 2 pcm/ $^{\circ}$ F of measured

The above list of parameters is representative of the startup physics test data typically available from commercial U.S. reactor measurements at zero power conditions; however, some of the cycles that were analyzed for U.S. EPR calculations are of European plants, from which certain startup physics test data is unavailable. The criteria for the parameters are based on the recommended test criteria provided in Reference A-2.

The results of the comparisons of SAV95 calculations with measured results are summarized in Table A-2.2. The measured data has been adjusted to reflect the SAV95 delayed neutron parameters.

The 18.2% deviation between the measured and calculated BOC HZP Shutdown Bank A of Plant A Cycle 12 is considered an anomaly and is therefore not considered when determining the applicability of the SAV95 control rod worth calculations. The conclusion that this data point is an anomaly is based on the fact that Shutdown Bank A meets the criteria in preceeding as well as subsequent cycles. Also, all other banks in Cycle 12 meet the acceptance criteria, including the total rod worth. This information supports the conclusion that the control rod worths calculated by SAV95 are acceptable.

A.2.4.2.3 Core Follow Measurements

Comparisons include two different plant/fuel types with additional data, as available from Siemens - KONVOI type reactors. A total of 24 cycles have been considered, which exceeds the criteria of a minimum of 9 cycles set forth in Reference A-1. Core follow predictions are compared to the available data measured at or near hot full power for each cycle of each plant/fuel type. The parameters compared are:

- 1) Critical boron concentrations

Criteria: Calculated within ± 50 ppm measured

Comparisons are performed for a minimum of one measured data point per 30 effective full power days (EFPD) throughout the cycle. The comparisons may use the trend of the measured data to avoid comparison with infrequent measurement anomalies.

- 2) Assembly average power distributions

Criteria: The root mean square (RMS) of the absolute differences between the calculated and measured assembly powers is < 0.05 for each map.

At least three comparison maps are provided per cycle, corresponding to the beginning-, middle-, and end-of-cycle conditions. These comparisons may be in a full-core format or, if the core loading is quarter-core symmetric, the symmetrically located measured powers may be averaged to allow comparisons in a quarter-core format.

3) Core average axial power distributions

Criteria: The root mean square (RMS) of the absolute differences between the calculated and measured core average axial powers is < 0.05 for each map. At least three comparisons are provided per cycle, corresponding to the beginning-, middle-, and end-of-cycle conditions.

Measured boron concentration and power distribution data are typically available from commercial reactor measurements at full power conditions as a function of cycle burnup. The criteria for these parameters are based on the recommended test criteria provided in Reference A-2.

The results of the comparison of SAV95 calculations with measured results are summarized in Table A-2.3. The results are within the specified criteria.

The HFP critical boron concentration in the core follow results for Plant A Cycle 1 is considered an anomalous data point and is therefore not considered when determining the applicability of SAV95 in predicting HFP boron concentrations. The deviation in the calculated versus measured values is of unknown origin; however, it is likely caused by insufficient modeling of the core follow because of a lack of first cycle data availability. Also, all of the other cycles analyzed have met the criteria and the HFP critical boron concentrations calculated by SAV95 are acceptable.

Plants G1 and G2 both use the Aeroball Measurement System and the POWERTRAX/S methodology for the calculation of the measured power distributions. Since this is the core monitoring system that the U.S. EPR will use,

a summary of the power distributions of all available maps (beyond the presented BOC, MOC, and EOC maps) from these two plants is provided in Table A-2.21.

Two maps in Plant G2, Cycle 1 do not meet the criteria for the axial power distribution. It is shown in Table A-2.21 that the axial offset during the data acquisition was over 7% in magnitude. This axial offset is not present in the PRISM model because some information was not available from the German customer to correctly model the rod positions. The difference in the axial offset between the actual plant conditions and the modeled conditions leads to larger difference in the measured to calculated axial power distribution comparison.

A.3.0 *Power Distribution Uncertainties for POWERTRAX/S*

A.3.1 Introduction

A three dimensional core power distribution is calculated by POWERTRAX/S from a combination of measured and calculated data. The power distribution calculated by POWERTRAX/S is referred to as the inferred power distribution to differentiate it from the specific measured and calculated data utilized by the code. Section A.3.1 presents a description of the methodology used to derive the inferred core power distribution in POWERTRAX/S. Section A.3.2 presents a description of the methodology used to derive an estimate of the combined calculated and measured uncertainties in the inferred core power distribution. The description of this methodology is provided only as a basis for presenting the calculated to measured power distribution comparisons in this document. The inferred power distribution reconstruction methodology and uncertainty analysis will be discussed in a future topical report and approval of that methodology is not requested at this time.

A.3.2 Inferred Relative Power Distribution Calculation

The Aeroball Measurement System (AMS) is used to obtain detector signals at numerous axial points in operable instrumented locations. The AMS for a 1300 MWe Siemens - KONVOI PWR consists of 28 probes that are inserted in the reactor core. After activation in the core the measurement signals of the

vanadium probes are stored with an axial resolution of 32 positions. The U.S. EPR design will utilize 40 probes with an axial resolution of 36 positions.

The core simulator PRISM calculates theoretical three dimensional power, burnup and neutron flux distributions and detector signals based on a physical core model which is continuously updated online in order to account for actual state parameters such as thermal reactor power, bank configurations, inlet temperature, etc. The number of axial nodes used in the PRISM model for incore monitoring corresponds to the axial resolution of the AMS, although the boundaries generally will not be identical due to consideration of the material boundaries of the fuel assemblies (FA). This is not necessarily the nodalization used in design calculations.

The inferred power distribution is generated by the module MEDIAN (**M**asured **D**ependent **I**nterpolation **A**lgorithm using **N**EM) using information from the theoretical PRISM calculation and the measured activation rate distribution. Radially the measured activation distribution corresponds exactly to the geometry of the calculation model. Axially the measured activation distribution is interpolated appropriately to match the nodal geometry of the calculation model.

MEDIAN then solves for the inferred power distribution in 2 steps:

- Determination of the node fluxes at the instrumented positions by Kalman-Filter-Technique
- Extrapolation of the fluxes to the non-instrumented locations by use of the nodal balance equation

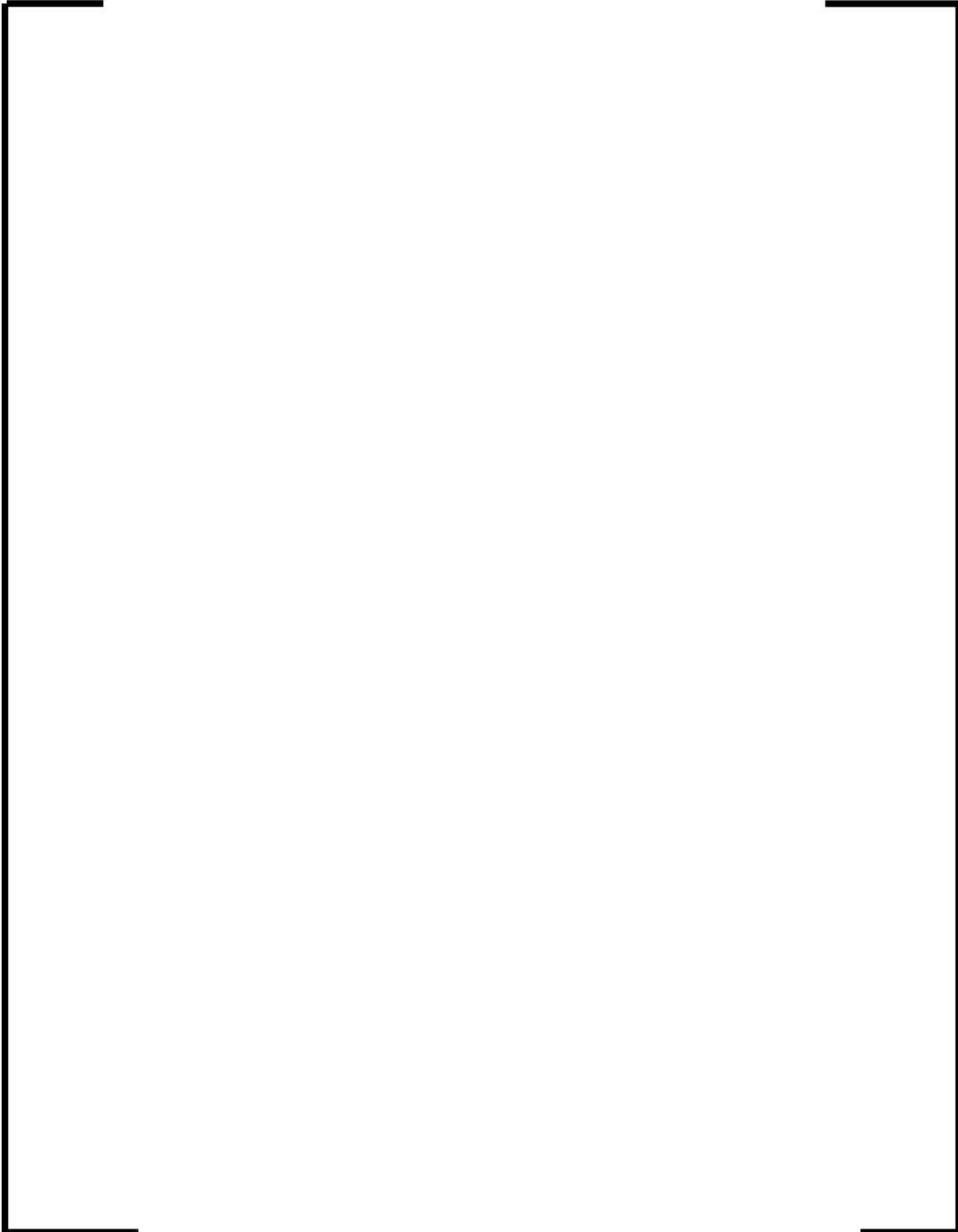
As a final step, spacer grid axial form functions for power and activation rates are applied to the non-instrumented locations. This adjustment is performed in a program external to PRISM/MEDIAN. See Section A.3.2.3.

A.3.2.1 Determination of the Optimal Node Fluxes

Using the Kalman-Filter-Technique MEDIAN adapts the group-wise neutron fluxes at the measured nodes to achieve optimal consistency between theoretical results and measurement. For the U.S. EPR, the measurement error of the

activation distribution is assumed zero in this derivation and the AMS measurement uncertainty is contained in the uncertainties derived in Section A.3.3.

In the following, the filter equations for the optimal fluxes are presented:



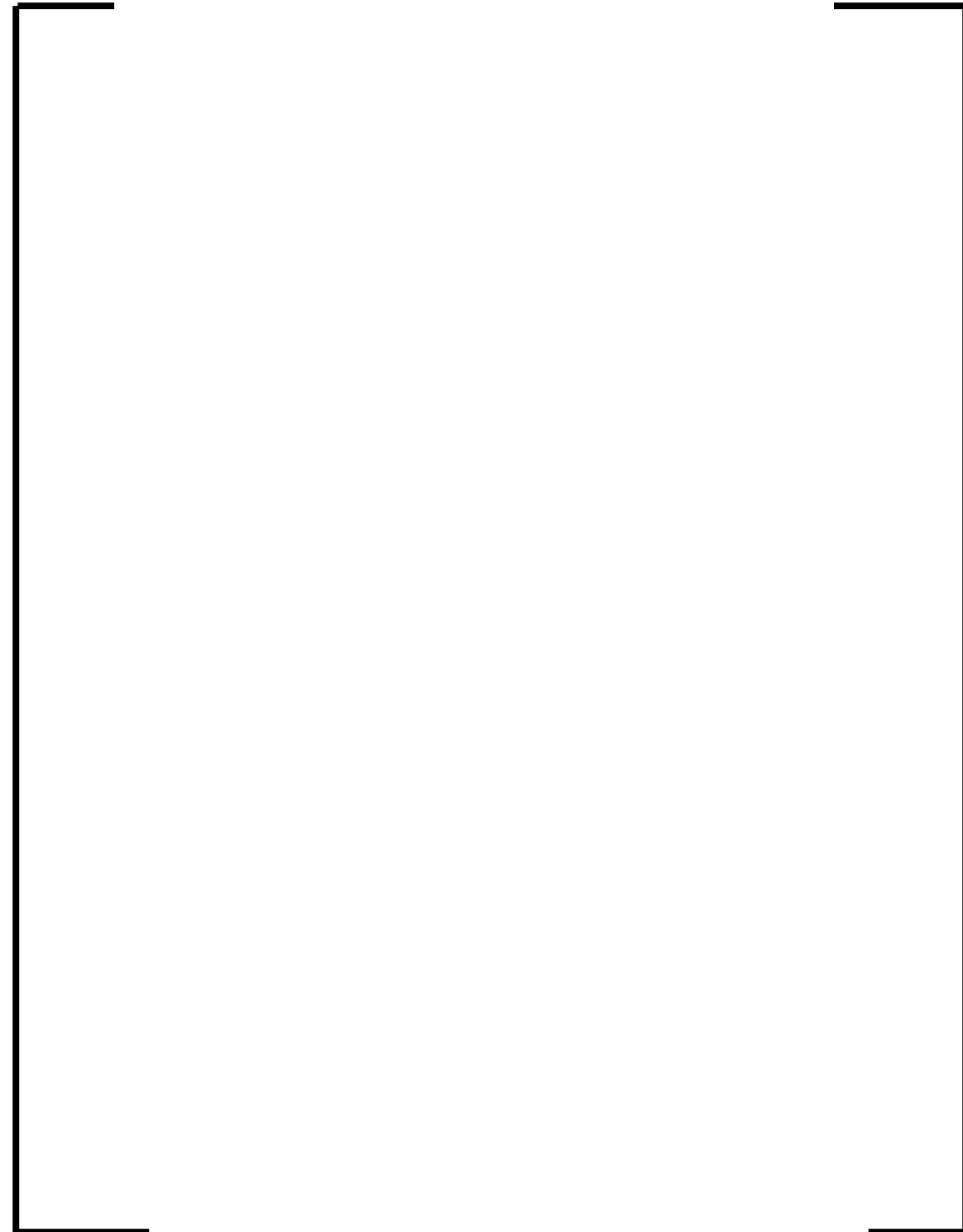


Simplistically the above described process adjusts the calculated fluxes in the measured nodes so that:

- The resulting activation rates agree with measurement.
- The variance between the original two group fluxes and the optimized fluxes is minimized.

A.3.2.2 Extrapolation of the Node Fluxes

After the optimal fluxes have been calculated in the instrumented nodes as described in A.3.2.1, the fluxes in the remaining non-instrumented nodes must be determined. The flux extrapolation is calculated by the physical models involved in the NEM method and not by a purely mathematical variance minimization approach. Therefore FA quantities like cross sections, flux and burnup gradients remain unchanged. By means of the optimal neutron fluxes in the instrumented FAs the nodal balance equation is modified and the flux distribution for the non-instrumented nodes n is determined by solving the following equation (see Reference A-1 Section 4.2):



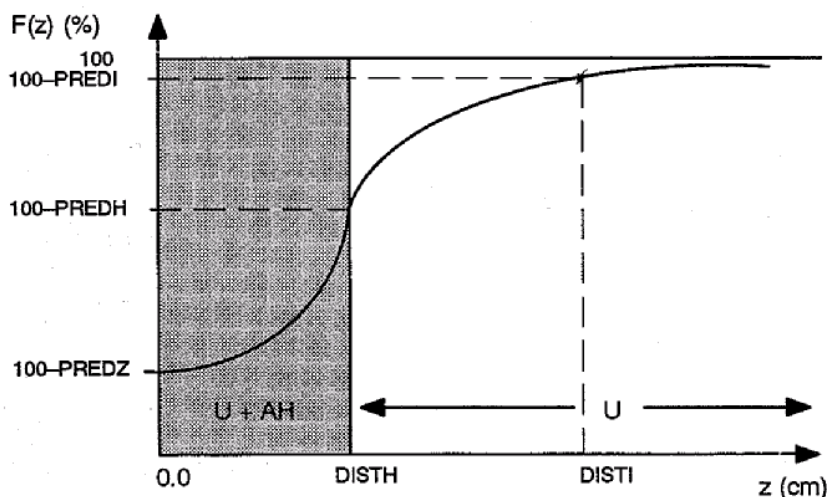
This inhomogeneous linear equation system in ϕ_g is now solved conserving the eigenvalue from the non-adapted solution and the optimal fluxes in the instrumented nodes. The result is a core wide node-wise 2-group flux

distribution. From this distribution other quantities such as nodal powers and pin powers can be derived.

A.3.2.3 Application of Spacer Grid Axial Form Functions

The 3D power distribution calculated in the instrumented nodes will necessarily include the flux depression effect due to the presence of grid spacers since the measured activation distributions include this effect. In the calculation of the 3D power distributions in the non-instrumented nodes, the flux depression effect becomes somewhat diluted since the cross sections and coupling coefficients of the non-adapted solution do not include this effect. In order to capture the flux depression effect due to the presence of grid spacers, POWERTRAX/S applies axial Spacer Grid Form Functions (SGFF) to the axial power distributions in non-instrumented locations using a post-processing program.

The SGFF parameters are dependent on burnup and material (Inconel or Zircaloy). Other dependencies such as varying fuel enrichments or special spacer grid designs have been shown to be negligible. The following sketch shows the qualitative behavior of the form function $F(z)$ as a function of the curve parameters DISTH, DISTI, PREDZ, PREDH, and PREDI:



DISTH = half thickness of the spacer grid, cm

DISTI = distance of the third point from the center of the spacer grid, cm

PREDZ = power reduction in % at the center of the spacer grid

PREDH = power reduction in % at the spacer grid edge (DISTH)

PREDI = power reduction in % at distance DISTI

After appropriate application of the SGFF at all spacer locations, a renormalization is performed such that the FA power is unchanged.

A.3.3 Inferred Relative Power Distribution Uncertainties

The methodology used to derive inferred relative power distribution uncertainties is essentially the same as the methodology described in Section 5.0 of Reference A-3 and details are not repeated herein. This methodology was further applied in Reference A-1.

The measurement uncertainties for the power distribution peaking factors $F_{\Delta h}$ and F_q are derived for an AMS incore measurement system. The methodology used to calculate the inferred relative power distribution in conjunction with the AMS monitoring system is described in Section A.3.2.

Data reduction and statistical treatment techniques are used to derive one-sided 95/95 relative uncertainties. The technique used in this analysis differs from that of Reference A-3 in that the statistical analysis only uses data from:

1. UO₂ only pin powers for the local peaking factor (LPF) uncertainty component.
2. Relative assembly powers > 0.9 for the assembly power distribution uncertainty component for $F_{\Delta h}$.
3. Relative nodal powers > 0.9 in assemblies w/ relative assembly power > 0.9 for the nodal power distribution uncertainty component for F_q .

Since the uncertainty is applied to the core limiting values, it is more important to use data based upon high powered locations. Only UO₂ pin powers were used for the LPF uncertainty component because the very low gadolinia pin powers skewed the statistics when differences were converted to percentages. Note that in Reference A-1 the database used for items 2 and 3 was reduced to relative

assembly powers > 1.0 , and the database used for item 3 excluded the top and bottom 10% or 15% of the axial core height. The methodology in Reference A-1 was not pursued in lieu of the more general approach described above which considers all axial locations.

A.3.3.1 Nodal and Assembly Power Distribution Uncertainties

The standard deviations of the relative uncertainty in the assembly ($F_{\Delta h}$) and nodal (F_q) power distributions will be obtained from 147 measurements taken over 10 cycles of operation at two independent reactors which utilize AMS incore monitoring systems:

1. G1 is a 177 assembly core with a 15x15 fuel lattice and an active fuel height of 9.83 feet. The G1 AMS includes 24 columns divided into 30 axial layers. G1 measured data from 76 maps in Cycles 26 through 30 will be used in the analysis. These maps are at or near hot full power conditions and include gadolinia fuel.
2. G2 is a 193 assembly core with an 18x18 fuel lattice and an active fuel height of 12.85 feet. The G2 AMS includes 28 columns divided into 32 axial layers. G2 measured data from 62 maps in Cycles 1 through 5 will be used in the analysis. These maps are at or near hot full power conditions and include gadolinia fuel.

Reference A-3 Section 5 should be referred to for details of the method used to derive these uncertainties.

A.3.3.2 Local Peaking Factor Uncertainty

The standard deviation of the relative uncertainty in the local peaking factor was determined by comparisons of calculated pin-by-pin fission rate distributions with critical experiment measurements performed by Babcock & Wilcox (Reference A-4). These comparisons included 6 distributions which cover a variety of lattice configurations, various enrichments and the inclusion of burnable absorbers.

Only UO_2 pin powers were used for the LPF uncertainty component because the very low gadolinia pin powers skewed the statistics when differences were converted to percentages. However, the gadolinia pin power differences did behave similarly to the UO_2 pin power differences. As the gadolinia burns out the gadolinia pin power percent differences would be expected to behave like the UO_2 pin power percent differences.

From comparisons of the calculated to measured pin-by-pin fission rate distributions, values for the combined uncertainties in calculation and measurement were determined. The uncertainties for the gadolinia-bearing assemblies are larger than those for the non-gadolinia-bearing assemblies. Conservatively, the final calculated local peaking factor uncertainty is determined by statistically combining the calculation uncertainties from the gadolinia-bearing assembly distributions only, resulting in a standard deviation of 1.335%. The mean value of +0.027 will be conservatively ignored.

An analysis was performed to determine the impact of changing the 2 group energy cutoff from 1.855 eV to 0.625 eV. The standard deviation for all pins (UO_2 and gadolinia) in the gadolinia-bearing assemblies was 1.456% and 1.469% for the 1.855 eV and the 0.625 eV cutoffs, respectively, i.e. difference less than 0.1%.

A.3.3.3 Combined Power Distribution Measurement Uncertainties

The standard deviations of the relative uncertainties associated with the assembly ($F_{\Delta h}$) and nodal (F_q) power distributions and the local peaking factor determined in Sections A.3.2.1 and A.3.2.2 are statistically combined and expressed in terms of relative standard deviations. A one-sided 95/95 tolerance factor is applied to the corresponding relative standard deviation, thereby resulting in the final relative uncertainty factor for each peaking factor. Any negative biases are also accounted for in the final relative uncertainty factors. Table A-3.1 provides a summary of the inputs used to derive the power distribution uncertainties.

Reference A-3 Section 5 should be referred to for details of the method used to combine these uncertainties. Final calculated U.S. EPR uncertainties will be provided as part of a future topical submittal.

A.4.0 *References*

- A-1. "Reactor Analysis System for PWRs," EMF-96-029(P)(A), Volumes 1 and 2
- A-2. "Reload Startup Physics Tests for Pressurized Water Reactors," ANSI/ANS-19.6.1-1995, American Nuclear Society, 1985.
- A-3. "Power Distribution Measurement Uncertainty For INPAX-W in Westinghouse Plants," EMF-93-164(P)(A),
- A-4. "Urania Gadolinia: Nuclear Model Development and Critical Experiment Benchmark", DOE/ET/34212-41, BAW-1810, April 1984.

Table A-2.1: Summary of SAV95 Validation Criteria and Results

Parameter	Criteria	SAV95 Result
Startup Physics Test		
ARO HZP Critical Boron Concentration	Maximum absolute difference <50 ppm	Maximum absolute difference 48 ppm
Total HZP Control Bank Worths	Maximum absolute difference <10%	Maximum absolute difference 8.49%
ARO HZP Isothermal Temperature Coefficient	Maximum absolute difference of <2.0 pcm/°F	Maximum absolute difference 0.990 pcm/°F
Core Follow Measurements		
HFP Critical Boron Concentrations	Maximum absolute difference measured and calculated <50 ppm	Maximum absolute difference measured and calculated <50 ppm
Assembly Average Power Distributions	Maximum RMS difference <5.0%	Maximum RMS difference 0.027
Core Average Axial Power Differences	Maximum RMS difference <5.0%	Maximum RMS difference 0.047

Table A-2.2: Results of SAV95 Calculations with Startup Physics Test Measurements

Description	Results	Criteria	Comments
Plant/fuel types	4	>3	Plants A, B, G1 and G2
Number of Westinghouse plant types	2	>1	Plants A and B
Number of Siemens - KONVOI plant types	2	>1	Plants G1 and G2
Number of evaluated cycles per plant type	14 cycles for Westinghouse reactors with 157 assemblies, 5 cycles for Siemens - KONVOI reactor with 193 assemblies, 5 cycles for Siemens - KONVOI with 177 assemblies	>3	13 Cycles for Plant A, 1 Cycle for Plant B, 5 Cycles for Plant G2, 5 Cycles for Plant G1
Total number of evaluated cycles	24	>9	
ARO HZP Critical Boron Concentrations	Maximum absolute difference of 48 ppm	Maximum absolute difference 50 ppm	See Table A-2.4
Individual HZP Control Bank Worths	Maximum absolute difference 12.06%*	Maximum absolute difference 15% or 100 pcm, whichever is larger	See Tables A-2.5 thru A-2.18. Data unavailable for Siemens - KONVOI reactors.
Total HZP Control Bank Worths	Maximum absolute difference 8.49%	Maximum absolute difference 10%	See Table A-2.19. Data unavailable for Siemens - KONVOI reactors.
ARO HZP Isothermal Temperature Coefficient	Maximum absolute difference 0.990 pcm/°F	Maximum absolute difference 2.0 pcm/°F	See Table A-2.20. Data unavailable for Siemens - KONVOI reactors.

* Excludes one anomalous data point, see Section A.2.4.2.2.

Table A-2.3: Results of SAV95 Calculations with Core Follow Measurements

Description	Results	Criteria	Comments
Plant/fuel types	4	>3	Plants A, B, G1
Number of Westinghouse plant types	2	>1	Plants A and B
Number of Siemens - KONVOI plant types	2	>1	Plants G1 and G2
Number of evaluated cycles per plant type	13 cycles for Westinghouse reactor with 157 assemblies, 5 cycles for Siemens - KONVOI with 193 assemblies, 5 cycles for Siemens - KONVOI with 177 assemblies	>3	12 cycles for Plant A, 1 cycles for Plant B, 5 cycles for Plant G2, 5 cycles for Plant G1
Total number of evaluated cycles	26	>9	
HFP Critical Boron Concentrations	Minimum of one measured data point per 30 EFPD for US plants... as available for European plants	Minimum of one measured data point per 30 EFPD	Plots provided in Figures A-2.3 – A-2.25, Frequency of data available for European plants does not meet 30 EFPD criteria
	Maximum absolute difference between trend of measured data and calculated data <50 ppm*	Maximum absolute difference 50 ppm	
Assembly Average Power Distributions	Maximum RMS difference of 0.027	Maximum RMS difference <0.05	Maps provided for BOC, MOC, and EOC conditions in Figures A-2.26 thru A-2.94
Core Average Axial Power Distributions	Maximum RMS difference of 0.047**	Maximum RMS difference <0.05	Plots provided for BOC, MOC, and EOC conditions in Figures 4.95 thru A-2.163

*Excludes one anomalous data point, see Section A.2.4.2.3.

**Excludes the G2 anomalous data, see Figure A-2.134.

Table A-2.4: Hot Zero Power All Rods Out Critical Boron Concentrations

Plant/Cycle	Calculated (ppm)	Measured (ppm)	Difference M - C (ppm)
A Cycle 1	1329	1353	24
A Cycle 2	1770	1764	-6
A Cycle 3	1859	1841	-18
A Cycle 4	1745	1718	-27
A Cycle 5	1975	1946	-29
A Cycle 6	1816	1842	26
A Cycle 7	2190	2224	34
A Cycle 8	2189	2206	17
A Cycle 9	2021	1997	-24
A Cycle 10	1895	1889	-6
A Cycle 11	2104	2090	-14
A Cycle 12	2072	2024	-48
A Cycle 13	2091	2061	-30
B Cycle 1	1148	1154	6
G2 Cycle 1	1444	1438	-6
G2 Cycle 2	1386	1419	33
G2 Cycle 3	1534	1556	22
G2 Cycle 4	1396	1408	12
G2 Cycle 5	1508	1541	33
G1 Cycle 26	1670	1688	18
G1 Cycle 27	1812	1779	-33
G1 Cycle 28	1636	1650	14
G1 Cycle 29	1117 ^a	1110	-7
G1 Cycle 30	1151 ^a	1156	5

^a30% B-10 enriched

Table A-2.5: Plant A Cycle 1 Hot Zero Power Rod Bank Worth

Bank	Measured (pcm)	Calculated (pcm)	M-C (pcm)	100*(M- C)/C (%)
Control A	683	674	9	1.3
Control C	972	986	-14	-1.5
Control D	458	457	1	0.1
Shutdown A	1131	1144	-13	-1.1
Shutdown B	966	981	-15	-1.5
Shutdown C	450	454	-4	-0.9
Shutdown D	556	576	-20	-3.5
Control B	1317	1343	-26	-1.9
Total	6533	6616	-83	-1.2

Table A-2.6: Plant A Cycle 2 Hot Zero Power Rod Bank Worth

Bank	Measured (pcm)	Calculated (pcm)	M-C (pcm)	100*(M- C)/C (%)
Control A	686	649	38	5.8
Control C	749	782	-33	-4.2
Control D	1020	1058	-39	-3.7
Shutdown A	1024	1022	1	0.1
Shutdown B	1015	1060	-44	-4.2
Shutdown C	427	407	20	5.0
Control B	1189	1211	-22	-1.8
Total	6110	6189	-79	-1.3

Table A-2.7: Plant A Cycle 3 Hot Zero Power Rod Bank Worth

Bank	Measured (pcm)	Calculated (pcm)	M-C (pcm)	100*(M- C)/C (%)
Control A	374	342	33	9.5
Control B	1183	1191	-8	-0.7
Control C	642	653	-11	-1.7
Control D	1217	1239	-22	-1.7
Shutdown B	768	796	-28	-3.5
Shutdown C	338	300	37	12.5
Shutdown A	1344	1347	-3	-0.3
Total	5866	5869	-3	0.0

Table A-2.8: Plant A Cycle 4 Hot Zero Power Rod Bank Worth

Bank	Measured (pcm)	Calculated (pcm)	M-C (pcm)	100*(M- C)/C (%)
Control A	378	385	-7	-1.7
Control C	763	733	30	4.1
Control D	928	930	-2	-0.2
Shutdown A	1236	1238	-2	-0.1
Shutdown B	773	759	14	1.9
Shutdown C	331	302	29	9.5
Control B	1320	1290	30	2.3
Total	5729	5636	93	1.6

Table A-2.9: Plant A Cycle 5 Hot Zero Power Rod Bank Worth

Bank	Measured (pcm)	Calculated (pcm)	M-C (pcm)	100*(M- C)/C (%)
Control A	395	331	64	19.2
Control C	914	859	55	6.4
Control D	1282	1195	87	7.3
Shutdown A	954	868	86	9.9
Shutdown B	999	951	48	5.1
Shutdown C	354	290	64	22.1
Control B	1352	1267	85	6.7
Total	6250	5761	489	8.5

Table A-2.10: Plant A Cycle 6 Hot Zero Power Rod Bank Worth

Bank	Measured (pcm)	Calculated (pcm)	M-C (pcm)	100*(M- C)/C (%)
Control A	346	349	-3	-0.9
Control C	1081	1110	-29	-2.6
Control D	901	932	-31	-3.3
Shutdown A	956	993	-37	-3.7
Shutdown B	746	790	-44	-5.5
Shutdown C	433	455	-22	-4.8
Control B	1201	1366	-165	-12.1
Total	5664	5994	-330	-5.5

Table A-2.11: Plant A Cycle 7 Hot Zero Power Rod Bank Worth

Bank	Measured (pcm)	Calculated (pcm)	M-C (pcm)	100*(M- C)/C (%)
Control B	1409	1449	-40	-2.7
Control A	293	270	23	8.4
Shutdown C	351	361	-10	-2.9
Shutdown A	1023	981	42	4.3
Control C	1023	987	36	3.7
Shutdown B	1047	1003	44	4.3
Control D	1072	991	81	8.2
Total	6218	6043	175	2.9

Table A-2.12: Plant A Cycle 8 Hot Zero Power Rod Bank Worth

Bank	Measured (pcm)	Calculated (pcm)	M-C (pcm)	100*(M- C)/C (%)
Control B	1109	1157	-48	-4.1
Control A	244	218	26	12.1
Shutdown C	299	272	27	9.8
Shutdown A	842	805	37	4.5
Control C	948	942	6	0.7
Shutdown B	996	1024	-28	-2.7
Control D	1074	1078	-4	-0.4
Total	5512	5496	16	0.3

Table A-2.13: Plant A Cycle 9 Hot Zero Power Rod Bank Worth

Bank	Measured (pcm)	Calculated (pcm)	M-C (pcm)	100*(M- C)/C (%)
Control B	1174	1154	20	1.7
Control A	319	281	38	13.6
Shutdown C	338	299	39	12.9
Shutdown A	891	841	50	5.9
Control C	974	986	-12	-1.2
Shutdown B	1006	1013	-7	-0.7
Control D	1018	1018	0	0.0
Total	5720	5593	127	2.3

Table A-2.14: Plant A Cycle 10 Hot Zero Power Rod Bank Worth

Bank	Measured (pcm)	Calculated (pcm)	M-C (pcm)	100*(M- C)/C (%)
Control B	1437	1411	26	1.9
Shutdown A	931	889	42	4.7
Shutdown B	1181	1156	24	2.1
Shutdown C	249	239	10	4.0
Control A	335	304	31	10.2
Control C	1117	1050	67	6.4
Control D	951	877	74	8.4
Total	6200	5926	274	4.6

Table A-2.15: Plant A Cycle 11 Hot Zero Power Rod Bank Worth

Bank	Measured (pcm)	Calculated (pcm)	M-C (pcm)	100*(M- C)/C (%)
Control B	1063	1044	19	1.8
Shutdown A	952	986	-34	-3.4
Shutdown B	866	882	-16	-1.8
Shutdown C	292	306	-14	-4.5
Control A	509	523	-14	-2.6
Control C	916	953	-37	-3.8
Control D	879	996	-117	-11.8
Total	5477	5689	-212	-3.7

Table A-2.16: Plant A Cycle 12 Hot Zero Power Rod Bank Worth

Bank	Measured (pcm)	Calculated (pcm)	M-C (pcm)	100*(M- C)/C (%)
Control B	1347	1236	111	9.0
Shutdown A	834	705	129	18.3
Shutdown B	1072	1207	-135	-11.2
Shutdown C	265	201	64	32.0
Control A	343	273	70	25.6
Control C	974	1021	-48	-4.7
Control D	1018	1004	14	1.4
Total	5851	5646	205	3.6

Table A-2.17: Plant A Cycle 13 Hot Zero Power Rod Bank Worth

Bank	Measured (pcm)	Calculated (pcm)	M-C (pcm)	100*(M- C)/C (%)
Control B	1127	1129	-2	-0.1
Shutdown A	1073	1001	73	7.2
Shutdown B	1015	1007	8	0.8
Shutdown C	300	267	34	12.6
Control A	408	360	49	13.5
Control C	878	845	33	3.9
Control D	1082	1043	39	3.7
Total	5886	5652	233	4.1

Table A-2.18: Plant B Cycle 1 Hot Zero Power Rod Bank Worth

Bank	Measured (pcm)	Calculated (pcm)	M-C (pcm)	100*(M- C)/C (%)
G1	504	493	11	2.2
G2	910	890	20	2.3
N1	973	967	6	0.6
N2	602	545	57	10.5
R	1443	1405	38	2.7
SA	486	476	10	2.1
SB	1187	1107	80	7.2
SC	692	687	5	0.7
Total	6797	6569	228	3.5

Table A-2.19: Summary of Total Bank Worths

Plant/Cycle	Measured (pcm)	Calculated (pcm)	M-C (pcm)	100*(M- C)/C (%)
A/1	6533	6616	-83	-1.3
A/2	6110	6189	-79	-1.3
A/3	5866	5869	-3	-0.1
A/4	5729	5636	93	1.7
A/5	6250	5761	489	8.5
A/6	5664	5994	-330	-5.5
A/7	6218	6043	175	2.9
A/8	5512	5496	16	0.3
A/9	5720	5593	127	2.3
A/10	6200	5926	274	4.6
A/11	5477	5689	-212	-3.7
A/12	5851	5646	205	3.6
A/13	5886	5652	233	4.1
B/1	6797	6569	228	3.5

Table A-2.20: Hot Zero Power All Rods Out Isothermal Temperature Coefficient

Plant/Cycle	Calculated (pcm/°F)	Measured (pcm/°F)	Difference M - C (pcm/°F)
A Cycle 1	-1.93	-1.50	0.41
A Cycle 2	-0.69	-0.82	-0.33
A Cycle 3	0.24	-0.53	-0.90
A Cycle 4	-1.07	-1.62	-0.70
A Cycle 5	2.04	1.17	-0.99
A Cycle 6	-3.75	-3.80	-0.25
A Cycle 7	-3.05	-2.85	-0.03
A Cycle 8	-3.34	-3.33	-0.39
A Cycle 9	-4.94	-5.49	-0.94
A Cycle 10	-5.68	-6.13	-0.61
A Cycle 11	-4.63	-5.03	-0.57
A Cycle 12	-5.95	-6.00	-0.27
A Cycle 13	-5.08	-5.25	-0.35
B Cycle 1	0.29	-0.13	-0.43

Data on HZP all rods out isothermal temperature coefficients were not available for Plants G1 and G2.

Table A-2.21 Power Distribution Summary for Plants G1 and G2

Plant	Cycle	Map	Burnup	Assembly RMS x 100	Axial RMS x 100	C-M Axial Offset
G1	26	32	1.66	1.2	2.0	-0.51
		37	2.36	1.1	2.1	-0.98
		40	2.90	1.1	2.1	-1.04
		46	3.51	1.2	2.2	-1.41
		49	4.00	1.0	2.3	-1.36
		53	4.76	1.0	2.5	-1.82
		57	5.30	1.0	2.6	-1.80
		60	5.85	1.2	2.6	-1.77
		66	6.94	0.9	2.6	-1.82
		73	8.31	1.1	2.5	-1.54
		79	9.48	1.1	2.4	-1.17
		84	10.57	1.1	2.2	-0.66
		87	10.99	1.0	2.2	-0.22
	27	15	0.20	1.3	2.6	-2.50
		18	0.71	1.1	2.2	-1.64
		30	1.54	1.0	1.9	-0.89
		35	2.27	1.0	2.2	-1.35
		46	3.61	0.9	2.3	-1.53
		53	4.63	1.0	2.4	-1.65
		61	5.79	1.0	2.7	-1.99
		70	6.92	1.0	2.5	-1.65
		76	8.22	1.1	2.3	-1.16
		82	9.32	0.9	2.3	-1.10
		90	10.67	0.9	2.6	-1.45
		94	11.30	1.0	2.2	-0.58
	28	21	0.72	1.3	2.0	-0.84
		25	1.55	1.2	2.2	-1.25
		29	2.41	1.1	2.0	-0.63
		35	3.50	0.9	2.0	-0.58
		52	4.70	1.1	2.3	-1.38
		58	5.91	1.1	2.3	-1.24
		64	6.92	1.2	2.3	-1.07
		75	8.30	1.1	2.2	-0.87
		86	9.31	1.1	2.2	-0.44
		93	10.48	0.8	2.2	-0.59
		96	11.02	0.8	2.3	-0.48
	29	23	0.25	1.5	2.6	-2.15
		30	0.88	1.5	2.2	-1.71
		35	1.16	1.6	2.4	-1.94

Codes and Methods Applicability Report
for the U.S. EPR

Page A-48

Plant	Cycle	Map	Burnup	Assembly RMS x 100	Axial RMS x 100	C-M Axial Offset
		41	1.45	1.6	2.4	-2.01
		46	1.93	1.4	2.2	-0.09
		47	2.28	1.3	2.1	-0.77
		54	3.49	1.2	2.1	-0.20
		66	4.68	1.2	2.1	-0.61
		81	5.76	1.2	2.1	-0.22
		86	6.55	1.1	2.1	-0.30
		89	7.05	1.1	2.2	-0.91
		91	7.71	1.1	2.2	-0.10
		94	8.21	1.0	2.2	-0.18
		99	8.95	1.1	2.2	-0.27
		102	9.31	1.1	2.4	-1.05
		108	10.02	1.0	2.2	-0.22
		111	10.61	1.1	2.3	-0.75
		115	11.16	1.0	2.3	-0.74
		118	11.86	0.9	2.5	-1.21
	30	21	0.34	0.8	2.0	-0.89
		22	0.62	0.9	2.0	-0.49
		25	1.21	0.8	2.0	-0.52
		26	1.44	0.9	1.9	-0.74
		30	2.29	0.9	2.1	0.26
		34	2.88	0.9	2.1	0.17
		36	3.40	0.9	2.3	0.52
		39	4.00	0.9	2.4	0.60
		44	4.76	0.9	2.4	0.63
		47	5.31	1.0	2.5	0.96
		50	5.85	1.0	2.5	0.86
		53	6.39	1.0	2.4	0.80
		57	6.90	1.1	2.3	0.61
		60	7.67	1.0	2.2	-0.27
		77	8.73	1.0	2.2	0.17
		80	9.29	1.1	2.3	0.55
		83	10.07	1.0	2.3	0.50
		85	10.61	0.9	2.2	0.42
		86	11.05	1.0	2.2	0.21
		90	11.80	0.9	2.1	-0.31
		92	12.04	0.9	2.3	0.53
G2	1	116	1.11	1.2	8.8	8.04
		194	5.49	0.8	5.0	1.60
		215	6.65	0.8	4.7	-1.50
		227	7.80	1.2	13.6	-11.81

Plant	Cycle	Map	Burnup	Assembly RMS x 100	Axial RMS x 100	C-M Axial Offset
		290	12.06	0.9	3.5	-1.50
		327	15.97	0.6	3.1	-0.40
	2	56	2.26	0.8	4.7	3.15
		63	3.28	0.7	4.2	2.97
		70	4.47	0.7	3.9	2.65
		80	5.56	0.8	3.4	1.90
		87	6.58	0.9	2.9	0.92
		100	7.31	0.9	2.7	0.59
		108	7.85	0.7	3.0	1.49
		111	8.11	0.7	3.9	2.52
		117	8.83	0.7	2.5	0.66
		124	9.39	0.7	2.5	0.65
		126	9.89	0.7	2.9	1.37
		130	10.41	0.7	2.4	-0.25
		133	10.99	0.7	2.4	-0.22
		146	11.61	0.6	2.6	-1.08
		150	12.02	0.7	3.2	-2.23
	3	25	0.29	0.7	3.2	2.50
		30	0.75	0.7	2.7	1.76
		36	1.65	0.8	3.2	2.08
		40	2.13	0.8	2.2	0.90
		48	3.42	0.7	2.1	-0.18
		55	4.52	0.7	2.8	-1.74
		63	5.77	0.7	2.6	-0.73
		71	6.29	0.8	2.8	-1.36
		76	6.89	1.0	3.7	-2.71
		78	7.37	0.7	2.7	-0.97
		80	7.82	0.7	2.8	-0.98
		84	8.38	0.8	3.0	-1.62
		87	8.90	0.8	3.6	-2.71
		94	9.98	0.8	3.6	-2.69
		103	11.24	0.8	3.3	-2.59
		109	12.33	0.8	3.4	-2.52
	4	19	0.14	1.0	4.4	2.97
		24	0.23	1.0	3.2	1.77
		29	0.89	1.0	3.3	2.06
		31	1.50	0.9	3.8	2.68
		35	2.21	0.9	2.7	1.26
		38	2.48	0.9	2.6	1.17
		41	3.07	1.0	2.3	0.50
		46	3.76	0.9	2.2	-0.56

Plant	Cycle	Map	Burnup	Assembly RMS x 100	Axial RMS x 100	C-M Axial Offset
		49	4.64	1.0	2.2	-0.04
		52	4.89	1.0	2.2	-0.37
		60	5.66	1.1	2.3	0.06
		66	6.03	1.2	4.6	2.57
		75	6.67	1.1	2.5	-0.84
		79	6.94	1.1	2.6	-0.96
		82	7.61	1.2	2.6	-1.36
		85	7.88	1.2	3.3	-2.54
		91	8.77	1.2	2.7	-1.88
		96	9.55	1.3	3.9	-3.35
		102	10.29	1.2	2.5	-1.62
		104	10.78	1.3	3.2	-2.55
		107	11.04	1.3	4.8	-4.20
	5	18	0.22	1.1	2.0	0.57
		23	0.82	1.1	1.9	-0.13
		25	1.31	1.1	1.9	0.02
		31	2.39	1.1	2.0	-0.80
		37	3.44	1.0	1.9	-0.17
		44	4.75	1.1	2.4	-1.46
		50	5.81	1.0	2.6	-1.76
		53	6.64	1.1	2.8	-1.76
		66	7.95	1.0	3.0	-2.31
		70	8.40	1.1	3.0	-2.34
		72	8.99	0.9	2.8	-2.11
		81	10.24	1.0	3.9	-3.50
		89	11.10	0.9	3.3	-2.30

Table A-3.1: Derivation of Inferred Power Distribution Uncertainties

Description	Results	Comments
Incore Monitoring System		AMS and POWERTRAX/S
Number of Reactors	2	G1 and G2
Number of cycles	10	5 cycles from Plant G1 5 cycles from Plant G2
Number of Maps	147	76 from Plant G1 71 from Plant G2
Number of pin-by-pin fission rate distributions used to calculate local peaking factor uncertainty	6	Included both Westinghouse and Combustion Engineering guide tube configurations, variety of enrichments, and burnable absorbers
Standard deviation of the relative uncertainty in the local peaking factor	1.335	

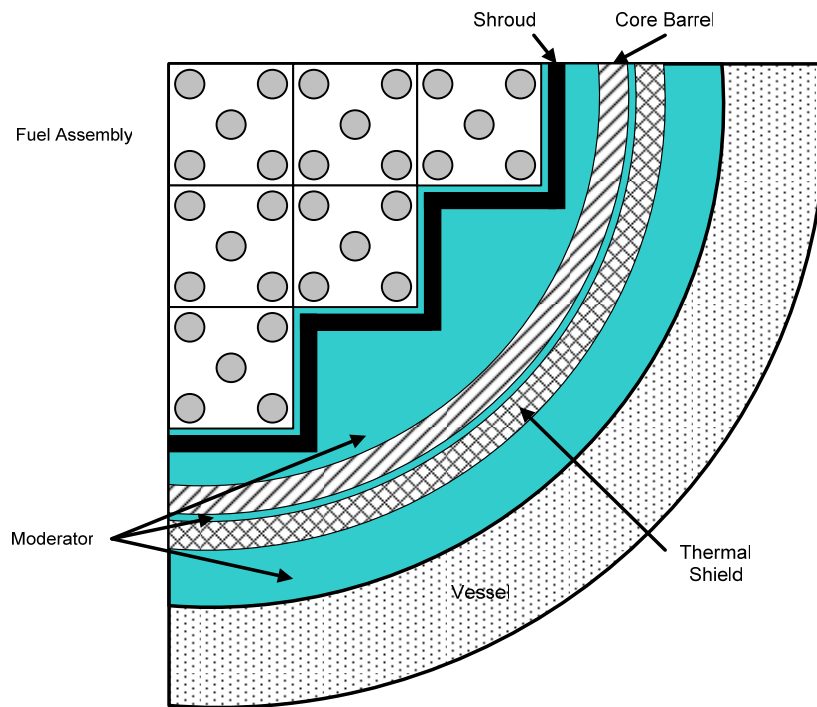
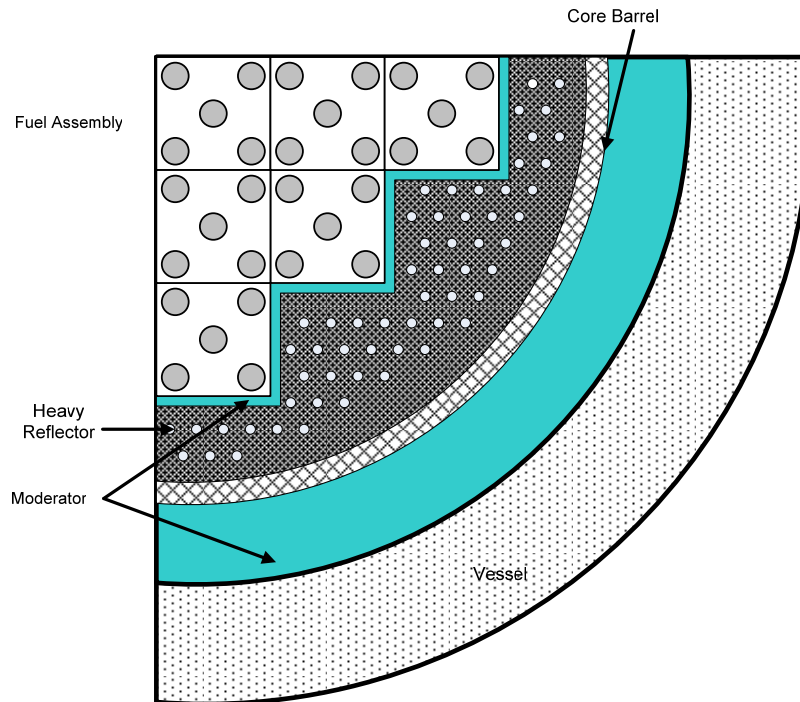
Figure A-1.1 Typical Layout of the Reflector in a Standard PWR**Figure A-1.2 Typical Layout of the Reflector in the EPR**

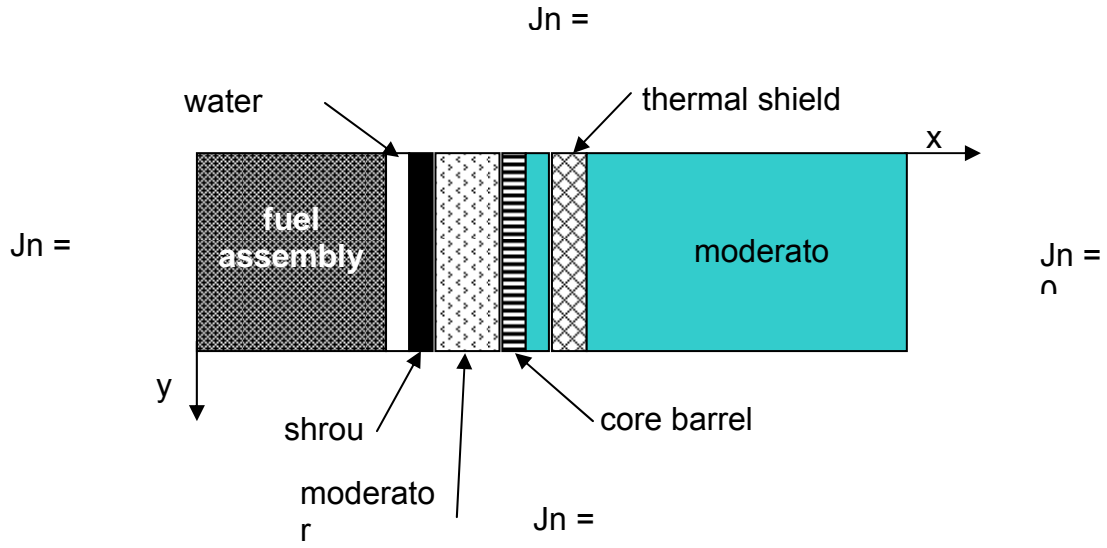
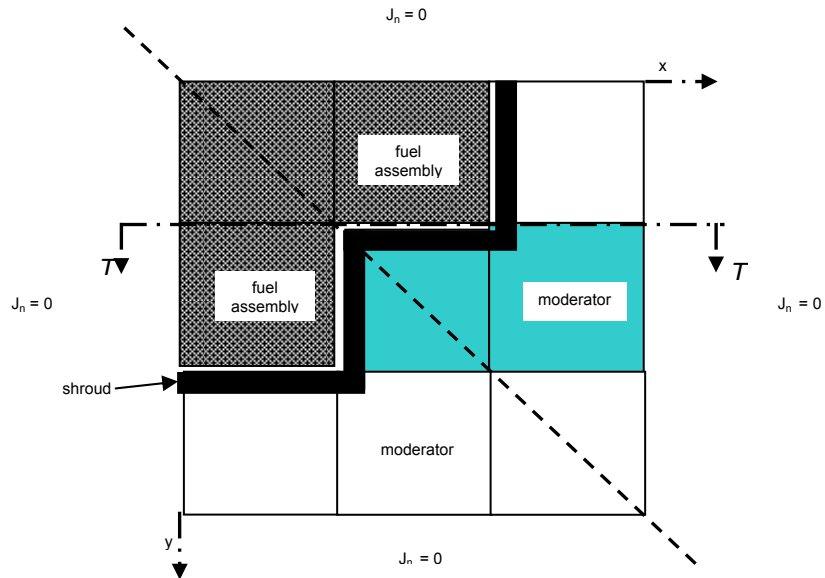
Figure A-1.3 1-D Reflector Model**Figure A-1.4 2-D Reflector Model**

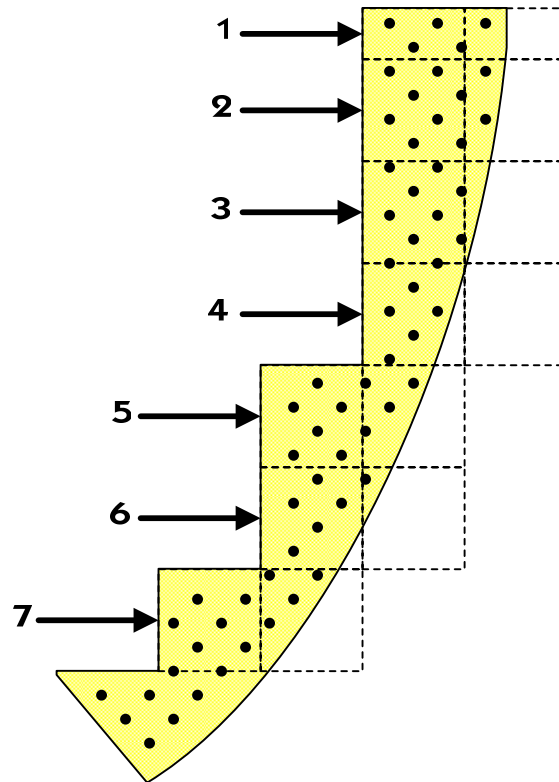
Figure A-1.5 U.S. EPR Reflector Geometry

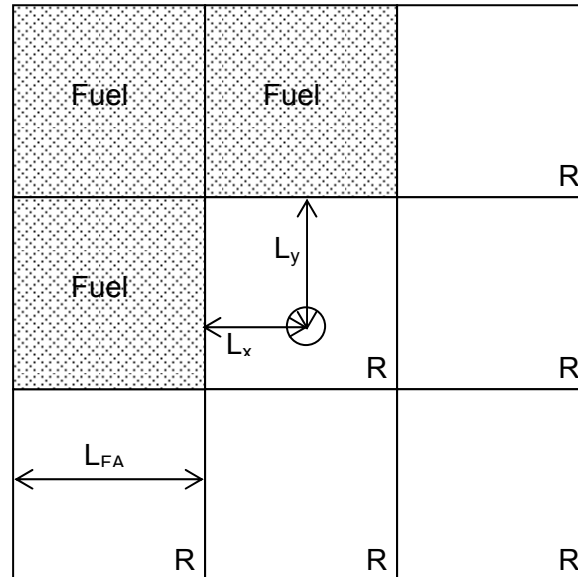
Figure A-1.6 Reflector Coolant Channel in Re-entrant Corner

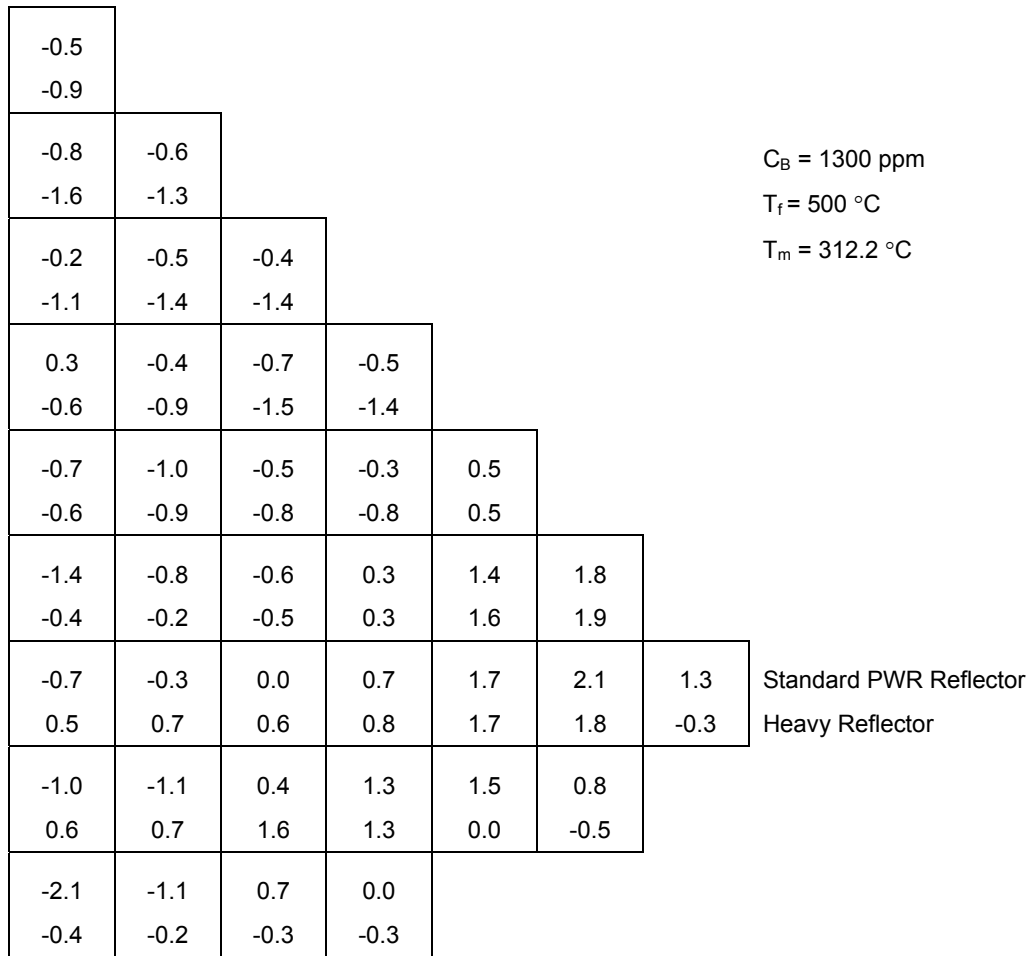
Figure A-1.7: Comparisons of the Differences between MCNP and PRISM Radial Powers for the Standard and Heavy Reflectors with the Standard Core Design

[illegible]

Figure A-1.8: Comparisons of the Differences between MCNP and PRISM Radial Powers for the Heavy Reflectors with the Different Core Designs

[illegible]

Figure A-1.9: Comparisons of the Differences between MCNP and PRISM Radial Powers for the Standard and Heavy Reflectors with the Standard Core Design at High Boron



[illegible]

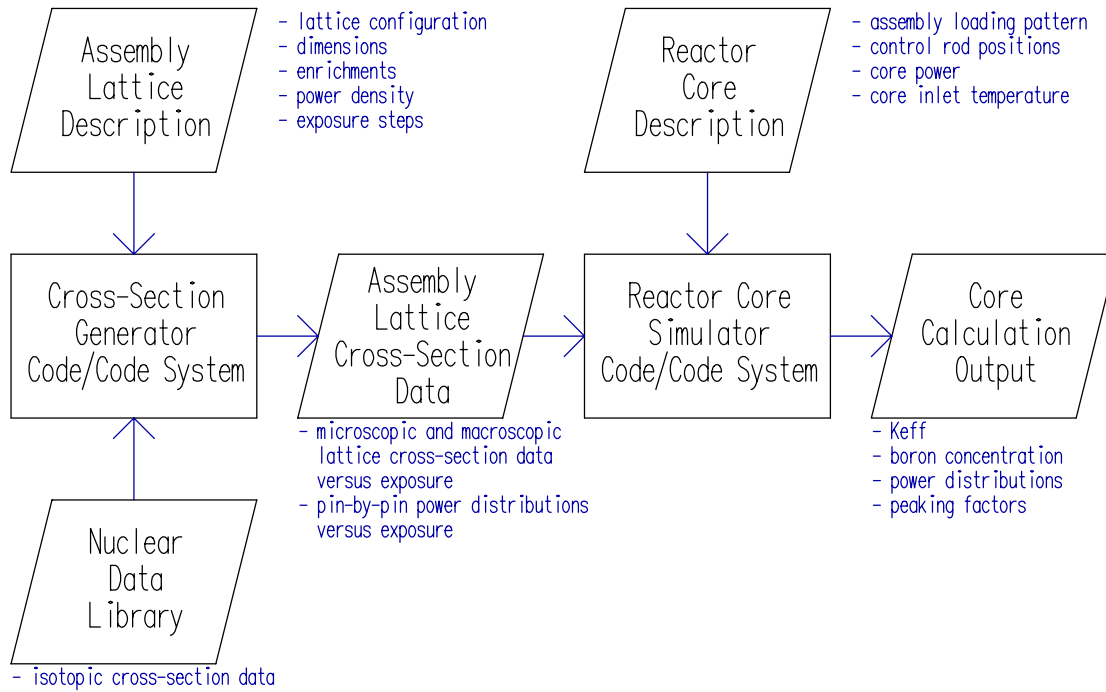
Figure A-2.1: SAV95 Calculation Flowchart

Figure A-2.2(a) Plant G2 Assembly Guide Tube Configuration

3	3	3	3	3	3	3	3	3	3	3	3	3	3	3	3	3	3
3	3	3	3	3	3	3	3	3	3	3	3	3	3	3	3	3	3
3	3	3	3	3	3	1	3	3	3	3	1	3	3	3	3	3	3
3	3	3	1	3	3	3	3	3	3	3	3	3	3	1	3	3	3
3	3	3	3	3	3	3	1	3	3	1	3	3	3	3	3	3	3
3	3	3	3	3	1	3	3	3	3	3	3	1	3	3	3	3	3
3	3	1	3	3	3	3	3	3	3	3	3	3	3	3	1	3	3
3	3	3	3	1	3	3	3	3	3	3	3	3	3	1	3	3	3
3	3	3	3	3	3	3	3	3	3	3	3	3	3	3	3	3	3
3	3	3	3	3	3	3	3	3	3	3	3	3	3	3	3	3	3
3	3	3	3	1	3	3	3	3	3	3	3	3	1	3	3	3	3
3	3	1	3	3	3	3	3	3	3	3	3	3	3	3	1	3	3
3	3	3	3	3	1	3	3	3	3	3	1	3	3	3	3	3	3
3	3	3	3	3	3	3	1	3	3	1	3	3	3	3	3	3	3
3	3	3	1	3	3	3	3	3	3	3	3	3	3	1	3	3	3
3	3	3	3	3	3	1	3	3	3	3	2	3	3	3	3	3	3
3	3	3	3	3	3	3	3	3	3	3	3	3	3	3	3	3	3
3	3	3	3	3	3	3	3	3	3	3	3	3	3	3	3	3	3



Guide tube location



Guide tube with instrument

UO₂ Rod

Figure A-2.2(b) Plant G1 Assembly Guide Tube Configuration

1	1	1	1	1	1	1	1	1	1	1	1	1	1	1
1	1	1	1	1	1	1	1	1	1	1	1	1	1	1
1	1	3	1	1	3	1	1	1	3	1	1	3	1	1
1	1	1	1	1	1	1	1	1	1	1	1	1	1	1
1	1	1	1	3	1	1	3	1	1	3	1	1	1	1
1	1	3	1	1	1	1	1	1	1	1	1	3	1	1
1	1	1	1	1	1	1	1	1	1	1	1	1	1	1
1	1	1	1	3	1	1	1	1	1	3	1	1	1	1
1	1	1	1	1	1	1	1	1	1	1	1	1	1	1
1	1	3	1	1	1	1	1	1	1	1	1	2	1	1
1	1	1	1	3	1	1	3	1	1	3	1	1	1	1
1	1	1	1	1	1	1	1	1	1	1	1	1	1	1
1	1	3	1	1	3	1	1	1	3	1	1	3	1	1
1	1	1	1	1	1	1	1	1	1	1	1	1	1	1
1	1	1	1	1	1	1	1	1	1	1	1	1	1	1

1

UO₂ Rod

2

Guide tube with instrument

3

Guide tube

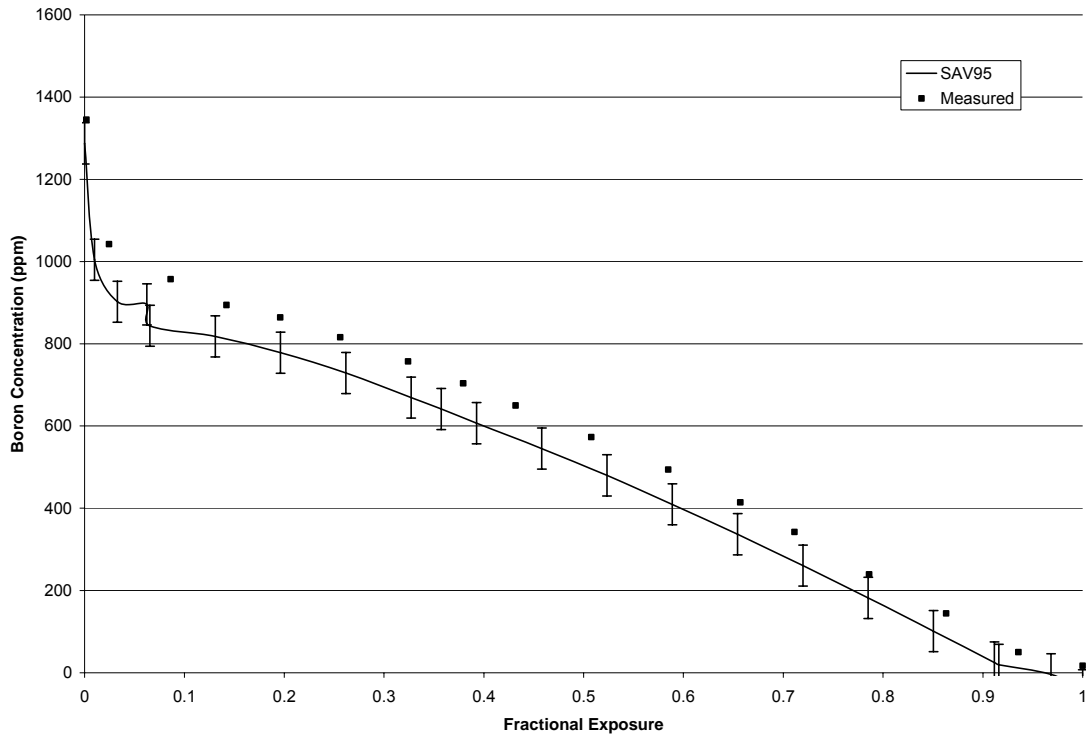
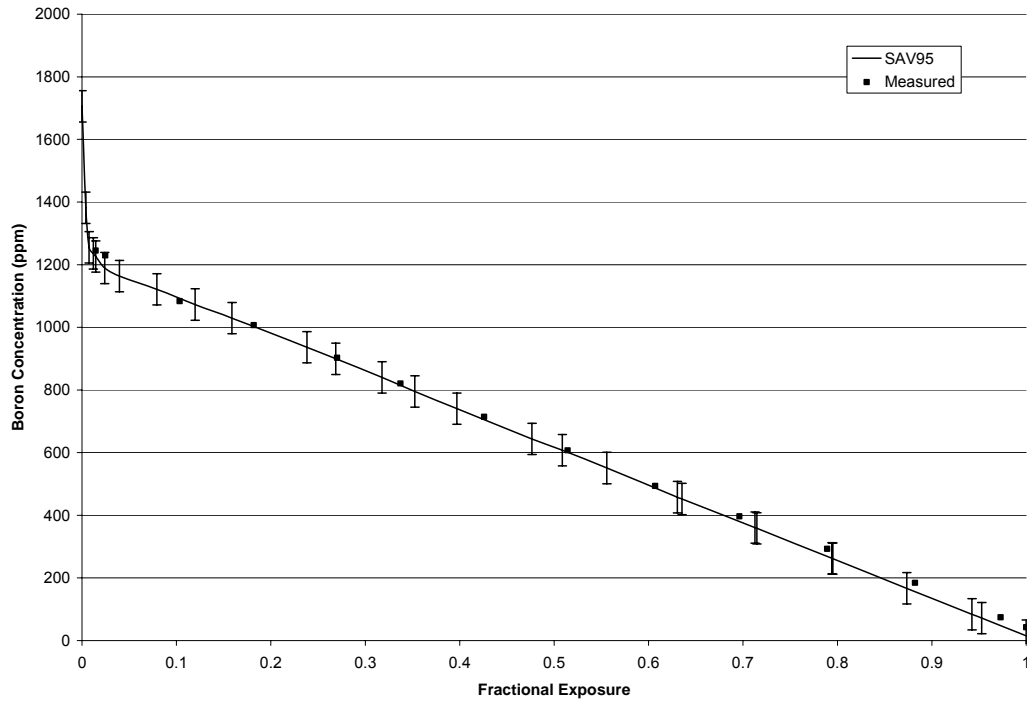
Figure A-2.3: Plant A Cycle 1 Critical Boron Concentration**Figure A-2.4: Plant A Cycle 2 Critical Boron Concentration**

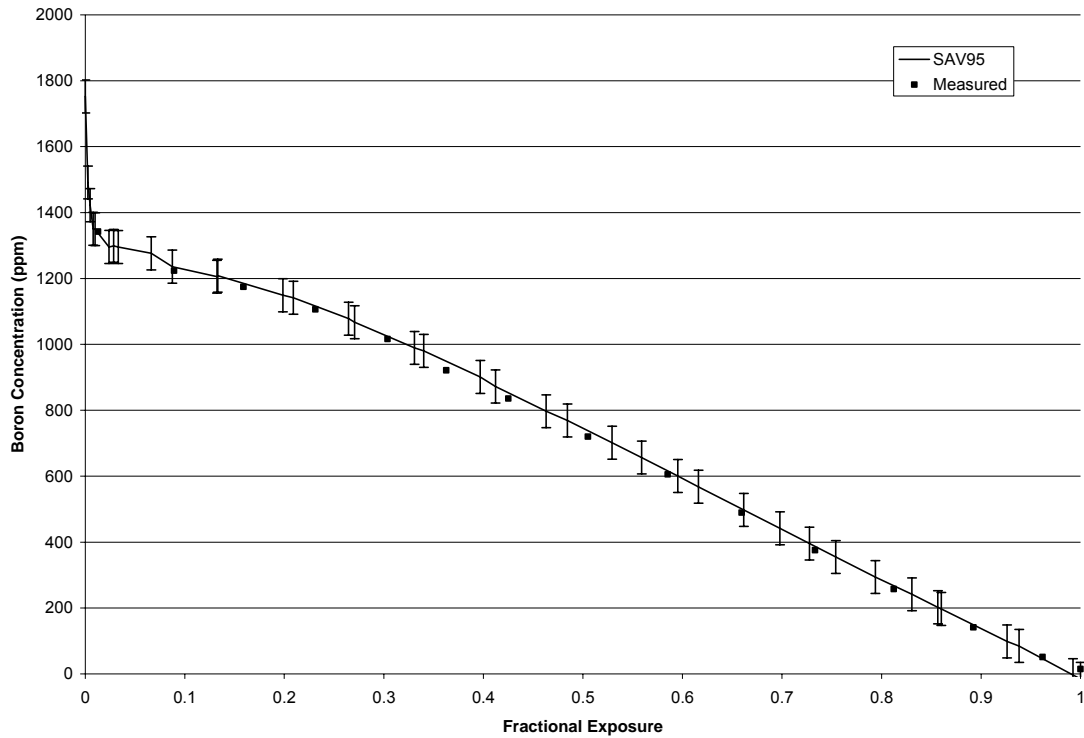
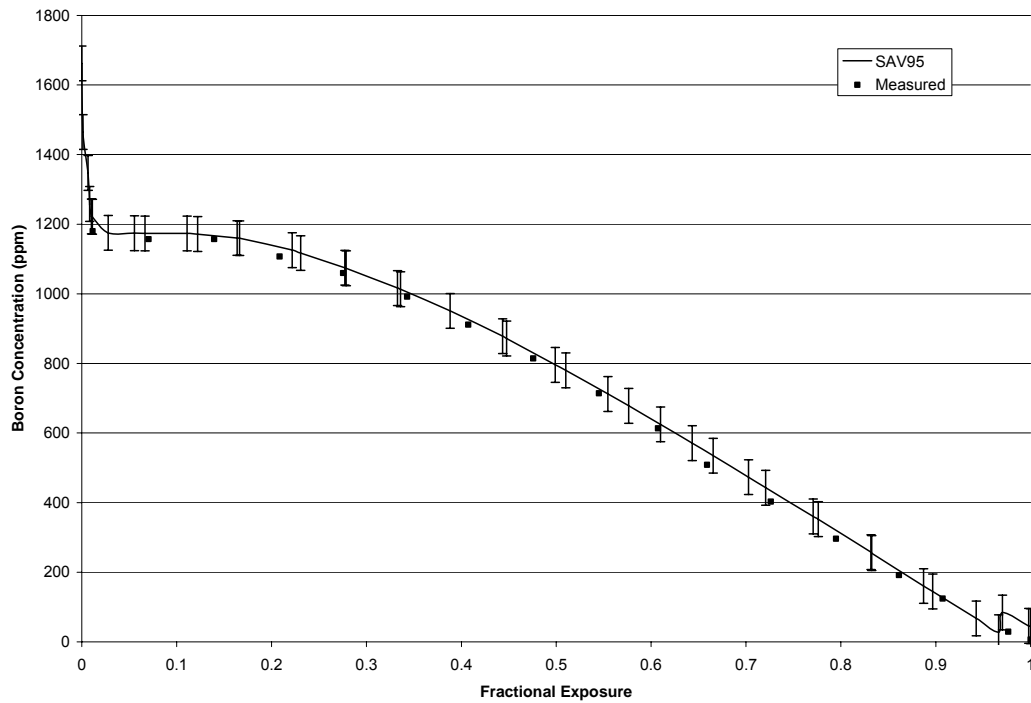
Figure A-2.5: Plant A Cycle 3 Critical Boron Concentration**Figure A-2.6: Plant A Cycle 4 Critical Boron Concentration**

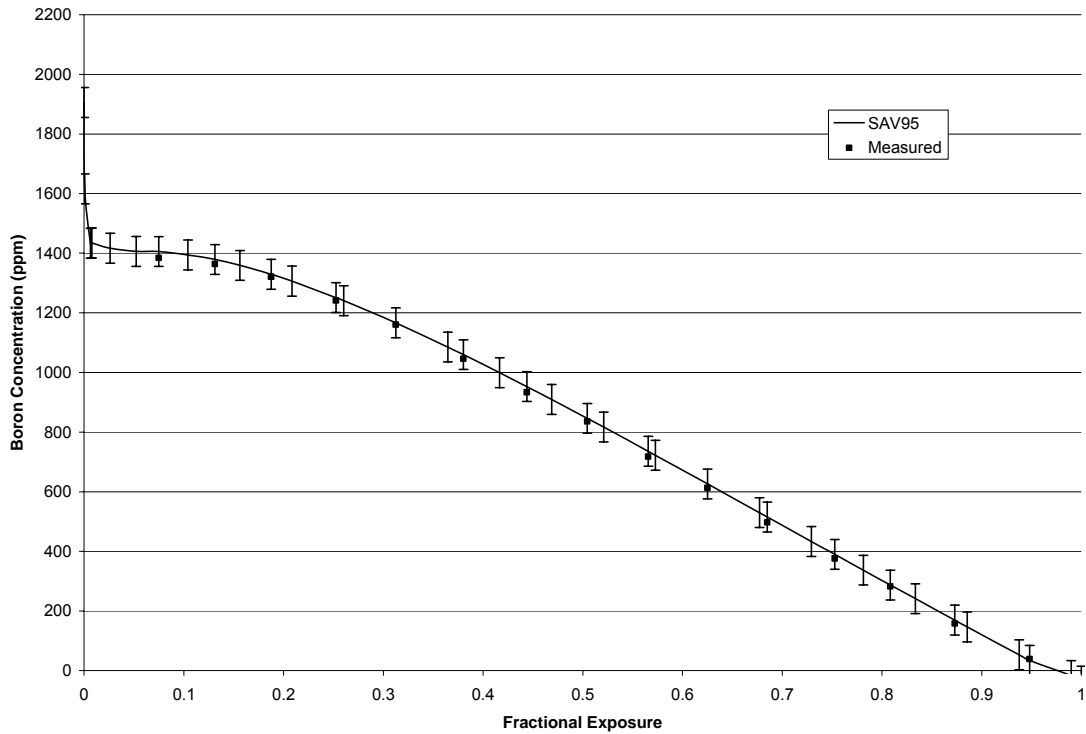
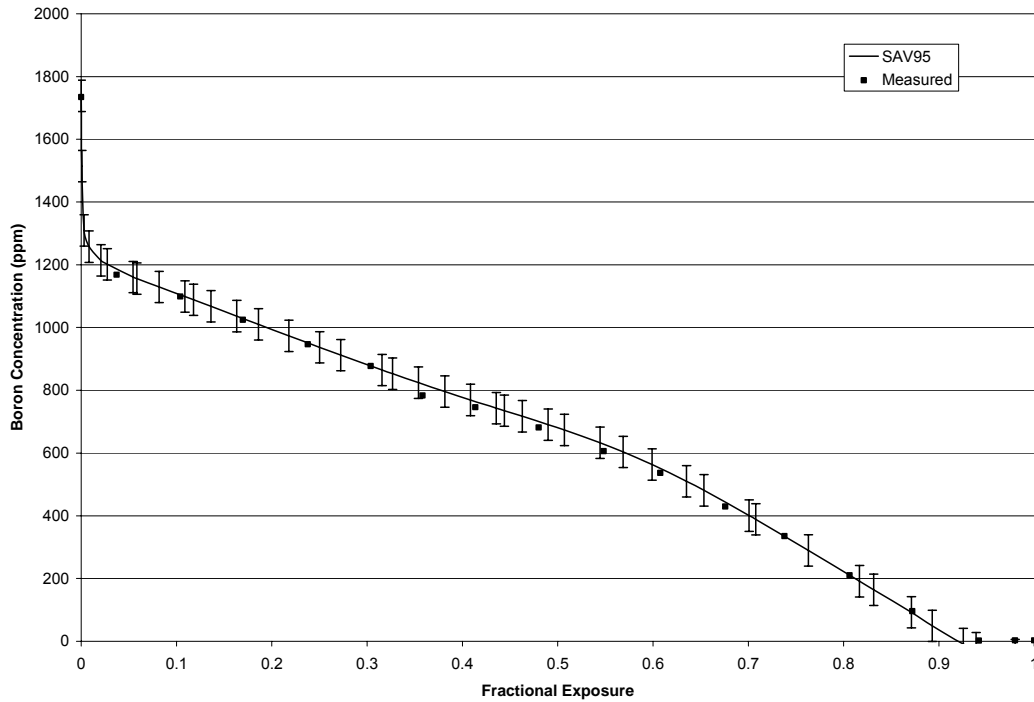
Figure A-2.7: Plant A Cycle 5 Critical Boron Concentration**Figure A-2.8: Plant A Cycle 6 Critical Boron Concentration**

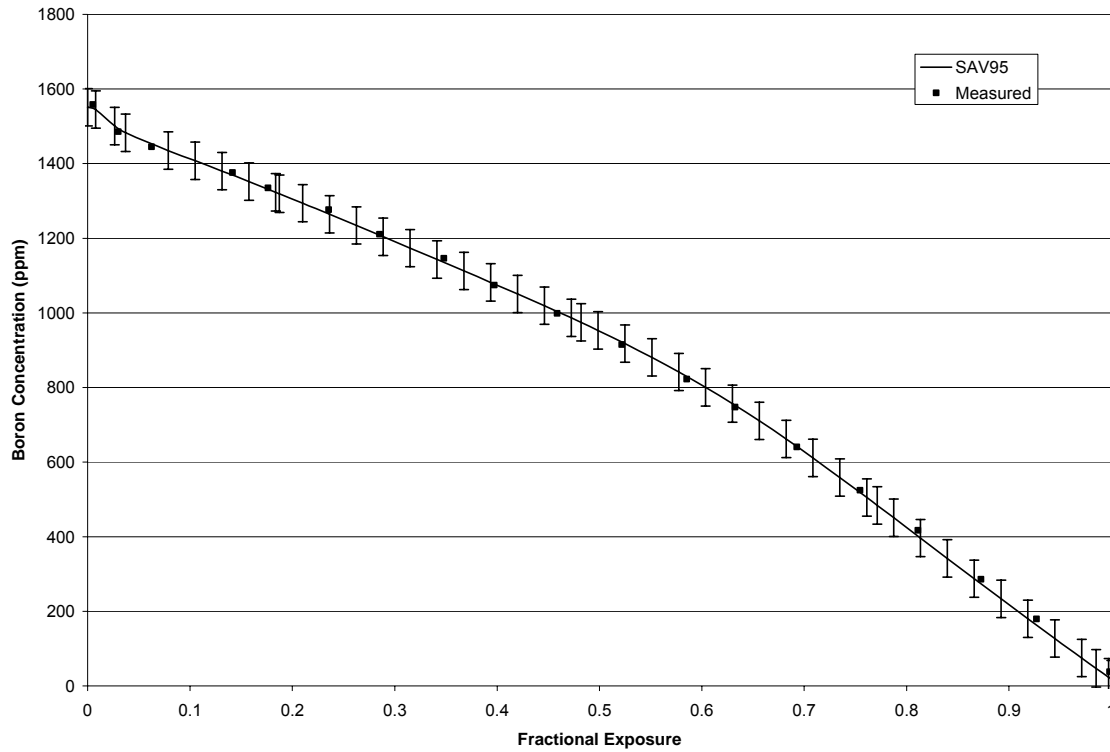
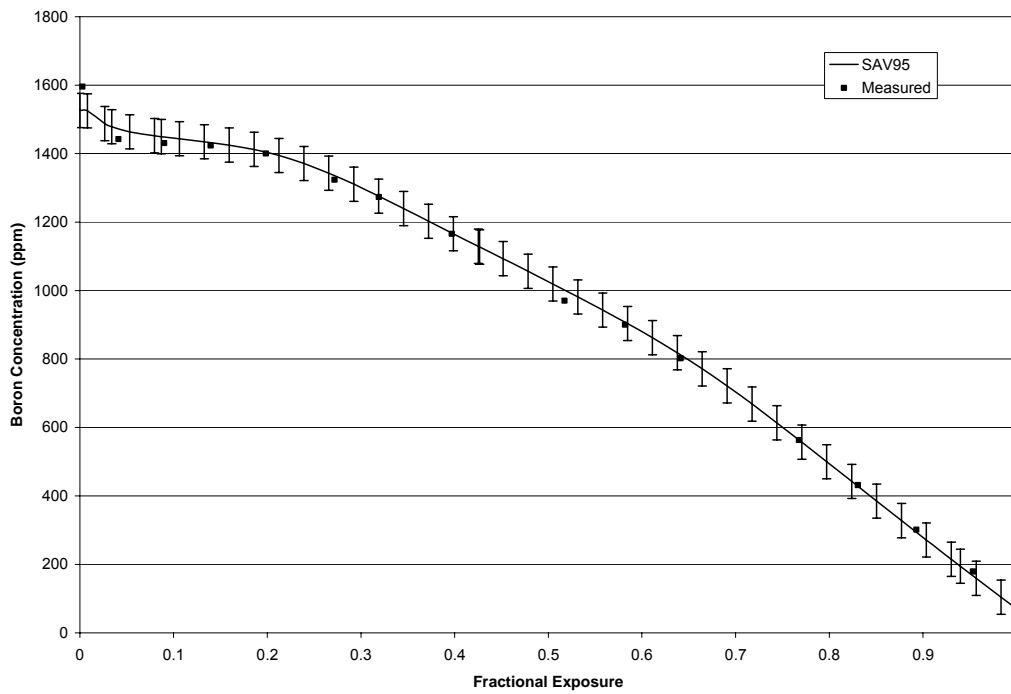
Figure A-2.9: Plant A Cycle 7 Critical Boron Concentration**Figure A-2.10: Plant A Cycle 8 Critical Boron Concentration**

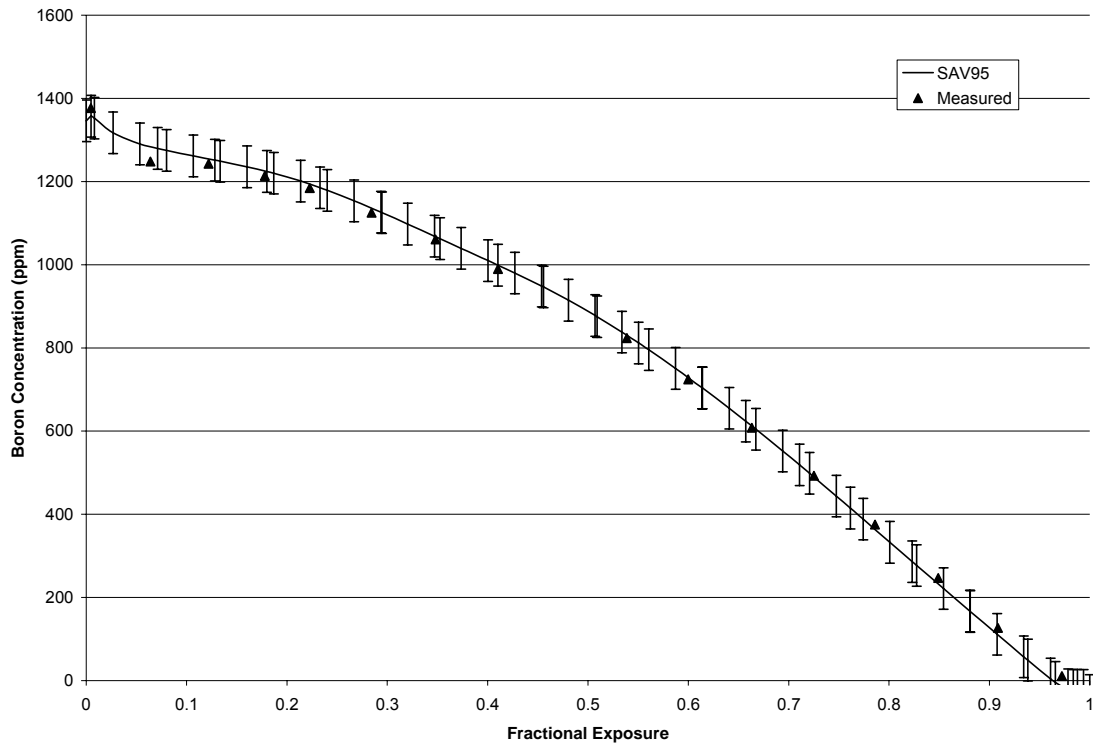
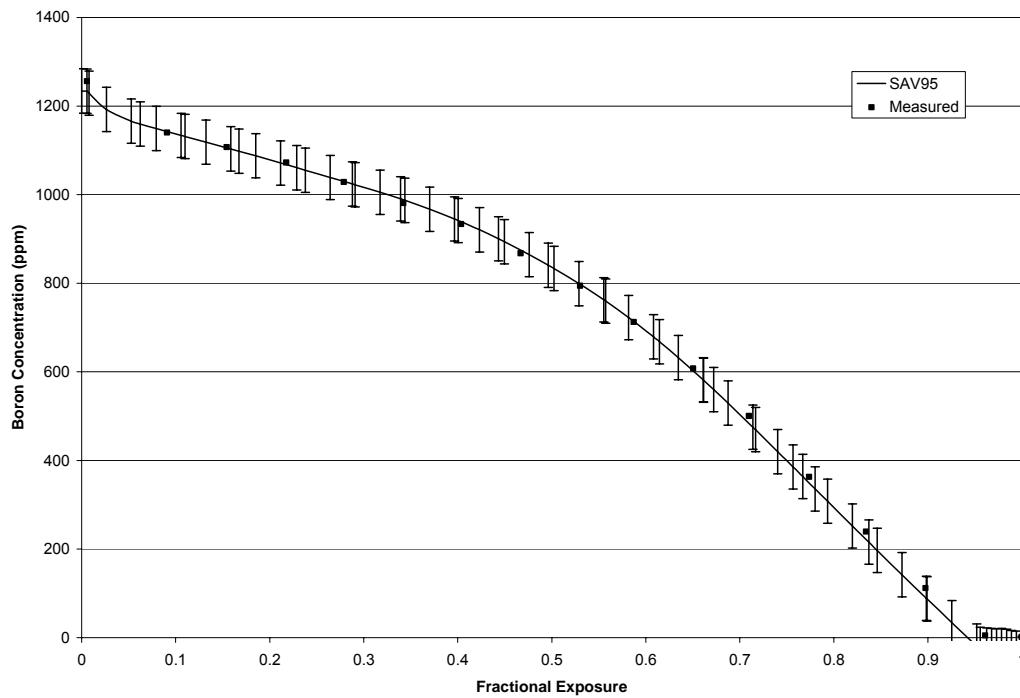
Figure A-2.11: Plant A Cycle 9 Critical Boron Concentration**Figure A-2.12: Plant A Cycle 10 Critical Boron Concentration**

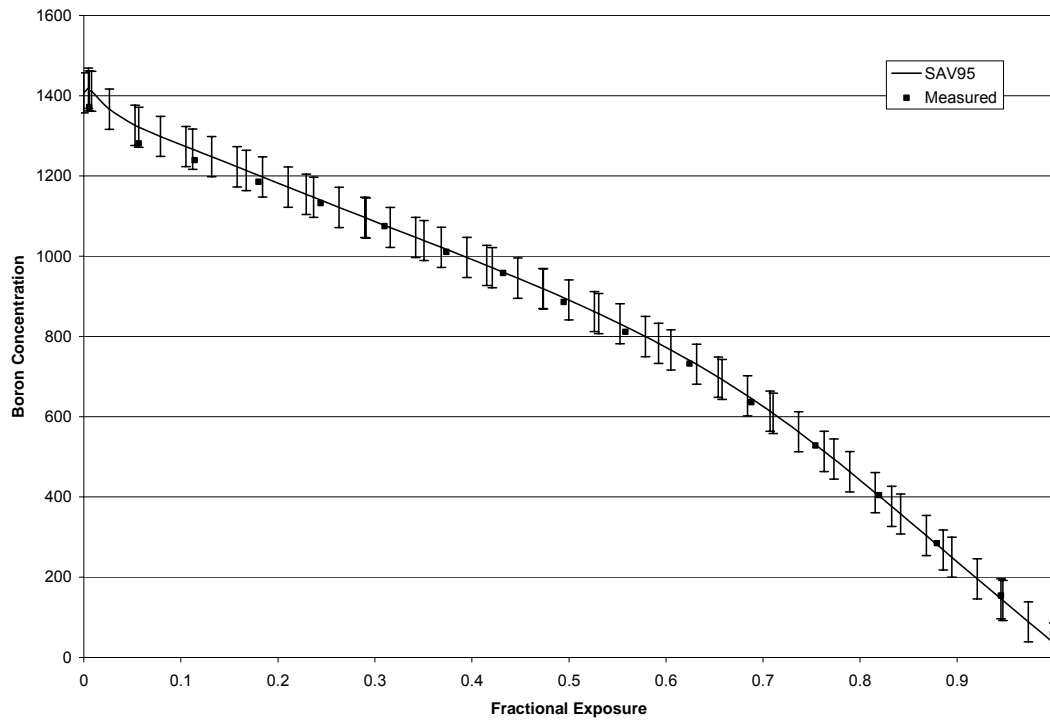
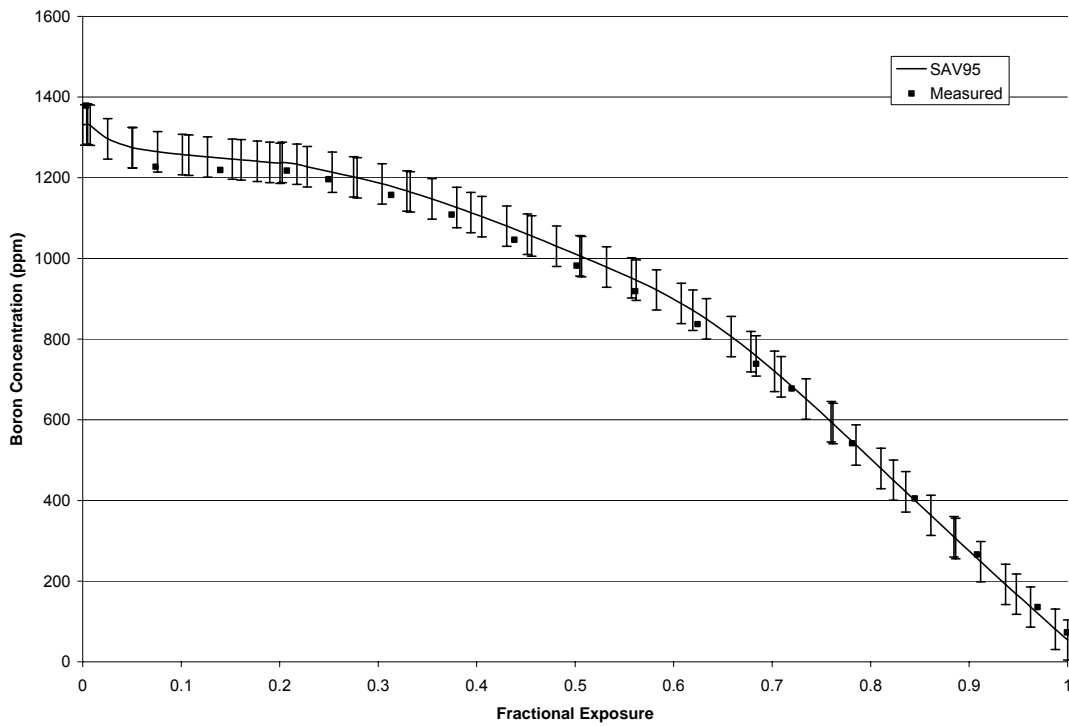
Figure A-2.13: Plant A Cycle 11 Critical Boron Concentration**Figure A-2.14: Plant A Cycle 12 Critical Boron Concentration**

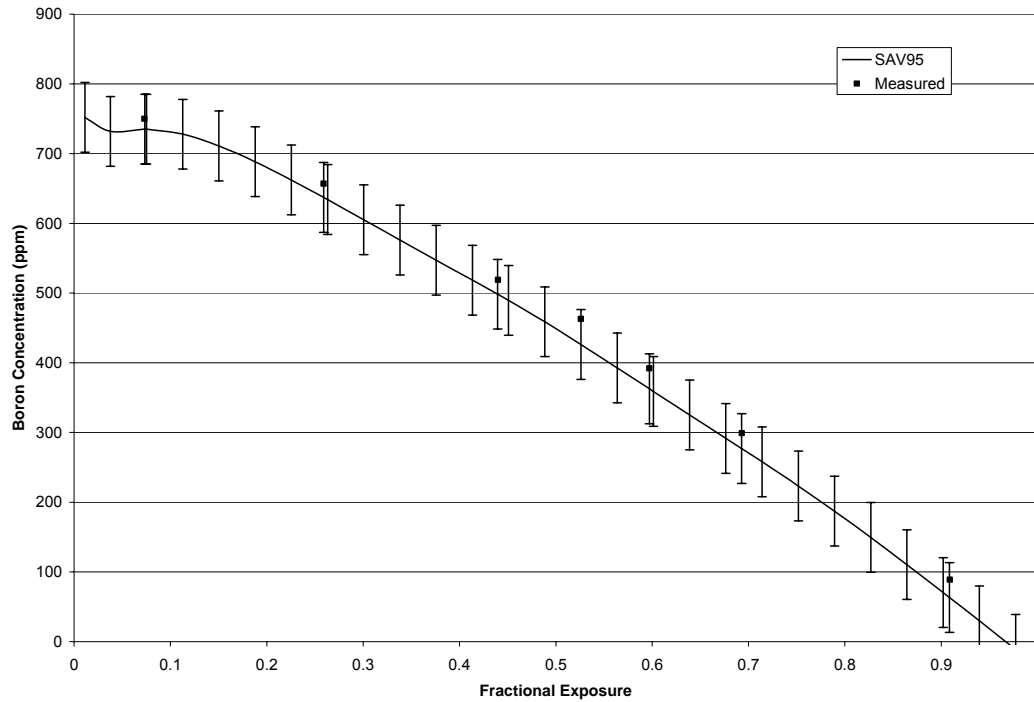
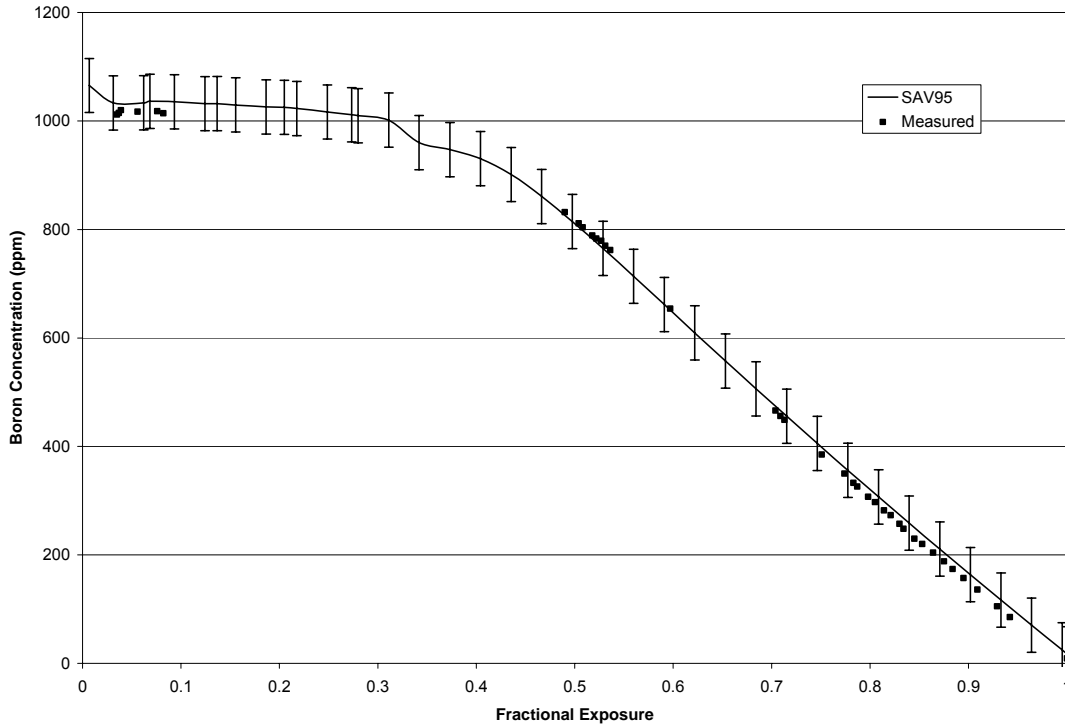
Figure A-2.15: Plant B Cycle 1 Critical Boron Concentration**Figure A-2.16: Plant G2 Cycle 1 Critical Boron Concentration**

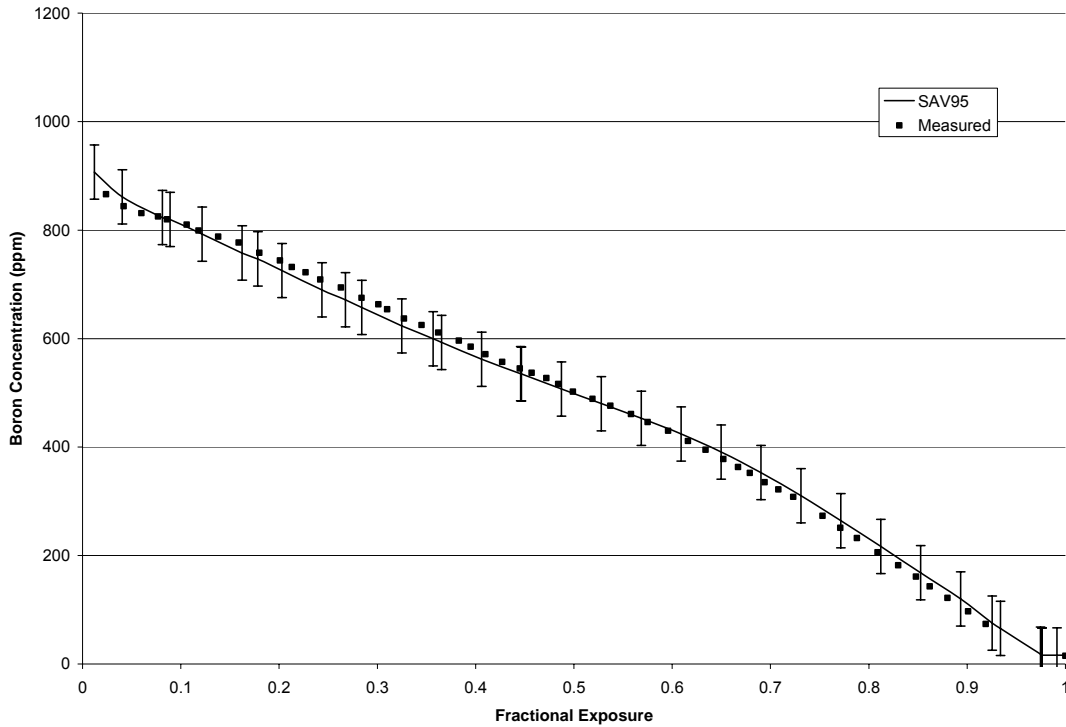
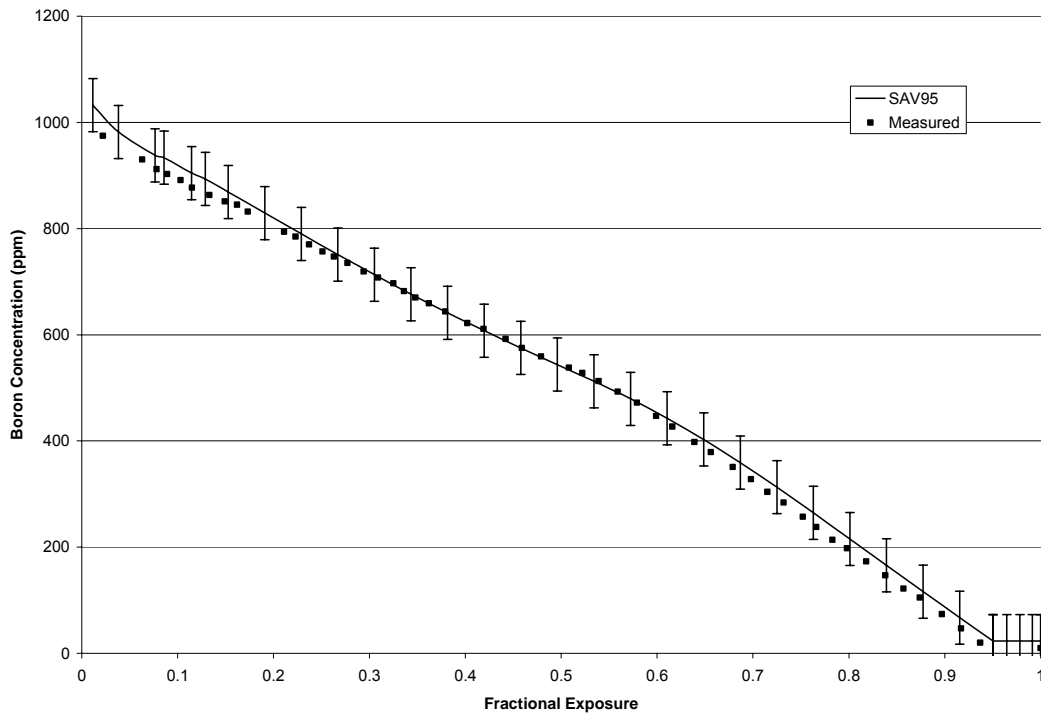
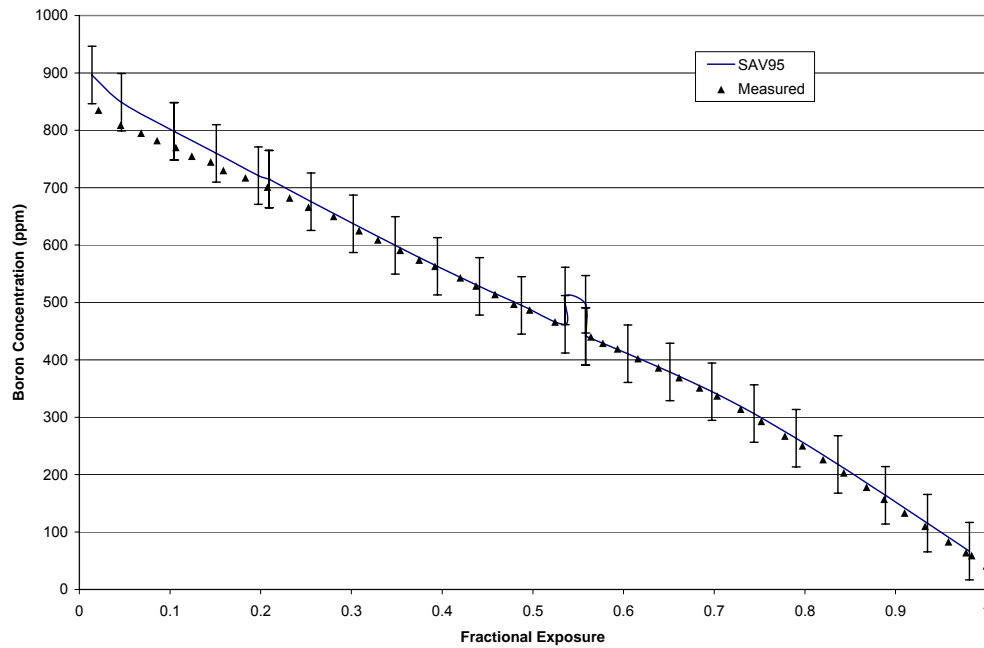
Figure A-2.17: Plant G2 Cycle 2 Critical Boron Concentration**Figure A-2.18: Plant G2 Cycle 3 Critical Boron Concentration**

Figure A-2.19: Plant G2 Cycle 4 Critical Boron Concentration

*The sudden rise in the calculated boron concentration is a result of a reduction in power to 93% and the insertion of a control rod bank for the rest of the cycle.

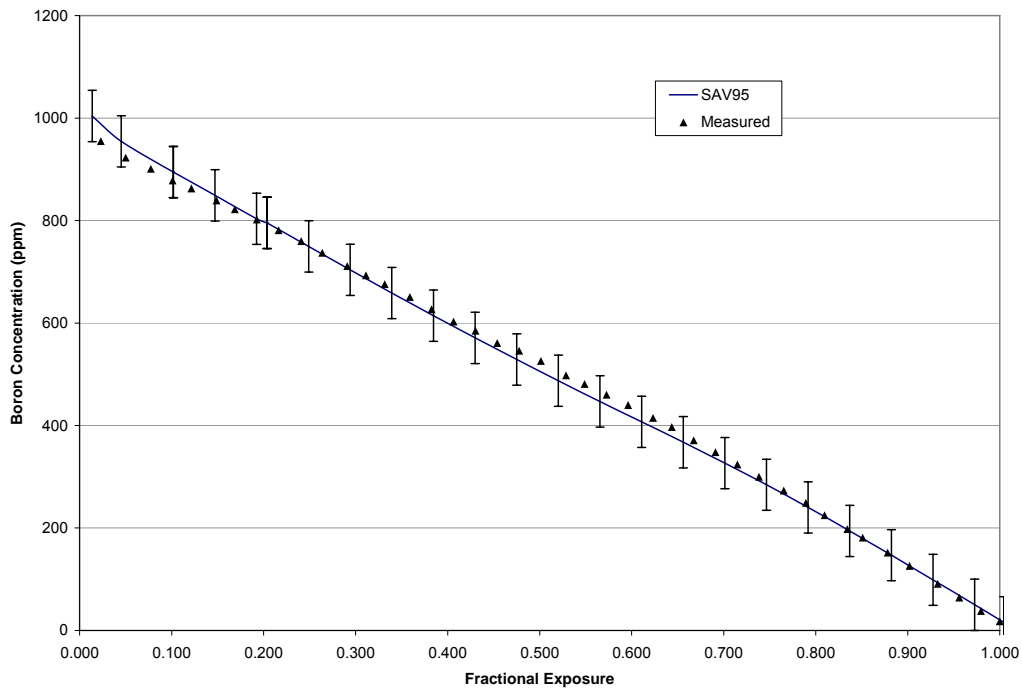
Figure A-2.20: Plant G2 Cycle 5 Critical Boron Concentration

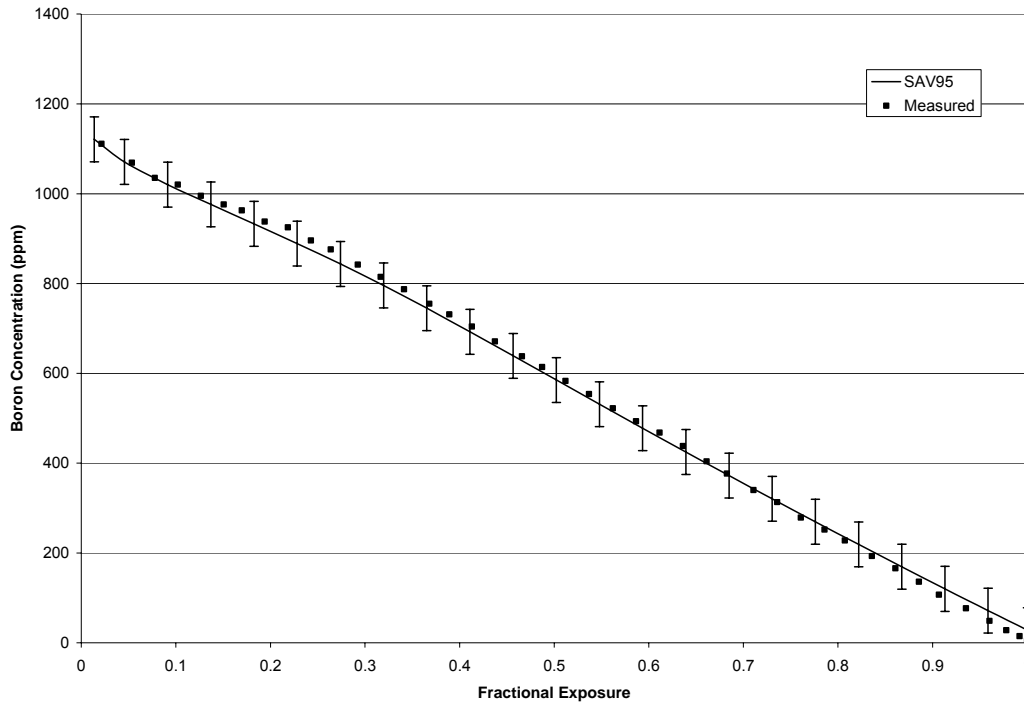
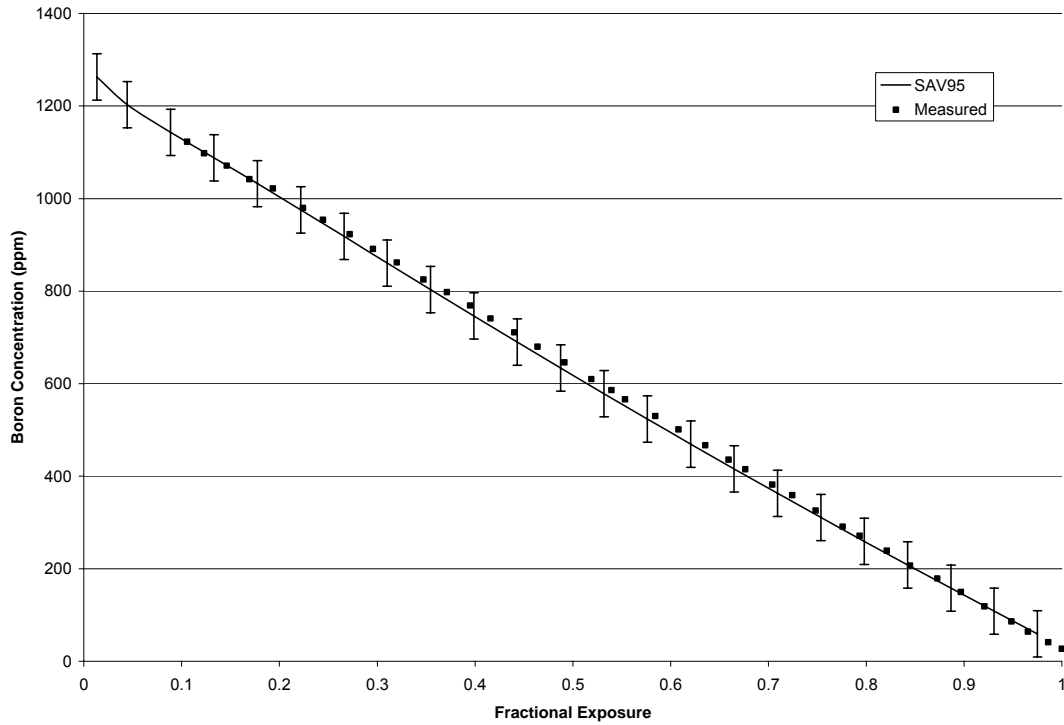
Figure A-2.21: Plant G1 Cycle 26 Critical Boron Concentration**Figure A-2.22: Plant G1 Cycle 27 Critical Boron Concentration**

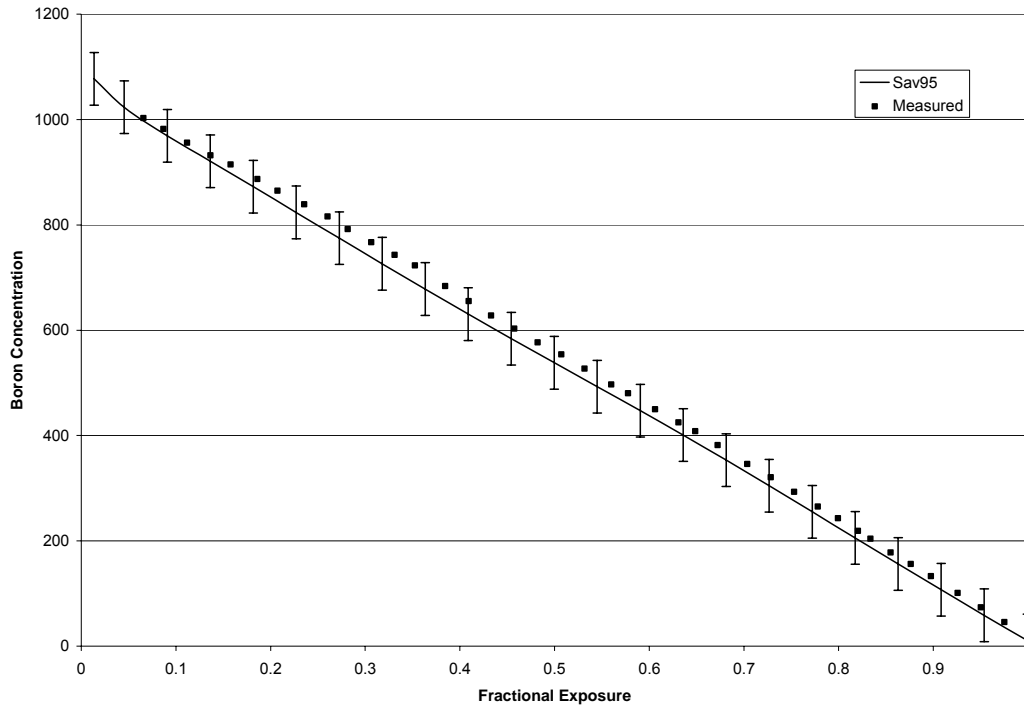
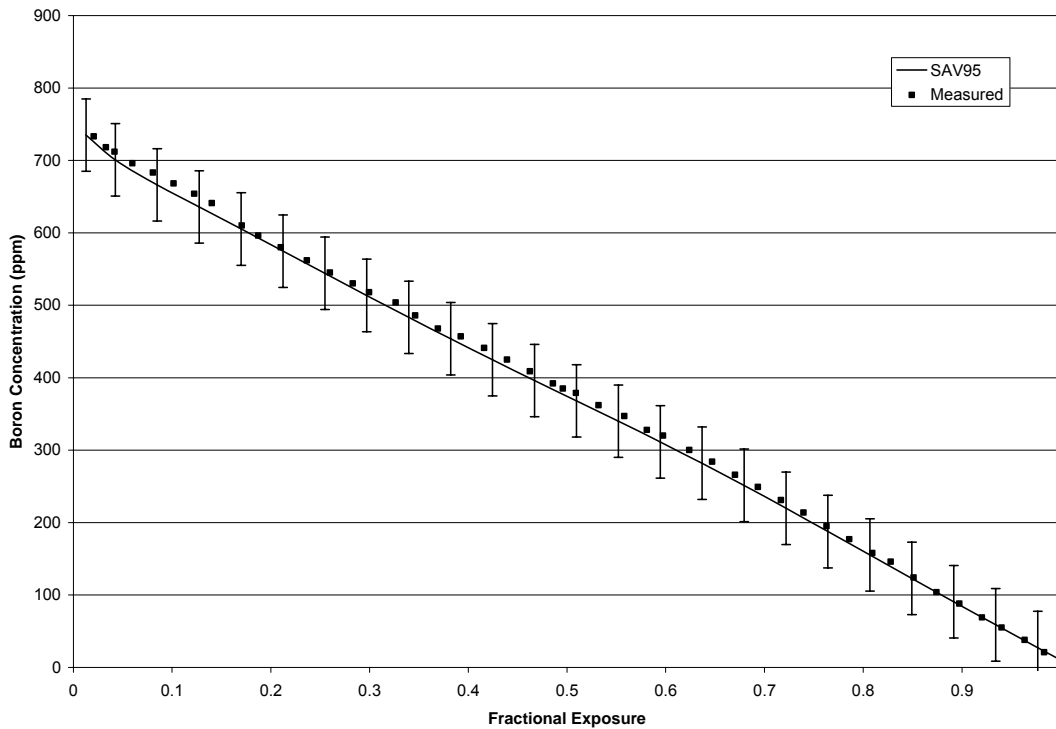
Figure A-2.23: Plant G1 Cycle 28 Critical Boron Concentration**Figure A-2.24: Plant G1 Cycle 29 Critical Boron Concentration**

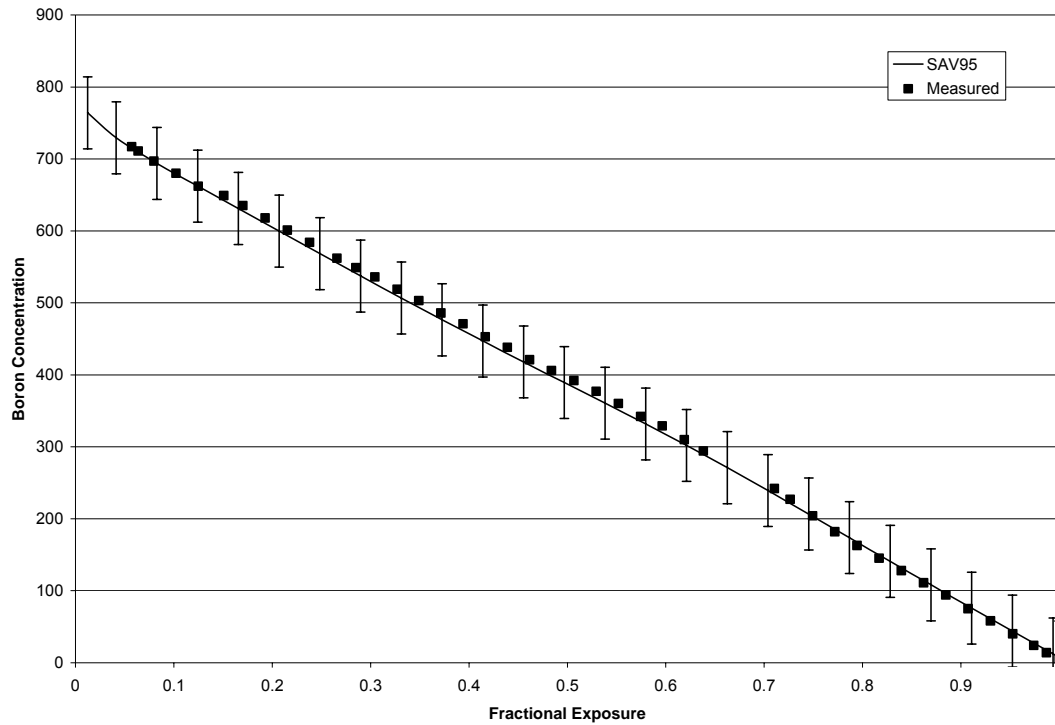
Figure A-2.25: Plant G1 Cycle 30 Critical Boron Concentration

Figure A-2.26: Plant A BOC 1 Assembly Power Distribution

	R	P	N	M	L	K	J	H	G	F	E	D	C	B	A
1							0.559	0.727	0.559						
							0.571	0.762	0.574						
							-0.011	-0.035	-0.015						
2					0.649	0.887	0.934	0.945	0.934	0.887	0.649		Calculated Power Measured Power Difference (C-M)		
					0.650	0.885	0.933	0.950	0.944	0.912	0.658				
					-0.001	0.002	0.001	-0.005	-0.010	-0.025	-0.009				
3				0.722	1.138	0.956	1.095	1.123	1.095	0.956	1.138	0.722			
				0.752	1.145	0.950	1.075	1.101	1.087	0.959	1.142	0.724			
				-0.030	-0.007	0.006	0.019	0.021	0.008	-0.002	-0.004	-0.002			
4			0.722	0.921	0.973	1.120	1.117	1.175	1.117	1.120	0.973	0.921	0.722		
			0.720	0.924	0.966	1.107	1.097	1.132	1.096	1.111	0.969	0.924	0.732		
			0.002	-0.003	0.007	0.013	0.020	0.043	0.021	0.009	0.004	-0.003	-0.010		
5		0.649	1.138	0.973	1.114	1.128	1.185	1.088	1.185	1.128	1.114	0.973	1.138	0.649	
		0.643	1.129	0.963	1.088	1.113	1.178	1.050	1.159	1.116	1.100	0.975	1.164	0.695	
		0.006	0.010	0.009	0.026	0.015	0.007	0.037	0.026	0.013	0.014	-0.002	-0.026	-0.046	
6		0.887	0.956	1.120	1.128	1.203	1.154	1.182	1.154	1.203	1.128	1.120	0.956	0.887	
		0.878	0.947	1.111	1.121	1.188	1.126	1.094	1.126	1.201	1.125	1.125	0.972	0.914	
		0.009	0.009	0.009	0.007	0.015	0.028	0.089	0.028	0.002	0.003	-0.005	-0.016	-0.027	
7	0.559	0.934	1.095	1.117	1.185	1.154	1.178	1.073	1.178	1.154	1.185	1.117	1.095	0.934	0.559
	0.552	0.923	1.081	1.108	1.181	1.147	1.173	1.050	1.177	1.151	1.184	1.121	1.106	0.949	0.573
	0.007	0.011	0.014	0.009	0.005	0.007	0.006	0.024	0.001	0.004	0.001	-0.004	-0.011	-0.015	-0.014
8	0.727	0.945	1.123	1.175	1.088	1.182	1.073	1.142	1.073	1.182	1.088	1.175	1.123	0.945	0.727
	0.719	0.932	1.105	1.167	1.093	1.179	1.069	1.132	1.069	1.171	1.085	1.177	1.130	0.956	0.755
	0.009	0.013	0.018	0.007	-0.005	0.003	0.005	0.009	0.005	0.011	0.003	-0.003	-0.008	-0.010	-0.028
9	0.559	0.934	1.095	1.117	1.185	1.154	1.178	1.073	1.178	1.154	1.185	1.117	1.095	0.934	0.559
	0.554	0.927	1.086	1.109	1.174	1.149	1.176	1.071	1.179	1.153	1.183	1.117	1.106	0.958	0.612
	0.005	0.007	0.009	0.008	0.012	0.005	0.002	0.002	-0.001	0.001	0.002	-0.001	-0.011	-0.024	-0.053
10		0.887	0.956	1.120	1.128	1.203	1.154	1.182	1.154	1.203	1.128	1.120	0.956	0.887	
		0.886	0.955	1.117	1.121	1.199	1.158	1.183	1.154	1.200	1.123	1.111	0.964	0.902	
		0.001	0.001	0.003	0.008	0.004	-0.003	-0.001	0.000	0.002	0.005	0.009	-0.008	-0.015	
11		0.649	1.138	0.973	1.114	1.128	1.185	1.088	1.185	1.128	1.114	0.973	1.138	0.649	
		0.654	1.155	0.977	1.102	1.123	1.181	1.089	1.185	1.125	1.106	0.973	1.157	0.659	
		-0.005	-0.017	-0.004	0.012	0.005	0.004	-0.001	0.000	0.003	0.008	0.000	-0.018	-0.011	
12		0.722	0.921	0.973	1.120	1.117	1.175	1.117	1.120	0.973	0.921	0.722			
		0.762	0.938	0.979	1.119	1.101	1.172	1.117	1.119	0.971	0.921	0.756			
		-0.040	-0.018	-0.006	0.001	0.015	0.003	-0.001	0.001	0.002	0.000	-0.034			
13			0.722	1.138	0.956	1.095	1.123	1.095	0.956	1.138	0.722				
			0.737	1.162	0.966	1.097	1.126	1.101	0.957	1.139	0.722				
			-0.015	-0.024	-0.010	-0.002	-0.003	-0.006	-0.001	-0.001	0.000				
14			0.649	0.887	0.934	0.945	0.934	0.887	0.649						
			0.686	0.907	0.944	0.953	0.951	0.894	0.651						
			-0.037	-0.020	-0.010	-0.007	-0.016	-0.007	-0.003						
15						0.559	0.727	0.559							
						0.565	0.735	0.567							
						-0.006	-0.008	-0.008							

Calculated Minus Measured Powers, RMS Difference = 0.016

Figure A-2.27: Plant A MOC 1 Assembly Power Distribution

	R	P	N	M	L	K	J	H	G	F	E	D	C	B	A
1							0.543 0.547 -0.004	0.689 0.705 -0.016	0.543 0.551 -0.008						
2					0.603 0.602 0.001	0.838 0.834 0.004	0.925 0.921 0.004	0.920 0.921 -0.001	0.925 0.933 -0.008	0.838 0.860 -0.023	0.603 0.613 -0.010		Calculated Power Measured Power Difference (C-M)		
3				0.669 0.686 -0.017	1.046 1.048 -0.002	0.982 0.975 0.006	1.064 1.047 0.017	1.121 1.102 0.019	1.064 1.062 0.002	0.982 0.989 -0.008	1.046 1.056 -0.009	0.669 0.676 -0.007			
4			0.669 0.669 0.001	0.883 0.885 -0.002	1.010 1.006 0.005	1.108 1.100 0.007	1.155 1.145 0.011	1.158 1.140 0.019	1.155 1.149 0.006	1.108 1.109 -0.001	1.010 1.015 -0.005	0.883 0.893 -0.010	0.669 0.681 -0.011		
5		0.603 0.599 0.004	1.046 1.044 0.003	1.010 1.005 0.005	1.111 1.096 0.016	1.178 1.171 0.006	1.188 1.188 -0.001	1.172 1.166 0.006	1.188 1.184 0.004	1.178 1.176 0.002	1.111 1.111 0.001	1.010 1.025 -0.014	1.046 1.070 -0.023	0.603 0.638 -0.035	
6			0.838 0.829 0.009	0.982 0.974 0.008	1.108 1.101 0.006	1.178 1.177 0.001	1.203 1.200 0.003	1.226 1.224 0.002	1.210 1.207 0.003	1.226 1.224 0.003	1.203 1.200 -0.002	1.178 1.116 -0.008	1.108 0.994 -0.013	0.982 0.855 -0.017	0.838
7	0.543 0.533 0.010	0.925 0.910 0.015	1.064 1.050 0.015	1.155 1.145 0.010	1.188 1.184 0.003	1.226 1.224 0.002	1.215 1.212 0.003	1.195 1.194 0.001	1.215 1.215 0.000	1.226 1.226 0.000	1.188 1.189 -0.001	1.155 1.159 -0.003	1.064 1.068 -0.003	0.925 0.929 -0.004	0.543 0.547 -0.003
8	0.689 0.675 0.014	0.920 0.898 0.022	1.121 1.079 0.041	1.158 1.143 0.015	1.172 1.173 -0.001	1.210 1.209 0.001	1.195 1.195 0.000	1.206 1.206 0.000	1.195 1.196 -0.001	1.210 1.211 -0.002	1.172 1.173 -0.001	1.158 1.157 0.001	1.121 1.115 0.006	0.920 0.899 0.021	0.689 0.695 -0.007
9	0.543 0.533 0.010	0.925 0.910 0.015	1.064 1.047 0.018	1.155 1.145 0.010	1.188 1.184 0.003	1.226 1.225 0.001	1.215 1.217 -0.001	1.195 1.197 -0.002	1.215 1.216 -0.001	1.226 1.233 -0.006	1.188 1.189 -0.001	1.155 1.155 0.001	1.064 1.065 0.000	0.925 0.931 -0.006	0.543 0.581 -0.038
10			0.838 0.832 0.005	0.982 0.979 0.003	1.108 1.103 0.004	1.178 1.173 0.005	1.203 1.202 0.001	1.226 1.232 -0.006	1.210 1.214 -0.005	1.226 1.229 -0.003	1.203 1.205 -0.002	1.178 1.177 0.001	1.108 1.103 0.004	0.982 0.984 -0.002	0.838 0.841 -0.004
11		0.603 0.604 -0.001	1.046 1.056 -0.010	1.010 1.012 -0.002	1.111 1.101 0.010	1.178 1.174 0.004	1.188 1.187 0.001	1.172 1.181 -0.009	1.188 1.191 -0.003	1.178 1.178 0.000	1.111 1.108 0.003	1.010 1.011 0.000	1.046 1.055 -0.008	0.603 0.607 -0.004	
12			0.669 0.700 -0.030	0.883 0.894 -0.011	1.010 1.013 -0.002	1.108 1.104 0.003	1.155 1.141 0.014	1.158 1.156 0.002	1.155 1.155 0.001	1.108 1.107 0.001	1.010 1.009 0.001	0.883 0.883 0.000	0.669 0.690 -0.020		
13				0.669 0.677 -0.008	1.046 1.058 -0.011	0.982 0.985 -0.004	1.064 1.061 0.003	1.121 1.118 0.003	1.064 1.062 0.003	0.982 0.980 0.002	1.046 1.045 0.002	0.669 0.669 0.001			
14					0.603 0.625 -0.022	0.838 0.846 -0.009	0.925 0.926 -0.001	0.920 0.917 0.002	0.925 0.920 0.005	0.838 0.835 0.003	0.603 0.602 0.002				
15							0.543 0.543 0.000	0.689 0.687 0.002	0.543 0.541 0.002						

Calculated Minus Measured Powers, RMS Difference = 0.010

Figure A-2.28: Plant A EOC 1 Assembly Power Distribution

	R	P	N	M	L	K	J	H	G	F	E	D	C	B	A
1							0.612 0.616 -0.004	0.748 0.754 -0.007	0.612 0.616 -0.005						
2					0.637 0.641 -0.004	0.874 0.879 -0.005	1.004 1.009 -0.005	0.971 0.972 -0.001	1.004 1.011 -0.007	0.874 0.894 -0.020	0.637 0.646 -0.009		Calculated Power Measured Power Difference (C-M)		
3				0.694 0.710 -0.016	1.037 1.044 -0.008	1.055 1.059 -0.005	1.060 1.069 -0.009	1.131 1.117 0.015	1.060 1.060 0.000	1.055 1.062 -0.007	1.037 1.045 -0.008	0.694 0.698 -0.005			
4			0.694 0.694 0.000	0.901 0.903 -0.002	1.075 1.074 0.001	1.085 1.085 0.000	1.150 1.151 -0.001	1.102 1.096 0.006	1.150 1.148 0.002	1.085 1.088 -0.003	1.075 1.079 -0.004	0.901 0.905 -0.005	0.694 0.703 -0.009		
5		0.637 0.634 0.003	1.037 1.035 0.001	1.075 1.068 0.007	1.084 1.073 0.011	1.154 1.148 0.007	1.107 1.108 -0.001	1.152 1.149 0.004	1.107 1.105 0.002	1.154 1.155 -0.001	1.084 1.087 -0.003	1.075 1.074 0.001	1.037 1.057 -0.020	0.637 0.684 -0.047	
6		0.874 0.867 0.007	1.055 1.045 0.009	1.085 1.070 0.015	1.154 1.123 0.031	1.107 1.092 0.014	1.161 1.152 0.008	1.108 1.103 0.005	1.161 1.156 0.005	1.107 1.105 0.001	1.154 1.155 0.000	1.085 1.088 -0.003	1.055 1.065 -0.010	0.874 0.893 -0.019	
7	0.612 0.606 0.006	1.004 0.994 0.010	1.060 1.049 0.011	1.150 1.135 0.015	1.107 1.088 0.019	1.161 1.146 0.015	1.108 1.096 0.012	1.153 1.147 0.006	1.108 1.099 0.009	1.161 1.155 0.005	1.107 1.105 0.002	1.150 1.149 0.001	1.060 1.061 -0.001	1.004 1.003 0.001	0.612 0.619 -0.007
8	0.748 0.741 0.007	0.971 0.962 0.009	1.131 1.120 0.012	1.102 1.090 0.012	1.152 1.134 0.018	1.108 1.098 0.011	1.153 1.147 0.006	1.109 1.112 -0.003	1.153 1.163 0.010	1.108 1.102 0.006	1.152 1.147 0.006	1.102 1.099 0.003	1.131 1.125 0.006	0.971 0.988 -0.017	0.748 0.769 -0.021
9	0.612 0.606 0.006	1.004 0.995 0.009	1.060 1.050 0.010	1.150 1.142 0.008	1.107 1.105 0.002	1.161 1.154 0.006	1.108 1.105 0.003	1.153 1.166 -0.012	1.108 1.159 -0.051	1.161 1.139 0.021	1.107 1.099 0.008	1.150 1.147 0.003	1.060 1.064 -0.004	1.004 1.023 -0.019	0.612 0.649 -0.037
10		0.874 0.868 0.006	1.055 1.040 0.014	1.085 1.081 0.004	1.154 1.150 0.004	1.107 1.099 0.008	1.161 1.146 0.014	1.108 1.107 0.001	1.161 1.171 -0.011	1.107 1.103 0.004	1.154 1.150 0.005	1.085 1.082 0.003	1.055 1.059 -0.005	0.874 0.884 -0.010	
11		0.637 0.640 -0.003	1.037 1.053 -0.017	1.075 1.082 -0.008	1.084 1.083 0.001	1.154 1.146 0.009	1.107 1.091 0.016	1.152 1.136 0.016	1.107 1.104 0.003	1.154 1.151 0.004	1.084 1.083 0.001	1.075 1.070 0.005	1.037 1.046 -0.009	0.637 0.643 -0.006	
12			0.694 0.751 -0.057	0.901 0.922 -0.021	1.075 1.080 -0.006	1.085 1.078 0.007	1.150 1.122 0.028	1.102 1.089 0.013	1.150 1.144 0.006	1.085 1.081 0.004	1.075 1.065 0.009	0.901 0.879 0.022	0.694 0.718 -0.024		
13				0.694 0.705 -0.012	1.037 1.048 -0.011	1.055 1.055 0.000	1.060 1.053 0.008	1.131 1.126 0.005	1.060 1.060 0.000	1.055 1.054 0.000	1.037 1.031 0.006	0.694 0.684 0.010			
14					0.637 0.656 -0.019	0.874 0.881 -0.007	1.004 1.004 0.000	0.971 0.973 -0.002	1.004 1.012 -0.008	0.874 0.877 -0.002	0.637 0.635 0.001				
15							0.612 0.613 -0.001	0.748 0.750 -0.002	0.612 0.615 -0.004						

Calculated Minus Measured Powers, RMS Difference = 0.012

Figure A-2.29: Plant A BOC 2 Assembly Power Distribution

	R	P	N	M	L	K	J	H	G	F	E	D	C	B	A
1							0.334 0.335 -0.002	0.395 0.403 -0.008	0.331 0.335 -0.005						
2					0.419 0.419 0.000	0.959 0.957 0.002	1.159 1.157 0.002	0.983 0.984 -0.001	1.146 1.159 -0.013	0.954 0.985 -0.031	0.418 0.426 -0.008		Calculated Power Measured Power Difference (C-M)		
3				0.403 0.415 -0.012	1.130 1.130 0.001	1.295 1.290 0.004	1.094 1.090 0.005	1.140 1.127 0.014	1.091 1.091 -0.001	1.291 1.300 -0.009	1.129 1.139 -0.010	0.403 0.412 -0.009			
4			0.403 0.407 -0.003	0.737 0.739 -0.002	1.284 1.275 0.009	1.067 1.063 0.004	1.176 1.172 0.003	1.275 1.273 0.002	1.176 1.171 0.005	1.066 1.053 0.013	1.281 1.284 -0.002	0.737 0.739 -0.002	0.403 0.406 -0.003		
5		0.418 0.420 -0.002	1.129 1.141 -0.012	1.281 1.283 -0.002	1.231 1.233 -0.002	1.135 1.131 0.003	1.016 1.014 0.002	0.986 0.984 0.002	1.024 1.019 0.005	1.140 1.133 0.007	1.231 1.239 -0.007	1.284 1.281 0.003	1.131 1.140 -0.010	0.419 0.439 -0.020	
6		0.954 0.951 0.004	1.291 1.286 0.005	1.066 1.058 0.008	1.139 1.117 0.022	1.160 1.150 0.010	1.267 1.263 0.004	1.207 1.207 0.000	1.289 1.281 0.008	1.161 1.143 0.017	1.135 1.132 0.003	1.067 1.069 -0.001	1.295 1.305 -0.010	0.959 0.974 -0.016	
7	0.331 0.329 0.002	1.146 1.138 0.008	1.091 1.076 0.015	1.176 1.163 0.013	1.024 1.008 0.016	1.289 1.278 0.011	1.199 1.199 0.000	1.212 1.211 0.001	1.201 1.197 0.004	1.269 1.259 0.010	1.017 1.014 0.003	1.176 1.177 -0.001	1.095 1.103 -0.008	1.159 1.175 -0.016	0.334 0.339 -0.005
8	0.395 0.394 0.001	0.983 0.980 0.003	1.140 1.143 -0.002	1.275 1.261 0.014	0.986 0.961 0.026	1.207 1.194 0.012	1.212 1.208 0.004	0.941 0.941 0.000	1.217 1.218 -0.001	1.208 1.203 0.006	0.987 0.984 0.003	1.275 1.276 0.000	1.141 1.147 -0.007	0.983 0.992 -0.009	0.395 0.402 -0.007
9	0.334 0.333 0.001	1.159 1.155 0.004	1.094 1.091 0.003	1.176 1.169 0.007	1.016 1.007 0.010	1.268 1.259 0.009	1.201 1.198 0.003	1.217 1.218 -0.001	1.203 1.217 -0.014	1.291 1.268 0.022	1.025 1.018 0.006	1.177 1.176 0.001	1.091 1.101 -0.010	1.146 1.169 -0.023	0.331 0.347 -0.017
10		0.959 0.955 0.003	1.295 1.288 0.007	1.067 1.065 0.002	1.135 1.133 0.002	1.161 1.158 0.003	1.290 1.288 0.002	1.208 1.202 0.006	1.269 1.264 0.005	1.162 1.148 0.013	1.140 1.136 0.004	1.066 1.059 0.007	1.292 1.306 -0.015	0.954 0.984 -0.030	
11		0.419 0.419 -0.001	1.131 1.135 -0.005	1.284 1.288 -0.003	1.231 1.236 -0.005	1.140 1.140 0.000	1.024 1.021 0.004	0.987 0.969 0.018	1.017 1.005 0.012	1.135 1.114 0.021	1.232 1.242 -0.010	1.282 1.291 -0.009	1.129 1.146 -0.017	0.418 0.427 -0.010	
12			0.403 0.421 -0.017	0.737 0.744 -0.007	1.281 1.287 -0.006	1.066 1.069 -0.003	1.177 1.177 0.001	1.275 1.261 0.014	1.176 1.166 0.010	1.067 1.060 0.007	1.284 1.289 -0.005	0.737 0.750 -0.013	0.404 0.421 -0.017		
13				0.403 0.407 -0.004	1.129 1.136 -0.007	1.291 1.295 -0.004	1.091 1.089 0.002	1.141 1.122 0.019	1.095 1.089 0.006	1.295 1.289 0.006	1.131 1.132 -0.001	0.403 0.406 -0.003			
14					0.418 0.428 -0.010	0.954 0.961 -0.006	1.146 1.151 -0.005	0.983 0.982 0.001	1.159 1.167 -0.008	0.959 0.960 -0.001	0.419 0.419 -0.001				
15							0.331 0.342 -0.011	0.395 0.398 -0.003	0.334 0.336 -0.003						

Calculated Minus Measured Powers, RMS Difference = 0.009

Codes and Methods Applicability Report
for the U.S. EPR

Figure A-2.30: Plant A MOC 2 Assembly Power Distribution

	R	P	N	M	L	K	J	H	G	F	E	D	C	B	A
1							0.354	0.418	0.351						
							0.354	0.418	0.355						
							0.000	0.000	-0.004						
2					0.436	0.944	1.130	0.968	1.122	0.942	0.436				
					0.439	0.946	1.131	0.970	1.137	0.976	0.446				
					-0.003	-0.002	-0.001	-0.002	-0.016	-0.034	-0.010				
												Calculated Power			
												Measured Power			
												Difference (C-M)			
3				0.426	1.102	1.305	1.078	1.121	1.076	1.303	1.102	0.427			
				0.440	1.110	1.308	1.078	1.113	1.083	1.322	1.116	0.432			
				-0.013	-0.008	-0.003	0.000	0.007	-0.007	-0.019	-0.014	-0.005			
4			0.427	0.751	1.268	1.053	1.162	1.299	1.163	1.053	1.267	0.751	0.426		
			0.431	0.759	1.275	1.056	1.161	1.296	1.165	1.059	1.277	0.757	0.430		
			-0.005	-0.007	-0.006	-0.003	0.001	0.003	-0.002	-0.007	-0.010	-0.005	-0.004		
5		0.436	1.102	1.267	1.192	1.117	1.028	1.007	1.034	1.120	1.192	1.268	1.102	0.436	
		0.438	1.114	1.272	1.200	1.116	1.026	1.004	1.031	1.119	1.199	1.273	1.114	0.452	
		-0.002	-0.012	-0.005	-0.008	0.001	0.002	0.003	0.003	0.002	-0.007	-0.005	-0.011	-0.016	
6		0.942	1.303	1.053	1.120	1.162	1.330	1.212	1.348	1.162	1.117	1.053	1.305	0.944	
		0.940	1.299	1.046	1.096	1.150	1.322	1.205	1.337	1.143	1.114	1.056	1.315	0.958	
		0.003	0.004	0.007	0.024	0.011	0.008	0.007	0.010	0.019	0.003	-0.003	-0.011	-0.014	
7	0.351	1.122	1.076	1.163	1.034	1.347	1.201	1.202	1.202	1.331	1.028	1.162	1.078	1.130	0.354
	0.350	1.116	1.063	1.150	1.018	1.333	1.197	1.197	1.197	1.318	1.024	1.163	1.085	1.144	0.358
	0.001	0.006	0.013	0.012	0.016	0.014	0.004	0.005	0.005	0.012	0.004	-0.001	-0.007	-0.014	-0.005
8	0.418	0.968	1.121	1.299	1.007	1.212	1.202	0.956	1.205	1.213	1.007	1.299	1.120	0.968	0.418
	0.418	0.967	1.125	1.287	0.983	1.198	1.195	0.953	1.202	1.200	1.002	1.298	1.125	0.968	0.424
	0.000	0.000	-0.005	0.012	0.024	0.014	0.007	0.003	0.003	0.013	0.005	0.002	-0.004	0.000	-0.005
9	0.354	1.130	1.078	1.162	1.028	1.330	1.202	1.205	1.203	1.348	1.034	1.163	1.076	1.122	0.351
	0.354	1.130	1.079	1.155	1.014	1.317	1.195	1.204	1.213	1.330	1.027	1.158	1.077	1.129	0.368
	0.000	0.000	-0.001	0.007	0.014	0.013	0.006	0.002	-0.010	0.018	0.007	0.005	-0.002	-0.008	-0.017
10		0.944	1.305	1.053	1.117	1.162	1.348	1.213	1.331	1.162	1.120	1.053	1.303	0.942	
		0.946	1.307	1.052	1.111	1.154	1.341	1.206	1.328	1.155	1.116	1.042	1.303	0.945	
		-0.002	-0.002	0.001	0.005	0.008	0.007	0.007	0.003	0.007	0.004	0.011	0.000	-0.003	
11		0.436	1.102	1.268	1.192	1.120	1.034	1.007	1.028	1.117	1.192	1.267	1.102	0.436	
		0.438	1.109	1.272	1.194	1.116	1.025	0.991	1.023	1.116	1.200	1.269	1.107	0.438	
		-0.002	-0.007	-0.004	-0.002	0.005	0.009	0.016	0.005	0.001	-0.008	-0.002	-0.005	-0.002	
12		0.426	0.751	1.267	1.053	1.163	1.299	1.162	1.053	1.268	0.751	0.427			
		0.440	0.756	1.269	1.049	1.147	1.287	1.158	1.053	1.273	0.756	0.440			
		-0.014	-0.005	-0.002	0.003	0.015	0.012	0.004	0.000	-0.005	-0.005	-0.013			
13			0.427	1.102	1.303	1.076	1.120	1.078	1.305	1.102	0.426				
			0.429	1.106	1.303	1.072	1.117	1.078	1.306	1.106	0.429				
			-0.002	-0.004	0.000	0.004	0.003	0.000	-0.001	-0.003	-0.002				
14				0.436	0.942	1.122	0.968	1.130	0.944	0.436					
				0.446	0.946	1.123	0.969	1.137	0.948	0.437					
				-0.010	-0.003	-0.001	-0.001	-0.008	-0.004	-0.001					
15							0.351	0.418	0.354						
							0.355	0.420	0.356						
							-0.003	-0.002	-0.002						

Calculated Minus Measured Powers, RMS Difference = 0.008

Figure A-2.31: Plant A EOC 2 Assembly Power Distribution

	R	P	N	M	L	K	J	H	G	F	E	D	C	B	A
1							0.393 0.394 -0.001	0.463 0.469 -0.006	0.391 0.396 -0.005						
2					0.468 0.469 -0.001	0.950 0.949 0.001	1.126 1.125 0.001	0.978 0.980 -0.002	1.121 1.136 -0.016	0.949 0.982 -0.034	0.468 0.479 -0.010		Calculated Power Measured Power Difference (C-M)		
3				0.465 0.475 -0.010	1.091 1.093 -0.002	1.307 1.304 0.002	1.071 1.068 0.003	1.110 1.099 0.011	1.070 1.076 -0.006	1.306 1.324 -0.018	1.091 1.103 -0.012	0.465 0.469 -0.004			
4			0.466 0.469 -0.003	0.778 0.782 -0.003	1.252 1.250 0.002	1.045 1.043 0.002	1.147 1.144 0.003	1.297 1.291 0.005	1.147 1.149 -0.002	1.045 1.051 -0.006	1.251 1.257 -0.006	0.778 0.781 -0.003	0.465 0.467 -0.002		
5		0.468 0.471 -0.002	1.091 1.100 -0.009	1.251 1.251 0.001	1.162 1.155 0.007	1.098 1.093 0.005	1.028 1.025 0.003	1.011 1.009 0.002	1.032 1.032 0.000	1.100 1.100 0.000	1.162 1.163 -0.001	1.252 1.249 0.003	1.091 1.096 -0.006	0.468 0.482 -0.014	
6		0.949 0.949 0.000	1.306 1.306 0.000	1.045 1.040 0.005	1.100 1.080 0.020	1.143 1.134 0.009	1.331 1.328 0.004	1.185 1.184 0.001	1.343 1.342 0.001	1.143 1.136 0.007	1.098 1.097 0.001	1.045 1.046 -0.001	1.306 1.312 -0.006	0.950 0.959 -0.009	
7	0.391 0.391 0.000	1.121 1.120 0.001	1.070 1.066 0.004	1.147 1.141 0.006	1.032 1.022 0.010	1.343 1.335 0.008	1.169 1.171 -0.002	1.164 1.166 -0.002	1.170 1.176 -0.007	1.331 1.332 0.000	1.028 1.028 -0.001	1.147 1.149 -0.002	1.071 1.075 -0.004	1.126 1.135 -0.009	0.393 0.396 -0.004
8	0.463 0.464 -0.001	0.978 0.980 -0.001	1.110 1.118 -0.008	1.297 1.291 0.006	1.011 1.000 0.011	1.185 1.178 0.007	1.164 1.162 0.002	0.951 0.952 -0.002	1.166 1.172 -0.006	1.186 1.190 -0.004	1.011 1.012 -0.002	1.297 1.298 -0.001	1.110 1.112 -0.002	0.978 0.981 -0.003	0.463 0.469 -0.006
9	0.393 0.393 0.000	1.126 1.124 0.002	1.071 1.070 0.001	1.147 1.141 0.005	1.028 1.017 0.011	1.331 1.321 0.010	1.170 1.166 0.004	1.166 1.167 -0.001	1.170 1.180 -0.010	1.343 1.336 0.007	1.032 1.031 0.001	1.147 1.146 0.001	1.070 1.071 -0.002	1.120 1.128 -0.008	0.391 0.406 -0.015
10		0.950 0.945 0.004	1.307 1.298 0.009	1.045 1.041 0.005	1.098 1.092 0.006	1.143 1.136 0.007	1.343 1.333 0.010	1.186 1.183 0.003	1.331 1.331 0.000	1.143 1.141 0.002	1.100 1.099 0.001	1.045 1.039 0.006	1.306 1.307 -0.001	0.949 0.952 -0.003	
11		0.468 0.467 0.001	1.091 1.089 0.002	1.252 1.249 0.003	1.162 1.160 0.002	1.100 1.096 0.004	1.032 1.026 0.006	1.011 1.005 0.005	1.028 1.026 0.002	1.098 1.097 0.000	1.162 1.166 -0.004	1.251 1.251 0.000	1.091 1.094 -0.003	0.468 0.470 -0.002	
12		0.465 0.472 -0.007	0.778 0.780 -0.001	1.251 1.250 0.002	1.045 1.042 0.003	1.147 1.138 0.009	1.297 1.289 0.008	1.147 1.143 0.004	1.045 1.043 0.002	1.252 1.251 0.001	0.778 0.779 -0.001	0.465 0.474 -0.009			
13			0.465 0.466 -0.001	1.091 1.092 -0.001	1.306 1.304 0.002	1.070 1.066 0.003	1.110 1.106 0.004	1.071 1.068 0.003	1.306 1.299 0.007	1.091 1.088 0.003	0.465 0.464 0.001				
14				0.468 0.475 -0.007	0.949 0.949 0.000	1.121 1.118 0.003	0.978 0.976 0.003	1.126 1.125 0.002	0.949 0.946 0.003	0.468 0.467 0.001					
15							0.391 0.390 0.000	0.463 0.462 0.001	0.393 0.393 0.000						

Calculated Minus Measured Powers, RMS Difference = 0.006

Codes and Methods Applicability Report
for the U.S. EPR

Figure A-2.32: Plant A BOC 3 Assembly Power Distribution

	R	P	N	M	L	K	J	H	G	F	E	D	C	B	A
1							0.306 0.307 -0.001	0.499 0.508 -0.009	0.306 0.306 0.000						
2					0.294 0.293 0.001	0.549 0.546 0.002	1.162 1.158 0.005	1.258 1.247 0.012	1.162 1.153 0.009	0.548 0.550 -0.003	0.293 0.294 -0.001		Calculated Power Measured Power Difference (C-M)		
3				0.323 0.330 -0.007	1.059 1.055 0.004	1.278 1.273 0.005	1.289 1.288 0.001	1.318 1.285 0.034	1.289 1.272 0.017	1.276 1.267 0.008	1.055 1.057 -0.002	0.321 0.336 -0.015			
4			0.321 0.322 -0.001	0.656 0.654 0.002	1.229 1.216 0.013	1.171 1.161 0.010	1.213 1.201 0.012	1.265 1.246 0.020	1.215 1.200 0.015	1.167 1.153 0.015	1.221 1.220 0.001	0.655 0.661 -0.005	0.323 0.326 -0.003		
5		0.293 0.294 -0.001	1.055 1.063 -0.008	1.222 1.217 0.004	1.161 1.150 0.011	0.977 0.966 0.011	1.393 1.376 0.017	0.958 0.949 0.009	1.394 1.383 0.011	0.975 0.969 0.006	1.161 1.164 -0.003	1.229 1.237 -0.009	1.059 1.070 -0.012	0.294 0.306 -0.011	
6		0.548 0.545 0.003	1.276 1.270 0.007	1.168 1.158 0.010	0.976 0.961 0.014	1.339 1.323 0.017	1.217 1.204 0.013	1.243 1.242 0.001	1.226 1.221 0.005	1.339 1.329 0.010	0.977 0.976 0.000	1.171 1.175 -0.005	1.278 1.290 -0.012	0.548 0.559 -0.010	
7	0.306 0.306 0.000	1.162 1.154 0.009	1.289 1.272 0.017	1.215 1.201 0.014	1.395 1.377 0.018	1.228 1.211 0.016	1.021 1.003 0.018	1.373 1.365 0.007	1.019 1.021 -0.002	1.217 1.218 -0.001	1.393 1.394 -0.001	1.213 1.212 0.000	1.289 1.298 -0.009	1.162 1.191 -0.028	0.306 0.313 -0.007
8	0.499 0.508 -0.009	1.259 1.252 0.006	1.318 1.301 0.018	1.266 1.251 0.015	0.958 0.946 0.012	1.244 1.231 0.013	1.379 1.366 0.013	0.983 0.979 0.004	1.373 1.372 0.001	1.243 1.254 -0.011	0.957 0.960 -0.003	1.265 1.265 0.000	1.318 1.315 0.003	1.258 1.275 -0.016	0.499 0.511 -0.012
9	0.306 0.307 -0.001	1.162 1.158 0.004	1.289 1.281 0.008	1.213 1.203 0.010	1.393 1.378 0.015	1.218 1.210 0.009	1.023 1.019 0.004	1.379 1.372 0.007	1.021 1.014 0.007	1.227 1.230 -0.003	1.394 1.396 -0.002	1.214 1.216 -0.002	1.289 1.297 -0.008	1.162 1.184 -0.022	0.306 0.327 -0.021
10		0.549 0.548 0.001	1.278 1.280 -0.002	1.171 1.168 0.003	0.976 0.971 0.005	1.340 1.337 0.003	1.228 1.233 -0.005	1.244 1.243 0.002	1.218 1.214 0.004	1.339 1.334 0.005	0.975 0.974 0.001	1.167 1.165 0.003	1.276 1.288 -0.012	0.548 0.566 -0.019	
11		0.294 0.295 -0.001	1.059 1.064 -0.005	1.229 1.230 -0.001	1.161 1.157 0.004	0.975 0.975 0.000	1.395 1.397 -0.002	0.958 0.958 0.000	1.393 1.390 0.003	0.976 0.965 0.011	1.161 1.158 0.003	1.221 1.225 -0.003	1.055 1.067 -0.013	0.293 0.299 -0.006	
12		0.323 0.335 -0.012	0.655 0.660 -0.004	1.222 1.226 -0.004	1.167 1.171 -0.003	1.215 1.215 -0.001	1.265 1.270 -0.005	1.213 1.219 -0.006	1.171 1.178 -0.007	1.228 1.235 -0.007	0.655 0.659 -0.003	0.321 0.338 -0.017			
13			0.321 0.324 -0.003	1.055 1.064 -0.009	1.276 1.286 -0.010	1.289 1.299 -0.010	1.318 1.331 -0.012	1.289 1.305 -0.016	1.278 1.306 -0.028	1.058 1.073 -0.014	0.323 0.326 -0.003				
14				0.293 0.305 -0.011	0.548 0.556 -0.008	1.162 1.179 -0.017	1.258 1.275 -0.017	1.162 1.179 -0.016	0.548 0.558 -0.009	0.294 0.298 -0.004					
15							0.306 0.320 -0.015	0.499 0.509 -0.009	0.306 0.311 -0.005						

Calculated Minus Measured Powers, RMS Difference = 0.010

Codes and Methods Applicability Report
for the U.S. EPR

Figure A-2.33: Plant A MOC 3 Assembly Power Distribution

	R	P	N	M	L	K	J	H	G	F	E	D	C	B	A
1							0.333 0.333 0.001	0.532 0.529 0.003	0.333 0.331 0.002						
2					0.322 0.323 -0.001	0.577 0.577 0.000	1.153 1.154 0.000	1.277 1.268 0.009	1.153 1.148 0.005	0.576 0.583 -0.007	0.322 0.324 -0.002		Calculated Power Measured Power Difference (C-M)		
3				0.357 0.369 -0.012	1.060 1.063 -0.003	1.309 1.313 -0.004	1.202 1.211 -0.010	1.205 1.184 0.021	1.201 1.190 0.012	1.308 1.301 0.007	1.058 1.060 -0.002	0.355 0.370 -0.015			
4			0.355 0.359 -0.003	0.701 0.704 -0.003	1.282 1.274 0.008	1.141 1.139 0.003	1.140 1.137 0.003	1.163 1.144 0.019	1.140 1.127 0.013	1.139 1.121 0.018	1.277 1.273 0.004	0.701 0.705 -0.004	0.357 0.359 -0.002		
5		0.322 0.325 -0.003	1.058 1.073 -0.015	1.277 1.281 -0.005	1.156 1.153 0.003	0.995 0.991 0.003	1.419 1.417 0.001	0.958 0.951 0.006	1.419 1.411 0.008	0.993 0.988 0.005	1.156 1.155 0.001	1.282 1.287 -0.005	1.060 1.067 -0.007	0.323 0.333 -0.010	
6		0.576 0.577 -0.001	1.308 1.312 -0.004	1.139 1.138 0.001	0.993 0.986 0.007	1.402 1.393 0.009	1.196 1.189 0.007	1.200 1.194 0.006	1.203 1.202 0.001	1.402 1.405 -0.003	0.995 0.993 0.002	1.141 1.138 0.003	1.309 1.313 -0.003	0.577 0.584 -0.008	
7	0.333 0.335 -0.002	1.153 1.152 0.001	1.201 1.196 0.005	1.140 1.135 0.005	1.419 1.410 0.009	1.203 1.193 0.010	1.026 1.011 0.015	1.407 1.400 0.008	1.025 1.031 -0.006	1.196 1.195 0.001	1.419 1.409 0.010	1.140 1.120 0.020	1.202 1.200 0.001	1.153 1.177 -0.024	0.333 0.340 -0.006
8	0.532 0.543 -0.011	1.277 1.275 0.002	1.205 1.189 0.016	1.163 1.155 0.008	0.958 0.952 0.005	1.201 1.192 0.009	1.411 1.398 0.013	1.024 1.018 0.006	1.407 1.402 0.005	1.200 1.195 0.005	0.958 0.952 0.006	1.163 1.152 0.012	1.205 1.193 0.013	1.277 1.284 -0.007	0.532 0.541 -0.009
9	0.333 0.335 -0.002	1.153 1.153 0.000	1.202 1.199 0.002	1.140 1.136 0.004	1.419 1.412 0.006	1.197 1.190 0.007	1.027 1.020 0.007	1.411 1.401 0.010	1.026 1.018 0.008	1.203 1.201 0.002	1.419 1.412 0.007	1.140 1.133 0.007	1.201 1.201 0.001	1.153 1.167 -0.014	0.333 0.354 -0.021
10		0.576 0.579 -0.002	1.309 1.320 -0.010	1.141 1.143 -0.002	0.994 0.991 0.003	1.402 1.395 0.007	1.203 1.195 0.008	1.201 1.193 0.008	1.197 1.188 0.008	1.402 1.391 0.011	0.992 0.986 0.007	1.139 1.128 0.011	1.308 1.311 -0.003	0.576 0.590 -0.014	
11		0.322 0.325 -0.002	1.060 1.071 -0.010	1.282 1.286 -0.004	1.156 1.151 0.006	0.992 0.990 0.003	1.419 1.415 0.004	0.958 0.953 0.005	1.419 1.410 0.009	0.994 0.978 0.016	1.156 1.149 0.007	1.277 1.274 0.003	1.058 1.065 -0.007	0.322 0.326 -0.004	
12		0.357 0.372 -0.016	0.701 0.707 -0.006	1.277 1.280 -0.003	1.139 1.141 -0.002	1.140 1.142 0.002	1.163 1.166 -0.002	1.140 1.142 -0.002	1.141 1.145 -0.004	1.141 1.145 -0.004	1.282 1.286 -0.004	0.701 0.704 -0.003	0.355 0.372 -0.017		
13			0.355 0.358 -0.003	1.058 1.066 -0.008	1.308 1.317 -0.009	1.201 1.210 -0.009	1.205 1.215 -0.010	1.202 1.215 -0.013	1.309 1.335 -0.026	1.060 1.072 -0.012	0.357 0.360 -0.003				
14				0.322 0.332 -0.010	0.576 0.583 -0.007	1.153 1.168 -0.015	1.277 1.293 -0.015	1.153 1.168 -0.015	0.577 0.586 -0.009	0.322 0.327 -0.004					
15							0.333 0.346 -0.013	0.532 0.541 -0.009	0.333 0.338 -0.005						

Calculated Minus Measured Powers, RMS Difference = 0.009

Figure A-2.34: Plant A EOC 3 Assembly Power Distribution

	R	P	N	M	L	K	J	H	G	F	E	D	C	B	A
1							0.387 0.392 -0.005	0.592 0.610 -0.017	0.387 0.390 -0.003						
2					0.376 0.378 -0.001	0.631 0.634 -0.003	1.163 1.170 -0.007	1.274 1.274 0.000	1.163 1.160 0.003	0.631 0.629 0.002	0.376 0.376 0.000		Calculated Power Measured Power Difference (C-M)		
3				0.416 0.431 -0.015	1.079 1.083 -0.004	1.301 1.306 -0.005	1.172 1.184 -0.012	1.166 1.145 0.021	1.172 1.161 0.010	1.301 1.293 0.008	1.078 1.079 -0.001	0.415 0.432 -0.018			
4			0.415 0.418 -0.003	0.759 0.761 -0.003	1.277 1.269 0.008	1.124 1.121 0.003	1.111 1.107 0.004	1.129 1.117 0.012	1.111 1.101 0.010	1.122 1.110 0.012	1.274 1.269 0.005	0.759 0.761 -0.002	0.416 0.416 0.000		
5		0.376 0.377 -0.001	1.078 1.090 -0.012	1.274 1.276 -0.002	1.146 1.141 0.004	1.000 0.995 0.005	1.369 1.355 0.013	0.963 0.956 0.008	1.369 1.361 0.008	0.998 0.992 0.007	1.146 1.139 0.007	1.277 1.271 0.006	1.079 1.078 0.001	0.376 0.386 -0.010	
6		0.631 0.627 0.004	1.301 1.294 0.007	1.122 1.118 0.005	0.998 0.994 0.005	1.346 1.339 0.008	1.154 1.145 0.009	1.155 1.147 0.008	1.158 1.158 0.000	1.347 1.342 0.005	1.000 0.994 0.006	1.124 1.116 0.008	1.301 1.294 0.007	0.631 0.631 0.001	
7	0.387 0.387 0.000	1.163 1.152 0.011	1.171 1.147 0.025	1.111 1.101 0.009	1.368 1.363 0.006	1.158 1.152 0.006	1.011 1.003 0.008	1.339 1.341 -0.002	1.011 1.030 -0.019	1.154 1.156 -0.002	1.369 1.361 0.007	1.111 1.096 0.015	1.172 1.160 0.012	1.163 1.158 0.005	0.387 0.385 0.002
8	0.592 0.602 -0.010	1.274 1.269 0.004	1.166 1.155 0.011	1.129 1.124 0.006	0.963 0.964 -0.001	1.155 1.153 0.002	1.341 1.338 0.003	1.017 1.018 -0.001	1.339 1.347 -0.001	1.155 1.156 -0.001	0.963 0.959 0.004	1.130 1.118 0.012	1.166 1.144 0.022	1.274 1.272 0.002	0.593 0.592 0.001
9	0.387 0.389 -0.002	1.163 1.162 0.000	1.172 1.170 0.002	1.111 1.109 0.002	1.368 1.364 0.005	1.154 1.151 0.002	1.012 1.010 0.001	1.341 1.343 -0.002	1.011 1.012 -0.001	1.158 1.158 0.000	1.369 1.366 0.002	1.111 1.108 0.003	1.172 1.169 0.003	1.163 1.168 -0.005	0.387 0.387 0.000
10		0.631 0.632 -0.001	1.301 1.308 -0.007	1.124 1.126 -0.003	0.999 0.999 0.000	1.346 1.345 0.002	1.158 1.157 0.001	1.155 1.158 -0.002	1.154 1.155 -0.002	1.346 1.347 0.000	0.998 0.998 0.000	1.122 1.125 -0.003	1.301 1.311 -0.010	0.631 0.648 -0.017	
11		0.376 0.379 -0.003	1.079 1.092 -0.013	1.277 1.284 -0.007	1.145 1.146 0.000	0.998 0.997 0.001	1.368 1.366 0.002	0.963 0.970 -0.006	1.368 1.372 -0.004	0.999 1.000 -0.001	1.146 1.141 0.004	1.274 1.281 -0.007	1.078 1.092 -0.014	0.376 0.383 -0.007	
12		0.416 0.437 -0.022	0.758 0.767 -0.008	1.274 1.278 -0.004	1.122 1.120 0.002	1.111 1.098 0.013	1.129 1.129 0.001	1.111 1.113 -0.002	1.124 1.127 -0.003	1.277 1.281 -0.004	0.759 0.768 -0.009	0.415 0.435 -0.020			
13			0.415 0.418 -0.003	1.078 1.084 -0.006	1.301 1.303 -0.003	1.172 1.171 0.000	1.166 1.169 -0.002	1.172 1.176 -0.004	1.301 1.307 -0.006	1.079 1.084 -0.004	0.416 0.419 -0.003				
14				0.376 0.385 -0.009	0.631 0.636 -0.004	1.163 1.171 -0.008	1.274 1.280 -0.006	1.163 1.168 -0.005	0.631 0.634 -0.003	0.376 0.378 -0.002					
15							0.387 0.399 -0.012	0.593 0.599 -0.006	0.387 0.390 -0.003						

Calculated Minus Measured Powers, RMS Difference = 0.008

Figure A-2.35: Plant A BOC 4 Assembly Power Distribution

	R	P	N	M	L	K	J	H	G	F	E	D	C	B	A
1							0.296 0.293 0.003	0.382 0.386 -0.004	0.296 0.291 0.004						
2					0.349 0.345 0.005	0.656 0.645 0.011	1.129 1.109 0.019	1.216 1.192 0.024	1.130 1.104 0.026	0.660 0.638 0.022	0.350 0.343 0.007	Calculated Power Measured Power Difference (C-M)			
3				0.364 0.370 -0.006	1.096 1.084 0.012	1.293 1.273 0.020	1.281 1.258 0.022	1.327 1.291 0.035	1.282 1.251 0.030	1.296 1.267 0.029	1.099 1.086 0.013	0.364 0.371 -0.007			
4			0.365 0.361 0.004	0.807 0.798 0.010	1.226 1.207 0.019	1.225 1.203 0.022	1.259 1.234 0.025	1.269 1.235 0.034	1.258 1.230 0.028	1.226 1.195 0.031	1.229 1.220 0.010	0.807 0.812 -0.005	0.364 0.369 -0.005		
5		0.350 0.346 0.005	1.100 1.090 0.010	1.231 1.210 0.021	0.925 0.899 0.026	1.169 1.146 0.023	1.175 1.155 0.021	1.230 1.210 0.020	1.172 1.157 0.014	1.167 1.158 0.009	0.924 0.929 -0.005	1.225 1.244 -0.019	1.095 1.118 -0.023	0.349 0.365 -0.016	
6		0.660 0.649 0.011	1.297 1.275 0.022	1.227 1.204 0.023	1.170 1.145 0.024	0.923 0.906 0.017	1.289 1.271 0.018	1.043 1.035 0.008	1.284 1.281 0.003	0.920 0.927 -0.006	1.167 1.178 -0.011	1.224 1.241 -0.017	1.292 1.319 -0.027	0.655 0.673 -0.018	
7	0.296 0.292 0.003	1.131 1.110 0.020	1.283 1.253 0.029	1.259 1.234 0.025	1.174 1.152 0.023	1.289 1.269 0.020	0.981 0.967 0.014	1.264 1.258 0.006	0.973 0.978 -0.004	1.285 1.296 -0.011	1.174 1.185 -0.012	1.258 1.272 -0.015	1.280 1.308 -0.028	1.128 1.163 -0.035	0.296 0.304 -0.008
8	0.382 0.386 -0.004	1.217 1.198 0.019	1.328 1.293 0.034	1.270 1.245 0.024	1.232 1.207 0.026	1.047 1.034 0.013	1.279 1.270 0.009	1.023 1.021 0.003	1.257 1.261 -0.004	1.041 1.050 -0.009	1.229 1.242 -0.014	1.268 1.287 -0.020	1.326 1.360 -0.034	1.215 1.248 -0.032	0.382 0.391 -0.010
9	0.296 0.294 0.002	1.129 1.118 0.011	1.281 1.268 0.013	1.260 1.248 0.012	1.177 1.166 0.012	1.293 1.285 0.008	0.984 0.982 0.002	1.272 1.273 -0.001	0.976 0.976 0.000	1.284 1.292 -0.008	1.172 1.184 -0.012	1.257 1.275 -0.018	1.281 1.307 -0.026	1.129 1.156 -0.026	0.296 0.302 -0.007
10		0.655 0.654 0.001	1.293 1.300 -0.006	1.225 1.227 -0.001	1.170 1.170 0.000	0.924 0.925 -0.001	1.289 1.298 -0.009	1.045 1.050 -0.004	1.289 1.295 -0.006	0.921 0.926 -0.005	1.168 1.181 -0.013	1.226 1.239 -0.013	1.296 1.320 -0.024	0.660 0.673 -0.013	
11		0.349 0.351 -0.002	1.096 1.110 -0.014	1.226 1.239 -0.012	0.926 0.935 -0.009	1.170 1.179 -0.010	1.174 1.183 -0.009	1.231 1.240 -0.009	1.176 1.181 -0.005	1.168 1.174 -0.005	0.925 0.939 -0.014	1.230 1.252 -0.023	1.099 1.124 -0.025	0.350 0.357 -0.007	
12		0.364 0.383 -0.019	0.807 0.822 -0.014	1.231 1.250 -0.019	1.227 1.241 -0.014	1.259 1.269 -0.010	1.269 1.273 -0.004	1.259 1.264 -0.005	1.224 1.230 -0.006	1.225 1.240 -0.015	0.807 0.827 -0.020	0.364 0.382 -0.018			
13			0.365 0.372 -0.007	1.100 1.123 -0.023	1.297 1.316 -0.019	1.282 1.292 -0.010	1.327 1.321 0.006	1.280 1.284 -0.003	1.292 1.292 0.001	1.095 1.103 -0.007	0.364 0.369 -0.005				
14				0.350 0.373 -0.023	0.660 0.674 -0.014	1.130 1.147 -0.017	1.216 1.227 -0.011	1.128 1.146 -0.017	0.655 0.659 -0.004	0.349 0.351 -0.002					
15							0.296 0.312 -0.016	0.382 0.388 -0.006	0.296 0.300 -0.004						

Calculated Minus Measured Powers, RMS Difference = 0.016

Codes and Methods Applicability Report
for the U.S. EPR

Figure A-2.36: Plant A MOC 4 Assembly Power Distribution

	R	P	N	M	L	K	J	H	G	F	E	D	C	B	A
1							0.311 0.318 -0.006	0.406 0.428 -0.022	0.311 0.316 -0.005						
2					0.371 0.374 -0.003	0.654 0.658 -0.004	1.114 1.122 -0.008	1.270 1.281 -0.011	1.114 1.118 -0.003	0.657 0.654 0.003	0.372 0.371 0.001		Calculated Power Measured Power Difference (C-M)		
3				0.394 0.407 -0.013	1.138 1.148 -0.010	1.343 1.348 -0.005	1.152 1.154 -0.002	1.365 1.367 -0.002	1.153 1.149 0.004	1.345 1.337 0.008	1.140 1.140 0.000	0.395 0.407 -0.012			
4			0.394 0.395 -0.001	0.839 0.844 -0.005	1.329 1.337 -0.008	1.157 1.157 0.000	1.084 1.078 0.006	1.067 1.046 0.020	1.083 1.071 0.013	1.158 1.140 0.018	1.332 1.329 0.003	0.839 0.839 0.000	0.394 0.394 0.000		
5		0.372 0.371 0.000	1.140 1.139 0.000	1.332 1.331 0.001	0.985 0.979 0.007	1.323 1.318 0.005	1.073 1.065 0.007	1.058 1.047 0.011	1.070 1.062 0.009	1.323 1.316 0.008	0.986 0.991 -0.005	1.329 1.322 0.007	1.139 1.141 -0.002	0.372 0.385 -0.013	
6		0.657 0.658 0.000	1.344 1.343 0.001	1.158 1.155 0.003	1.323 1.318 0.005	0.986 0.981 0.005	1.393 1.385 0.008	1.013 1.006 0.008	1.390 1.383 0.007	0.986 0.981 0.005	1.323 1.320 0.003	1.158 1.151 0.007	1.343 1.342 0.002	0.654 0.658 -0.003	
7	0.311 0.315 -0.004	1.114 1.118 -0.004	1.153 1.150 0.002	1.083 1.080 0.003	1.071 1.066 0.005	1.392 1.387 0.005	1.000 0.995 0.005	1.323 1.318 0.005	0.996 0.993 0.003	1.392 1.388 0.004	1.072 1.066 0.006	1.084 1.069 0.015	1.153 1.147 0.005	1.114 1.118 -0.004	0.312 0.313 -0.002
8	0.405 0.422 -0.017	1.269 1.278 -0.009	1.364 1.363 0.001	1.066 1.063 0.003	1.059 1.053 0.005	1.015 1.011 0.004	1.333 1.330 0.004	1.024 1.020 0.004	1.319 1.316 0.004	1.013 1.011 0.001	1.058 1.054 0.005	1.067 1.058 0.009	1.365 1.357 0.008	1.270 1.283 -0.013	0.406 0.413 -0.007
9	0.311 0.316 -0.005	1.113 1.122 -0.009	1.152 1.157 -0.005	1.084 1.083 0.001	1.073 1.063 0.010	1.394 1.390 0.005	1.001 1.000 0.001	1.329 1.325 0.004	0.997 0.991 0.006	1.390 1.407 -0.016	1.070 1.069 0.002	1.083 1.075 0.009	1.153 1.151 0.002	1.115 1.129 -0.014	0.311 0.331 -0.019
10		0.653 0.660 -0.006	1.342 1.358 -0.015	1.157 1.161 -0.004	1.323 1.320 0.003	0.987 0.986 0.001	1.392 1.403 -0.011	1.014 1.011 0.003	1.393 1.389 0.004	0.986 0.986 0.000	1.323 1.312 0.011	1.158 1.135 0.023	1.345 1.341 0.004	0.657 0.670 -0.012	
11		0.371 0.376 -0.004	1.138 1.154 -0.016	1.329 1.336 -0.008	0.985 0.980 0.005	1.323 1.319 0.005	1.071 1.064 0.007	1.059 1.042 0.017	1.073 1.068 0.005	1.323 1.327 -0.004	0.986 0.974 0.012	1.332 1.322 0.010	1.140 1.140 0.000	0.372 0.374 -0.003	
12		0.394 0.413 -0.019	0.839 0.847 -0.008	1.332 1.334 -0.003	1.158 1.154 0.004	1.083 1.065 0.018	1.066 1.056 0.010	1.084 1.080 0.004	1.157 1.156 0.002	1.329 1.325 0.004	0.839 0.842 -0.003	0.394 0.406 -0.011			
13			0.394 0.398 -0.003	1.140 1.148 -0.009	1.344 1.347 -0.003	1.153 1.150 0.003	1.364 1.360 0.004	1.152 1.152 0.001	1.343 1.341 0.002	1.138 1.137 0.002	0.394 0.394 0.000				
14				0.372 0.389 -0.017	0.657 0.664 -0.007	1.114 1.123 -0.009	1.269 1.276 -0.006	1.114 1.123 -0.010	0.653 0.655 -0.001	0.371 0.371 0.000					
15							0.311 0.328 -0.017	0.406 0.411 -0.005	0.311 0.314 -0.003						

Calculated Minus Measured Powers, RMS Difference = 0.008

Figure A-4.37: Plant A EOC 4 Assembly Power Distribution

	R	P	N	M	L	K	J	H	G	F	E	D	C	B	A
1							0.358	0.456	0.357						
							0.368	0.485	0.367						
							-0.011	-0.029	-0.010						
2					0.420	0.693	1.111	1.251	1.111	0.696	0.420				
					0.423	0.700	1.128	1.270	1.124	0.703	0.423				
					-0.003	-0.007	-0.017	-0.019	-0.013	-0.008	-0.003				
												Calculated Power			
												Measured Power			
												Difference (C-M)			
3				0.444	1.138	1.312	1.110	1.335	1.110	1.312	1.138	0.444			
				0.464	1.144	1.321	1.125	1.340	1.113	1.314	1.144	0.454			
				-0.021	-0.006	-0.009	-0.015	-0.005	-0.003	-0.002	-0.006	-0.011			
4			0.444	0.863	1.299	1.120	1.054	1.037	1.054	1.120	1.301	0.863	0.444		
			0.443	0.864	1.286	1.117	1.054	1.028	1.049	1.108	1.304	0.864	0.444		
			0.001	-0.001	0.013	0.002	0.000	0.009	0.005	0.012	-0.003	0.000	0.000		
5		0.419	1.138	1.300	1.003	1.341	1.055	1.039	1.054	1.341	1.004	1.299	1.138	0.420	
		0.418	1.135	1.297	1.000	1.336	1.051	1.033	1.050	1.342	1.019	1.287	1.139	0.433	
		0.001	0.003	0.003	0.004	0.005	0.005	0.006	0.004	0.000	-0.015	0.013	0.000	-0.013	
6		0.696	1.312	1.119	1.341	1.009	1.373	1.016	1.372	1.009	1.341	1.120	1.312	0.694	
		0.694	1.306	1.115	1.335	1.004	1.365	1.008	1.367	1.009	1.345	1.116	1.313	0.701	
		0.002	0.006	0.004	0.005	0.005	0.008	0.007	0.005	0.000	-0.003	0.004	-0.001	-0.007	
7	0.357	1.111	1.109	1.053	1.054	1.372	1.010	1.314	1.008	1.373	1.056	1.055	1.110	1.111	0.358
	0.361	1.111	1.101	1.048	1.049	1.365	1.004	1.306	1.001	1.371	1.053	1.046	1.110	1.126	0.363
	-0.004	0.001	0.008	0.005	0.005	0.007	0.005	0.008	0.007	0.002	0.003	0.009	0.000	-0.014	-0.006
8	0.456	1.251	1.335	1.037	1.039	1.016	1.319	1.039	1.312	1.016	1.040	1.038	1.335	1.251	0.456
	0.472	1.255	1.331	1.033	1.034	1.011	1.312	1.034	1.307	1.017	1.036	1.032	1.329	1.265	0.465
	-0.016	-0.004	0.004	0.004	0.004	0.005	0.006	0.005	0.005	-0.001	0.004	0.006	0.006	-0.014	-0.010
9	0.358	1.111	1.109	1.054	1.055	1.373	1.010	1.317	1.009	1.372	1.054	1.054	1.110	1.111	0.357
	0.362	1.114	1.109	1.050	1.044	1.365	1.006	1.310	1.003	1.361	1.046	1.047	1.111	1.128	0.378
	-0.005	-0.003	0.001	0.004	0.011	0.008	0.004	0.007	0.005	0.012	0.008	0.007	-0.001	-0.017	-0.021
10	0.693	1.312	1.119	1.341	1.009	1.372	1.016	1.373	1.009	1.341	1.120	1.312	0.696		
	0.695	1.313	1.119	1.336	1.005	1.370	1.009	1.360	0.996	1.327	1.104	1.314	0.712		
	-0.002	-0.001	0.000	0.004	0.004	0.001	0.007	0.013	0.013	0.014	0.016	-0.002	-0.016		
11	0.420	1.138	1.299	1.003	1.340	1.054	1.039	1.056	1.341	1.004	1.301	1.138	0.420		
	0.422	1.146	1.304	1.004	1.337	1.047	1.026	1.041	1.312	0.996	1.295	1.142	0.424		
	-0.002	-0.008	-0.005	-0.001	0.004	0.007	0.013	0.014	0.029	0.008	0.006	-0.004	-0.005		
12	0.444	0.863	1.300	1.119	1.054	1.037	1.054	1.120	1.299	0.863	0.444				
	0.460	0.870	1.305	1.117	1.039	1.025	1.045	1.109	1.292	0.864	0.456				
	-0.016	-0.007	-0.005	0.002	0.015	0.012	0.010	0.011	0.007	-0.001	-0.013				
13	0.444	1.138	1.312	1.110	1.335	1.110	1.312	1.138	0.444						
	0.447	1.147	1.315	1.105	1.319	1.107	1.308	1.134	0.443						
	-0.004	-0.009	-0.003	0.004	0.016	0.002	0.004	0.004	0.000						
14	0.419	0.696	1.111	1.251	1.111	0.693	0.420								
	0.436	0.702	1.119	1.257	1.131	0.697	0.420								
	-0.016	-0.007	-0.008	-0.005	-0.020	-0.004	0.000								
15	0.357	0.456	0.358												
	0.375	0.462	0.364												
	-0.018	-0.007	-0.006												

Calculated Minus Measured Powers, RMS Difference = 0.009

Figure A-2.38: Plant A BOC 5 Assembly Power Distribution

	R	P	N	M	L	K	J	H	G	F	E	D	C	B	A
1							0.284	0.364	0.281						
							0.288	0.385	0.286						
							-0.005	-0.021	-0.005						
2					0.310	0.657	1.161	1.245	1.156	0.650	0.309				
					0.306	0.654	1.166	1.258	1.164	0.654	0.309				
					0.003	0.003	-0.004	-0.014	-0.007	-0.005	0.000				
												Calculated Power			
												Measured Power			
												Difference (C-M)			
3				0.317	1.087	1.275	1.305	0.878	1.303	1.271	1.084	0.317			
				0.322	1.073	1.262	1.302	0.882	1.301	1.266	1.079	0.320			
				-0.005	0.014	0.013	0.003	-0.005	0.002	0.004	0.005	-0.004			
4			0.317	0.770	1.232	1.264	1.128	1.107	1.129	1.264	1.231	0.769	0.316		
			0.318	0.762	1.203	1.240	1.107	1.080	1.113	1.251	1.217	0.763	0.315		
			-0.002	0.008	0.029	0.024	0.021	0.028	0.016	0.012	0.014	0.006	0.001		
5		0.309	1.085	1.232	0.885	1.345	1.204	1.343	1.204	1.344	0.884	1.231	1.085	0.309	
		0.313	1.101	1.223	0.856	1.311	1.171	1.309	1.178	1.318	0.861	1.218	1.085	0.321	
		-0.004	-0.017	0.009	0.029	0.033	0.033	0.034	0.027	0.026	0.023	0.013	0.001	-0.012	
6		0.650	1.271	1.264	1.345	1.191	1.203	1.245	1.202	1.189	1.343	1.263	1.273	0.654	
		0.656	1.278	1.255	1.316	1.164	1.173	1.211	1.168	1.161	1.316	1.246	1.273	0.665	
		-0.006	-0.007	0.009	0.029	0.028	0.030	0.034	0.034	0.028	0.027	0.016	0.000	-0.011	
7	0.281	1.156	1.303	1.130	1.205	1.203	1.178	1.342	1.175	1.200	1.202	1.126	1.303	1.159	0.283
	0.287	1.171	1.313	1.125	1.188	1.181	1.152	1.304	1.127	1.170	1.178	1.102	1.308	1.192	0.291
	-0.006	-0.015	-0.010	0.004	0.017	0.022	0.026	0.038	0.048	0.030	0.024	0.024	-0.005	-0.033	-0.008
8	0.364	1.244	0.878	1.107	1.343	1.245	1.341	0.907	1.333	1.241	1.341	1.106	0.876	1.243	0.363
	0.382	1.266	0.887	1.106	1.329	1.227	1.317	0.887	1.300	1.219	1.323	1.097	0.884	1.280	0.376
	-0.018	-0.022	-0.010	0.001	0.014	0.018	0.024	0.019	0.033	0.022	0.017	0.008	-0.008	-0.037	-0.013
9	0.284	1.161	1.305	1.127	1.204	1.202	1.175	1.332	1.171	1.199	1.203	1.128	1.302	1.155	0.281
	0.291	1.181	1.323	1.131	1.192	1.188	1.158	1.313	1.148	1.189	1.195	1.128	1.314	1.179	0.301
	-0.007	-0.021	-0.019	-0.003	0.012	0.014	0.016	0.019	0.023	0.010	0.008	0.000	-0.013	-0.024	-0.021
10	0.656	1.274	1.264	1.344	1.190	1.201	1.241	1.199	1.187	1.342	1.262	1.269	0.649		
	0.670	1.304	1.273	1.337	1.180	1.186	1.236	1.194	1.185	1.339	1.267	1.279	0.652		
	-0.013	-0.030	-0.009	0.006	0.009	0.015	0.005	0.005	0.003	0.004	-0.005	-0.010	-0.003		
11	0.309	1.086	1.231	0.884	1.344	1.203	1.341	1.201	1.341	0.883	1.230	1.083	0.309		
	0.315	1.108	1.241	0.875	1.341	1.206	1.359	1.212	1.351	0.875	1.238	1.095	0.311		
	-0.006	-0.022	-0.010	0.010	0.002	-0.002	-0.019	-0.011	-0.009	0.008	-0.009	-0.012	-0.003		
12	0.316	0.769	1.230	1.263	1.128	1.106	1.126	1.262	1.230	0.768	0.316				
	0.333	0.777	1.236	1.270	1.136	1.124	1.147	1.284	1.248	0.788	0.329				
	-0.017	-0.009	-0.006	-0.008	-0.008	-0.018	-0.021	-0.022	-0.018	-0.019	-0.013				
13	0.316	1.084	1.269	1.302	0.876	1.302	1.272	1.084	0.316						
	0.320	1.095	1.288	1.330	0.902	1.345	1.310	1.110	0.323						
	-0.003	-0.011	-0.019	-0.028	-0.026	-0.043	-0.039	-0.026	-0.007						
14	0.309	0.649	1.155	1.243	1.158	0.653	0.309								
	0.313	0.664	1.197	1.295	1.218	0.678	0.317								
	-0.005	-0.015	-0.042	-0.052	-0.059	-0.025	-0.009								
15	0.281	0.363	0.283												
	0.311	0.383	0.297												
	-0.030	-0.019	-0.014												

Calculated Minus Measured Powers, RMS Difference = 0.019

Codes and Methods Applicability Report
for the U.S. EPR

Figure A-2.39: Plant A MOC 5 Assembly Power Distribution

	R	P	N	M	L	K	J	H	G	F	E	D	C	B	A
1							0.306 0.308 -0.003	0.386 0.390 -0.004	0.303 0.306 -0.003						
2					0.342 0.344 -0.002	0.689 0.693 -0.005	1.177 1.188 -0.011	1.242 1.255 -0.014	1.174 1.187 -0.013	0.682 0.695 -0.013	0.342 0.346 -0.004		Calculated Power Measured Power Difference (C-M)		
3				0.351 0.364 -0.013	1.126 1.134 -0.007	1.345 1.352 -0.007	1.387 1.399 -0.012	0.913 0.923 -0.010	1.386 1.397 -0.010	1.343 1.354 -0.011	1.125 1.136 -0.011	0.351 0.361 -0.010			
4			0.351 0.355 -0.004	0.812 0.817 -0.005	1.307 1.306 0.002	1.224 1.222 0.002	1.077 1.074 0.003	1.049 1.031 0.018	1.079 1.076 0.003	1.225 1.228 -0.003	1.308 1.314 -0.006	0.812 0.818 -0.005	0.351 0.353 -0.002		
5		0.342 0.346 -0.004	1.125 1.143 -0.018	1.307 1.313 -0.006	0.912 0.902 0.010	1.384 1.377 0.007	1.109 1.103 0.006	1.319 1.305 0.014	1.110 1.101 0.009	1.384 1.379 0.005	0.912 0.911 0.001	1.308 1.312 -0.005	1.126 1.135 -0.009	0.342 0.352 -0.011	
6		0.682 0.688 -0.006	1.342 1.354 -0.012	1.224 1.229 -0.004	1.384 1.384 0.001	1.106 1.100 0.006	1.076 1.066 0.009	1.118 1.103 0.015	1.076 1.060 0.016	1.105 1.093 0.012	1.384 1.374 0.010	1.224 1.219 0.005	1.345 1.352 -0.007	0.687 0.698 -0.011	
7	0.303 0.308 -0.005	1.174 1.185 -0.011	1.386 1.395 -0.009	1.079 1.082 -0.003	1.110 1.109 0.001	1.076 1.070 0.006	1.064 1.052 0.012	1.325 1.303 0.022	1.063 1.033 0.030	1.075 1.056 0.019	1.109 1.094 0.015	1.077 1.056 0.021	1.387 1.395 -0.007	1.177 1.205 -0.028	0.306 0.313 -0.007
8	0.386 0.402 -0.015	1.242 1.255 -0.013	0.913 0.915 -0.002	1.049 1.051 -0.002	1.319 1.321 -0.003	1.118 1.111 0.007	1.325 1.310 0.015	0.889 0.874 0.015	1.320 1.291 0.029	1.117 1.097 0.020	1.319 1.303 0.016	1.049 1.041 0.008	0.913 0.920 -0.007	1.242 1.265 -0.023	0.386 0.397 -0.010
9	0.306 0.311 -0.005	1.177 1.189 -0.012	1.387 1.397 -0.010	1.077 1.079 -0.002	1.109 1.106 0.004	1.076 1.067 0.009	1.062 1.048 0.015	1.320 1.298 0.022	1.061 1.033 0.028	1.075 1.054 0.021	1.110 1.098 0.012	1.079 1.077 0.002	1.387 1.397 -0.010	1.174 1.194 -0.019	0.303 0.324 -0.021
10		0.688 0.695 -0.007	1.345 1.360 -0.015	1.224 1.225 -0.001	1.384 1.375 0.009	1.106 1.094 0.012	1.075 1.056 0.019	1.117 1.104 0.012	1.075 1.060 0.015	1.105 1.091 0.014	1.385 1.372 0.012	1.225 1.226 -0.001	1.343 1.350 -0.007	0.682 0.687 -0.005	
11		0.342 0.345 -0.003	1.126 1.135 -0.009	1.307 1.306 0.002	0.912 0.894 0.018	1.385 1.372 0.012	1.110 1.103 0.007	1.319 1.322 -0.004	1.109 1.103 0.006	1.384 1.372 0.012	0.912 0.895 0.017	1.308 1.306 0.002	1.126 1.132 -0.006	0.342 0.344 -0.002	
12		0.351 0.360 -0.009	0.811 0.811 0.001	1.307 1.300 0.007	1.225 1.219 0.006	1.079 1.077 0.002	1.049 1.049 0.000	1.077 1.077 0.001	1.224 1.221 0.003	1.308 1.303 0.005	0.812 0.812 0.000	0.351 0.361 -0.010			
13			0.351 0.350 0.001	1.125 1.123 0.002	1.343 1.343 0.000	1.387 1.391 -0.004	0.913 0.913 0.000	1.387 1.394 -0.007	1.345 1.352 -0.007	1.126 1.128 -0.002	0.351 0.351 0.000				
14				0.342 0.342 0.000	0.682 0.686 -0.003	1.174 1.189 -0.015	1.242 1.255 -0.013	1.177 1.192 -0.015	0.686 0.692 -0.005	0.342 0.343 -0.001					
15							0.303 0.328 -0.024	0.386 0.395 -0.008	0.306 0.310 -0.004						

Calculated Minus Measured Powers, RMS Difference = 0.011

Figure A-2.40: Plant A EOC 5 Assembly Power Distribution

	R	P	N	M	L	K	J	H	G	F	E	D	C	B	A
1							0.365 0.371 -0.006	0.451 0.470 -0.018	0.362 0.369 -0.006						
2					0.403 0.405 -0.001	0.732 0.734 -0.002	1.168 1.175 -0.006	1.222 1.237 -0.015	1.166 1.175 -0.009	0.726 0.724 0.002	0.404 0.405 -0.001		Calculated Power Measured Power Difference (C-M)		
3				0.417 0.434 -0.017	1.135 1.139 -0.004	1.295 1.296 -0.001	1.333 1.330 0.003	0.946 0.958 -0.012	1.333 1.341 -0.008	1.294 1.297 -0.003	1.135 1.140 -0.005	0.417 0.429 -0.011			
4			0.417 0.420 -0.003	0.862 0.866 -0.004	1.288 1.281 0.007	1.172 1.172 0.000	1.053 1.055 -0.002	1.035 1.040 -0.005	1.055 1.057 -0.003	1.173 1.171 0.002	1.289 1.289 -0.001	0.862 0.864 -0.002	0.417 0.418 -0.001		
5		0.404 0.405 -0.002	1.135 1.145 -0.010	1.288 1.293 -0.005	0.940 0.946 -0.006	1.377 1.380 -0.004	1.084 1.091 -0.007	1.287 1.293 -0.005	1.085 1.085 -0.001	1.377 1.375 0.003	0.940 0.937 0.003	1.288 1.281 0.007	1.135 1.138 -0.003	0.403 0.417 -0.014	
6		0.726 0.723 0.003	1.294 1.288 0.006	1.173 1.167 0.006	1.377 1.363 0.014	1.088 1.085 0.003	1.058 1.060 -0.001	1.090 1.094 -0.004	1.058 1.056 0.002	1.088 1.083 0.005	1.377 1.370 0.007	1.172 1.165 0.007	1.295 1.296 -0.001	0.730 0.736 -0.006	
7	0.362 0.362 0.000	1.166 1.159 0.007	1.333 1.310 0.022	1.055 1.047 0.008	1.085 1.079 0.006	1.058 1.055 0.003	1.046 1.044 0.002	1.301 1.297 0.004	1.046 1.036 0.010	1.058 1.050 0.008	1.084 1.075 0.009	1.053 1.038 0.016	1.333 1.335 -0.002	1.168 1.177 -0.008	0.365 0.369 -0.004
8	0.451 0.459 -0.008	1.222 1.224 -0.001	0.946 0.948 -0.002	1.035 1.034 0.001	1.287 1.288 -0.001	1.090 1.087 0.002	1.301 1.296 0.005	0.915 0.911 0.004	1.298 1.289 0.009	1.090 1.081 0.009	1.288 1.279 0.009	1.035 1.031 0.004	0.946 0.956 -0.010	1.222 1.236 -0.014	0.451 0.461 -0.009
9	0.365 0.367 -0.002	1.168 1.170 -0.001	1.333 1.333 0.000	1.053 1.053 0.000	1.084 1.085 -0.001	1.058 1.055 0.003	1.046 1.040 0.006	1.298 1.291 0.007	1.045 1.039 0.006	1.058 1.045 0.013	1.085 1.077 0.008	1.055 1.052 0.002	1.333 1.340 -0.008	1.166 1.180 -0.014	0.362 0.385 -0.023
10		0.731 0.731 0.000	1.295 1.292 0.003	1.172 1.171 0.001	1.377 1.374 0.003	1.088 1.082 0.006	1.058 1.048 0.010	1.090 1.083 0.007	1.058 1.049 0.010	1.088 1.074 0.015	1.378 1.369 0.009	1.173 1.167 0.006	1.294 1.297 -0.003	0.726 0.726 0.000	
11		0.404 0.405 -0.001	1.135 1.142 -0.007	1.288 1.290 -0.002	0.940 0.935 0.005	1.378 1.369 0.008	1.085 1.076 0.009	1.288 1.284 0.003	1.085 1.073 0.011	1.377 1.347 0.031	0.940 0.939 0.001	1.289 1.292 -0.003	1.135 1.143 -0.008	0.404 0.405 -0.002	
12		0.417 0.436 -0.019	0.862 0.866 -0.005	1.289 1.286 0.002	1.173 1.166 0.007	1.055 1.037 0.018	1.035 1.029 0.006	1.054 1.047 0.007	1.173 1.161 0.012	1.289 1.287 0.002	0.862 0.871 -0.009	0.417 0.432 -0.015			
13			0.417 0.418 -0.001	1.135 1.134 0.001	1.294 1.292 0.002	1.333 1.332 0.001	0.946 0.950 -0.004	1.333 1.332 0.001	1.295 1.285 0.010	1.135 1.131 0.004	0.417 0.418 -0.001				
14				0.404 0.404 -0.001	0.726 0.729 -0.003	1.166 1.178 -0.012	1.222 1.234 -0.011	1.168 1.176 -0.008	0.730 0.729 0.001	0.403 0.402 0.001					
15							0.362 0.387 -0.025	0.451 0.461 -0.009	0.365 0.369 -0.004						

Calculated Minus Measured Powers, RMS Difference = 0.008

Figure A-2.41: Plant A BOC 6 Assembly Power Distribution

	R	P	N	M	L	K	J	H	G	F	E	D	C	B	A
1							0.292 0.292 0.001	0.324 0.333 -0.008	0.273 0.274 0.000						
2					0.326 0.325 0.000	0.538 0.534 0.004	1.162 1.149 0.012	0.987 0.978 0.009	1.146 1.140 0.007	0.539 0.545 -0.007	0.326 0.328 -0.002		Calculated Power Measured Power Difference (C-M)		
3				0.477 0.491 -0.014	1.245 1.248 -0.003	1.276 1.268 0.008	1.134 1.118 0.016	1.280 1.252 0.028	1.130 1.116 0.014	1.275 1.267 0.008	1.246 1.249 -0.003	0.477 0.492 -0.015			
4		0.477 0.476 0.001	1.328 1.331 -0.003	1.376 1.377 -0.001	1.149 1.140 0.009	1.239 1.219 0.020	1.151 1.122 0.029	1.240 1.220 0.020	1.150 1.129 0.021	1.376 1.378 -0.002	1.328 1.339 -0.011	0.477 0.480 -0.003			
5		0.325 0.322 0.003	1.245 1.238 0.007	1.376 1.371 0.006	0.881 0.877 0.004	1.101 1.090 0.011	1.296 1.277 0.019	1.140 1.125 0.016	1.297 1.285 0.012	1.102 1.097 0.005	0.880 0.893 -0.013	1.375 1.386 -0.010	1.245 1.254 -0.009	0.326 0.334 -0.008	
6		0.537 0.531 0.006	1.274 1.260 0.014	1.149 1.136 0.013	1.102 1.082 0.020	1.191 1.180 0.011	1.156 1.149 0.006	1.181 1.176 0.006	1.156 1.154 0.002	1.191 1.190 0.001	1.100 1.102 -0.002	1.148 1.148 0.000	1.276 1.277 -0.002	0.538 0.539 -0.001	
7	0.273 0.273 0.000	1.145 1.132 0.013	1.129 1.108 0.022	1.239 1.223 0.016	1.297 1.281 0.016	1.156 1.152 0.004	0.846 0.858 -0.011	1.277 1.283 -0.006	0.845 0.855 -0.010	1.154 1.156 -0.002	1.295 1.291 0.004	1.238 1.225 0.013	1.133 1.127 0.006	1.161 1.160 0.001	0.292 0.293 -0.001
8	0.324 0.336 -0.012	0.987 0.981 0.006	1.279 1.261 0.018	1.151 1.139 0.012	1.140 1.128 0.012	1.181 1.179 0.002	1.277 1.282 -0.006	0.855 0.862 -0.006	1.271 1.284 -0.013	1.179 1.182 -0.003	1.138 1.136 0.003	1.149 1.140 0.008	1.279 1.264 0.015	0.987 0.997 -0.010	0.324 0.330 -0.006
9	0.292 0.294 -0.002	1.161 1.159 0.002	1.134 1.130 0.004	1.239 1.235 0.004	1.296 1.295 0.001	1.155 1.155 -0.001	0.845 0.849 -0.004	1.271 1.282 -0.011	0.843 0.863 -0.020	1.154 1.151 0.003	1.295 1.291 0.004	1.238 1.233 0.005	1.129 1.131 -0.002	1.146 1.164 -0.018	0.273 0.289 -0.016
10		0.538 0.539 -0.001	1.276 1.284 -0.008	1.149 1.153 -0.004	1.100 1.103 -0.003	1.190 1.192 -0.002	1.154 1.159 -0.005	1.179 1.182 -0.003	1.153 1.158 -0.005	1.189 1.189 0.000	1.101 1.100 0.001	1.149 1.139 0.010	1.275 1.284 -0.009	0.539 0.557 -0.018	
11		0.325 0.329 -0.003	1.245 1.261 -0.016	1.375 1.387 -0.012	0.880 0.886 -0.006	1.100 1.102 -0.002	1.294 1.290 0.004	1.137 1.127 0.010	1.293 1.290 0.003	1.099 1.097 0.002	0.880 0.891 -0.011	1.375 1.390 -0.014	1.245 1.266 -0.021	0.326 0.333 -0.007	
12		0.477 0.497 -0.020	1.327 1.342 -0.016	1.374 1.382 -0.007	1.147 1.148 -0.001	1.236 1.227 0.008	1.146 1.137 0.008	1.235 1.234 0.001	1.147 1.152 -0.006	1.147 1.152 -0.017	1.374 1.390 -0.017	1.327 1.352 -0.025	0.477 0.504 -0.027		
13			0.477 0.481 -0.004	1.243 1.247 -0.005	1.271 1.271 0.000	1.124 1.120 0.005	1.272 1.256 0.016	1.129 1.129 0.000	1.272 1.283 -0.011	1.243 1.257 -0.014	0.476 0.483 -0.007				
14				0.325 0.326 -0.001	0.535 0.536 -0.001	1.136 1.141 -0.004	0.975 0.975 0.000	1.152 1.163 -0.011	0.535 0.540 -0.004	0.325 0.328 -0.003					
15							0.269 0.284 -0.015	0.318 0.322 -0.004	0.288 0.291 -0.003						

Calculated Minus Measured Powers, RMS Difference = 0.010

Codes and Methods Applicability Report
for the U.S. EPR

Figure A-2.42: Plant A MOC 6 Assembly Power Distribution

	R	P	N	M	L	K	J	H	G	F	E	D	C	B	A
1							0.297 0.291 0.006	0.331 0.325 0.007	0.278 0.275 0.003						
2					0.337 0.336 0.002	0.546 0.538 0.008	1.125 1.103 0.022	0.958 0.938 0.020	1.115 1.105 0.010	0.548 0.563 -0.015	0.338 0.342 -0.005		Calculated Power Measured Power Difference (C-M)		
3				0.471 0.493 -0.022	1.225 1.226 -0.001	1.344 1.330 0.013	1.088 1.065 0.023	1.401 1.358 0.043	1.086 1.068 0.018	1.344 1.339 0.005	1.226 1.235 -0.009	0.472 0.498 -0.026			
4			0.472 0.472 0.000	1.293 1.300 -0.007	1.422 1.416 0.006	1.100 1.086 0.013	1.175 1.150 0.025	1.102 1.066 0.036	1.176 1.152 0.024	1.101 1.079 0.021	1.423 1.423 0.000	1.293 1.300 -0.007	0.471 0.472 -0.001		
5		0.337 0.337 0.001	1.225 1.226 -0.001	1.423 1.424 -0.002	0.891 0.890 0.001	1.045 1.033 0.012	1.409 1.382 0.027	1.106 1.087 0.019	1.410 1.391 0.019	1.046 1.036 0.011	0.891 0.894 -0.004	1.422 1.414 0.008	1.225 1.225 0.000	0.338 0.350 -0.012	
6		0.546 0.545 0.002	1.343 1.342 0.001	1.100 1.095 0.006	1.046 1.030 0.016	1.109 1.102 0.007	1.105 1.102 0.003	1.146 1.141 0.005	1.105 1.098 0.007	1.108 1.102 0.007	1.045 1.040 0.005	1.099 1.092 0.007	1.343 1.337 0.006	0.546 0.543 0.003	
7	0.278 0.280 -0.002	1.114 1.111 0.003	1.085 1.085 0.001	1.176 1.169 0.007	1.410 1.402 0.007	1.105 1.110 -0.004	0.897 0.925 -0.028	1.439 1.451 -0.013	0.895 0.897 -0.002	1.104 1.101 0.003	1.408 1.402 0.006	1.175 1.165 0.009	1.088 1.075 0.013	1.125 1.107 0.018	0.297 0.293 0.004
8	0.331 0.346 -0.015	0.958 0.948 0.010	1.401 1.364 0.037	1.102 1.089 0.013	1.106 1.102 0.004	1.146 1.150 -0.004	1.439 1.455 -0.016	0.980 0.989 -0.009	1.433 1.444 -0.011	1.145 1.143 0.001	1.105 1.100 0.005	1.101 1.091 0.010	1.400 1.378 0.022	0.958 0.950 0.008	0.331 0.332 -0.001
9	0.297 0.297 -0.001	1.125 1.115 0.010	1.088 1.072 0.016	1.175 1.167 0.008	1.409 1.411 -0.002	1.104 1.105 -0.001	0.895 0.898 -0.003	1.433 1.445 -0.012	0.894 0.912 -0.018	1.104 1.097 0.007	1.409 1.404 0.005	1.176 1.171 0.005	1.086 1.084 0.001	1.115 1.125 -0.010	0.279 0.296 -0.018
10		0.546 0.541 0.005	1.344 1.333 0.011	1.100 1.100 0.000	1.045 1.049 -0.003	1.109 1.108 0.001	1.104 1.091 0.013	1.144 1.145 -0.001	1.103 1.108 -0.004	1.108 1.107 0.001	1.046 1.045 0.001	1.100 1.099 0.002	1.344 1.356 -0.012	0.548 0.565 -0.017	
11		0.338 0.339 -0.001	1.225 1.239 -0.014	1.422 1.442 -0.020	0.891 0.909 -0.018	1.046 1.052 -0.006	1.408 1.408 0.001	1.105 1.105 0.000	1.407 1.409 -0.002	1.045 1.043 0.002	0.891 0.896 -0.005	1.423 1.441 -0.018	1.226 1.248 -0.022	0.338 0.345 -0.007	
12		0.471 0.499 -0.028	1.293 1.321 -0.028	1.423 1.447 -0.024	1.100 1.110 -0.011	1.175 1.179 -0.004	1.100 1.103 -0.003	1.174 1.177 -0.003	1.099 1.105 -0.005	1.422 1.440 -0.018	1.293 1.321 -0.028	0.472 0.496 -0.025			
13			0.472 0.480 -0.008	1.225 1.244 -0.018	1.342 1.357 -0.016	1.084 1.092 -0.009	1.396 1.404 -0.008	1.086 1.089 -0.003	1.342 1.351 -0.009	1.225 1.237 -0.013	0.471 0.477 -0.006				
14				0.337 0.342 -0.004	0.546 0.553 -0.006	1.110 1.125 -0.014	0.951 0.956 -0.005	1.121 1.118 0.003	0.545 0.546 -0.001	0.337 0.339 -0.002					
15							0.276 0.292 -0.016	0.327 0.331 -0.004	0.294 0.294 0.000						

Calculated Minus Measured Powers, RMS Difference = 0.013

Figure A-2.43: Plant A EOC 6 Assembly Power Distribution

	R	P	N	M	L	K	J	H	G	F	E	D	C	B	A
1							0.342 0.338 0.004	0.381 0.376 0.005	0.323 0.323 0.000						
2					0.386 0.382 0.004	0.591 0.584 0.007	1.108 1.095 0.013	0.951 0.936 0.015	1.101 1.106 -0.005	0.593 0.630 -0.037	0.386 0.399 -0.013		Calculated Power Measured Power Difference (C-M)		
3				0.515 0.532 -0.017	1.219 1.205 0.014	1.347 1.332 0.015	1.044 1.036 0.008	1.394 1.343 0.051	1.043 1.034 0.009	1.348 1.361 -0.013	1.220 1.242 -0.022	0.516 0.550 -0.034			
4			0.516 0.516 -0.001	1.292 1.285 0.007	1.462 1.422 0.040	1.070 1.053 0.016	1.116 1.104 0.012	1.050 1.045 0.005	1.117 1.109 0.008	1.070 1.059 0.011	1.463 1.470 -0.008	1.292 1.309 -0.017	0.515 0.520 -0.004		
5		0.386 0.390 -0.004	1.220 1.227 -0.008	1.462 1.463 -0.001	0.942 0.936 0.006	1.027 1.019 0.008	1.404 1.385 0.020	1.058 1.051 0.006	1.405 1.396 0.009	1.028 1.022 0.006	0.942 0.938 0.004	1.462 1.467 -0.005	1.220 1.224 -0.005	0.386 0.390 -0.003	
6		0.592 0.601 -0.009	1.347 1.366 -0.018	1.070 1.081 -0.011	1.028 1.039 -0.011	1.078 1.086 -0.008	1.066 1.074 -0.008	1.101 1.104 -0.003	1.066 1.064 0.003	1.078 1.074 0.004	1.027 1.024 0.003	1.070 1.070 0.000	1.347 1.349 -0.001	0.591 0.595 -0.004	
7	0.323 0.329 -0.007	1.101 1.116 -0.015	1.043 1.075 -0.032	1.117 1.132 -0.015	1.405 1.423 -0.018	1.066 1.086 -0.019	0.930 0.968 -0.039	1.440 1.454 -0.014	0.929 0.924 0.005	1.066 1.063 0.004	1.405 1.400 0.005	1.116 1.112 0.004	1.044 1.040 0.005	1.108 1.121 -0.013	0.342 0.347 -0.005
8	0.381 0.394 -0.013	0.951 0.947 0.004	1.394 1.360 0.034	1.050 1.048 0.002	1.058 1.074 -0.016	1.101 1.116 -0.015	1.440 1.461 -0.021	1.019 1.026 -0.007	1.438 1.437 0.001	1.101 1.099 0.002	1.058 1.055 0.003	1.049 1.042 0.007	1.394 1.364 0.030	0.951 0.952 -0.001	0.381 0.389 -0.008
9	0.342 0.343 -0.001	1.108 1.098 0.011	1.044 1.027 0.017	1.116 1.109 0.007	1.404 1.400 0.005	1.066 1.070 -0.004	0.929 0.933 -0.004	1.438 1.440 -0.002	0.929 0.931 -0.002	1.067 1.063 0.004	1.405 1.405 0.000	1.117 1.121 -0.004	1.043 1.044 -0.001	1.102 1.116 -0.014	0.323 0.352 -0.029
10		0.591 0.582 0.009	1.347 1.320 0.027	1.070 1.064 0.006	1.028 1.031 -0.003	1.078 1.079 -0.001	1.067 1.056 0.011	1.102 1.100 0.002	1.067 1.065 0.002	1.078 1.077 0.001	1.029 1.034 -0.006	1.071 1.094 -0.023	1.348 1.363 -0.015	0.594 0.602 -0.008	
11		0.386 0.383 0.004	1.220 1.211 0.008	1.462 1.467 -0.004	0.942 0.964 -0.021	1.029 1.034 -0.005	1.405 1.400 0.006	1.058 1.060 -0.001	1.405 1.398 0.007	1.028 1.021 0.007	0.942 0.945 -0.002	1.463 1.464 -0.001	1.220 1.236 -0.015	0.387 0.392 -0.005	
12		0.515 0.517 -0.001	1.292 1.299 -0.007	1.463 1.475 -0.012	1.071 1.075 -0.004	1.118 1.110 0.007	1.050 1.044 0.006	1.117 1.106 0.011	1.071 1.054 0.016	1.463 1.438 0.025	1.292 1.257 0.035	0.516 0.542 -0.026			
13			0.516 0.519 -0.003	1.221 1.227 -0.007	1.348 1.352 -0.003	1.043 1.043 0.001	1.395 1.385 0.010	1.045 1.029 0.016	1.348 1.312 0.036	1.220 1.194 0.027	0.516 0.504 0.012				
14				0.387 0.389 -0.003	0.593 0.596 -0.003	1.100 1.107 -0.006	0.948 0.944 0.004	1.107 1.089 0.018	0.591 0.578 0.013	0.386 0.378 0.008					
15							0.321 0.342 -0.021	0.378 0.381 -0.003	0.340 0.337 0.004						

Calculated Minus Measured Powers, RMS Difference = 0.014

Figure A-2.44: Plant A BOC 7 Assembly Power Distribution

	R	P	N	M	L	K	J	H	G	F	E	D	C	B	A
1							0.256 0.252 0.003	0.320 0.321 0.000	0.257 0.254 0.003						
2					0.268 0.266 0.002	0.484 0.477 0.006	1.079 1.064 0.015	1.145 1.129 0.016	1.086 1.069 0.017	0.516 0.507 0.009	0.278 0.275 0.004		Calculated Power Measured Power Difference (C-M)		
3				0.379 0.385 -0.006	1.153 1.145 0.007	1.246 1.232 0.014	1.206 1.186 0.019	1.159 1.138 0.021	1.211 1.189 0.021	1.265 1.243 0.022	1.167 1.155 0.012	0.381 0.387 -0.006			
4			0.381 0.378 0.003	1.221 1.215 0.006	1.318 1.307 0.011	1.230 1.216 0.014	1.289 1.270 0.019	0.855 0.841 0.014	1.293 1.269 0.024	1.237 1.204 0.033	1.324 1.312 0.013	1.221 1.224 -0.003	0.379 0.381 -0.002		
5		0.278 0.276 0.002	1.167 1.156 0.011	1.324 1.315 0.009	1.227 1.216 0.011	1.250 1.237 0.013	1.186 1.167 0.019	1.325 1.308 0.017	1.188 1.171 0.017	1.253 1.235 0.018	1.228 1.218 0.010	1.318 1.331 -0.013	1.153 1.162 -0.009	0.268 0.269 -0.001	
6		0.515 0.514 0.001	1.265 1.260 0.004	1.237 1.230 0.006	1.252 1.239 0.013	1.276 1.270 0.006	1.160 1.156 0.004	1.174 1.165 0.009	1.161 1.152 0.009	1.277 1.268 0.009	1.250 1.246 0.005	1.231 1.236 -0.005	1.246 1.257 -0.011	0.484 0.488 -0.004	
7	0.257 0.260 -0.003	1.085 1.091 -0.005	1.210 1.212 -0.002	1.293 1.294 -0.001	1.187 1.191 -0.003	1.159 1.166 -0.006	0.848 0.867 -0.019	1.357 1.361 -0.004	0.849 0.848 0.001	1.160 1.155 0.005	1.186 1.184 0.002	1.289 1.293 -0.004	1.206 1.219 -0.013	1.080 1.096 -0.016	0.256 0.259 -0.003
8	0.320 0.333 -0.012	1.145 1.155 -0.010	1.159 1.164 -0.005	0.855 0.860 -0.005	1.324 1.345 -0.021	1.172 1.181 -0.010	1.351 1.363 -0.012	0.896 0.898 -0.002	1.357 1.355 0.002	1.173 1.168 0.005	1.325 1.322 0.003	0.856 0.859 -0.004	1.159 1.182 -0.023	1.145 1.162 -0.017	0.321 0.326 -0.006
9	0.256 0.259 -0.003	1.080 1.088 -0.007	1.207 1.212 -0.005	1.289 1.293 -0.003	1.186 1.187 -0.001	1.158 1.161 -0.002	0.846 0.847 -0.001	1.351 1.352 -0.001	0.848 0.846 0.001	1.160 1.153 0.007	1.188 1.182 0.006	1.294 1.291 0.003	1.213 1.223 -0.010	1.086 1.105 -0.019	0.257 0.271 -0.013
10		0.484 0.486 -0.001	1.247 1.251 -0.004	1.231 1.231 0.000	1.250 1.246 0.004	1.276 1.274 0.003	1.159 1.152 0.007	1.172 1.170 0.002	1.159 1.155 0.004	1.277 1.268 0.009	1.253 1.241 0.012	1.238 1.218 0.019	1.266 1.269 -0.003	0.516 0.527 -0.011	
11		0.269 0.269 -0.001	1.153 1.157 -0.003	1.319 1.317 0.002	1.229 1.214 0.015	1.253 1.251 0.002	1.187 1.191 -0.003	1.324 1.326 -0.002	1.186 1.184 0.002	1.250 1.239 0.011	1.229 1.216 0.013	1.325 1.319 0.006	1.168 1.172 -0.004	0.278 0.281 -0.002	
12		0.379 0.385 -0.006	1.221 1.224 -0.003	1.325 1.326 -0.003	1.237 1.245 -0.008	1.293 1.314 -0.022	0.855 0.861 -0.006	1.289 1.296 -0.007	1.231 1.234 -0.004	1.319 1.320 -0.001	1.222 1.223 -0.002	0.381 0.394 -0.013			
13			0.381 0.382 -0.001	1.167 1.173 -0.006	1.265 1.277 -0.012	1.211 1.227 -0.016	1.159 1.166 -0.008	1.206 1.222 -0.017	1.246 1.265 -0.018	1.153 1.162 -0.009	0.379 0.380 -0.001				
14				0.278 0.280 -0.002	0.515 0.522 -0.007	1.085 1.109 -0.024	1.145 1.169 -0.024	1.080 1.112 -0.033	0.484 0.493 -0.009	0.268 0.271 -0.003					
15							0.257 0.278 -0.021	0.320 0.330 -0.010	0.255 0.263 -0.007						

Calculated Minus Measured Powers, RMS Difference = 0.011

Figure A-2.45: Plant A MOC 7 Assembly Power Distribution

	R	P	N	M	L	K	J	H	G	F	E	D	C	B	A
1							0.265	0.332	0.266						
							0.268	0.343	0.269						
							-0.003	-0.010	-0.004						
2					0.287	0.497	1.054	1.158	1.058	0.526	0.296				
					0.286	0.498	1.061	1.166	1.068	0.543	0.300				
					0.001	-0.001	-0.007	-0.008	-0.010	-0.017	-0.004				
												Calculated Power			
												Measured Power			
												Difference (C-M)			
3				0.400	1.145	1.302	1.167	1.114	1.170	1.317	1.155	0.401			
				0.401	1.141	1.302	1.175	1.110	1.170	1.319	1.159	0.416			
				-0.001	0.005	0.000	-0.008	0.003	0.000	-0.002	-0.004	-0.014			
4			0.401	1.223	1.387	1.199	1.364	0.892	1.367	1.203	1.392	1.223	0.400		
			0.400	1.217	1.371	1.193	1.362	0.887	1.359	1.186	1.384	1.224	0.400		
			0.001	0.006	0.015	0.006	0.003	0.005	0.009	0.017	0.008	-0.001	0.000		
5		0.296	1.155	1.392	1.183	1.188	1.147	1.400	1.148	1.190	1.184	1.387	1.145	0.287	
		0.297	1.159	1.390	1.176	1.182	1.139	1.391	1.140	1.177	1.166	1.384	1.147	0.293	
		-0.001	-0.004	0.002	0.007	0.006	0.009	0.009	0.009	0.013	0.017	0.003	-0.001	-0.006	
6		0.525	1.316	1.203	1.190	1.307	1.103	1.117	1.104	1.308	1.188	1.199	1.302	0.497	
		0.526	1.319	1.202	1.182	1.307	1.106	1.110	1.098	1.300	1.179	1.194	1.303	0.502	
		-0.001	-0.003	0.001	0.007	0.000	-0.002	0.007	0.006	0.008	0.009	0.005	-0.001	-0.005	
7	0.266	1.058	1.170	1.367	1.148	1.103	0.842	1.357	0.843	1.103	1.147	1.364	1.167	1.054	0.265
	0.270	1.064	1.172	1.369	1.151	1.111	0.869	1.367	0.844	1.102	1.142	1.356	1.167	1.076	0.271
	-0.004	-0.006	-0.002	-0.002	-0.002	-0.009	-0.026	-0.010	-0.001	0.001	0.005	0.009	-0.001	-0.022	-0.006
8	0.332	1.158	1.114	0.892	1.399	1.116	1.354	0.900	1.357	1.117	1.400	0.892	1.114	1.158	0.332
	0.350	1.167	1.114	0.892	1.409	1.123	1.369	0.905	1.361	1.124	1.397	0.886	1.103	1.188	0.344
	-0.018	-0.008	0.000	0.000	-0.009	-0.007	-0.015	-0.005	-0.004	-0.007	0.003	0.006	0.011	-0.030	-0.012
9	0.265	1.055	1.168	1.365	1.147	1.103	0.841	1.354	0.842	1.103	1.148	1.368	1.171	1.058	0.266
	0.268	1.055	1.160	1.355	1.137	1.100	0.843	1.357	0.840	1.097	1.141	1.359	1.170	1.079	0.290
	-0.003	0.000	0.008	0.009	0.010	0.002	-0.002	-0.004	0.002	0.006	0.007	0.009	0.001	-0.020	-0.025
10	0.497	1.302	1.199	1.188	1.307	1.103	1.116	1.103	1.308	1.190	1.204	1.317	0.525		
	0.492	1.280	1.185	1.175	1.300	1.099	1.120	1.102	1.300	1.178	1.187	1.314	0.530		
	0.005	0.022	0.014	0.013	0.007	0.004	-0.004	0.001	0.008	0.012	0.017	0.003	-0.005		
11	0.287	1.146	1.387	1.185	1.190	1.148	1.399	1.147	1.188	1.185	1.392	1.155	0.296		
	0.284	1.135	1.372	1.165	1.181	1.149	1.421	1.151	1.179	1.168	1.377	1.156	0.297		
	0.003	0.011	0.015	0.020	0.009	0.000	-0.021	-0.003	0.009	0.017	0.016	-0.001	-0.001		
12	0.400	1.223	1.392	1.204	1.367	0.892	1.364	1.199	1.387	1.223	0.401				
	0.407	1.215	1.381	1.197	1.362	0.894	1.370	1.199	1.376	1.201	0.422				
	-0.007	0.008	0.011	0.007	0.005	-0.002	-0.005	0.001	0.011	0.022	-0.021				
13		0.401	1.155	1.317	1.170	1.114	1.167	1.302	1.146	0.400					
		0.399	1.149	1.313	1.169	1.104	1.177	1.315	1.145	0.395					
		0.003	0.006	0.004	0.001	0.010	-0.010	-0.013	0.000	0.005					
14		0.296	0.525	1.058	1.158	1.054	0.497	0.287							
		0.295	0.527	1.072	1.174	1.090	0.506	0.289							
		0.001	-0.001	-0.014	-0.016	-0.035	-0.009	-0.001							
15						0.266	0.332	0.265							
						0.290	0.342	0.273							
						-0.024	-0.009	-0.008							

Calculated Minus Measured Powers, RMS Difference = 0.010

Figure A-2.46: Plant A EOC 7 Assembly Power Distribution

	R	P	N	M	L	K	J	H	G	F	E	D	C	B	A
1							0.283	0.350	0.283						
							0.287	0.366	0.287						
							-0.004	-0.016	-0.004						
2					0.317	0.520	1.030	1.115	1.031	0.545	0.324				
					0.323	0.525	1.037	1.124	1.033	0.535	0.327				
					-0.006	-0.005	-0.008	-0.009	-0.003	0.010	-0.003				
												Calculated Power			
												Measured Power			
												Difference (C-M)			
3					0.433	1.140	1.294	1.142	1.088	1.142	1.300	1.144	0.433		
					0.453	1.167	1.311	1.145	1.088	1.147	1.311	1.166	0.468		
					-0.020	-0.027	-0.017	-0.003	0.000	-0.005	-0.011	-0.023	-0.035		
4					0.433	1.219	1.421	1.184	1.412	0.926	1.412	1.185	1.422	1.219	0.433
					0.439	1.246	1.461	1.200	1.419	0.928	1.420	1.201	1.442	1.249	0.442
					-0.006	-0.027	-0.039	-0.016	-0.007	-0.002	-0.009	-0.016	-0.021	-0.030	-0.010
5					0.324	1.144	1.422	1.174	1.178	1.135	1.381	1.135	1.178	1.174	1.421
					0.326	1.152	1.440	1.189	1.187	1.134	1.379	1.137	1.183	1.173	1.449
					-0.002	-0.008	-0.018	-0.014	-0.009	0.001	0.001	-0.003	-0.005	0.001	-0.028
6					0.544	1.300	1.185	1.178	1.371	1.090	1.081	1.090	1.371	1.178	1.184
					0.549	1.310	1.192	1.176	1.378	1.096	1.073	1.089	1.375	1.185	1.204
					-0.005	-0.010	-0.007	0.002	-0.007	-0.007	0.008	0.000	-0.005	-0.008	-0.019
7					0.283	1.030	1.142	1.412	1.135	1.089	0.846	1.285	0.846	1.089	1.135
					0.293	1.046	1.152	1.418	1.137	1.099	0.875	1.290	0.846	1.092	1.144
					-0.010	-0.016	-0.010	-0.006	-0.002	-0.009	-0.030	-0.005	0.001	-0.003	-0.009
8					0.350	1.115	1.088	0.926	1.381	1.080	1.283	0.880	1.284	1.080	1.380
					0.382	1.137	1.097	0.925	1.377	1.080	1.287	0.876	1.270	1.079	1.382
					-0.033	-0.022	-0.009	0.000	0.003	0.001	-0.005	0.004	0.015	0.002	-0.002
9					0.283	1.030	1.143	1.412	1.135	1.089	0.846	1.282	0.846	1.089	1.134
					0.292	1.042	1.146	1.400	1.117	1.076	0.836	1.257	0.817	1.080	1.130
					-0.009	-0.012	-0.004	0.012	0.018	0.013	0.009	0.026	0.029	0.009	0.005
10					0.520	1.294	1.184	1.178	1.371	1.089	1.080	1.089	1.371	1.178	1.185
					0.520	1.301	1.160	1.156	1.347	1.067	1.057	1.074	1.367	1.168	1.171
					0.000	-0.007	0.025	0.022	0.024	0.022	0.023	0.015	0.004	0.010	0.014
11					0.317	1.140	1.421	1.175	1.178	1.135	1.381	1.135	1.178	1.175	1.422
					0.298	1.041	1.339	1.150	1.155	1.115	1.339	1.128	1.199	1.155	1.412
					0.019	0.098	0.082	0.025	0.023	0.020	0.042	0.007	-0.021	0.020	0.009
12					0.433	1.219	1.422	1.185	1.412	0.926	1.412	1.184	1.421	1.219	0.433
					0.228	1.093	1.356	1.159	1.408	0.921	1.415	1.193	1.419	1.216	0.433
					0.205	0.126	0.066	0.026	0.004	0.005	-0.003	-0.009	0.002	0.002	0.000
13					0.433	1.144	1.300	1.142	1.088	1.142	1.294	1.139	0.433		
					0.402	1.102	1.278	1.143	1.102	1.154	1.310	1.145	0.433		
					0.031	0.042	0.022	-0.001	-0.014	-0.012	-0.017	-0.006	-0.001		
14					0.324	0.544	1.030	1.115	1.029	0.520	0.317				
					0.315	0.541	1.048	1.136	1.049	0.527	0.319				
					0.009	0.003	-0.018	-0.021	-0.019	-0.007	-0.003				
15							0.283	0.350	0.282						
							0.318	0.363	0.289						
							-0.035	-0.013	-0.006						

Calculated Minus Measured Powers, RMS Difference = 0.027

Codes and Methods Applicability Report
for the U.S. EPR

Figure A-2.47: Plant A BOC 8 Assembly Power Distribution

	R	P	N	M	L	K	J	H	G	F	E	D	C	B	A
1							0.266 0.259 0.007	0.351 0.350 0.001	0.272 0.270 0.002						
2					0.284 0.273 0.011	0.489 0.470 0.019	1.073 1.036 0.037	1.141 1.122 0.018	1.074 1.066 0.008	0.489 0.495 -0.006	0.284 0.283 0.000		Calculated Power Measured Power Difference (C-M)		
3				0.404 0.412 -0.008	1.051 1.015 0.037	1.046 1.003 0.043	1.246 1.182 0.065	1.259 1.244 0.015	1.244 1.235 0.009	1.042 1.047 -0.005	1.049 1.043 0.006	0.404 0.401 0.003			
4			0.403 0.384 0.019	1.110 1.074 0.036	1.142 1.088 0.055	1.285 1.240 0.045	1.240 1.192 0.047	1.284 1.213 0.071	1.231 1.214 0.016	1.280 1.311 -0.031	1.142 1.123 0.019	1.112 1.098 0.015	0.404 0.401 0.003		
5		0.283 0.269 0.013	1.046 0.980 0.066	1.127 1.092 0.035	1.307 1.292 0.015	1.240 1.217 0.023	1.302 1.288 0.014	1.275 1.251 0.024	1.290 1.272 0.018	1.236 1.212 0.024	1.310 1.222 0.088	1.129 1.114 0.015	1.046 1.044 0.001	0.282 0.294 -0.011	
6		0.487 0.481 0.006	1.038 1.014 0.023	1.274 1.246 0.028	1.233 1.194 0.039	1.343 1.324 0.020	1.217 1.213 0.005	1.240 1.247 -0.006	1.212 1.205 0.007	1.343 1.318 0.025	1.236 1.203 0.034	1.276 1.264 0.012	1.040 1.043 -0.003	0.486 0.496 -0.010	
7	0.272 0.273 -0.002	1.072 1.077 -0.005	1.241 1.252 -0.011	1.228 1.221 0.006	1.288 1.275 0.013	1.211 1.205 0.007	1.181 1.190 -0.009	1.106 1.112 -0.006	1.178 1.187 -0.010	1.214 1.195 0.019	1.298 1.282 0.016	1.234 1.234 0.000	1.241 1.258 -0.017	1.068 1.103 -0.034	0.265 0.271 -0.006
8	0.351 0.355 -0.004	1.139 1.148 -0.010	1.257 1.267 -0.010	1.282 1.286 -0.004	1.273 1.277 -0.004	1.238 1.233 0.005	1.102 1.098 0.004	0.869 0.869 0.000	1.095 1.095 0.000	1.235 1.187 0.048	1.271 1.261 0.010	1.279 1.289 -0.010	1.254 1.280 -0.026	1.136 1.104 0.032	0.350 0.348 0.002
9	0.266 0.269 -0.003	1.071 1.083 -0.012	1.245 1.260 -0.015	1.238 1.246 -0.008	1.300 1.300 0.000	1.215 1.203 0.011	1.174 1.152 0.022	1.091 1.093 -0.002	1.171 1.208 -0.037	1.208 1.220 -0.012	1.286 1.300 -0.014	1.226 1.250 -0.024	1.239 1.265 -0.026	1.070 1.083 -0.013	0.271 0.288 -0.017
10		0.488 0.496 -0.008	1.045 1.068 -0.023	1.284 1.300 -0.016	1.238 1.242 -0.004	1.341 1.320 0.021	1.208 1.135 0.073	1.234 1.226 0.008	1.212 1.224 -0.012	1.340 1.349 -0.009	1.231 1.258 -0.027	1.273 1.324 -0.051	1.037 1.070 -0.033	0.487 0.510 -0.024	
11		0.284 0.290 -0.006	1.050 1.077 -0.027	1.141 1.163 -0.022	1.306 1.329 -0.023	1.231 1.235 -0.004	1.286 1.281 0.005	1.271 1.298 -0.027	1.299 1.310 -0.012	1.237 1.221 0.017	1.305 1.345 -0.039	1.126 1.164 -0.038	1.045 1.074 -0.029	0.282 0.292 -0.010	
12		0.404 0.425 -0.021	1.109 1.137 -0.028	1.126 1.150 -0.023	1.273 1.294 -0.021	1.227 1.250 -0.023	1.281 1.311 -0.030	1.237 1.258 -0.021	1.283 1.304 -0.021	1.141 1.173 -0.032	1.109 1.147 -0.038	0.403 0.402 0.001			
13			0.403 0.413 -0.010	1.045 1.073 -0.028	1.037 1.061 -0.024	1.240 1.272 -0.032	1.256 1.304 -0.048	1.244 1.266 -0.022	1.044 1.086 -0.042	1.050 1.085 -0.035	0.404 0.418 -0.014				
14				0.282 0.299 -0.017	0.487 0.501 -0.014	1.071 1.097 -0.026	1.138 1.154 -0.016	1.071 1.045 0.026	0.487 0.493 -0.005	0.284 0.291 -0.008					
15							0.272 0.285 -0.014	0.351 0.357 -0.006	0.266 0.263 0.003						

Calculated Minus Measured Powers, RMS Difference = 0.025

Figure A-2.48: Plant A MOC 8 Assembly Power Distribution

	R	P	N	M	L	K	J	H	G	F	E	D	C	B	A
1							0.284 0.284 0.000	0.375 0.377 -0.001	0.291 0.292 -0.002						
2					0.278 0.277 0.001	0.491 0.489 0.002	1.106 1.103 0.003	1.210 1.215 -0.005	1.108 1.116 -0.008	0.492 0.502 -0.011	0.278 0.280 -0.003		Calculated Power Measured Power Difference (C-M)		
3				0.383 0.401 -0.018	0.983 0.981 0.002	1.007 1.001 0.007	1.337 1.326 0.011	1.240 1.250 -0.009	1.336 1.342 -0.007	1.004 1.014 -0.009	0.982 0.986 -0.003	0.383 0.385 -0.002			
4			0.383 0.380 0.003	1.054 1.050 0.003	1.071 1.057 0.014	1.339 1.327 0.012	1.186 1.173 0.013	1.361 1.327 0.034	1.180 1.177 0.003	1.336 1.353 -0.017	1.071 1.067 0.004	1.055 1.042 0.013	0.383 0.377 0.006		
5		0.277 0.275 0.003	0.981 0.970 0.011	1.060 1.051 0.009	1.386 1.370 0.016	1.187 1.179 0.008	1.206 1.206 0.001	1.190 1.181 0.009	1.198 1.193 0.006	1.185 1.177 0.007	1.389 1.365 0.024	1.061 1.033 0.028	0.981 0.962 0.019	0.277 0.273 0.004	
6		0.491 0.489 0.001	1.003 0.997 0.006	1.332 1.321 0.011	1.183 1.161 0.022	1.429 1.424 0.006	1.181 1.186 -0.005	1.331 1.332 -0.001	1.177 1.174 0.003	1.429 1.410 0.019	1.185 1.167 0.018	1.334 1.308 0.025	1.005 0.991 0.014	0.490 0.487 0.003	
7	0.290 0.292 -0.002	1.107 1.110 -0.002	1.334 1.335 -0.001	1.179 1.178 0.001	1.198 1.197 0.001	1.177 1.184 -0.007	1.307 1.335 -0.028	1.123 1.133 -0.010	1.305 1.316 -0.011	1.179 1.173 0.006	1.205 1.191 0.013	1.185 1.160 0.024	1.335 1.327 0.009	1.106 1.109 -0.004	0.284 0.284 0.000
8	0.375 0.382 -0.006	1.210 1.217 -0.007	1.240 1.246 -0.006	1.360 1.367 -0.007	1.189 1.202 -0.013	1.330 1.338 -0.008	1.121 1.129 -0.008	0.900 0.904 -0.003	1.115 1.117 0.002	1.328 1.322 0.006	1.188 1.184 0.004	1.359 1.355 0.004	1.239 1.243 -0.004	1.210 1.194 0.017	0.375 0.373 0.003
9	0.284 0.287 -0.003	1.106 1.114 -0.007	1.337 1.347 -0.010	1.186 1.193 -0.007	1.206 1.211 -0.005	1.180 1.180 0.000	1.302 1.297 0.005	1.113 1.109 0.004	1.299 1.297 0.002	1.175 1.178 -0.002	1.197 1.201 -0.004	1.179 1.188 -0.009	1.334 1.345 -0.010	1.108 1.112 -0.004	0.290 0.297 -0.006
10		0.490 0.495 -0.004	1.007 1.019 -0.012	1.339 1.346 -0.007	1.186 1.187 -0.001	1.428 1.421 0.007	1.175 1.154 0.021	1.327 1.313 0.013	1.178 1.170 0.008	1.428 1.419 0.008	1.182 1.192 -0.009	1.332 1.363 -0.031	1.003 1.019 -0.016	0.491 0.504 -0.013	
11		0.278 0.280 -0.002	0.983 0.990 -0.007	1.071 1.074 -0.004	1.386 1.386 0.000	1.182 1.179 0.003	1.197 1.188 0.009	1.188 1.175 0.013	1.205 1.192 0.013	1.186 1.157 0.029	1.386 1.401 -0.015	1.060 1.075 -0.015	0.981 0.994 -0.012	0.277 0.282 -0.005	
12			0.383 0.385 -0.002	1.054 1.058 -0.004	1.060 1.063 -0.003	1.332 1.333 -0.002	1.179 1.179 0.000	1.360 1.359 0.001	1.186 1.184 0.002	1.339 1.335 0.004	1.071 1.077 -0.007	1.054 1.062 -0.009	0.383 0.382 0.001		
13				0.383 0.385 -0.002	0.981 0.988 -0.007	1.003 1.009 -0.006	1.334 1.344 -0.009	1.240 1.252 -0.012	1.337 1.347 -0.010	1.007 1.020 -0.012	0.983 0.992 -0.009	0.383 0.387 -0.004			
14					0.277 0.286 -0.009	0.491 0.497 -0.006	1.108 1.122 -0.014	1.211 1.224 -0.014	1.106 1.118 -0.012	0.490 0.497 -0.006	0.278 0.281 -0.003				
15							0.290 0.305 -0.015	0.375 0.383 -0.008	0.284 0.289 -0.004						

Calculated Minus Measured Powers, RMS Difference = 0.011

Figure A-2.49: Plant A EOC 8 Assembly Power Distribution

	R	P	N	M	L	K	J	H	G	F	E	D	C	B	A
1							0.323	0.413	0.330						
							0.325	0.424	0.336						
							-0.003	-0.010	-0.007						
2					0.328	0.546	1.090	1.153	1.092	0.547	0.329				
					0.333	0.548	1.093	1.173	1.114	0.562	0.335				
					-0.005	-0.002	-0.003	-0.021	-0.022	-0.014	-0.006				
												Calculated Power			
												Measured Power			
												Difference (C-M)			
3					0.425	1.000	1.029	1.379	1.198	1.379	1.027	1.000	0.425		
					0.460	1.020	1.032	1.362	1.231	1.404	1.049	1.015	0.432		
					-0.034	-0.020	-0.003	0.017	-0.033	-0.025	-0.022	-0.015	-0.007		
4					0.426	1.039	1.043	1.371	1.158	1.373	1.155	1.371	1.043	1.040	0.426
					0.429	1.062	1.057	1.379	1.152	1.335	1.161	1.407	1.050	1.034	0.422
					-0.003	-0.023	-0.015	-0.008	0.007	0.038	-0.006	-0.036	-0.007	0.006	0.004
5					0.329	1.001	1.037	1.311	1.118	1.146	1.144	1.117	1.312	1.037	1.000
					0.328	0.996	1.049	1.346	1.131	1.162	1.141	1.144	1.120	1.297	1.010
					0.001	0.006	-0.012	-0.035	-0.013	-0.016	0.002	-0.002	-0.003	0.015	0.027
6					0.547	1.028	1.371	1.116	1.329	1.133	1.360	1.132	1.329	1.118	1.371
					0.549	1.029	1.373	1.105	1.331	1.139	1.370	1.134	1.320	1.104	1.349
					-0.002	-0.001	-0.002	0.012	-0.002	-0.005	-0.010	-0.002	0.009	0.014	0.022
7					0.330	1.093	1.380	1.156	1.142	1.132	1.362	1.139	1.362	1.134	1.147
					0.334	1.101	1.388	1.160	1.144	1.132	1.360	1.142	1.370	1.122	1.132
					-0.004	-0.008	-0.008	-0.004	-0.001	0.000	0.003	-0.003	-0.008	0.012	0.015
8					0.414	1.154	1.199	1.373	1.144	1.360	1.138	0.964	1.135	1.360	1.145
					0.425	1.164	1.206	1.381	1.158	1.359	1.132	0.960	1.132	1.323	1.128
					-0.011	-0.010	-0.007	-0.008	-0.014	0.001	0.006	0.003	0.003	0.038	0.017
9					0.323	1.091	1.380	1.159	1.147	1.134	1.361	1.134	1.133	1.143	1.157
					0.327	1.099	1.386	1.160	1.135	1.122	1.342	1.125	1.377	1.115	1.131
					-0.004	-0.008	-0.006	-0.001	0.012	0.011	0.019	0.009	-0.017	0.018	0.012
10					0.546	1.029	1.372	1.118	1.330	1.132	1.360	1.134	1.330	1.117	1.372
					0.550	1.034	1.374	1.112	1.310	1.094	1.327	1.119	1.307	1.109	1.364
					-0.004	-0.005	-0.002	0.007	0.020	0.039	0.033	0.015	0.023	0.009	0.008
11					0.328	1.000	1.043	1.311	1.117	1.143	1.145	1.148	1.119	1.312	1.038
					0.332	1.015	1.050	1.312	1.106	1.115	1.096	1.119	1.081	1.316	1.041
					-0.004	-0.015	-0.007	-0.001	0.011	0.027	0.049	0.028	0.037	-0.004	-0.004
12					0.426	1.040	1.037	1.372	1.156	1.374	1.159	1.373	1.043	1.040	0.426
					0.451	1.054	1.040	1.367	1.146	1.360	1.148	1.360	1.046	1.055	0.430
					-0.026	-0.015	-0.003	0.005	0.011	0.014	0.012	0.012	-0.003	-0.015	-0.004
13					0.426	1.001	1.028	1.380	1.199	1.380	1.029	1.000	0.426		
					0.430	1.008	1.032	1.388	1.223	1.382	1.036	1.006	0.430		
					-0.004	-0.006	-0.003	-0.008	-0.024	-0.002	-0.007	-0.006	-0.004		
14					0.329	0.548	1.093	1.154	1.091	0.546	0.329				
					0.335	0.552	1.103	1.162	1.080	0.546	0.330				
					-0.007	-0.004	-0.010	-0.008	0.011	0.001	-0.001				
15							0.330	0.414	0.323						
							0.340	0.418	0.322						
							-0.010	-0.004	0.001						

Calculated Minus Measured Powers, RMS Difference = 0.014

Figure A-2.50: Plant A BOC 9 Assembly Power Distribution

	R	P	N	M	L	K	J	H	G	F	E	D	C	B	A
1							0.281	0.355	0.287						
							0.285	0.370	0.294						
							-0.004	-0.015	-0.007						
2					0.322	0.537	1.109	1.161	1.105	0.534	0.320				
					0.319	0.536	1.117	1.181	1.128	0.550	0.327				
					0.003	0.001	-0.007	-0.020	-0.023	-0.016	-0.007				
												Calculated Power			
												Measured Power			
												Difference (C-M)			
3				0.419	1.099	1.152	1.238	1.163	1.221	1.145	1.094	0.416			
				0.429	1.086	1.143	1.236	1.183	1.243	1.171	1.112	0.420			
				-0.009	0.013	0.008	0.002	-0.020	-0.022	-0.027	-0.018	-0.004			
4			0.416	1.157	1.188	1.239	1.253	0.894	1.246	1.232	1.185	1.157	0.419		
			0.407	1.141	1.154	1.225	1.240	0.867	1.257	1.272	1.198	1.155	0.419		
			0.009	0.016	0.035	0.014	0.013	0.028	-0.011	-0.040	-0.013	0.002	0.000		
5		0.321	1.096	1.186	1.272	1.175	1.211	1.278	1.213	1.167	1.273	1.189	1.100	0.322	
		0.314	1.063	1.177	1.298	1.175	1.208	1.277	1.221	1.180	1.269	1.168	1.100	0.341	
		0.007	0.033	0.009	-0.026	0.000	0.002	0.001	-0.008	-0.013	0.003	0.021	0.000	-0.018	
6		0.535	1.147	1.234	1.167	1.236	1.192	1.270	1.187	1.238	1.176	1.240	1.153	0.538	
		0.533	1.139	1.222	1.140	1.226	1.194	1.290	1.196	1.250	1.174	1.232	1.157	0.550	
		0.002	0.008	0.012	0.027	0.009	-0.001	-0.020	-0.009	-0.012	0.002	0.008	-0.004	-0.012	
7	0.288	1.108	1.226	1.252	1.211	1.182	1.287	1.175	1.296	1.196	1.211	1.254	1.239	1.110	0.281
	0.291	1.116	1.243	1.247	1.196	1.172	1.285	1.178	1.294	1.188	1.203	1.243	1.249	1.148	0.289
	-0.003	-0.009	-0.016	0.004	0.015	0.010	0.003	-0.003	0.001	0.007	0.008	0.011	-0.010	-0.038	-0.008
8	0.356	1.163	1.166	0.893	1.270	1.263	1.161	0.959	1.180	1.272	1.278	0.895	1.164	1.162	0.355
	0.363	1.170	1.170	0.889	1.251	1.247	1.149	0.955	1.176	1.240	1.265	0.892	1.168	1.160	0.361
	-0.007	-0.007	-0.005	0.004	0.019	0.016	0.012	0.005	0.004	0.031	0.013	0.003	-0.004	0.002	-0.005
9	0.282	1.110	1.236	1.245	1.204	1.187	1.282	1.165	1.292	1.186	1.212	1.246	1.222	1.106	0.287
	0.283	1.112	1.235	1.240	1.195	1.169	1.256	1.157	1.314	1.168	1.207	1.254	1.235	1.121	0.309
	-0.002	-0.003	0.001	0.005	0.009	0.019	0.027	0.009	-0.022	0.018	0.005	-0.007	-0.012	-0.016	-0.021
10		0.536	1.149	1.235	1.172	1.232	1.180	1.264	1.192	1.237	1.168	1.233	1.146	0.534	
		0.536	1.144	1.230	1.162	1.205	1.121	1.239	1.183	1.222	1.170	1.256	1.163	0.547	
		0.001	0.006	0.005	0.010	0.027	0.059	0.025	0.009	0.016	-0.003	-0.023	-0.017	-0.013	
11		0.322	1.097	1.186	1.269	1.163	1.205	1.269	1.210	1.177	1.274	1.186	1.095	0.321	
		0.322	1.100	1.186	1.268	1.149	1.179	1.250	1.192	1.142	1.284	1.206	1.109	0.326	
		0.000	-0.002	0.000	0.001	0.014	0.026	0.019	0.017	0.035	-0.010	-0.019	-0.013	-0.005	
12		0.416	1.154	1.182	1.229	1.241	0.894	1.258	1.242	1.190	1.158	0.416			
		0.428	1.159	1.184	1.224	1.228	0.889	1.250	1.233	1.200	1.190	0.412			
		-0.012	-0.005	-0.001	0.005	0.013	0.005	0.008	0.009	-0.010	-0.032	0.004			
13			0.417	1.092	1.144	1.223	1.170	1.244	1.155	1.101	0.420				
			0.419	1.099	1.146	1.226	1.180	1.247	1.154	1.109	0.427				
			-0.002	-0.007	-0.003	-0.003	-0.010	-0.003	0.001	-0.008	-0.007				
14				0.320	0.534	1.108	1.165	1.114	0.539	0.323					
				0.335	0.539	1.117	1.175	1.125	0.541	0.325					
				-0.014	-0.005	-0.009	-0.010	-0.011	-0.002	-0.002					
15							0.288	0.356	0.282						
							0.297	0.361	0.285						
							-0.009	-0.005	-0.003						

Calculated Minus Measured Powers, RMS Difference = 0.015

Figure A-2.51: Plant A MOC 9 Assembly Power Distribution

	R	P	N	M	L	K	J	H	G	F	E	D	C	B	A
1							0.296	0.377	0.303						
							0.302	0.390	0.308						
							-0.005	-0.013	-0.005						
2					0.315	0.529	1.125	1.241	1.122	0.527	0.314				
					0.316	0.533	1.138	1.250	1.134	0.543	0.321				
					-0.002	-0.004	-0.013	-0.009	-0.012	-0.016	-0.008				
												Calculated Power			
												Measured Power			
												Difference (C-M)			
3				0.397	1.050	1.101	1.317	1.118	1.302	1.096	1.047	0.395			
				0.416	1.053	1.106	1.338	1.111	1.306	1.115	1.064	0.406			
				-0.019	-0.003	-0.005	-0.021	0.007	-0.004	-0.018	-0.017	-0.011			
4			0.395	1.089	1.119	1.380	1.175	0.850	1.170	1.374	1.117	1.089	0.397		
			0.391	1.086	1.103	1.370	1.160	0.798	1.164	1.405	1.130	1.097	0.399		
			0.004	0.003	0.016	0.010	0.015	0.052	0.006	-0.031	-0.013	-0.008	-0.002		
5		0.314	1.048	1.117	1.380	1.157	1.121	1.164	1.123	1.149	1.380	1.119	1.050	0.315	
		0.310	1.030	1.112	1.386	1.150	1.104	1.141	1.115	1.153	1.380	1.116	1.049	0.314	
		0.004	0.018	0.006	-0.006	0.007	0.018	0.024	0.008	-0.004	0.000	0.003	0.001	0.001	
6		0.528	1.098	1.376	1.149	1.410	1.166	1.416	1.160	1.411	1.157	1.380	1.102	0.529	
		0.525	1.091	1.365	1.132	1.397	1.159	1.403	1.153	1.404	1.152	1.374	1.102	0.535	
		0.002	0.008	0.011	0.018	0.013	0.007	0.013	0.007	0.007	0.005	0.006	0.000	-0.006	
7	0.303	1.124	1.306	1.174	1.122	1.158	1.375	1.147	1.381	1.168	1.121	1.175	1.317	1.125	0.296
	0.305	1.127	1.307	1.170	1.115	1.154	1.383	1.143	1.375	1.156	1.111	1.165	1.318	1.155	0.302
	-0.001	-0.002	-0.001	0.004	0.007	0.004	-0.008	0.003	0.006	0.012	0.010	0.011	-0.001	-0.030	-0.006
8	0.377	1.242	1.120	0.850	1.160	1.411	1.137	0.944	1.150	1.417	1.164	0.850	1.118	1.241	0.377
	0.382	1.247	1.123	0.848	1.157	1.396	1.128	0.936	1.138	1.384	1.150	0.845	1.104	1.211	0.379
	-0.005	-0.005	-0.003	0.002	0.003	0.014	0.009	0.007	0.011	0.032	0.014	0.005	0.013	0.030	-0.002
9	0.297	1.126	1.316	1.171	1.119	1.164	1.372	1.140	1.378	1.160	1.122	1.170	1.302	1.123	0.303
	0.299	1.132	1.321	1.166	1.084	1.141	1.337	1.125	1.372	1.127	1.113	1.174	1.303	1.130	0.337
	-0.002	-0.006	-0.005	0.006	0.035	0.023	0.034	0.016	0.006	0.033	0.009	-0.004	-0.001	-0.007	-0.034
10	0.529	1.101	1.379	1.156	1.408	1.157	1.412	1.166	1.411	1.149	1.374	1.097	0.527		
	0.535	1.116	1.387	1.154	1.379	1.100	1.384	1.150	1.380	1.152	1.401	1.111	0.542		
	-0.006	-0.016	-0.008	0.002	0.030	0.057	0.027	0.016	0.031	-0.002	-0.026	-0.014	-0.015		
11	0.315	1.050	1.119	1.379	1.148	1.119	1.159	1.121	1.158	1.381	1.117	1.047	0.314		
	0.320	1.072	1.141	1.419	1.147	1.101	1.165	1.109	1.114	1.396	1.134	1.057	0.319		
	-0.006	-0.022	-0.022	-0.040	0.001	0.018	-0.006	0.012	0.044	-0.015	-0.017	-0.010	-0.005		
12	0.395	1.089	1.116	1.373	1.168	0.850	1.179	1.382	1.120	1.089	0.395				
	0.413	1.111	1.134	1.370	1.141	0.849	1.179	1.377	1.130	1.107	0.388				
	-0.018	-0.022	-0.017	0.003	0.026	0.001	0.000	0.005	-0.010	-0.017	0.007				
13	0.397	1.047	1.097	1.304	1.122	1.321	1.103	1.050	0.397						
	0.403	1.058	1.101	1.304	1.134	1.340	1.123	1.066	0.404						
	-0.007	-0.011	-0.004	-0.001	-0.012	-0.019	-0.020	-0.015	-0.007						
14	0.314	0.527	1.124	1.243	1.127	0.530	0.315								
	0.319	0.532	1.139	1.267	1.166	0.545	0.322								
	-0.005	-0.005	-0.015	-0.024	-0.039	-0.015	-0.007								
15	0.303	0.377	0.297												
	0.318	0.388	0.307												
	-0.015	-0.011	-0.010												

Calculated Minus Measured Powers, RMS Difference = 0.016

Figure A-2.52: Plant A EOC 9 Assembly Power Distribution

	R	P	N	M	L	K	J	H	G	F	E	D	C	B	A
1							0.342 0.342 0.000	0.426 0.439 -0.014	0.349 0.354 -0.005						
2					0.358 0.357 0.001	0.582 0.576 0.006	1.145 1.132 0.013	1.244 1.241 0.004	1.147 1.153 -0.007	0.582 0.602 -0.020	0.358 0.364 -0.006		Calculated Power Measured Power Difference (C-M)		
3				0.431 0.456 -0.025	1.047 1.050 -0.003	1.107 1.096 0.011	1.407 1.373 0.033	1.145 1.128 0.016	1.401 1.401 0.001	1.108 1.117 -0.010	1.047 1.052 -0.005	0.430 0.429 0.001			
4			0.430 0.430 -0.001	1.077 1.087 -0.010	1.096 1.091 0.004	1.346 1.338 0.008	1.166 1.151 0.015	0.898 0.879 0.019	1.164 1.162 0.002	1.345 1.358 -0.012	1.095 1.096 0.000	1.077 1.069 0.008	0.431 0.429 0.002		
5		0.358 0.357 0.001	1.047 1.042 0.005	1.095 1.101 -0.006	1.415 1.439 -0.024	1.114 1.117 -0.003	1.077 1.079 -0.002	1.116 1.113 0.003	1.079 1.079 0.000	1.109 1.109 0.000	1.415 1.406 0.009	1.096 1.076 0.020	1.047 1.043 0.004	0.358 0.372 -0.014	
6		0.582 0.583 -0.001	1.108 1.106 0.001	1.346 1.342 0.003	1.110 1.094 0.016	1.333 1.328 0.005	1.097 1.097 0.000	1.324 1.328 -0.004	1.091 1.096 -0.005	1.333 1.328 0.004	1.114 1.107 0.007	1.346 1.336 0.010	1.108 1.105 0.003	0.582 0.586 -0.004	
7	0.349 0.356 -0.007	1.146 1.155 -0.009	1.402 1.404 -0.001	1.167 1.168 -0.001	1.079 1.078 0.001	1.091 1.090 0.001	1.328 1.328 0.000	1.089 1.094 -0.005	1.330 1.351 -0.021	1.097 1.086 0.011	1.076 1.066 0.010	1.165 1.163 0.003	1.406 1.405 0.001	1.145 1.150 -0.006	0.341 0.342 -0.001
8	0.426 0.448 -0.023	1.244 1.262 -0.017	1.146 1.154 -0.008	0.898 0.904 -0.006	1.115 1.128 -0.013	1.324 1.324 0.000	1.084 1.080 0.005	0.940 0.937 0.003	1.091 1.084 0.007	1.324 1.267 0.057	1.116 1.095 0.021	0.898 0.891 0.007	1.144 1.141 0.003	1.244 1.222 0.022	0.426 0.424 0.001
9	0.342 0.350 -0.008	1.145 1.160 -0.014	1.407 1.419 -0.012	1.164 1.171 -0.007	1.077 1.078 -0.001	1.097 1.091 0.007	1.328 1.309 0.018	1.086 1.078 0.008	1.329 1.336 -0.007	1.091 1.088 0.003	1.078 1.068 0.009	1.164 1.158 0.006	1.401 1.400 0.001	1.146 1.148 -0.001	0.349 0.366 -0.017
10		0.582 0.589 -0.007	1.108 1.118 -0.010	1.347 1.357 -0.010	1.116 1.118 -0.003	1.334 1.319 0.016	1.092 1.052 0.040	1.324 1.302 0.021	1.097 1.089 0.008	1.333 1.319 0.013	1.109 1.101 0.009	1.345 1.339 0.006	1.108 1.110 -0.002	0.582 0.592 -0.010	
11		0.358 0.364 -0.006	1.049 1.068 -0.020	1.097 1.112 -0.015	1.417 1.433 -0.016	1.110 1.106 0.004	1.077 1.059 0.018	1.114 1.100 0.014	1.077 1.066 0.011	1.114 1.093 0.022	1.415 1.404 0.011	1.095 1.101 -0.006	1.047 1.053 -0.007	0.358 0.362 -0.003	
12		0.430 0.456 -0.026	1.078 1.096 -0.018	1.096 1.104 -0.008	1.346 1.341 0.005	1.163 1.146 0.017	0.898 0.894 0.004	1.167 1.165 0.002	1.345 1.346 0.000	1.095 1.105 -0.009	1.077 1.115 -0.039	0.430 0.437 -0.007			
13			0.431 0.436 -0.005	1.047 1.050 -0.003	1.108 1.107 0.001	1.402 1.400 0.002	1.147 1.156 -0.009	1.407 1.411 -0.004	1.107 1.123 -0.016	1.047 1.061 -0.014	0.431 0.442 -0.011				
14				0.358 0.356 0.003	0.582 0.582 0.000	1.146 1.151 -0.004	1.244 1.245 -0.002	1.144 1.136 0.008	0.582 0.584 -0.003	0.358 0.362 -0.004					
15							0.349 0.362 -0.013	0.425 0.429 -0.004	0.342 0.341 0.001						

Calculated Minus Measured Powers, RMS Difference = 0.012

Figure A-2.53: Plant A BOC 10 Assembly Power Distribution

	R	P	N	M	L	K	J	H	G	F	E	D	C	B	A
1							0.297 0.300 -0.003	0.381 0.381 0.000	0.299 0.302 -0.003						
2					0.276 0.278 -0.001	0.564 0.568 -0.005	1.151 1.165 -0.015	1.095 1.114 -0.020	1.150 1.167 -0.017	0.564 0.572 -0.008	0.277 0.280 -0.003				
3				0.411 0.414 -0.004	0.845 0.846 -0.001	1.229 1.235 -0.006	1.297 1.313 -0.016	0.864 0.898 -0.034	1.292 1.311 -0.019	1.227 1.240 -0.013	0.848 0.856 -0.008	0.411 0.420 -0.009			
4		0.412 0.408 0.003	1.171 1.163 0.008	1.290 1.283 0.007	1.358 1.356 0.002	1.270 1.205 -0.001	1.274 1.259 0.012	1.185 1.196 -0.004	1.267 1.364 -0.008	1.268 1.364 -0.008	1.223 1.295 -0.005	1.290 1.177 -0.007	0.845 0.413 -0.002	0.276 0.281 -0.005	
5		0.277 0.274 0.003	0.847 0.837 0.009	1.290 1.276 0.014	1.223 1.203 0.020	1.270 1.263 0.007	1.274 1.277 -0.003	1.185 1.178 0.007	1.267 1.265 0.002	1.268 1.265 0.003	1.223 1.218 0.004	1.290 1.295 -0.005	0.845 0.848 -0.003	0.276 0.281 -0.005	
6		0.564 0.559 0.005	1.226 1.213 0.013	1.355 1.343 0.012	1.267 1.268 0.000	0.873 0.864 0.010	1.274 1.255 0.019	1.162 1.142 0.020	1.266 1.264 0.002	0.874 0.862 0.012	1.270 1.263 0.007	1.358 1.355 0.003	1.229 1.228 0.001	0.564 0.566 -0.002	
7	0.298 0.298 0.000	1.149 1.141 0.008	1.291 1.273 0.018	1.192 1.176 0.016	1.267 1.246 0.021	1.266 1.240 0.026	1.234 1.191 0.043	1.148 1.138 0.010	1.234 1.262 -0.028	1.275 1.273 0.002	1.275 1.269 0.006	1.204 1.197 0.008	1.298 1.294 0.004	1.151 1.155 -0.004	0.298 0.300 -0.003
8	0.380 0.389 -0.008	1.094 1.092 0.002	0.863 0.856 0.007	1.270 1.250 0.019	1.184 1.146 0.038	1.160 1.136 0.024	1.148 1.126 0.022	0.800 0.796 0.004	1.149 1.155 -0.006	1.164 1.147 0.016	1.186 1.179 0.007	1.272 1.264 0.007	0.864 0.856 0.009	1.095 1.118 -0.023	0.381 0.388 -0.008
9	0.297 0.299 -0.002	1.150 1.153 -0.003	1.296 1.298 -0.003	1.202 1.194 0.008	1.273 1.258 0.015	1.274 1.257 0.017	1.234 1.222 0.011	1.148 1.147 0.001	1.234 1.251 -0.017	1.267 1.258 0.009	1.268 1.267 0.001	1.194 1.193 0.001	1.292 1.297 -0.005	1.150 1.168 -0.018	0.298 0.306 -0.007
10		0.564 0.569 -0.006	1.228 1.249 -0.021	1.357 1.352 0.004	1.269 1.254 0.016	0.873 0.863 0.011	1.267 1.261 0.006	1.163 1.155 0.008	1.275 1.279 -0.004	0.874 0.878 -0.004	1.268 1.282 -0.014	1.356 1.354 0.001	1.228 1.238 -0.010	0.564 0.580 -0.016	
11		0.276 0.278 -0.002	0.845 0.848 -0.004	1.289 1.278 0.012	1.222 1.193 0.029	1.267 1.247 0.020	1.268 1.248 0.019	1.186 1.158 0.028	1.274 1.275 -0.001	1.270 1.291 -0.021	1.223 1.272 -0.049	1.290 1.313 -0.022	0.848 0.861 -0.013	0.277 0.283 -0.006	
12		0.411 0.413 -0.003	1.171 1.159 0.011	1.290 1.272 0.018	1.355 1.337 0.018	1.193 1.171 0.022	1.270 1.259 0.012	1.203 1.209 -0.006	1.357 1.377 -0.020	1.289 1.319 -0.029	1.171 1.190 -0.019	0.412 0.422 -0.010			
13			0.412 0.409 0.003	0.847 0.843 0.004	1.227 1.221 0.006	1.291 1.289 0.002	0.863 0.869 -0.005	1.296 1.314 -0.017	1.228 1.246 -0.018	0.844 0.860 -0.016	0.411 0.418 -0.007				
14				0.277 0.287 -0.011	0.564 0.568 -0.004	1.150 1.164 -0.014	1.095 1.112 -0.018	1.150 1.178 -0.028	0.563 0.574 -0.011	0.276 0.282 -0.005					
15							0.299 0.320 -0.021	0.381 0.391 -0.010	0.297 0.305 -0.007						

Calculated Minus Measured Powers, RMS Difference = 0.014

Figure A-2.54: Plant A MOC 10 Assembly Power Distribution

	R	P	N	M	L	K	J	H	G	F	E	D	C	B	A
1							0.303 0.307 -0.005	0.393 0.407 -0.013	0.304 0.308 -0.004						
2					0.283 0.285 -0.002	0.566 0.570 -0.004	1.122 1.133 -0.010	1.177 1.189 -0.012	1.123 1.130 -0.007	0.567 0.570 -0.004	0.284 0.285 -0.001		Calculated Power Measured Power Difference (C-M)		
3				0.400 0.414 -0.014	0.819 0.825 -0.006	1.308 1.315 -0.008	1.387 1.398 -0.011	0.882 0.888 -0.006	1.383 1.386 -0.002	1.307 1.308 -0.001	0.822 0.822 0.000	0.400 0.409 -0.009			
4			0.401 0.403 -0.002	1.101 1.107 -0.006	1.361 1.361 0.000	1.282 1.285 -0.003	1.118 1.118 0.001	1.140 1.117 0.023	1.112 1.105 0.007	1.281 1.277 0.005	1.361 1.352 0.009	1.101 1.089 0.011	0.399 0.395 0.004		
5		0.284 0.285 -0.001	0.821 0.825 -0.004	1.361 1.365 -0.004	1.190 1.201 -0.011	1.419 1.423 -0.004	1.358 1.365 -0.007	1.067 1.062 0.005	1.353 1.347 0.006	1.417 1.411 0.006	1.190 1.176 0.014	1.360 1.329 0.031	0.819 0.810 0.009	0.283 0.292 -0.009	
6		0.566 0.567 0.000	1.307 1.305 0.002	1.281 1.272 0.009	1.417 1.385 0.032	0.897 0.889 0.008	1.151 1.148 0.003	1.043 1.044 -0.001	1.146 1.141 0.005	0.897 0.901 -0.005	1.419 1.407 0.012	1.282 1.264 0.018	1.308 1.297 0.010	0.566 0.566 0.000	
7	0.304 0.308 -0.004	1.122 1.126 -0.004	1.383 1.381 0.002	1.111 1.104 0.007	1.353 1.335 0.018	1.146 1.134 0.012	1.133 1.121 0.012	1.273 1.264 0.009	1.133 1.116 0.017	1.151 1.143 0.009	1.359 1.345 0.013	1.119 1.101 0.018	1.387 1.381 0.006	1.123 1.126 -0.003	0.303 0.304 -0.001
8	0.393 0.409 -0.016	1.177 1.185 -0.008	0.882 0.882 0.000	1.140 1.135 0.005	1.066 1.053 0.014	1.042 1.035 0.007	1.272 1.265 0.007	0.874 0.873 0.002	1.273 1.275 -0.002	1.044 1.037 0.007	1.067 1.058 0.009	1.140 1.132 0.008	0.882 0.886 -0.004	1.177 1.174 0.003	0.393 0.394 -0.001
9	0.303 0.307 -0.004	1.122 1.128 -0.005	1.387 1.389 -0.003	1.117 1.121 -0.003	1.358 1.372 -0.014	1.151 1.151 0.000	1.133 1.130 0.003	1.273 1.279 -0.006	1.133 1.166 -0.033	1.146 1.139 0.007	1.354 1.342 0.012	1.112 1.106 0.006	1.383 1.386 -0.003	1.122 1.129 -0.006	0.304 0.309 -0.005
10		0.566 0.568 -0.001	1.307 1.306 0.001	1.281 1.284 -0.002	1.419 1.422 -0.003	0.897 0.893 0.003	1.146 1.134 0.012	1.044 1.035 0.008	1.151 1.154 -0.003	0.897 0.891 0.005	1.417 1.398 0.020	1.281 1.271 0.010	1.307 1.311 -0.004	0.566 0.581 -0.014	
11		0.283 0.285 -0.002	0.819 0.826 -0.006	1.360 1.365 -0.004	1.190 1.187 0.003	1.417 1.410 0.007	1.353 1.336 0.017	1.067 1.033 0.034	1.358 1.349 0.009	1.419 1.418 0.001	1.190 1.150 0.040	1.361 1.358 0.004	0.822 0.826 -0.004	0.284 0.288 -0.004	
12		0.400 0.420 -0.020	1.101 1.110 -0.009	1.361 1.364 -0.002	1.281 1.280 0.001	1.112 1.106 0.006	1.140 1.131 0.009	1.118 1.117 0.000	1.281 1.283 -0.002	1.360 1.360 0.000	1.101 1.135 -0.034	0.401 0.414 -0.013			
13			0.401 0.403 -0.003	0.822 0.825 -0.003	1.307 1.312 -0.005	1.383 1.392 -0.008	0.882 0.889 -0.007	1.387 1.402 -0.015	1.307 1.316 -0.009	0.818 0.823 -0.005	0.400 0.408 -0.008				
14				0.284 0.287 -0.003	0.567 0.572 -0.006	1.123 1.142 -0.020	1.177 1.201 -0.024	1.122 1.155 -0.033	0.566 0.575 -0.009	0.283 0.286 -0.003					
15							0.304 0.327 -0.022	0.394 0.406 -0.012	0.303 0.312 -0.009						

Calculated Minus Measured Powers, RMS Difference = 0.011

Figure A-2.55: Plant A EOC 10 Assembly Power Distribution

	R	P	N	M	L	K	J	H	G	F	E	D	C	B	A
1							0.360 0.364 -0.004	0.464 0.470 -0.006	0.362 0.366 -0.004						
2					0.330 0.335 -0.005	0.614 0.621 -0.006	1.135 1.145 -0.011	1.220 1.234 -0.014	1.136 1.148 -0.012	0.616 0.626 -0.010	0.331 0.334 -0.003		Calculated Power Measured Power Difference (C-M)		
3				0.433 0.450 -0.017	0.823 0.837 -0.014	1.270 1.282 -0.013	1.380 1.389 -0.009	0.943 0.961 -0.018	1.379 1.388 -0.009	1.271 1.274 -0.003	0.826 0.829 -0.003	0.434 0.447 -0.013			
4			0.434 0.442 -0.008	1.042 1.060 -0.018	1.254 1.274 -0.020	1.202 1.213 -0.012	1.094 1.099 -0.005	1.134 1.121 0.013	1.090 1.087 0.004	1.203 1.191 0.012	1.255 1.246 0.008	1.042 1.033 0.009	0.433 0.428 0.004		
5		0.331 0.335 -0.004	0.826 0.842 -0.016	1.255 1.267 -0.013	1.113 1.122 -0.009	1.363 1.373 -0.010	1.338 1.352 -0.014	1.066 1.066 -0.001	1.336 1.334 0.002	1.363 1.361 0.001	1.113 1.104 0.009	1.254 1.224 0.030	0.823 0.813 0.010	0.330 0.333 -0.002	
6		0.616 0.616 0.000	1.271 1.271 0.000	1.203 1.201 0.001	1.363 1.352 0.011	0.942 0.940 0.002	1.154 1.157 -0.002	1.064 1.068 -0.004	1.151 1.149 0.002	0.942 0.959 -0.017	1.363 1.358 0.004	1.202 1.188 0.014	1.269 1.260 0.010	0.614 0.612 0.003	
7	0.362 0.365 -0.004	1.136 1.134 0.002	1.379 1.363 0.016	1.091 1.085 0.006	1.336 1.328 0.008	1.151 1.145 0.006	1.161 1.152 0.009	1.353 1.341 0.013	1.161 1.132 0.028	1.154 1.148 0.006	1.337 1.328 0.009	1.094 1.080 0.014	1.380 1.376 0.004	1.135 1.130 0.005	0.360 0.360 0.000
8	0.465 0.482 -0.018	1.220 1.225 -0.005	0.943 0.940 -0.003	1.134 1.130 0.004	1.065 1.061 0.005	1.063 1.058 0.005	1.353 1.345 0.009	0.987 0.979 0.008	1.353 1.341 0.012	1.065 1.059 0.006	1.066 1.058 0.007	1.134 1.131 0.003	0.943 0.960 -0.017	1.220 1.237 -0.018	0.464 0.469 -0.005
9	0.360 0.365 -0.005	1.135 1.138 -0.003	1.380 1.379 0.000	1.093 1.092 0.001	1.338 1.336 0.001	1.154 1.150 0.004	1.160 1.155 0.006	1.353 1.347 0.007	1.160 1.164 -0.004	1.151 1.134 0.017	1.336 1.321 0.015	1.091 1.084 0.006	1.379 1.386 -0.007	1.136 1.147 -0.011	0.362 0.362 0.000
10		0.615 0.616 -0.001	1.270 1.269 0.001	1.202 1.201 0.001	1.363 1.360 0.003	0.942 0.937 0.005	1.151 1.144 0.007	1.064 1.053 0.011	1.154 1.147 0.008	0.942 0.930 0.011	1.363 1.341 0.022	1.202 1.184 0.018	1.271 1.271 0.000	0.615 0.627 -0.011	
11		0.331 0.332 -0.002	0.824 0.828 -0.005	1.254 1.256 -0.002	1.113 1.110 0.002	1.363 1.354 0.009	1.336 1.319 0.017	1.066 1.037 0.029	1.338 1.324 0.013	1.363 1.356 0.007	1.113 1.083 0.030	1.255 1.244 0.011	0.826 0.827 -0.002	0.331 0.334 -0.003	
12		0.433 0.449 -0.015	1.042 1.048 -0.006	1.255 1.254 0.001	1.203 1.197 0.005	1.091 1.078 0.013	1.134 1.123 0.011	1.093 1.090 0.003	1.202 1.201 0.000	1.254 1.249 0.005	1.042 1.053 -0.011	0.434 0.447 -0.013			
13			0.434 0.436 -0.002	0.826 0.826 -0.001	1.271 1.270 0.000	1.379 1.380 -0.001	0.943 0.946 -0.003	1.380 1.391 -0.011	1.270 1.282 -0.012	0.823 0.826 -0.003	0.434 0.437 -0.003				
14				0.331 0.332 -0.001	0.616 0.619 -0.003	1.136 1.149 -0.013	1.220 1.236 -0.016	1.135 1.158 -0.024	0.614 0.623 -0.009	0.330 0.333 -0.003					
15							0.362 0.383 -0.021	0.465 0.476 -0.011	0.360 0.368 -0.008						

Calculated Minus Measured Powers, RMS Difference = 0.010

Figure A-2.56: Plant A BOC 11 Assembly Power Distribution

	R	P	N	M	L	K	J	H	G	F	E	D	C	B	A
1							0.311 0.308 0.003	0.364 0.357 0.007	0.313 0.309 0.004						
2					0.374 0.373 0.001	0.936 0.932 0.004	1.163 1.156 0.008	1.075 1.063 0.012	1.168 1.156 0.012	0.939 0.931 0.008	0.375 0.374 0.001		Calculated Power Measured Power Difference (C-M)		
3				0.439 0.442 -0.003	1.096 1.093 0.003	1.172 1.170 0.002	1.190 1.187 0.003	1.165 1.147 0.018	1.197 1.185 0.012	1.174 1.165 0.009	1.097 1.097 0.000	0.440 0.456 -0.015			
4			0.440 0.444 -0.004	1.162 1.165 -0.003	1.167 1.162 0.005	1.058 1.059 -0.001	1.094 1.097 -0.003	1.241 1.251 -0.010	1.093 1.089 0.005	1.055 1.039 0.016	1.167 1.165 0.003	1.162 1.170 -0.008	0.439 0.443 -0.004		
5		0.375 0.377 -0.002	1.097 1.110 -0.014	1.167 1.178 -0.011	1.036 1.061 -0.025	1.152 1.160 -0.008	1.297 1.303 -0.007	1.195 1.202 -0.008	1.283 1.281 0.002	1.126 1.114 0.012	1.036 1.031 0.004	1.167 1.175 -0.007	1.096 1.107 -0.011	0.374 0.392 -0.018	
6		0.939 0.937 0.002	1.174 1.172 0.002	1.055 1.050 0.004	1.126 1.111 0.015	1.082 1.081 0.001	1.153 1.161 -0.008	1.138 1.154 -0.016	1.138 1.140 -0.002	1.082 1.057 0.025	1.152 1.141 0.011	1.058 1.054 0.004	1.172 1.178 -0.006	0.936 0.949 -0.013	
7	0.313 0.314 -0.001	1.168 1.162 0.007	1.197 1.182 0.015	1.093 1.081 0.012	1.283 1.264 0.019	1.138 1.134 0.004	1.235 1.246 -0.011	1.074 1.090 -0.016	1.235 1.253 -0.018	1.153 1.152 0.001	1.297 1.286 0.011	1.094 1.075 0.019	1.190 1.177 0.001	1.163 1.177 -0.014	0.311 0.315 -0.004
8	0.364 0.374 -0.010	1.075 1.073 0.002	1.165 1.156 0.009	1.241 1.225 0.016	1.195 1.159 0.036	1.138 1.131 0.007	1.074 1.083 -0.009	1.259 1.286 -0.027	1.074 1.111 -0.036	1.138 1.150 -0.012	1.194 1.188 0.006	1.241 1.230 0.011	1.164 1.162 0.003	1.075 1.076 0.000	0.364 0.369 -0.004
9	0.311 0.313 -0.002	1.163 1.163 0.000	1.191 1.189 0.002	1.094 1.093 0.001	1.297 1.309 -0.012	1.153 1.155 -0.002	1.235 1.244 -0.009	1.074 1.107 -0.033	1.235 1.341 -0.106	1.138 1.114 0.024	1.283 1.266 0.017	1.093 1.082 0.011	1.197 1.196 0.001	1.168 1.178 -0.010	0.313 0.327 -0.014
10		0.936 0.938 -0.002	1.172 1.176 -0.004	1.058 1.057 0.001	1.152 1.147 0.005	1.082 1.074 0.008	1.138 1.128 0.010	1.138 1.142 -0.004	1.153 1.175 -0.022	1.082 1.072 0.010	1.126 1.109 0.017	1.055 1.033 0.022	1.174 1.174 -0.001	0.939 0.958 -0.019	
11		0.374 0.377 -0.003	1.096 1.109 -0.013	1.167 1.166 0.001	1.036 1.012 0.024	1.126 1.108 0.018	1.283 1.259 0.024	1.195 1.167 0.028	1.297 1.287 0.010	1.152 1.130 0.022	1.036 1.016 0.019	1.167 1.169 -0.002	1.097 1.103 -0.006	0.375 0.380 -0.005	
12			0.439 0.472 -0.033	1.162 1.169 -0.007	1.167 1.157 0.011	1.055 1.039 0.016	1.093 1.064 0.029	1.241 1.222 0.019	1.094 1.086 0.008	1.058 1.052 0.006	1.167 1.173 -0.006	1.162 1.204 -0.042	0.440 0.452 -0.012		
13				0.440 0.440 0.000	1.097 1.088 0.009	1.174 1.163 0.011	1.197 1.185 0.012	1.165 1.158 0.006	1.190 1.191 0.000	1.172 1.169 0.003	1.096 1.100 -0.004	0.439 0.448 -0.009			
14					0.375 0.373 0.002	0.939 0.934 0.005	1.168 1.169 -0.001	1.075 1.081 -0.005	1.163 1.183 -0.019	0.936 0.942 -0.006	0.374 0.376 -0.002				
15							0.313 0.329 -0.015	0.364 0.370 -0.006	0.311 0.316 -0.005						

Calculated Minus Measured Powers, RMS Difference = 0.015

Figure A-2.57: Plant A MOC 11 Assembly Power Distribution

	R	P	N	M	L	K	J	H	G	F	E	D	C	B	A
1							0.339 0.342 -0.003	0.405 0.420 -0.015	0.341 0.344 -0.003						
2					0.400 0.399 0.002	0.985 0.983 0.002	1.202 1.203 -0.001	1.210 1.215 -0.005	1.205 1.208 -0.003	0.987 0.988 -0.001	0.401 0.402 -0.001		Calculated Power Measured Power Difference (C-M)		
3				0.455 0.462 -0.007	1.153 1.148 0.005	1.265 1.260 0.005	1.135 1.131 0.005	1.116 1.113 0.002	1.140 1.138 0.002	1.266 1.265 0.002	1.154 1.160 -0.006	0.456 0.469 -0.013			
4			0.456 0.452 0.004	1.154 1.145 0.009	1.249 1.234 0.015	1.015 1.009 0.007	1.032 1.030 0.002	1.286 1.281 0.005	1.032 1.026 0.005	1.013 1.001 0.012	1.249 1.255 -0.006	1.154 1.173 -0.019	0.455 0.463 -0.008		
5		0.401 0.398 0.003	1.154 1.144 0.009	1.249 1.235 0.014	0.979 0.956 0.023	1.049 1.043 0.006	1.305 1.311 -0.006	1.111 1.111 0.001	1.293 1.288 0.005	1.028 1.019 0.009	0.979 0.983 -0.004	1.249 1.280 -0.031	1.153 1.175 -0.022	0.401 0.412 -0.011	
6		0.987 0.979 0.008	1.266 1.255 0.012	1.013 1.005 0.008	1.028 1.027 0.000	0.974 0.972 0.002	1.060 1.064 -0.003	1.048 1.049 -0.001	1.049 1.047 0.002	0.974 0.950 0.024	1.049 1.042 0.007	1.015 1.019 -0.003	1.265 1.280 -0.015	0.985 1.004 -0.019	
7	0.341 0.342 -0.001	1.205 1.198 0.007	1.140 1.124 0.016	1.032 1.022 0.010	1.293 1.284 0.009	1.049 1.047 0.002	1.316 1.326 -0.010	1.049 1.056 -0.007	1.316 1.334 -0.018	1.060 1.056 0.004	1.305 1.293 0.012	1.032 1.010 0.022	1.136 1.139 -0.004	1.202 1.232 -0.030	0.339 0.346 -0.007
8	0.405 0.418 -0.013	1.210 1.210 0.001	1.116 1.108 0.007	1.286 1.274 0.012	1.111 1.093 0.018	1.048 1.041 0.007	1.049 1.049 0.000	1.362 1.367 -0.004	1.050 1.056 -0.007	1.048 1.048 -0.001	1.111 1.103 0.008	1.286 1.272 0.014	1.116 1.108 0.007	1.210 1.213 -0.003	0.406 0.411 -0.006
9	0.339 0.341 -0.003	1.202 1.202 0.000	1.136 1.133 0.003	1.032 1.027 0.005	1.305 1.299 0.006	1.060 1.053 0.007	1.316 1.308 0.008	1.050 1.049 0.001	1.316 1.326 -0.010	1.049 1.047 0.002	1.293 1.284 0.009	1.031 1.021 0.010	1.140 1.140 0.000	1.205 1.221 -0.015	0.341 0.360 -0.019
10		0.985 0.986 -0.001	1.265 1.266 -0.001	1.015 1.013 0.002	1.049 1.043 0.006	0.974 0.963 0.010	1.049 1.031 0.018	1.048 1.038 0.010	1.060 1.056 0.004	0.974 0.967 0.006	1.028 1.018 0.009	1.013 0.990 0.023	1.266 1.270 -0.003	0.987 1.010 -0.023	
11		0.401 0.402 -0.001	1.153 1.159 -0.006	1.249 1.251 -0.002	0.979 0.972 0.007	1.028 1.017 0.010	1.293 1.273 0.020	1.112 1.095 0.016	1.305 1.294 0.011	1.049 1.039 0.010	0.979 0.978 0.001	1.249 1.251 -0.002	1.154 1.163 -0.010	0.401 0.407 -0.006	
12			0.455 0.469 -0.014	1.154 1.161 -0.007	1.249 1.251 -0.002	1.013 1.007 0.006	1.032 1.011 0.021	1.286 1.274 0.012	1.032 1.027 0.005	1.015 1.014 0.002	1.249 1.256 -0.007	1.154 1.174 -0.021	0.456 0.472 -0.016		
13				0.456 0.459 -0.003	1.154 1.163 -0.009	1.266 1.272 -0.005	1.140 1.140 0.000	1.116 1.117 -0.001	1.136 1.139 -0.003	1.265 1.266 -0.001	1.153 1.158 -0.005	0.455 0.460 -0.005			
14					0.401 0.418 -0.017	0.987 1.000 -0.013	1.205 1.222 -0.016	1.210 1.223 -0.013	1.202 1.218 -0.016	0.985 0.992 -0.007	0.401 0.402 -0.002				
15							0.341 0.364 -0.023	0.405 0.414 -0.009	0.339 0.344 -0.005						

Calculated Minus Measured Powers, RMS Difference = 0.010

Figure A-2.58: Plant A EOC 11 Assembly Power Distribution

	R	P	N	M	L	K	J	H	G	F	E	D	C	B	A
1							0.362 0.368 -0.007	0.431 0.450 -0.019	0.363 0.370 -0.006						
2					0.445 0.447 -0.002	0.986 0.992 -0.006	1.120 1.130 -0.011	1.156 1.168 -0.013	1.121 1.129 -0.008	0.986 0.989 -0.003	0.445 0.447 -0.001		Calculated Power Measured Power Difference (C-M)		
3				0.511 0.521 -0.010	1.172 1.176 -0.003	1.325 1.330 -0.006	1.079 1.087 -0.007	1.052 1.057 -0.004	1.082 1.085 -0.003	1.325 1.325 0.000	1.172 1.176 -0.004	0.512 0.528 -0.016			
4			0.512 0.516 -0.004	1.199 1.203 -0.004	1.364 1.358 0.007	1.024 1.025 -0.001	1.014 1.018 -0.004	1.335 1.345 -0.010	1.015 1.015 0.000	1.023 1.012 0.011	1.365 1.360 0.004	1.199 1.198 0.000	0.511 0.512 -0.001		
5		0.445 0.447 -0.002	1.172 1.188 -0.015	1.365 1.370 -0.005	1.004 1.004 0.000	1.031 1.031 -0.001	1.300 1.300 0.000	1.074 1.079 -0.006	1.294 1.294 0.001	1.014 1.006 0.008	1.004 0.996 0.007	1.364 1.351 0.014	1.172 1.177 -0.004	0.445 0.468 -0.024	
6		0.986 0.982 0.004	1.325 1.319 0.006	1.023 1.021 0.003	1.014 1.015 -0.001	0.943 0.944 -0.001	1.009 1.016 -0.007	0.995 1.011 -0.016	1.002 1.002 0.000	0.943 0.930 0.013	1.031 1.022 0.008	1.024 1.018 0.006	1.325 1.327 -0.003	0.986 0.997 -0.011	
7	0.363 0.365 -0.002	1.121 1.112 0.010	1.082 1.055 0.027	1.015 1.002 0.012	1.294 1.284 0.011	1.002 1.002 0.001	1.275 1.289 -0.014	0.996 1.002 -0.006	1.275 1.271 0.004	1.009 1.002 0.007	1.300 1.291 0.009	1.014 1.007 0.007	1.079 1.078 0.001	1.120 1.126 -0.006	0.361 0.364 -0.002
8	0.431 0.447 -0.017	1.155 1.153 0.002	1.052 1.041 0.012	1.335 1.317 0.018	1.074 1.052 0.022	0.995 0.988 0.007	0.996 0.997 -0.001	1.323 1.326 -0.003	0.996 0.997 0.001	0.995 0.991 0.005	1.074 1.068 0.006	1.335 1.329 0.007	1.052 1.047 0.006	1.156 1.162 -0.006	0.431 0.434 -0.003
9	0.361 0.365 -0.004	1.120 1.119 0.001	1.079 1.074 0.005	1.014 1.005 0.009	1.300 1.283 0.016	1.009 1.001 0.008	1.275 1.271 0.004	0.996 0.997 -0.001	1.275 1.286 -0.011	1.002 0.998 0.004	1.294 1.289 0.006	1.014 1.012 0.003	1.082 1.085 -0.003	1.121 1.133 -0.012	0.364 0.367 -0.004
10		0.986 0.986 0.000	1.325 1.324 0.001	1.024 1.020 0.004	1.031 1.021 0.009	0.943 0.934 0.009	1.002 0.996 0.007	0.995 0.991 0.005	1.009 1.006 0.003	0.943 0.936 0.007	1.014 1.008 0.006	1.023 1.020 0.003	1.325 1.334 -0.010	0.986 1.011 -0.024	
11		0.445 0.446 -0.002	1.172 1.180 -0.008	1.364 1.364 0.001	1.004 0.993 0.011	1.014 1.001 0.013	1.294 1.273 0.021	1.074 1.062 0.012	1.300 1.288 0.012	1.031 1.014 0.016	1.004 0.995 0.009	1.365 1.363 0.002	1.172 1.179 -0.006	0.445 0.451 -0.006	
12		0.511 0.535 -0.024	1.199 1.204 -0.005	1.365 1.357 0.008	1.023 1.009 0.014	1.014 0.979 0.036	1.335 1.318 0.017	1.014 1.008 0.006	1.024 1.017 0.007	1.364 1.358 0.006	1.199 1.198 0.001	0.512 0.517 -0.006			
13			0.512 0.512 0.000	1.172 1.167 0.005	1.325 1.317 0.008	1.082 1.075 0.007	1.052 1.054 -0.002	1.079 1.088 -0.009	1.325 1.320 0.005	1.172 1.169 0.003	0.511 0.510 0.001				
14				0.445 0.444 0.001	0.986 0.987 -0.001	1.121 1.134 -0.012	1.155 1.177 -0.022	1.120 1.164 -0.044	0.986 1.000 -0.014	0.445 0.447 -0.002					
15							0.363 0.387 -0.024	0.431 0.444 -0.014	0.361 0.375 -0.014						

Calculated Minus Measured Powers, RMS Difference = 0.010

Figure A-2.59: Plant A BOC 12 Assembly Power Distribution

	R	P	N	M	L	K	J	H	G	F	E	D	C	B	A
1							0.272 0.276 -0.004	0.334 0.346 -0.012	0.275 0.280 -0.005						
2					0.318 0.320 -0.001	0.692 0.696 -0.004	1.070 1.080 -0.010	1.025 1.038 -0.013	1.076 1.089 -0.013	0.691 0.697 -0.006	0.314 0.317 -0.003		Calculated Power Measured Power Difference (C-M)		
3				0.384 0.390 -0.006	0.985 0.990 -0.004	1.172 1.177 -0.005	1.193 1.200 -0.007	1.270 1.285 -0.015	1.189 1.201 -0.012	1.173 1.182 -0.009	0.987 0.999 -0.012	0.384 0.401 -0.018			
4			0.384 0.383 0.001	1.002 0.999 0.003	1.178 1.180 -0.001	1.250 1.250 0.000	1.221 1.231 -0.010	1.201 1.225 -0.024	1.224 1.233 -0.009	1.255 1.256 -0.001	1.184 1.192 -0.007	1.002 1.017 -0.015	0.384 0.389 -0.005		
5		0.314 0.313 0.001	0.987 0.989 -0.003	1.184 1.167 0.017	1.253 1.206 0.047	1.228 1.213 0.015	1.199 1.207 -0.008	1.262 1.259 0.003	1.211 1.211 0.001	1.235 1.236 -0.001	1.253 1.251 0.002	1.178 1.195 -0.016	0.985 1.000 -0.014	0.318 0.329 -0.010	
6		0.691 0.686 0.005	1.173 1.163 0.010	1.255 1.236 0.019	1.235 1.204 0.031	1.194 1.175 0.019	1.214 1.197 0.017	1.222 1.179 0.043	1.221 1.212 0.010	1.194 1.199 -0.005	1.228 1.229 -0.001	1.250 1.255 -0.005	1.172 1.185 -0.013	0.692 0.705 -0.013	
7	0.275 0.275 0.000	1.076 1.069 0.008	1.189 1.175 0.014	1.224 1.210 0.015	1.211 1.195 0.016	1.221 1.207 0.014	1.190 1.179 0.011	1.204 1.187 0.016	1.190 1.191 -0.001	1.214 1.213 0.001	1.199 1.196 0.003	1.221 1.212 0.010	1.193 1.204 -0.011	1.070 1.097 -0.027	0.272 0.278 -0.007
8	0.334 0.341 -0.007	1.025 1.022 0.003	1.269 1.262 0.007	1.201 1.194 0.007	1.262 1.254 0.007	1.222 1.212 0.010	1.204 1.193 0.011	1.188 1.177 0.011	1.204 1.198 0.006	1.222 1.217 0.005	1.262 1.257 0.005	1.201 1.199 0.002	1.269 1.279 -0.009	1.025 1.040 -0.016	0.334 0.342 -0.007
9	0.272 0.273 -0.001	1.070 1.068 0.001	1.193 1.191 0.002	1.221 1.220 0.002	1.199 1.204 -0.005	1.214 1.208 0.006	1.190 1.181 0.010	1.204 1.192 0.011	1.190 1.184 0.007	1.221 1.213 0.008	1.211 1.204 0.007	1.224 1.218 0.006	1.189 1.196 -0.007	1.076 1.095 -0.019	0.275 0.287 -0.012
10		0.692 0.692 0.000	1.172 1.172 0.000	1.250 1.247 0.002	1.228 1.222 0.005	1.194 1.185 0.009	1.221 1.208 0.013	1.222 1.206 0.016	1.214 1.201 0.013	1.194 1.182 0.012	1.235 1.223 0.012	1.255 1.234 0.021	1.173 1.178 -0.005	0.691 0.711 -0.020	
11		0.318 0.319 -0.001	0.985 0.990 -0.005	1.178 1.176 0.002	1.253 1.238 0.014	1.235 1.223 0.012	1.211 1.195 0.017	1.262 1.235 0.027	1.199 1.184 0.015	1.228 1.211 0.017	1.253 1.246 0.007	1.184 1.187 -0.003	0.987 0.997 -0.010	0.313 0.319 -0.005	
12		0.384 0.400 -0.016	1.002 1.006 -0.004	1.184 1.180 0.004	1.255 1.247 0.008	1.224 1.209 0.016	1.201 1.191 0.010	1.221 1.217 0.004	1.250 1.248 0.002	1.178 1.186 -0.008	1.002 1.030 -0.028	0.384 0.402 -0.018			
13			0.384 0.385 -0.001	0.987 0.990 -0.003	1.173 1.174 -0.001	1.189 1.190 -0.001	1.269 1.274 -0.004	1.193 1.203 -0.009	1.172 1.180 -0.008	0.985 0.994 -0.009	0.384 0.390 -0.007				
14				0.313 0.325 -0.012	0.691 0.698 -0.007	1.076 1.090 -0.014	1.025 1.040 -0.015	1.070 1.100 -0.031	0.692 0.704 -0.012	0.318 0.322 -0.004					
15							0.275 0.292 -0.017	0.334 0.343 -0.009	0.272 0.280 -0.008						

Calculated Minus Measured Powers, RMS Difference = 0.012

Figure A-2.60: Plant A MOC 12 Assembly Power Distribution

	R	P	N	M	L	K	J	H	G	F	E	D	C	B	A
1							0.268 0.246 0.021	0.318 0.224 0.094	0.270 0.247 0.023						
2					0.350 0.352 -0.002	0.711 0.709 0.002	1.069 1.054 0.015	0.943 0.907 0.035	1.072 1.048 0.024	0.709 0.701 0.008	0.345 0.345 0.000	Calculated Power Measured Power Difference (C-M)			
3				0.428 0.444 -0.016	1.115 1.129 -0.014	1.301 1.311 -0.011	1.326 1.337 -0.010	1.213 1.210 0.002	1.322 1.315 0.007	1.300 1.297 0.003	1.115 1.125 -0.010	0.428 0.450 -0.023			
4			0.428 0.430 -0.002	1.120 1.132 -0.013	1.297 1.310 -0.014	1.178 1.186 -0.008	1.165 1.176 -0.011	1.320 1.345 -0.025	1.167 1.168 -0.002	1.181 1.172 0.009	1.301 1.310 -0.010	1.120 1.141 -0.022	0.428 0.436 -0.009		
5		0.345 0.346 -0.001	1.115 1.123 -0.008	1.301 1.306 -0.005	1.155 1.145 0.011	1.115 1.115 0.000	1.256 1.264 -0.008	1.154 1.160 -0.006	1.267 1.269 -0.003	1.120 1.118 0.002	1.155 1.163 -0.008	1.297 1.322 -0.026	1.115 1.140 -0.026	0.350 0.374 -0.023	
6		0.709 0.713 -0.004	1.300 1.308 -0.008	1.181 1.184 -0.003	1.120 1.118 0.002	1.238 1.236 0.002	1.081 1.078 0.003	1.042 1.034 0.008	1.087 1.088 -0.001	1.238 1.229 0.009	1.115 1.117 -0.002	1.178 1.189 -0.011	1.301 1.321 -0.020	0.711 0.727 -0.016	
7	0.270 0.276 -0.005	1.072 1.082 -0.010	1.322 1.329 -0.007	1.167 1.171 -0.004	1.266 1.269 -0.002	1.086 1.083 0.003	1.161 1.151 0.010	1.006 1.006 0.000	1.161 1.182 -0.021	1.081 1.085 -0.004	1.256 1.258 -0.003	1.165 1.163 0.002	1.326 1.339 -0.013	1.069 1.087 -0.018	0.268 0.273 -0.005
8	0.318 0.337 -0.019	0.943 0.956 -0.014	1.213 1.224 -0.011	1.320 1.330 -0.010	1.154 1.160 -0.006	1.042 1.039 0.002	1.006 0.999 0.007	0.968 0.966 0.002	1.006 1.010 -0.005	1.042 1.045 -0.003	1.154 1.157 -0.003	1.320 1.324 -0.004	1.213 1.219 -0.007	0.943 0.964 -0.022	0.318 0.328 -0.010
9	0.268 0.274 -0.006	1.069 1.084 -0.015	1.326 1.341 -0.015	1.165 1.176 -0.011	1.256 1.274 -0.018	1.081 1.075 0.006	1.161 1.148 0.013	1.006 1.001 0.005	1.161 1.160 0.001	1.086 1.089 -0.002	1.266 1.272 -0.005	1.167 1.171 -0.005	1.322 1.341 -0.019	1.072 1.104 -0.032	0.270 0.292 -0.022
10		0.711 0.720 -0.009	1.301 1.316 -0.015	1.178 1.185 -0.007	1.115 1.113 0.002	1.238 1.211 0.027	1.086 1.055 0.031	1.042 1.037 0.005	1.081 1.081 0.000	1.238 1.241 -0.003	1.120 1.125 -0.006	1.181 1.176 0.005	1.300 1.324 -0.024	0.709 0.741 -0.032	
11		0.350 0.356 -0.005	1.115 1.134 -0.020	1.297 1.301 -0.004	1.155 1.148 0.008	1.120 1.066 0.054	1.266 1.175 0.092	1.154 1.171 -0.017	1.256 1.258 -0.002	1.115 1.118 -0.003	1.155 1.179 -0.023	1.301 1.329 -0.029	1.115 1.145 -0.031	0.345 0.356 -0.011	
12			0.428 0.462 -0.034	1.119 1.115 0.004	1.301 1.256 0.044	1.181 1.073 0.107	1.167 0.907 0.259	1.320 1.236 0.084	1.165 1.152 0.013	1.178 1.190 -0.012	1.297 1.329 -0.032	1.120 1.169 -0.049	0.428 0.456 -0.028		
13				0.428 0.420 0.008	1.115 1.078 0.036	1.300 1.213 0.087	1.322 1.202 0.120	1.213 1.167 0.046	1.326 1.342 -0.015	1.301 1.328 -0.027	1.115 1.143 -0.028	0.428 0.442 -0.015			
14					0.345 0.374 -0.029	0.709 0.683 0.026	1.072 1.033 0.039	0.943 0.945 -0.002	1.069 1.155 -0.086	0.711 0.743 -0.032	0.350 0.362 -0.011				
15							0.270 0.295 -0.025	0.318 0.328 -0.010	0.268 0.286 -0.018						

Calculated Minus Measured Powers, RMS Difference = 0.033

Codes and Methods Applicability Report
for the U.S. EPR

Figure A-2.61: Plant A EOC 12 Assembly Power Distribution

	R	P	N	M	L	K	J	H	G	F	E	D	C	B	A
1							0.300	0.354	0.303						
							0.305	0.374	0.307						
							-0.004	-0.019	-0.004						
2					0.390	0.734	1.039	0.923	1.042	0.732	0.384				
					0.394	0.738	1.043	0.930	1.044	0.729	0.383				
					-0.004	-0.004	-0.004	-0.007	-0.002	0.003	0.001				
												Calculated Power			
												Measured Power			
												Difference (C-M)			
3				0.468	1.095	1.279	1.280	1.154	1.278	1.278	1.094	0.468			
				0.495	1.114	1.288	1.274	1.158	1.275	1.267	1.094	0.487			
				-0.026	-0.019	-0.008	0.006	-0.004	0.003	0.011	0.001	-0.019			
4			0.468	1.126	1.261	1.132	1.128	1.312	1.128	1.132	1.263	1.126	0.468		
			0.477	1.149	1.279	1.141	1.136	1.329	1.123	1.101	1.253	1.131	0.470		
			-0.009	-0.023	-0.018	-0.009	-0.008	-0.017	0.005	0.031	0.010	-0.005	-0.002		
5		0.384	1.094	1.263	1.115	1.098	1.287	1.145	1.291	1.100	1.115	1.261	1.095	0.390	
		0.390	1.119	1.278	1.108	1.104	1.304	1.148	1.285	1.085	1.107	1.264	1.099	0.403	
		-0.006	-0.025	-0.016	0.007	-0.006	-0.017	-0.003	0.007	0.015	0.008	-0.003	-0.004	-0.014	
6		0.732	1.278	1.132	1.100	1.286	1.106	1.064	1.109	1.286	1.098	1.132	1.279	0.734	
		0.741	1.296	1.145	1.114	1.294	1.109	1.050	1.102	1.267	1.085	1.121	1.273	0.733	
		-0.010	-0.018	-0.013	-0.014	-0.008	-0.003	0.015	0.007	0.019	0.013	0.011	0.007	0.001	
7	0.303	1.042	1.278	1.128	1.291	1.109	1.256	1.056	1.256	1.106	1.287	1.128	1.280	1.039	0.300
	0.310	1.055	1.287	1.137	1.301	1.114	1.259	1.055	1.267	1.098	1.269	1.100	1.266	1.029	0.290
	-0.007	-0.013	-0.009	-0.009	-0.010	-0.005	-0.003	0.001	-0.010	0.008	0.018	0.028	0.015	0.010	0.010
8	0.354	0.923	1.154	1.312	1.145	1.064	1.056	1.024	1.056	1.064	1.145	1.312	1.154	0.923	0.354
	0.374	0.938	1.165	1.321	1.151	1.067	1.056	1.022	1.052	1.055	1.130	1.292	1.145	0.918	0.317
	-0.020	-0.015	-0.011	-0.009	-0.005	-0.002	0.000	0.003	0.004	0.010	0.015	0.020	0.009	0.005	0.037
9	0.300	1.039	1.280	1.128	1.287	1.106	1.256	1.056	1.256	1.109	1.291	1.128	1.278	1.042	0.303
	0.308	1.053	1.293	1.135	1.290	1.105	1.253	1.050	1.242	1.096	1.274	1.110	1.255	0.992	0.160
	-0.007	-0.014	-0.012	-0.007	-0.002	0.001	0.004	0.006	0.014	0.013	0.018	0.019	0.023	0.049	0.143
10	0.734	1.279	1.132	1.098	1.286	1.109	1.064	1.106	1.286	1.100	1.132	1.278	0.732		
	0.742	1.292	1.137	1.097	1.281	1.104	1.059	1.097	1.271	1.085	1.112	1.271	0.749		
	-0.008	-0.013	-0.006	0.001	0.005	0.005	0.005	0.009	0.015	0.015	0.015	0.020	0.007	-0.017	
11	0.390	1.095	1.261	1.115	1.100	1.292	1.145	1.287	1.098	1.115	1.263	1.094	0.384		
	0.395	1.110	1.267	1.105	1.093	1.281	1.144	1.280	1.085	1.103	1.253	1.097	0.388		
	-0.005	-0.015	-0.006	0.010	0.007	0.010	0.002	0.007	0.013	0.012	0.009	-0.003	-0.004		
12	0.468	1.126	1.263	1.132	1.128	1.312	1.128	1.132	1.261	1.126	0.468				
	0.492	1.137	1.263	1.126	1.107	1.307	1.128	1.129	1.257	1.124	0.487				
	-0.023	-0.011	0.000	0.006	0.021	0.005	0.000	0.002	0.004	0.003	-0.020				
13	0.468	1.094	1.278	1.278	1.154	1.280	1.279	1.095	0.468						
	0.471	1.100	1.281	1.278	1.161	1.294	1.287	1.098	0.469						
	-0.004	-0.006	-0.002	0.000	-0.006	-0.013	-0.008	-0.002	-0.001						
14	0.384	0.732	1.042	0.923	1.039	0.734	0.390								
	0.396	0.740	1.055	0.940	1.074	0.746	0.393								
	-0.013	-0.008	-0.014	-0.016	-0.035	-0.012	-0.003								
15	0.303	0.354	0.300												
	0.321	0.365	0.310												
	-0.018	-0.010	-0.010												

Calculated Minus Measured Powers, RMS Difference = 0.017

Figure A-2.62: Plant B BOC 1 Assembly Power Distribution

	R	P	N	M	L	K	J	H	G	F	E	D	C	B	A
1							0.546 0.570 -0.024	0.713 0.771 -0.057	0.546 0.574 -0.028						
2					0.560 0.561 -0.001	0.854 0.857 -0.003	0.881 0.892 -0.011	0.867 0.886 -0.019	0.881 0.905 -0.024	0.854 0.894 -0.040	0.560 0.579 -0.019		Calculated Power Measured Power Difference (C-M)		
3				0.611 0.644 -0.034	0.818 0.819 -0.001	1.004 1.000 0.004	1.062 1.060 0.003	1.190 1.176 0.013	1.062 1.067 -0.004	1.004 1.017 -0.013	0.818 0.836 -0.018	0.611 0.651 -0.040			
4			0.611 0.623 -0.012	0.800 0.805 -0.005	1.028 1.002 0.026	1.126 1.110 0.016	1.296 1.282 0.014	1.201 1.195 0.005	1.296 1.290 0.006	1.126 1.114 0.012	1.028 1.027 0.001	0.800 0.807 -0.006	0.611 0.616 -0.006		
5		0.560 0.571 -0.011	0.818 0.847 -0.029	1.028 1.027 0.001	1.138 1.117 0.022	1.323 1.299 0.024	1.222 1.198 0.024	1.203 1.191 0.012	1.222 1.212 0.012	1.323 1.311 0.012	1.138 1.121 0.017	1.028 1.010 0.018	0.818 0.827 -0.009	0.560 0.600 -0.040	
6		0.854 0.859 -0.005	1.004 1.004 0.000	1.126 1.112 0.014	1.323 1.286 0.036	1.208 1.186 0.022	1.263 1.245 0.018	1.174 1.166 0.008	1.263 1.254 0.009	1.208 1.203 0.005	1.323 1.308 0.014	1.126 1.115 0.012	1.004 1.012 -0.008	0.854 0.885 -0.031	
7	0.546 0.564 -0.018	0.881 0.884 -0.003	1.062 1.043 0.020	1.296 1.274 0.022	1.222 1.198 0.024	1.263 1.242 0.020	1.157 1.146 0.011	1.138 1.127 0.011	1.157 1.146 0.011	1.263 1.249 0.013	1.222 1.205 0.017	1.296 1.273 0.023	1.062 1.064 -0.002	0.881 0.922 -0.041	0.546 0.572 -0.026
8	0.713 0.762 -0.048	0.867 0.875 -0.008	1.190 1.167 0.022	1.201 1.181 0.020	1.203 1.182 0.022	1.174 1.156 0.018	1.138 1.123 0.015	1.103 1.090 0.013	1.138 1.125 0.014	1.174 1.156 0.018	1.203 1.184 0.020	1.201 1.181 0.019	1.190 1.171 0.018	0.867 0.881 -0.014	0.713 0.747 -0.033
9	0.546 0.563 -0.017	0.881 0.883 -0.002	1.062 1.050 0.012	1.296 1.279 0.017	1.222 1.206 0.015	1.263 1.245 0.018	1.157 1.139 0.015	1.138 1.123 0.015	1.157 1.145 0.012	1.263 1.227 0.036	1.222 1.198 0.024	1.296 1.277 0.019	1.062 1.061 0.001	0.881 0.907 -0.026	0.546 0.598 -0.051
10		0.854 0.850 0.004	1.004 0.990 0.014	1.126 1.114 0.012	1.323 1.306 0.016	1.208 1.191 0.016	1.263 1.238 0.025	1.174 1.158 0.016	1.263 1.244 0.019	1.208 1.182 0.026	1.323 1.296 0.026	1.126 1.104 0.022	1.004 1.010 -0.006	0.854 0.889 -0.035	
11		0.560 0.560 0.000	0.818 0.824 -0.006	1.028 1.026 0.002	1.138 1.124 0.014	1.323 1.309 0.014	1.222 1.207 0.015	1.203 1.197 0.007	1.222 1.205 0.016	1.323 1.291 0.032	1.138 1.117 0.022	1.028 1.019 0.009	0.818 0.830 -0.012	0.560 0.575 -0.016	
12		0.611 0.649 -0.038	0.800 0.813 -0.013	1.028 1.032 -0.004	1.126 1.123 0.003	1.296 1.279 0.017	1.201 1.190 0.011	1.296 1.286 0.010	1.126 1.112 0.014	1.028 1.017 0.011	0.800 0.798 0.002	0.611 0.645 -0.034			
13			0.611 0.623 -0.012	0.818 0.838 -0.020	1.004 1.018 -0.014	1.062 1.068 -0.005	1.190 1.179 0.010	1.062 1.067 -0.004	1.004 0.998 0.005	0.818 0.814 0.004	0.611 0.608 0.002				
14				0.560 0.608 -0.048	0.854 0.888 -0.034	0.881 0.915 -0.034	0.867 0.894 -0.027	0.881 0.925 -0.044	0.854 0.869 -0.015	0.560 0.563 -0.004					
15							0.546 0.611 -0.064	0.713 0.758 -0.044	0.546 0.576 -0.030						

Calculated Minus Measured Powers, RMS Difference = 0.021

Figure A-2.63: Plant B MOC 1 Assembly Power Distribution

	R	P	N	M	L	K	J	H	G	F	E	D	C	B	A
1							0.573 0.587 -0.014	0.721 0.756 -0.035	0.573 0.591 -0.018						
2					0.595 0.596 -0.001	0.865 0.866 -0.001	0.953 0.959 -0.006	0.889 0.898 -0.009	0.953 0.972 -0.019	0.865 0.899 -0.034	0.595 0.615 -0.020		Calculated Power Measured Power Difference (C-M)		
3				0.647 0.674 -0.027	0.912 0.914 -0.001	1.034 1.031 0.002	1.030 1.027 0.002	1.141 1.120 0.021	1.030 1.035 -0.005	1.034 1.053 -0.019	0.912 0.938 -0.025	0.647 0.688 -0.041			
4			0.647 0.654 -0.006	0.831 0.834 -0.003	1.050 1.029 0.021	1.067 1.057 0.009	1.208 1.202 0.005	1.123 1.123 0.000	1.208 1.211 -0.003	1.067 1.074 -0.007	1.050 1.063 -0.012	0.831 0.845 -0.014	0.647 0.658 -0.010		
5		0.595 0.601 -0.005	0.912 0.927 -0.014	1.050 1.050 0.000	1.067 1.060 0.007	1.214 1.203 0.011	1.146 1.139 0.007	1.266 1.261 0.005	1.146 1.219 0.000	1.214 1.219 -0.005	1.067 1.067 0.000	1.050 1.043 0.007	0.912 0.926 -0.014	0.595 0.635 -0.040	
6		0.865 0.866 -0.002	1.034 1.033 0.001	1.067 1.056 0.011	1.214 1.186 0.027	1.123 1.105 0.018	1.251 1.235 0.016	1.183 1.173 0.010	1.251 1.248 0.003	1.123 1.134 -0.011	1.214 1.214 0.000	1.067 1.064 0.003	1.034 1.042 -0.009	0.865 0.887 -0.023	
7	0.573 0.582 -0.009	0.953 0.953 -0.001	1.030 1.022 0.007	1.208 1.189 0.019	1.146 1.120 0.026	1.251 1.226 0.025	1.194 1.170 0.024	1.317 1.300 0.018	1.194 1.181 0.013	1.251 1.245 0.006	1.146 1.139 0.007	1.208 1.193 0.015	1.030 1.028 0.001	0.953 0.973 -0.020	0.573 0.587 -0.014
8	0.721 0.748 -0.027	0.889 0.888 0.001	1.141 1.113 0.028	1.123 1.099 0.024	1.266 1.224 0.042	1.183 1.157 0.025	1.317 1.293 0.024	1.225 1.206 0.018	1.317 1.302 0.016	1.183 1.172 0.011	1.266 1.254 0.012	1.123 1.110 0.013	1.141 1.121 0.020	0.889 0.893 -0.003	0.721 0.742 -0.021
9	0.573 0.581 -0.008	0.953 0.951 0.002	1.030 1.017 0.012	1.208 1.194 0.013	1.146 1.140 0.006	1.251 1.233 0.018	1.194 1.173 0.020	1.317 1.297 0.021	1.194 1.179 0.014	1.251 1.227 0.024	1.146 1.134 0.012	1.208 1.199 0.008	1.030 1.029 0.001	0.953 0.971 -0.018	0.573 0.613 -0.040
10		0.865 0.862 0.003	1.034 1.026 0.008	1.067 1.061 0.005	1.214 1.207 0.007	1.123 1.110 0.013	1.251 1.225 0.026	1.183 1.161 0.022	1.251 1.232 0.019	1.123 1.108 0.015	1.214 1.206 0.008	1.067 1.062 0.004	1.034 1.042 -0.008	0.865 0.885 -0.020	
11		0.595 0.597 -0.002	0.912 0.921 -0.009	1.050 1.055 -0.005	1.067 1.067 0.000	1.214 1.205 0.009	1.146 1.127 0.019	1.266 1.236 0.030	1.146 1.128 0.018	1.214 1.198 0.015	1.067 1.069 -0.002	1.050 1.055 -0.004	0.912 0.927 -0.015	0.595 0.607 -0.012	
12		0.647 0.681 -0.034	0.831 0.846 -0.015	1.050 1.059 -0.009	1.067 1.066 0.001	1.208 1.191 0.016	1.123 1.105 0.018	1.208 1.194 0.014	1.067 1.058 0.009	1.050 1.049 0.002	0.831 0.835 -0.004	0.647 0.677 -0.030			
13			0.647 0.660 -0.013	0.912 0.932 -0.019	1.034 1.046 -0.012	1.030 1.031 -0.001	1.141 1.125 0.016	1.030 1.025 0.004	1.034 1.025 0.009	0.912 0.910 0.003	0.647 0.648 -0.001				
14				0.595 0.633 -0.038	0.865 0.890 -0.025	0.953 0.978 -0.025	0.889 0.903 -0.013	0.953 0.972 -0.019	0.865 0.868 -0.004	0.595 0.596 0.000					
15							0.573 0.623 -0.050	0.721 0.749 -0.028	0.573 0.589 -0.016						

Calculated Minus Measured Powers, RMS Difference = 0.017

Codes and Methods Applicability Report
for the U.S. EPR

Page A-113

Figure A-2.64: Plant B EOC 1 Assembly Power Distribution

	R	P	N	M	L	K	J	H	G	F	E	D	C	B	A
1							0.672	0.816	0.672						
							0.679	0.832	0.680						
							-0.007	-0.016	-0.008						
2					0.695	0.957	1.114	0.985	1.114	0.957	0.695		Calculated Power		
					0.694	0.956	1.117	0.985	1.122	0.971	0.705		Measured Power		
					0.002	0.001	-0.003	0.000	-0.007	-0.014	-0.010		Difference (C-M)		
3				0.744	1.092	1.103	1.045	1.137	1.045	1.103	1.092	0.744			
				0.757	1.088	1.100	1.046	1.113	1.044	1.112	1.107	0.767			
				-0.013	0.004	0.002	-0.001	0.024	0.000	-0.009	-0.015	-0.023			
4			0.744	0.901	1.099	1.043	1.127	1.037	1.127	1.043	1.099	0.901	0.744		
			0.734	0.893	1.074	1.037	1.131	1.049	1.133	1.049	1.105	0.903	0.746		
			0.011	0.008	0.024	0.005	-0.004	-0.012	-0.006	-0.006	-0.006	-0.003	-0.001		
5		0.695	1.092	1.099	1.029	1.114	1.023	1.114	1.023	1.114	1.029	1.099	1.092	0.695	
		0.686	1.072	1.089	1.031	1.115	1.030	1.124	1.028	1.115	1.028	1.079	1.094	0.723	
		0.009	0.021	0.010	-0.002	0.000	-0.008	-0.011	-0.006	-0.001	0.002	0.020	-0.002	-0.027	
6		0.957	1.103	1.043	1.114	1.014	1.089	1.014	1.089	1.014	1.114	1.043	1.103	0.957	
		0.951	1.093	1.033	1.100	1.012	1.096	1.028	1.096	1.010	1.110	1.035	1.097	0.956	
		0.006	0.009	0.009	0.014	0.002	-0.007	-0.014	-0.006	0.004	0.004	0.008	0.006	0.001	
7	0.672	1.114	1.045	1.127	1.023	1.089	1.011	1.103	1.011	1.089	1.023	1.127	1.045	1.114	0.672
	0.677	1.114	1.047	1.120	1.015	1.088	1.018	1.113	1.020	1.094	1.022	1.123	1.031	1.089	0.663
	-0.005	0.000	-0.002	0.007	0.008	0.002	-0.006	-0.010	-0.009	-0.004	0.001	0.004	0.014	0.025	0.009
8	0.816	0.985	1.137	1.037	1.114	1.014	1.103	1.017	1.103	1.014	1.114	1.037	1.137	0.985	0.816
	0.830	0.982	1.117	1.028	1.101	1.012	1.107	1.024	1.115	1.026	1.115	1.031	1.113	0.966	0.816
	-0.014	0.002	0.020	0.009	0.012	0.002	-0.003	-0.007	-0.011	-0.013	-0.002	0.006	0.023	0.018	0.000
9	0.672	1.114	1.045	1.127	1.023	1.089	1.011	1.103	1.011	1.089	1.023	1.127	1.045	1.114	0.672
	0.676	1.111	1.036	1.126	1.037	1.093	1.012	1.108	1.025	1.086	1.022	1.126	1.041	1.119	0.699
	-0.004	0.004	0.009	0.002	-0.015	-0.004	-0.001	-0.005	-0.013	0.003	0.000	0.002	0.004	-0.005	-0.027
10		0.957	1.103	1.043	1.114	1.014	1.089	1.014	1.089	1.014	1.114	1.043	1.103	0.957	
		0.951	1.089	1.041	1.118	1.014	1.081	1.011	1.090	1.012	1.116	1.048	1.107	0.963	
		0.006	0.013	0.002	-0.004	0.000	0.009	0.003	0.000	0.002	-0.002	-0.005	-0.005	-0.006	
11		0.695	1.092	1.099	1.029	1.114	1.023	1.114	1.023	1.114	1.029	1.099	1.092	0.695	
		0.694	1.095	1.102	1.033	1.113	1.017	1.106	1.016	1.104	1.035	1.104	1.102	0.701	
		0.001	-0.002	-0.004	-0.004	0.001	0.006	0.008	0.007	0.010	-0.006	-0.005	-0.010	-0.006	
12		0.744	0.901	1.099	1.043	1.127	1.037	1.127	1.043	1.099	0.901	0.744			
		0.762	0.910	1.106	1.044	1.118	1.026	1.115	1.034	1.096	0.900	0.760			
		-0.017	-0.009	-0.007	-0.001	0.009	0.012	0.012	0.009	0.003	0.001	-0.016			
13			0.744	1.092	1.103	1.045	1.137	1.045	1.103	1.092	0.744				
			0.752	1.105	1.108	1.041	1.115	1.029	1.090	1.085	0.741				
			-0.008	-0.013	-0.006	0.003	0.021	0.016	0.012	0.007	0.003				
14				0.695	0.957	1.114	0.985	1.114	0.957	0.695					
				0.716	0.969	1.125	0.978	1.092	0.943	0.688					
				-0.020	-0.012	-0.011	0.006	0.023	0.014	0.007					
15							0.672	0.816	0.672						
							0.704	0.823	0.667						
							-0.032	-0.007	0.005						

Calculated Minus Measured Powers, RMS Difference = 0.010

Figure A-2.65: Plant G2 BOC 1 Assembly Power Distribution

	1	2	3	4	5	6	7	8	9	10	11	12	13	14	15
P					0.395 0.390 0.4	0.533 0.529 0.4	0.558 0.556 0.2	0.579 0.578 0.0	0.563 0.563 0.0	0.543 0.543 0.0	0.404 0.404 0.1				
O			0.376 0.370 0.6	0.651 0.644 0.8	1.124 1.113 1.2	1.237 1.228 0.8	1.187 1.184 0.3	1.317 1.321 -0.4	1.199 1.200 -0.1	1.262 1.265 -0.3	1.160 1.159 0.2	0.667 0.665 0.2	0.380 0.379 0.1	Calculated Power Measured Power Difference (C-M)*100	
N		0.380 0.368 1.2	0.975 0.960 1.5	1.304 1.291 1.3	1.009 1.004 0.5	0.887 0.871 1.6	1.064 1.062 0.2	1.109 1.111 -0.2	1.074 1.076 -0.2	0.912 0.909 0.3	1.076 1.068 0.8	1.329 1.325 0.4	0.975 0.977 -0.1	0.376 0.376 -0.1	
M		0.667 0.655 1.3	1.329 1.311 1.8	1.118 1.105 1.3	1.072 1.064 0.9	1.231 1.231 0.1	1.044 1.058 -1.4	1.249 1.263 -1.4	1.050 1.058 -0.8	1.249 1.253 -0.5	1.092 1.069 2.3	1.118 1.115 0.3	1.304 1.311 -0.7	0.651 0.655 -0.4	
L	0.404 0.396 0.8	1.160 1.143 1.8	1.076 1.059 1.7	1.092 1.074 1.8	1.274 1.267 0.7	1.064 1.066 -0.3	1.092 1.103 -1.1	1.105 1.127 -2.2	1.095 1.111 -1.6	1.068 1.094 -2.6	1.274 1.282 -0.8	1.072 1.078 -0.6	1.009 1.023 -1.4	1.124 1.136 -1.2	0.395 0.397 -0.3
K	0.543 0.528 1.5	1.262 1.247 1.6	0.912 0.898 1.4	1.249 1.238 1.0	1.068 1.066 0.2	1.085 1.094 -0.8	1.145 1.158 -1.3	1.300 1.323 -2.3	1.146 1.162 -1.6	1.085 1.103 -1.7	1.064 1.076 -1.3	1.231 1.249 -1.8	0.887 0.895 -0.8	1.237 1.249 -1.3	0.533 0.537 -0.3
J	0.563 0.555 0.8	1.199 1.191 0.8	1.074 1.061 1.3	1.050 1.044 0.6	1.095 1.097 -0.2	1.146 1.167 -2.1	1.346 1.368 -2.2	1.255 1.273 -1.8	1.346 1.367 -2.1	1.145 1.160 -1.5	1.092 1.106 -1.5	1.044 1.072 -2.8	1.064 1.072 -0.8	1.187 1.192 -0.5	0.558 0.559 -0.1
H	0.579 0.573 0.6	1.317 1.307 1.1	1.109 1.086 2.3	1.249 1.245 0.4	1.105 1.108 -0.3	1.300 1.319 -1.9	1.255 1.272 -1.7	1.177 1.195 -1.8	1.255 1.272 -1.7	1.300 1.319 -1.9	1.105 1.114 -0.9	1.249 1.257 -0.9	1.109 1.101 0.9	1.317 1.317 0.0	0.579 0.577 0.2
G	0.558 0.554 0.4	1.187 1.180 0.7	1.064 1.058 0.6	1.044 1.055 -1.1	1.092 1.098 -0.6	1.145 1.157 -1.2	1.346 1.366 -2.0	1.255 1.273 -1.8	1.346 1.366 -2.0	1.146 1.161 -1.5	1.095 1.099 -0.4	1.050 1.050 0.1	1.074 1.066 0.8	1.199 1.188 1.0	0.563 0.556 0.7
F	0.533 0.530 0.3	1.236 1.234 0.2	0.887 0.884 0.3	1.231 1.235 -0.4	1.063 1.069 -0.6	1.085 1.101 -1.5	1.146 1.162 -1.7	1.300 1.325 -2.5	1.145 1.158 -1.3	1.085 1.093 -0.7	1.068 1.068 0.0	1.249 1.243 0.6	0.912 0.902 1.0	1.262 1.250 1.2	0.543 0.530 1.3
E	0.395 0.392 0.2	1.124 1.121 0.3	1.009 1.010 -0.1	1.072 1.066 0.6	1.274 1.275 -0.1	1.068 1.096 -2.8	1.095 1.113 -1.8	1.105 1.134 -2.9	1.092 1.103 -1.1	1.063 1.067 -0.3	1.274 1.270 0.4	1.092 1.079 1.3	1.076 1.065 1.1	1.160 1.149 1.1	0.404 0.398 0.6
D		0.651 0.645 0.6	1.304 1.291 1.3	1.118 1.099 2.0	1.092 1.062 3.0	1.249 1.250 -0.1	1.050 1.056 -0.6	1.249 1.261 -1.2	1.044 1.052 -0.8	1.231 1.231 0.1	1.072 1.067 0.6	1.118 1.111 0.7	1.329 1.321 0.9	0.667 0.661 0.6	
C		0.376 0.370 0.6	0.975 0.958 1.8	1.329 1.292 3.7	1.076 1.054 2.2	0.912 0.902 0.9	1.074 1.072 0.2	1.109 1.108 0.1	1.064 1.061 0.3	0.887 0.874 1.3	1.009 1.008 0.1	1.304 1.299 0.5	0.975 0.970 0.5	0.380 0.376 0.3	
B		0.379 0.372 0.8	0.667 0.653 1.5	1.160 1.144 1.6	1.262 1.255 0.8	1.199 1.194 0.4	1.317 1.318 0.0	1.187 1.183 0.4	1.236 1.230 0.6	1.124 1.117 0.7	0.651 0.647 0.4	0.376 0.373 0.3			
A				0.404 0.399 0.5	0.543 0.538 0.5	0.563 0.560 0.3	0.579 0.577 0.2	0.558 0.555 0.3	0.533 0.530 0.3	0.395 0.392 0.3					

Calculated Minus Measured Powers, RMS Abs. Difference *100 = 1.2

Figure A-2.66: Plant G2 MOC 1 Assembly Power Distribution

	1	2	3	4	5	6	7	8	9	10	11	12	13	14	15
P					0.328 0.337 -0.9	0.449 0.457 -0.8	0.487 0.492 -0.5	0.498 0.502 -0.3	0.490 0.492 -0.1	0.452 0.454 -0.1	0.330 0.331 -0.1				
O			0.336 0.341 -0.5	0.556 0.567 -1.1	0.936 0.967 -3.1	1.056 1.074 -1.8	1.105 1.116 -1.1	1.143 1.150 -0.6	1.116 1.120 -0.4	1.066 1.067 -0.2	0.941 0.943 -0.2	0.557 0.563 -0.5	0.336 0.339 -0.3	Calculated Power Measured Power Difference (C-M)*100	
N		0.336 0.342 -0.6	0.884 0.895 -1.0	1.137 1.151 -1.3	1.088 1.103 -1.5	1.008 1.018 -1.0	1.131 1.138 -0.7	1.189 1.193 -0.4	1.162 1.163 -0.1	1.018 1.017 0.1	1.093 1.090 0.3	1.139 1.158 -1.9	0.884 0.891 -0.7	0.336 0.337 -0.2	
M		0.557 0.563 -0.6	1.139 1.146 -0.7	1.178 1.182 -0.4	1.231 1.237 -0.6	1.348 1.355 -0.7	1.103 1.110 -0.7	1.379 1.381 -0.2	1.111 1.111 0.0	1.355 1.350 0.5	1.234 1.207 2.8	1.178 1.175 0.3	1.137 1.139 -0.2	0.556 0.557 -0.1	
L	0.330 0.334 -0.4	0.941 0.949 -0.8	1.093 1.095 -0.2	1.234 1.225 0.9	1.408 1.405 0.3	1.129 1.128 0.1	1.239 1.239 0.1	1.265 1.262 0.4	1.242 1.242 -0.1	1.131 1.141 -1.0	1.408 1.401 0.7	1.231 1.228 0.3	1.088 1.087 0.1	0.936 0.936 0.0	0.328 0.328 0.0
K	0.452 0.461 -0.8	1.066 1.077 -1.2	1.018 1.020 -0.2	1.355 1.350 0.5	1.131 1.126 0.5	1.233 1.226 0.7	1.260 1.254 0.5	1.288 1.284 0.5	1.260 1.258 0.3	1.233 1.232 0.0	1.129 1.126 0.2	1.348 1.347 0.1	1.008 1.006 0.2	1.056 1.055 0.1	0.449 0.449 0.0
J	0.490 0.497 -0.7	1.116 1.139 -2.2	1.162 1.163 -0.1	1.111 1.106 0.5	1.242 1.233 0.9	1.260 1.245 1.5	1.284 1.276 0.8	1.260 1.254 0.6	1.284 1.278 0.5	1.260 1.255 0.5	1.239 1.236 0.3	1.103 1.106 -0.3	1.131 1.128 0.4	1.105 1.104 0.1	0.487 0.487 0.0
H	0.498 0.501 -0.2	1.143 1.145 -0.1	1.189 1.173 1.6	1.379 1.370 1.0	1.265 1.257 0.8	1.288 1.280 0.9	1.260 1.253 0.7	1.118 1.112 0.6	1.260 1.252 0.8	1.288 1.278 1.1	1.265 1.257 0.8	1.379 1.374 0.6	1.189 1.180 0.9	1.143 1.144 -0.1	0.498 0.499 -0.1
G	0.487 0.486 0.1	1.105 1.101 0.4	1.131 1.122 0.9	1.103 1.100 0.3	1.239 1.234 0.5	1.260 1.255 0.5	1.284 1.280 0.4	1.260 1.255 0.5	1.284 1.274 1.0	1.260 1.239 2.1	1.242 1.230 1.1	1.111 1.105 0.6	1.162 1.160 0.2	1.116 1.127 -1.1	0.490 0.493 -0.3
F	0.449 0.447 0.2	1.056 1.051 0.5	1.008 1.001 0.6	1.348 1.342 0.6	1.129 1.126 0.3	1.233 1.233 0.0	1.260 1.261 -0.1	1.288 1.289 -0.1	1.260 1.254 0.5	1.233 1.223 1.0	1.131 1.123 0.8	1.355 1.346 0.9	1.018 1.015 0.3	1.066 1.069 -0.3	0.452 0.454 -0.2
E	0.328 0.326 0.2	0.936 0.930 0.6	1.088 1.081 0.7	1.231 1.224 0.7	1.408 1.404 0.4	1.131 1.140 -1.0	1.242 1.248 -0.6	1.265 1.278 -1.2	1.239 1.239 0.1	1.129 1.125 0.3	1.408 1.400 0.8	1.234 1.220 1.5	1.093 1.089 0.4	0.941 0.943 -0.2	0.330 0.331 -0.1
D		0.556 0.552 0.4	1.137 1.128 0.9	1.178 1.168 1.1	1.234 1.223 1.2	1.355 1.354 0.1	1.111 1.113 -0.2	1.379 1.382 -0.3	1.103 1.098 0.5	1.348 1.350 -0.2	1.231 1.233 -0.2	1.178 1.178 0.1	1.139 1.142 -0.3	0.557 0.561 -0.3	
C		0.336 0.332 0.3	0.884 0.876 0.9	1.139 1.127 1.3	1.093 1.085 0.9	1.018 1.015 0.3	1.162 1.162 0.0	1.189 1.192 -0.3	1.131 1.135 -0.3	1.008 1.022 -1.4	1.088 1.101 -1.2	1.137 1.147 -0.9	0.884 0.892 -0.8	0.336 0.342 -0.6	
B		0.336 0.333 0.3	0.557 0.552 0.5	0.941 0.936 0.5	1.066 1.063 0.3	1.116 1.117 -0.1	1.143 1.147 -0.4	1.105 1.113 -0.8	1.056 1.072 -1.6	0.936 0.959 -2.4	0.556 0.564 -0.9	0.336 0.340 -0.4			
A				0.330 0.329 0.2	0.452 0.451 0.1	0.490 0.490 -0.1	0.498 0.501 -0.2	0.487 0.491 -0.4	0.449 0.455 -0.6	0.328 0.335 -0.7					

Calculated Minus Measured Powers, RMS Abs. Difference *100 = 0.8

Codes and Methods Applicability Report
for the U.S. EPR

Page A-116

Figure A-2.67: Plant G2 EOC 1 Assembly Power Distribution

	1	2	3	4	5	6	7	8	9	10	11	12	13	14	15
P					0.471 0.474 -0.3	0.608 0.613 -0.5	0.636 0.640 -0.4	0.640 0.642 -0.2	0.634 0.634 0.0	0.604 0.603 0.1	0.466 0.465 0.1				
O			0.469 0.469 0.0	0.694 0.696 -0.2	1.051 1.059 -0.8	1.139 1.149 -1.0	1.158 1.166 -0.8	1.170 1.174 -0.4	1.154 1.154 -0.1	1.129 1.127 0.2	1.037 1.034 0.3	0.688 0.688 -0.1	0.467 0.468 -0.1	Calculated Power Measured Power Difference (C-M)*100	
N		0.467 0.463 0.4	0.989 0.987 0.3	1.170 1.172 -0.1	1.118 1.125 -0.7	1.045 1.061 -1.6	1.141 1.151 -1.0	1.154 1.157 -0.4	1.137 1.136 0.1	1.035 1.030 0.4	1.090 1.081 0.9	1.161 1.169 -0.8	0.989 0.991 -0.2	0.469 0.469 0.0	
M		0.688 0.685 0.2	1.161 1.157 0.4	1.142 1.139 0.3	1.160 1.162 -0.2	1.235 1.243 -0.8	1.054 1.064 -1.0	1.244 1.246 -0.2	1.052 1.050 0.1	1.229 1.221 0.7	1.152 1.122 3.0	1.142 1.134 0.7	1.170 1.169 0.1	0.694 0.694 0.0	
L	0.466 0.466 0.0	1.037 1.036 0.1	1.090 1.085 0.5	1.152 1.142 1.0	1.245 1.242 0.3	1.047 1.048 -0.1	1.133 1.134 -0.1	1.143 1.138 0.5	1.131 1.132 -0.1	1.046 1.055 -1.0	1.245 1.238 0.6	1.160 1.157 0.3	1.118 1.118 0.0	1.051 1.052 -0.1	0.471 0.471 -0.1
K	0.604 0.605 -0.1	1.129 1.134 -0.5	1.035 1.034 0.1	1.229 1.224 0.5	1.046 1.043 0.3	1.120 1.118 0.2	1.127 1.125 0.2	1.129 1.126 0.3	1.127 1.126 0.1	1.120 1.121 -0.2	1.047 1.047 0.0	1.235 1.239 -0.4	1.045 1.047 -0.3	1.139 1.142 -0.3	0.608 0.610 -0.1
J	0.634 0.639 -0.5	1.154 1.137 -2.1	1.137 1.137 0.0	1.052 1.129 0.2	1.131 1.123 0.2	1.127 1.123 0.3	1.122 1.120 0.2	1.106 1.103 0.3	1.122 1.119 0.3	1.127 1.125 0.2	1.133 1.135 -0.2	1.054 1.067 -1.3	1.141 1.146 -0.5	1.158 1.162 -0.5	0.636 0.638 -0.2
H	0.640 0.642 -0.2	1.170 1.171 -0.1	1.154 1.139 1.5	1.244 1.242 0.2	1.143 1.143 0.0	1.129 1.128 0.1	1.106 1.104 0.1	1.006 1.003 0.3	1.106 1.100 0.6	1.129 1.120 0.9	1.143 1.139 0.3	1.244 1.246 -0.2	1.154 1.157 -0.3	1.170 1.175 -0.5	0.640 0.642 -0.2
G	0.636 0.637 0.0	1.158 1.158 0.0	1.141 1.139 0.2	1.054 1.064 -1.0	1.133 1.137 -0.4	1.127 1.130 -0.3	1.122 1.123 -0.1	1.106 1.102 0.3	1.122 1.113 1.0	1.127 1.104 2.3	1.131 1.122 0.9	1.052 1.049 0.2	1.137 1.139 -0.2	1.154 1.166 -1.2	0.634 0.636 -0.2
F	0.608 0.608 0.1	1.139 1.138 0.1	1.045 1.044 0.1	1.235 1.238 -0.3	1.047 1.051 -0.4	1.120 1.127 -0.8	1.127 1.131 -0.4	1.129 1.128 0.1	1.127 1.122 0.5	1.120 1.110 1.0	1.046 1.039 0.7	1.229 1.223 0.6	1.035 1.033 0.2	1.129 1.129 0.0	0.604 0.600 0.4
E	0.471 0.470 0.1	1.051 1.049 0.2	1.118 1.116 0.3	1.160 1.158 0.2	1.245 1.247 -0.2	1.046 1.065 -2.0	1.131 1.139 -0.8	1.143 1.146 -0.3	1.133 1.132 0.1	1.047 1.044 0.3	1.245 1.239 0.5	1.152 1.143 0.9	1.090 1.086 0.5	1.037 1.035 0.2	0.466 0.464 0.2
D		0.694 0.691 0.3	1.170 1.165 0.6	1.142 1.134 0.8	1.152 1.137 1.5	1.229 1.230 -0.2	1.052 1.055 -0.3	1.244 1.247 -0.3	1.054 1.057 -0.3	1.235 1.237 -0.2	1.160 1.160 0.0	1.142 1.140 0.2	1.161 1.160 0.1	0.688 0.687 0.1	
C		0.469 0.466 0.3	0.989 0.983 0.6	1.161 1.152 0.8	1.090 1.082 0.9	1.035 1.033 0.2	1.137 1.138 -0.1	1.154 1.157 -0.3	1.141 1.146 -0.5	1.045 1.053 -0.9	1.118 1.124 -0.6	1.170 1.174 -0.3	0.989 0.991 -0.1	0.467 0.468 -0.1	
B		0.467 0.464 0.3	0.688 0.683 0.5	1.037 1.032 0.5	1.129 1.127 0.3	1.154 1.154 -0.1	1.170 1.173 -0.3	1.158 1.164 -0.6	1.139 1.148 -0.9	1.051 1.064 -1.3	0.694 0.699 -0.4	0.469 0.471 -0.2			
A					0.466 0.464 0.2	0.604 0.603 0.1	0.634 0.634 0.0	0.640 0.642 -0.2	0.636 0.639 -0.3	0.608 0.613 -0.4	0.471 0.475 -0.4				

Calculated Minus Measured Powers, RMS Abs. Difference *100 = 0.6

Codes and Methods Applicability Report
for the U.S. EPR

Page A-117

Figure A-2.68: Plant G2 BOC 2 Assembly Power Distribution

	1	2	3	4	5	6	7	8	9	10	11	12	13	14	15
P					0.399 0.395 0.4	0.521 0.515 0.6	0.517 0.512 0.5	0.510 0.506 0.4	0.513 0.508 0.5	0.514 0.509 0.5	0.392 0.387 0.5				
O			0.388 0.385 0.3	0.690 0.684 0.6	1.340 1.327 1.2	1.271 1.258 1.3	1.380 1.369 1.1	1.248 1.239 0.8	1.370 1.360 1.0	1.252 1.241 1.2	1.312 1.296 1.6	0.678 0.666 1.1	0.385 0.379 0.6	Calculated Power Measured Power Difference (C-M)*100	
N		0.385 0.380 0.5	1.168 1.161 0.7	1.363 1.355 0.8	1.391 1.380 1.1	0.946 0.931 1.5	0.919 0.914 0.6	0.983 0.978 0.5	0.912 0.906 0.6	0.928 0.918 0.9	1.338 1.322 1.5	1.344 1.317 2.7	1.168 1.151 1.7	0.388 0.383 0.5	
M		0.678 0.676 0.2	1.344 1.342 0.2	1.100 1.098 0.2	1.002 0.999 0.3	0.997 0.995 0.2	1.266 1.274 -0.7	1.073 1.076 -0.3	1.256 1.253 0.4	0.986 0.977 0.9	0.988 0.978 1.0	1.100 1.086 1.4	1.363 1.349 1.4	0.690 0.683 0.6	
L	0.392 0.392 0.0	1.312 1.313 -0.1	1.338 1.341 -0.4	0.988 0.992 -0.4	1.196 1.201 -0.5	0.911 0.916 -0.5	1.103 1.112 -0.9	1.340 1.357 -1.7	1.099 1.099 0.0	0.908 0.897 1.1	1.196 1.186 1.0	1.002 0.994 0.8	1.391 1.383 0.8	1.340 1.334 0.6	0.399 0.397 0.2
K	0.514 0.515 -0.1	1.252 1.254 -0.2	0.928 0.929 -0.1	0.986 0.990 -0.4	0.908 0.915 -0.7	1.257 1.274 -1.7	1.064 1.076 -1.2	1.058 1.066 -0.9	1.062 1.064 -0.2	1.257 1.254 0.3	0.911 0.908 0.3	0.997 0.995 0.2	0.946 0.944 0.2	1.271 1.270 0.1	0.521 0.520 0.1
J	0.513 0.513 0.0	1.370 1.371 -0.1	0.912 0.912 0.0	1.256 1.262 -0.6	1.099 1.112 -1.3	1.062 1.091 -2.9	1.311 1.331 -1.9	1.093 1.102 -0.9	1.311 1.316 -0.5	1.064 1.064 0.0	1.103 1.104 -0.1	1.266 1.276 -0.9	0.919 0.922 -0.3	1.380 1.383 -0.3	0.517 0.517 0.0
H	0.510 0.509 0.1	1.248 1.245 0.2	0.983 0.979 0.4	1.073 1.076 -0.3	1.340 1.351 -1.2	1.058 1.072 -1.5	1.093 1.105 -1.2	0.838 0.845 -0.6	1.093 1.096 -0.4	1.058 1.057 0.0	1.340 1.342 -0.2	1.073 1.078 -0.4	0.983 0.990 -0.7	1.248 1.253 -0.6	0.510 0.511 -0.1
G	0.517 0.515 0.2	1.380 1.377 0.3	0.919 0.917 0.2	1.266 1.268 -0.2	1.103 1.109 -0.6	1.064 1.074 -1.0	1.311 1.325 -1.3	1.093 1.101 -0.9	1.311 1.316 -0.5	1.062 1.056 0.5	1.099 1.099 0.0	1.256 1.259 -0.3	0.912 0.915 -0.3	1.370 1.378 -0.8	0.513 0.514 -0.1
F	0.521 0.519 0.2	1.271 1.269 0.2	0.946 0.944 0.2	0.997 0.998 0.0	0.911 0.916 -0.4	1.257 1.268 -1.1	1.062 1.073 -1.1	1.058 1.070 -1.3	1.064 1.072 -0.8	1.257 1.260 -0.3	0.908 0.909 -0.1	0.986 0.988 -0.2	0.928 0.929 -0.1	1.252 1.255 -0.2	0.514 0.512 0.2
E	0.399 0.397 0.2	1.340 1.336 0.4	1.391 1.388 0.3	1.002 1.001 0.1	1.196 1.203 -0.6	0.908 0.917 -0.9	1.099 1.113 -1.4	1.340 1.369 -2.9	1.103 1.118 -1.5	0.911 0.916 -0.5	1.196 1.199 -0.3	0.988 0.992 -0.4	1.338 1.340 -0.3	1.312 1.312 0.0	0.392 0.391 0.1
D		0.690 0.686 0.4	1.363 1.356 0.6	1.100 1.096 0.5	0.988 0.995 -0.7	0.986 0.993 -0.7	1.256 1.269 -1.3	1.073 1.089 -1.6	1.266 1.293 -2.6	0.997 1.002 -0.4	1.002 1.001 0.1	1.100 1.099 0.2	1.344 1.341 0.2	0.678 0.675 0.3	
C		0.388 0.384 0.3	1.168 1.157 1.1	1.344 1.324 2.0	1.338 1.337 0.1	0.928 0.930 -0.2	0.912 0.916 -0.5	0.983 0.989 -0.6	0.919 0.924 -0.4	0.946 0.939 0.6	1.391 1.382 0.8	1.363 1.356 0.7	1.168 1.161 0.7	0.385 0.380 0.5	
B		0.385 0.381 0.4	0.678 0.671 0.7	1.312 1.309 0.3	1.252 1.254 -0.2	1.370 1.375 -0.4	1.247 1.252 -0.4	1.380 1.380 -0.1	1.271 1.264 0.7	1.340 1.324 1.6	0.690 0.683 0.6	0.388 0.384 0.3			
A				0.392 0.391 0.1	0.514 0.514 0.0	0.513 0.511 -0.1	0.510 0.511 0.0	0.517 0.516 0.1	0.521 0.518 0.3	0.399 0.395 0.4					

Calculated Minus Measured Powers, RMS Abs. Difference *100 = 0.8

Codes and Methods Applicability Report
for the U.S. EPR

Figure A-2.69: Plant G2 MOC 2 Assembly Power Distribution

	1	2	3	4	5	6	7	8	9	10	11	12	13	14	15
P					0.397 0.390 0.7	0.519 0.513 0.6	0.505 0.501 0.4	0.506 0.503 0.3	0.507 0.504 0.3	0.524 0.520 0.4	0.402 0.398 0.4				
O			0.403 0.398 0.5	0.690 0.679 1.0	1.246 1.219 2.7	1.256 1.242 1.4	1.259 1.251 0.8	1.221 1.215 0.6	1.265 1.258 0.7	1.271 1.261 1.0	1.268 1.254 1.4	0.699 0.689 1.0	0.405 0.400 0.5	Calculated Power Measured Power Difference (C-M)*100	
N		0.405 0.398 0.7	1.146 1.135 1.1	1.408 1.395 1.3	1.399 1.385 1.4	0.923 0.919 0.4	0.886 0.885 0.1	0.945 0.944 0.1	0.890 0.886 0.3	0.936 0.929 0.7	1.441 1.425 1.5	1.421 1.397 2.4	1.146 1.132 1.4	0.403 0.399 0.4	
M		0.699 0.694 0.5	1.421 1.415 0.7	1.108 1.105 0.3	1.001 0.999 0.2	0.985 0.987 -0.2	1.301 1.313 -1.2	1.061 1.068 -0.6	1.301 1.300 0.1	0.992 0.986 0.7	1.010 1.005 0.5	1.108 1.098 1.0	1.408 1.397 1.1	0.690 0.685 0.4	
L	0.402 0.400 0.3	1.268 1.263 0.4	1.441 1.440 0.1	1.010 1.017 -0.7	1.267 1.272 -0.5	0.924 0.929 -0.6	1.088 1.099 -1.1	1.383 1.404 -2.2	1.088 1.090 -0.2	0.925 0.914 1.1	1.267 1.258 0.9	1.001 0.996 0.5	1.399 1.394 0.5	1.246 1.243 0.3	0.397 0.396 0.1
K	0.524 0.519 0.6	1.271 1.268 0.3	0.936 0.936 -0.1	0.992 0.996 -0.4	0.925 0.931 -0.5	1.320 1.331 -1.1	1.051 1.060 -0.9	1.036 1.044 -0.9	1.050 1.052 -0.3	1.320 1.316 0.4	0.924 0.922 0.2	0.985 0.985 0.0	0.923 0.924 -0.1	1.256 1.258 -0.2	0.519 0.520 -0.1
J	0.507 0.507 0.1	1.265 1.270 -0.5	0.890 0.891 -0.1	1.301 1.306 -0.5	1.088 1.096 -0.8	1.050 1.064 -1.4	1.345 1.358 -1.2	1.066 1.073 -0.7	1.345 1.349 -0.4	1.051 1.051 0.0	1.088 1.090 -0.2	1.301 1.309 -0.8	0.886 0.892 -0.6	1.259 1.266 -0.8	0.505 0.508 -0.3
H	0.506 0.505 0.1	1.221 1.220 0.1	0.945 0.945 0.1	1.061 1.064 -0.3	1.383 1.390 -0.8	1.036 1.044 -0.9	1.066 1.074 -0.9	0.838 0.843 -0.5	1.066 1.069 -0.3	1.036 1.035 0.0	1.383 1.386 -0.3	1.061 1.069 -0.7	0.945 0.961 -1.6	1.221 1.234 -1.3	0.506 0.510 -0.4
G	0.505 0.503 0.1	1.259 1.256 0.3	0.886 0.885 0.1	1.301 1.305 -0.3	1.088 1.093 -0.5	1.051 1.058 -0.7	1.345 1.356 -1.1	1.066 1.074 -0.8	1.345 1.349 -0.4	1.050 1.044 0.6	1.088 1.090 -0.1	1.301 1.308 -0.7	0.890 0.899 -0.9	1.265 1.283 -1.8	0.507 0.511 -0.4
F	0.519 0.517 0.2	1.256 1.251 0.6	0.923 0.920 0.3	0.985 0.985 0.0	0.924 0.927 -0.3	1.320 1.329 -0.9	1.050 1.061 -1.1	1.036 1.049 -1.4	1.051 1.059 -0.9	1.320 1.324 -0.4	0.925 0.928 -0.3	0.992 0.996 -0.4	0.936 0.941 -0.5	1.271 1.276 -0.5	0.524 0.522 0.3
E	0.397 0.394 0.3	1.246 1.238 0.9	1.399 1.389 1.0	1.001 0.997 0.4	1.267 1.269 -0.2	0.925 0.933 -0.7	1.088 1.103 -1.5	1.383 1.418 -3.6	1.088 1.105 -1.7	0.924 0.931 -0.7	1.267 1.271 -0.4	1.010 1.013 -0.3	1.441 1.444 -0.3	1.268 1.270 -0.3	0.402 0.402 0.0
D		0.690 0.682 0.7	1.408 1.392 1.6	1.108 1.097 1.2	1.010 1.012 -0.2	0.992 0.997 -0.4	1.301 1.314 -1.2	1.061 1.078 -1.7	1.301 1.325 -2.4	0.985 0.994 -0.9	1.001 1.003 -0.2	1.108 1.109 -0.1	1.421 1.422 -0.1	0.699 0.700 -0.1	
C		0.403 0.397 0.6	1.146 1.126 2.0	1.421 1.386 3.6	1.441 1.427 1.4	0.936 0.934 0.2	0.890 0.893 -0.4	0.945 0.953 -0.7	0.886 0.894 -0.8	0.923 0.929 -0.6	1.399 1.395 0.4	1.408 1.404 0.3	1.146 1.145 0.1	0.405 0.406 -0.1	
B		0.405 0.398 0.7	0.699 0.686 1.3	1.268 1.255 1.2	1.271 1.266 0.5	1.265 1.266 -0.1	1.221 1.225 -0.4	1.259 1.262 -0.3	1.256 1.253 0.3	1.246 1.229 1.7	0.690 0.685 0.5	0.403 0.401 0.1			
A					0.402 0.399 0.4	0.524 0.522 0.2	0.507 0.507 0.0	0.506 0.507 -0.1	0.505 0.505 0.0	0.519 0.517 0.2	0.397 0.393 0.4				

Calculated Minus Measured Powers, RMS Abs. Difference *100 = 0.9

Codes and Methods Applicability Report
for the U.S. EPR

Figure A-2.70: Plant G2 EOC 2 Assembly Power Distribution

	1	2	3	4	5	6	7	8	9	10	11	12	13	14	15
P					0.432 0.428 0.4	0.568 0.565 0.3	0.555 0.553 0.2	0.558 0.556 0.2	0.551 0.548 0.3	0.563 0.560 0.3	0.429 0.427 0.3				
O			0.424 0.423 0.1	0.698 0.694 0.4	1.210 1.193 1.7	1.259 1.254 0.6	1.256 1.254 0.3	1.239 1.235 0.4	1.242 1.235 0.7	1.247 1.238 0.9	1.203 1.195 0.9	0.695 0.692 0.4	0.423 0.421 0.2	Calculated Power Measured Power Difference (C-M)*100	
N		0.423 0.425 -0.2	1.092 1.093 -0.1	1.335 1.334 0.1	1.363 1.360 0.3	0.941 0.947 -0.6	0.912 0.915 -0.3	0.959 0.959 0.0	0.879 0.874 0.5	0.928 0.920 0.8	1.356 1.344 1.2	1.332 1.327 0.5	1.092 1.087 0.5	0.424 0.422 0.2	
M		0.695 0.696 -0.1	1.332 1.335 -0.3	1.070 1.075 -0.5	1.006 1.010 -0.4	1.006 1.012 -0.6	1.314 1.324 -1.0	1.061 1.065 -0.4	1.300 1.292 0.8	0.998 0.983 1.5	1.002 0.988 1.4	1.070 1.062 0.8	1.335 1.328 0.6	0.698 0.695 0.2	
L	0.429 0.427 0.2	1.203 1.202 0.1	1.356 1.361 -0.5	1.002 1.016 -1.4	1.292 1.299 -0.7	0.953 0.958 -0.5	1.091 1.099 -0.8	1.362 1.379 -1.7	1.087 1.080 0.8	0.950 0.921 2.9	1.292 1.272 2.0	1.006 0.999 0.7	1.363 1.358 0.5	1.210 1.208 0.2	0.432 0.432 0.0
K	0.563 0.556 0.7	1.247 1.241 0.6	0.928 0.929 -0.1	0.998 1.003 -0.4	0.950 0.953 -0.3	1.333 1.334 -0.1	1.055 1.057 -0.2	1.037 1.039 -0.2	1.053 1.047 0.7	1.333 1.314 1.9	0.953 0.945 0.8	1.006 1.004 0.2	0.941 0.941 0.0	1.259 1.260 -0.1	0.568 0.568 -0.1
J	0.551 0.547 0.4	1.242 1.235 0.7	0.879 0.877 0.2	1.300 1.300 0.0	1.087 1.087 0.0	1.053 1.050 0.3	1.341 1.338 0.3	1.070 1.067 0.3	1.341 1.332 0.9	1.055 1.046 0.9	1.091 1.087 0.4	1.314 1.324 -1.0	0.912 0.917 -0.5	1.256 1.261 -0.5	0.555 0.557 -0.2
H	0.558 0.556 0.2	1.239 1.235 0.4	0.959 0.961 -0.2	1.061 1.061 0.0	1.362 1.361 0.2	1.037 1.035 0.2	1.070 1.067 0.2	0.868 0.865 0.3	1.070 1.062 0.8	1.037 1.027 1.0	1.362 1.356 0.6	1.061 1.064 -0.3	0.959 0.969 -1.0	1.239 1.247 -0.8	0.558 0.561 -0.3
G	0.555 0.554 0.1	1.256 1.254 0.3	0.912 0.912 0.0	1.314 1.312 0.2	1.091 1.090 0.1	1.055 1.054 0.1	1.341 1.338 0.2	1.070 1.066 0.4	1.341 1.329 1.2	1.053 1.032 2.2	1.087 1.080 0.7	1.300 1.300 0.0	0.879 0.882 -0.3	1.242 1.252 -1.1	0.551 0.553 -0.2
F	0.568 0.567 0.1	1.259 1.257 0.2	0.941 0.941 0.0	1.006 1.006 0.0	0.953 0.953 -0.1	1.333 1.333 0.0	1.053 1.054 -0.1	1.037 1.037 0.0	1.055 1.052 0.2	1.333 1.325 0.8	0.950 0.949 0.2	0.998 0.999 -0.1	0.928 0.931 -0.3	1.247 1.249 -0.2	0.563 0.558 0.5
E	0.432 0.432 0.0	1.210 1.209 0.1	1.363 1.362 0.1	1.006 1.006 -0.1	1.292 1.294 -0.1	0.950 0.955 -0.5	1.087 1.091 -0.4	1.362 1.367 -0.5	1.091 1.097 -0.6	0.953 0.956 -0.4	1.292 1.296 -0.3	1.002 1.006 -0.4	1.356 1.361 -0.5	1.203 1.206 -0.3	0.429 0.429 0.0
D		0.698 0.697 0.0	1.335 1.334 0.1	1.070 1.070 0.0	1.002 1.004 -0.2	0.998 1.002 -0.4	1.300 1.306 -0.6	1.061 1.070 -0.9	1.314 1.334 -2.0	1.006 1.019 -1.3	1.006 1.013 -0.8	1.070 1.076 -0.6	1.332 1.339 -0.7	0.695 0.700 -0.4	
C		0.424 0.424 0.0	1.092 1.091 0.1	1.332 1.330 0.2	1.356 1.358 -0.2	0.928 0.932 -0.3	0.879 0.883 -0.4	0.959 0.968 -0.9	0.912 0.925 -1.3	0.941 0.963 -2.2	1.363 1.374 -1.0	1.335 1.343 -0.8	1.092 1.099 -0.8	0.423 0.429 -0.6	
B		0.423 0.423 0.0	0.695 0.696 -0.1	1.203 1.206 -0.2	1.247 1.252 -0.4	1.242 1.249 -0.7	1.239 1.249 -0.9	1.256 1.268 -1.2	1.259 1.270 -1.1	1.210 1.209 0.2		0.698 0.700 -0.2	0.424 0.427 -0.3		
A					0.429 0.431 -0.1	0.563 0.565 -0.2	0.551 0.554 -0.3	0.558 0.562 -0.4	0.555 0.560 -0.5	0.568 0.572 -0.4	0.432 0.433 -0.1				

Calculated Minus Measured Powers, RMS Abs. Difference *100 = 0.7

Codes and Methods Applicability Report
for the U.S. EPR

Figure A-2.71: Plant G2 BOC 3 Assembly Power Distribution

	1	2	3	4	5	6	7	8	9	10	11	12	13	14	15
P					0.279 0.282 -0.3	0.330 0.331 -0.1	0.341 0.341 0.0	0.350 0.349 0.1	0.344 0.343 0.1	0.334 0.332 0.2	0.281 0.279 0.2				
O			0.283 0.284 -0.1	0.513 0.516 -0.4	1.100 1.121 -2.1	1.069 1.071 -0.2	1.076 1.076 0.1	1.223 1.222 0.1	1.092 1.089 0.3	1.084 1.078 0.5	1.110 1.101 0.9	0.517 0.513 0.4	0.283 0.281 0.2	Calculated Power Measured Power Difference (C-M)*100	
N		0.283 0.285 -0.2	1.053 1.055 -0.2	1.207 1.208 0.0	1.188 1.187 0.1	1.176 1.158 1.8	1.087 1.085 0.2	1.003 1.002 0.0	1.127 1.125 0.2	1.194 1.187 0.7	1.199 1.186 1.3	1.215 1.208 0.8	1.053 1.048 0.5	0.283 0.281 0.1	
M		0.517 0.516 0.1	1.216 1.212 0.4	1.237 1.231 0.6	1.226 1.220 0.6	1.372 1.366 0.5	0.992 0.998 -0.6	1.303 1.311 -0.7	1.001 1.002 -0.1	1.383 1.377 0.7	1.234 1.207 2.7	1.237 1.226 1.1	1.207 1.202 0.5	0.512 0.510 0.2	
L	0.281 0.282 0.0	1.110 1.107 0.3	1.199 1.192 0.8	1.234 1.218 1.7	1.243 1.235 0.8	1.259 1.255 0.4	1.406 1.413 -0.7	1.261 1.280 -1.8	1.411 1.421 -0.9	1.263 1.272 -0.9	1.243 1.238 0.5	1.226 1.223 0.3	1.187 1.186 0.1	1.100 1.100 0.0	0.278 0.278 0.0
K	0.334 0.338 -0.4	1.084 1.081 0.3	1.195 1.188 0.7	1.383 1.374 0.9	1.264 1.256 0.8	1.240 1.235 0.4	1.236 1.237 -0.1	1.000 1.004 -0.5	1.245 1.250 -0.5	1.239 1.243 -0.5	1.258 1.261 -0.3	1.371 1.378 -0.7	1.175 1.180 -0.5	1.069 1.072 -0.3	0.329 0.330 0.0
J	0.344 0.343 0.1	1.092 1.122 1.3	1.127 1.122 0.6	1.001 0.996 0.5	1.412 1.405 0.7	1.246 1.238 0.8	1.265 1.264 0.2	1.379 1.381 -0.2	1.262 1.263 -0.1	1.234 1.236 -0.2	1.405 1.412 -0.7	0.992 1.009 -1.7	1.087 1.097 -1.0	1.076 1.080 -0.4	0.341 0.341 0.0
H	0.350 0.349 0.1	1.223 1.221 0.2	1.003 1.006 -0.4	1.303 1.302 0.1	1.261 1.259 0.2	0.999 0.998 0.2	1.379 1.379 0.0	1.007 1.007 0.0	1.372 1.369 0.3	0.997 0.993 0.4	1.260 1.261 0.0	1.303 1.311 -0.8	1.002 1.011 -0.9	1.223 1.223 0.0	0.350 0.349 0.0
G	0.341 0.340 0.1	1.076 1.075 0.1	1.087 1.088 -0.1	0.992 0.991 0.1	1.406 1.407 -0.1	1.235 1.238 -0.3	1.262 1.265 -0.3	1.371 1.372 -0.1	1.259 1.253 0.6	1.243 1.223 2.0	1.410 1.403 0.7	1.001 0.999 0.1	1.127 1.124 0.2	1.092 1.075 1.7	0.344 0.343 0.2
F	0.330 0.329 0.1	1.069 1.069 0.0	1.176 1.176 0.0	1.371 1.373 -0.2	1.258 1.263 -0.5	1.239 1.248 -0.9	1.244 1.252 -0.8	0.997 1.002 -0.5	1.233 1.233 0.0	1.238 1.231 0.7	1.263 1.258 0.4	1.383 1.382 0.1	1.194 1.193 0.1	1.083 1.083 0.1	0.334 0.338 -0.5
E	0.279 0.278 0.1	1.100 1.098 0.2	1.188 1.186 0.1	1.226 1.226 0.0	1.243 1.250 -0.7	1.263 1.285 -2.2	1.410 1.427 -1.6	1.260 1.277 -1.7	1.404 1.411 -0.6	1.258 1.256 0.2	1.243 1.241 0.1	1.234 1.234 0.0	1.199 1.200 -0.2	1.110 1.112 -0.3	0.281 0.283 -0.2
D		0.512 0.510 0.2	1.207 1.203 0.4	1.237 1.233 0.4	1.234 1.236 -0.2	1.383 1.394 -1.1	1.001 1.008 -0.7	1.302 1.313 -1.0	0.992 0.998 -0.6	1.371 1.368 0.3	1.225 1.225 0.0	1.237 1.240 -0.3	1.215 1.220 -0.4	0.517 0.519 -0.2	
C		0.283 0.281 0.2	1.053 1.046 0.7	1.215 1.201 1.5	1.199 1.196 0.3	1.194 1.197 -0.3	1.127 1.131 -0.4	1.002 1.005 -0.3	1.087 1.086 0.0	1.175 1.156 1.9	1.187 1.191 -0.4	1.207 1.214 -0.7	1.052 1.060 -0.7	0.283 0.286 -0.3	
B		0.283 0.281 0.2	0.517 0.513 0.4	1.110 1.107 0.2	1.083 1.085 -0.2	1.092 1.095 -0.3	1.223 1.227 -0.4	1.076 1.078 -0.2	1.069 1.073 -0.4	1.099 1.126 -2.7	0.512 0.519 -0.6	0.282 0.285 -0.2			
A					0.281 0.281 0.1	0.334 0.334 0.0	0.344 0.345 -0.1	0.350 0.351 -0.1	0.341 0.342 -0.1	0.329 0.331 -0.2	0.278 0.283 -0.5				

Calculated Minus Measured Powers, RMS Abs. Difference *100 = 0.7

Codes and Methods Applicability Report
for the U.S. EPR

Figure A-2.72: Plant G2 MOC 3 Assembly Power Distribution

	1	2	3	4	5	6	7	8	9	10	11	12	13	14	15
P					0.308 0.312 -0.3	0.385 0.386 -0.1	0.403 0.403 0.0	0.401 0.400 0.1	0.400 0.399 0.2	0.381 0.378 0.3	0.303 0.301 0.2				
O			0.305 0.308 -0.2	0.531 0.536 -0.5	1.084 1.100 -1.7	1.161 1.163 -0.1	1.189 1.188 0.1	1.243 1.239 0.4	1.183 1.177 0.6	1.148 1.139 0.9	1.063 1.053 1.0	0.524 0.521 0.3	0.304 0.302 0.1	Calculated Power Measured Power Difference (C-M)*100	
N		0.304 0.307 -0.4	1.034 1.039 -0.5	1.222 1.226 -0.4	1.131 1.133 -0.2	1.163 1.152 1.1	1.132 1.132 0.0	1.027 1.025 0.1	1.127 1.121 0.5	1.148 1.138 1.0	1.091 1.077 1.4	1.212 1.208 0.4	1.034 1.030 0.4	0.305 0.305 0.1	
M		0.524 0.527 -0.3	1.212 1.214 -0.3	1.151 1.152 -0.1	1.139 1.140 0.0	1.407 1.406 0.1	1.025 1.038 -1.3	1.397 1.396 0.1	1.019 1.015 0.4	1.398 1.384 1.4	1.131 1.100 3.0	1.151 1.142 1.0	1.222 1.218 0.4	0.531 0.531 0.0	
L	0.303 0.306 -0.3	1.063 1.067 -0.4	1.091 1.090 0.1	1.131 1.127 0.4	1.136 1.134 0.3	1.182 1.180 0.2	1.448 1.447 0.0	1.243 1.237 0.5	1.447 1.443 0.4	1.180 1.184 -0.4	1.136 1.130 0.7	1.139 1.138 0.1	1.131 1.132 -0.1	1.084 1.086 -0.2	0.308 0.309 -0.1
K	0.381 0.389 -0.8	1.148 1.152 -0.5	1.148 1.149 -0.1	1.398 1.394 0.4	1.180 1.176 0.4	1.147 1.140 0.7	1.165 1.160 0.5	0.986 0.982 0.4	1.172 1.169 0.4	1.147 1.146 0.0	1.182 1.184 -0.2	1.407 1.416 -0.9	1.163 1.171 -0.8	1.161 1.167 -0.6	0.385 0.387 -0.2
J	0.400 0.403 -0.2	1.183 1.128 0.2	1.127 1.018 -0.2	1.019 1.439 0.1	1.447 1.158 0.8	1.173 1.158 1.4	1.206 1.198 0.8	1.421 1.412 0.9	1.203 1.198 0.6	1.164 1.161 0.3	1.447 1.454 -0.7	1.025 1.049 -2.4	1.132 1.146 -1.5	1.189 1.198 -0.9	0.403 0.405 -0.3
H	0.401 0.402 -0.1	1.243 1.246 -0.2	1.027 1.035 -0.9	1.397 1.398 -0.1	1.243 1.241 0.2	0.986 0.982 0.4	1.421 1.413 0.7	1.029 1.023 0.6	1.414 1.402 1.3	0.985 0.974 1.0	1.242 1.240 0.2	1.396 1.408 -1.1	1.026 1.042 -1.6	1.243 1.251 -0.7	0.401 0.403 -0.3
G	0.403 0.403 -0.1	1.189 1.191 -0.2	1.132 1.136 -0.4	1.025 1.029 -0.3	1.448 1.449 -0.2	1.165 1.166 -0.1	1.203 1.201 0.2	1.414 1.406 0.8	1.201 1.186 1.5	1.171 1.135 3.6	1.446 1.432 1.4	1.019 1.020 -0.1	1.127 1.131 -0.5	1.183 1.180 0.3	0.400 0.403 -0.3
F	0.385 0.385 0.0	1.161 1.162 0.0	1.163 1.165 -0.2	1.407 1.409 -0.2	1.182 1.188 -0.6	1.146 1.155 -0.8	1.171 1.175 -0.4	0.985 0.983 0.1	1.164 1.157 0.7	1.146 1.133 1.3	1.180 1.174 0.6	1.398 1.397 0.1	1.148 1.152 -0.4	1.148 1.154 -0.7	0.381 0.389 -0.8
E	0.308 0.308 0.0	1.084 1.082 0.2	1.131 1.129 0.1	1.139 1.141 -0.1	1.136 1.144 -0.8	1.180 1.205 -2.5	1.446 1.457 -1.1	1.242 1.246 -0.5	1.447 1.447 0.0	1.182 1.178 0.4	1.136 1.135 0.1	1.131 1.133 -0.3	1.091 1.096 -0.5	1.063 1.071 -0.8	0.303 0.307 -0.4
D		0.531 0.529 0.2	1.222 1.216 0.7	1.151 1.145 0.6	1.131 1.132 -0.1	1.398 1.406 -0.9	1.019 1.025 -0.6	1.396 1.402 -0.5	1.025 1.034 -0.9	1.407 1.402 0.5	1.139 1.141 -0.2	1.151 1.157 -0.6	1.212 1.222 -1.0	0.524 0.530 -0.6	
C		0.305 0.303 0.2	1.034 1.023 1.1	1.212 1.192 2.0	1.091 1.085 0.6	1.148 1.149 -0.1	1.127 1.129 -0.2	1.026 1.028 -0.2	1.132 1.130 0.2	1.163 1.144 1.9	1.131 1.136 -0.5	1.222 1.233 -1.1	1.034 1.047 -1.3	0.304 0.312 -0.8	
B		0.304 0.301 0.3	0.524 0.518 0.6	1.063 1.057 0.6	1.148 1.145 0.2	1.183 1.183 0.0	1.243 1.243 0.0	1.189 1.189 -0.1	1.161 1.164 -0.3	1.084 1.112 -2.8		0.531 0.540 -0.9	0.305 0.310 -0.5		
A					0.303 0.302 0.1	0.381 0.380 0.1	0.400 0.400 0.0	0.401 0.401 0.0	0.402 0.404 -0.1	0.385 0.388 -0.3	0.308 0.314 -0.6				

Calculated Minus Measured Powers, RMS Abs. Difference *100 = 0.8

Codes and Methods Applicability Report
for the U.S. EPR

Page A-122

Figure A-2.73: Plant G2 EOC 3 Assembly Power Distribution

	1	2	3	4	5	6	7	8	9	10	11	12	13	14	15
P					0.368 0.367 0.1	0.471 0.469 0.3	0.491 0.488 0.3	0.479 0.477 0.2	0.494 0.492 0.2	0.475 0.472 0.3	0.371 0.369 0.2				
O			0.363 0.363 0.0	0.593 0.592 0.1	1.115 1.112 0.2	1.249 1.237 1.2	1.270 1.262 0.8	1.265 1.258 0.7	1.282 1.276 0.7	1.259 1.251 0.8	1.120 1.112 0.8	0.595 0.592 0.3	0.364 0.362 0.2	Calculated Power Measured Power Difference (C-M)*100	
N		0.364 0.367 -0.3	1.082 1.080 0.1	1.264 1.260 0.5	1.115 1.107 0.7	1.136 1.117 1.9	1.092 1.086 0.6	1.022 1.020 0.2	1.125 1.121 0.3	1.148 1.143 0.5	1.121 1.111 1.0	1.268 1.261 0.8	1.082 1.077 0.5	0.364 0.363 0.1	
M		0.595 0.595 0.0	1.268 1.264 0.4	1.136 1.133 0.3	1.093 1.089 0.3	1.335 1.331 0.5	0.989 1.002 -1.3	1.339 1.339 -0.1	0.993 0.994 0.0	1.343 1.339 0.4	1.098 1.081 1.7	1.136 1.130 0.6	1.264 1.262 0.2	0.593 0.594 -0.1	
L	0.371 0.370 0.1	1.120 1.114 0.6	1.121 1.116 0.4	1.098 1.097 0.1	1.071 1.068 0.3	1.096 1.095 0.2	1.342 1.343 -0.1	1.149 1.146 0.3	1.345 1.349 -0.3	1.099 1.114 -1.5	1.071 1.074 -0.3	1.093 1.098 -0.5	1.115 1.119 -0.4	1.115 1.118 -0.4	0.368 0.370 -0.2
K	0.475 0.474 0.1	1.259 1.247 1.2	1.148 1.142 0.7	1.343 1.337 0.6	1.099 1.095 0.4	1.061 1.056 0.5	1.073 1.071 0.2	0.934 0.933 0.1	1.080 1.082 -0.3	1.061 1.068 -0.8	1.097 1.107 -1.0	1.336 1.352 -1.6	1.136 1.146 -1.0	1.249 1.255 -0.6	0.472 0.474 -0.2
J	0.494 0.488 0.6	1.282 1.256 2.6	1.125 1.118 0.7	0.993 0.991 0.2	1.345 1.339 0.6	1.080 1.068 1.2	1.109 1.105 0.4	1.321 1.318 0.3	1.108 1.109 -0.1	1.073 1.078 -0.5	1.343 1.359 -1.6	0.989 1.022 -3.3	1.092 1.106 -1.3	1.270 1.277 -0.7	0.491 0.493 -0.2
H	0.479 0.476 0.3	1.265 1.255 1.0	1.022 1.028 -0.6	1.339 1.343 -0.4	1.149 1.151 -0.2	0.934 0.933 0.1	1.321 1.319 0.2	0.976 0.975 0.2	1.318 1.313 0.5	0.934 0.930 0.4	1.149 1.154 -0.5	1.339 1.354 -1.5	1.022 1.036 -1.4	1.265 1.264 0.1	0.479 0.480 -0.1
G	0.491 0.489 0.2	1.270 1.266 0.4	1.092 1.094 -0.2	0.989 1.002 -1.3	1.343 1.352 -1.0	1.073 1.080 -0.7	1.108 1.112 -0.4	1.318 1.316 0.2	1.107 1.100 0.7	1.080 1.057 2.3	1.346 1.339 0.7	0.994 0.996 -0.3	1.125 1.125 0.0	1.283 1.261 2.2	0.494 0.493 0.1
F	0.472 0.471 0.1	1.249 1.247 0.2	1.136 1.138 -0.3	1.336 1.344 -0.9	1.097 1.109 -1.3	1.061 1.077 -1.6	1.080 1.089 -0.9	0.934 0.936 -0.2	1.073 1.071 0.2	1.061 1.054 0.7	1.099 1.097 0.2	1.343 1.343 0.0	1.149 1.150 -0.2	1.259 1.259 0.0	0.475 0.484 -0.9
E	0.368 0.368 0.1	1.115 1.112 0.2	1.115 1.115 0.0	1.093 1.098 -0.5	1.071 1.086 -1.5	1.099 1.138 -3.9	1.346 1.363 -1.7	1.149 1.153 -0.3	1.343 1.347 -0.4	1.097 1.095 0.1	1.071 1.071 0.1	1.098 1.101 -0.3	1.121 1.126 -0.5	1.120 1.127 -0.7	0.371 0.375 -0.4
D		0.593 0.591 0.2	1.264 1.257 0.7	1.136 1.131 0.5	1.098 1.103 -0.5	1.343 1.359 -1.6	0.994 1.003 -0.9	1.339 1.347 -0.7	0.989 1.004 -1.5	1.336 1.330 0.5	1.093 1.093 0.0	1.136 1.140 -0.4	1.268 1.278 -1.0	0.595 0.604 -0.8	
C		0.364 0.360 0.3	1.082 1.068 1.4	1.268 1.244 2.4	1.121 1.116 0.5	1.148 1.152 -0.3	1.125 1.128 -0.4	1.022 1.024 -0.2	1.092 1.087 0.6	1.136 1.108 2.8	1.115 1.112 0.3	1.265 1.270 -0.6	1.082 1.095 -1.3	0.364 0.377 -1.3	
B		0.364 0.360 0.4	0.595 0.588 0.7	1.120 1.114 0.6	1.259 1.257 0.2	1.283 1.282 0.1	1.265 1.263 0.3	1.270 1.264 0.6	1.249 1.240 0.9	1.115 1.125 -1.0		0.593 0.598 -0.5	0.364 0.368 -0.5		
A					0.371 0.369 0.1	0.475 0.474 0.1	0.494 0.494 0.0	0.479 0.479 0.1	0.491 0.489 0.1	0.472 0.470 0.1	0.368 0.370 -0.2				

Calculated Minus Measured Powers, RMS Abs. Difference *100 = 0.8

Codes and Methods Applicability Report
for the U.S. EPR

Figure A-2.74: Plant G2 BOC 4 Assembly Power Distribution

	1	2	3	4	5	6	7	8	9	10	11	12	13	14	15
P					0.270 0.275 -0.5	0.352 0.357 -0.5	0.340 0.343 -0.3	0.357 0.359 -0.2	0.337 0.338 -0.1	0.357 0.357 0.0	0.267 0.267 0.0				
O			0.319 0.325 -0.6	0.970 0.987 -1.7	0.989 1.012 -2.3	1.290 1.306 -1.6	1.110 1.120 -1.0	1.206 1.213 -0.7	1.120 1.123 -0.3	1.284 1.284 -0.1	0.997 0.996 0.1	0.985 0.987 -0.2	0.324 0.324 0.0	Calculated Power Measured Power Difference (C-M)*100	
N		0.316 0.331 -1.5	0.917 0.934 -1.7	1.310 1.327 -1.7	1.211 1.225 -1.4	1.189 1.197 -0.8	0.896 0.903 -0.8	0.885 0.889 -0.4	0.933 0.934 -0.1	1.206 1.204 0.1	1.230 1.225 0.5	1.340 1.348 -0.8	0.947 0.947 0.0	0.322 0.321 0.1	
M		0.965 0.980 -1.4	1.309 1.320 -1.1	1.222 1.227 -0.5	1.008 1.013 -0.5	1.337 1.348 -1.0	1.197 1.213 -1.6	1.313 1.317 -0.4	1.207 1.208 -0.1	1.349 1.347 0.2	1.022 1.003 2.0	1.241 1.233 0.8	1.332 1.326 0.6	0.981 0.975 0.6	
L	0.265 0.265 -0.1	0.986 0.989 -0.3	1.217 1.215 0.1	1.013 1.002 1.2	1.282 1.281 0.1	0.994 0.998 -0.4	1.389 1.394 -0.5	1.045 1.038 0.7	1.387 1.390 -0.3	0.998 1.010 -1.2	1.289 1.282 0.6	1.016 1.008 0.8	1.221 1.212 1.0	0.996 0.988 0.8	0.272 0.269 0.2
K	0.355 0.354 0.0	1.277 1.276 0.1	1.199 1.194 0.5	1.344 1.336 0.7	0.995 0.994 0.1	1.164 1.170 -0.6	1.234 1.238 -0.4	1.212 1.211 0.1	1.232 1.233 -0.1	1.166 1.167 -0.1	0.997 0.991 0.6	1.343 1.329 1.4	1.194 1.181 1.3	1.295 1.284 1.2	0.354 0.350 0.3
J	0.336 0.335 0.2	1.117 1.115 0.2	0.931 0.922 0.9	1.205 1.195 0.9	1.386 1.387 0.0	1.233 1.252 -1.9	0.991 0.997 -0.5	1.326 1.329 -0.3	0.989 0.989 0.0	1.235 1.232 0.3	1.392 1.381 1.1	1.199 1.178 2.1	0.898 0.886 1.3	1.113 1.102 1.1	0.341 0.337 0.3
H	0.357 0.353 0.4	1.206 1.191 1.5	0.885 0.865 2.0	1.314 1.293 2.1	1.046 1.039 0.7	1.214 1.218 -0.3	1.333 1.338 -0.5	0.953 0.955 -0.2	1.326 1.328 -0.2	1.213 1.212 0.1	1.046 1.040 0.6	1.315 1.301 1.5	0.886 0.869 1.7	1.208 1.199 0.9	0.358 0.356 0.2
G	0.340 0.335 0.5	1.112 1.095 1.7	0.898 0.879 1.9	1.199 1.163 3.6	1.393 1.378 1.5	1.238 1.237 0.1	0.994 0.997 -0.2	1.334 1.338 -0.4	0.992 0.994 -0.2	1.234 1.241 -0.6	1.389 1.388 0.1	1.208 1.203 0.4	0.934 0.930 0.4	1.121 1.127 -0.6	0.338 0.338 0.0
F	0.354 0.348 0.5	1.295 1.276 1.9	1.194 1.175 1.9	1.343 1.323 2.0	0.998 0.993 0.6	1.169 1.175 -0.5	1.236 1.242 -0.5	1.216 1.219 -0.4	1.238 1.239 -0.2	1.169 1.171 -0.2	0.999 1.000 -0.1	1.350 1.353 -0.2	1.206 1.209 -0.3	1.285 1.290 -0.5	0.357 0.356 0.1
E	0.272 0.268 0.4	0.996 0.983 1.3	1.221 1.207 1.5	1.016 1.007 0.9	1.290 1.292 -0.2	0.999 1.020 -2.0	1.390 1.402 -1.2	1.047 1.053 -0.5	1.393 1.392 0.2	0.999 1.000 -0.1	1.290 1.295 -0.5	1.023 1.028 -0.5	1.231 1.240 -0.9	0.997 1.005 -0.8	0.267 0.269 -0.1
D		0.981 0.970 1.1	1.332 1.319 1.3	1.242 1.232 1.0	1.023 1.021 0.1	1.351 1.359 -0.8	1.208 1.213 -0.4	1.316 1.316 0.1	1.200 1.186 1.5	1.344 1.345 -0.1	1.016 1.023 -0.6	1.242 1.254 -1.3	1.341 1.359 -1.8	0.985 1.003 -1.7	
C		0.322 0.319 0.4	0.947 0.938 1.0	1.341 1.328 1.3	1.231 1.226 0.5	1.207 1.207 -0.1	0.934 0.935 -0.1	0.887 0.887 0.0	0.899 0.899 0.0	1.194 1.204 -1.0	1.222 1.236 -1.5	1.332 1.352 -2.0	0.947 0.966 -1.9	0.324 0.338 -1.4	
B		0.324 0.321 0.3	0.985 0.978 0.8	0.997 0.993 0.4	1.285 1.284 0.1	1.121 1.122 -0.1	1.209 1.212 -0.3	1.114 1.119 -0.6	1.296 1.310 -1.4	0.996 1.017 -2.0		0.981 0.999 -1.7	0.322 0.328 -0.6		
A					0.267 0.266 0.1	0.357 0.356 0.1	0.338 0.338 0.0	0.358 0.359 -0.1	0.341 0.342 -0.2	0.354 0.357 -0.4	0.272 0.276 -0.4				

Calculated Minus Measured Powers, RMS Abs. Difference *100 = 1.0

Figure A-2.75: Plant G2 MOC 4 Assembly Power Distribution

	1	2	3	4	5	6	7	8	9	10	11	12	13	14	15
P					0.273 0.276 -0.3	0.357 0.360 -0.3	0.359 0.361 -0.2	0.376 0.376 -0.1	0.356 0.355 0.1	0.356 0.354 0.2	0.269 0.267 0.2				
O			0.331 0.336 -0.5	0.931 0.942 -1.1	0.919 0.933 -1.4	1.193 1.202 -0.9	1.123 1.128 -0.5	1.176 1.177 -0.1	1.128 1.125 0.3	1.184 1.177 0.7	0.923 0.914 0.8	0.940 0.933 0.7	0.334 0.331 0.3	Calculated Power Measured Power Difference (C-M)*100	
N		0.328 0.342 -1.5	0.909 0.922 -1.3	1.311 1.322 -1.1	1.143 1.151 -0.9	1.128 1.135 -0.7	0.900 0.904 -0.4	0.899 0.901 -0.1	0.927 0.925 0.2	1.138 1.130 0.8	1.155 1.139 1.6	1.333 1.328 0.5	0.930 0.922 0.9	0.332 0.329 0.4	
M		0.928 0.940 -1.2	1.310 1.318 -0.8	1.188 1.188 -0.1	1.006 1.009 -0.3	1.401 1.408 -0.6	1.206 1.216 -1.0	1.395 1.399 -0.3	1.212 1.213 0.0	1.409 1.401 0.8	1.016 0.980 3.5	1.200 1.180 2.0	1.327 1.309 1.8	0.938 0.925 1.3	
L	0.267 0.268 -0.1	0.917 0.920 -0.3	1.147 1.145 0.2	1.010 0.996 1.4	1.364 1.362 0.3	1.034 1.038 -0.4	1.469 1.475 -0.7	1.070 1.072 -0.2	1.465 1.474 -0.8	1.036 1.055 -1.9	1.369 1.355 1.4	1.011 0.997 1.4	1.149 1.132 1.7	0.924 0.910 1.3	0.274 0.270 0.4
K	0.355 0.356 0.0	1.181 1.183 -0.2	1.135 1.133 0.3	1.406 1.398 0.8	1.034 1.035 -0.1	1.164 1.172 -0.8	1.222 1.230 -0.8	1.209 1.214 -0.5	1.220 1.226 -0.5	1.165 1.168 -0.4	1.036 1.028 0.8	1.405 1.383 2.2	1.131 1.113 1.8	1.196 1.179 1.8	0.358 0.353 0.5
J	0.355 0.356 -0.1	1.127 1.134 -0.8	0.926 0.923 0.3	1.212 1.206 0.6	1.465 1.469 -0.4	1.221 1.245 -2.4	1.021 1.031 -1.0	1.422 1.430 -0.8	1.019 1.023 -0.4	1.223 1.223 0.0	1.471 1.457 1.4	1.209 1.181 2.8	0.902 0.885 1.8	1.126 1.110 1.6	0.360 0.356 0.4
H	0.376 0.374 0.2	1.176 1.168 0.8	0.899 0.888 1.2	1.396 1.377 1.9	1.071 1.068 0.3	1.211 1.219 -0.8	1.428 1.438 -1.0	1.022 1.028 -0.6	1.422 1.428 -0.3	1.210 1.213 0.5	1.072 1.067 0.5	1.398 1.379 1.9	0.901 0.881 2.0	1.178 1.167 1.1	0.376 0.374 0.2
G	0.360 0.356 0.4	1.124 1.111 1.3	0.901 0.885 1.7	1.208 1.169 3.9	1.471 1.458 1.3	1.225 1.229 -0.4	1.024 1.031 -0.7	1.429 1.438 -0.9	1.022 1.029 -0.7	1.222 1.235 -1.3	1.468 1.470 -0.2	1.215 1.211 0.4	0.929 0.926 0.3	1.130 1.141 -1.1	0.356 0.357 -0.1
F	0.358 0.354 0.4	1.196 1.181 1.5	1.130 1.115 1.5	1.405 1.386 1.9	1.037 1.035 0.2	1.167 1.179 -1.2	1.223 1.235 -1.1	1.212 1.220 -0.8	1.225 1.231 -0.6	1.168 1.174 -0.6	1.038 1.042 -0.4	1.411 1.414 -0.3	1.140 1.144 -0.4	1.186 1.192 -0.6	0.357 0.356 0.1
E	0.274 0.271 0.3	0.923 0.914 1.0	1.149 1.137 1.1	1.011 1.006 0.6	1.370 1.378 -0.8	1.038 1.070 -3.2	1.468 1.488 -2.0	1.073 1.081 -0.8	1.473 1.474 -0.2	1.038 1.041 -0.3	1.371 1.378 -0.6	1.017 1.024 -0.7	1.157 1.166 -1.0	0.924 0.933 -0.9	0.269 0.271 -0.2
D		0.938 0.928 0.9	1.327 1.315 1.2	1.200 1.193 0.8	1.017 1.019 -0.3	1.411 1.426 -1.5	1.215 1.224 -1.0	1.399 1.401 -0.2	1.210 1.198 1.1	1.407 1.408 -0.1	1.013 1.020 -0.7	1.202 1.214 -1.3	1.336 1.354 -1.8	0.942 0.959 -1.7	
C		0.332 0.329 0.3	0.931 0.921 1.0	1.334 1.319 1.5	1.156 1.153 0.3	1.140 1.144 -0.4	0.929 0.933 -0.4	0.901 0.903 -0.2	0.903 0.903 0.0	1.132 1.138 -0.6	1.150 1.163 -1.3	1.329 1.348 -1.9	0.932 0.950 -1.8	0.334 0.349 -1.4	
B		0.334 0.331 0.3	0.941 0.933 0.8	0.924 0.921 0.3	1.185 1.187 -0.1	1.130 1.133 -0.3	1.178 1.182 -0.3	1.126 1.131 -0.5	1.198 1.208 -1.0	0.925 0.943 -1.9	0.939 0.955 -1.6	0.333 0.339 -0.7			
A					0.269 0.269 0.1	0.357 0.357 0.0	0.356 0.357 -0.1	0.376 0.378 -0.1	0.360 0.362 -0.2	0.359 0.362 -0.4	0.275 0.279 -0.4				

Calculated Minus Measured Powers, RMS Abs. Difference *100 = 1.1

Codes and Methods Applicability Report
for the U.S. EPR

Figure A-2.76: Plant G2 EOC 4 Assembly Power Distribution

	1	2	3	4	5	6	7	8	9	10	11	12	13	14	15
P					0.318 0.319 -0.1	0.426 0.426 0.0	0.451 0.451 -0.1	0.467 0.469 -0.1	0.445 0.446 -0.1	0.420 0.421 -0.1	0.313 0.314 -0.1				
O			0.376 0.379 -0.3	0.972 0.975 -0.3	0.947 0.949 -0.2	1.251 1.250 0.2	1.303 1.303 0.0	1.308 1.310 -0.2	1.302 1.305 -0.3	1.242 1.244 -0.2	0.956 0.957 0.0	0.981 0.982 -0.1	0.376 0.376 0.0	Calculated Power Measured Power Difference (C-M)*100	
N		0.375 0.388 -1.3	0.963 0.972 -0.9	1.346 1.350 -0.4	1.095 1.093 0.1	1.130 1.126 0.4	0.985 0.986 -0.1	0.982 0.986 -0.4	0.988 0.993 -0.5	1.141 1.146 -0.4	1.133 1.130 0.3	1.362 1.366 -0.4	0.971 0.968 0.3	0.372 0.370 0.2	
M		0.981 0.990 -0.9	1.358 1.364 -0.6	1.119 1.121 -0.2	0.882 0.883 -0.2	1.341 1.342 -0.1	1.201 1.205 -0.4	1.448 1.455 -0.7	1.203 1.215 -1.1	1.349 1.360 -1.1	0.893 0.877 1.6	1.119 1.110 0.8	1.345 1.334 1.1	0.969 0.960 0.9	
L	0.314 0.314 0.0	0.958 0.959 0.0	1.135 1.134 0.1	0.894 0.892 0.2	0.783 0.785 -0.2	0.907 0.913 -0.6	1.438 1.447 -0.9	1.068 1.077 -0.9	1.436 1.460 -2.4	0.908 0.946 -3.8	0.782 0.785 -0.2	0.880 0.874 0.6	1.092 1.078 1.3	0.944 0.933 1.1	0.317 0.313 0.4
K	0.421 0.419 0.2	1.245 1.236 0.9	1.144 1.138 0.6	1.351 1.347 0.5	0.909 0.914 -0.5	1.058 1.072 -1.5	1.171 1.185 -1.5	1.179 1.192 -1.3	1.170 1.186 -1.6	1.057 1.072 -1.6	0.906 0.905 0.1	1.339 1.321 1.8	1.128 1.111 1.7	1.249 1.229 2.0	0.425 0.419 0.6
J	0.445 0.440 0.5	1.303 1.287 1.6	0.989 0.978 1.1	1.204 1.197 0.7	1.437 1.445 -0.9	1.170 1.208 -3.8	1.021 1.039 -1.8	1.449 1.467 -1.8	1.020 1.031 -1.1	1.170 1.178 -0.8	1.437 1.427 1.0	1.200 1.171 2.9	0.984 0.963 2.1	1.301 1.277 2.4	0.450 0.443 0.7
H	0.467 0.460 0.7	1.309 1.284 2.5	0.982 0.962 2.0	1.448 1.421 2.7	1.067 1.065 0.2	1.179 1.194 -1.4	1.452 1.471 -1.8	1.054 1.066 -1.2	1.449 1.462 -1.4	1.178 1.187 -0.8	1.067 1.064 0.3	1.447 1.423 2.4	0.981 0.954 2.8	1.308 1.284 2.4	0.467 0.461 0.6
G	0.450 0.442 0.8	1.302 1.274 2.7	0.984 0.959 2.5	1.200 1.150 5.0	1.437 1.422 1.5	1.171 1.180 -0.9	1.022 1.034 -1.2	1.452 1.467 -1.5	1.021 1.032 -1.1	1.170 1.189 -1.9	1.436 1.438 -0.2	1.203 1.196 0.8	0.988 0.978 1.0	1.301 1.293 0.8	0.445 0.442 0.3
F	0.425 0.418 0.8	1.249 1.225 2.4	1.128 1.106 2.1	1.339 1.313 2.6	0.906 0.905 0.1	1.058 1.077 -1.9	1.170 1.188 -1.8	1.179 1.191 -1.2	1.170 1.178 -0.8	1.058 1.064 -0.7	0.908 0.910 -0.2	1.349 1.346 0.3	1.141 1.139 0.3	1.242 1.239 0.4	0.420 0.420 0.0
E	0.317 0.312 0.5	0.944 0.930 1.4	1.092 1.076 1.6	0.880 0.873 0.6	0.782 0.791 -0.9	0.908 0.954 -4.7	1.435 1.465 -2.9	1.067 1.075 -0.9	1.437 1.434 0.3	0.906 0.906 0.0	0.782 0.783 -0.1	0.893 0.896 -0.3	1.133 1.137 -0.4	0.956 0.961 -0.5	0.313 0.315 -0.1
D		0.969 0.956 1.3	1.345 1.329 1.5	1.118 1.111 0.7	0.892 0.899 -0.6	1.348 1.373 -2.4	1.203 1.217 -1.4	1.447 1.447 0.0	1.200 1.179 2.1	1.339 1.330 0.9	0.880 0.881 -0.2	1.119 1.125 -0.6	1.362 1.374 -1.2	0.981 0.995 -1.3	
C		0.372 0.368 0.4	0.970 0.960 1.1	1.362 1.347 1.4	1.132 1.133 0.0	1.141 1.149 -0.8	0.987 0.993 -0.6	0.981 0.982 -0.1	0.984 0.979 0.5	1.128 1.124 0.3	1.092 1.095 -0.3	1.345 1.356 -1.1	0.971 0.985 -1.4	0.376 0.391 -1.5	
B		0.376 0.373 0.3	0.981 0.974 0.7	0.956 0.955 0.1	1.242 1.245 -0.3	1.301 1.304 -0.3	1.307 1.307 0.0	1.301 1.300 0.2	1.249 1.250 -0.2	0.944 0.956 -1.2	0.969 0.979 -1.0	0.372 0.378 -0.6			
A					0.313 0.313 0.0	0.420 0.421 -0.1	0.444 0.446 -0.1	0.467 0.468 -0.1	0.450 0.451 -0.1	0.425 0.427 -0.2	0.317 0.320 -0.3				

Calculated Minus Measured Powers, RMS Abs. Difference *100 = 1.3

Codes and Methods Applicability Report
for the U.S. EPR

Figure A-2.77: Plant G2 BOC 5 Assembly Power Distribution

	1	2	3	4	5	6	7	8	9	10	11	12	13	14	15
P					0.275 0.282 -0.7	0.393 0.397 -0.4	0.407 0.407 0.0	0.393 0.391 0.2	0.418 0.415 0.3	0.383 0.379 0.3	0.272 0.269 0.2				
O			0.309 0.312 -0.3	0.642 0.653 -1.1	1.216 1.257 -4.1	1.058 1.066 -0.8	1.206 1.203 0.3	1.302 1.294 0.8	1.228 1.218 1.0	1.064 1.054 1.0	1.225 1.213 1.1	0.611 0.609 0.2	0.305 0.303 0.1	Calculated Power Measured Power Difference (C-M)*100	
N		0.305 0.309 -0.4	1.172 1.178 -0.6	1.340 1.346 -0.6	1.269 1.277 -0.8	1.233 1.224 0.9	1.150 1.141 0.9	0.939 0.931 0.8	1.203 1.192 1.2	1.255 1.240 1.5	1.274 1.258 1.6	1.334 1.339 -0.5	1.173 1.169 0.4	0.309 0.307 0.2	
M		0.612 0.612 0.0	1.336 1.332 0.5	1.036 1.029 0.7	1.264 1.258 0.6	1.367 1.356 1.2	0.991 0.977 1.4	1.098 1.086 1.2	1.006 0.996 1.0	1.385 1.366 2.0	1.274 1.234 4.0	1.039 1.026 1.2	1.342 1.331 1.1	0.643 0.638 0.5	
L	0.272 0.271 0.1	1.225 1.220 0.6	1.275 1.262 1.3	1.272 1.242 3.0	0.950 0.941 1.0	1.170 1.162 0.8	1.261 1.250 1.0	0.974 0.967 0.7	1.266 1.258 0.8	1.183 1.181 0.2	0.960 0.947 1.3	1.279 1.264 1.5	1.268 1.255 1.3	1.217 1.206 1.1	0.276 0.274 0.2
K	0.383 0.383 0.0	1.065 1.063 0.2	1.255 1.245 1.0	1.385 1.369 1.5	1.182 1.176 0.7	0.990 0.989 0.1	1.188 1.184 0.3	1.413 1.407 0.6	1.185 1.179 0.6	0.990 0.984 0.6	1.177 1.165 1.2	1.374 1.359 1.6	1.235 1.222 1.3	1.062 1.052 1.0	0.396 0.393 0.3
J	0.418 0.419 -0.1	1.228 1.236 -0.8	1.204 1.196 0.8	1.008 1.001 0.7	1.270 1.270 0.0	1.191 1.206 -1.5	0.952 0.955 -0.3	1.213 1.211 0.1	0.952 0.949 0.3	1.185 1.179 0.7	1.261 1.250 1.1	0.992 0.980 1.2	1.153 1.139 1.4	1.212 1.203 0.9	0.416 0.414 0.2
H	0.393 0.392 0.1	1.302 1.294 0.8	0.939 0.920 1.9	1.098 1.088 1.0	0.974 0.974 0.0	1.414 1.421 -0.7	1.213 1.218 -0.5	0.858 0.859 -0.1	1.217 1.214 0.3	1.413 1.405 0.8	0.974 0.967 0.6	1.098 1.087 1.1	0.939 0.924 1.5	1.302 1.299 0.3	0.393 0.392 0.0
G	0.407 0.406 0.1	1.207 1.200 0.6	1.150 1.139 1.1	0.990 0.980 1.0	1.258 1.258 0.0	1.183 1.190 -0.6	0.952 0.957 -0.6	1.217 1.221 -0.4	0.954 0.953 0.0	1.185 1.179 0.6	1.264 1.259 0.5	1.004 1.001 0.3	1.201 1.201 0.0	1.221 1.242 -2.1	0.408 0.410 -0.2
F	0.394 0.394 0.0	1.060 1.059 0.1	1.234 1.232 0.1	1.366 1.366 0.0	1.168 1.175 -0.7	0.987 0.998 -1.1	1.184 1.195 -1.1	1.413 1.422 -0.9	1.185 1.187 -0.2	0.987 0.986 0.1	1.179 1.177 0.1	1.381 1.380 0.0	1.251 1.253 -0.2	1.059 1.063 -0.4	0.379 0.375 0.4
E	0.277 0.278 -0.1	1.223 1.228 -0.5	1.270 1.277 -0.7	1.262 1.272 -1.0	0.948 0.961 -1.2	1.178 1.205 -2.7	1.263 1.281 -1.8	0.972 0.986 -1.4	1.259 1.261 -0.2	1.170 1.169 0.1	0.949 0.950 -0.1	1.267 1.270 -0.3	1.270 1.274 -0.4	1.221 1.225 -0.4	0.271 0.270 0.0
D		0.640 0.646 -0.5	1.338 1.352 -1.5	1.034 1.048 -1.4	1.269 1.287 -1.9	1.380 1.402 -2.2	1.004 1.016 -1.2	1.096 1.103 -0.6	0.990 0.982 0.8	1.368 1.362 0.6	1.266 1.269 -0.4	1.036 1.042 -0.6	1.332 1.340 -0.8	0.610 0.614 -0.4	
C		0.305 0.309 -0.4	1.168 1.186 -1.9	1.333 1.362 -2.9	1.271 1.292 -2.1	1.250 1.268 -1.8	1.200 1.212 -1.3	0.938 0.943 -0.5	1.151 1.149 0.2	1.235 1.222 1.3	1.272 1.284 -1.2	1.343 1.358 -1.5	1.172 1.184 -1.2	0.304 0.308 -0.4	
B		0.304 0.309 -0.5	0.610 0.621 -1.1	1.221 1.240 -1.9	1.059 1.073 -1.4	1.220 1.233 -1.3	1.301 1.310 -0.9	1.212 1.218 -0.6	1.062 1.072 -1.1	1.219 1.262 -4.3		0.643 0.657 -1.3	0.309 0.313 -0.4		
A					0.271 0.275 -0.4	0.379 0.384 -0.5	0.408 0.412 -0.4	0.393 0.396 -0.3	0.416 0.420 -0.3	0.396 0.402 -0.5	0.276 0.283 -0.7				

Calculated Minus Measured Powers, RMS Abs. Difference *100 = 1.1

Codes and Methods Applicability Report
for the U.S. EPR

Figure A-2.78: Plant G2 MOC 5 Assembly Power Distribution

	1	2	3	4	5	6	7	8	9	10	11	12	13	14	15
P					0.294 0.301 -0.7	0.423 0.428 -0.4	0.445 0.445 0.0	0.429 0.427 0.2	0.456 0.453 0.3	0.412 0.409 0.3	0.291 0.289 0.2				
O			0.342 0.348 -0.6	0.666 0.680 -1.4	1.173 1.212 -3.9	1.043 1.050 -0.7	1.249 1.245 0.4	1.284 1.275 0.9	1.269 1.258 1.1	1.050 1.040 1.0	1.183 1.173 1.0	0.636 0.635 0.1	0.337 0.337 0.1	Calculated Power Measured Power Difference (C-M)*100	
N		0.338 0.350 -1.3	1.191 1.207 -1.6	1.389 1.401 -1.2	1.226 1.236 -0.9	1.201 1.190 1.1	1.137 1.127 1.1	0.938 0.930 0.8	1.183 1.171 1.1	1.219 1.206 1.4	1.231 1.216 1.4	1.384 1.389 -0.5	1.191 1.187 0.4	0.342 0.340 0.2	
M		0.637 0.644 -0.7	1.386 1.391 -0.5	1.047 1.047 0.1	1.242 1.240 0.2	1.421 1.410 1.1	0.988 0.978 1.1	1.082 1.071 1.0	1.001 0.991 1.0	1.436 1.415 2.1	1.250 1.214 3.7	1.049 1.037 1.1	1.390 1.379 1.2	0.666 0.661 0.5	
L	0.291 0.293 -0.2	1.183 1.186 -0.3	1.232 1.228 0.5	1.249 1.229 2.0	0.955 0.949 0.6	1.149 1.143 0.6	1.221 1.213 0.8	0.964 0.957 0.7	1.225 1.216 0.9	1.158 1.153 0.5	0.962 0.949 1.3	1.255 1.241 1.4	1.225 1.213 1.2	1.173 1.162 1.1	0.294 0.292 0.2
K	0.412 0.417 -0.5	1.050 1.053 -0.3	1.220 1.215 0.4	1.436 1.424 1.2	1.158 1.154 0.4	0.975 0.976 0.0	1.151 1.149 0.3	1.428 1.420 0.8	1.149 1.142 0.7	0.975 0.969 0.6	1.154 1.142 1.2	1.426 1.410 1.7	1.202 1.189 1.3	1.046 1.036 1.0	0.426 0.422 0.3
J	0.456 0.459 -0.3	1.269 1.277 -0.8	1.183 1.177 0.6	1.002 0.997 0.5	1.228 1.229 0.0	1.154 1.168 -1.4	0.938 0.941 -0.3	1.168 1.165 0.2	0.938 0.934 0.4	1.149 1.142 0.7	1.221 1.211 1.1	0.989 0.980 0.9	1.139 1.123 1.6	1.255 1.243 1.2	0.455 0.452 0.3
H	0.429 0.428 0.1	1.284 1.275 0.9	0.937 0.919 1.8	1.082 1.071 1.1	0.964 0.963 0.1	1.429 1.433 -0.4	1.169 1.171 -0.3	0.854 0.854 0.0	1.171 1.167 0.4	1.429 1.418 1.1	0.964 0.957 0.7	1.082 1.071 1.1	0.938 0.921 1.7	1.284 1.276 0.8	0.429 0.428 0.1
G	0.445 0.444 0.1	1.249 1.241 0.8	1.137 1.123 1.4	0.987 0.975 1.2	1.220 1.218 0.2	1.149 1.153 -0.4	0.938 0.942 -0.4	1.172 1.173 -0.1	0.939 0.938 0.2	1.149 1.140 0.9	1.225 1.218 0.7	1.000 0.997 0.4	1.181 1.179 0.2	1.263 1.278 -1.5	0.446 0.447 -0.1
F	0.424 0.423 0.0	1.045 1.042 0.2	1.201 1.198 0.3	1.420 1.417 0.3	1.148 1.152 -0.4	0.974 0.983 -0.9	1.149 1.157 -0.8	1.429 1.433 -0.4	1.150 1.149 0.0	0.974 0.971 0.3	1.156 1.154 0.2	1.433 1.431 0.2	1.217 1.219 -0.1	1.047 1.049 -0.2	0.409 0.404 0.5
E	0.295 0.296 -0.1	1.178 1.180 -0.3	1.227 1.232 -0.5	1.242 1.249 -0.8	0.954 0.965 -1.1	1.156 1.181 -2.5	1.224 1.238 -1.4	0.963 0.972 -0.9	1.220 1.220 0.0	1.149 1.147 0.2	0.955 0.955 -0.1	1.247 1.250 -0.3	1.229 1.235 -0.5	1.181 1.186 -0.5	0.290 0.290 0.0
D		0.664 0.669 -0.5	1.387 1.399 -1.3	1.046 1.059 -1.3	1.248 1.264 -1.6	1.434 1.452 -1.9	1.000 1.010 -1.0	1.081 1.085 -0.4	0.988 0.982 0.6	1.422 1.413 0.9	1.244 1.248 -0.3	1.047 1.055 -0.8	1.383 1.395 -1.2	0.636 0.644 -0.8	
C		0.338 0.342 -0.4	1.188 1.205 -1.7	1.384 1.412 -2.9	1.230 1.249 -1.8	1.217 1.232 -1.5	1.181 1.191 -1.0	0.937 0.941 -0.3	1.139 1.132 0.6	1.202 1.184 1.8	1.228 1.240 -1.1	1.392 1.410 -1.8	1.191 1.210 -1.8	0.337 0.348 -1.1	
B		0.337 0.342 -0.5	0.636 0.647 -1.1	1.181 1.198 -1.7	1.047 1.059 -1.2	1.263 1.273 -1.0	1.284 1.289 -0.6	1.255 1.259 -0.3	1.047 1.055 -0.8	1.175 1.219 -4.4		0.667 0.683 -1.6	0.342 0.349 -0.7		
A					0.290 0.294 -0.4	0.409 0.414 -0.5	0.446 0.451 -0.4	0.429 0.432 -0.3	0.455 0.458 -0.3	0.426 0.432 -0.6	0.295 0.303 -0.9				

Calculated Minus Measured Powers, RMS Abs. Difference *100 = 1.0

Codes and Methods Applicability Report
for the U.S. EPR

Figure A-2.79: Plant G2 EOC 5 Assembly Power Distribution

	1	2	3	4	5	6	7	8	9	10	11	12	13	14	15
P					0.327 0.337 -1.0	0.478 0.486 -0.8	0.513 0.516 -0.3	0.490 0.490 0.0	0.519 0.518 0.1	0.459 0.458 0.1	0.319 0.319 0.1				
O			0.376 0.383 -0.7	0.694 0.711 -1.6	1.150 1.194 -4.4	1.060 1.074 -1.3	1.336 1.339 -0.2	1.301 1.297 0.4	1.335 1.329 0.7	1.050 1.044 0.6	1.145 1.140 0.5	0.660 0.661 -0.1	0.370 0.371 0.0	Calculated Power Measured Power Difference (C-M)*100	
N		0.371 0.382 -1.1	1.181 1.196 -1.5	1.396 1.412 -1.6	1.182 1.196 -1.4	1.176 1.177 -0.1	1.168 1.165 0.4	0.962 0.958 0.4	1.168 1.160 0.7	1.170 1.162 0.8	1.162 1.153 0.9	1.384 1.392 -0.8	1.181 1.180 0.1	0.376 0.376 0.0	
M		0.660 0.667 -0.7	1.386 1.391 -0.6	1.032 1.034 -0.2	1.195 1.197 -0.2	1.394 1.388 0.6	0.991 0.983 0.8	1.078 1.068 1.0	0.989 0.982 0.7	1.392 1.377 1.5	1.192 1.170 2.2	1.032 1.026 0.6	1.396 1.390 0.6	0.694 0.692 0.2	
L	0.319 0.322 -0.3	1.145 1.148 -0.3	1.163 1.159 0.4	1.191 1.177 1.4	0.939 0.935 0.4	1.114 1.108 0.6	1.187 1.176 1.1	0.962 0.948 1.4	1.185 1.175 0.9	1.117 1.117 0.1	0.944 0.937 0.7	1.204 1.197 0.7	1.180 1.173 0.7	1.150 1.143 0.6	0.327 0.326 0.1
K	0.459 0.467 -0.7	1.050 1.051 -0.2	1.170 1.166 0.5	1.392 1.380 1.2	1.117 1.112 0.5	0.962 0.959 0.3	1.126 1.119 0.7	1.425 1.411 1.4	1.123 1.114 0.8	0.961 0.957 0.5	1.117 1.110 0.7	1.396 1.387 0.9	1.176 1.169 0.7	1.062 1.055 0.7	0.480 0.478 0.2
J	0.519 0.521 -0.2	1.335 1.336 -0.1	1.168 1.158 1.0	0.991 0.985 0.6	1.188 1.184 0.4	1.127 1.130 -0.4	0.939 0.936 0.2	1.147 1.140 0.7	0.938 0.933 0.6	1.124 1.116 0.8	1.186 1.179 0.7	0.991 0.990 0.0	1.169 1.159 0.9	1.340 1.330 1.0	0.523 0.521 0.3
H	0.490 0.488 0.1	1.301 1.288 1.3	0.961 0.941 2.0	1.078 1.069 0.9	0.962 0.960 0.2	1.426 1.423 0.3	1.148 1.145 0.3	0.869 0.865 0.4	1.150 1.142 0.8	1.425 1.410 1.5	0.962 0.955 0.6	1.078 1.070 0.8	0.962 0.949 1.3	1.301 1.291 1.0	0.490 0.488 0.2
G	0.513 0.511 0.2	1.336 1.326 1.0	1.168 1.158 1.0	0.991 0.990 0.0	1.186 1.186 0.0	1.124 1.125 -0.1	0.939 0.939 -0.1	1.150 1.147 0.4	0.940 0.934 0.6	1.123 1.109 1.5	1.185 1.176 0.9	0.990 0.985 0.5	1.168 1.162 0.6	1.332 1.336 -0.4	0.509 0.509 0.0
F	0.478 0.478 0.0	1.061 1.059 0.3	1.177 1.175 0.2	1.394 1.394 0.0	1.114 1.118 -0.4	0.961 0.968 -0.6	1.123 1.127 -0.3	1.426 1.423 0.3	1.124 1.120 0.4	0.961 0.955 0.6	1.117 1.112 0.5	1.392 1.386 0.5	1.170 1.168 0.2	1.048 1.047 0.1	0.457 0.453 0.3
E	0.328 0.329 -0.1	1.154 1.155 -0.1	1.183 1.186 -0.3	1.195 1.202 -0.6	0.939 0.948 -0.9	1.117 1.136 -1.9	1.185 1.194 -0.8	0.962 0.965 -0.4	1.186 1.185 0.1	1.115 1.111 0.4	0.939 0.939 0.1	1.191 1.192 -0.1	1.162 1.164 -0.1	1.145 1.147 -0.2	0.319 0.319 0.0
D		0.692 0.696 -0.4	1.395 1.404 -0.8	1.032 1.041 -1.0	1.192 1.203 -1.1	1.392 1.404 -1.2	0.990 0.997 -0.7	1.078 1.081 -0.3	0.991 0.993 -0.2	1.395 1.387 0.8	1.196 1.199 -0.3	1.032 1.038 -0.6	1.385 1.394 -1.0	0.660 0.667 -0.7	
C		0.373 0.376 -0.3	1.180 1.191 -1.1	1.386 1.406 -2.0	1.163 1.174 -1.1	1.170 1.180 -1.0	1.168 1.174 -0.7	0.962 0.965 -0.3	1.169 1.165 0.4	1.177 1.158 1.9	1.183 1.193 -1.0	1.397 1.414 -1.6	1.181 1.198 -1.6	0.371 0.381 -1.1	
B		0.370 0.375 -0.4	0.660 0.669 -0.8	1.145 1.156 -1.1	1.048 1.056 -0.8	1.332 1.338 -0.7	1.302 1.305 -0.4	1.340 1.344 -0.3	1.062 1.071 -0.8	1.151 1.196 -4.5		0.695 0.712 -1.7	0.376 0.384 -0.8		
A				0.319 0.322 -0.3	0.457 0.461 -0.4	0.510 0.513 -0.4	0.490 0.493 -0.3	0.523 0.527 -0.4	0.480 0.487 -0.7	0.328 0.338 -1.0					

Calculated Minus Measured Powers, RMS Abs. Difference *100 = 0.9

Codes and Methods Applicability Report
for the U.S. EPR

Figure A-2.80: Plant G1 BOC 26 Assembly Power Distribution

	1	2	3	4	5	6	7	8	9	10	11	12	13	14	15
P						0.248 0.247 0.2	0.345 0.343 0.2	0.387 0.385 0.2	0.343 0.342 0.1	0.247 0.249 -0.2					
O				0.282 0.280 0.1	0.504 0.501 0.3	1.073 1.066 0.7	1.314 1.305 0.9	1.343 1.334 0.9	1.304 1.297 0.8	1.059 1.053 0.7	0.493 0.488 0.5	0.276 0.273 0.3	Calculated Power Measured Power Difference (C-M)*100		
N			0.375 0.373 0.2	1.144 1.139 0.5	1.354 1.346 0.8	0.984 0.978 0.6	1.323 1.314 0.9	1.015 1.007 0.8	1.304 1.293 1.1	0.968 0.959 1.0	1.315 1.296 1.9	1.131 1.116 1.5	0.375 0.371 0.4		
M		0.277 0.275 0.1	1.131 1.124 0.7	1.199 1.196 0.3	1.275 1.269 0.6	1.399 1.390 0.9	1.035 1.028 0.7	1.417 1.404 1.2	1.029 1.019 0.9	1.387 1.371 1.6	1.262 1.242 2.0	1.199 1.184 1.5	1.144 1.132 1.3	0.282 0.280 0.2	
L		0.493 0.491 0.2	1.315 1.310 0.5	1.263 1.269 -0.6	1.034 1.030 0.5	1.436 1.426 1.0	1.118 1.109 0.9	0.922 0.915 0.7	1.116 1.107 1.0	1.435 1.421 1.4	1.034 1.023 1.1	1.274 1.262 1.2	1.353 1.340 1.3	0.504 0.502 0.2	
K	0.247 0.246 0.1	1.060 1.054 0.5	0.969 0.964 0.4	1.388 1.382 0.6	1.435 1.423 1.3	1.359 1.346 1.3	0.966 0.958 0.8	1.370 1.358 1.2	0.967 0.960 0.7	1.358 1.348 1.0	1.435 1.425 1.1	1.398 1.389 0.9	0.984 0.977 0.7	1.072 1.075 -0.2	0.248 0.250 -0.2
J	0.343 0.341 0.2	1.305 1.297 0.7	1.304 1.296 0.8	1.029 1.022 0.7	1.117 1.106 1.1	0.968 0.955 1.3	1.115 1.105 1.0	1.096 1.088 0.8	1.114 1.107 0.7	0.965 0.960 0.5	1.117 1.113 0.4	1.034 1.034 0.0	1.323 1.329 -0.6	1.314 1.336 -2.3	0.345 0.350 -0.5
H	0.387 0.385 0.2	1.343 1.335 0.7	1.015 1.007 0.8	1.417 1.405 1.2	0.922 0.914 0.8	1.369 1.355 1.3	1.094 1.086 0.8	0.780 0.776 0.4	1.092 1.087 0.5	1.368 1.360 0.7	0.922 0.921 0.0	1.416 1.420 -0.4	1.015 1.023 -0.8	1.343 1.357 -1.4	0.387 0.390 -0.3
G	0.345 0.343 0.2	1.314 1.310 0.4	1.323 1.309 1.4	1.034 1.024 1.0	1.117 1.108 0.9	0.965 0.959 0.6	1.113 1.109 0.4	1.091 1.088 0.2	1.112 1.110 0.3	0.967 0.961 0.6	1.116 1.119 -0.3	1.028 1.036 -0.8	1.304 1.317 -1.3	1.304 1.320 -1.6	0.343 0.347 -0.4
F	0.248 0.245 0.3	1.072 1.059 1.4	0.984 0.962 2.3	1.398 1.381 1.7	1.435 1.425 1.0	1.358 1.353 0.4	0.966 0.966 0.0	1.367 1.370 -0.3	0.965 0.969 -0.5	1.358 1.365 -0.7	1.435 1.446 -1.1	1.387 1.406 -1.9	0.968 0.984 -1.6	1.059 1.076 -1.7	0.247 0.251 -0.4
E		0.504 0.497 0.6	1.353 1.335 1.9	1.274 1.263 1.1	1.033 1.030 0.4	1.434 1.434 0.0	1.116 1.120 -0.4	0.922 0.929 -0.7	1.117 1.132 -1.5	1.435 1.455 -1.9	1.034 1.050 -1.7	1.262 1.292 -3.0	1.315 1.346 -3.1	0.493 0.505 -1.2	
D		0.282 0.279 0.3	1.144 1.134 1.0	1.199 1.194 0.5	1.262 1.264 -0.2	1.387 1.392 -0.5	1.028 1.036 -0.7	1.417 1.431 -1.5	1.035 1.063 -2.8	1.398 1.426 -2.8	1.274 1.302 -2.7	1.199 1.232 -3.3	1.131 1.177 -4.6	0.276 0.286 -0.9	
C			0.375 0.374 0.2	1.130 1.129 0.2	1.315 1.316 -0.2	0.968 0.976 -0.8	1.304 1.315 -1.1	1.016 1.021 -0.5	1.323 1.345 -2.2	0.984 1.003 -1.9	1.354 1.382 -2.9	1.144 1.174 -3.0	0.375 0.388 -1.3		
B				0.276 0.277 -0.1	0.493 0.498 -0.5	1.059 1.078 -1.8	1.305 1.329 -2.4	1.343 1.361 -1.8	1.314 1.335 -2.1	1.072 1.092 -2.0	0.504 0.514 -1.1	0.282 0.289 -0.7			
A						0.247 0.259 -1.2	0.343 0.352 -0.8	0.387 0.393 -0.7	0.345 0.351 -0.6	0.248 0.253 -0.5					

Calculated Minus Measured Powers, RMS Abs. Difference *100 = 1.2

Codes and Methods Applicability Report
for the U.S. EPR

Figure A-2.81: Plant G1 MOC 26 Assembly Power Distribution

	1	2	3	4	5	6	7	8	9	10	11	12	13	14	15
P						0.265 0.266 0.0	0.358 0.358 0.0	0.395 0.395 0.0	0.357 0.359 -0.1	0.268 0.272 -0.4					
O				0.307 0.308 -0.1	0.535 0.537 -0.2	1.060 1.061 -0.1	1.243 1.243 0.0	1.265 1.263 0.2	1.241 1.239 0.2	1.061 1.058 0.3	0.538 0.534 0.5	0.308 0.304 0.4	Calculated Power Measured Power Difference (C-M)*100		
N			0.396 0.398 -0.2	1.131 1.135 -0.4	1.385 1.388 -0.3	0.977 0.979 -0.2	1.277 1.277 0.0	1.002 1.000 0.2	1.266 1.259 0.7	0.978 0.970 0.8	1.397 1.377 2.0	1.134 1.116 1.7	0.396 0.390 0.5		
M		0.308 0.310 -0.2	1.134 1.140 -0.6	1.142 1.147 -0.6	1.229 1.234 -0.5	1.342 1.345 -0.3	1.035 1.037 -0.2	1.472 1.467 0.5	1.033 1.027 0.6	1.343 1.327 1.6	1.231 1.205 2.6	1.142 1.121 2.0	1.131 1.114 1.7	0.306 0.303 0.3	
L		0.538 0.540 -0.2	1.397 1.406 -0.9	1.232 1.250 -1.9	1.006 1.010 -0.5	1.368 1.369 -0.2	1.124 1.124 0.0	0.967 0.965 0.3	1.125 1.119 0.6	1.370 1.357 1.3	1.005 0.993 1.3	1.229 1.214 1.5	1.385 1.367 1.8	0.535 0.531 0.4	
K	0.268 0.267 0.0	1.061 1.061 0.0	0.978 0.980 -0.2	1.343 1.348 -0.5	1.370 1.370 0.0	1.320 1.319 0.1	0.999 0.998 0.1	1.474 1.469 0.5	1.000 0.996 0.4	1.320 1.312 0.8	1.368 1.357 1.1	1.342 1.331 1.1	0.977 0.970 0.8	1.060 1.056 0.4	0.265 0.266 0.0
J	0.357 0.356 0.2	1.241 1.235 0.6	1.266 1.261 0.5	1.033 1.031 0.3	1.125 1.122 0.3	1.001 0.997 0.3	1.165 1.162 0.3	1.156 1.153 0.3	1.164 1.161 0.3	0.998 0.996 0.3	1.124 1.121 0.3	1.035 1.033 0.2	1.276 1.276 0.0	1.243 1.252 -0.9	0.358 0.359 -0.2
H	0.395 0.391 0.4	1.265 1.253 1.2	1.003 0.994 0.9	1.472 1.460 1.2	0.967 0.962 0.6	1.474 1.466 0.8	1.155 1.151 0.3	0.855 0.854 0.1	1.153 1.152 0.1	1.473 1.470 0.3	0.967 0.968 -0.1	1.472 1.473 -0.1	1.002 1.006 -0.4	1.265 1.270 -0.5	0.394 0.394 0.0
G	0.358 0.353 0.5	1.243 1.227 1.6	1.277 1.256 2.1	1.035 1.022 1.3	1.124 1.114 1.0	0.999 0.993 0.5	1.164 1.161 0.3	1.152 1.152 0.0	1.163 1.165 -0.2	1.000 1.002 -0.2	1.125 1.129 -0.4	1.033 1.040 -0.7	1.266 1.275 -0.9	1.241 1.250 -0.9	0.357 0.360 -0.3
F	0.265 0.261 0.5	1.060 1.038 2.2	0.977 0.949 2.9	1.342 1.318 2.4	1.367 1.352 1.6	1.320 1.312 0.8	1.000 0.999 0.1	1.473 1.476 -0.3	0.998 1.005 -0.7	1.320 1.329 -1.0	1.370 1.379 -0.9	1.343 1.359 -1.7	0.978 0.992 -1.5	1.061 1.075 -1.4	0.268 0.271 -0.4
E		0.535 0.524 1.1	1.385 1.354 3.1	1.229 1.208 2.1	1.005 0.992 1.3	1.370 1.361 0.8	1.125 1.125 0.0	0.967 0.974 -0.7	1.124 1.141 -1.7	1.368 1.387 -2.0	1.005 1.021 -1.5	1.232 1.259 -2.8	1.397 1.429 -3.2	0.538 0.550 -1.2	
D		0.306 0.301 0.6	1.131 1.110 2.1	1.142 1.122 1.9	1.231 1.211 2.0	1.343 1.335 0.8	1.033 1.035 -0.2	1.472 1.484 -1.2	1.035 1.067 -3.2	1.342 1.370 -2.7	1.229 1.253 -2.4	1.142 1.168 -2.6	1.134 1.176 -4.2	0.308 0.318 -1.0	
C			0.396 0.390 0.6	1.134 1.120 1.4	1.397 1.385 1.2	0.978 0.977 0.0	1.266 1.269 -0.3	1.003 1.003 0.0	1.277 1.296 -1.9	0.977 0.995 -1.8	1.385 1.411 -2.6	1.131 1.157 -2.6	0.396 0.408 -1.2		
B				0.308 0.306 0.2	0.538 0.538 0.0	1.061 1.071 -1.0	1.241 1.255 -1.4	1.265 1.275 -1.0	1.243 1.260 -1.6	1.060 1.078 -1.7	0.535 0.546 -1.1	0.307 0.314 -0.7			
A						0.268 0.279 -1.2	0.357 0.364 -0.7	0.395 0.400 -0.5	0.358 0.363 -0.5	0.265 0.270 -0.4					

Calculated Minus Measured Powers, RMS Abs. Difference *100 = 1.2

Codes and Methods Applicability Report
for the U.S. EPR

Page A-131

Figure A-2.82: Plant G1 EOC 26 Assembly Power Distribution

	1	2	3	4	5	6	7	8	9	10	11	12	13	14	15
P						0.304 0.306 -0.2	0.398 0.400 -0.2	0.434 0.435 -0.2	0.398 0.399 -0.1	0.306 0.311 -0.5					
O				0.343 0.345 -0.1	0.574 0.578 -0.3	1.075 1.082 -0.7	1.226 1.233 -0.8	1.243 1.247 -0.4	1.226 1.223 0.2	1.076 1.075 0.0	0.575 0.573 0.3	0.344 0.341 0.3	Calculated Power Measured Power Difference (C-M)*100		
N			0.434 0.434 0.0	1.131 1.134 -0.4	1.355 1.364 -0.9	0.983 0.991 -0.8	1.256 1.267 -1.1	1.004 1.009 -0.5	1.254 1.253 0.0	0.983 0.979 0.4	1.358 1.346 1.2	1.131 1.120 1.1	0.434 0.429 0.5		
M		0.344 0.343 0.1	1.131 1.126 0.4	1.142 1.145 -0.4	1.205 1.213 -0.9	1.307 1.321 -1.4	1.034 1.052 -1.8	1.438 1.448 -1.0	1.034 1.035 -0.1	1.307 1.300 0.7	1.205 1.189 1.6	1.142 1.129 1.4	1.131 1.117 1.3	0.343 0.340 0.4	
L		0.575 0.574 0.1	1.358 1.357 0.1	1.205 1.211 -0.6	1.007 1.016 -0.9	1.325 1.339 -1.5	1.119 1.131 -1.3	0.978 0.985 -0.7	1.119 1.122 -0.2	1.326 1.322 0.4	1.007 0.999 0.8	1.205 1.193 1.2	1.355 1.338 1.7	0.574 0.568 0.6	
K	0.306 0.305 0.1	1.076 1.072 0.3	0.983 0.982 0.0	1.307 1.313 -0.6	1.326 1.345 -1.9	1.288 1.305 -1.7	1.006 1.017 -1.0	1.444 1.454 -1.0	1.007 1.011 -0.3	1.288 1.287 0.1	1.325 1.319 0.6	1.307 1.296 1.1	0.983 0.969 1.4	1.075 1.064 1.1	0.304 0.302 0.2
J	0.398 0.395 0.3	1.226 1.218 0.7	1.254 1.249 0.4	1.034 1.035 -0.1	1.119 1.129 -0.9	1.008 1.026 -1.8	1.168 1.180 -1.2	1.160 1.169 -0.8	1.168 1.174 -0.6	1.006 1.008 -0.2	1.119 1.117 0.1	1.034 1.030 0.4	1.256 1.248 0.8	1.226 1.223 0.3	0.398 0.397 0.2
H	0.434 0.429 0.5	1.243 1.231 1.3	1.005 0.996 0.9	1.438 1.431 0.6	0.978 0.979 -0.1	1.444 1.452 -0.9	1.159 1.167 -0.7	0.902 0.908 -0.6	1.158 1.166 -0.7	1.443 1.453 -0.9	0.978 0.980 -0.2	1.438 1.436 0.1	1.005 1.003 0.2	1.243 1.240 0.3	0.434 0.432 0.2
G	0.398 0.392 0.6	1.226 1.208 1.8	1.256 1.234 2.1	1.034 1.023 1.2	1.119 1.113 0.6	1.006 1.006 0.0	1.167 1.171 -0.3	1.157 1.163 -0.6	1.167 1.177 -0.9	1.007 1.022 -1.4	1.119 1.122 -0.3	1.034 1.035 -0.1	1.254 1.255 -0.1	1.226 1.226 0.0	0.398 0.398 0.0
F	0.304 0.298 0.6	1.075 1.049 2.6	0.983 0.951 3.2	1.307 1.283 2.4	1.325 1.311 1.4	1.288 1.282 0.6	1.007 1.007 0.0	1.443 1.449 -0.5	1.006 1.012 -0.7	1.288 1.295 -0.7	1.326 1.319 0.7	1.307 1.310 -0.3	0.983 0.988 -0.5	1.076 1.080 -0.4	0.306 0.307 -0.1
E		0.574 0.561 1.3	1.355 1.323 3.3	1.204 1.182 2.2	1.007 0.993 1.3	1.326 1.317 0.9	1.119 1.118 0.2	0.978 0.981 -0.3	1.119 1.129 -1.0	1.325 1.335 -1.0	1.007 1.012 -0.5	1.205 1.217 -1.1	1.358 1.373 -1.5	0.575 0.581 -0.6	
D		0.343 0.336 0.7	1.131 1.108 2.3	1.142 1.122 2.1	1.205 1.184 2.1	1.307 1.296 1.1	1.034 1.032 0.2	1.438 1.440 -0.2	1.034 1.054 -2.0	1.307 1.321 -1.4	1.205 1.216 -1.2	1.142 1.157 -1.4	1.131 1.157 -2.6	0.344 0.350 -0.6	
C			0.434 0.426 0.7	1.131 1.115 1.6	1.358 1.344 1.4	0.983 0.979 0.3	1.254 1.251 0.3	1.005 0.994 1.1	1.256 1.262 -0.6	0.983 0.991 -0.8	1.355 1.368 -1.3	1.131 1.144 -1.4	0.434 0.441 -0.8		
B				0.344 0.341 0.3	0.575 0.574 0.1	1.076 1.083 -0.7	1.226 1.236 -1.1	1.244 1.245 -0.1	1.226 1.231 -0.5	1.075 1.082 -0.7	0.574 0.580 -0.5	0.343 0.347 -0.4			
A						0.306 0.318 -1.2	0.398 0.404 -0.6	0.434 0.436 -0.3	0.398 0.400 -0.2	0.304 0.306 -0.2					

Calculated Minus Measured Powers, RMS Abs. Difference *100 = 1.0

Codes and Methods Applicability Report
for the U.S. EPR

Figure A-2.83: Plant G1 BOC 27 Assembly Power Distribution

	1	2	3	4	5	6	7	8	9	10	11	12	13	14	15
P						0.233 0.230 0.3	0.331 0.327 0.4	0.389 0.384 0.5	0.329 0.324 0.5	0.233 0.226 0.7					
O				0.189 0.186 0.2	0.502 0.496 0.7	1.176 1.160 1.6	1.326 1.308 1.8	1.104 1.092 1.3	1.313 1.302 1.1	1.167 1.154 1.3	0.503 0.499 0.4	0.190 0.189 0.1	Calculated Power Measured Power Difference (C-M)*100		
N			0.249 0.245 0.4	0.740 0.730 1.0	1.310 1.291 1.9	1.207 1.190 1.7	1.055 1.040 1.5	1.490 1.472 1.8	1.030 1.020 1.0	1.201 1.192 0.9	1.323 1.315 0.8	0.743 0.740 0.3	0.249 0.249 0.0		
M		0.190 0.188 0.2	0.743 0.730 1.3	1.324 1.303 2.0	1.053 1.041 1.2	1.115 1.100 1.5	1.483 1.455 2.8	1.000 0.988 1.3	1.478 1.466 1.3	1.114 1.108 0.5	1.055 1.054 0.1	1.324 1.318 0.6	0.740 0.740 0.0	0.189 0.189 -0.1	
L		0.503 0.498 0.4	1.323 1.309 1.3	1.055 1.049 0.5	1.064 1.057 0.7	1.485 1.470 1.6	1.127 1.113 1.3	1.168 1.157 1.1	1.125 1.118 0.7	1.483 1.478 0.6	1.064 1.063 0.2	1.053 1.054 -0.1	1.310 1.311 -0.1	0.502 0.504 -0.2	
K	0.233 0.231 0.2	1.167 1.157 1.0	1.201 1.192 0.9	1.113 1.110 0.3	1.483 1.490 -0.7	1.008 1.000 0.8	1.285 1.272 1.2	1.294 1.284 1.0	1.283 1.278 0.5	1.009 1.008 0.1	1.486 1.487 -0.1	1.115 1.120 -0.5	1.207 1.218 -1.1	1.176 1.182 -0.6	0.233 0.234 -0.1
J	0.329 0.326 0.3	1.312 1.301 1.2	1.030 1.022 0.8	1.478 1.468 1.0	1.124 1.117 0.8	1.282 1.254 2.8	1.353 1.339 1.5	1.354 1.347 0.8	1.356 1.288 0.2	1.286 1.288 -0.2	1.127 1.131 -0.4	1.484 1.489 -0.5	1.055 1.062 -0.7	1.326 1.334 -0.8	0.331 0.330 0.1
H	0.389 0.386 0.3	1.104 1.094 1.0	1.490 1.477 1.2	1.000 0.993 0.7	1.168 1.160 0.8	1.293 1.279 1.4	1.353 1.344 0.8	1.035 1.033 0.2	1.359 1.361 -0.2	1.295 1.300 -0.5	1.169 1.175 -0.6	1.001 1.004 -0.4	1.490 1.493 -0.3	1.104 1.101 0.3	0.389 0.377 1.3
G	0.331 0.328 0.3	1.326 1.311 1.5	1.055 1.048 0.8	1.484 1.475 0.9	1.127 1.122 0.5	1.285 1.280 0.5	1.354 1.353 0.1	1.357 1.360 -0.3	1.357 1.365 -0.8	1.284 1.299 -1.5	1.125 1.135 -0.9	1.478 1.487 -0.8	1.030 1.034 -0.3	1.313 1.312 0.1	0.329 0.326 0.2
F	0.234 0.232 0.2	1.176 1.166 1.0	1.207 1.200 0.7	1.115 1.111 0.4	1.485 1.482 0.3	1.008 1.010 -0.1	1.283 1.288 -0.5	1.295 1.302 -0.8	1.286 1.298 -1.2	1.009 1.021 -1.2	1.484 1.497 -1.3	1.114 1.124 -1.0	1.201 1.209 -0.8	1.167 1.171 -0.4	0.233 0.233 0.0
E		0.502 0.499 0.3	1.310 1.302 0.8	1.053 1.051 0.2	1.064 1.064 0.0	1.483 1.489 -0.6	1.125 1.134 -0.9	1.169 1.182 -1.3	1.127 1.145 -1.7	1.486 1.506 -2.0	1.064 1.077 -1.2	1.055 1.069 -1.4	1.323 1.337 -1.4	0.503 0.508 -0.5	
D		0.189 0.188 0.1	0.740 0.738 0.2	1.324 1.321 0.3	1.055 1.060 -0.5	1.114 1.123 -0.9	1.478 1.495 -1.7	1.001 1.016 -1.5	1.484 1.518 -3.5	1.115 1.135 -2.0	1.053 1.069 -1.5	1.324 1.338 -1.4	0.743 0.757 -1.4	0.190 0.193 -0.3	
C			0.249 0.249 0.0	0.743 0.745 -0.2	1.323 1.331 -0.8	1.201 1.214 -1.3	1.030 1.046 -1.6	1.490 1.515 -2.4	1.055 1.076 -2.1	1.207 1.228 -2.1	1.310 1.329 -1.8	0.740 0.751 -1.1	0.249 0.253 -0.4		
B				0.190 0.192 -0.1	0.503 0.508 -0.5	1.167 1.183 -1.6	1.313 1.346 -3.3	1.104 1.127 -2.2	1.326 1.351 -2.4	1.176 1.197 -2.0	0.502 0.511 -0.8	0.189 0.192 -0.3			
A						0.233 0.234 -0.1	0.329 0.335 -0.7	0.389 0.397 -0.8	0.331 0.338 -0.7	0.234 0.238 -0.4					

Calculated Minus Measured Powers, RMS Abs. Difference *100 = 1.1

Codes and Methods Applicability Report
for the U.S. EPR

Figure A-2.84: Plant G1 MOC 27 Assembly Power Distribution

	1	2	3	4	5	6	7	8	9	10	11	12	13	14	15
P						0.264 0.263 0.1	0.367 0.365 0.1	0.431 0.430 0.1	0.365 0.364 0.1	0.264 0.260 0.5					
O				0.223 0.222 0.1	0.541 0.540 0.2	1.173 1.168 0.5	1.301 1.296 0.5	1.097 1.094 0.2	1.294 1.297 -0.2	1.168 1.163 0.5	0.541 0.539 0.2	0.223 0.223 0.1	Calculated Power Measured Power Difference (C-M)*100		
N			0.289 0.288 0.1	0.781 0.777 0.4	1.306 1.300 0.6	1.196 1.191 0.5	1.047 1.041 0.5	1.437 1.431 0.6	1.032 1.030 0.2	1.193 1.189 0.4	1.313 1.307 0.5	0.782 0.779 0.3	0.289 0.288 0.1		
M		0.223 0.223 0.0	0.782 0.778 0.3	1.310 1.301 0.9	1.061 1.059 0.2	1.106 1.102 0.5	1.436 1.423 1.3	1.007 1.002 0.5	1.433 1.429 0.4	1.106 1.104 0.2	1.062 1.059 0.3	1.310 1.302 0.8	0.781 0.778 0.2	0.223 0.223 0.0	
L		0.541 0.541 0.1	1.313 1.309 0.4	1.062 1.061 0.1	1.069 1.073 -0.4	1.438 1.435 0.2	1.118 1.114 0.5	1.173 1.169 0.4	1.117 1.115 0.2	1.436 1.434 0.3	1.069 1.067 0.2	1.061 1.060 0.1	1.306 1.303 0.3	0.541 0.542 0.0	
K	0.264 0.264 0.0	1.168 1.166 0.3	1.193 1.192 0.1	1.106 1.111 -0.5	1.436 1.465 -2.8	1.013 1.013 0.0	1.270 1.266 0.4	1.282 1.278 0.4	1.269 1.268 0.1	1.013 1.014 -0.1	1.438 1.438 0.0	1.106 1.108 -0.2	1.196 1.200 -0.4	1.173 1.172 0.1	0.264 0.264 0.0
J	0.365 0.364 0.1	1.294 1.290 0.5	1.032 1.029 0.3	1.433 1.431 0.2	1.117 1.117 0.0	1.269 1.248 2.0	1.323 1.314 0.9	1.326 1.322 0.3	1.325 1.325 -0.1	1.271 1.274 -0.3	1.119 1.122 -0.3	1.436 1.438 -0.2	1.046 1.048 -0.2	1.301 1.302 0.0	0.367 0.364 0.3
H	0.432 0.430 0.2	1.097 1.091 0.5	1.437 1.427 0.9	1.007 1.001 0.6	1.173 1.166 0.6	1.281 1.270 1.1	1.324 1.319 0.6	1.056 1.056 0.0	1.329 1.333 -0.4	1.282 1.290 -0.7	1.173 1.179 -0.6	1.007 1.010 -0.3	1.437 1.436 0.1	1.097 1.090 0.7	0.431 0.417 1.4
G	0.367 0.364 0.2	1.302 1.295 0.6	1.047 1.035 1.1	1.436 1.421 1.5	1.118 1.110 0.8	1.270 1.263 0.7	1.324 1.321 0.3	1.327 1.330 -0.3	1.325 1.334 -0.9	1.270 1.288 -1.8	1.117 1.126 -0.9	1.433 1.440 -0.7	1.032 1.034 -0.3	1.294 1.291 0.3	0.365 0.362 0.3
F	0.264 0.261 0.3	1.173 1.155 1.8	1.196 1.167 2.9	1.107 1.090 1.6	1.438 1.423 1.5	1.013 1.008 0.5	1.269 1.269 0.0	1.282 1.287 -0.6	1.271 1.282 -1.1	1.014 1.025 -1.1	1.436 1.446 -0.9	1.106 1.116 -1.0	1.193 1.201 -0.8	1.168 1.172 -0.4	0.264 0.265 0.0
E		0.541 0.532 0.9	1.306 1.279 2.7	1.061 1.044 1.7	1.069 1.056 1.3	1.436 1.428 0.8	1.117 1.119 -0.2	1.173 1.182 -0.9	1.118 1.134 -1.6	1.438 1.456 -1.8	1.069 1.081 -1.2	1.062 1.078 -1.6	1.312 1.328 -1.5	0.541 0.547 -0.6	
D		0.223 0.219 0.4	0.781 0.766 1.4	1.310 1.284 2.6	1.062 1.043 1.9	1.106 1.101 0.5	1.433 1.438 -0.5	1.007 1.018 -1.1	1.436 1.469 -3.4	1.106 1.126 -1.9	1.061 1.076 -1.5	1.310 1.325 -1.5	0.782 0.799 -1.7	0.223 0.228 -0.4	
C			0.289 0.285 0.4	0.782 0.771 1.1	1.313 1.299 1.3	1.193 1.192 0.1	1.032 1.040 -0.8	1.437 1.452 -1.5	1.047 1.064 -1.7	1.196 1.215 -1.9	1.306 1.324 -1.8	0.780 0.792 -1.2	0.289 0.295 -0.6		
B				0.223 0.222 0.2	0.541 0.540 0.2	1.168 1.172 -0.4	1.294 1.316 -2.2	1.097 1.112 -1.5	1.301 1.320 -1.9	1.173 1.191 -1.8	0.541 0.550 -0.9	0.223 0.226 -0.4			
A						0.264 0.264 0.0	0.365 0.370 -0.5	0.432 0.438 -0.6	0.367 0.372 -0.6	0.264 0.268 -0.4					

Calculated Minus Measured Powers, RMS Abs. Difference *100 = 1.0

Codes and Methods Applicability Report
for the U.S. EPR

Page A-134

Figure A-2.85: Plant G1 EOC 27 Assembly Power Distribution

	1	2	3	4	5	6	7	8	9	10	11	12	13	14	15
P						0.303 0.302 0.1	0.411 0.410 0.1	0.482 0.482 0.1	0.410 0.410 0.0	0.304 0.303 0.1					
O				0.269 0.267 0.2	0.590 0.588 0.2	1.174 1.171 0.4	1.281 1.278 0.3	1.094 1.093 0.1	1.278 1.281 -0.3	1.172 1.171 0.1	0.590 0.588 0.2	0.270 0.269 0.1	Calculated Power Measured Power Difference (C-M)*100		
N			0.348 0.343 0.5	0.843 0.837 0.6	1.312 1.307 0.5	1.184 1.180 0.4	1.038 1.034 0.3	1.383 1.380 0.3	1.031 1.030 0.1	1.183 1.180 0.3	1.314 1.308 0.5	0.843 0.840 0.3	0.348 0.346 0.1		
M		0.270 0.266 0.4	0.843 0.826 1.7	1.345 1.336 0.9	1.077 1.075 0.2	1.096 1.094 0.3	1.381 1.373 0.7	1.005 1.002 0.3	1.381 1.378 0.3	1.097 1.094 0.3	1.078 1.072 0.5	1.345 1.338 0.7	0.843 0.839 0.3	0.269 0.268 0.1	
L		0.590 0.586 0.4	1.314 1.305 0.9	1.078 1.080 -0.3	1.073 1.079 -0.6	1.382 1.384 -0.2	1.097 1.095 0.2	1.154 1.152 0.2	1.096 1.095 0.1	1.382 1.379 0.2	1.073 1.070 0.3	1.077 1.074 0.3	1.312 1.306 0.5	0.591 0.589 0.1	
K	0.304 0.303 0.2	1.172 1.166 0.6	1.183 1.180 0.3	1.097 1.102 -0.5	1.382 1.410 -2.9	1.004 1.008 -0.4	1.232 1.232 0.0	1.242 1.242 0.0	1.231 1.231 -0.1	1.004 1.005 -0.1	1.382 1.382 0.1	1.096 1.095 0.1	1.184 1.181 0.3	1.174 1.171 0.3	0.303 0.302 0.1
J	0.410 0.408 0.2	1.278 1.271 0.7	1.031 1.027 0.4	1.381 1.380 0.1	1.096 1.099 -0.2	1.231 1.223 0.8	1.266 1.264 0.2	1.267 1.268 -0.1	1.267 1.270 -0.3	1.232 1.236 -0.4	1.097 1.100 -0.3	1.381 1.382 -0.1	1.038 1.038 -0.1	1.281 1.284 -0.3	0.411 0.408 0.3
H	0.482 0.479 0.3	1.094 1.086 0.7	1.383 1.373 1.0	1.005 0.999 0.5	1.154 1.150 0.4	1.241 1.236 0.5	1.267 1.265 0.1	1.040 1.042 -0.2	1.269 1.276 -0.6	1.242 1.250 -0.8	1.154 1.161 -0.7	1.005 1.008 -0.4	1.383 1.383 0.0	1.094 1.089 0.5	0.482 0.470 1.2
G	0.411 0.407 0.4	1.281 1.272 0.9	1.038 1.025 1.3	1.381 1.366 1.4	1.097 1.088 0.8	1.232 1.226 0.5	1.266 1.266 0.0	1.269 1.274 -0.5	1.267 1.278 -1.0	1.231 1.249 -1.8	1.096 1.107 -1.1	1.380 1.389 -0.9	1.031 1.034 -0.3	1.278 1.276 0.2	0.410 0.407 0.3
F	0.303 0.299 0.4	1.174 1.154 2.0	1.184 1.155 2.9	1.096 1.079 1.8	1.382 1.366 1.6	1.004 0.999 0.6	1.231 1.231 0.0	1.242 1.249 -0.7	1.232 1.245 -1.3	1.004 1.018 -1.4	1.382 1.402 -2.1	1.096 1.107 -1.0	1.183 1.189 -0.6	1.172 1.174 -0.2	0.304 0.304 0.0
E		0.591 0.579 1.1	1.312 1.283 2.8	1.077 1.057 2.0	1.073 1.056 1.7	1.382 1.372 1.0	1.096 1.098 -0.2	1.154 1.164 -1.0	1.097 1.112 -1.6	1.382 1.402 -2.0	1.073 1.087 -1.4	1.077 1.089 -1.1	1.314 1.322 -0.9	0.590 0.593 -0.3	
D		0.269 0.264 0.5	0.843 0.825 1.8	1.345 1.315 3.0	1.078 1.048 3.0	1.096 1.087 0.9	1.380 1.385 -0.5	1.005 1.019 -1.4	1.381 1.413 -3.2	1.096 1.115 -1.9	1.077 1.092 -1.5	1.345 1.359 -1.4	0.843 0.851 -0.8	0.270 0.272 -0.2	
C			0.348 0.341 0.7	0.843 0.828 1.5	1.314 1.294 2.0	1.183 1.178 0.4	1.031 1.040 -0.9	1.383 1.410 -2.6	1.038 1.058 -2.0	1.184 1.204 -2.0	1.312 1.330 -1.9	0.842 0.853 -1.0	0.348 0.351 -0.4		
B			0.270 0.266 0.4	0.590 0.585 0.5	1.172 1.173 -0.1	1.278 1.298 -2.0	1.094 1.112 -1.8	1.281 1.303 -2.2	1.174 1.193 -1.9	0.590 0.599 -0.9	0.269 0.273 -0.4				
A					0.304 0.303 0.1	0.410 0.415 -0.5	0.482 0.490 -0.7	0.411 0.418 -0.7	0.303 0.308 -0.5						

Calculated Minus Measured Powers, RMS Abs. Difference *100 = 1.0

Codes and Methods Applicability Report
for the U.S. EPR

Figure A-2.86: Plant G1 BOC 28 Assembly Power Distribution

	1	2	3	4	5	6	7	8	9	10	11	12	13	14	15
P						0.270 0.266 0.4	0.384 0.378 0.6	0.434 0.426 0.8	0.385 0.377 0.8	0.281 0.275 0.6					
O				0.297 0.295 0.2	0.515 0.510 0.5	1.203 1.187 1.6	1.314 1.292 2.2	1.463 1.436 2.7	1.312 1.284 2.8	1.203 1.182 2.1	0.518 0.512 0.6	0.300 0.298 0.3	Calculated Power Measured Power Difference (C-M)*100		
N			0.382 0.383 0.0	1.172 1.167 0.5	1.420 1.408 1.1	1.063 1.050 1.3	1.280 1.258 2.2	0.989 0.973 1.6	1.268 1.248 2.1	1.063 1.050 1.3	1.434 1.420 1.4	1.179 1.170 0.9	0.382 0.381 0.2		
M		0.300 0.301 -0.1	1.179 1.186 -0.7	1.074 1.071 0.3	1.001 0.996 0.4	1.302 1.287 1.5	1.171 1.145 2.6	0.941 0.926 1.5	1.168 1.154 1.4	1.301 1.289 1.1	1.004 1.000 0.4	1.074 1.068 0.6	1.172 1.169 0.4	0.297 0.297 0.0	
L		0.518 0.517 0.1	1.434 1.433 0.1	1.004 1.004 0.0	1.203 1.208 -0.4	1.170 1.165 0.6	1.404 1.389 1.6	1.014 1.004 1.0	1.402 1.390 1.1	1.170 1.164 0.6	1.203 1.200 0.4	1.001 1.000 0.1	1.420 1.419 0.1	0.515 0.517 -0.1	
K	0.281 0.278 0.3	1.203 1.193 0.9	1.063 1.061 0.2	1.301 1.308 -0.7	1.170 1.200 -3.0	0.962 0.963 -0.1	1.012 1.006 0.6	1.170 1.162 0.8	1.010 1.006 0.5	0.963 0.961 0.2	1.171 1.171 -0.1	1.302 1.306 -0.4	1.063 1.072 -0.8	1.203 1.208 -0.5	0.270 0.271 -0.1
J	0.385 0.376 0.9	1.312 1.294 1.8	1.268 1.258 1.0	1.168 1.166 0.1	1.402 1.405 -0.3	1.010 0.998 1.2	1.469 1.458 1.1	0.977 0.972 0.4	1.470 1.467 0.3	1.013 1.014 -0.1	1.405 1.409 -0.5	1.171 1.177 -0.6	1.280 1.289 -0.8	1.313 1.323 -0.9	0.384 0.385 0.0
H	0.434 0.413 2.1	1.463 1.433 2.9	0.989 0.978 1.2	0.941 0.935 0.6	1.014 1.010 0.4	1.170 1.163 0.8	0.977 0.972 0.4	0.765 0.764 0.1	0.979 0.980 -0.1	1.171 1.174 -0.3	1.014 1.022 -0.8	0.941 0.949 -0.8	0.989 0.997 -0.8	1.463 1.465 -0.3	0.434 0.427 0.7
G	0.384 0.375 0.9	1.314 1.296 1.7	1.280 1.264 1.6	1.171 1.161 1.0	1.405 1.397 0.8	1.013 1.009 0.4	1.471 1.468 0.3	0.979 0.980 -0.1	1.472 1.476 -0.4	1.011 1.015 -0.4	1.402 1.422 -2.0	1.168 1.185 -1.7	1.268 1.283 -1.5	1.312 1.323 -1.1	0.385 0.386 -0.1
F	0.270 0.265 0.5	1.203 1.184 1.9	1.063 1.045 1.8	1.302 1.289 1.3	1.171 1.164 0.6	0.963 0.961 0.2	1.011 1.012 -0.1	1.171 1.175 -0.3	1.013 1.021 -0.8	0.963 0.977 -1.4	1.170 1.207 -3.7	1.301 1.329 -2.8	1.063 1.084 -2.0	1.203 1.221 -1.8	0.281 0.285 -0.4
E		0.515 0.508 0.7	1.420 1.401 1.8	1.001 0.993 0.8	1.203 1.199 0.5	1.170 1.170 0.0	1.402 1.405 -0.3	1.014 1.020 -0.5	1.405 1.417 -1.2	1.171 1.188 -1.7	1.204 1.229 -2.6	1.004 1.028 -2.3	1.434 1.471 -3.7	0.518 0.531 -1.3	
D		0.297 0.294 0.3	1.172 1.162 1.1	1.074 1.067 0.7	1.004 1.005 -0.1	1.301 1.303 -0.3	1.168 1.173 -0.5	0.941 0.946 -0.5	1.171 1.182 -1.1	1.302 1.320 -1.8	1.001 1.021 -2.0	1.074 1.100 -2.7	1.179 1.228 -4.8	0.300 0.311 -1.1	
C			0.382 0.380 0.2	1.179 1.175 0.4	1.434 1.434 0.0	1.063 1.067 -0.4	1.268 1.276 -0.8	0.989 0.994 -0.5	1.280 1.292 -1.2	1.063 1.078 -1.5	1.420 1.445 -2.5	1.173 1.200 -2.7	0.382 0.395 -1.3		
B				0.300 0.300 0.0	0.518 0.519 -0.1	1.203 1.209 -0.6	1.312 1.333 -2.1	1.462 1.476 -1.4	1.313 1.327 -1.4	1.203 1.219 -1.6	0.515 0.524 -0.9	0.297 0.304 -0.7			
A						0.281 0.280 0.1	0.385 0.389 -0.4	0.434 0.438 -0.5	0.384 0.389 -0.5	0.270 0.274 -0.4					

Calculated Minus Measured Powers, RMS Abs. Difference *100 = 1.3

Codes and Methods Applicability Report
for the U.S. EPR

Figure A-2.87: Plant G1 MOC 28 Assembly Power Distribution

	1	2	3	4	5	6	7	8	9	10	11	12	13	14	15
P						0.303 0.300 0.3	0.431 0.425 0.5	0.478 0.471 0.7	0.430 0.423 0.8	0.312 0.308 0.4					
O				0.304 0.304 -0.1	0.520 0.518 0.2	1.193 1.183 1.0	1.381 1.364 1.7	1.449 1.426 2.3	1.379 1.351 2.9	1.190 1.170 2.0	0.521 0.513 0.8	0.306 0.302 0.4	Calculated Power Measured Power Difference (C-M)*100		
N			0.381 0.386 -0.5	1.088 1.092 -0.5	1.313 1.311 0.2	1.039 1.032 0.7	1.272 1.256 1.5	1.009 0.995 1.4	1.263 1.242 2.0	1.039 1.023 1.5	1.322 1.302 1.9	1.092 1.076 1.6	0.381 0.376 0.5		
M		0.306 0.311 -0.5	1.092 1.113 -0.5	1.006 1.013 -0.7	0.964 0.966 -0.2	1.265 1.258 0.7	1.180 1.163 1.7	0.982 0.970 1.2	1.177 1.163 1.4	1.264 1.248 1.5	0.966 0.954 1.2	1.006 0.992 1.4	1.088 1.073 1.5	0.304 0.300 0.4	
L		0.521 0.525 -0.4	1.322 1.334 -1.3	0.966 0.976 -1.0	1.173 1.181 -0.8	1.170 1.168 0.1	1.502 1.491 1.1	1.066 1.057 0.9	1.499 1.486 1.4	1.169 1.159 1.1	1.173 1.161 1.2	0.964 0.953 1.0	1.313 1.296 1.7	0.520 0.514 0.6	
K	0.312 0.311 0.1	1.190 1.191 -0.1	1.039 1.044 -0.5	1.264 1.275 -1.1	1.169 1.189 -2.0	0.990 0.992 -0.3	1.037 1.034 0.3	1.192 1.186 0.6	1.035 1.029 0.6	0.990 0.984 0.6	1.170 1.162 0.7	1.265 1.255 1.0	1.039 1.028 1.1	1.193 1.179 1.4	0.303 0.299 0.4
J	0.430 0.425 0.5	1.379 1.372 0.7	1.263 1.261 0.1	1.177 1.181 -0.3	1.499 1.505 -0.6	1.035 1.031 0.3	1.427 1.423 0.4	0.976 0.973 0.2	1.428 1.424 0.4	1.037 1.035 0.2	1.502 1.497 0.4	1.180 1.175 0.5	1.272 1.263 0.9	1.381 1.370 1.1	0.431 0.423 0.7
H	0.478 0.464 1.4	1.449 1.434 1.6	1.009 1.005 0.5	0.982 0.981 0.1	1.066 1.067 0.0	1.192 1.190 0.2	0.976 0.975 0.1	0.789 0.789 0.0	0.978 0.979 -0.1	1.193 1.194 -0.2	1.066 1.070 -0.4	0.982 0.983 -0.1	1.009 1.006 0.4	1.449 1.431 1.8	0.478 0.460 1.8
G	0.431 0.424 0.6	1.381 1.371 1.0	1.272 1.264 0.8	1.180 1.176 0.4	1.502 1.500 0.2	1.037 1.037 0.0	1.428 1.429 -0.1	0.978 0.981 -0.3	1.429 1.434 -0.6	1.035 1.041 -0.6	1.500 1.517 -1.8	1.177 1.188 -1.0	1.263 1.266 -0.4	1.379 1.374 0.5	0.430 0.425 0.5
F	0.303 0.300 0.3	1.193 1.182 1.0	1.039 1.032 0.8	1.265 1.260 0.5	1.170 1.168 0.2	0.990 0.991 -0.1	1.035 1.038 -0.3	1.193 1.198 -0.6	1.037 1.046 -0.8	0.990 1.005 -1.5	1.169 1.206 -3.7	1.264 1.286 -2.2	1.039 1.051 -1.3	1.190 1.197 -0.7	0.312 0.312 -0.1
E		0.520 0.516 0.3	1.313 1.304 0.9	0.964 0.960 0.4	1.173 1.171 0.2	1.169 1.171 -0.2	1.500 1.505 -0.5	1.066 1.073 -0.7	1.502 1.514 -1.2	1.170 1.186 -1.6	1.173 1.196 -2.3	0.966 0.983 -1.7	1.322 1.349 -2.7	0.521 0.530 -0.9	
D		0.304 0.302 0.2	1.088 1.082 0.6	1.006 1.001 0.5	0.966 0.966 0.0	1.264 1.267 -0.3	1.177 1.184 -0.6	0.982 0.989 -0.7	1.180 1.188 -0.8	1.265 1.281 -1.6	0.964 0.981 -1.8	1.006 1.028 -2.2	1.092 1.135 -4.3	0.306 0.316 -1.0	
C			0.381 0.380 0.1	1.092 1.089 0.2	1.322 1.322 0.0	1.039 1.043 -0.4	1.263 1.273 -1.0	1.009 1.022 -1.2	1.272 1.285 -1.4	1.039 1.054 -1.4	1.313 1.335 -2.2	1.088 1.111 -2.4	0.381 0.393 -1.2		
B			0.306 0.306 0.0	0.521 0.522 -0.1	1.190 1.195 -0.5	1.379 1.397 -1.8	1.449 1.466 -1.6	1.381 1.397 -1.6	1.193 1.208 -1.6	0.520 0.528 -0.9	0.304 0.310 -0.6				
A					0.312 0.310 0.1	0.430 0.434 -0.4	0.478 0.484 -0.5	0.431 0.436 -0.5	0.303 0.307 -0.4						

Calculated Minus Measured Powers, RMS Abs. Difference *100 = 1.1

Codes and Methods Applicability Report
for the U.S. EPR

Page A-137

Figure A-2.88: Plant G1 EOC 28 Assembly Power Distribution

	1	2	3	4	5	6	7	8	9	10	11	12	13	14	15
P						0.338 0.335 0.3	0.468 0.463 0.5	0.512 0.505 0.6	0.467 0.461 0.6	0.345 0.341 0.5					
O				0.340 0.339 0.1	0.554 0.551 0.3	1.183 1.172 1.1	1.364 1.347 1.6	1.391 1.374 1.7	1.363 1.345 1.7	1.180 1.166 1.4	0.554 0.549 0.6	0.342 0.339 0.3	Calculated Power Measured Power Difference (C-M)*100		
N			0.421 0.423 -0.1	1.105 1.104 0.1	1.296 1.290 0.6	1.032 1.023 1.0	1.239 1.221 1.7	1.003 0.990 1.3	1.234 1.220 1.4	1.032 1.021 1.0	1.300 1.288 1.2	1.107 1.098 0.9	0.421 0.419 0.3		
M		0.342 0.344 -0.2	1.107 1.115 -0.7	1.035 1.038 -0.3	0.978 0.977 0.1	1.240 1.229 1.1	1.157 1.133 2.4	0.990 0.977 1.3	1.156 1.145 1.1	1.239 1.229 1.0	0.979 0.972 0.7	1.035 1.028 0.7	1.105 1.098 0.7	0.340 0.339 0.1	
L		0.554 0.556 -0.2	1.300 1.306 -0.7	0.979 0.987 -0.8	1.172 1.179 -0.7	1.153 1.150 0.3	1.473 1.460 1.4	1.065 1.056 0.9	1.472 1.462 1.0	1.153 1.146 0.6	1.172 1.166 0.5	0.978 0.974 0.4	1.296 1.289 0.6	0.554 0.552 0.2	
K	0.345 0.345 0.0	1.180 1.182 -0.2	1.032 1.036 -0.4	1.239 1.250 -1.1	1.153 1.177 -2.4	0.995 0.998 -0.3	1.035 1.031 0.3	1.184 1.179 0.5	1.033 1.030 0.3	0.996 0.994 0.2	1.153 1.152 0.1	1.240 1.238 0.2	1.032 1.030 0.3	1.183 1.181 0.2	0.338 0.337 0.1
J	0.467 0.465 0.3	1.363 1.360 0.2	1.234 1.236 -0.2	1.156 1.161 -0.5	1.472 1.480 -0.8	1.033 1.029 0.4	1.387 1.383 0.3	0.979 0.978 0.1	1.387 1.388 -0.1	1.035 1.037 -0.3	1.473 1.477 -0.4	1.157 1.160 -0.2	1.239 1.240 -0.2	1.364 1.369 -0.6	0.468 0.466 0.2
H	0.512 0.504 0.8	1.391 1.385 0.6	1.003 1.002 0.1	0.990 0.991 -0.1	1.065 1.066 -0.1	1.184 1.183 0.1	0.979 0.979 0.0	0.819 0.821 -0.1	0.981 0.985 -0.4	1.184 1.193 -0.9	1.064 1.074 -0.9	0.990 0.996 -0.6	1.003 1.006 -0.3	1.391 1.387 0.4	0.512 0.500 1.1
G	0.468 0.465 0.3	1.364 1.361 0.3	1.239 1.235 0.3	1.157 1.156 0.2	1.473 1.472 0.1	1.035 1.034 0.0	1.387 1.389 -0.1	0.981 0.984 -0.4	1.388 1.398 -1.1	1.033 1.050 -1.6	1.472 1.496 -2.4	1.156 1.169 -1.3	1.234 1.242 -0.8	1.362 1.364 -0.2	0.467 0.465 0.2
F	0.338 0.336 0.2	1.183 1.178 0.5	1.032 1.028 0.5	1.240 1.236 0.4	1.153 1.150 0.2	0.995 0.995 0.1	1.033 1.035 -0.1	1.184 1.188 -0.4	1.035 1.042 -0.8	0.996 1.012 -1.6	1.153 1.190 -3.7	1.239 1.258 -1.9	1.032 1.042 -1.0	1.180 1.187 -0.7	0.345 0.346 -0.1
E		0.554 0.551 0.3	1.296 1.289 0.7	0.978 0.973 0.4	1.172 1.168 0.4	1.153 1.151 0.2	1.472 1.473 -0.1	1.065 1.067 -0.2	1.473 1.477 -0.4	1.153 1.164 -1.1	1.172 1.189 -1.7	0.979 0.988 -0.9	1.300 1.314 -1.4	0.554 0.559 -0.5	
D		0.340 0.339 0.2	1.105 1.099 0.6	1.035 1.029 0.6	0.979 0.973 0.6	1.239 1.237 0.3	1.156 1.157 -0.1	0.990 0.991 -0.2	1.157 1.150 0.7	1.240 1.245 -0.5	0.978 0.987 -0.9	1.035 1.046 -1.1	1.107 1.126 -1.9	0.342 0.347 -0.5	
C			0.421 0.419 0.2	1.107 1.101 0.6	1.300 1.294 0.6	1.032 1.030 0.1	1.234 1.239 -0.4	1.003 1.014 -1.1	1.239 1.243 -0.4	1.032 1.038 -0.5	1.296 1.306 -1.0	1.105 1.116 -1.1	0.421 0.427 -0.6		
B				0.342 0.341 0.2	0.554 0.552 0.2	1.180 1.177 0.3	1.362 1.370 -0.8	1.391 1.400 -0.8	1.364 1.370 -0.7	1.183 1.190 -0.7	0.554 0.558 -0.4	0.340 0.343 -0.3			
A						0.345 0.340 0.5	0.467 0.467 0.0	0.512 0.514 -0.2	0.468 0.470 -0.2	0.338 0.340 -0.2					

Calculated Minus Measured Powers, RMS Abs. Difference *100 = 0.8

Figure A-2.89: Plant G1 BOC 29 Assembly Power Distribution

	1	2	3	4	5	6	7	8	9	10	11	12	13	14	15
P						0.234 0.235 0.0	0.336 0.336 0.1	0.367 0.364 0.3	0.337 0.331 0.6	0.236 0.225 1.0					
O				0.253 0.253 0.0	0.488 0.488 -0.1	1.125 1.126 -0.1	1.251 1.250 0.1	1.353 1.345 0.8	1.248 1.232 1.7	1.127 1.106 2.0	0.492 0.485 0.7	0.256 0.253 0.3	Calculated Power Measured Power Difference (C-M)*100		
N			0.333 0.333 0.0	1.083 1.081 0.2	1.257 1.257 0.0	1.036 1.039 -0.4	1.267 1.271 -0.4	1.069 1.068 0.1	1.247 1.237 1.0	1.037 1.026 1.1	1.284 1.267 1.7	1.091 1.077 1.4	0.333 0.329 0.3		
M		0.256 0.257 0.0	1.091 1.093 -0.2	0.985 0.979 0.6	1.349 1.352 -0.3	1.273 1.282 -0.9	1.291 1.306 -1.5	1.223 1.227 -0.4	1.287 1.285 0.2	1.274 1.266 0.8	1.355 1.337 1.8	0.985 0.972 1.3	1.083 1.072 1.1	0.253 0.252 0.2	
L		0.493 0.491 0.1	1.284 1.278 0.6	1.356 1.337 1.9	1.323 1.329 -0.6	1.257 1.272 -1.5	1.017 1.031 -1.4	1.169 1.179 -1.0	1.016 1.021 -0.5	1.258 1.257 0.0	1.323 1.315 0.8	1.349 1.340 0.8	1.257 1.247 1.0	0.488 0.485 0.2	
K	0.236 0.234 0.2	1.127 1.121 0.5	1.037 1.036 0.1	1.275 1.280 -0.6	1.258 1.291 -3.3	0.956 0.979 -2.4	1.363 1.388 -2.5	0.949 0.962 -1.2	1.364 1.377 -1.4	0.955 0.962 -0.7	1.257 1.260 -0.3	1.272 1.272 0.0	1.036 1.036 0.0	1.125 1.121 0.4	0.234 0.234 0.1
J	0.337 0.332 0.5	1.248 1.240 0.9	1.247 1.245 0.2	1.287 1.297 -0.9	1.017 1.040 -2.2	1.365 1.419 -5.4	1.025 1.049 -2.4	1.465 1.489 -2.4	1.023 1.039 -1.6	1.362 1.380 -1.8	1.017 1.027 -1.0	1.291 1.296 -0.5	1.267 1.269 -0.1	1.251 1.250 0.1	0.336 0.333 0.3
H	0.367 0.352 1.5	1.354 1.341 1.3	1.069 1.068 0.2	1.224 1.228 -0.5	1.169 1.185 -1.5	0.951 0.969 -1.8	1.469 1.494 -2.5	0.964 0.980 -1.6	1.464 1.492 -2.8	0.949 0.971 -2.2	1.168 1.186 -1.8	1.223 1.230 -0.7	1.069 1.071 -0.2	1.353 1.344 0.9	0.367 0.355 1.2
G	0.336 0.332 0.4	1.251 1.253 -0.1	1.268 1.266 0.2	1.291 1.293 -0.2	1.018 1.025 -0.7	1.364 1.377 -1.3	1.026 1.038 -1.2	1.468 1.489 -2.1	1.024 1.049 -2.4	1.364 1.428 -6.4	1.017 1.039 -2.3	1.287 1.299 -1.2	1.247 1.250 -0.3	1.248 1.247 0.1	0.337 0.335 0.3
F	0.235 0.233 0.2	1.125 1.120 0.6	1.036 1.030 0.6	1.273 1.269 0.4	1.257 1.257 0.0	0.956 0.958 -0.3	1.365 1.370 -0.5	0.950 0.956 -0.6	1.363 1.380 -1.7	0.955 0.975 -2.0	1.258 1.276 -1.8	1.274 1.283 -0.9	1.037 1.045 -0.8	1.127 1.132 -0.5	0.236 0.236 -0.1
E		0.488 0.485 0.3	1.257 1.245 1.3	1.349 1.338 1.0	1.323 1.314 1.0	1.258 1.251 0.7	1.017 1.012 0.5	1.169 1.164 0.6	1.018 1.019 -0.1	1.257 1.263 -0.6	1.323 1.325 -0.2	1.355 1.349 0.6	1.284 1.301 -1.7	0.492 0.500 -0.7	
D		0.253 0.251 0.2	1.083 1.071 1.2	0.985 0.973 1.2	1.356 1.344 1.1	1.275 1.259 1.6	1.287 1.266 2.2	1.223 1.197 2.6	1.291 1.277 1.4	1.273 1.268 0.5	1.349 1.349 0.0	0.985 0.992 -0.7	1.091 1.137 -4.6	0.256 0.265 -0.8	
C			0.333 0.329 0.4	1.091 1.076 1.5	1.284 1.265 2.0	1.037 1.016 2.0	1.247 1.210 3.7	1.069 1.022 4.8	1.268 1.239 2.9	1.036 1.025 1.1	1.257 1.252 0.6	1.083 1.089 -0.6	0.333 0.341 -0.8		
B			0.256 0.253 0.4	0.493 0.483 0.9	1.127 1.097 3.0	1.248 1.214 3.5	1.354 1.309 4.5	1.251 1.221 3.0	1.125 1.107 1.8	0.488 0.485 0.3	0.253 0.254 -0.1				
A						0.236 0.227 0.9	0.337 0.327 1.0	0.367 0.356 1.0	0.336 0.329 0.8	0.235 0.231 0.4					

Calculated Minus Measured Powers, RMS Abs. Difference *100 = 1.5

Codes and Methods Applicability Report
for the U.S. EPR

Figure A-2.90: Plant G1 MOC 29 Assembly Power Distribution

	1	2	3	4	5	6	7	8	9	10	11	12	13	14	15
P						0.260 0.260 0.0	0.365 0.364 0.1	0.393 0.390 0.3	0.372 0.366 0.6	0.266 0.258 0.8					
O				0.285 0.286 0.0	0.525 0.526 -0.1	1.118 1.119 -0.1	1.265 1.263 0.2	1.304 1.296 0.9	1.287 1.270 1.7	1.138 1.117 2.0	0.533 0.523 1.0	0.289 0.283 0.5	Calculated Power Measured Power Difference (C-M)*100		
N			0.365 0.365 -0.1	1.105 1.107 -0.1	1.314 1.318 -0.3	1.012 1.015 -0.3	1.170 1.172 -0.1	1.027 1.024 0.4	1.211 1.199 1.2	1.032 1.016 1.6	1.339 1.312 2.7	1.112 1.092 2.1	0.365 0.359 0.6		
M		0.289 0.289 0.0	1.112 1.116 -0.3	1.014 1.014 0.0	1.300 1.304 -0.5	1.206 1.214 -0.8	1.215 1.228 -1.4	1.172 1.173 -0.1	1.229 1.222 0.8	1.219 1.202 1.7	1.308 1.274 3.4	1.014 0.996 1.8	1.105 1.089 1.6	0.285 0.282 0.3	
L		0.533 0.532 0.1	1.339 1.335 0.4	1.308 1.298 1.0	1.262 1.270 -0.8	1.213 1.226 -1.2	1.016 1.026 -1.0	1.161 1.166 -0.5	1.019 1.018 0.1	1.218 1.209 0.9	1.262 1.245 1.7	1.300 1.284 1.6	1.314 1.299 1.5	0.525 0.522 0.3	
K	0.266 0.264 0.2	1.138 1.133 0.5	1.032 1.031 0.1	1.219 1.224 -0.4	1.218 1.241 -2.4	0.982 1.000 -1.8	1.453 1.472 -1.9	0.992 0.999 -0.8	1.455 1.460 -0.5	0.982 0.981 0.1	1.213 1.207 0.6	1.206 1.198 0.8	1.012 1.006 0.6	1.118 1.118 0.0	0.260 0.261 -0.1
J	0.372 0.366 0.5	1.287 1.278 0.8	1.211 1.208 0.3	1.229 1.235 -0.6	1.019 1.035 -1.6	1.456 1.500 -4.5	1.051 1.068 -1.8	1.437 1.453 -1.6	1.050 1.058 -0.8	1.452 1.459 -0.6	1.016 1.017 -0.1	1.215 1.213 0.2	1.170 1.168 0.2	1.265 1.284 -1.9	0.365 0.368 -0.2
H	0.393 0.380 1.3	1.304 1.293 1.2	1.027 1.023 0.4	1.172 1.173 -0.1	1.161 1.171 -1.0	0.992 1.006 -1.4	1.439 1.458 -1.9	0.968 0.979 -1.1	1.437 1.452 -1.6	0.991 1.002 -1.0	1.161 1.166 -0.6	1.171 1.172 0.0	1.027 1.027 0.0	1.304 1.304 0.1	0.393 0.387 0.5
G	0.365 0.362 0.3	1.265 1.269 -0.4	1.171 1.160 1.0	1.215 1.210 0.5	1.016 1.018 -0.2	1.453 1.463 -1.0	1.051 1.061 -1.0	1.439 1.455 -1.6	1.050 1.065 -1.5	1.455 1.488 -3.3	1.019 1.026 -0.7	1.229 1.229 0.0	1.211 1.208 0.3	1.287 1.283 0.4	0.372 0.370 0.2
F	0.260 0.258 0.3	1.118 1.106 1.3	1.012 0.992 2.0	1.206 1.193 1.3	1.213 1.207 0.6	0.982 0.984 -0.1	1.456 1.464 -0.9	0.992 1.002 -1.0	1.453 1.471 -1.8	0.982 0.993 -1.1	1.218 1.218 -0.1	1.219 1.211 0.8	1.032 1.028 0.4	1.138 1.134 0.4	0.266 0.265 0.1
E		0.525 0.518 0.7	1.314 1.291 2.3	1.300 1.281 1.8	1.262 1.248 1.5	1.218 1.214 0.4	1.019 1.024 -0.4	1.161 1.173 -1.2	1.016 1.031 -1.6	1.213 1.224 -1.1	1.262 1.259 0.3	1.308 1.281 2.7	1.339 1.332 0.6	0.533 0.532 0.1	
D		0.285 0.281 0.4	1.105 1.087 1.8	1.014 0.998 1.7	1.308 1.281 2.8	1.219 1.211 0.9	1.229 1.232 -0.3	1.172 1.185 -1.3	1.215 1.250 -3.5	1.206 1.221 -1.5	1.300 1.305 -0.5	1.014 1.014 0.1	1.112 1.127 -1.4	0.289 0.291 -0.2	
C			0.365 0.359 0.5	1.112 1.096 1.6	1.339 1.321 1.8	1.032 1.027 0.5	1.211 1.213 -0.1	1.027 1.036 -0.9	1.171 1.184 -1.4	1.012 1.023 -1.0	1.314 1.322 -0.8	1.105 1.110 -0.4	0.365 0.368 -0.3		
B				0.289 0.285 0.3	0.533 0.529 0.5	1.138 1.135 0.3	1.287 1.291 -0.4	1.304 1.312 -0.8	1.265 1.276 -1.1	1.118 1.128 -1.0	0.525 0.529 -0.4	0.285 0.287 -0.2			
A						0.266 0.266 0.0	0.372 0.373 -0.1	0.393 0.396 -0.3	0.365 0.368 -0.3	0.260 0.263 -0.2					

Calculated Minus Measured Powers, RMS Abs. Difference *100 = 1.2

Codes and Methods Applicability Report
for the U.S. EPR

Figure A-2.91: Plant G1 EOC 29 Assembly Power Distribution

	1	2	3	4	5	6	7	8	9	10	11	12	13	14	15
P						0.306 0.304 0.2	0.417 0.414 0.3	0.440 0.436 0.5	0.423 0.416 0.7	0.311 0.302 0.8					
O				0.329 0.327 0.2	0.577 0.574 0.4	1.137 1.130 0.7	1.286 1.277 0.9	1.280 1.269 1.2	1.302 1.285 1.7	1.151 1.132 1.9	0.582 0.573 0.9	0.331 0.326 0.4	Calculated Power Measured Power Difference (C-M)*100		
N			0.405 0.403 0.2	1.115 1.106 0.8	1.327 1.319 0.9	1.016 1.012 0.5	1.156 1.150 0.5	1.022 1.016 0.7	1.190 1.178 1.2	1.030 1.017 1.3	1.340 1.320 2.0	1.118 1.104 1.4	0.405 0.401 0.4		
M		0.331 0.329 0.2	1.118 1.115 0.3	1.007 0.997 0.9	1.253 1.245 0.9	1.172 1.169 0.3	1.188 1.193 -0.5	1.154 1.151 0.3	1.199 1.191 0.8	1.182 1.169 1.2	1.258 1.238 2.1	1.007 0.996 1.1	1.115 1.105 1.0	0.329 0.327 0.2	
L		0.582 0.577 0.5	1.340 1.326 1.4	1.258 1.234 2.4	1.217 1.207 1.0	1.182 1.179 0.3	1.014 1.015 -0.1	1.149 1.148 0.1	1.016 1.014 0.2	1.185 1.179 0.6	1.217 1.208 0.9	1.253 1.245 0.8	1.327 1.319 0.9	0.577 0.576 0.2	
K	0.311 0.308 0.2	1.151 1.142 0.9	1.030 1.022 0.8	1.181 1.171 1.1	1.185 1.180 0.5	0.984 0.984 0.0	1.431 1.433 -0.2	0.995 0.997 -0.2	1.433 1.435 -0.2	0.984 0.984 -0.1	1.182 1.181 0.2	1.172 1.170 0.2	1.016 1.015 0.1	1.137 1.137 0.1	0.306 0.307 -0.1
J	0.423 0.419 0.4	1.302 1.294 0.8	1.190 1.184 0.6	1.199 1.194 0.5	1.016 1.015 0.1	1.433 1.439 -0.6	1.035 1.039 -0.4	1.367 1.374 -0.6	1.035 1.041 -0.6	1.431 1.440 -0.8	1.014 1.018 -0.5	1.188 1.190 -0.2	1.156 1.155 0.1	1.286 1.296 -1.0	0.417 0.418 -0.1
H	0.440 0.433 0.8	1.280 1.278 0.3	1.022 1.020 0.2	1.154 1.151 0.3	1.149 1.149 0.0	0.995 0.998 -0.3	1.369 1.375 -0.6	0.957 0.964 -0.7	1.367 1.382 -1.5	0.995 1.009 -1.4	1.149 1.160 -1.1	1.154 1.159 -0.6	1.022 1.026 -0.3	1.280 1.280 0.0	0.440 0.435 0.6
G	0.417 0.419 -0.2	1.286 1.306 -2.1	1.156 1.154 0.2	1.188 1.185 0.3	1.014 1.013 0.1	1.431 1.434 -0.2	1.035 1.041 -0.6	1.368 1.381 -1.3	1.035 1.052 -1.7	1.433 1.477 -4.4	1.016 1.030 -1.4	1.199 1.206 -0.8	1.190 1.195 -0.4	1.302 1.304 -0.2	0.423 0.422 0.1
F	0.306 0.306 0.0	1.137 1.136 0.1	1.016 1.006 1.0	1.172 1.165 0.7	1.182 1.178 0.4	0.984 0.984 -0.1	1.433 1.439 -0.6	0.995 1.005 -0.9	1.431 1.451 -2.0	0.984 1.000 -1.6	1.185 1.194 -0.9	1.182 1.185 -0.4	1.030 1.035 -0.5	1.151 1.155 -0.4	0.311 0.312 -0.1
E		0.577 0.575 0.3	1.327 1.315 1.2	1.253 1.243 1.0	1.217 1.208 0.9	1.185 1.183 0.2	1.016 1.020 -0.4	1.149 1.160 -1.1	1.014 1.029 -1.6	1.182 1.197 -1.5	1.217 1.224 -0.7	1.258 1.252 0.7	1.340 1.350 -1.0	0.582 0.587 -0.5	
D		0.329 0.327 0.2	1.114 1.104 1.0	1.007 0.997 1.0	1.258 1.241 1.7	1.181 1.176 0.5	1.199 1.202 -0.3	1.154 1.164 -1.0	1.188 1.216 -2.9	1.172 1.189 -1.7	1.253 1.266 -1.3	1.007 1.017 -1.0	1.118 1.147 -2.9	0.331 0.337 -0.6	
C			0.405 0.402 0.3	1.118 1.108 1.0	1.340 1.329 1.1	1.030 1.027 0.3	1.190 1.191 -0.1	1.022 1.025 -0.2	1.156 1.166 -1.0	1.016 1.028 -1.2	1.327 1.342 -1.4	1.115 1.128 -1.4	0.405 0.413 -0.8		
B			0.331 0.329 0.2	0.582 0.579 0.3	1.151 1.149 0.1	1.302 1.308 -0.6	1.280 1.285 -0.5	1.286 1.295 -0.9	1.137 1.148 -1.1	0.577 0.584 -0.6	0.329 0.333 -0.4				
A						0.311 0.311 0.0	0.423 0.424 -0.2	0.440 0.443 -0.2	0.417 0.420 -0.3	0.306 0.309 -0.3					

Calculated Minus Measured Powers, RMS Abs. Difference *100 = 0.9

Codes and Methods Applicability Report
for the U.S. EPR

Page A-141

Figure A-2.92: Plant G1 BOC 30 Assembly Power Distribution

	1	2	3	4	5	6	7	8	9	10	11	12	13	14	15
P						0.213 0.211 0.1	0.401 0.400 0.1	0.374 0.374 0.0	0.406 0.406 0.0	0.216 0.212 0.3					
O				0.269 0.267 0.1	0.425 0.422 0.3	0.889 0.883 0.5	1.349 1.343 0.6	1.315 1.315 0.0	1.365 1.375 -1.1	0.901 0.901 0.0	0.432 0.432 0.0	0.274 0.274 0.0	Calculated Power Measured Power Difference (C-M)*100		
N			0.363 0.363 0.0	1.178 1.171 0.6	1.354 1.345 1.0	1.204 1.195 0.9	0.975 0.967 0.8	1.008 1.004 0.4	1.002 1.002 0.0	1.224 1.223 0.1	1.384 1.382 0.2	1.190 1.190 0.0	0.363 0.364 -0.1		
M		0.274 0.274 0.0	1.190 1.197 -0.7	1.023 1.016 0.7	1.336 1.325 1.1	1.353 1.341 1.3	1.028 1.013 1.5	1.416 1.406 1.0	1.037 1.035 0.2	1.366 1.364 0.2	1.347 1.343 0.3	1.023 1.025 -0.2	1.177 1.182 -0.5	0.269 0.271 -0.2	
L		0.432 0.430 0.3	1.384 1.374 1.0	1.347 1.324 2.3	1.221 1.210 1.1	1.279 1.271 0.8	1.489 1.479 1.0	1.062 1.058 0.4	1.496 1.494 0.2	1.286 1.286 0.0	1.221 1.222 -0.1	1.336 1.341 -0.6	1.354 1.362 -0.8	0.425 0.431 -0.6	
K	0.216 0.213 0.3	0.901 0.893 0.8	1.224 1.214 0.9	1.366 1.355 1.1	1.286 1.285 0.1	0.990 0.990 0.0	1.017 1.016 0.1	1.142 1.141 0.1	1.019 1.020 -0.1	0.990 0.992 -0.3	1.279 1.285 -0.5	1.353 1.362 -0.9	1.204 1.219 -1.4	0.889 0.908 -1.9	0.212 0.218 -0.5
J	0.406 0.399 0.7	1.365 1.350 1.4	1.002 0.995 0.7	1.037 1.033 0.4	1.496 1.497 -0.1	1.019 1.030 -1.1	1.455 1.459 -0.4	0.999 1.001 -0.2	1.454 1.457 -0.3	1.016 1.021 -0.4	1.489 1.497 -0.8	1.028 1.038 -1.0	0.975 0.989 -1.4	1.349 1.400 -5.1	0.401 0.411 -1.0
H	0.374 0.359 1.5	1.315 1.304 1.1	1.008 1.002 0.5	1.416 1.409 0.6	1.062 1.061 0.1	1.142 1.144 -0.2	0.999 1.001 -0.2	0.759 0.761 -0.2	0.997 1.001 -0.4	1.141 1.147 -0.6	1.062 1.068 -0.6	1.416 1.425 -0.9	1.008 1.019 -1.1	1.315 1.333 -1.7	0.374 0.371 0.3
G	0.401 0.400 0.2	1.349 1.364 -1.6	0.975 0.971 0.4	1.028 1.024 0.4	1.489 1.485 0.4	1.016 1.016 0.0	1.453 1.453 0.0	0.997 0.998 -0.1	1.452 1.457 -0.5	1.018 1.030 -1.1	1.495 1.502 -0.6	1.037 1.042 -0.5	1.002 1.008 -0.6	1.364 1.374 -0.9	0.406 0.407 -0.1
F	0.212 0.212 0.0	0.889 0.887 0.1	1.204 1.192 1.3	1.353 1.343 1.0	1.279 1.273 0.6	0.990 0.987 0.2	1.018 1.017 0.1	1.141 1.140 0.1	1.016 1.015 0.0	0.989 0.991 -0.1	1.286 1.283 0.3	1.366 1.365 0.1	1.223 1.228 -0.4	0.901 0.906 -0.5	0.216 0.217 -0.1
E		0.425 0.422 0.2	1.354 1.341 1.3	1.336 1.325 1.1	1.221 1.211 1.0	1.286 1.281 0.5	1.496 1.493 0.3	1.062 1.059 0.2	1.489 1.480 0.9	1.279 1.274 0.5	1.220 1.215 0.5	1.347 1.337 1.0	1.383 1.389 -0.6	0.432 0.435 -0.3	
D		0.269 0.267 0.2	1.178 1.167 1.0	1.023 1.014 0.8	1.347 1.331 1.6	1.366 1.361 0.5	1.037 1.038 -0.1	1.415 1.411 0.4	1.028 1.013 1.5	1.353 1.346 0.7	1.335 1.333 0.3	1.023 1.025 -0.3	1.190 1.211 -2.1	0.274 0.278 -0.3	
C			0.363 0.361 0.2	1.190 1.183 0.8	1.384 1.378 0.6	1.224 1.227 -0.4	1.002 1.012 -1.0	1.008 1.021 -1.3	0.975 0.973 0.1	1.204 1.203 0.1	1.354 1.354 0.0	1.177 1.181 -0.3	0.363 0.367 -0.4		
B				0.274 0.273 0.1	0.432 0.433 -0.1	0.901 0.910 -1.0	1.364 1.401 -3.6	1.315 1.334 -1.9	1.349 1.356 -0.7	0.889 0.891 -0.2	0.425 0.425 -0.1	0.269 0.269 -0.1			
A						0.216 0.217 -0.2	0.406 0.414 -0.8	0.374 0.380 -0.5	0.401 0.405 -0.3	0.212 0.214 -0.1					

Calculated Minus Measured Powers, RMS Abs. Difference *100 = 0.9

Codes and Methods Applicability Report
for the U.S. EPR

Page A-142

Figure A-2.93: Plant G1 MOC 30 Assembly Power Distribution

	1	2	3	4	5	6	7	8	9	10	11	12	13	14	15
P						0.238 0.237 0.1	0.429 0.428 0.1	0.409 0.409 0.0	0.434 0.436 -0.2	0.241 0.238 0.3					
O				0.291 0.291 0.0	0.455 0.453 0.2	0.893 0.889 0.4	1.313 1.308 0.5	1.356 1.359 -0.2	1.330 1.348 -1.8	0.905 0.904 0.1	0.462 0.459 0.3	0.296 0.294 0.2	Calculated Power Measured Power Difference (C-M)*100		
N			0.380 0.382 -0.3	1.152 1.152 0.0	1.372 1.367 0.5	1.172 1.164 0.8	0.977 0.968 0.9	1.033 1.028 0.5	1.009 1.008 0.1	1.191 1.185 0.6	1.395 1.382 1.3	1.162 1.152 1.0	0.380 0.377 0.3		
M		0.296 0.299 -0.3	1.162 1.181 -1.9	0.993 0.993 0.0	1.269 1.263 0.5	1.298 1.286 1.3	1.049 1.025 2.4	1.515 1.499 1.6	1.059 1.051 0.8	1.310 1.299 1.2	1.278 1.259 1.9	0.993 0.984 0.9	1.152 1.145 0.7	0.291 0.291 0.1	
L		0.462 0.462 0.0	1.395 1.396 -0.1	1.278 1.266 1.3	1.166 1.163 0.4	1.241 1.234 0.7	1.553 1.538 1.5	1.101 1.092 0.9	1.559 1.549 1.0	1.247 1.238 0.9	1.166 1.156 1.0	1.269 1.261 0.8	1.372 1.366 0.6	0.455 0.456 -0.1	
K	0.241 0.239 0.2	0.905 0.902 0.4	1.191 1.189 0.2	1.310 1.309 0.2	1.247 1.257 -1.0	0.991 0.993 -0.2	1.017 1.015 0.3	1.144 1.139 0.4	1.019 1.015 0.4	0.990 0.986 0.4	1.241 1.236 0.5	1.298 1.295 0.4	1.172 1.168 0.4	0.893 0.905 -1.2	0.238 0.241 -0.4
J	0.434 0.427 0.7	1.330 1.320 0.9	1.009 1.006 0.4	1.059 1.058 0.0	1.559 1.567 -0.8	1.019 1.031 -1.1	1.384 1.388 -0.4	0.975 0.974 0.1	1.384 1.382 0.2	1.017 1.016 0.1	1.552 1.553 0.0	1.049 1.052 -0.3	0.977 0.987 -0.9	1.313 1.362 -4.9	0.429 0.438 -0.9
H	0.409 0.393 1.6	1.356 1.346 1.0	1.033 1.029 0.4	1.515 1.512 0.2	1.101 1.102 -0.1	1.143 1.147 -0.4	0.974 0.976 -0.1	0.770 0.770 0.0	0.973 0.973 0.0	1.143 1.144 -0.1	1.101 1.103 -0.2	1.515 1.521 -0.6	1.033 1.042 -0.9	1.356 1.373 -1.7	0.409 0.405 0.4
G	0.429 0.426 0.3	1.313 1.328 -1.5	0.977 0.973 0.4	1.049 1.045 0.4	1.552 1.549 0.3	1.017 1.017 0.1	1.384 1.384 0.0	0.973 0.973 0.0	1.383 1.384 -0.1	1.019 1.023 -0.4	1.559 1.563 -0.4	1.059 1.062 -0.3	1.009 1.016 -0.6	1.330 1.340 -1.0	0.434 0.435 -0.1
F	0.238 0.236 0.1	0.893 0.888 0.5	1.172 1.152 2.0	1.298 1.286 1.2	1.241 1.234 0.7	0.990 0.988 0.3	1.019 1.018 0.1	1.143 1.142 0.1	1.017 1.016 0.1	0.990 0.991 0.0	1.247 1.249 -0.3	1.310 1.311 -0.1	1.191 1.198 -0.7	0.905 0.912 -0.7	0.241 0.243 -0.1
E		0.455 0.451 0.4	1.372 1.355 1.6	1.269 1.257 1.2	1.166 1.157 0.9	1.247 1.243 0.4	1.559 1.559 0.0	1.101 1.100 0.1	1.552 1.547 0.5	1.241 1.239 0.2	1.166 1.164 0.1	1.278 1.269 0.9	1.395 1.408 -1.3	0.462 0.467 -0.5	
D		0.291 0.289 0.3	1.152 1.140 1.1	0.993 0.984 0.9	1.278 1.263 1.5	1.310 1.308 0.2	1.059 1.062 -0.3	1.515 1.518 -0.3	1.049 1.038 1.1	1.298 1.297 0.1	1.269 1.272 -0.4	0.993 1.001 -0.8	1.162 1.197 -3.5	0.296 0.303 -0.6	
C			0.380 0.377 0.3	1.162 1.155 0.6	1.395 1.391 0.4	1.191 1.198 -0.7	1.009 1.024 -1.5	1.033 1.052 -1.8	0.977 0.983 -0.5	1.172 1.177 -0.5	1.372 1.380 -0.9	1.152 1.163 -1.2	0.380 0.387 -0.7		
B				0.296 0.296 0.1	0.462 0.463 -0.2	0.905 0.918 -1.3	1.330 1.374 -4.5	1.356 1.384 -2.8	1.313 1.329 -1.6	0.893 0.900 -0.7	0.455 0.458 -0.3	0.291 0.294 -0.3			
A						0.241 0.244 -0.3	0.434 0.445 -1.1	0.409 0.417 -0.8	0.429 0.435 -0.6	0.238 0.240 -0.2					

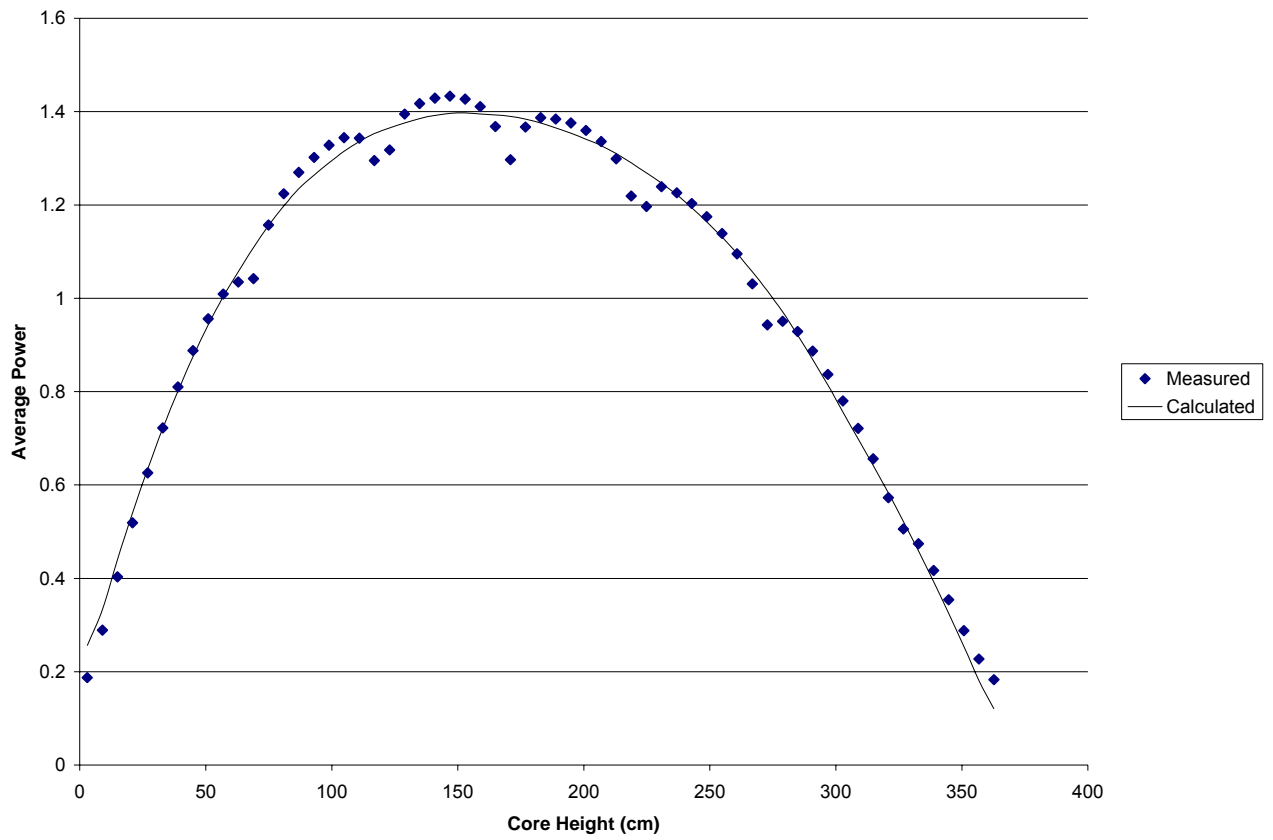
Calculated Minus Measured Powers, RMS Abs. Difference *100 = 1.0

Codes and Methods Applicability Report
for the U.S. EPR

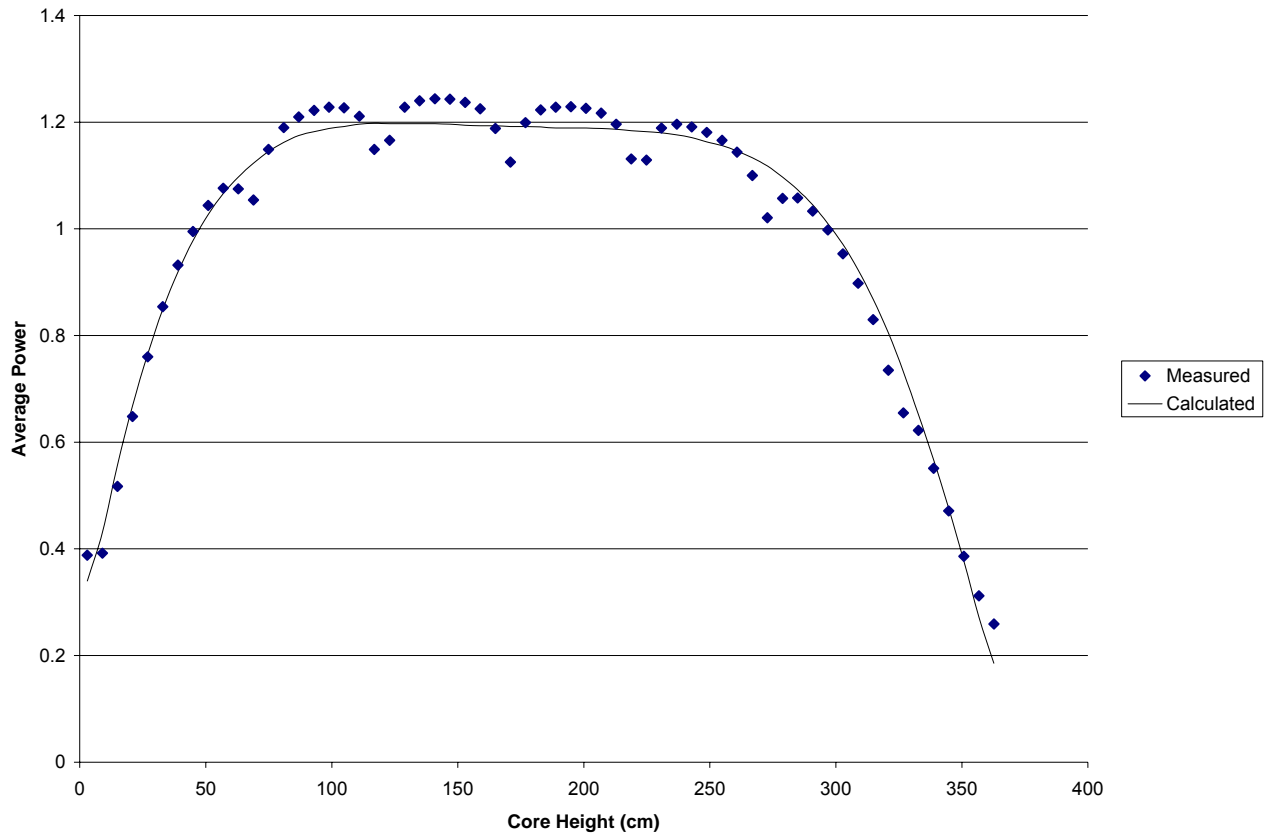
Figure A-2.94: Plant G1 EOC 30 Assembly Power Distribution

	1	2	3	4	5	6	7	8	9	10	11	12	13	14	15
P						0.285 0.283 0.2	0.485 0.482 0.2	0.465 0.464 0.1	0.486 0.486 -0.1	0.285 0.283 0.2					
O				0.333 0.331 0.1	0.508 0.504 0.3	0.935 0.929 0.7	1.316 1.308 0.8	1.380 1.378 0.2	1.316 1.327 -1.1	0.934 0.933 0.0	0.507 0.506 0.2	0.335 0.334 0.1	Calculated Power Measured Power Difference (C-M)*100		
N			0.417 0.419 -0.2	1.151 1.148 0.3	1.375 1.366 0.9	1.167 1.156 1.1	1.021 1.009 1.1	1.050 1.044 0.7	1.019 1.017 0.2	1.166 1.163 0.3	1.376 1.370 0.6	1.153 1.149 0.5	0.417 0.415 0.2		
M		0.335 0.338 -0.3	1.153 1.173 -1.9	0.981 0.977 0.4	1.221 1.210 1.1	1.252 1.237 1.6	1.048 1.025 2.3	1.497 1.481 1.6	1.047 1.041 0.6	1.252 1.246 0.6	1.222 1.215 0.6	0.981 0.977 0.4	1.151 1.146 0.4	0.333 0.332 0.1	
L		0.507 0.507 0.1	1.376 1.372 0.3	1.222 1.200 2.2	1.127 1.115 1.2	1.194 1.181 1.3	1.504 1.486 1.8	1.084 1.075 0.9	1.505 1.497 0.8	1.196 1.191 0.5	1.127 1.122 0.4	1.221 1.216 0.4	1.375 1.369 0.6	0.508 0.508 0.0	
K	0.285 0.283 0.2	0.934 0.930 0.4	1.166 1.161 0.6	1.252 1.242 1.1	1.196 1.189 0.7	0.984 0.978 0.6	1.010 1.003 0.7	1.134 1.128 0.6	1.011 1.007 0.4	0.984 0.982 0.2	1.194 1.192 0.2	1.252 1.249 0.3	1.167 1.160 0.7	0.935 0.942 -0.7	0.285 0.287 -0.2
J	0.486 0.480 0.5	1.316 1.310 0.6	1.019 1.015 0.4	1.047 1.042 0.5	1.505 1.500 0.5	1.011 1.010 0.1	1.341 1.337 0.4	0.979 0.976 0.3	1.341 1.339 0.1	1.010 1.011 0.0	1.504 1.506 -0.2	1.048 1.051 -0.3	1.021 1.028 -0.8	1.316 1.351 -3.5	0.485 0.489 -0.5
H	0.465 0.453 1.2	1.380 1.377 0.3	1.050 1.049 0.2	1.497 1.494 0.3	1.084 1.081 0.2	1.134 1.132 0.2	0.978 0.976 0.2	0.810 0.809 0.1	0.977 0.978 -0.1	1.134 1.138 -0.4	1.084 1.088 -0.4	1.497 1.504 -0.7	1.050 1.057 -0.7	1.380 1.389 -0.9	0.465 0.458 0.7
G	0.485 0.485 -0.1	1.316 1.339 -2.4	1.021 1.023 -0.2	1.048 1.047 0.1	1.504 1.502 0.2	1.010 1.009 0.1	1.340 1.339 0.1	0.977 0.977 0.0	1.340 1.344 -0.4	1.011 1.022 -1.1	1.505 1.514 -0.9	1.047 1.053 -0.6	1.019 1.025 -0.6	1.316 1.323 -0.7	0.486 0.485 0.0
F	0.285 0.286 -0.1	0.935 0.939 -0.3	1.167 1.160 0.7	1.252 1.249 0.3	1.194 1.193 0.1	0.984 0.983 0.1	1.011 1.010 0.1	1.134 1.132 0.2	1.010 1.009 0.1	0.984 0.987 -0.3	1.195 1.203 -0.8	1.252 1.258 -0.6	1.166 1.176 -0.9	0.934 0.941 -0.8	0.285 0.287 -0.2
E		0.508 0.508 0.0	1.375 1.372 0.3	1.221 1.220 0.1	1.127 1.127 0.0	1.195 1.196 -0.1	1.505 1.504 0.1	1.084 1.080 0.4	1.504 1.494 1.0	1.194 1.192 0.2	1.127 1.128 -0.2	1.222 1.221 0.1	1.376 1.394 -1.8	0.507 0.515 -0.7	
D		0.333 0.333 0.0	1.151 1.151 0.0	0.981 0.982 -0.1	1.222 1.225 -0.4	1.252 1.256 -0.4	1.047 1.049 -0.1	1.497 1.490 0.8	1.048 1.027 2.1	1.252 1.247 0.6	1.221 1.224 -0.4	0.981 0.993 -1.1	1.153 1.195 -4.2	0.335 0.344 -0.9	
C			0.417 0.417 -0.1	1.153 1.157 -0.4	1.376 1.382 -0.7	1.166 1.175 -0.9	1.019 1.028 -0.9	1.050 1.053 -0.2	1.021 1.017 0.4	1.167 1.167 0.0	1.375 1.381 -0.6	1.151 1.164 -1.3	0.417 0.426 -1.0		
B				0.335 0.337 -0.2	0.507 0.511 -0.4	0.934 0.947 -1.3	1.316 1.351 -3.5	1.380 1.395 -1.5	1.316 1.321 -0.5	0.935 0.938 -0.3	0.508 0.510 -0.3	0.333 0.336 -0.3			
A						0.285 0.288 -0.3	0.486 0.494 -0.9	0.465 0.470 -0.5	0.485 0.488 -0.3	0.285 0.286 -0.1					

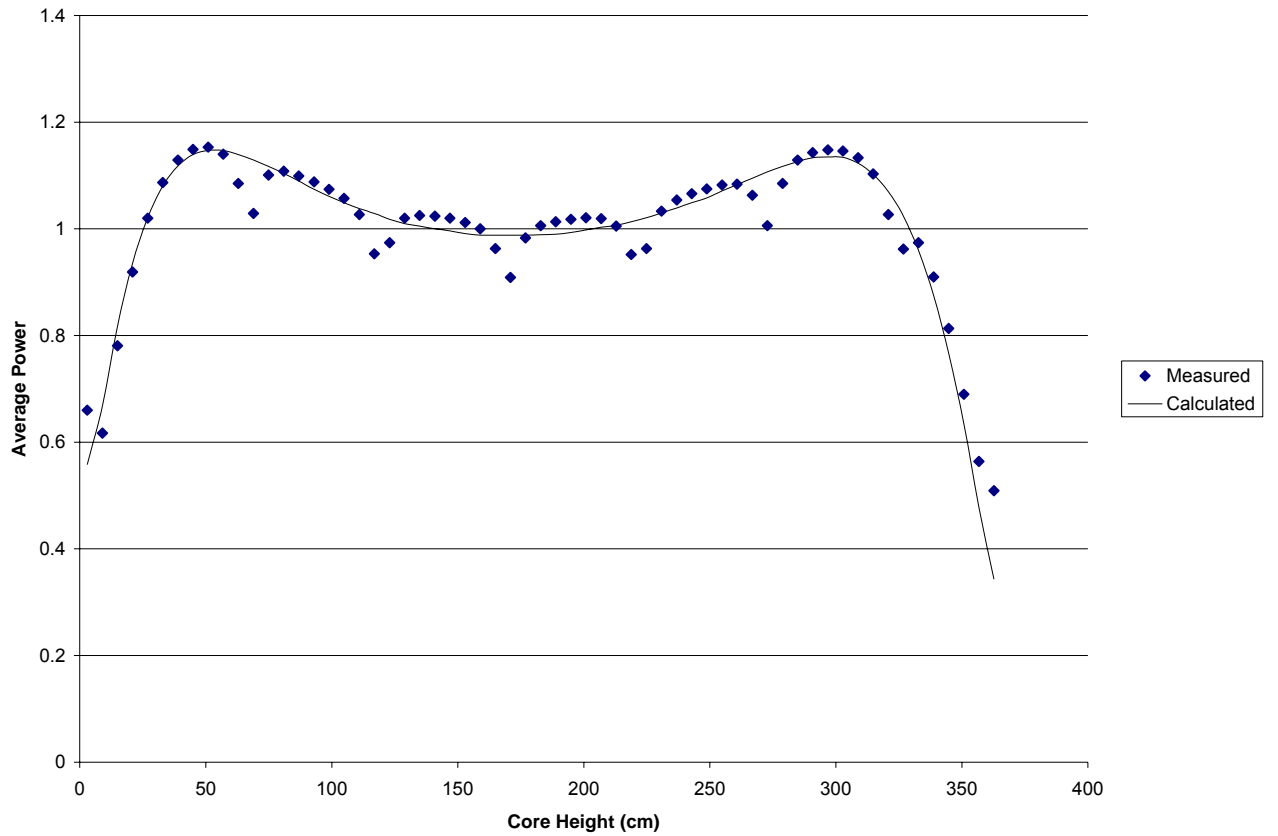
Calculated Minus Measured Powers, RMS Abs. Difference *100 = 0.9

Figure A-2.95: Plant A BOC 1 Axial Power Distribution

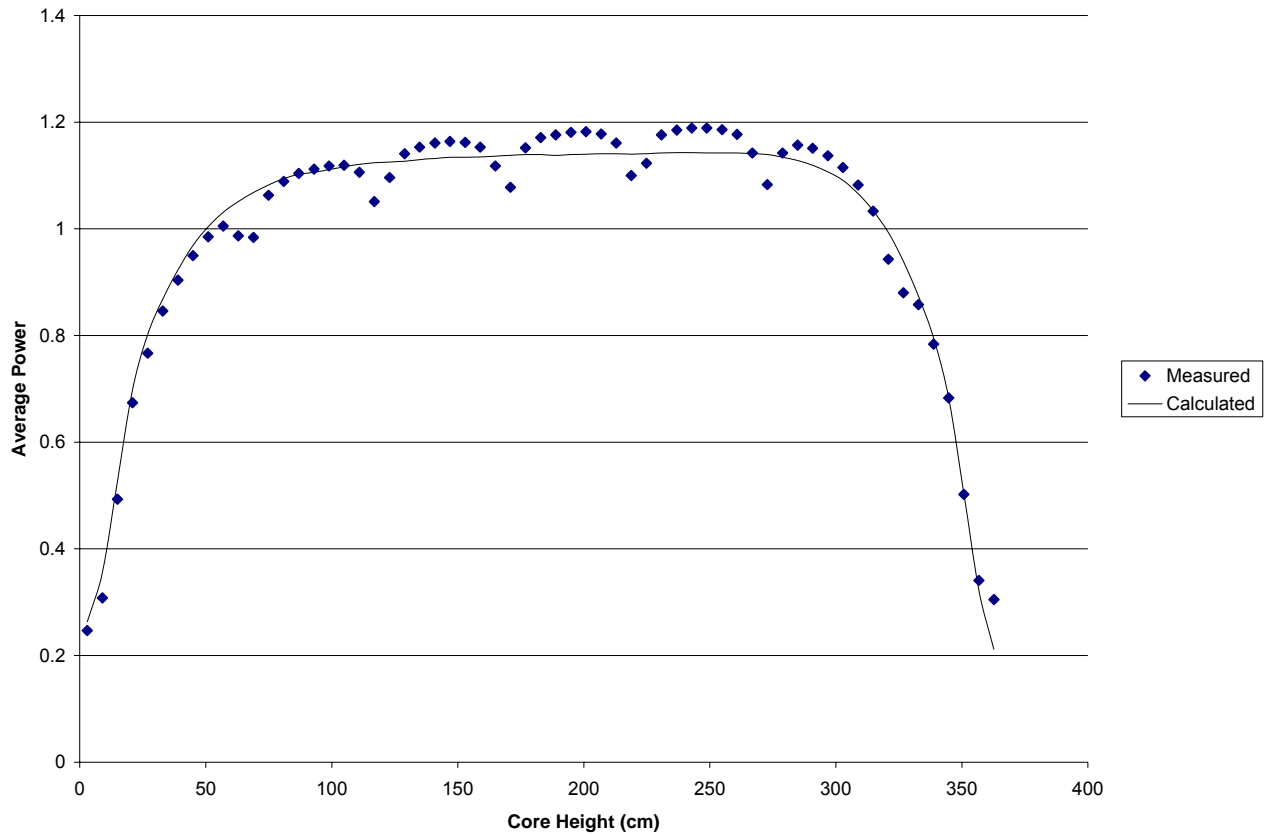
RMS = 0.034

Figure A-2.96: Plant A MOC 1 Axial Power Distribution

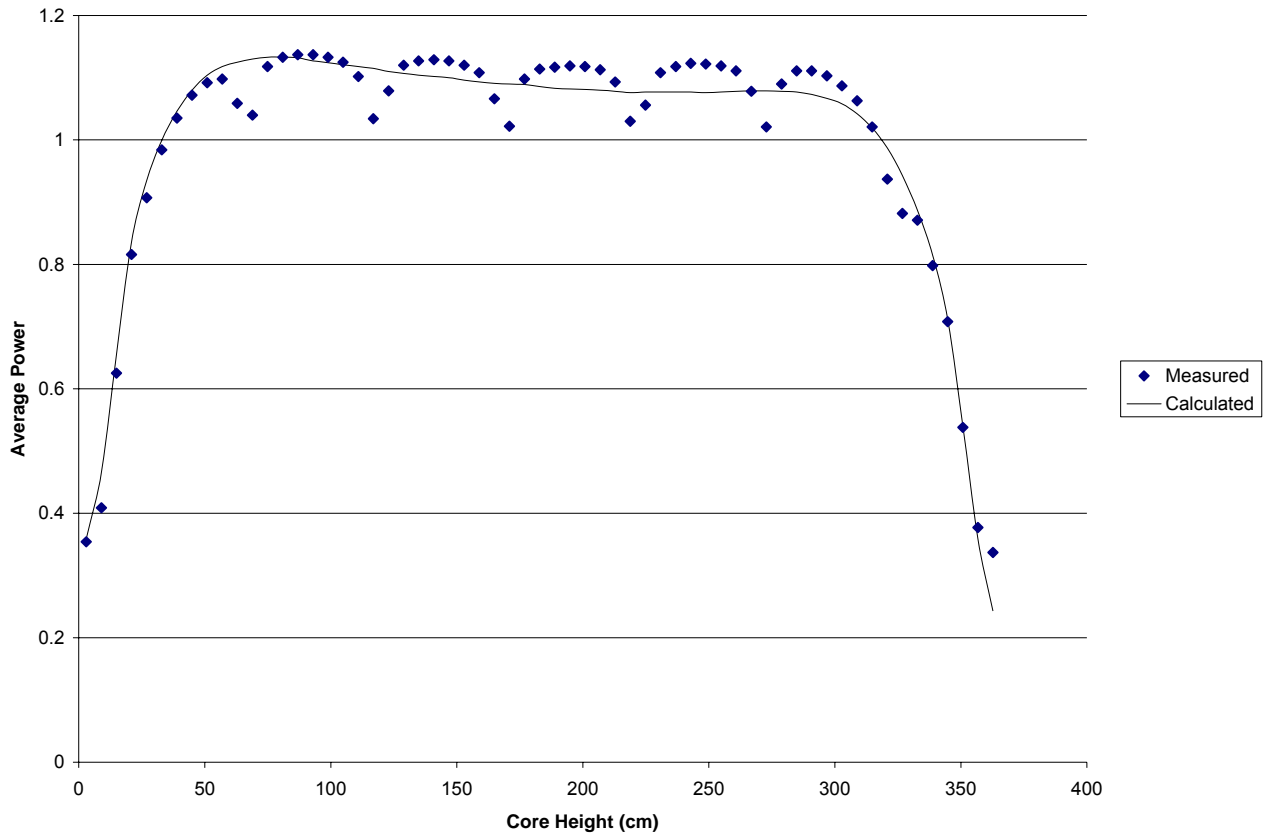
RMS = 0.037

Figure A-2.97: Plant A EOC 1 Axial Power Distribution

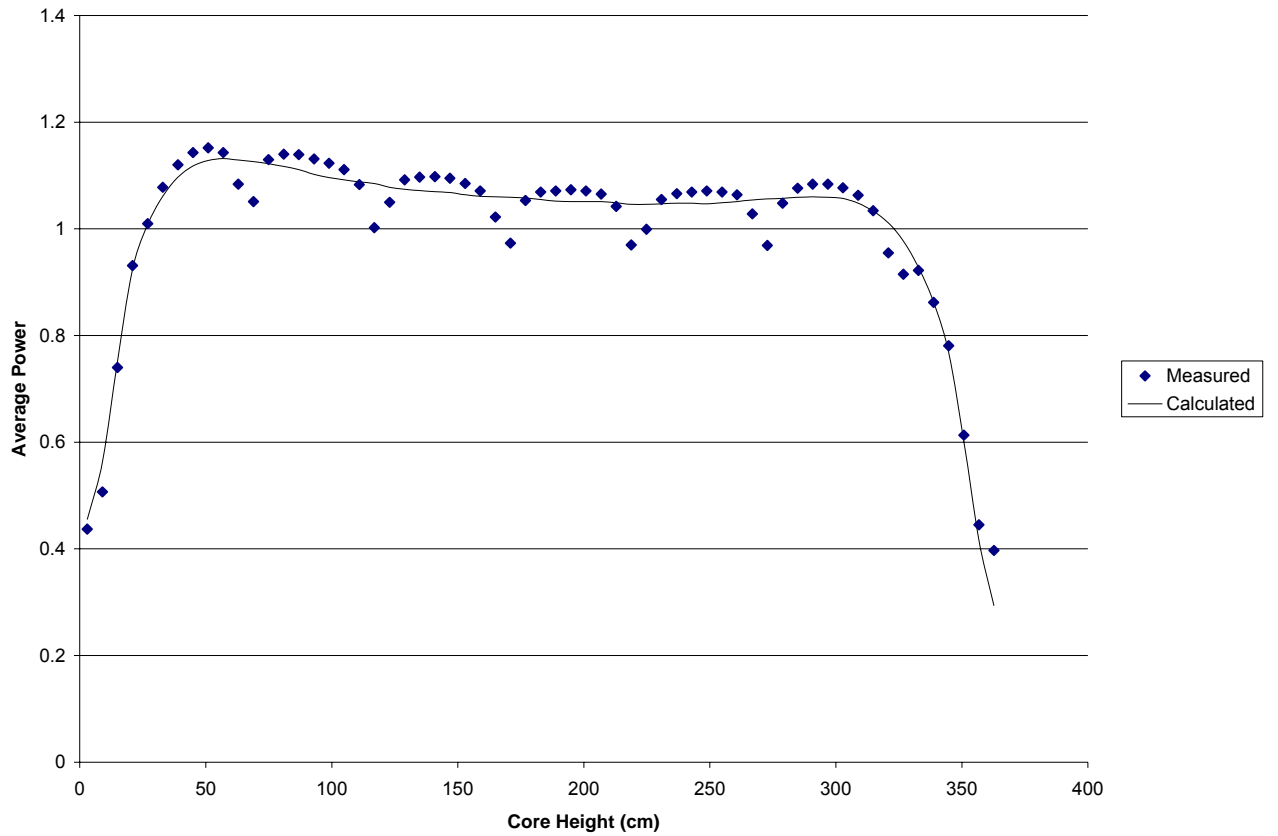
RMS = 0.044

Figure A-2.98: Plant A BOC 2 Axial Power Distribution

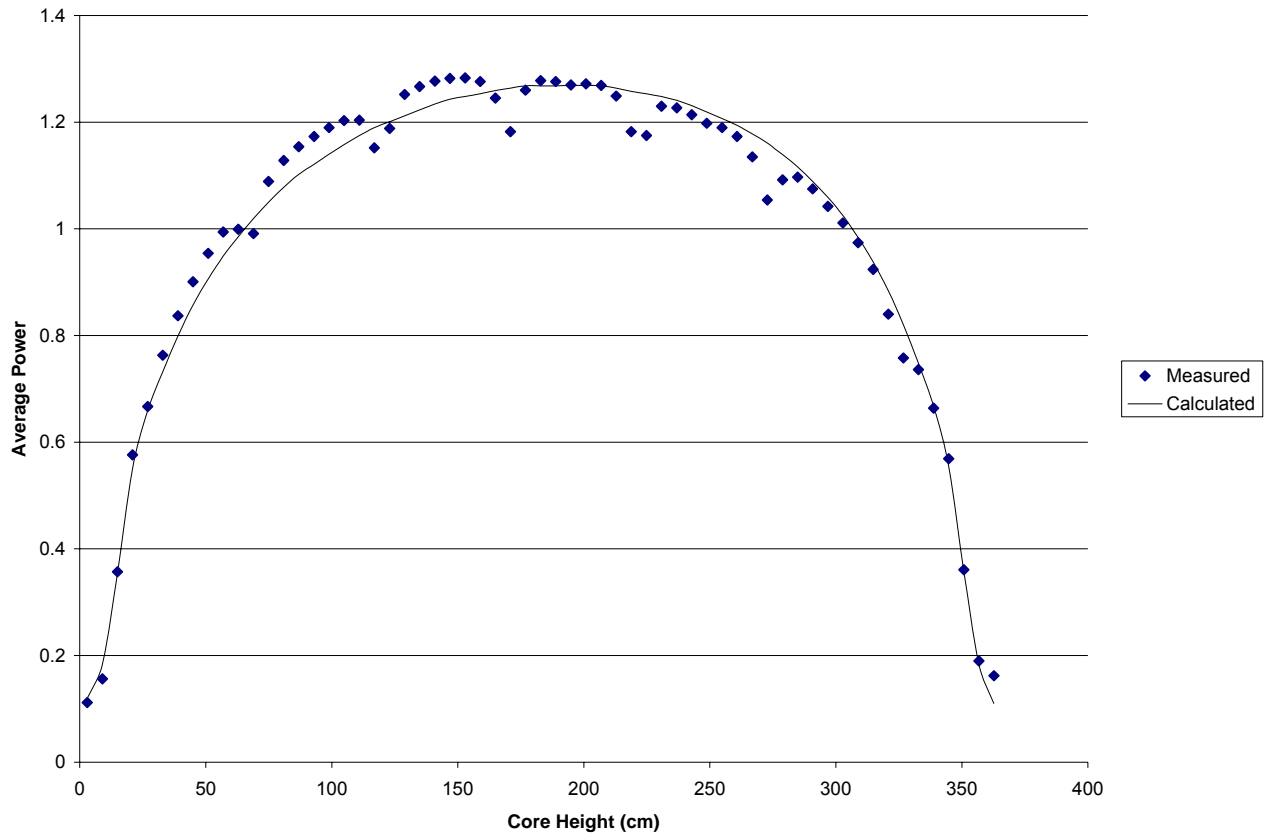
RMS = 0.035

Figure A-2.99: Plant A MOC 2 Axial Power Distribution

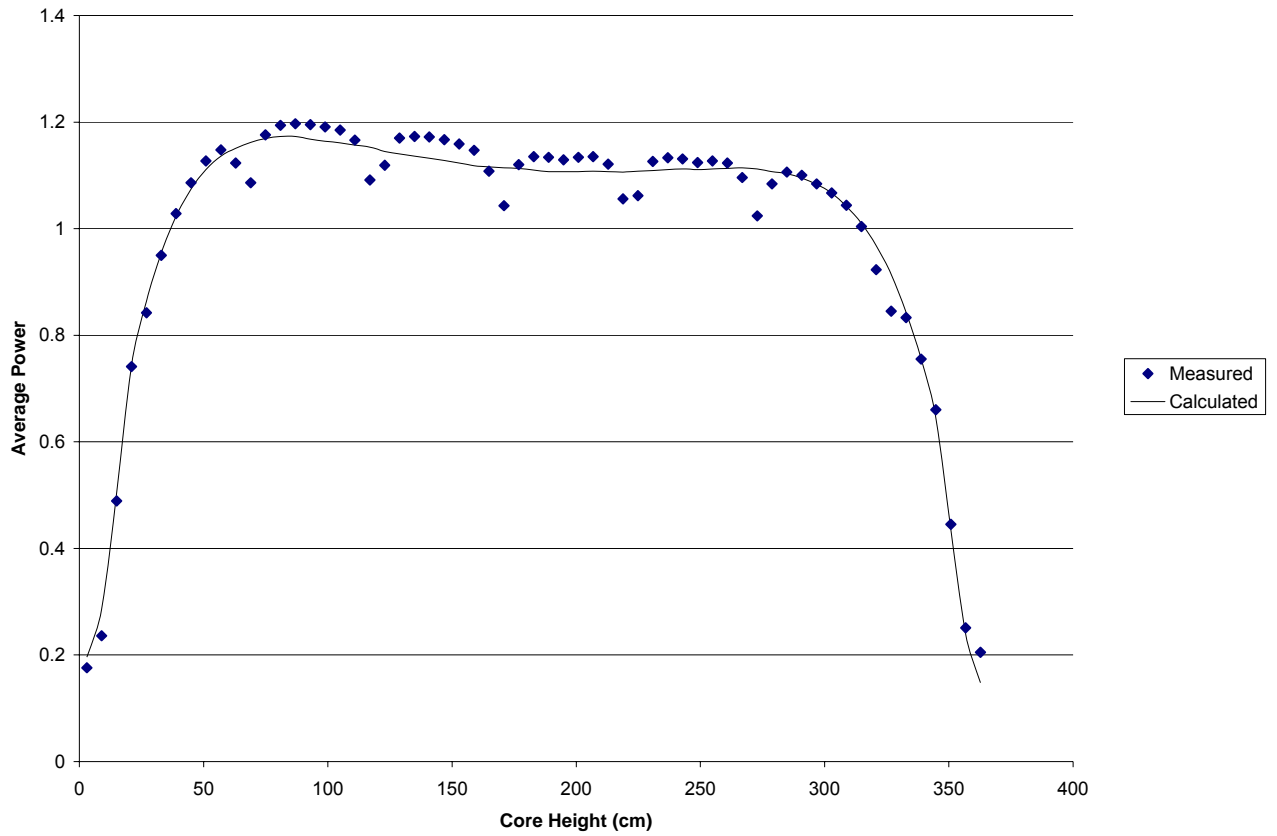
RMS = 0.036

Figure A-2.100: Plant A EOC 2 Axial Power Distribution

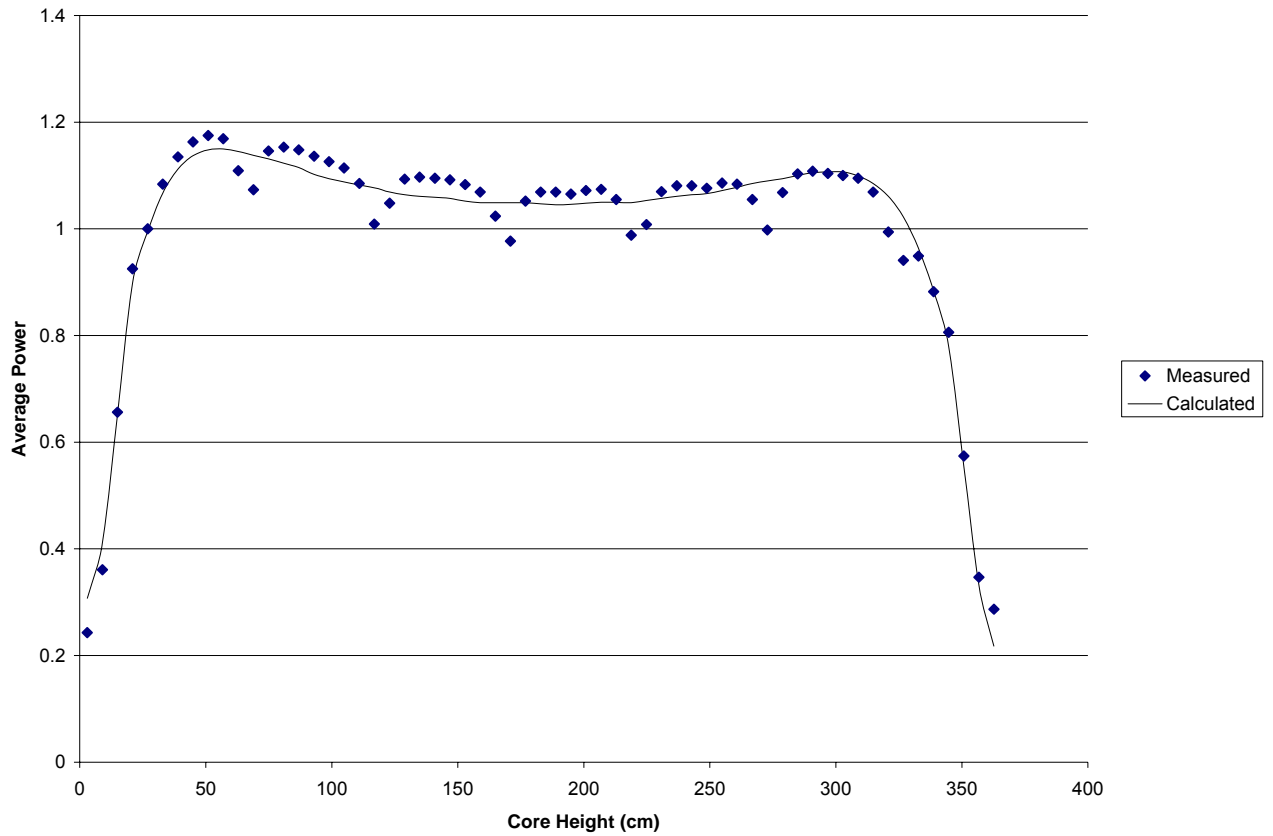
RMS = 0.036

Figure A-2.101: Plant A BOC 3 Axial Power Distribution

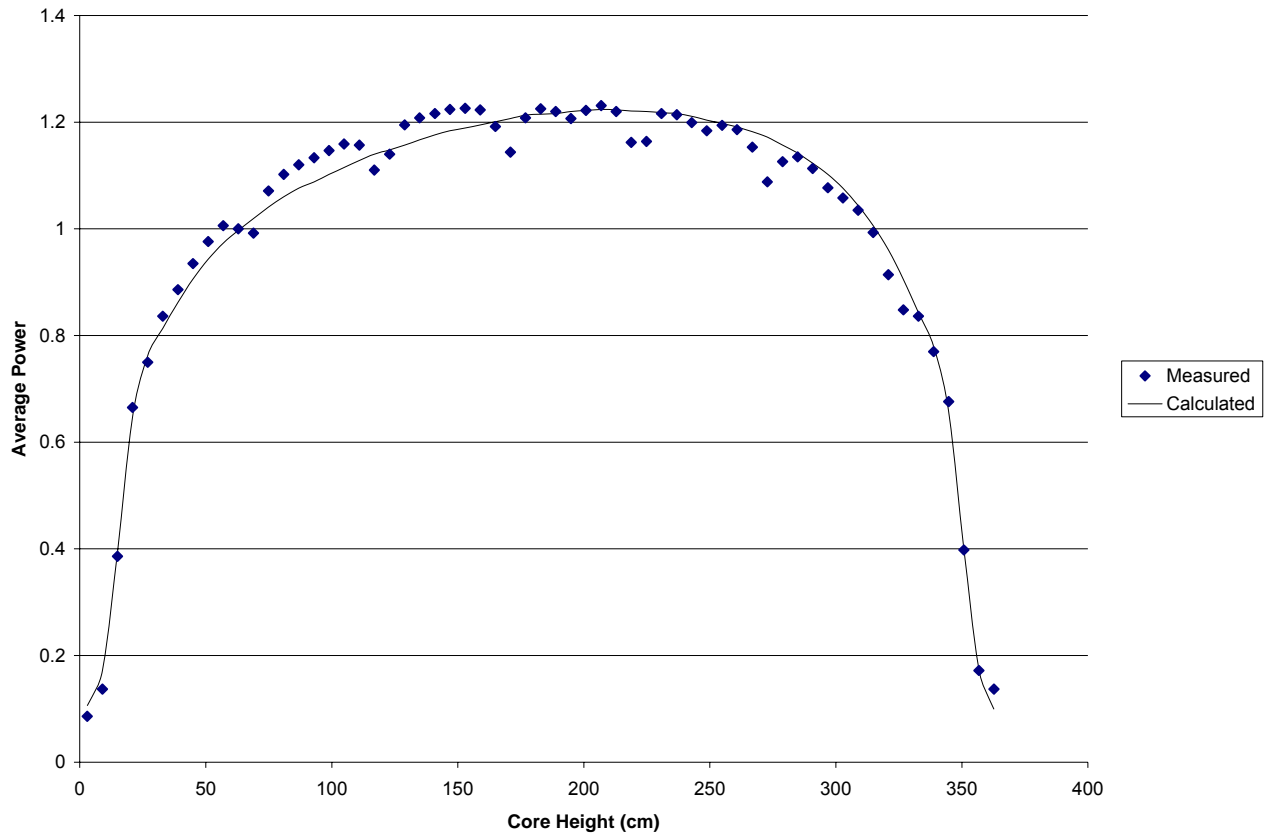
RMS = 0.037

Figure A-2.102: Plant A MOC 3 Axial Power Distribution

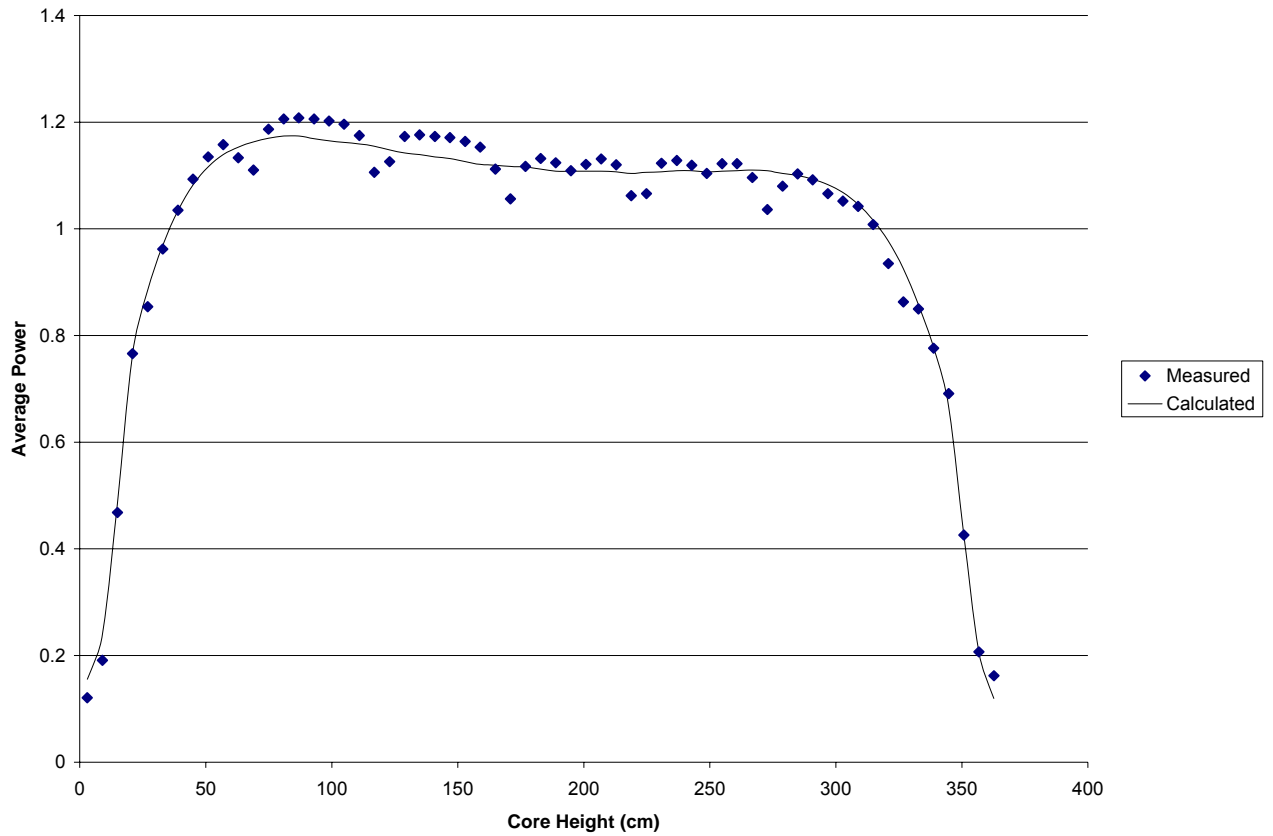
RMS = 0.031

Figure A-2.103: Plant A EOC 3 Axial Power Distribution

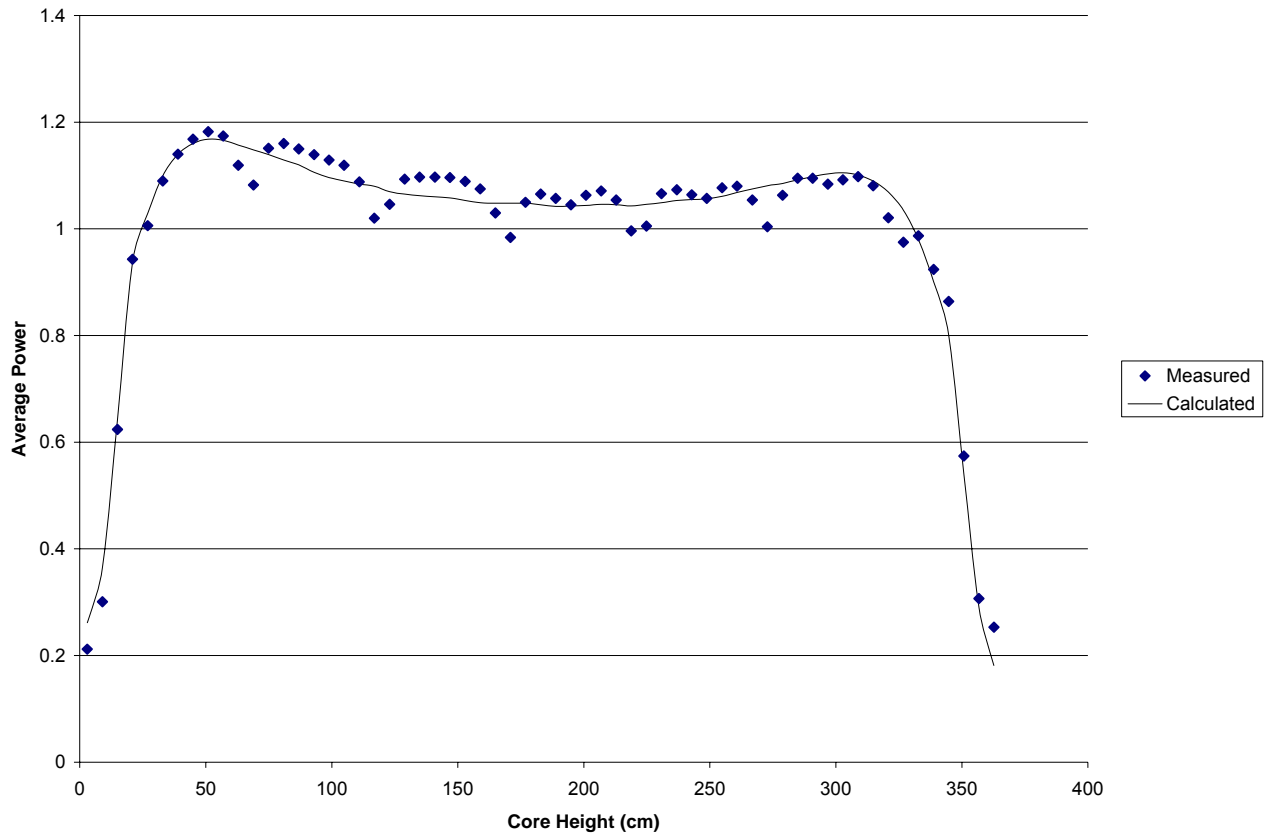
RMS = 0.035

Figure A-2.104: Plant A BOC 4 Axial Power Distribution

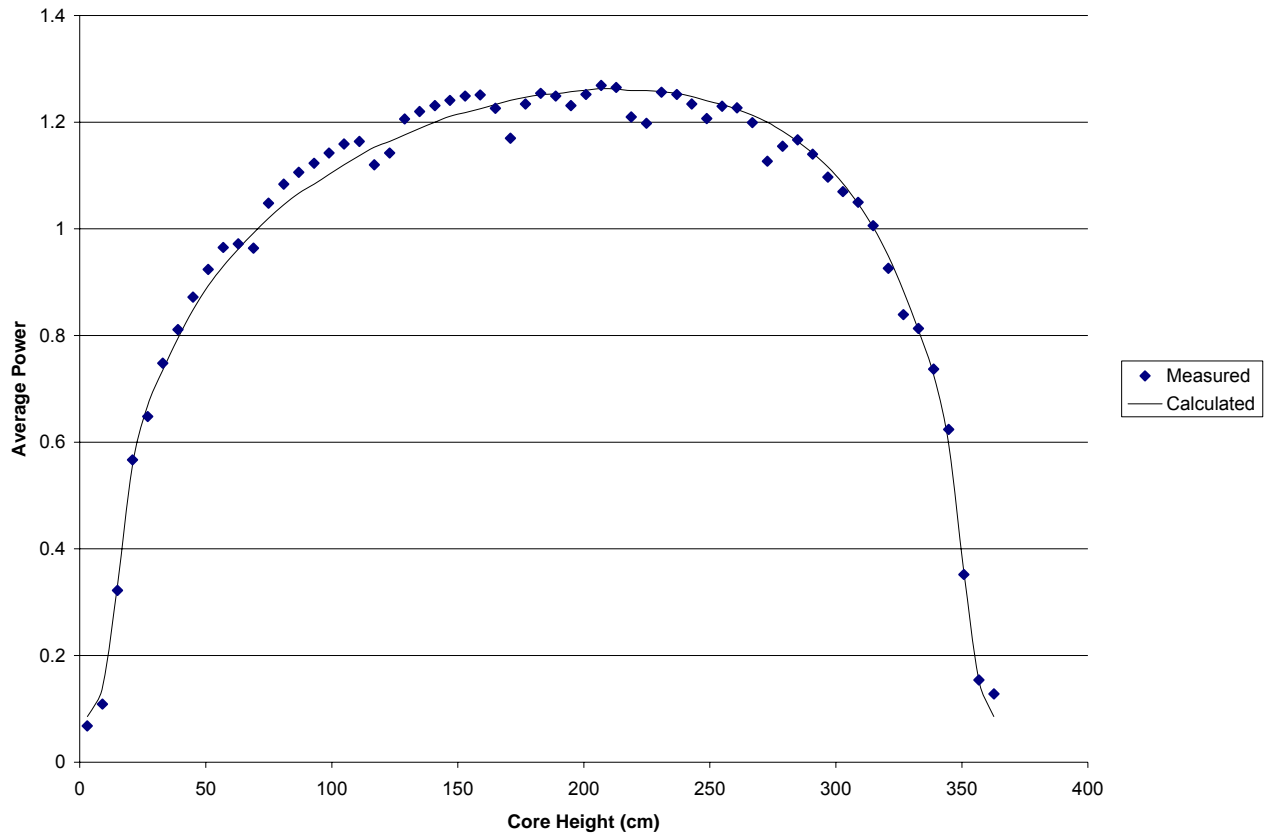
RMS = 0.031

Figure A-2.105: Plant A MOC 4 Axial Power Distribution

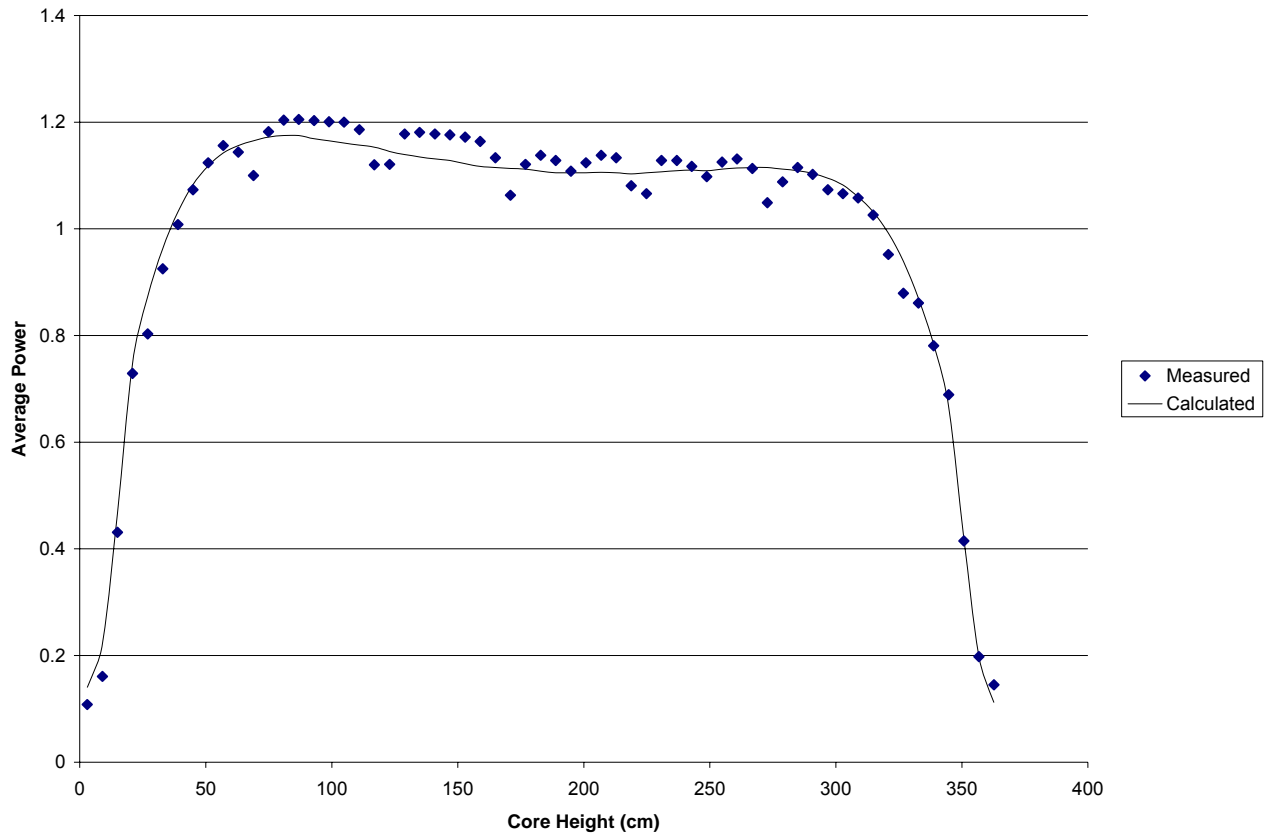
RMS = 0.029

Figure A-2.106: Plant A EOC 4 Axial Power Distribution

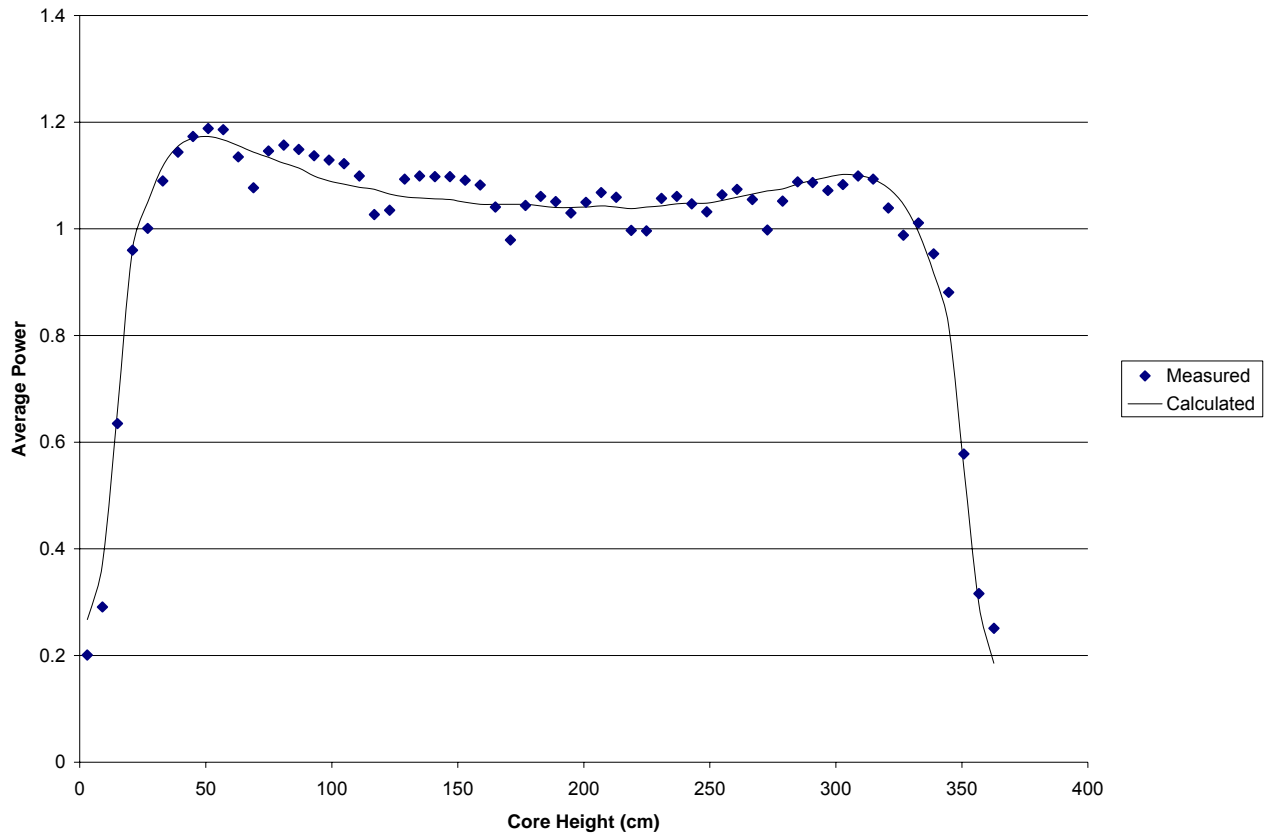
RMS = 0.033

Figure A-2.107: Plant A BOC 5 Axial Power Distribution

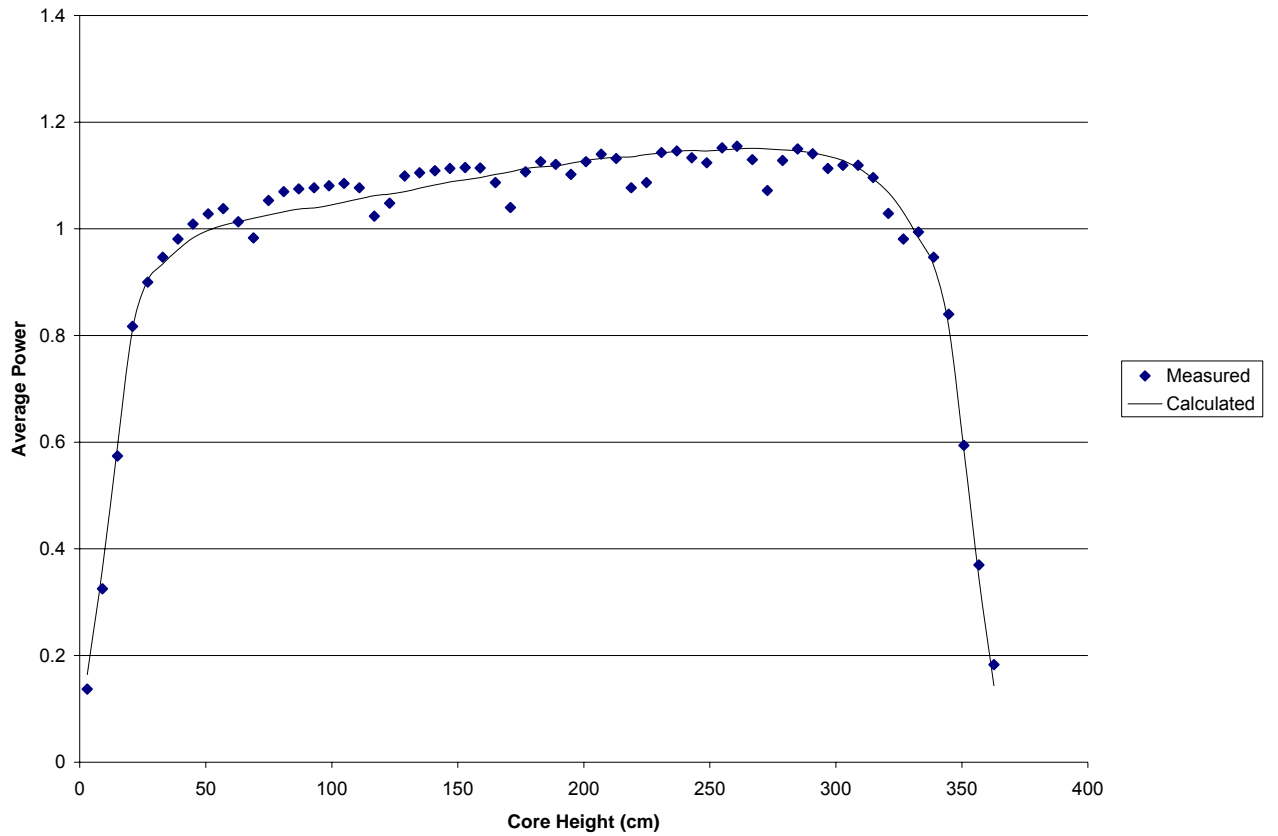
RMS = 0.028

Figure A-2.108: Plant A MOC 5 Axial Power Distribution

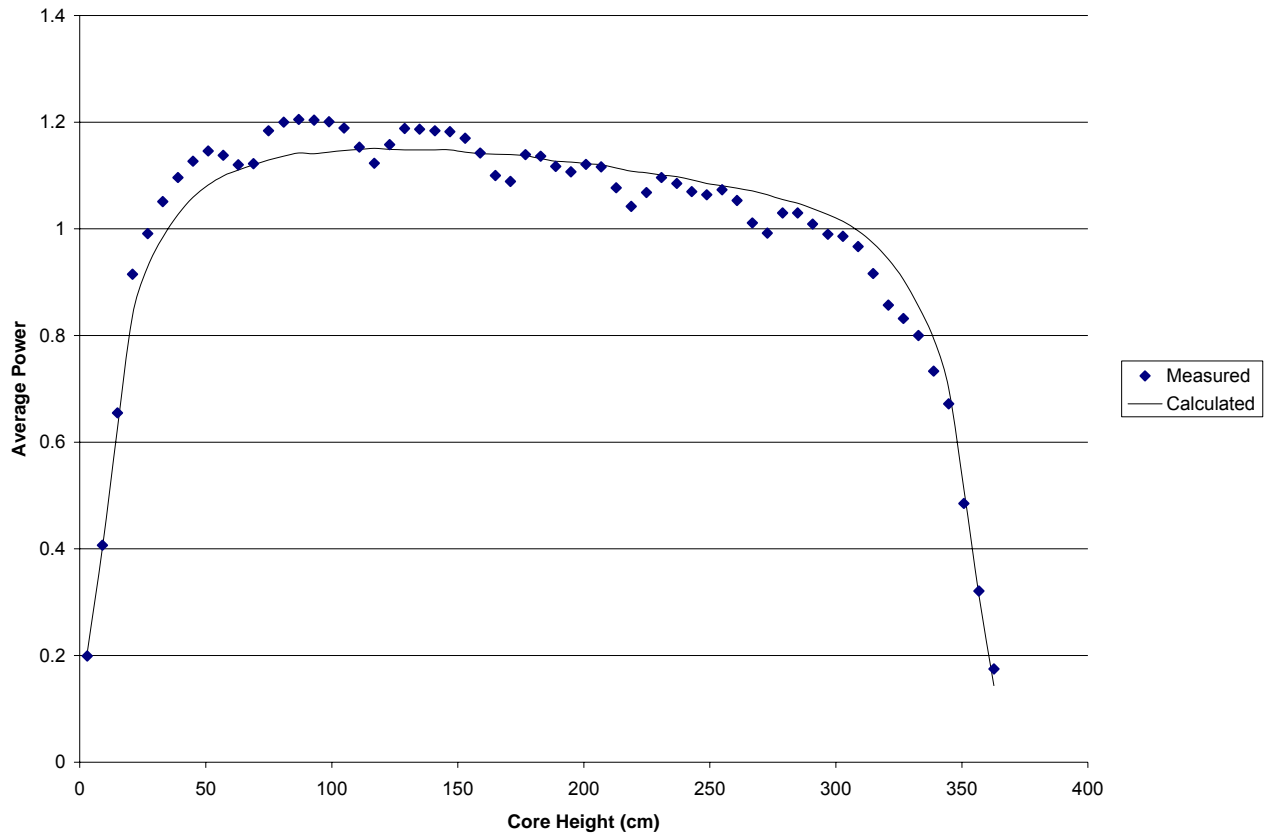
RMS = 0.032

Figure A-2.109: Plant A EOC 5 Axial Power Distribution

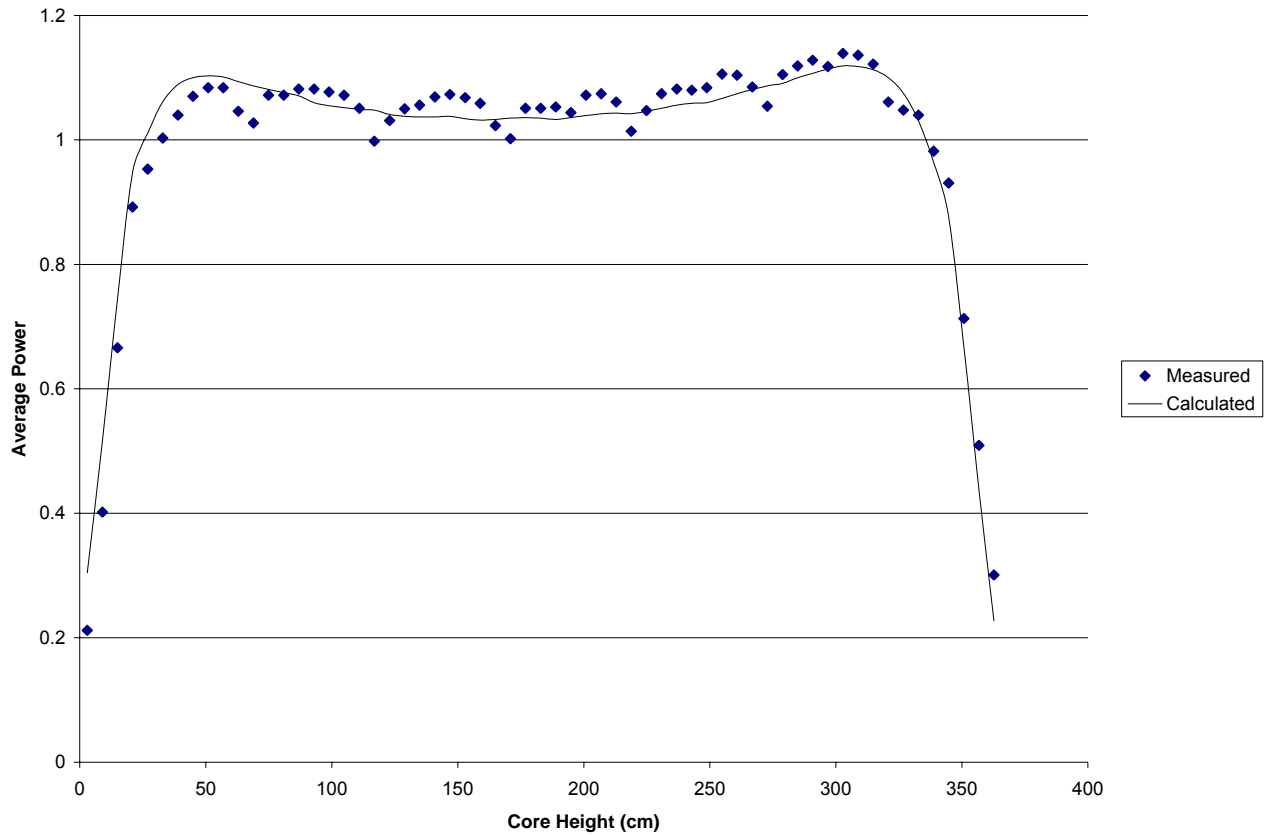
RMS = 0.035

Figure A-2.110: Plant A BOC 6 Axial Power Distribution

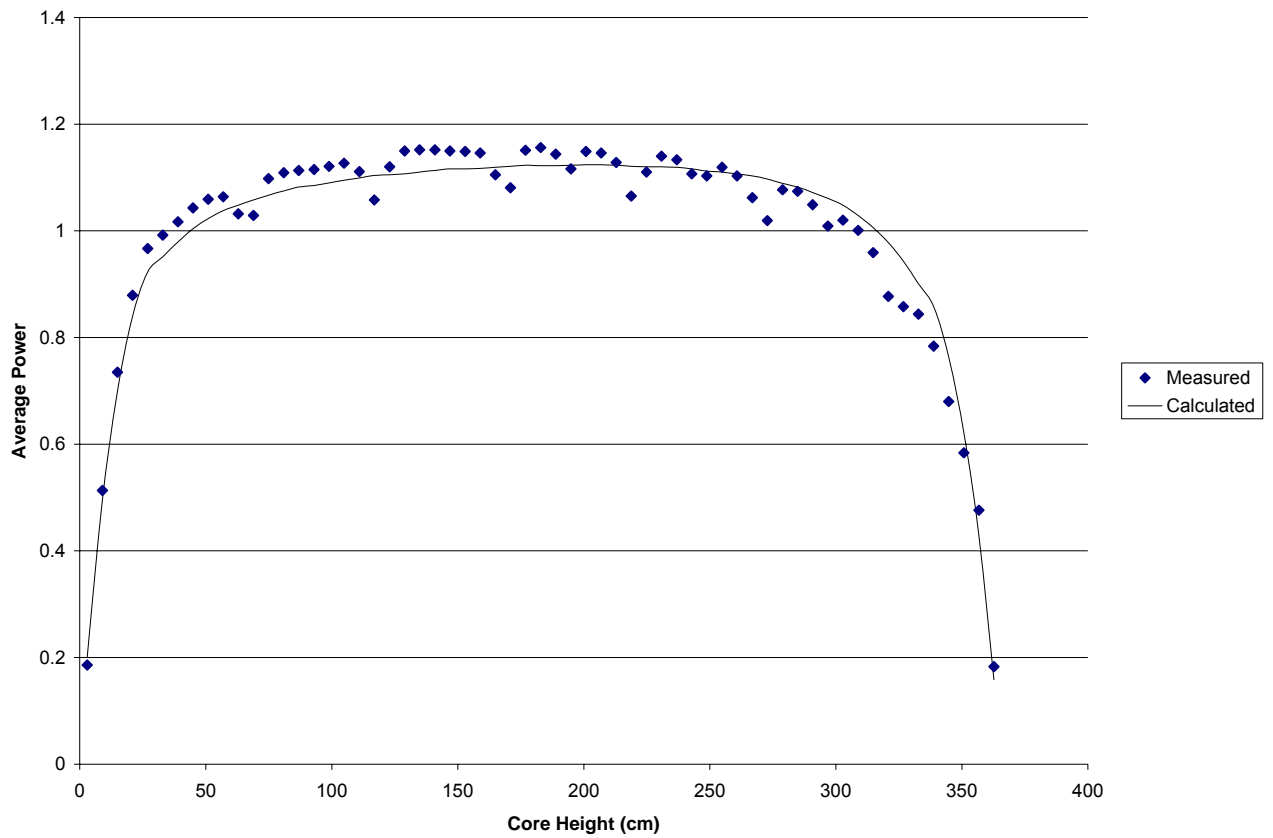
RMS = 0.028

Figure A-2.111: Plant A MOC 6 Axial Power Distribution

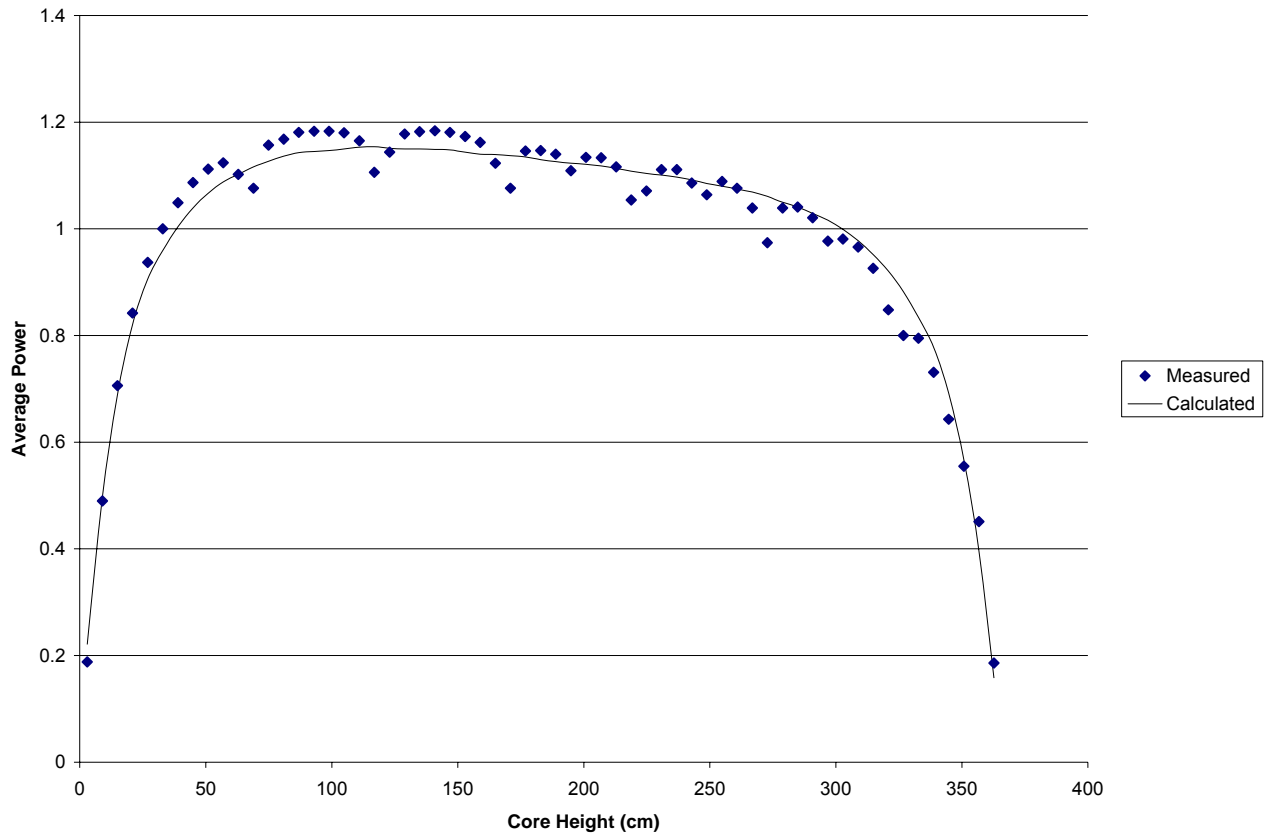
RMS = 0.043

Figure A-2.112: Plant A EOC 6 Axial Power Distribution

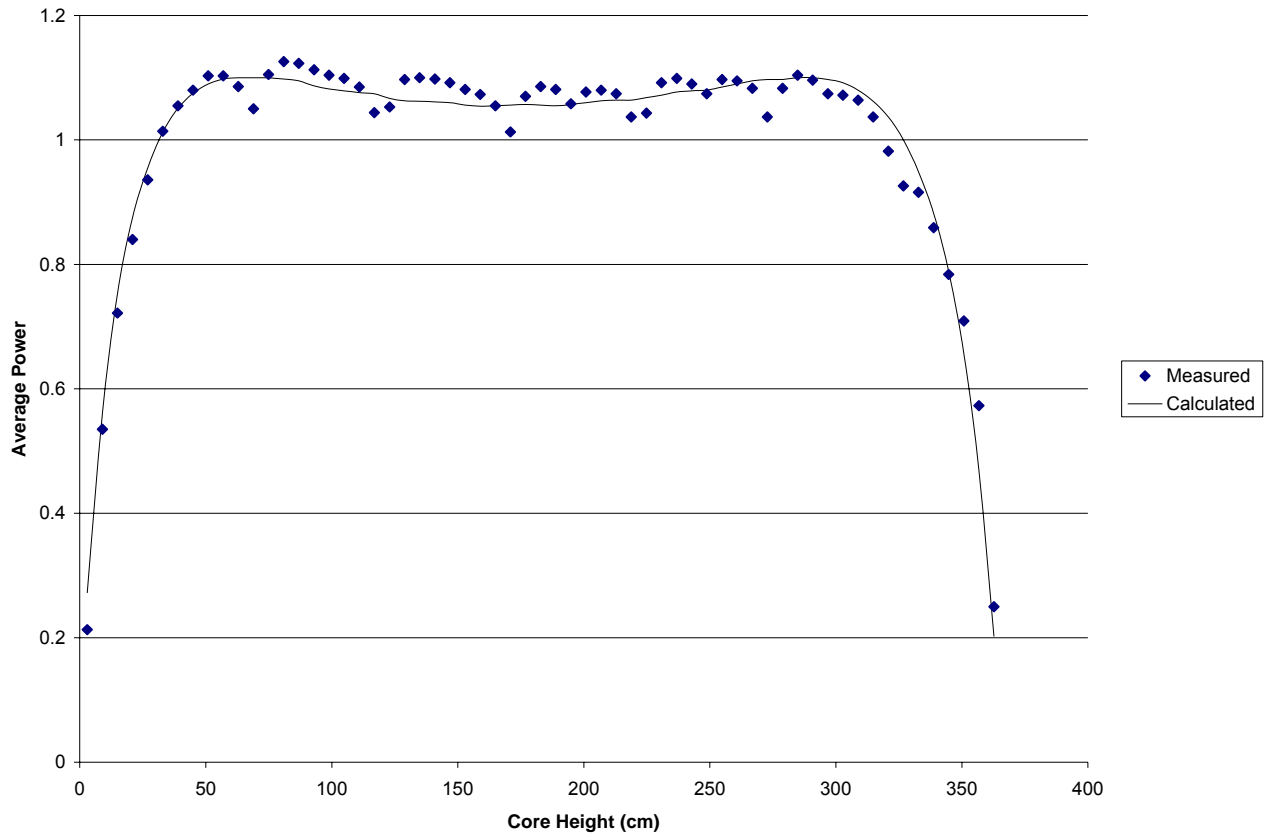
RMS = 0.038

Figure A-2.113: Plant A BOC 7 Axial Power Distribution

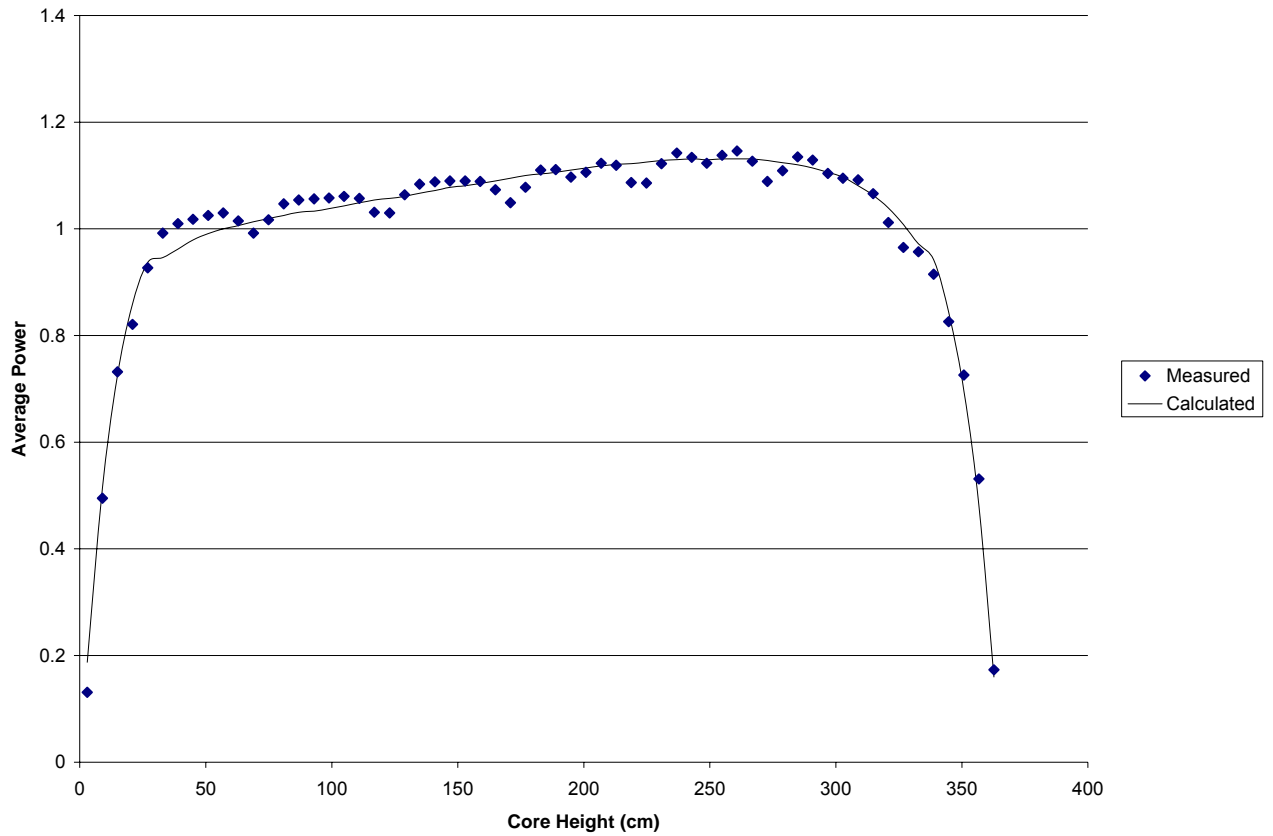
RMS = 0.039

Figure A-2.114: Plant A MOC 7 Axial Power Distribution

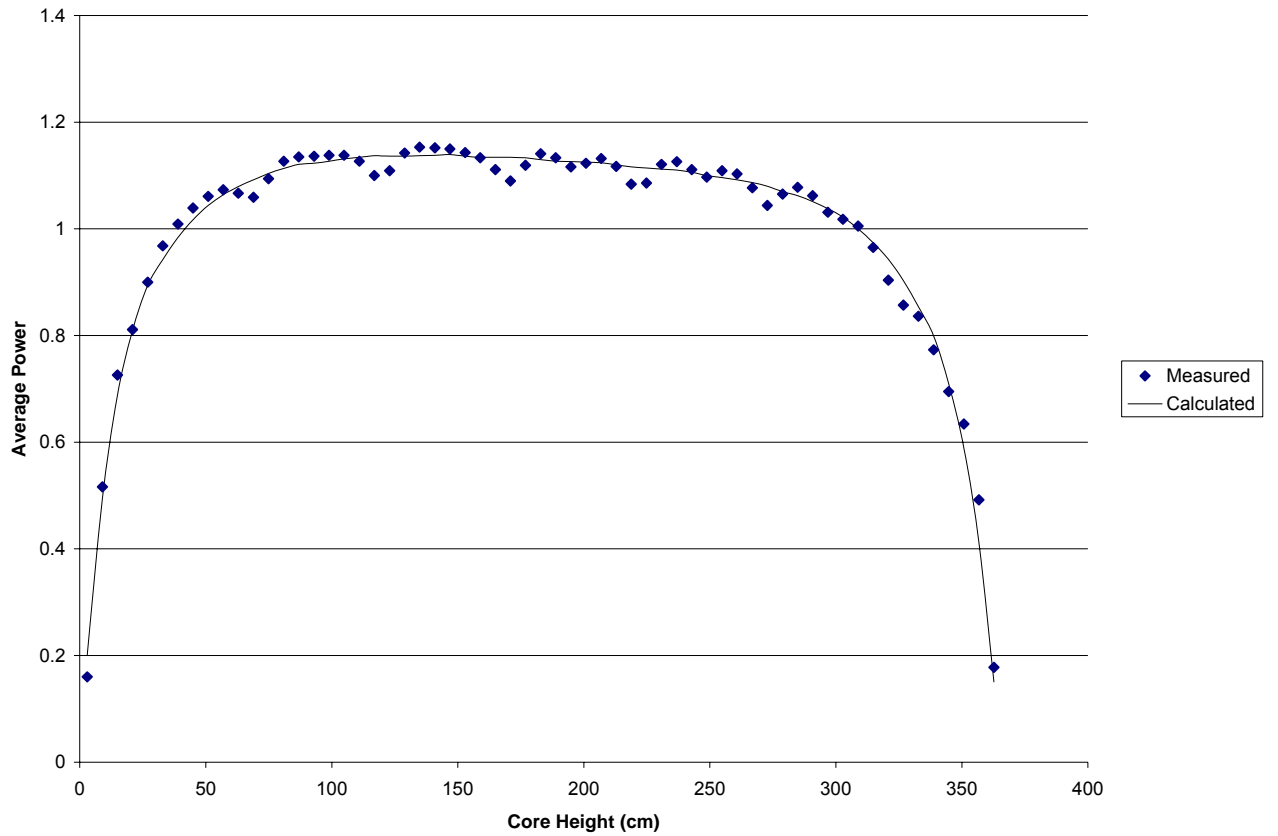
RMS = 0.034

Figure A-2.115: Plant A EOC 7 Axial Power Distribution

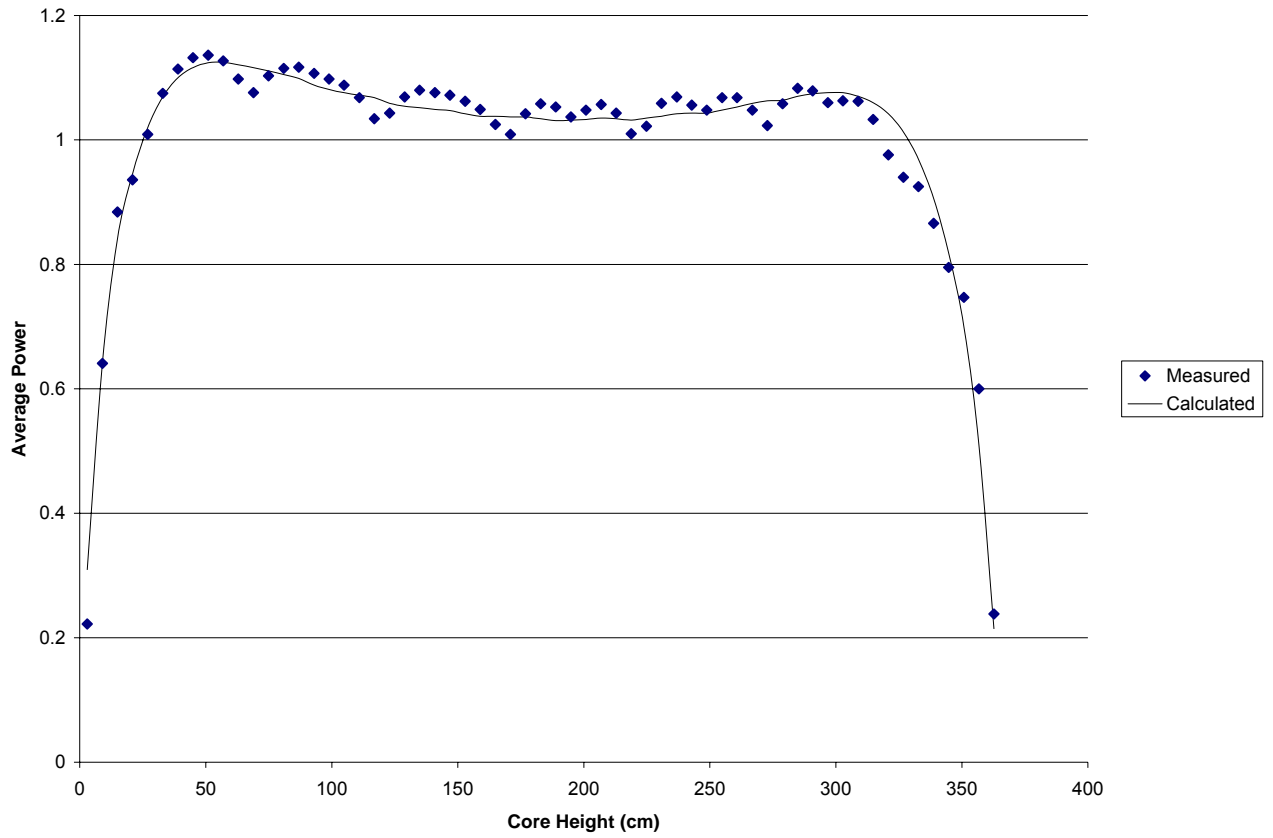
RMS = 0.031

Figure A-2.116: Plant A BOC 8 Axial Power Distribution

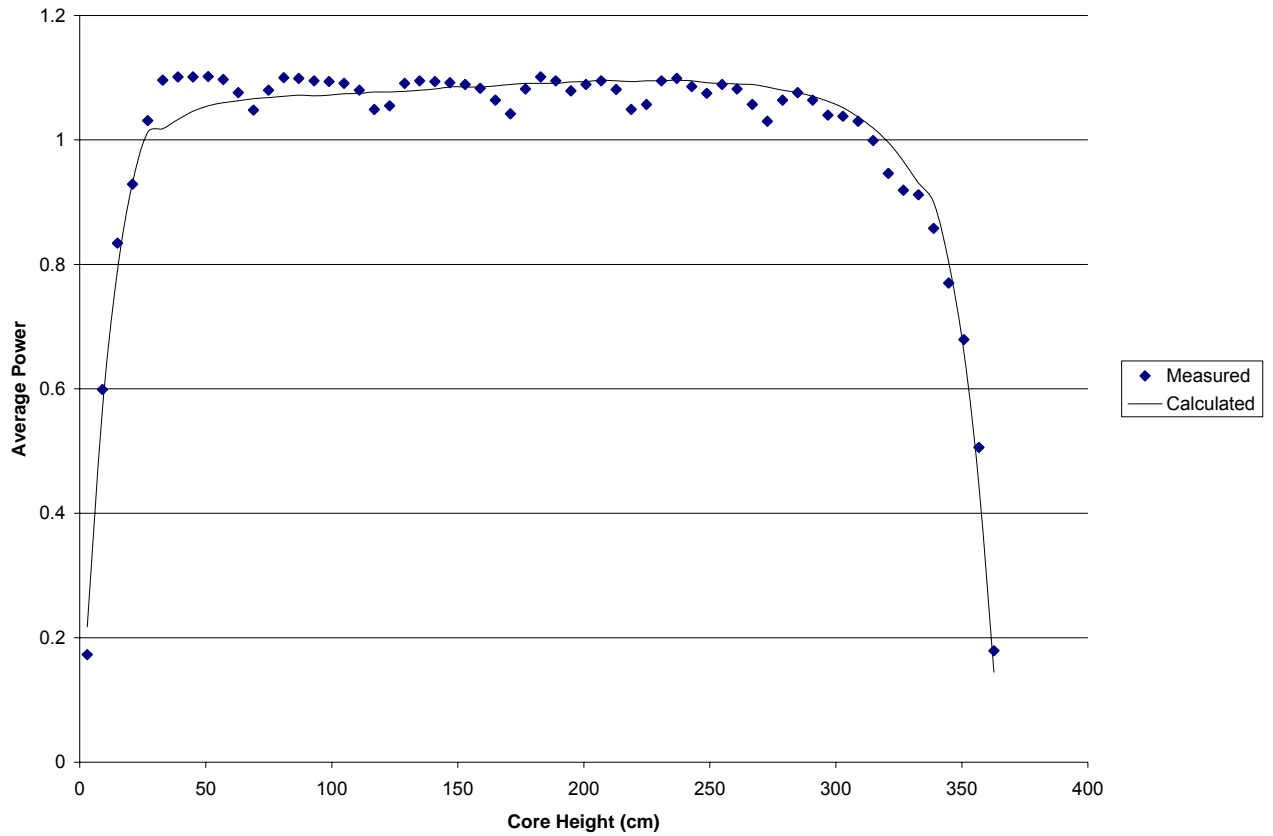
RMS = 0.024

Figure A-2.117: Plant A MOC 8 Axial Power Distribution

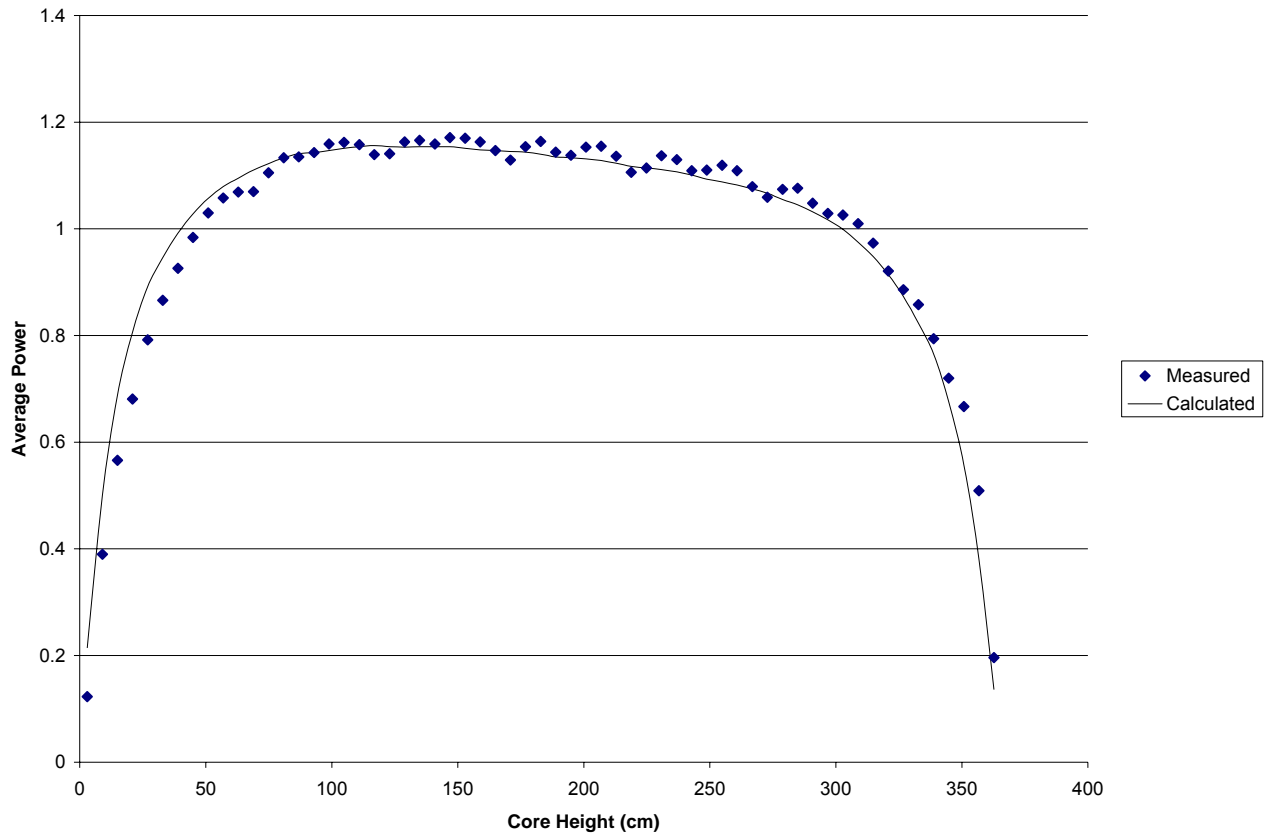
RMS = 0.023

Figure A-2.118: Plant A EOC 8 Axial Power Distribution

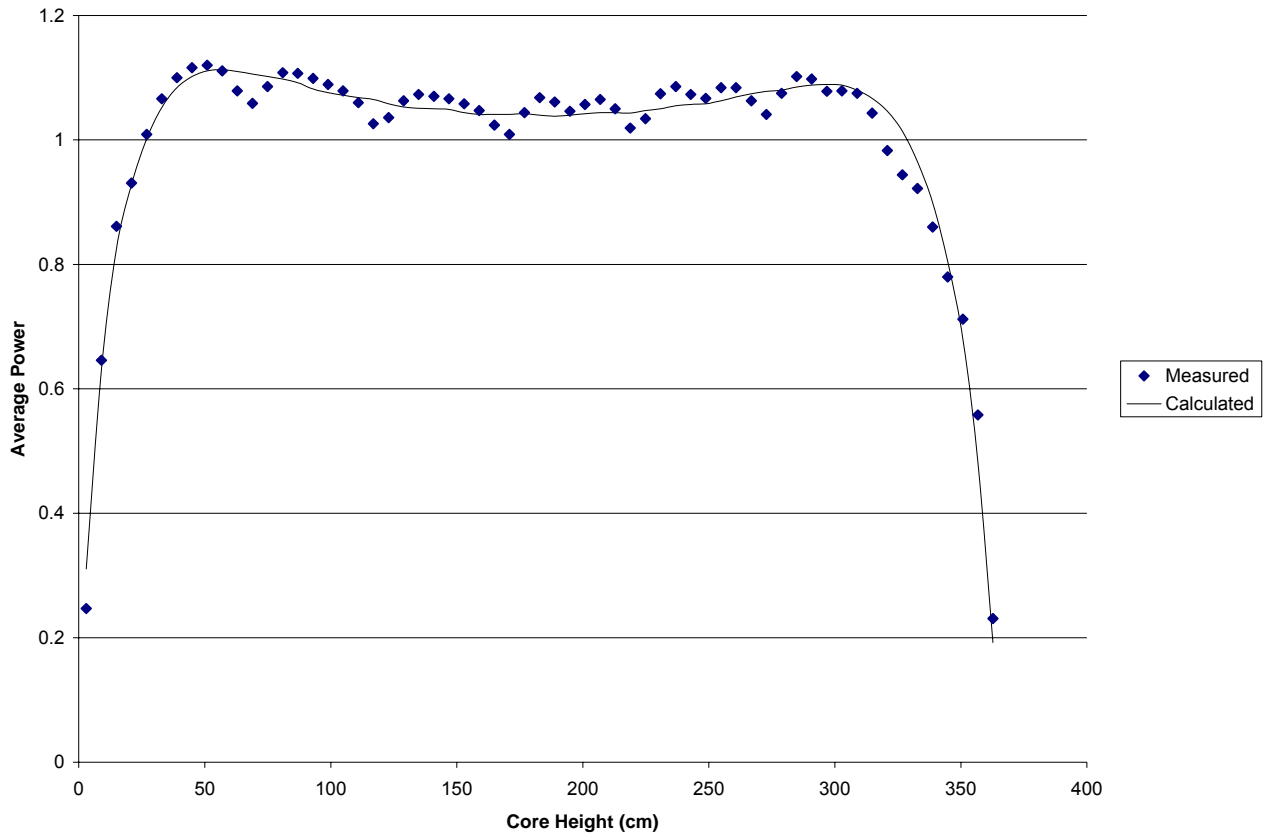
RMS = 0.029

Figure A-2.119: Plant A BOC 9 Axial Power Distribution

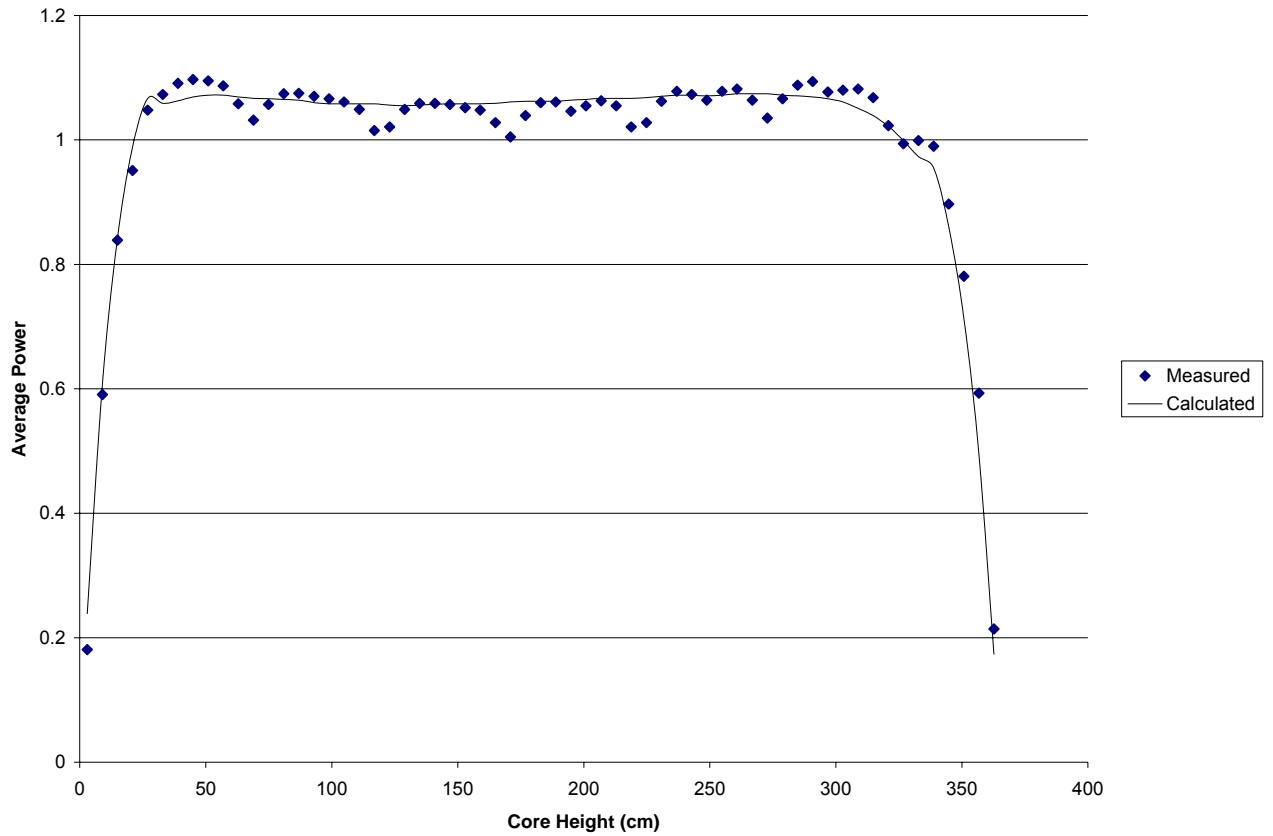
RMS = 0.030

Figure A-2.120: Plant A MOC 9 Axial Power Distribution

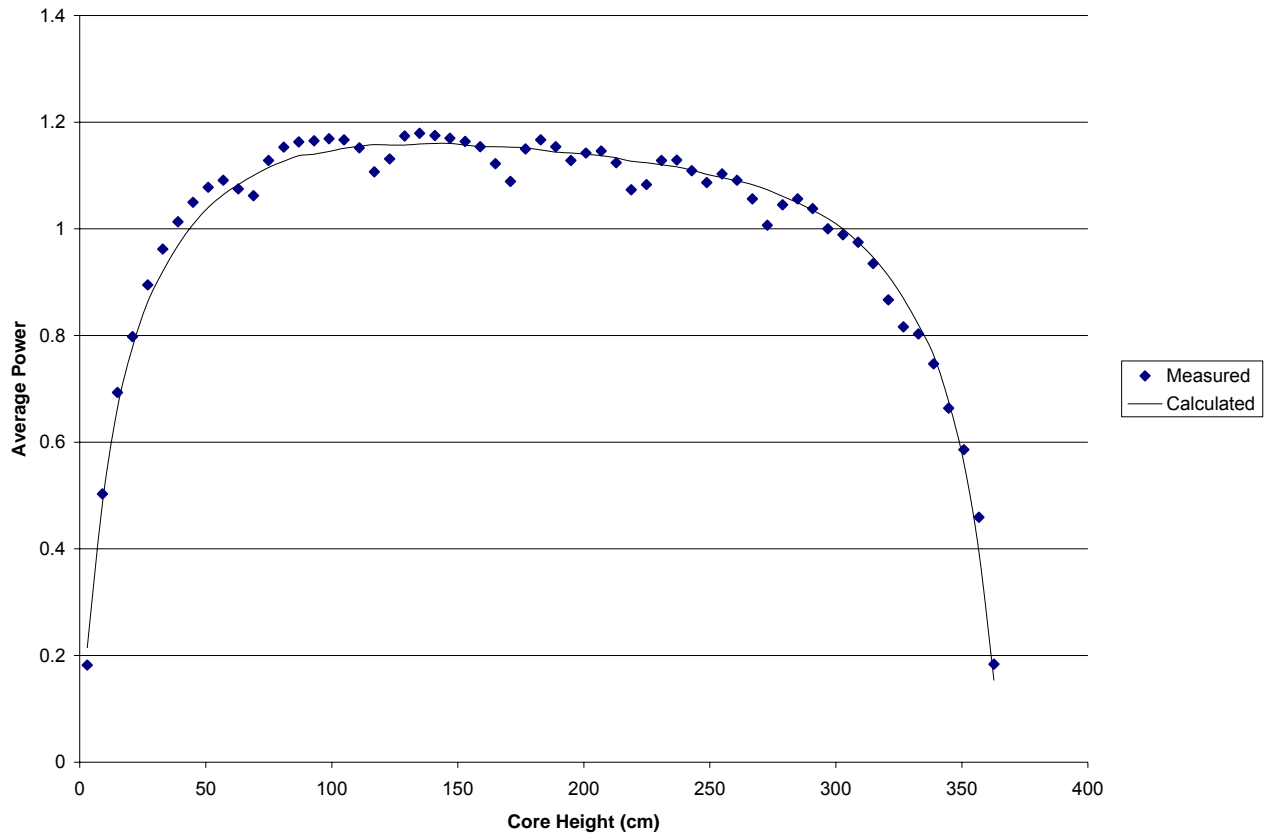
RMS = 0.045

Figure A-2.121: Plant A EOC 9 Axial Power Distribution

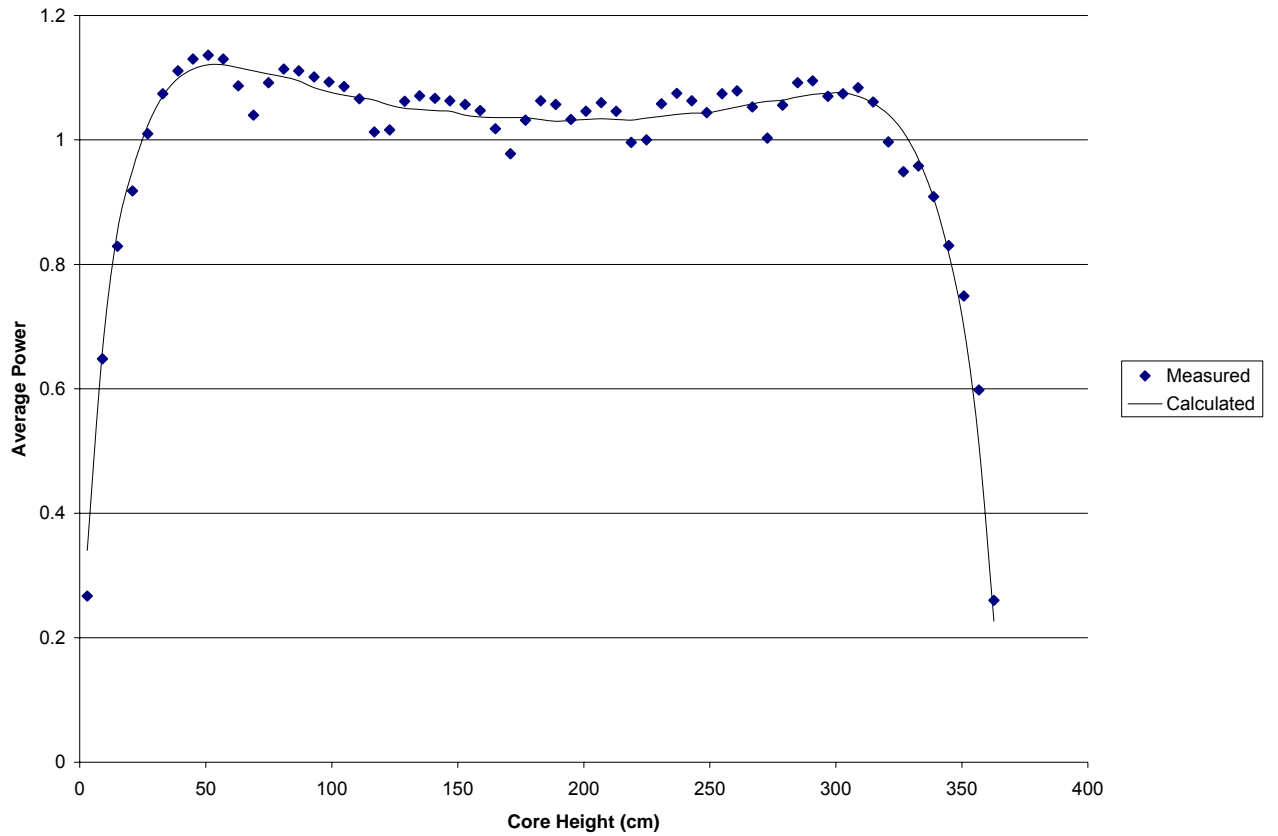
RMS = 0.027

Figure A-2.122: Plant A BOC 10 Axial Power Distribution

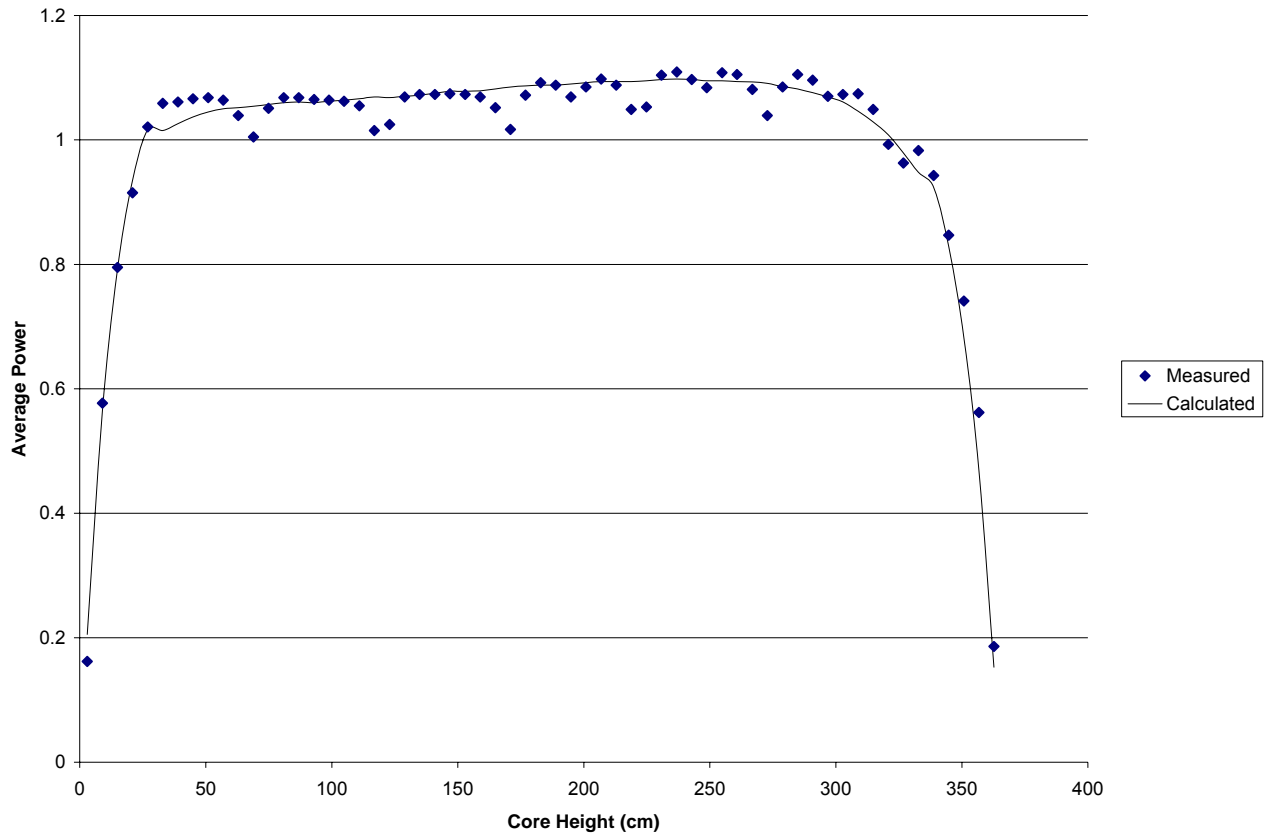
RMS = 0.028

Figure A-2.123: Plant A MOC 10 Axial Power Distribution

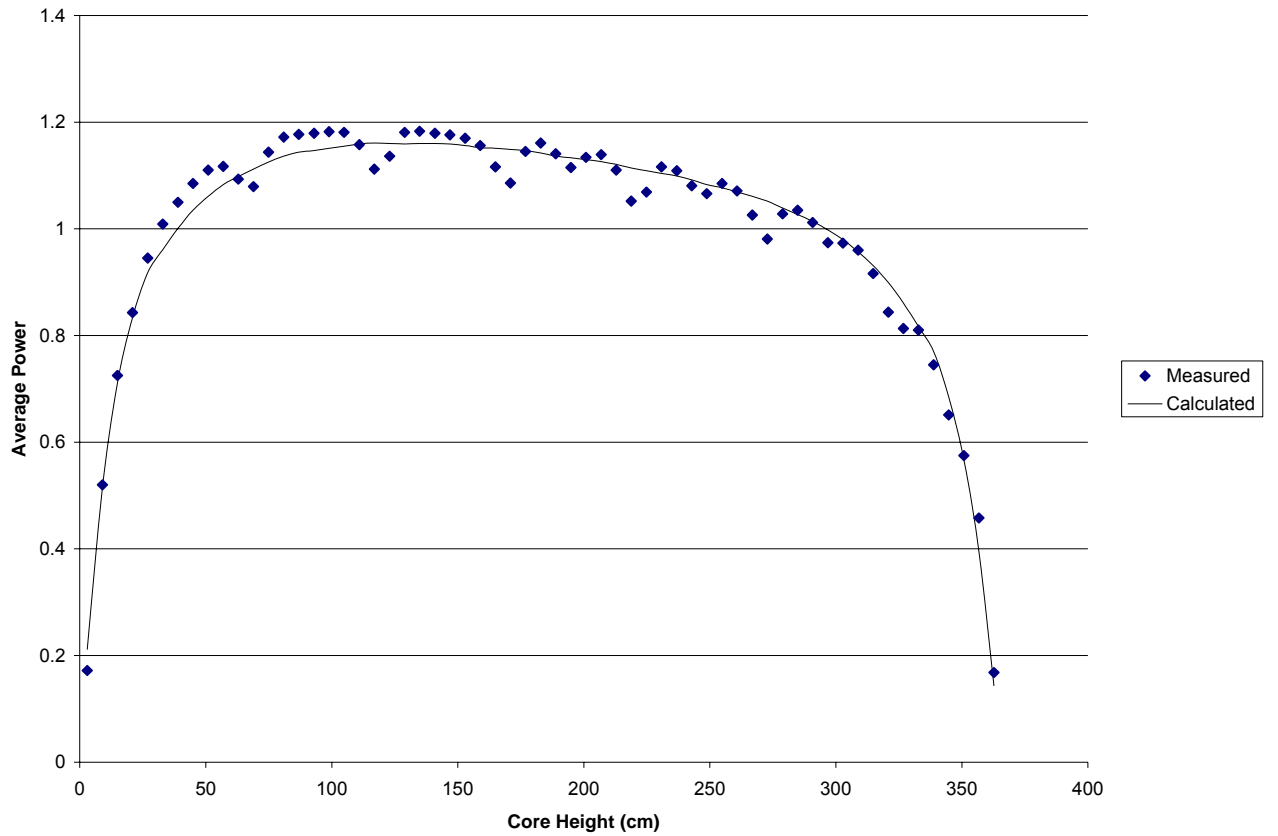
RMS = 0.028

Figure A-2.124: Plant A EOC 10 Axial Power Distribution

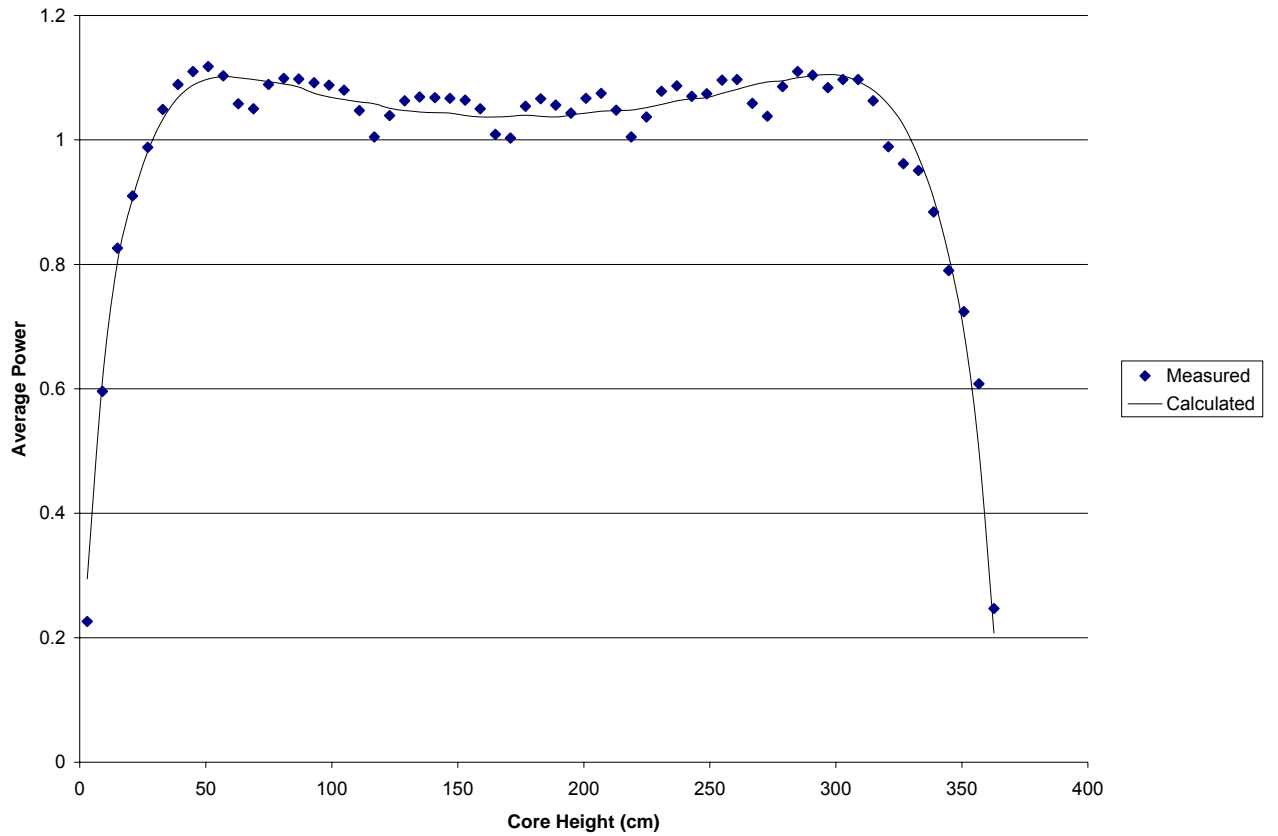
RMS = 0.030

Figure A-2.125: Plant A BOC 11 Axial Power Distribution

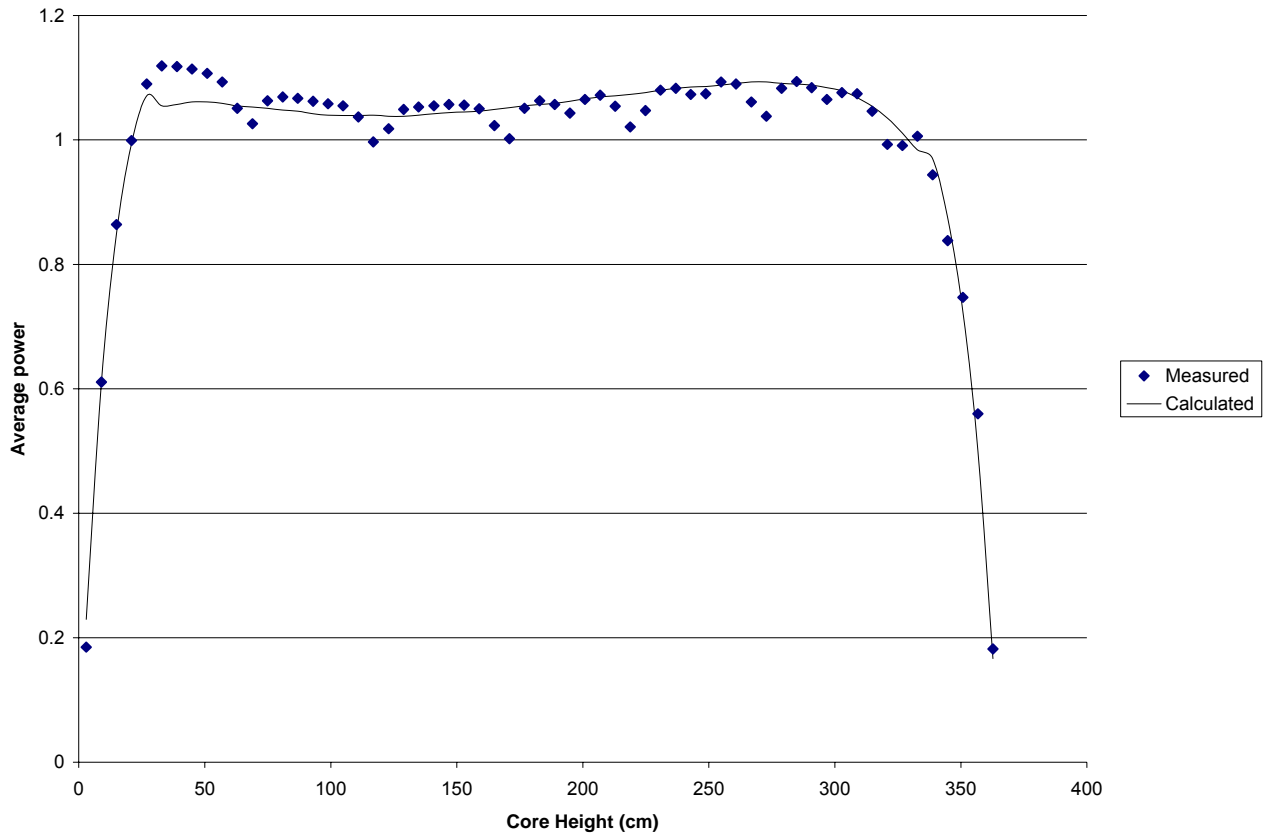
RMS = 0.028

Figure A-2.126: Plant A MOC 11 Axial Power Distribution

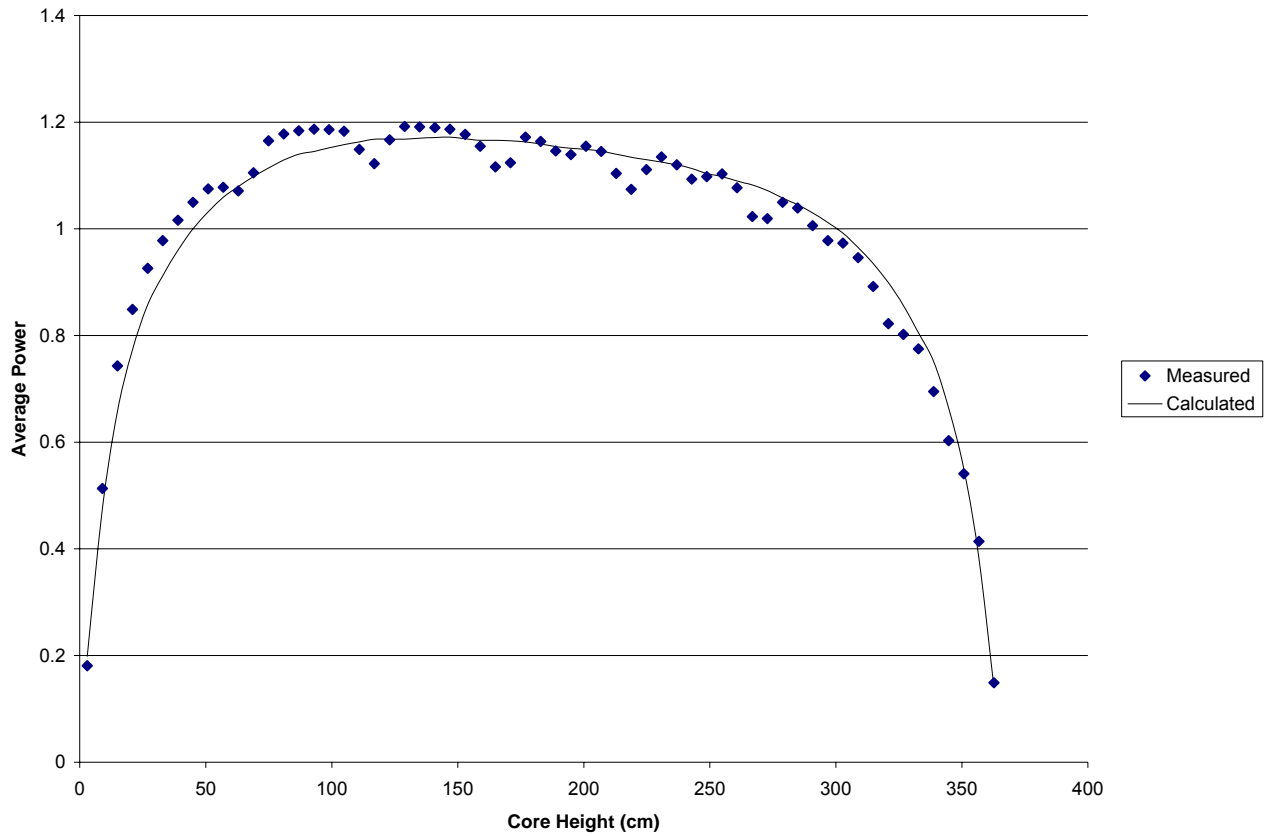
RMS = 0.030

Figure A-2.127: Plant A EOC 11 Axial Power Distribution

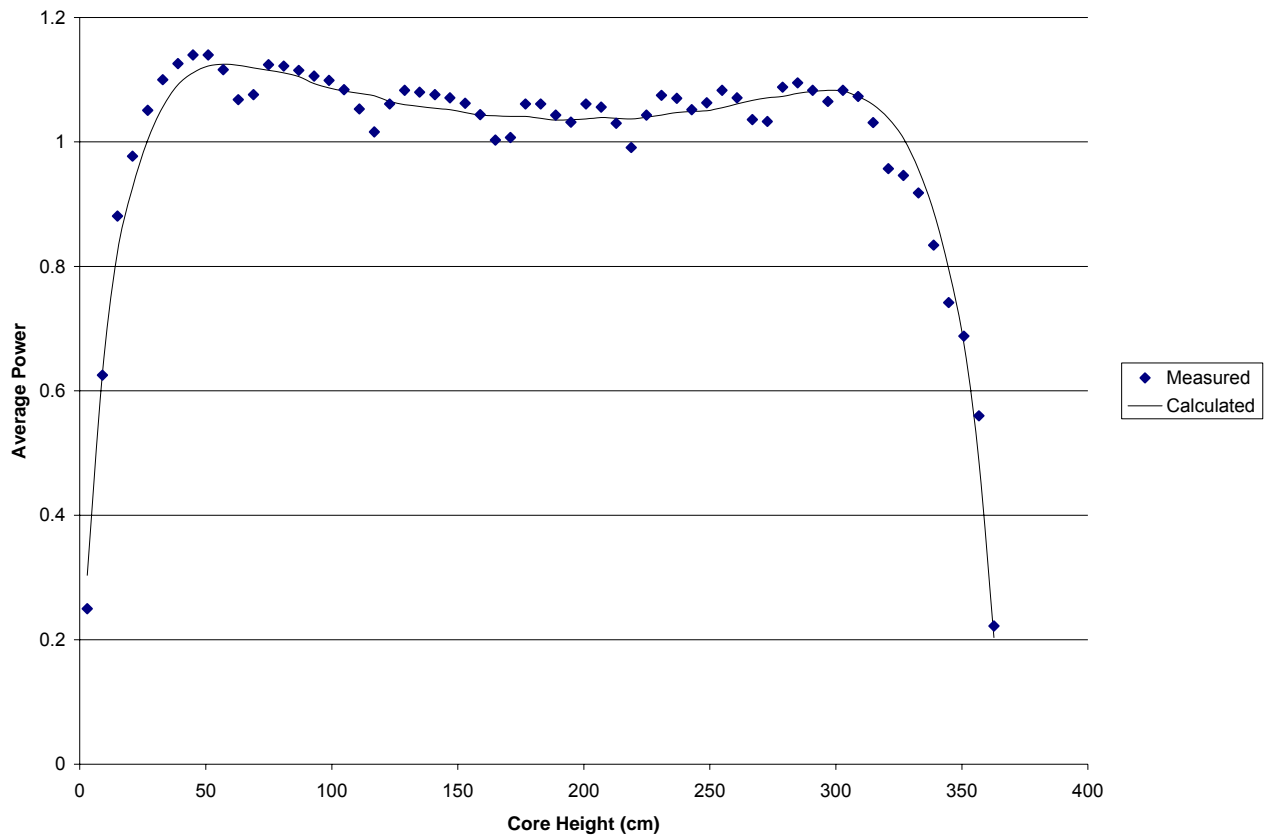
RMS = 0.030

Figure A-2.128: Plant A BOC 12 Axial Power Distribution

RMS = 0.027

Figure A-2.129: Plant A MOC 12 Axial Power Distribution

RMS = 0.037

Figure A-2.130: Plant A EOC 12 Axial Power Distribution

RMS = 0.032

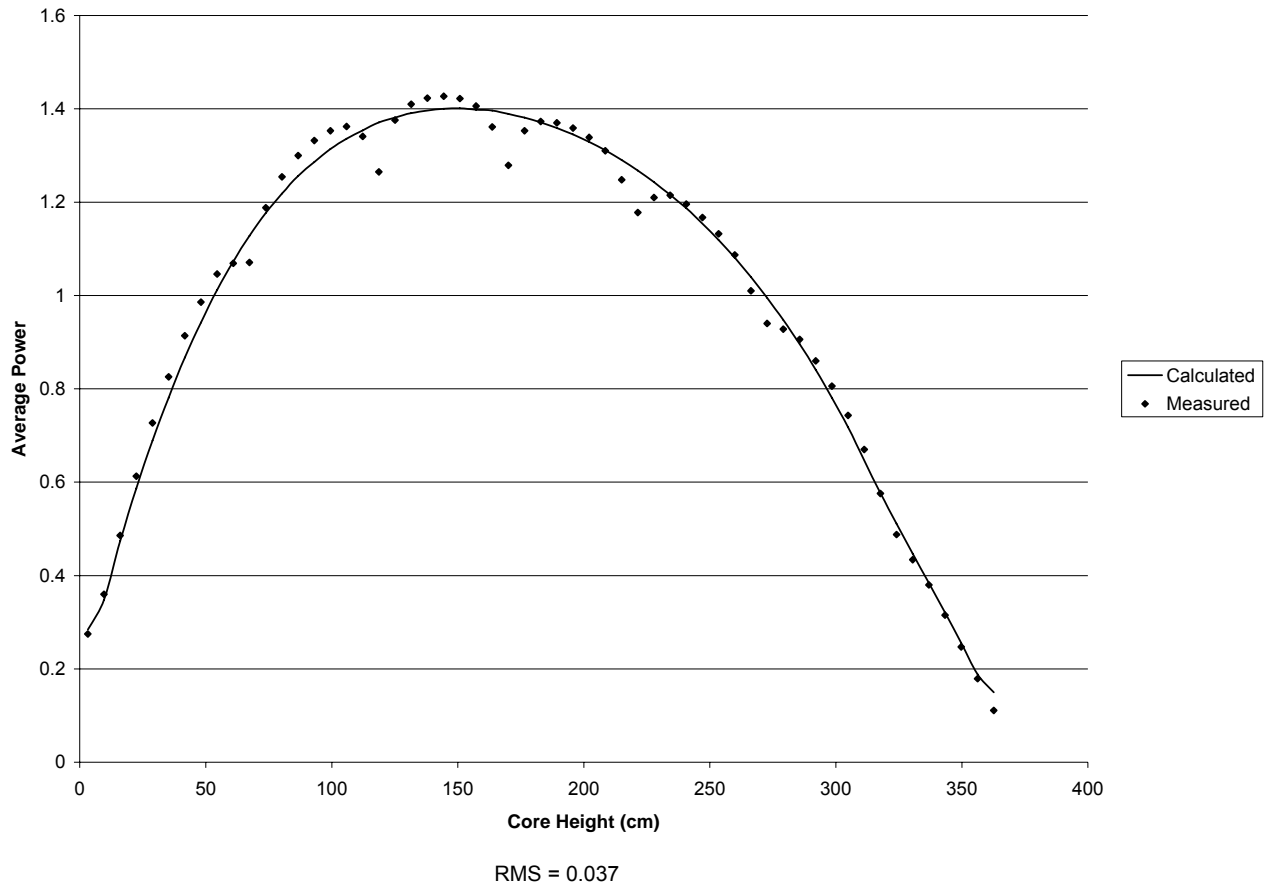
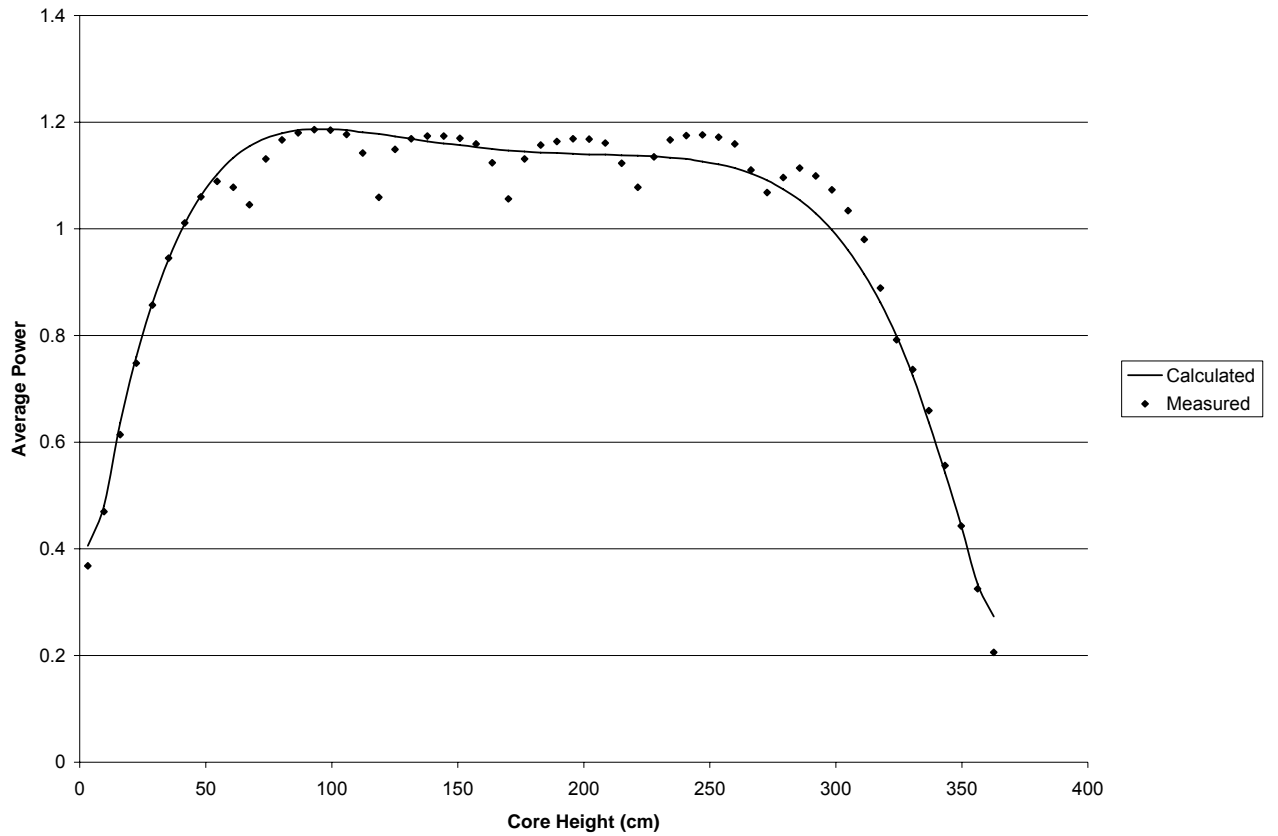
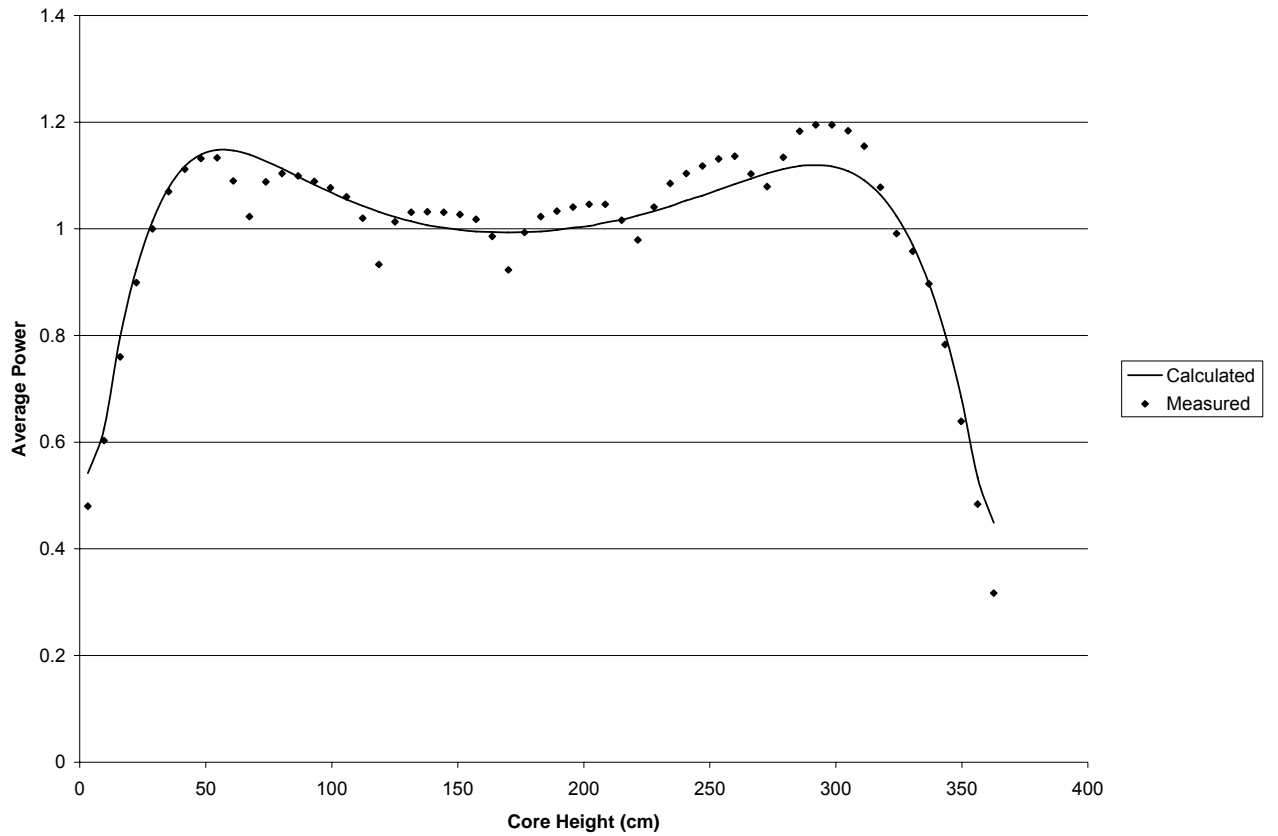
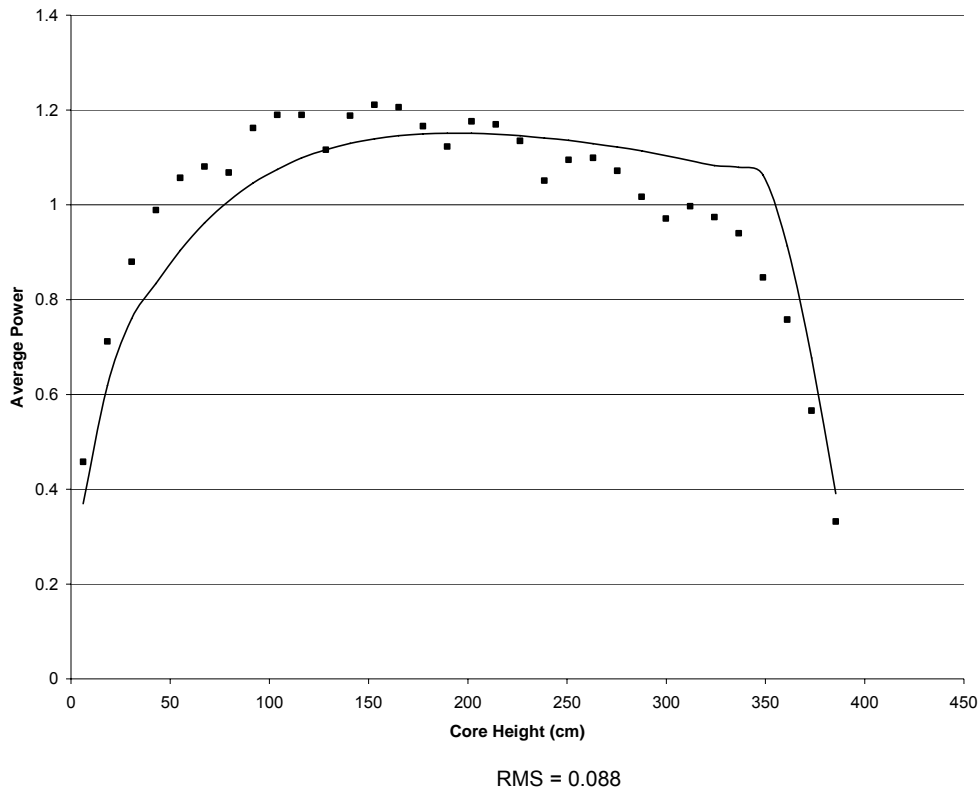
Figure A-2.131: Plant B BOC 1 Axial Power Distribution

Figure A-2.132: Plant B MOC 1 Axial Power Distribution

RMS = 0.043

Figure A-2.133: Plant B EOC 1 Axial Power Distribution

RMS = 0.044

Figure A-2.134: Plant G2 BOC 1 Axial Power Distribution***Notes –**

- The inaccuracy of the calculated power distribution is due to the use of a design depletion since core follow data was unavailable.
- The bump in the upper fuel region results from an extended gadolinia cutback region which was implemented in this cycle and shortened in subsequent cycles.

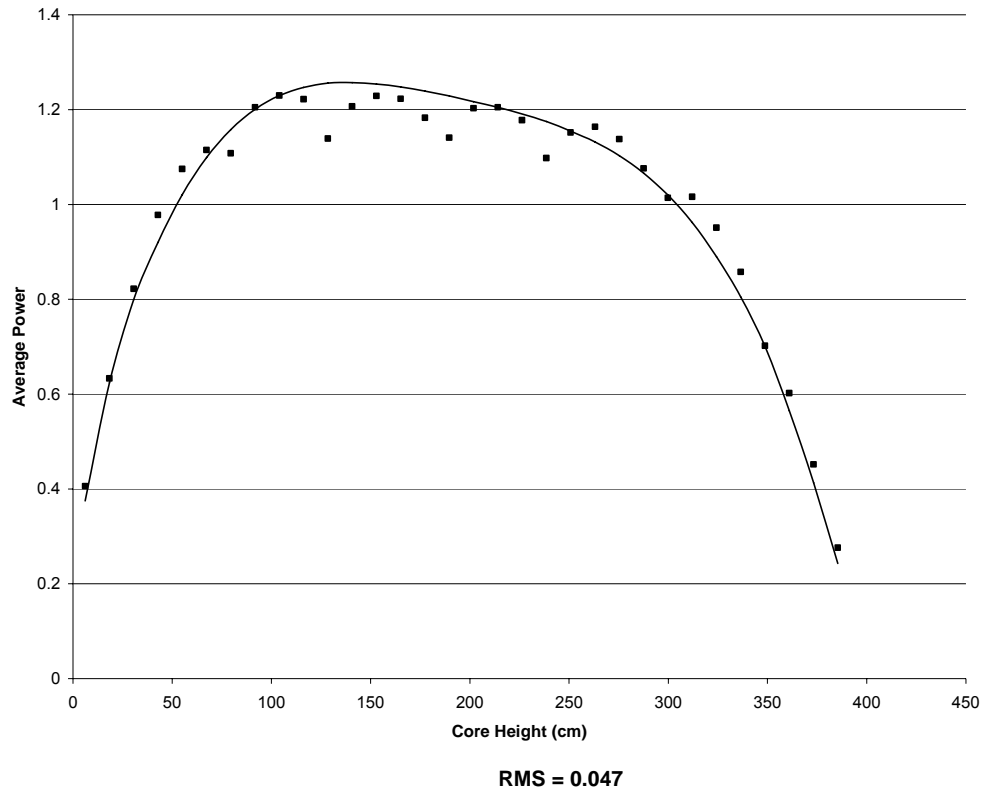
Figure A-2.135: Plant G2 MOC 1 Axial Power Distribution

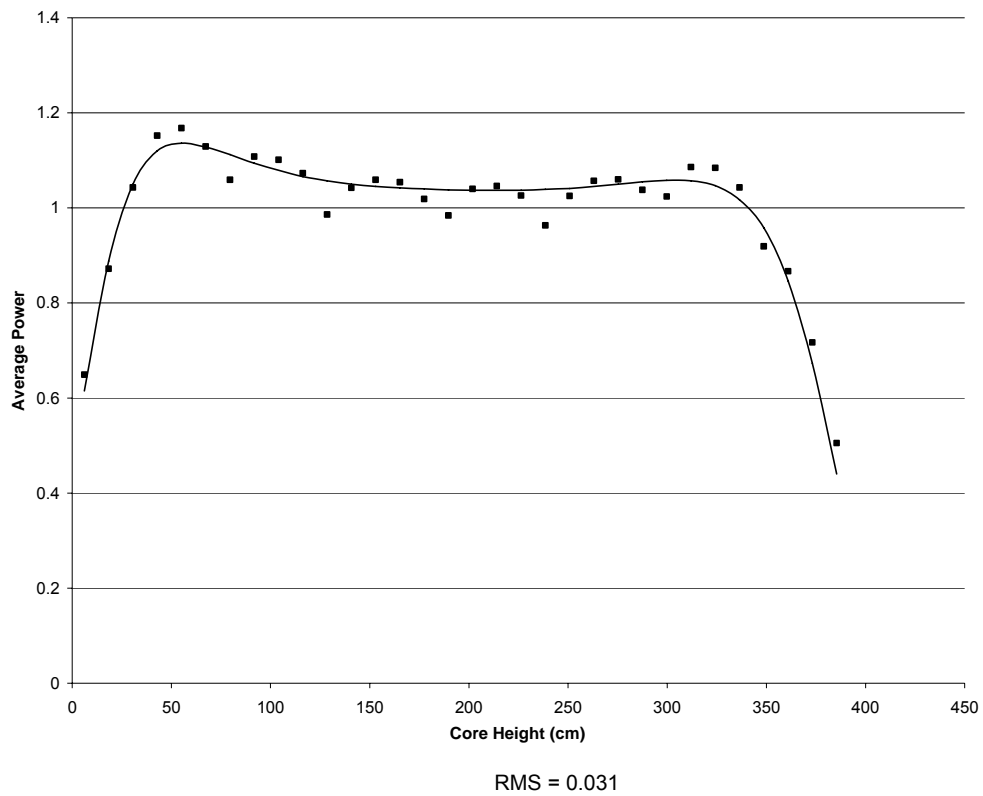
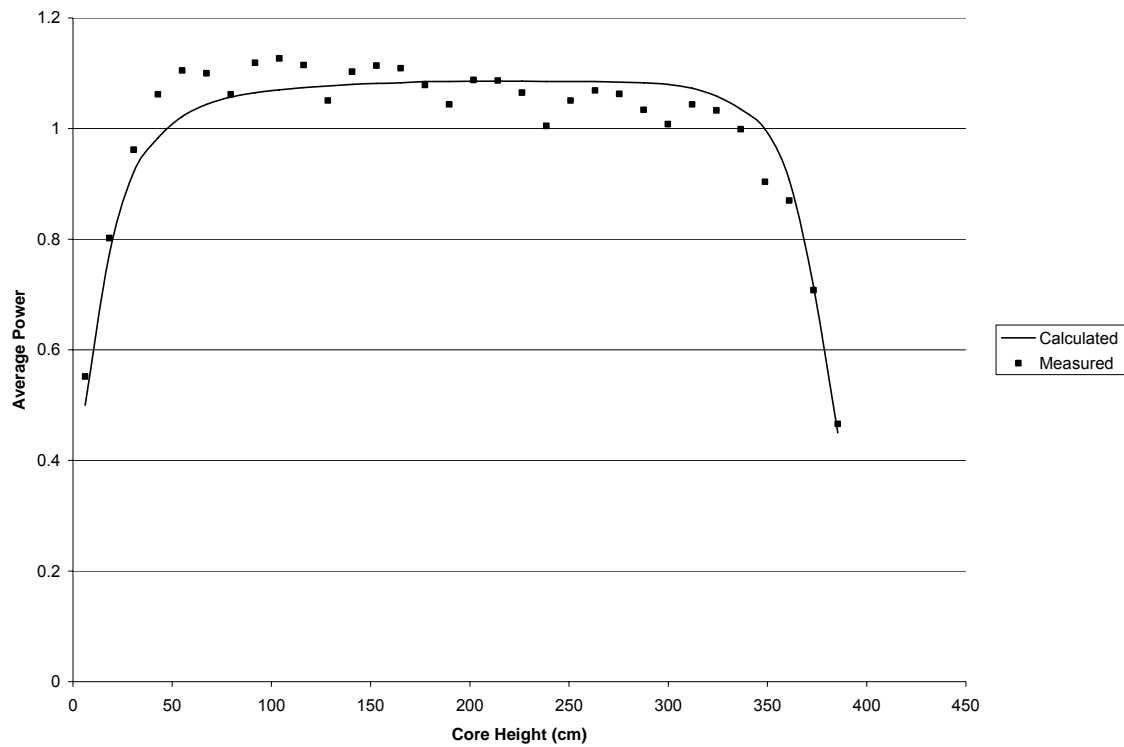
Figure A-2.136 Plant G2 EOC 1 Axial Power Distribution

Figure A-2.137 Plant G2 BOC 2 Axial Power Distribution

RMS = 0.047

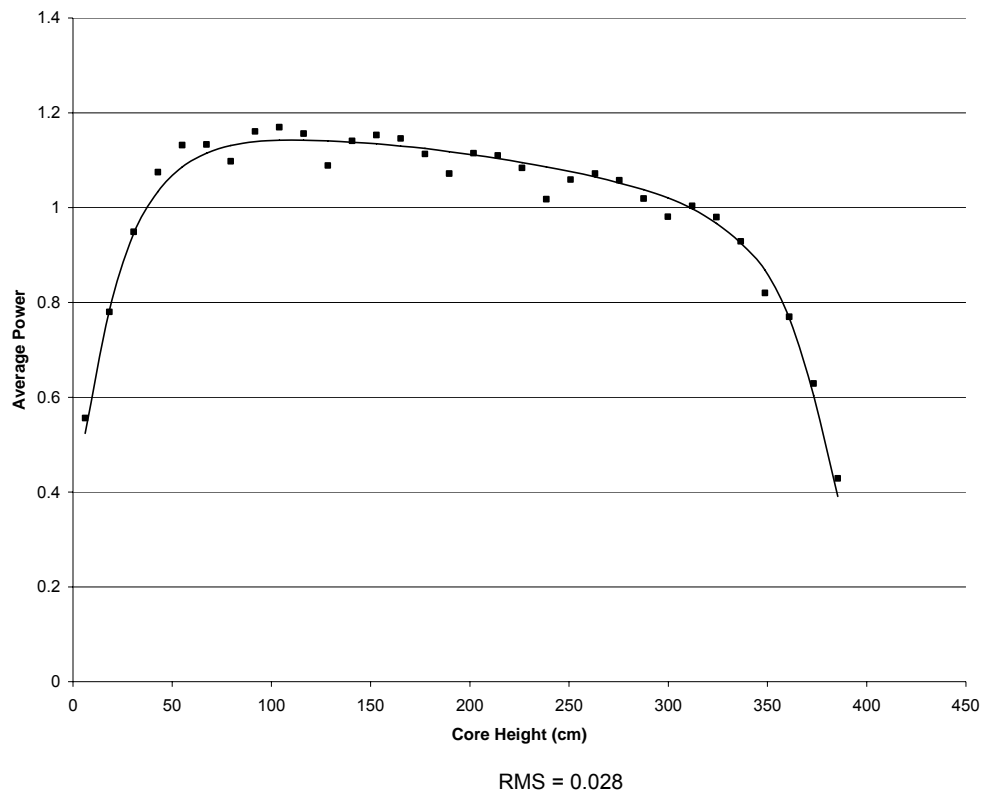
Figure A-2.138 Plant G2 MOC 2 Axial Power Distribution

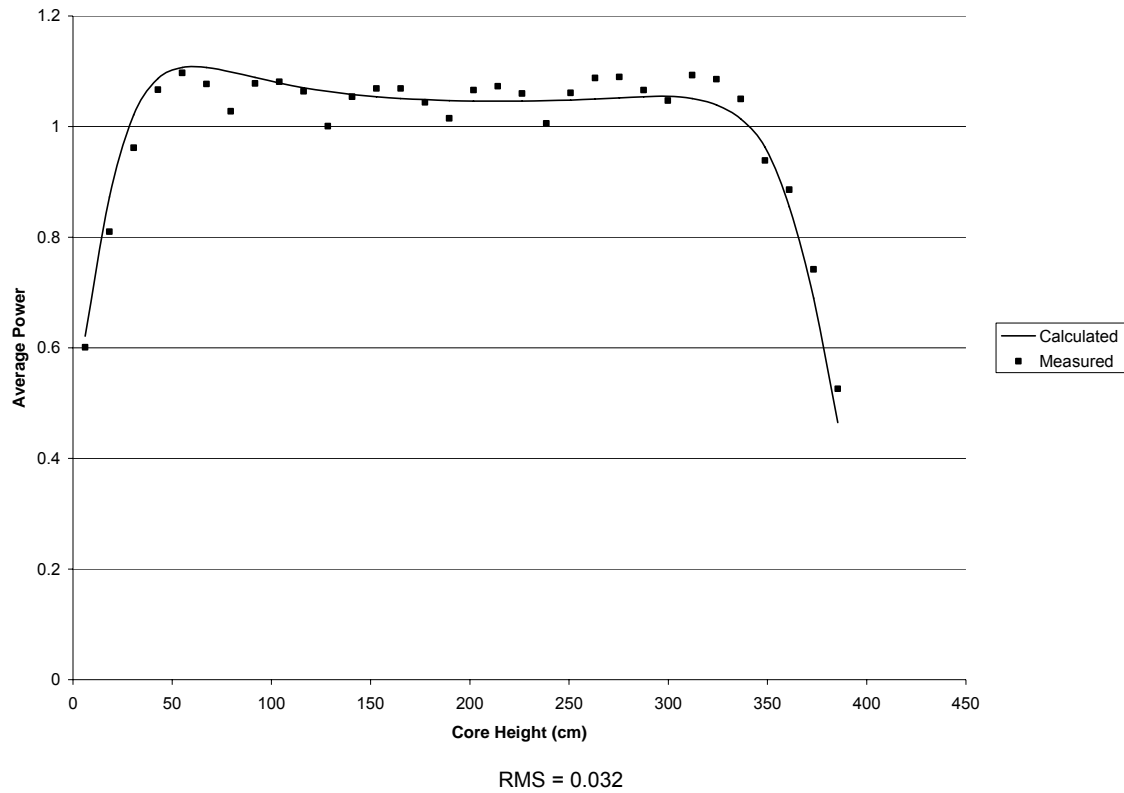
Figure A-2.139: Plant G2 EOC 2 Axial Power Distribution

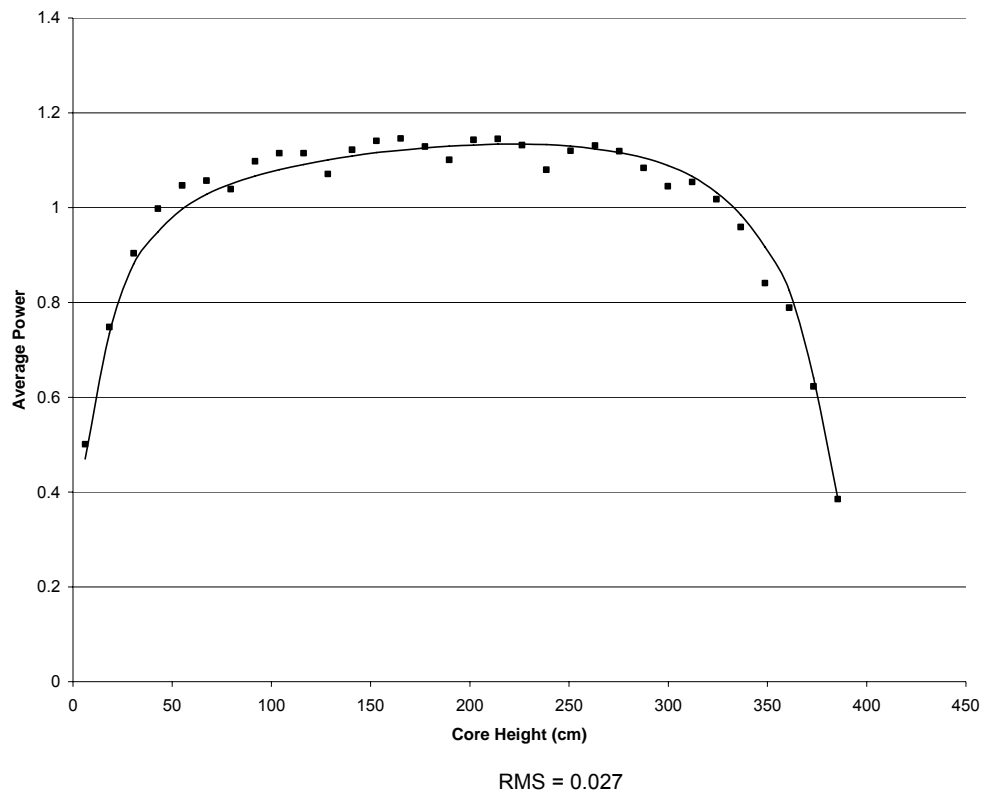
Figure A-2.140: Plant G2 BOC 3 Axial Power Distribution

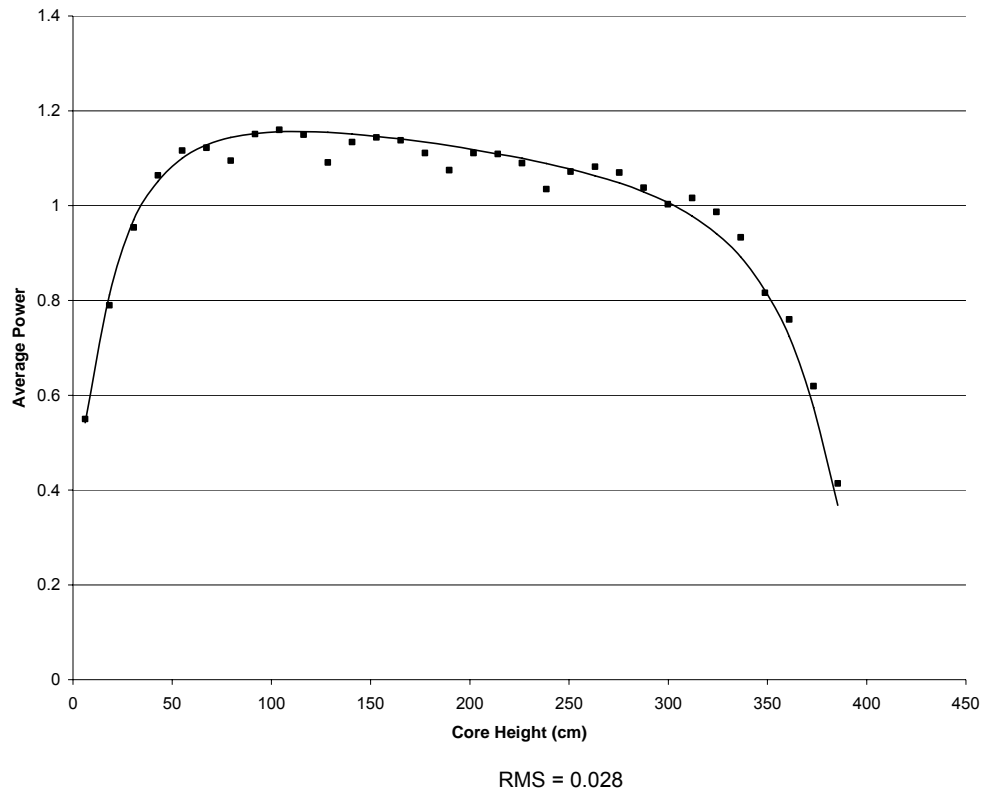
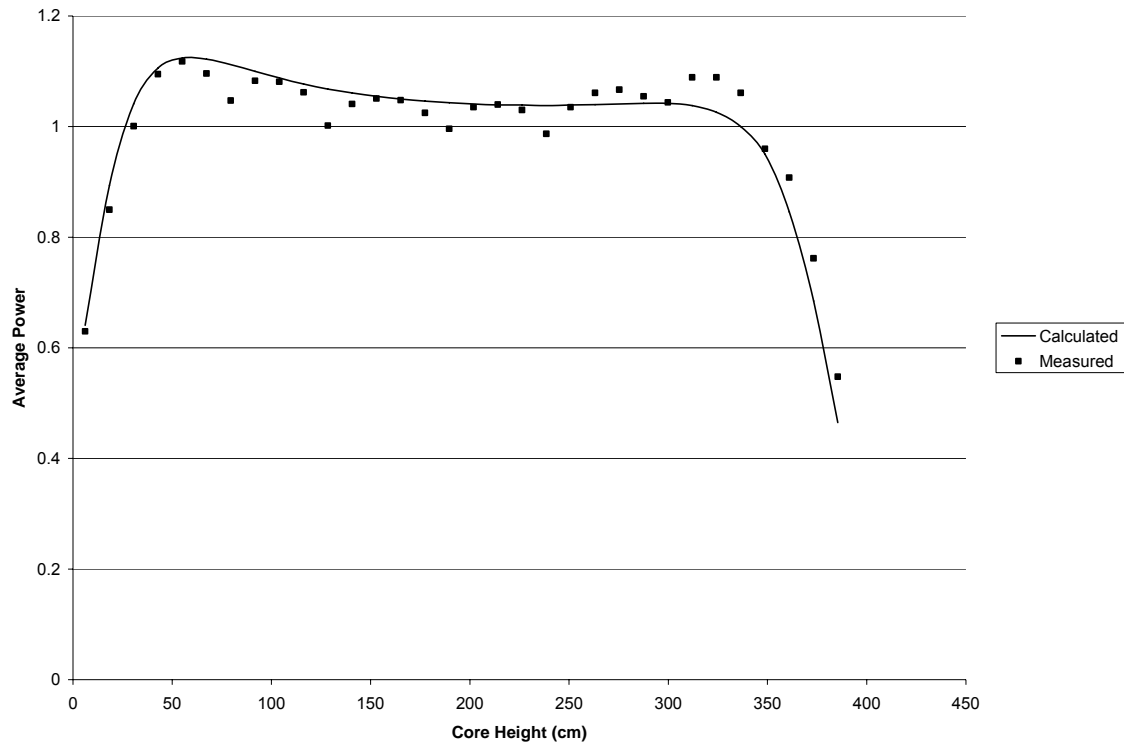
Figure A-2.141: Plant G2 MOC 3 Axial Power Distribution

Figure A-2.142: Plant G2 EOC 3 Axial Power Distribution

RMS = 0.034

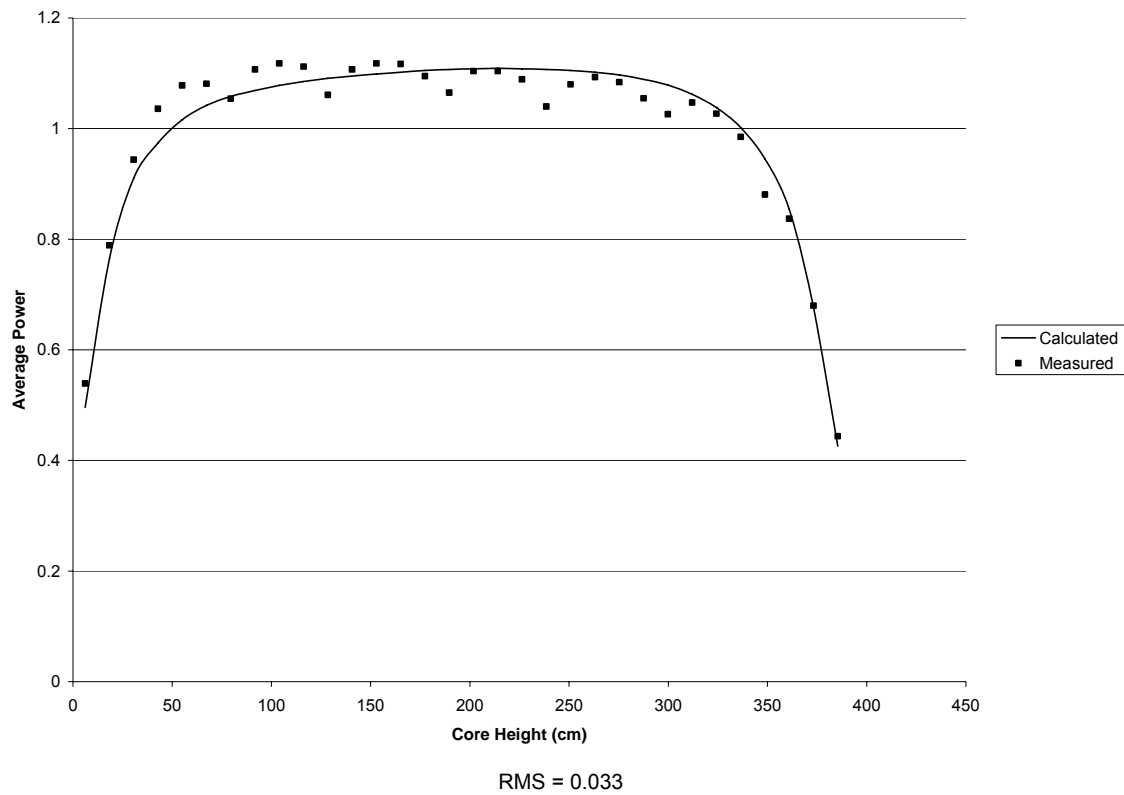
Figure A-2.143: Plant G2 BOC 4 Axial Power Distribution

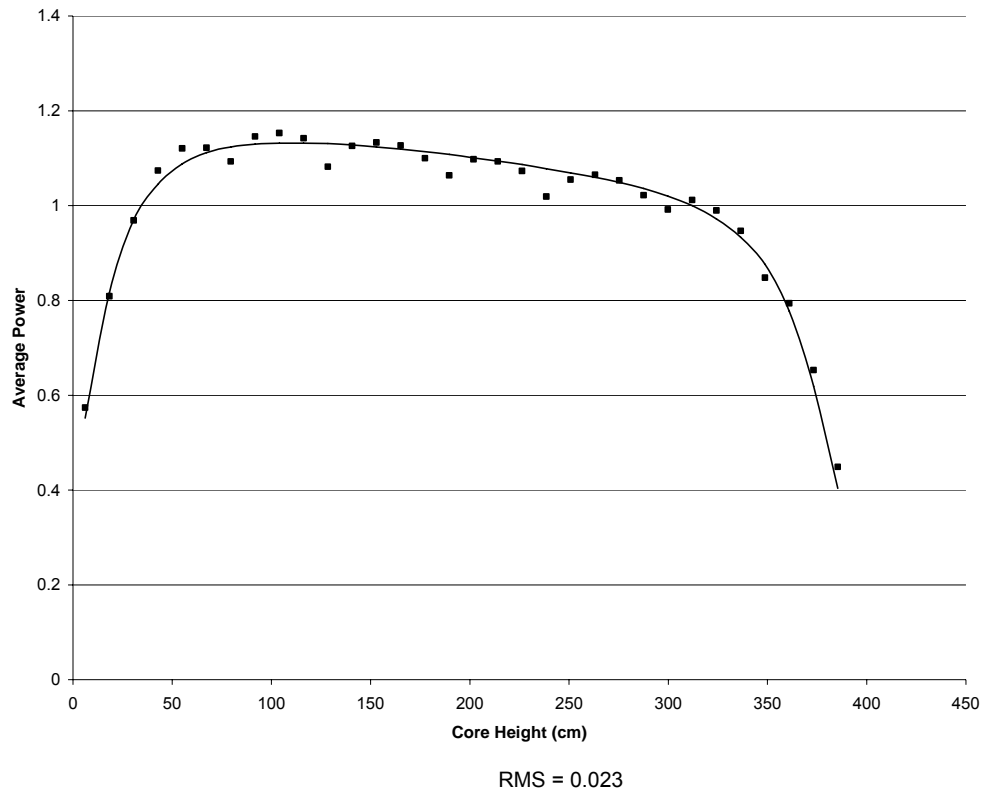
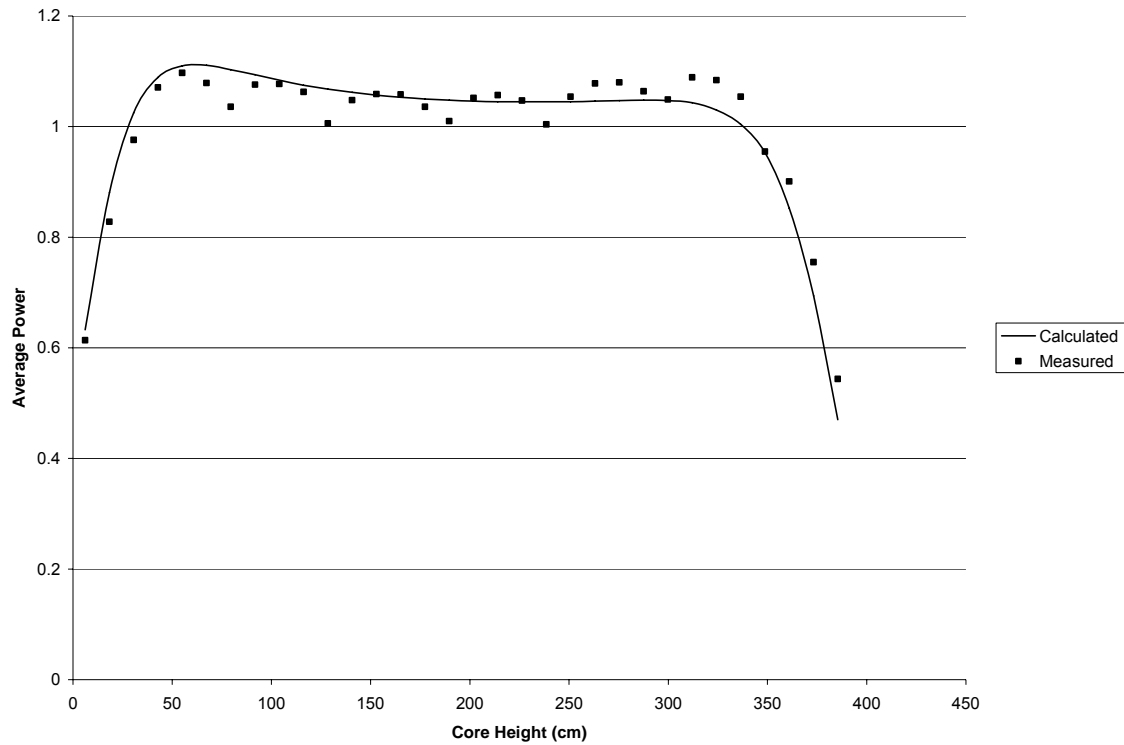
Figure A-2.144: Plant G2 MOC 4 Axial Power Distribution

Figure A-2.145: Plant G2 EOC 4 Axial Power Distribution

RMS = 0.032

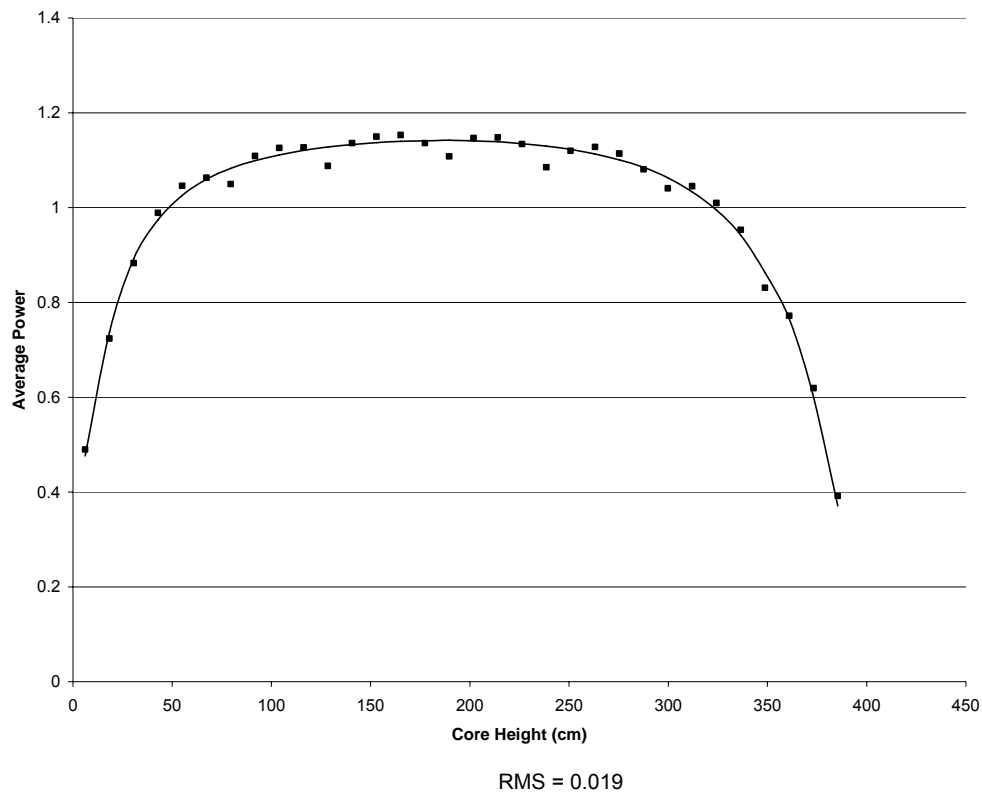
Figure A-2.146: Plant G2 BOC 5 Axial Power Distribution

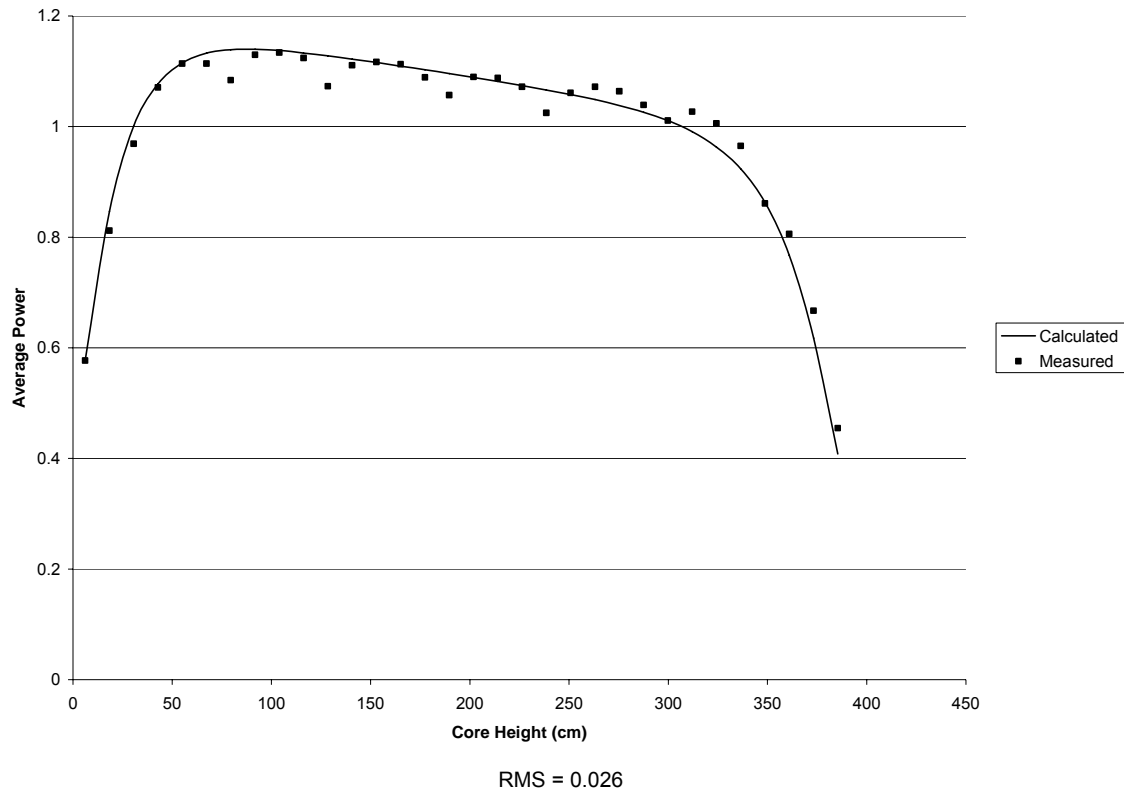
Figure A-2.147: Plant G2 MOC 5 Axial Power Distribution

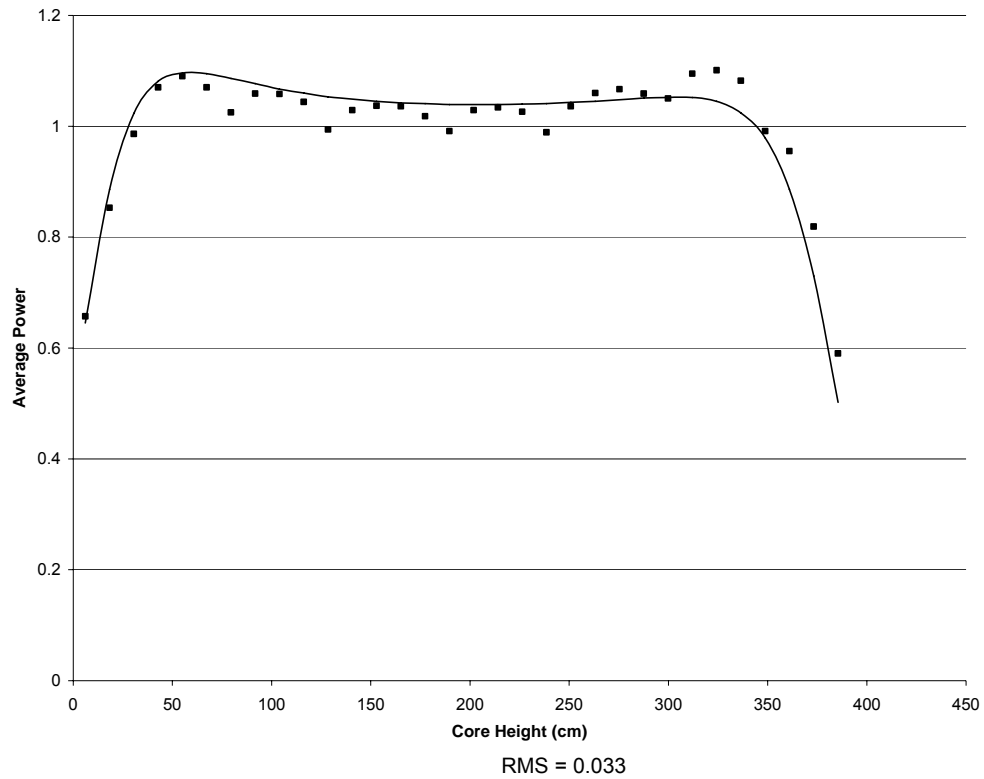
Figure A-2.148: Plant G2 EOC 5 Axial Power Distribution

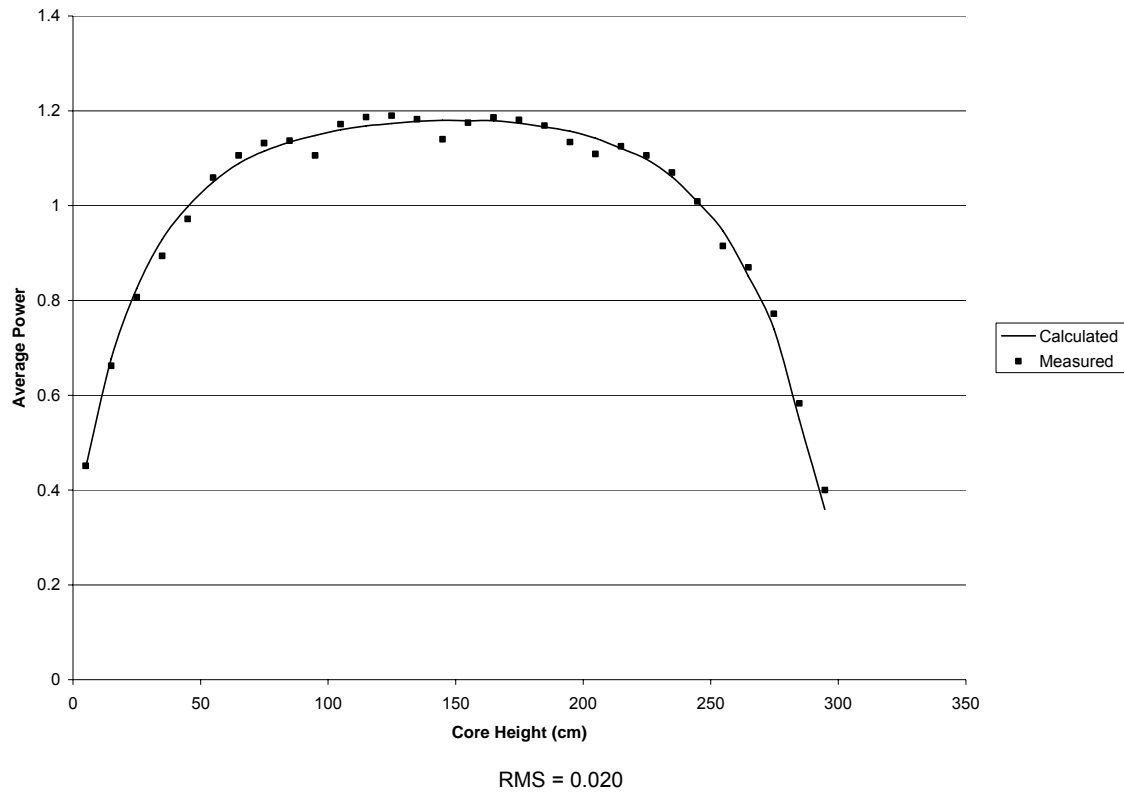
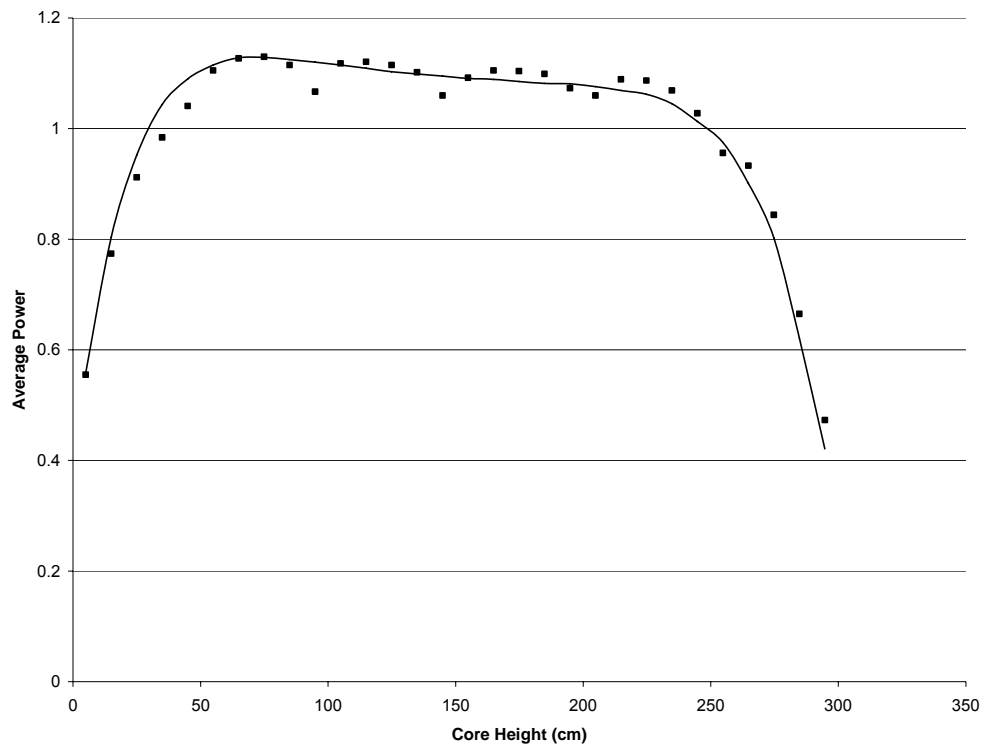
Figure A-2.149: Plant G1 BOC 26 Axial Power Distribution

Figure A-2.150: Plant G1 MOC 26 Axial Power Distribution

RMS = 0.026

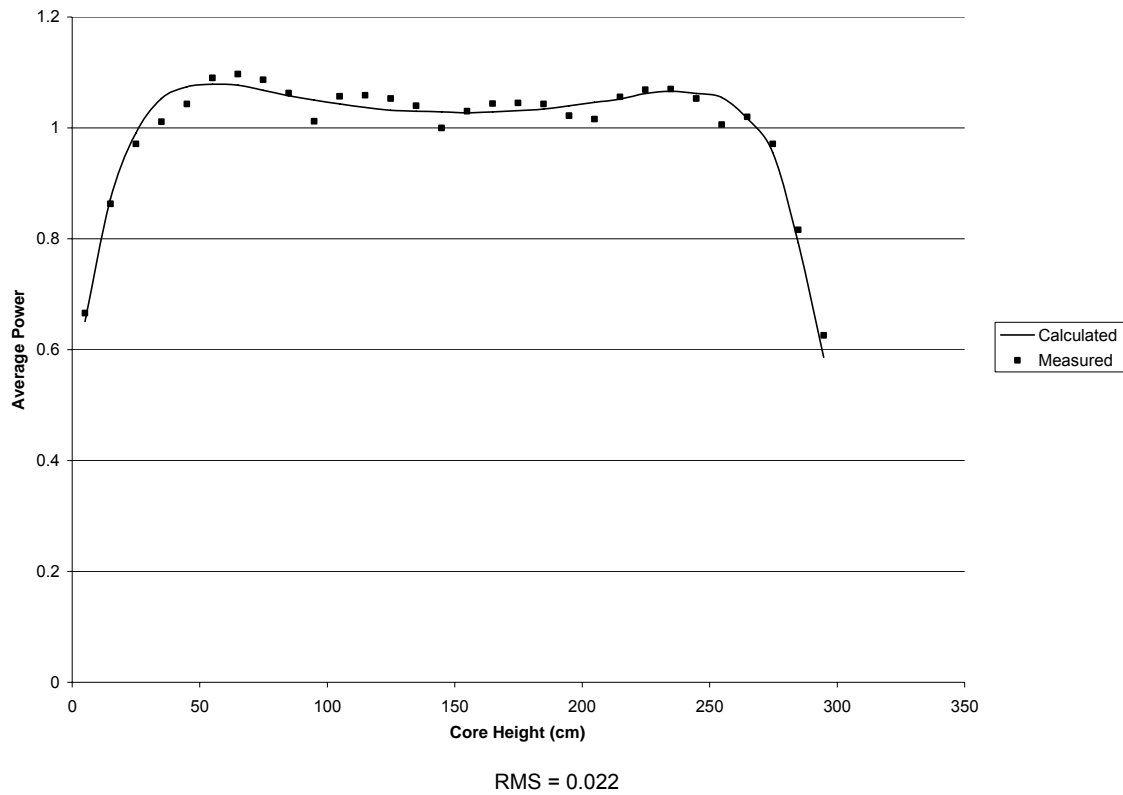
Figure A-2.151: Plant G1 EOC 26 Axial Power Distribution

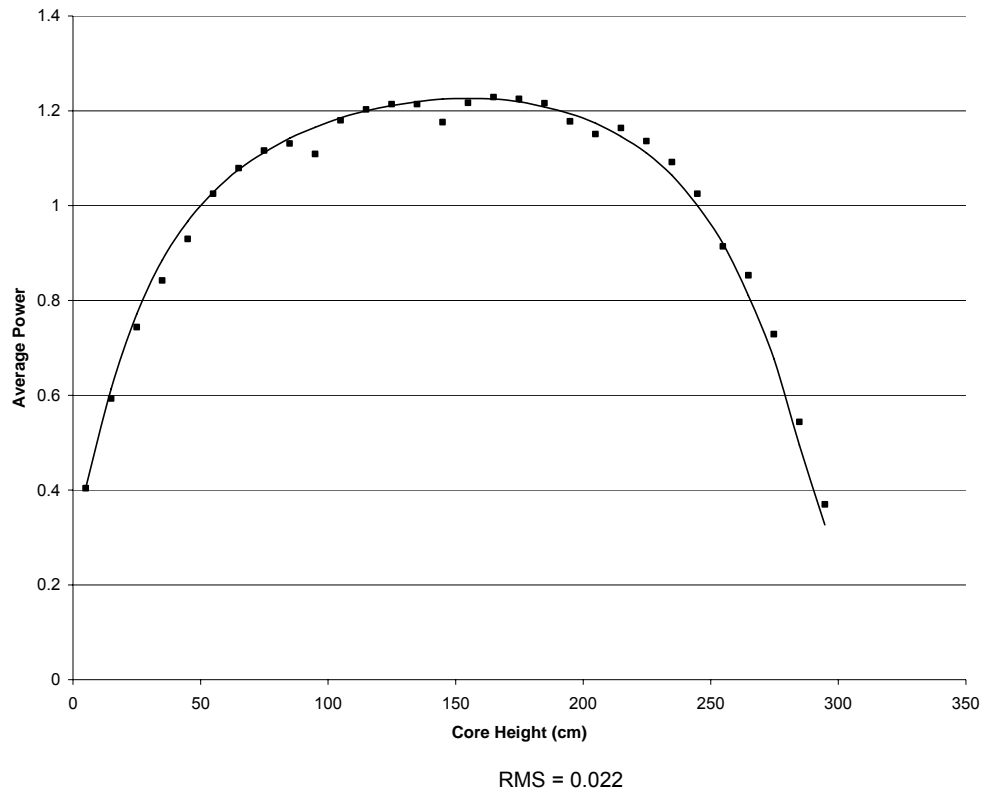
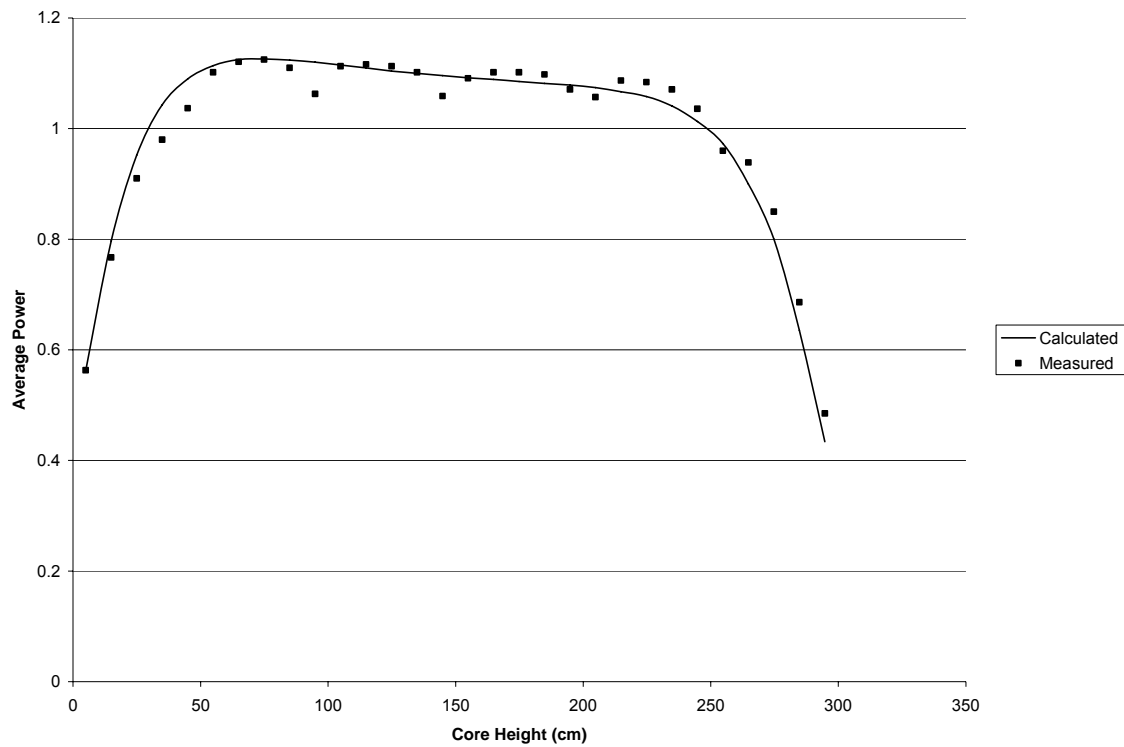
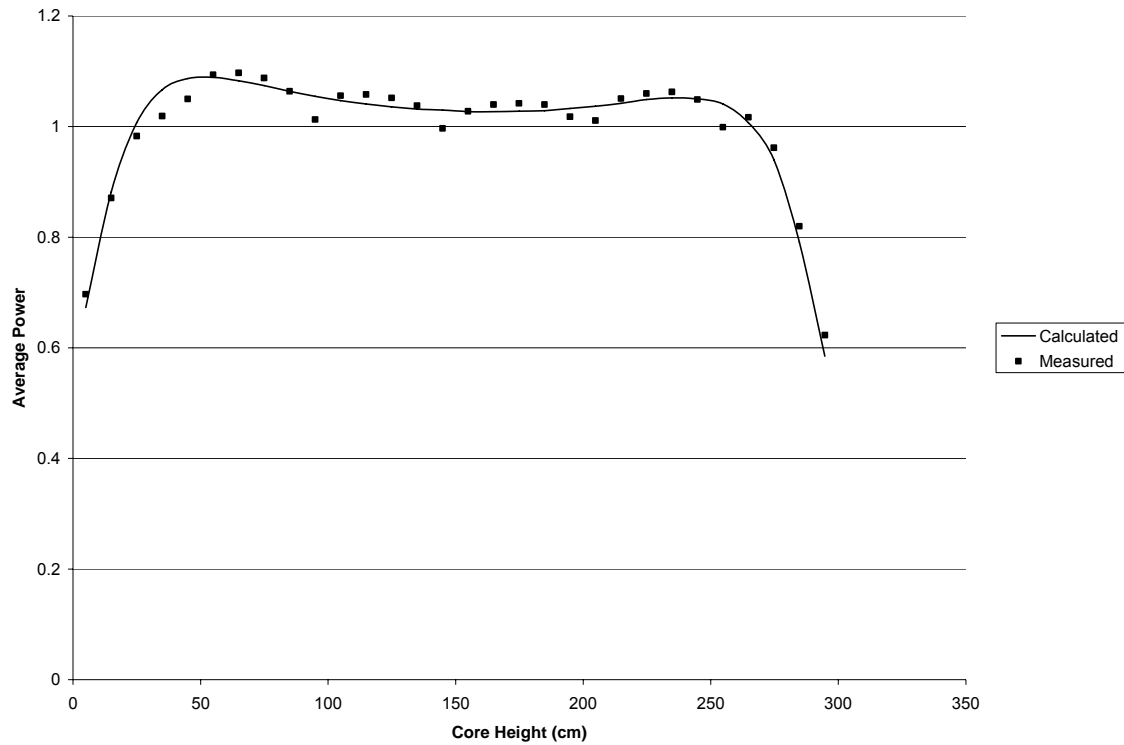
Figure A-2.152: Plant G1 BOC 27 Axial Power Distribution

Figure A-2.153: Plant G1 MOC 27 Axial Power Distribution

RMS = 0.027

Figure A-2.154: Plant G1 EOC 27 Axial Power Distribution

RMS = 0.022

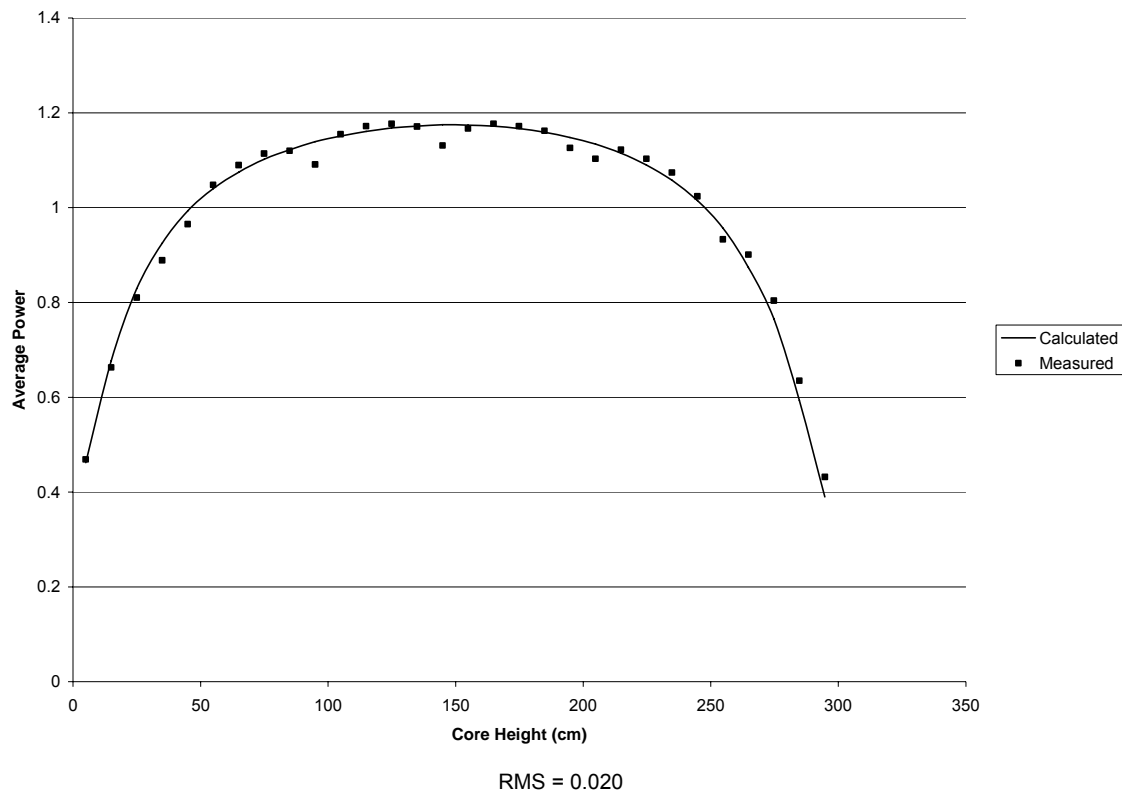
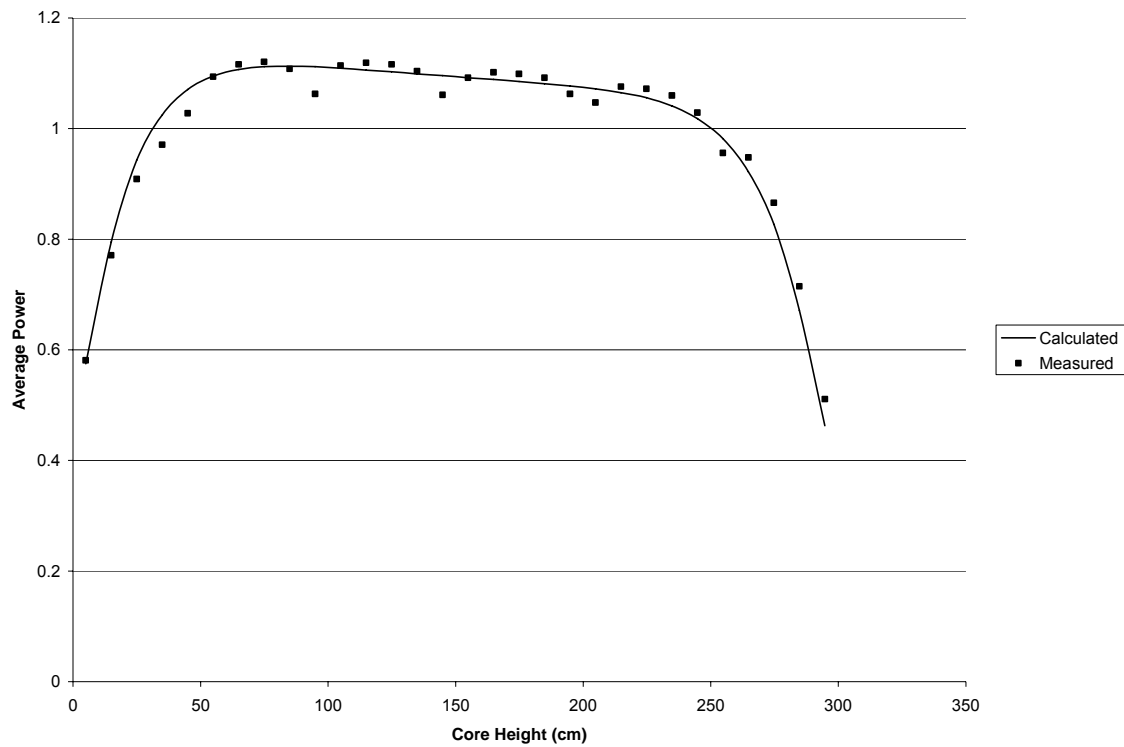
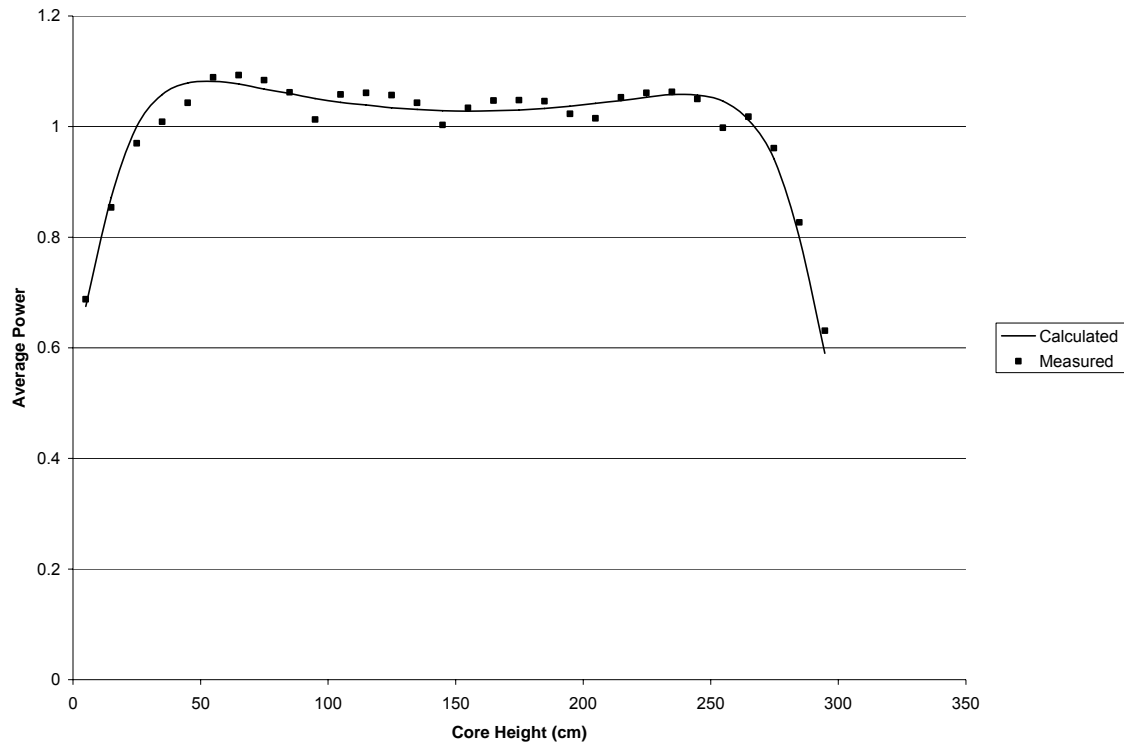
Figure A-2.155: Plant G1 BOC 28 Axial Power Distribution

Figure A-2.156: Plant G1 MOC 28 Axial Power Distribution

RMS = 0.023

Figure A-2.157: Plant G1 EOC 28 Axial Power Distribution

RMS = 0.023

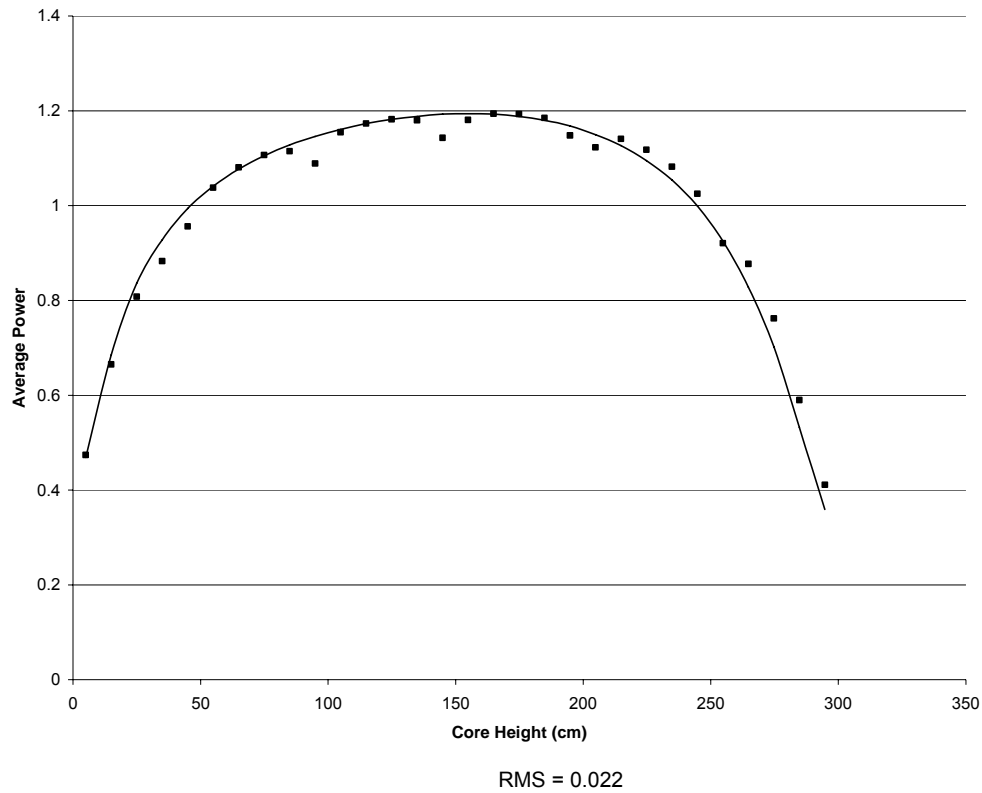
Figure A-2.158: Plant G1 BOC 29 Axial Power Distribution

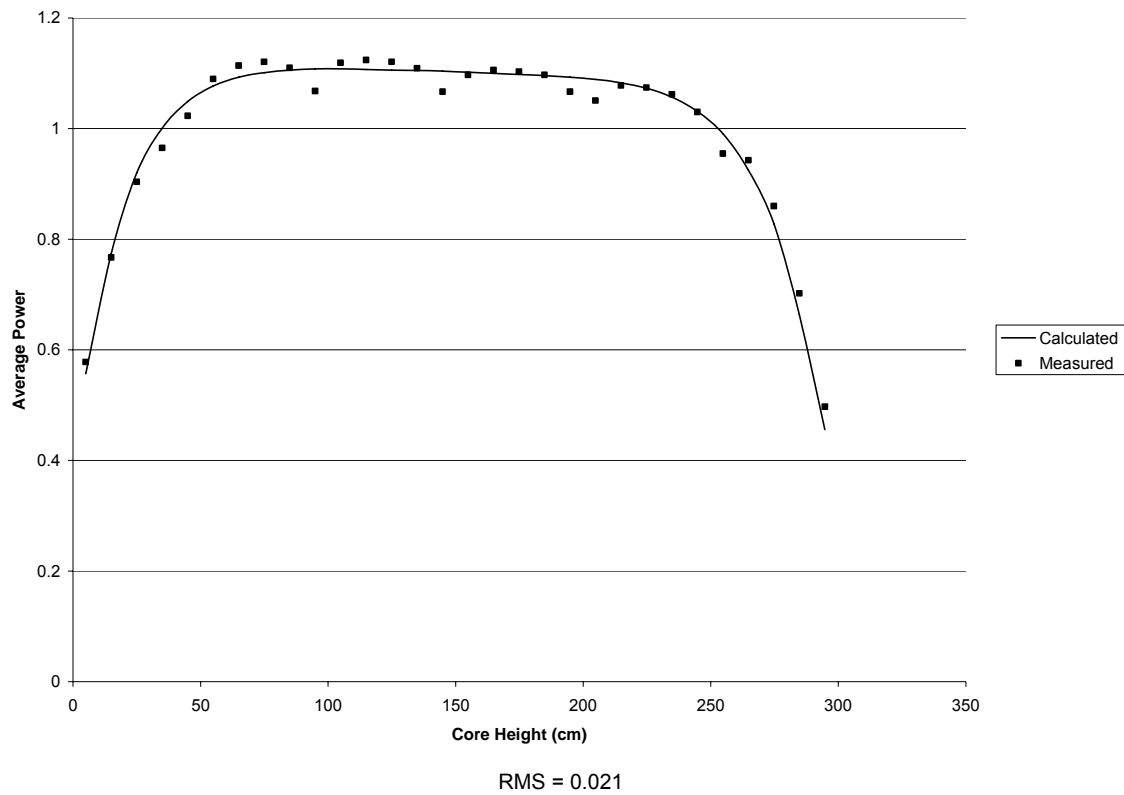
Figure A-2.159: Plant G1 MOC 29 Axial Power Distribution

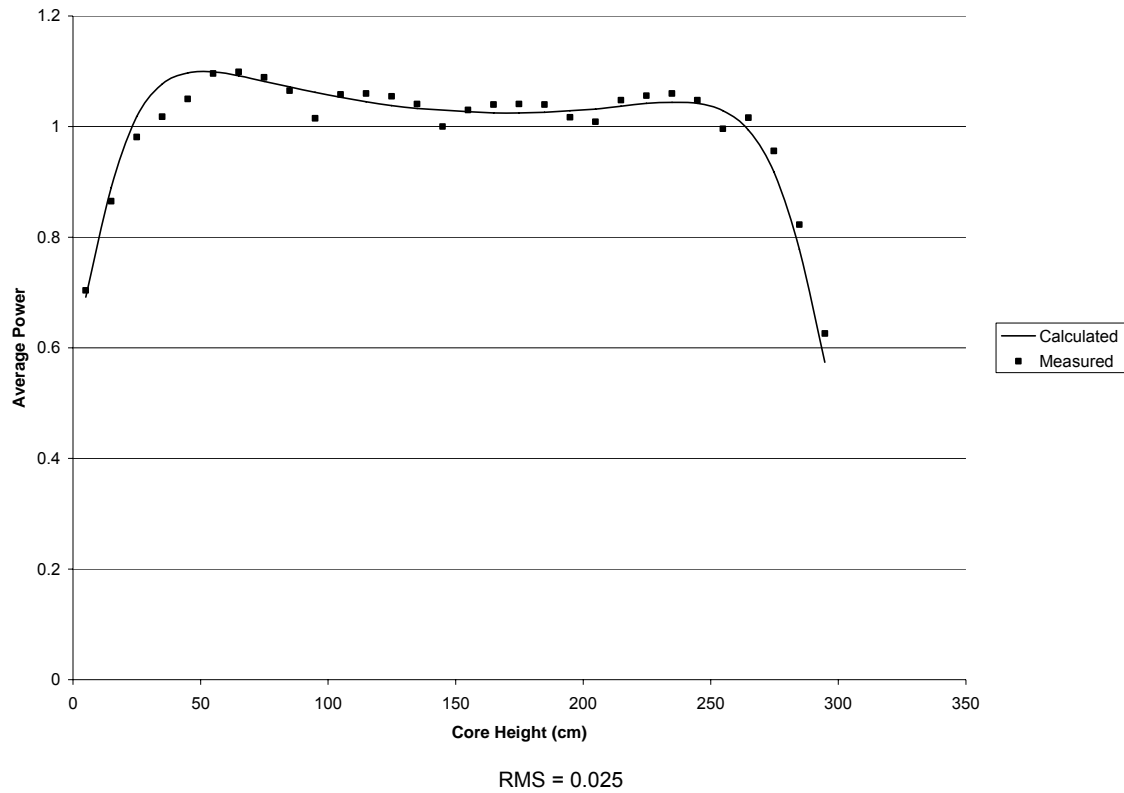
Figure A-2.160: Plant G1 EOC 29 Axial Power Distribution

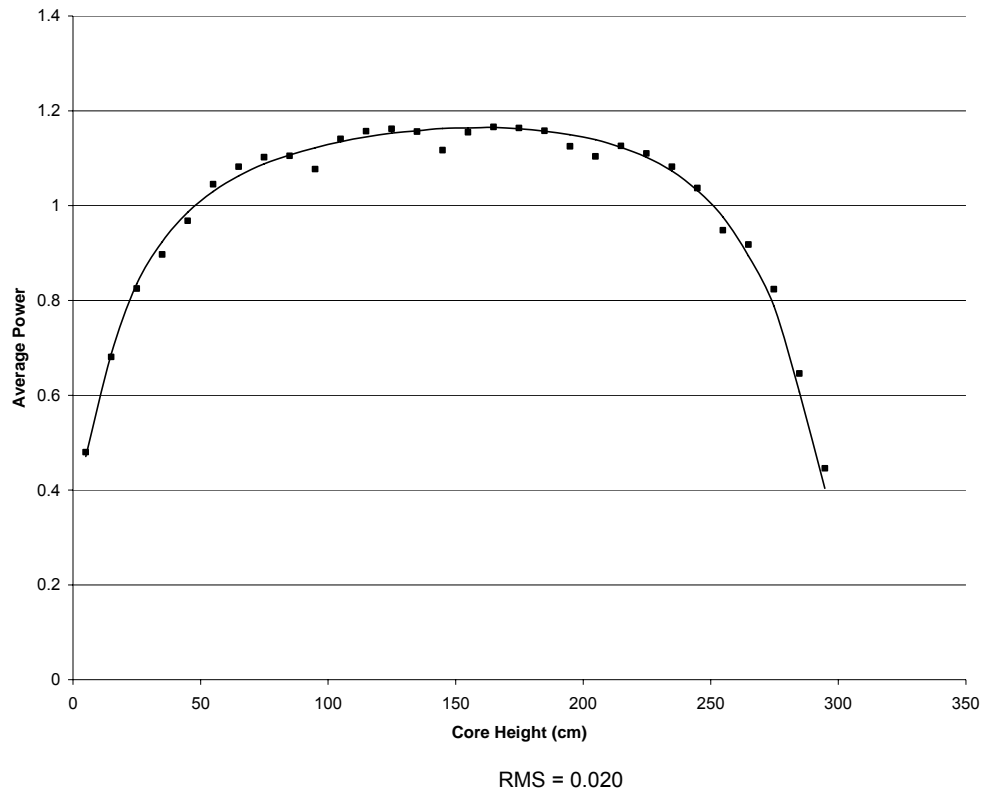
Figure A-2.161: Plant G1 BOC 30 Axial Power Distribution

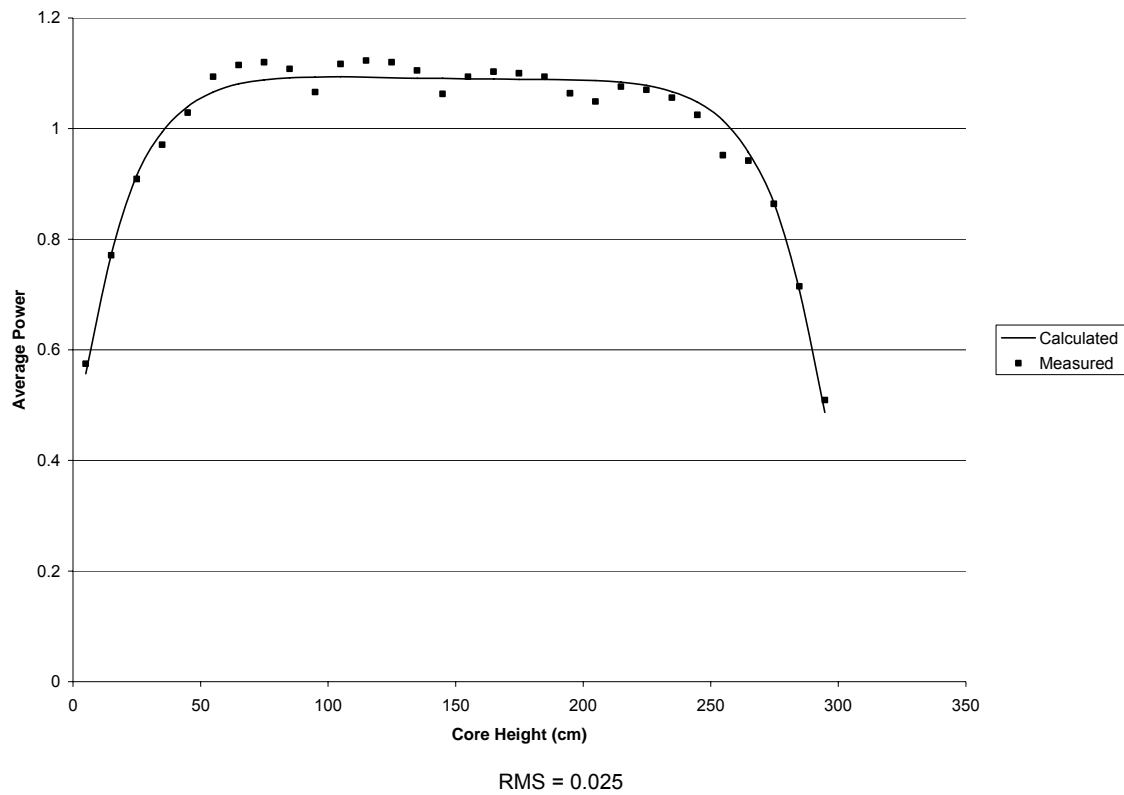
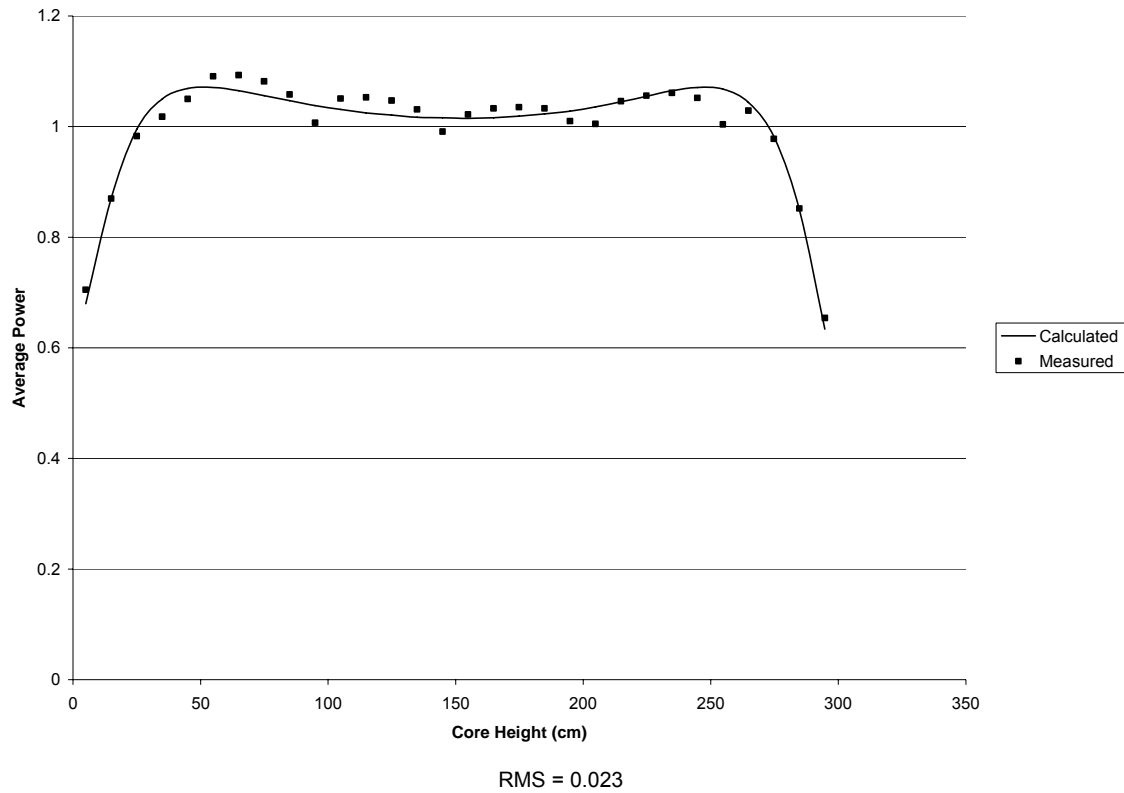
Figure A-2.162: Plant G1 MOC 30 Axial Power Distribution

Figure A-2.163: Plant G1 EOC 30 Axial Power Distribution

APPENDIX B

COPERNIC Sample Calculation

APPENDIX B
LIST OF TABLES

Table B-1 Typical U.S. EPR Fuel Rod Characteristics.....	B-3
Table B-2 Typical U.S. EPR Thermal-Hydraulic Conditions.....	B-4
Table B-3 Normalized Axial Transient Power Distribution.....	B-4

LIST OF FIGURES

Figure B-1 Power History Envelope for Bounding and Max Pressure Rod for U.S. EPR	B-5
Figure B-2 Sample U.S. EPR Internal Gas Pressure	B-5
Figure B-3 Normalized Transient Axial Power Distribution for U.S. EPR	B-6
Figure B-4 U.S. EPR Local Linear Heat Rate at Fuel Melt and 1% Cladding Strain.....	B-6
Figure B-5 U.S. EPR Creep Collapse Analysis.....	B-7
Figure B-6 U.S. EPR Peak Cladding Oxide Thickness	B-7

Fuel performance codes are used in a wide variety of disciplines: thermal, mechanical, nuclear and material. The COPENIC code (Reference B-1) is no exception. It is used primarily as a design tool for light water reactor fuel rods. The following design criteria are used with the COPENIC code to verify fuel rod designs.

- Fuel Rod Internal Gas Pressure: The internal gas pressure of the peak fuel rod in the reactor is limited to a value below that which would cause (1) the fuel-cladding gap to increase due to outward cladding creep during steady-state operation and (2) extensive DNB propagation to occur.
- Fuel Melting: Fuel melting during normal operation and anticipated operational occurrences is precluded.
- Cladding Strain: The maximum uniform hoop strain (elastic plus plastic) shall not exceed 1%; steady-state creep-down and irradiation growth are excluded.
- Creep Collapse Initialization: Cladding collapse is precluded during the fuel rod design life.
- Cladding Peak Oxide Thickness: The cladding peak oxide thickness shall not exceed a best- estimate predicted value of 100 microns.

These design criteria satisfy the fuel cycle review recommendations defined in Regulatory Guide 1.70 (4.4.1) and the licensing requirements defined in 10 CFR 50.46 and SRP 4.2.

The COPENIC code is also used to provide data for analyses that have no explicit basis in the regulations. These include best-estimate fuel temperatures for nuclear analysis codes such as PRISM (Reference B-2) and initialization data for core thermal-hydraulic codes such as LYNXT (Reference B-3). The COPENIC code also provides best-estimate fuel performance predictions for other similar analyses as appropriate.

The manner in which the COPENIC code is applied to the fuel rod design criteria is detailed in Section 12 of Reference B-1. The sample calculations provided in this appendix are intended to demonstrate the ability of COPENIC to analyze typical U.S. EPR fuel designs. The calculations were performed on a standard uranium dioxide fuel rod using U.S. EPR fuel rod geometries and M5[®] cladding and duplicate those in Section 12 of Reference B-1. The fuel rod characteristics and thermal hydraulic

conditions for this typical fuel rod are listed in Tables B-1 and B-2. Table B-3 provides the normalized transient axial power distribution. Figures B-1 to B-6 provide the COPENIC results for this typical rod.

B.1. REFERENCES

- B-1. COPENIC Fuel Rod Design Computer Code, BAW-10231P-A, Rev. 1, January 2004.

Table B-1 – Typical U.S. EPR Fuel Rod Characteristics

Typical Pellet Characteristics			
	Nominal	UTL	LTL
Outside Diameter: (in/mm)	0.3225/8.192	[]
Inside diameter: : (in/mm)	0.00	---	---
Dish and Chamfer Vol.: (%)	1.0	---	---
Roughness (RMS): (µin/mm)	[]	---	---
Density (As-Fabricated): (%)	96.0	---	---
Densification (Resinter): (%)	---	[]	---
Open Porosity Fraction: (frac.)	---	---	---
Grain Size (mean): (µm/mm)	[]	---	---
Enrichment: (wt.%)	4.00	---	---
Typical Cladding Characteristics:			
Outside Diameter: (in/mm)	0.374/9.500	[]
Inside diameter: : (in/mm)	0.329/8.360	[]
Length: (in/mm) (No End Cap Intrusions)	178.142/4525	[]
I.D. Roughness (RMS): (µin/mm)	[]	---	---
Typical Cladding Characteristics:			
Total stack Length: (in/mm)	165.35/4200		
Upper Plenum Volume: (in ³ /mm ³)	0.586/9600	[]
Lower Plenum volume: (in ³ /mm ³)	0.317/5200	[]
He Backfill Pres.: (psia/Mpa)	[]	[]
Residual Pressure: (psia/Mpa)	---	---	---

Table B-2 – Typical U.S. EPR Thermal-Hydraulic Conditions

Mass Flux: ($\text{lb}_m \cdot \text{h}^{-1} \cdot \text{ft}^{-2}$ / $\text{kg} \cdot \text{s}^{-1} \cdot \text{m}^{-2}$)	2.74×10^6 / 3719
Hydraulic Dia.: (in./mm)	.4366 / 11.09
Equiv. Heated Dia.: (in/mm)	.4882 / 12.40
Coolant Inlet Temp.: ($^{\circ}\text{F}/^{\circ}\text{C}$)	563.9 / 295.5
Coolant Pressure: (psia/MPa)	2248 / 15.50
Heat Produced Within Fuel: (frac.)	.974

Table B-3 – Normalized Axial Transient Power Distribution

Axial Elevation (inch) (mm)		Typical Power Distribution
3.76	95.4	.259
11.27	286.4	.300
18.79	477.3	.616
26.31	668.2	1.113
33.82	859.1	1.549
41.34	1050.0	1.700
48.86	1240.9	1.691
56.37	1431.8	1.662
63.89	1622.7	1.609
71.40	1813.6	1.531
78.92	2004.6	1.431
86.44	2195.4	1.311
93.95	2386.4	1.176
101.47	2577.3	1.032
108.98	2768.2	.886
116.50	2959.1	.743
124.02	3150.0	.610
131.53	3340.9	.492
139.05	3531.8	.396
146.56	3722.7	.314
154.08	3913.6	.267
161.60	4104.6	.259



Figure B-1: Power History Envelope for Bounding and Max Pressure Rod for U.S. EPR

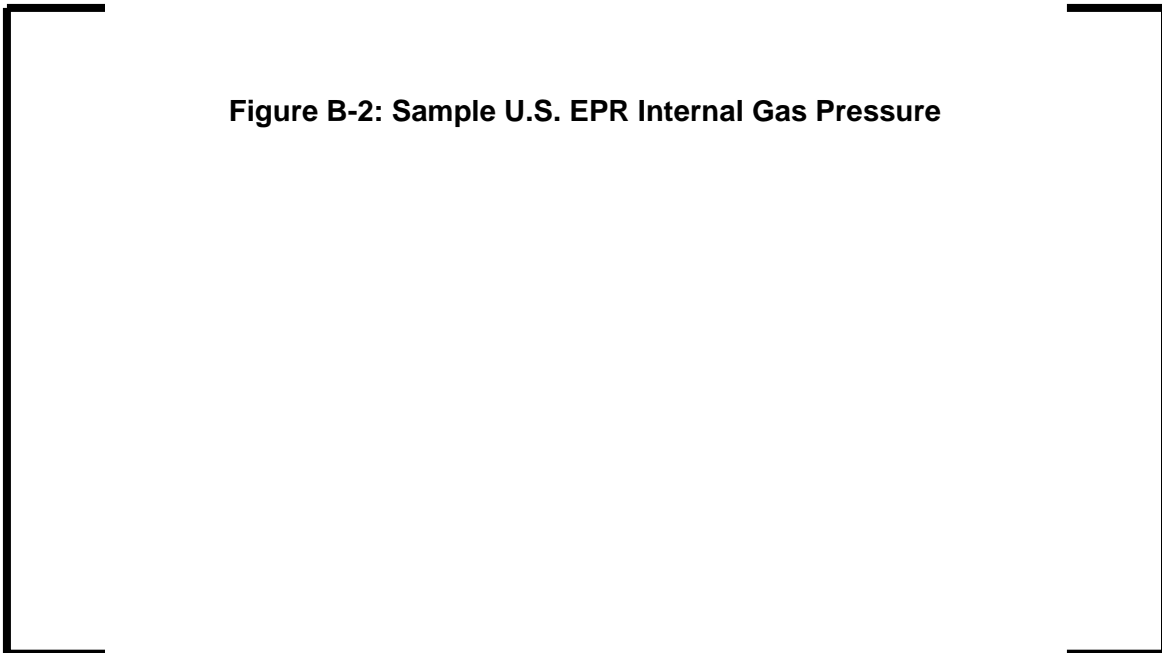


Figure B-2: Sample U.S. EPR Internal Gas Pressure

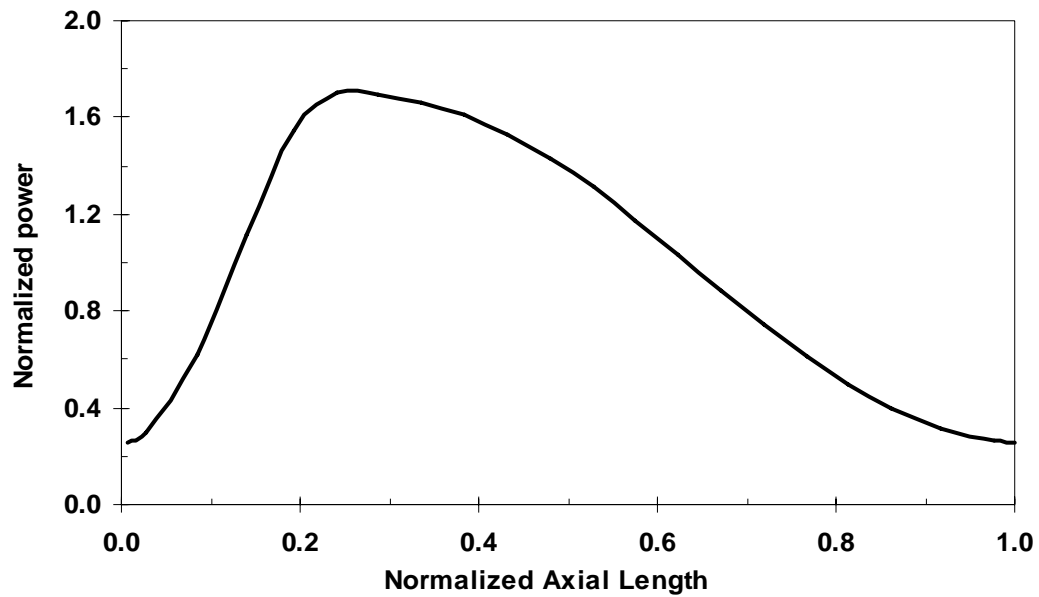


Figure B-3: Normalized Transient Axial Power Distribution for U.S. EPR



Figure B-4: U.S. EPR Local Linear Heat Rate at Fuel Melt and 1% Cladding Strain



Figure B-5: U.S. EPR Creep Collapse Analysis



Figure B-6: U.S. EPR Peak Cladding Oxide Thickness

APPENDIX C

SMALL BREAK LOCA SAMPLE CALCULATION

TABLE OF CONTENTS

	<u>Page</u>
C.1. INTRODUCTION	C-1
C.2. S-RELAP5 MODEL	C-1
C.3. INITIAL CONDITIONS AND OTHER INPUT PARAMETERS	C-3
C.4. BREAK SPECTRUM.....	C-4
C.5. 4.0-INCH BREAK (LIMITING CASE)	C-5
C.6. RESULTS/SUMMARY/CONCLUSION	C-7
C.7. REFERENCES	C-9

LIST OF TABLES

Table C-1 Input Parameters	C-10
Table C-2 Safety Classified I&C Signals Considered for SBLOCA Analysis	C-11
Table C-3 Break Spectrum- Peak Cladding Temperature	C-12
Table C-4 Limiting Break Sequence of Events	C-12

LIST OF FIGURES

Figure C-1 U.S. EPR Vessel Nodalization.....	C-13
Figure C-2 U.S. EPR Steam Generator Nodalization	C-14
Figure C-3 U.S. EPR Loop Nodalization	C-15
Figure C-4 Break Flow Rate for 4.0 Inch Break.....	C-16
Figure C-5 Break Void Fraction for 4.0 Inch Break.....	C-17
Figure C-6 Primary and Secondary System Pressures for 4.0 Inch Break.....	C-18
Figure C-7 Steam Generators Pressures for 4.0 Inch Break.....	C-19
Figure C-8 Steam Generators Total Mass Inventories for 4.0 Inch Break.....	C-20
Figure C-9 MSRT Flow Rate for 4.0 Inch Break.....	C-21
Figure C-10 Loop Seal Void Fraction for 4.0 Inch Break.....	C-22
Figure C-11 Total MHSI Flow (Loops 3 and 4) for 4.0 Inch Break.....	C-23
Figure C-12 Hot Assembly Collapsed Liquid Level for 4.0 Inch Break	C-24
Figure C-13 Total Accumulator Flow for 4.0 Inch Break.....	C-25
Figure C-14 Total RCS and RV Mass Inventories.....	C-26
Figure C-15 Vapor and Clad Temperature for Hot Node with 4.0 Inch Break	C-27

C.1. Introduction

This appendix presents the application of the S-RELAP5 SBLOCA methodology (Reference C-1) to the U.S. EPR. The U.S. EPR has four loops with 4 hot-legs, 4 cold-legs, and 4 vertical U-tube steam generators. The reactor vessel contains a downcomer, upper and lower plena, and a reactor core with 241 fuel assemblies. The hot-legs connect the reactor vessel with the vertical U-tube steam generators. Feedwater is injected into the downcomer of each steam generator. The Main Steam Relief Trains (MSRTs) are used to cool the primary system at a rate of 180 °F/hr. There are four EFW pumps; all are motor driven. The SIS contains four MHSI pumps, four accumulators, and four LHSI pumps.

C.2. S-RELAP5 MODEL

The reactor coolant system of the plant is modeled in S-RELAP5 as a network of control volumes interconnected by flow paths. The model includes four accumulators, a pressurizer, and four steam generators in which both the primary and secondary sides are modeled. All the loops are modeled explicitly to provide an accurate representation of the plant. Figure C-1 and Figure C-2 are nodalization diagrams for the reactor vessel and secondary system. Figure C-3 presents the nodalization of the loops.

Decay heat is determined from reactor kinetics equations with actinide and decay heating as prescribed by Appendix K to 10 CFR Part 50.

The calculations assume a loss of off-site power concurrent with reactor scram. The single failure criterion required by Appendix K is satisfied by assuming the loss of one diesel generator. This results in the disabling of one MHSI pump, one LHSI pump and one motor-driven EFW pump. In addition, one SIS train is assumed to be off line for service, leaving active only two MHSI pumps, two LHSI pumps and two emergency feedwater pumps. All four accumulators are assumed to inject.

The actuation of the EFW pumps on LOOP and Safety injection (SI) signal was neglected. The EFW was not actuated on the low and the wide range level signal because the level in each steam generator never dropped to the EFW actuation signal for the breaks analyzed.

MHSI is initiated on a SI actuation signal. The flow of water begins following a delay to account for the maximum time required to start up emergency diesel generators and actuate equipment. The two active trains of MHSI are assumed to inject into Loop 4 (the broken loop) and into Loop 3 (the intact loop adjacent to the broken loop). The adjacent loop was chosen because it provides the greatest opportunity for injected ECCS to flow directly to the break and bypass the core.

The MFW system and the RCPs are assumed to be tripped-off at reactor scram, coincident with an assumed LOOP.

The axial power shape used is a conservatively top-skewed, End of Cycle (EOC) shape. The power peak occurs at a normalized distance of 0.8089. The power in the hot rod is assumed at the technical specification peaking limits for the US U.S. EPR. The sample problem assumes peaking limits of $F_q = 2.6$ and $F_{\Delta H} = 1.7$.

[

]

The RCPs are modeled to reflect how the fluid is distributed vertically in the pumps to incorporate the physical elevation of the impeller into the model and to allow the fluid in the pump volutes (the pump discharge regions) to overflow into the discharge cold-legs. The pump model consists of a PUMP component representing the region from the pump suction to the impeller outlet and a

BRANCH component representing the pump volute. The flow area of the PUMP component is set to that of the pump suction piping.

Heat removal in the SGs is due to the MSRT opening at a SG pressure of 1406.9 psia. The MSRT system provides a controlled primary system cooldown at a rate of 180 °F/h down to a pressure to SG pressure of 892 psia. Steam generator tube plugging was set to 5% symmetrically.

The core is modeled with a two-dimensional component having 28 axial nodes and three radial nodes. The fuel pin model utilizes a radial nodalization having eight intervals in the pellet. This is for compatibility with the RODEX2 fuel code, which is used to generate the EOC burn-up conditions that are input to S-RELAP5. The Baker-Just metal water reaction correlation is used for all fuel rod heat structures. The rupture model was invoked for the hot rod.

The limiting case was identified via a break spectrum analysis. The initial conditions for the analysis are presented in Table C-1.

C.3. INITIAL CONDITIONS AND OTHER INPUT PARAMETERS

Table C-1 provides a listing of the initial conditions for the S-RELAP5 analysis of the SBLOCA event.

Table C-2 presents the safety classified I&C signals considered for this SBLOCA analysis. Degraded conditions are used to establish an uncertainty offset for signals unless the action occurs before degraded conditions occur. Mitigating systems are assumed to be actuated in the analyses at setpoints with allowance for instrument inaccuracy in accordance with Regulatory Guide 1.105. The Protection System (PS) scram trip credited in the SBLOCA analysis is generated on low pressurizer pressure. Conservative scram characteristics are assumed, i.e., maximum time delay with the most reactive rod held out of the core.

C.4. BREAK SPECTRUM

The sample problem analysis for the SBLOCA covers a range of breaks located in the pump discharge cold-leg. It includes 2.0, 2.5, 3.0, 3.5, 4.0 and 4.5-inch-diameter breaks. The 4.0-inch break produced the limiting PCT. (See Table C-3.)

The 2.0-inch, 2.5-inch and 3.0-inch breaks are small enough that MHSI flow is sufficient to prevent core uncover. The 3.5-inch, 4.0-inch and 4.5-inch breaks depressurize to the accumulator injection setpoint. There was a mild heatup for the 3.5-inch break before loop seal clearing, but there was no secondary heatup.

The analyses are terminated when the reactor vessel mass starts to increase, the vessel downcomer is filled to the elevation of the cold-leg nozzles, the SIS flow exceeds the break flow, and the core collapsed level shows an increasing trend.

The 4.0 -inch break is large enough to cause the system to depressurize to the accumulator injection pressure at 1194 seconds. The injected water causes a momentary increase in pressure so the accumulators stop discharging. The primary continues to depressurize causing a sustained accumulator injection between 1282 and 1352 seconds.

For the 4.0-inch break, the first core heatup occurs around 350 seconds due to loop seal plugging. This leads to a temporary depression in core level (Figure C-12). Following the loop seal clearing in Loop 2, the collapsed core level increases and leads to core quench. A core boil-off starts at about 750 seconds. The boil-off leads to a deeper and prolonged core uncover from about 750 seconds to about 1100 seconds when the core level starts a slow recovery. The recovery becomes more pronounced due to the large amount of liquid injected by the accumulators between 1282 and 1352 seconds. The sustained accumulator discharge occurs after the PCT turn-around. The cladding temperature recovers primarily on MHSI flow alone (see Table C-4, Sequence of events). By the time the calculation is terminated, the accumulators have ceased to discharge and the flow from two MHSI trains exceeds the break flow.

The 4.0-inch break is the limiting break. The 4.0-inch break causes a longer period of core uncover than do the 3.5-inch and 4.5-inch breaks. The rate of depressurization to the accumulator discharge pressure is slower than that for the 4.5 inch break; and, therefore, the amount of time the hot rod spends uncovered is greater.

The 4.5-inch break behaves similarly to the 4.0-inch break. The 4.5-inch break, unlike the 4.0-inch break, recovers as soon as accumulator discharge begins.

C.5. 4.0-INCH BREAK (LIMITING CASE)

Table C-4 presents the sequence of events for this break case. Cladding temperatures rise steadily from about 750 seconds to about 1000 seconds, when cladding quench occurs.

Break flow is plotted in Figure C-4. The break flow is driven by the combination of system pressure and the void fraction at the break (Figure C-5). Until the loop seal clears, break flow mirrors the primary pressure. At that time, the flow transitions from liquid to steam and the mass flow out the break drops precipitously (see Figure C-4).

Figure C-6 shows the pressure traces for the RCS and the secondary side of one of the four steam generators. The behavior is typical of limiting SBLOCA events. The primary pressure drops rapidly to saturation at about 50 seconds. From 50 seconds to about 550 seconds, corresponding to the loop seal clearing, the primary pressure is controlled by the MSRT opening and closing to control the RCS depressurization. The primary pressure again falls as the core level drops and the boil-off rate decreases. At about 800 seconds, once the break flow transitions to steam, the energy removal by the break is sufficient to depressurize the primary system below the SG secondary side pressure. Primary pressure increases when the accumulators start to discharge because the volumetric flow through the break decreases with decreasing void fraction at the break due to the accumulator water and condensate. Figure C-7 shows the pressure traces in all the four SGs. Figure C-8 shows the inventories of the SGs. The inventory of SG2

decreases more than the others because flow through the MSRT in SG2 persists for a longer period. This is attributed to the fact that the seal in loop 2 clears first and therefore, SG2 removes more energy from the primary system.

Figure C-9 shows MSRT flow. Because break flow is not sufficient to offset decay heat, heat transfer to the SGs causes SG pressure increases to the MSRT opening setpoint of 1406.87 psia. The MSRV opens and the SG pressure drops because the Main Steam Relief Control Valve (MSRCV) is fully open at that time and energy removal is high. From then on, the MSRCV modulates to maintain a primary cooldown rate of 180 °F/hr.

Figure C-10 shows void fraction in the horizontal legs of the loop seals. As expected because of the loop seal biasing methodology, only one loop (Loop 2) clears first at 544 seconds. This is defined as a void fraction in the horizontal leg that is greater than 0.97.

Loop 1 clears at 1334 seconds, followed almost immediately by the broken loop (Loop 4) at 1336 seconds and Loop 3 at 1346 seconds. After the initial clearing, some of the four loops experienced some carryover of liquid from the vertical segments of the seal; however, there is always at least one loop seal that is open.

Figure C-11 shows the combined MHSI flow for this case. MHSI flow increases as the system depressurizes when the break flow transitions to steam.

Collapsed liquid level for the hot fuel assembly is shown in Figure C-12. The core uncovers before loop seal clearing at about 300 seconds. The two-phase level recovers to the top of core after loop seal clearing. The core uncovers again at about 720 seconds and the two-phase level recovers to the top of core at about 1400 seconds.

Figure C-13 presents the total accumulator flow into all four loops. The accumulators start injecting at 1194 seconds and stop at 1216 seconds when pressure increases slightly in the primary system due to the change in break flow from steam to liquid. The accumulators start injecting again at 1282 seconds, and

the flow stops at 1352 seconds. As the core refloods, the steam generation rate increases and system pressure rises. The pressure rise reduces MHSI flow and the accumulator discharge ceases.

Figure C-14 presents the RCS and RPV inventory. At 2000 seconds, the RPV inventory shows a slight increase while the RCS inventory exhibits a plateau, consistent with the vessel pressure and the MHSI flow.

Figure C-15 shows the steam and cladding temperatures for the fuel segment experiencing the maximum PCT of 1128.7 °F. Cladding temperature starts to recover with MHSI flow alone. It approaches saturation when accumulators discharge toward the end of the PCT recovery.

The analysis is terminated at 2000 seconds, at which time conditions are stable, pumped injection exceeds the break flow and decay heat is being removed by the combination of the MHSI and break flow.

C.6. RESULTS/SUMMARY/CONCLUSION

AREVA NP's, NRC-approved, SBLOCA evaluation methodology was used to perform a SBLOCA sample problem analysis for the U.S. EPR plant design. The analysis covered a spectrum of breaks in the pump discharge cold leg piping. The analyses assumed the worst-case failure of a diesel generator that takes out one entire train of SIS injection and EFW (no EFW injection was assumed). Additionally, it assumed another train of SIS injection was unavailable because of preventive maintenance. EOC fuel conditions were assumed as calculated by RODEX2-2A. Peak cladding temperature was calculated for the hot rod using S-RELAP5.

The analyses showed the following:

1. The highest PCT, 1128.7 °F, is calculated for a 4-inch break. This value is well below the 2200 °F PCT limit specified in 10CFR50.46(b)(1).
2. The total cladding oxidation at the peak location is 0.0443 %, well below the 17% limit specified in 10CFR50.46(b)(2).

3. The hydrogen generated in the core by cladding oxidation (0.00118%) during these accidents is less than 1% limit specified in 10CFR50.46 (b)(3).
4. The calculation shows that the core retains a coolable geometry. There is no clad rupture for any of the four fuel rods in the three core region. Thus the coolable geometry criterion in 10CFR50.46 (b)(4) is satisfied.

Other observations are:

1. Sensitivity studies performed in Reference 1 for a three-loop Westinghouse plant indicate that the solution is converged with respect to time step size, restart application, loop seal biasing, pump application, core radial flow, and nodalization. Therefore no additional sensitivity studies are required for the SBLOCA analysis of the U.S. EPR.
2. SBLOCA events in the U.S. EPR exhibit all the phenomena encountered in a U.S. PWR plant. The limiting break exhibits all five phases of a small break LOCA: blowdown, natural circulation, loop seal clearance, boil off and core recovery. As such, the U.S. EPR behaves in the same manner as other U.S. PWRs during a SBLOCA event.

The overall conclusion is that the current SBLOCA evaluation methodology is applicable to the U.S. EPR. The U.S. EPR is similar to other U.S. PWRs for which the methodology was used successfully to analyze SBLOCA events.

C.7. References

- C-1. "PWR Small-Break LOCA Evaluation Model, S-RELAP5 Based," AREVA NP Report EMF-2328 (P)(A), Revision 0, March 2001.

Table C-1 Input Parameters

Parameter	EPR Value
Core power	4500.0 MWth + 2%= 4590 MWth
Axial power shape and power peaking	An EOC top skewed
Loop flow rate/per loop	119,670 gpm
Reactor vessel Average temperature	596.0 °F
Primary pressure (Pressurizer Pressure)	2250 psia
Initial Pressurizer Liquid Level	56%
Secondary pressure	1108 psia, consistent with the plugging level
Initial SG Level	49 % NR
SG Secondary Side Inventory	179,500 lbm/SG
Accumulator pressure	652.7 psia
Accumulator level	Accumulator Liquid Volume: 1324 ft ³ , Accumulator Total Volume: 1942 ft ³
Accumulator temperature	90.5°F
MHSI fluid temperature	140°F
SG tube plugging ¹	5%
EFW Flow	Assumed not to inject

¹ Performing the SBLOCA analysis at higher tube plugging levels is conservative because the initial primary system mass inventory is reduced.

Table C-2. Safety Classified I&C Signals Considered for SBLOCA Analysis

Signal	Setpoint
Reactor Trip, on low PZR pressure	1958 psia – 43.51 = 1914.49 psia Degraded conditions 43.51 psi Trip Delay = 0.9 seconds
Turbine Trip, on RT signal	1958 psia – 43.51 psia Degraded conditions 43.51 psi Trip Delay = 0.3 seconds
Beginning of Rod Insertion	1.2 seconds after RT signal (0.9+0.3 seconds), 3.5 seconds for complete rod insertion (seismic conditions)
MFW Isolation	1.2 seconds after RT
Safety Injection, on low-low PZR pressure	1667.96 - 43.51 = 1624.45 psia Degraded conditions 43.51 psi Trip Delay = 0.9 seconds 40 seconds delay for SIS pump start up (includes diesel delay + pump startup)
RCP trip	RCP trip on LOOP at the time of scram
MSRT opening and pressure control, (partial cooldown signal simultaneously with SI signal)	1385.13 + 21.76 psia before beginning of partial cooldown. 870.24 + 21.76 psia after the end of partial cooldown. Time delay: 2 seconds
EFWS	EFW assumed not to inject

Table C-3 Break Spectrum- Peak Cladding Temperature

Break Size	Break Area (ft²)	PCT (°F)	Time of PCT (sec)
2 in	0.0218	No Heatup	N/A
2.5 in	0.0341	No Heatup	N/A
3.0 in	0.0491	No Heatup	N/A
3.5 in	0.0668	704.99	681.54
4.0 in	0.0873	1128.7	1056.1
4.5 in	0.1104	1011.3	893.15

Table C-4 Limiting Break Sequence of Events

Event	Time (sec)
Break initiation	0.0
Reactor and RCP trip (with delay)	18.7
SIAS trip (with delay)	71.69
MHSI Injection Began	479.0
Loop seal clearing – Loop 2 (Void >0.97)	544
Break uncover (Void >0.97)	552
Emergency Feedwater initiated	N/A
PCT occurs (1128.7 °F, Node 31)	1056.1
Accumulator injection	1194-1218 1282-1352
Loop seal clearing – Loop 1 (Void >0.97)	1332
Loop seal clearing – Loop 4 (Void >0.97)	1336
Loop seal clearing – Loop 3 (Void >0.97)	1346
End of Calculation	2000

Figure C-1 U.S. EPR Vessel Nodalization

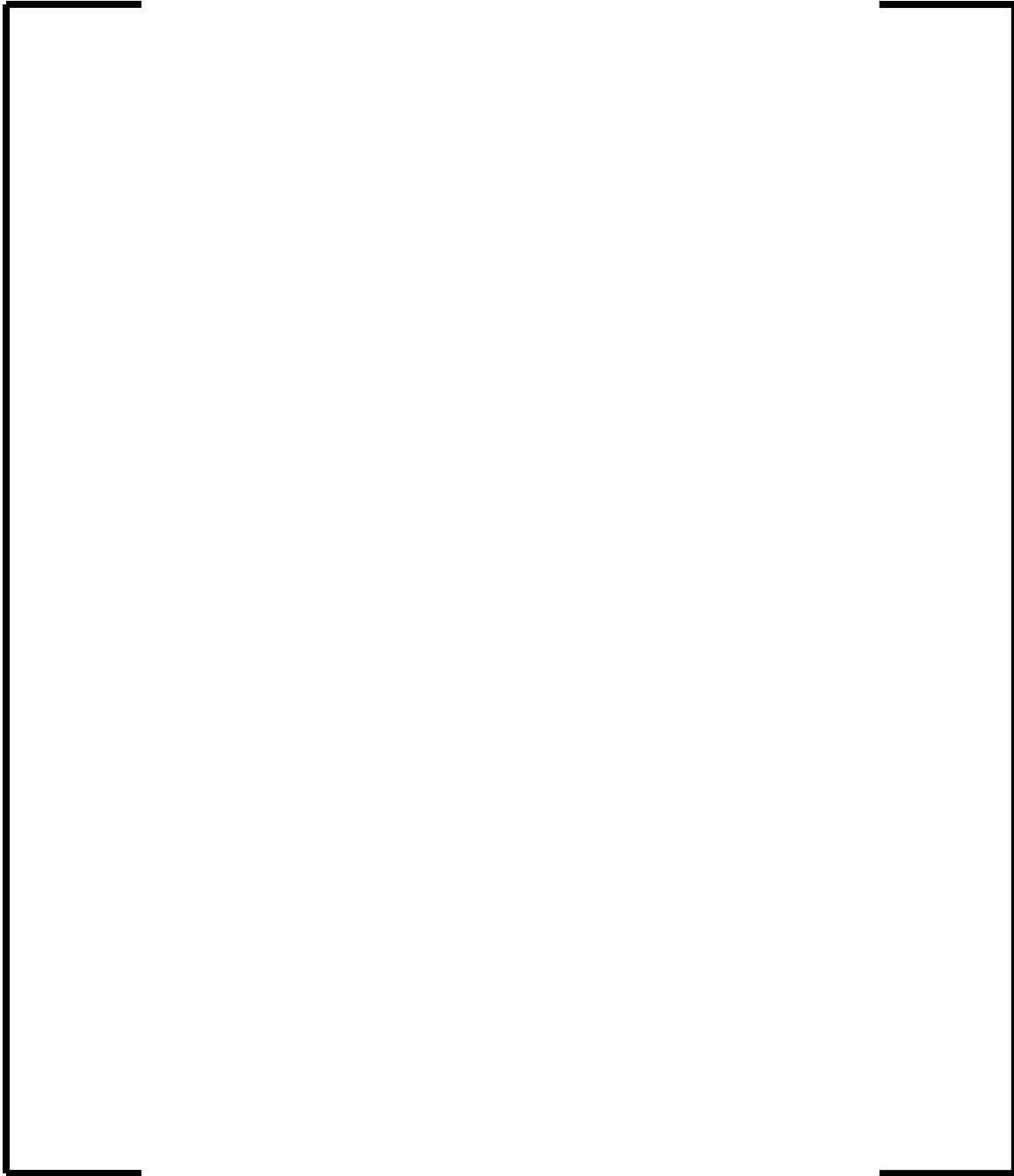


Figure C-2 U.S. EPR Steam Generator Nodalization

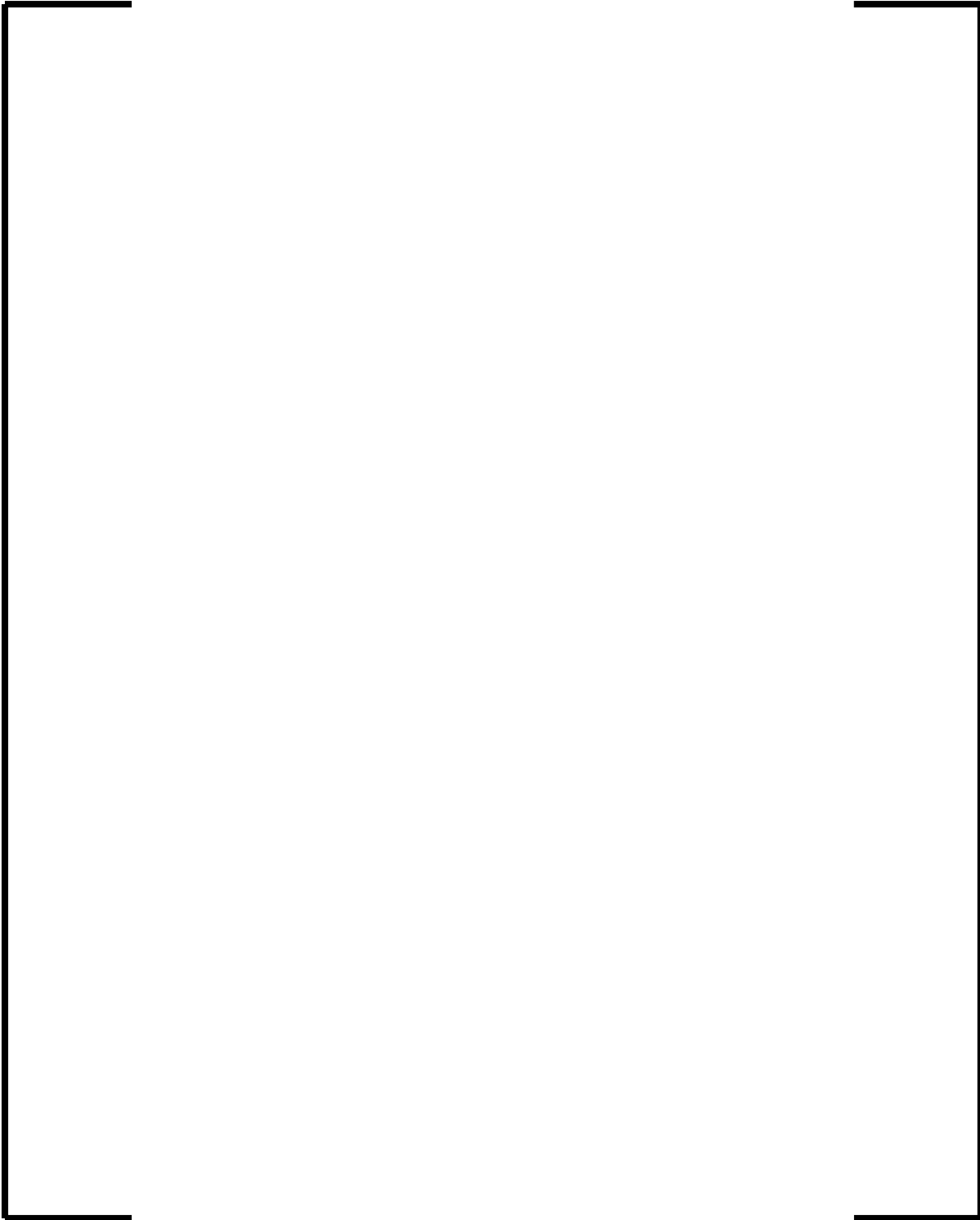


Figure C-3 U.S. EPR Loop Nodalization

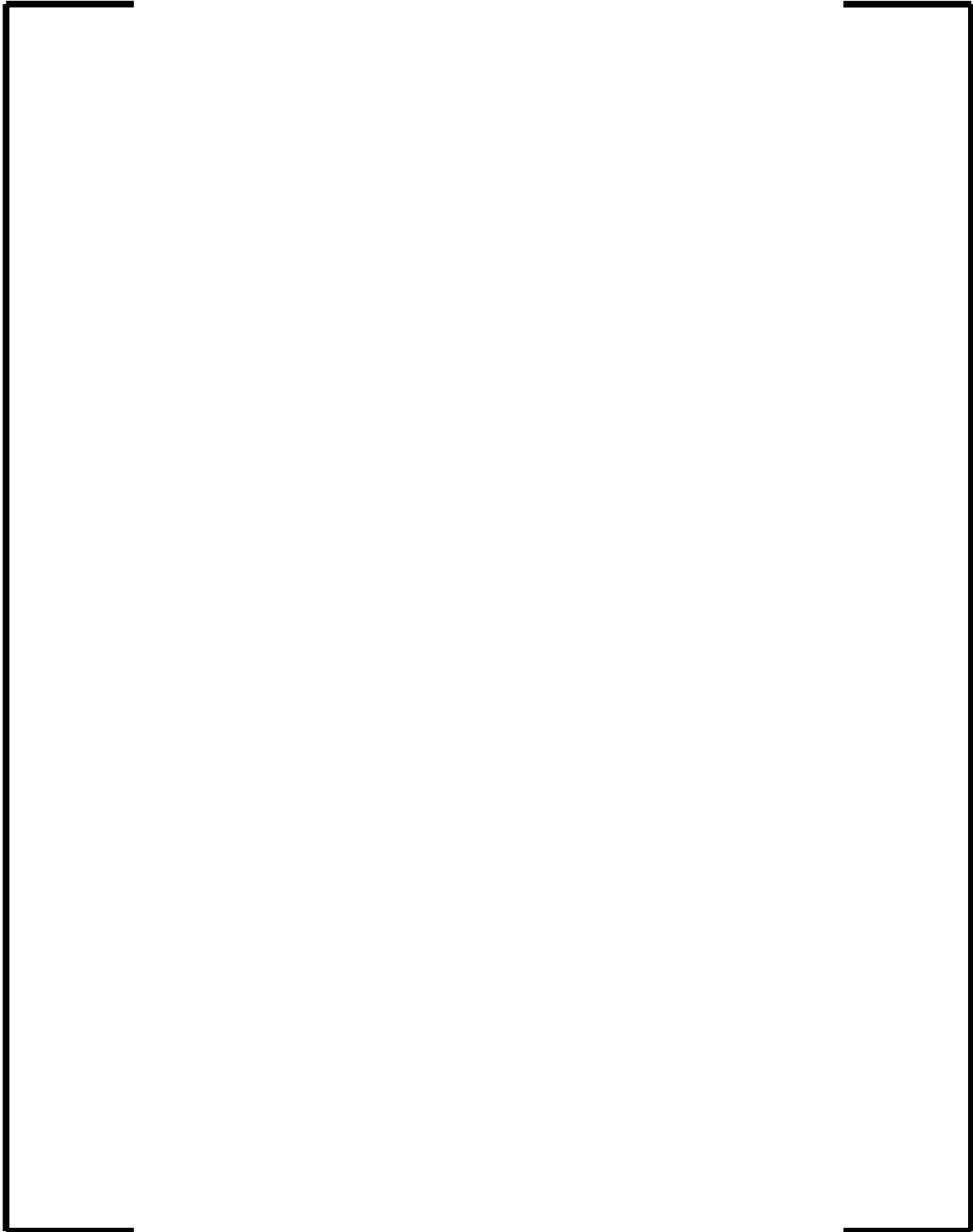


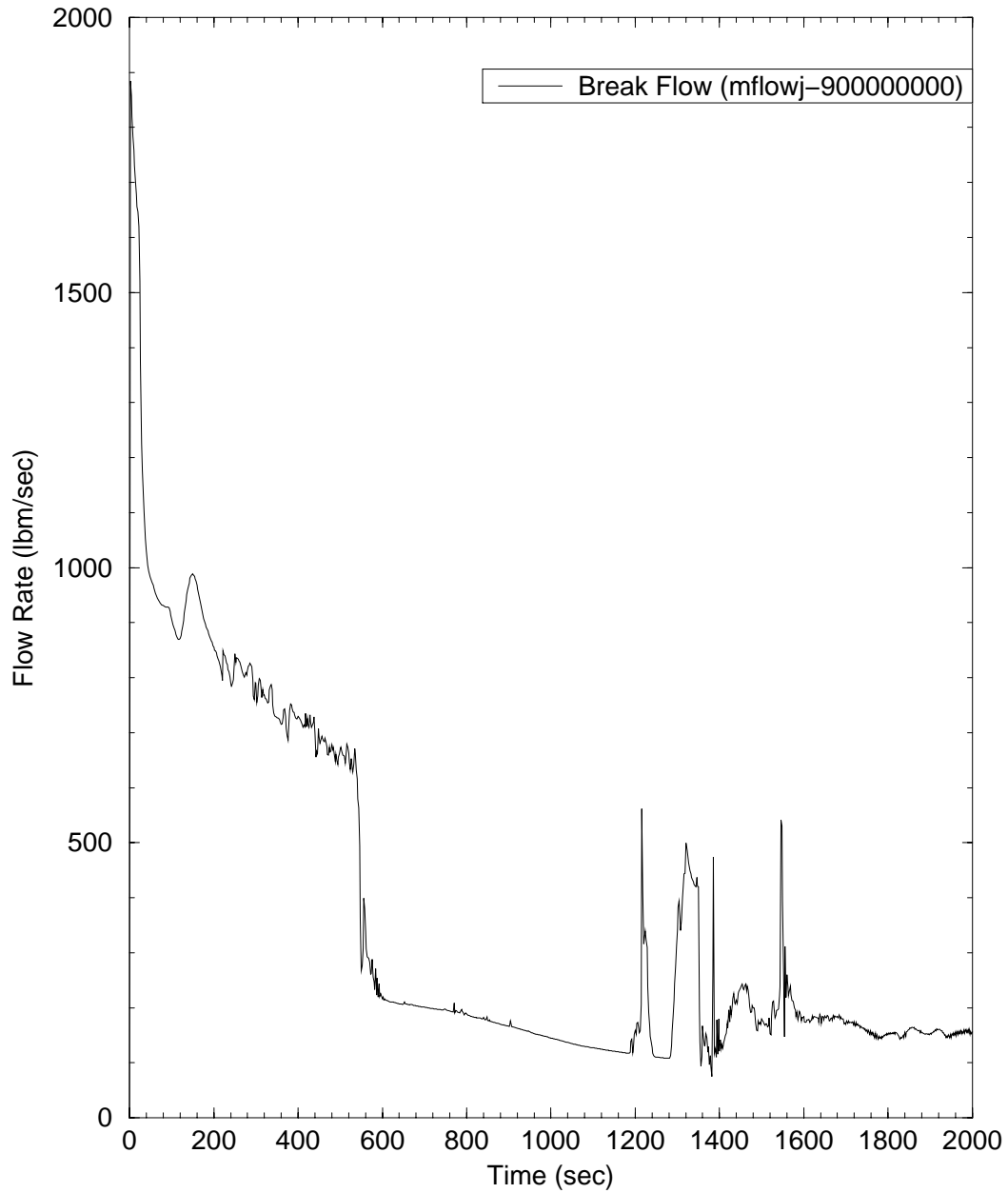
Figure C-4 Break Flow Rate for 4.0 Inch Break

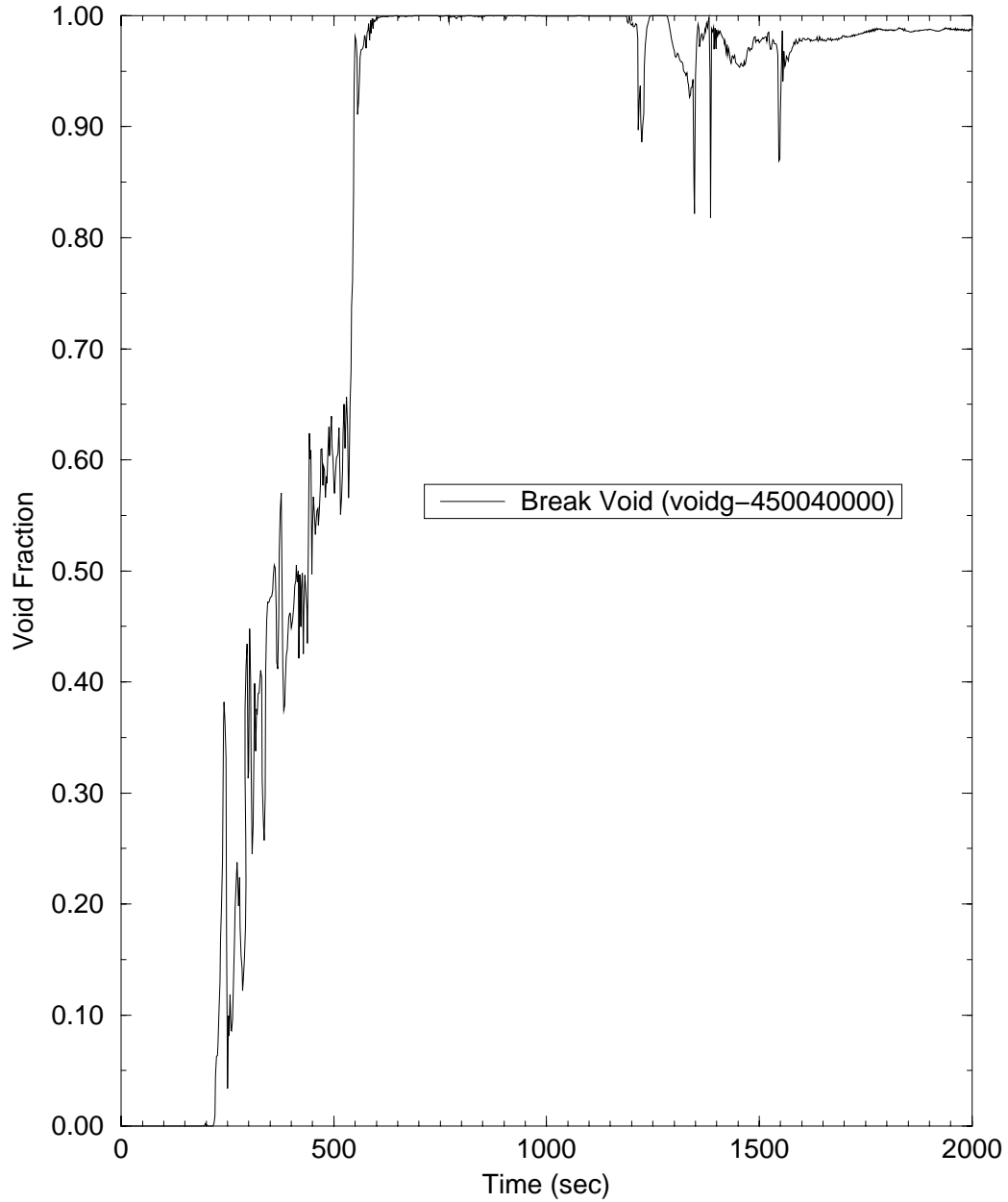
Figure C-5 Break Void Fraction for 4.0 Inch Break

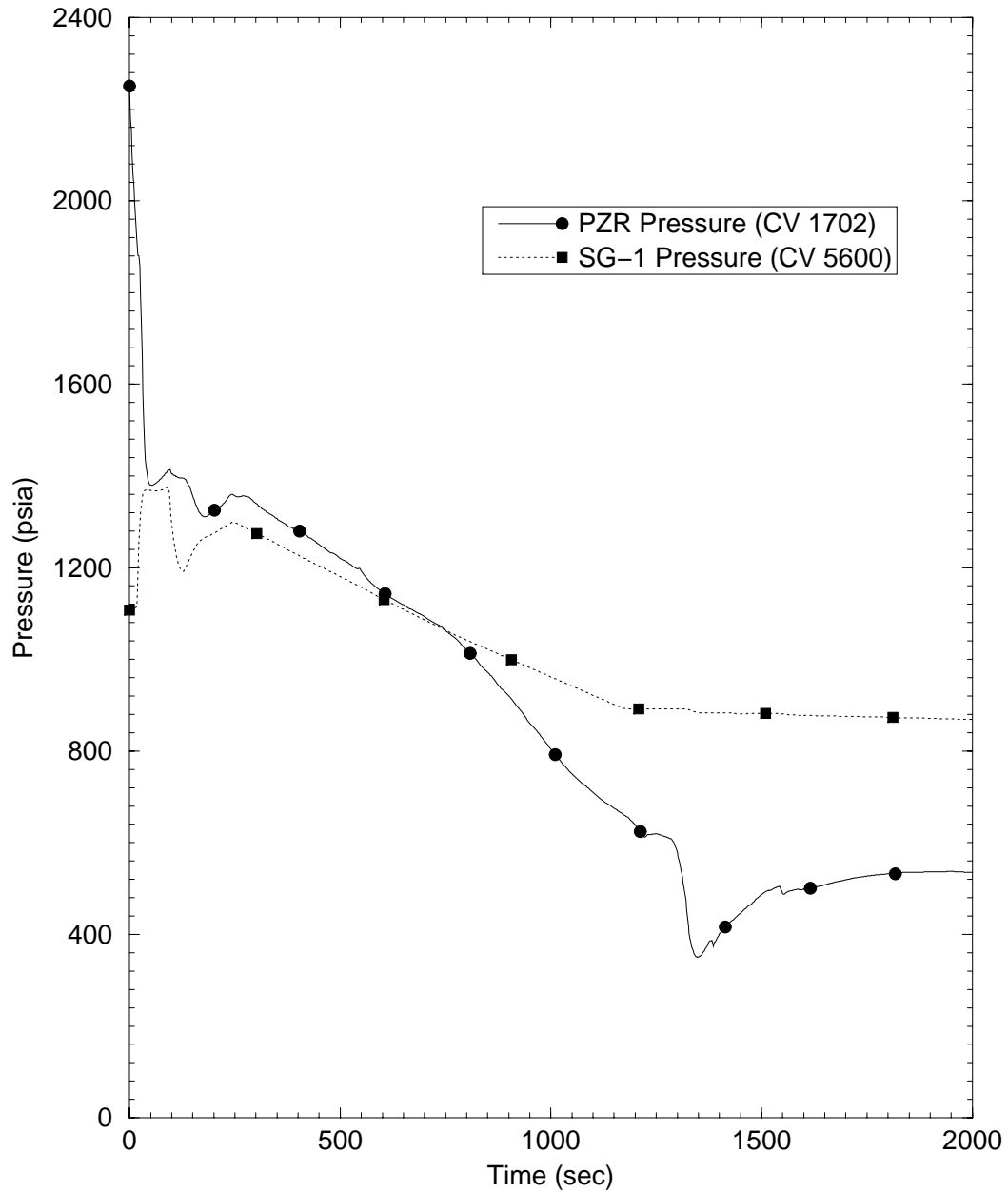
Figure C-6 Primary and Secondary System Pressures for 4.0 Inch Break

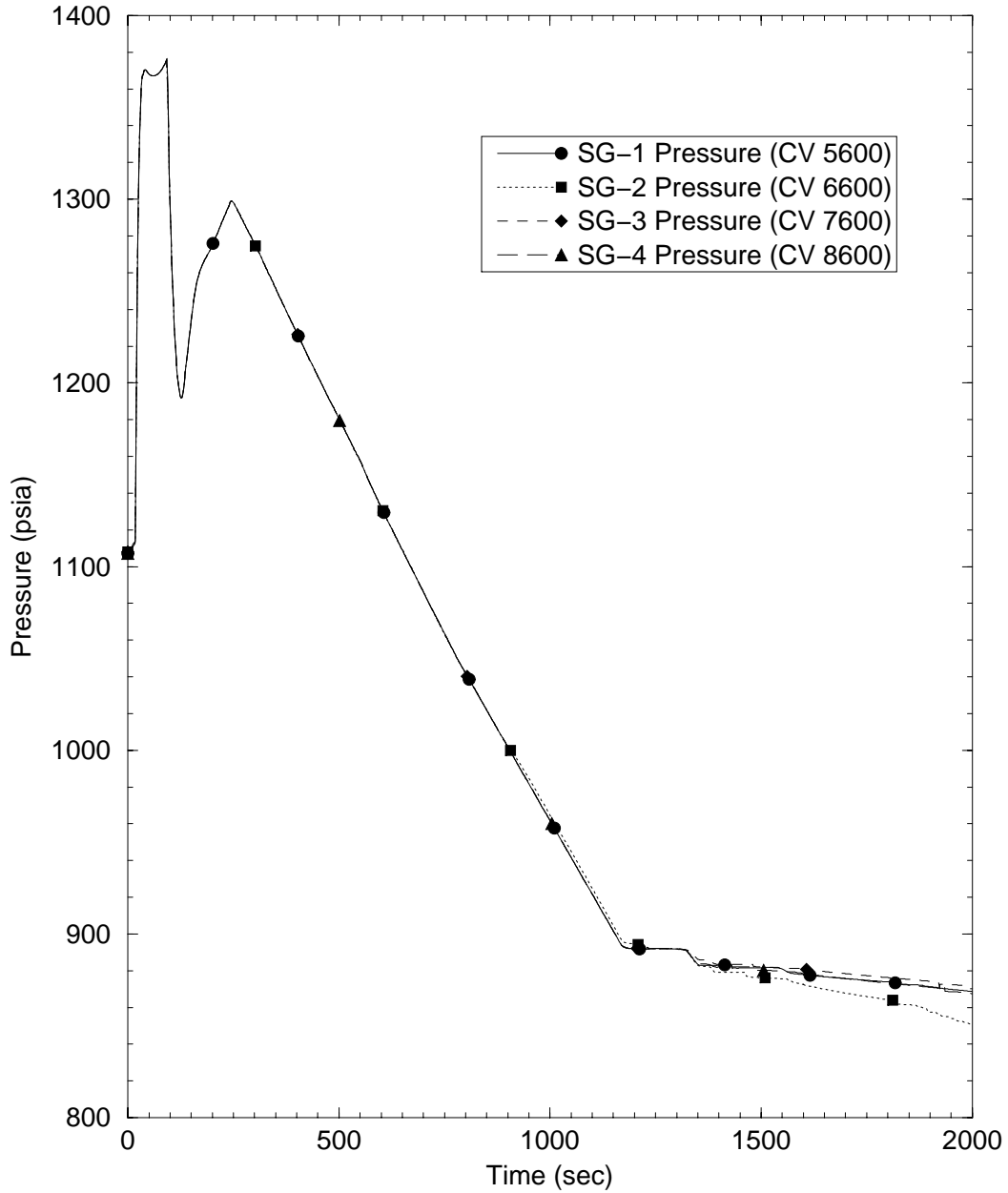
Figure C-7 Steam Generator Pressures for 4.0 Inch Break

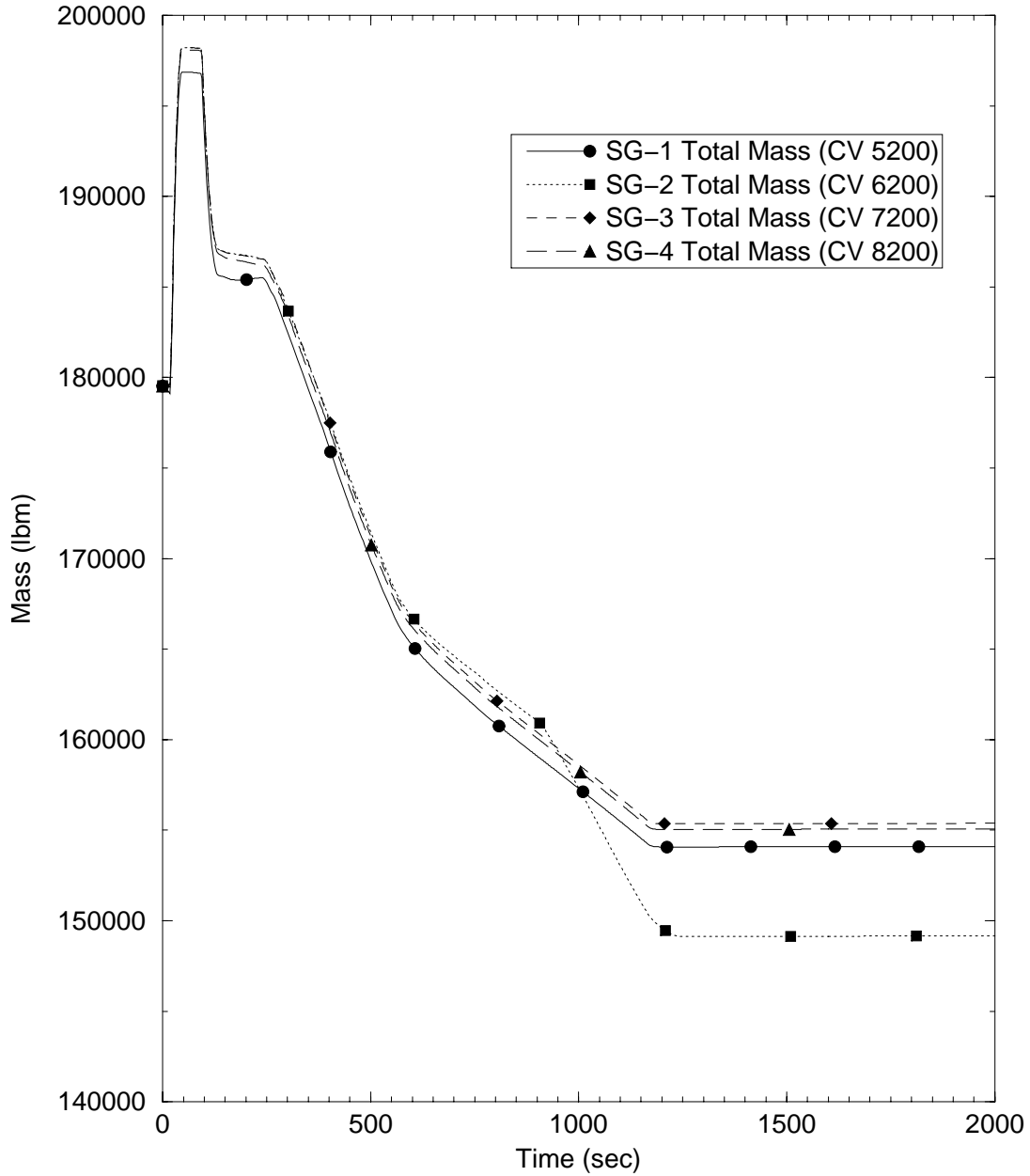
Figure C-8 Steam Generator Total Mass Inventories for 4.0 Inch Break

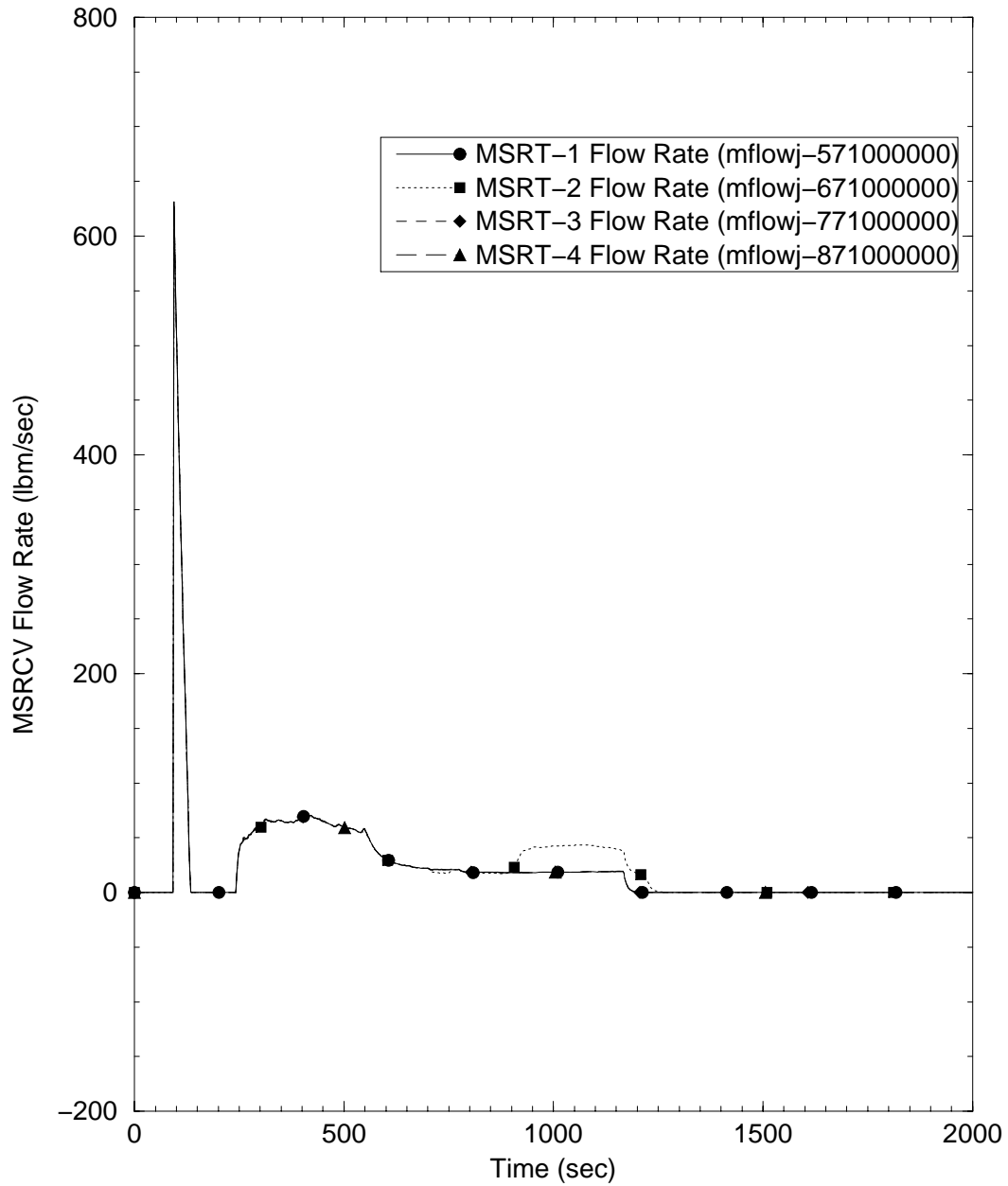
Figure C-9 MSRT Flow Rate for 4.0 Inch Break

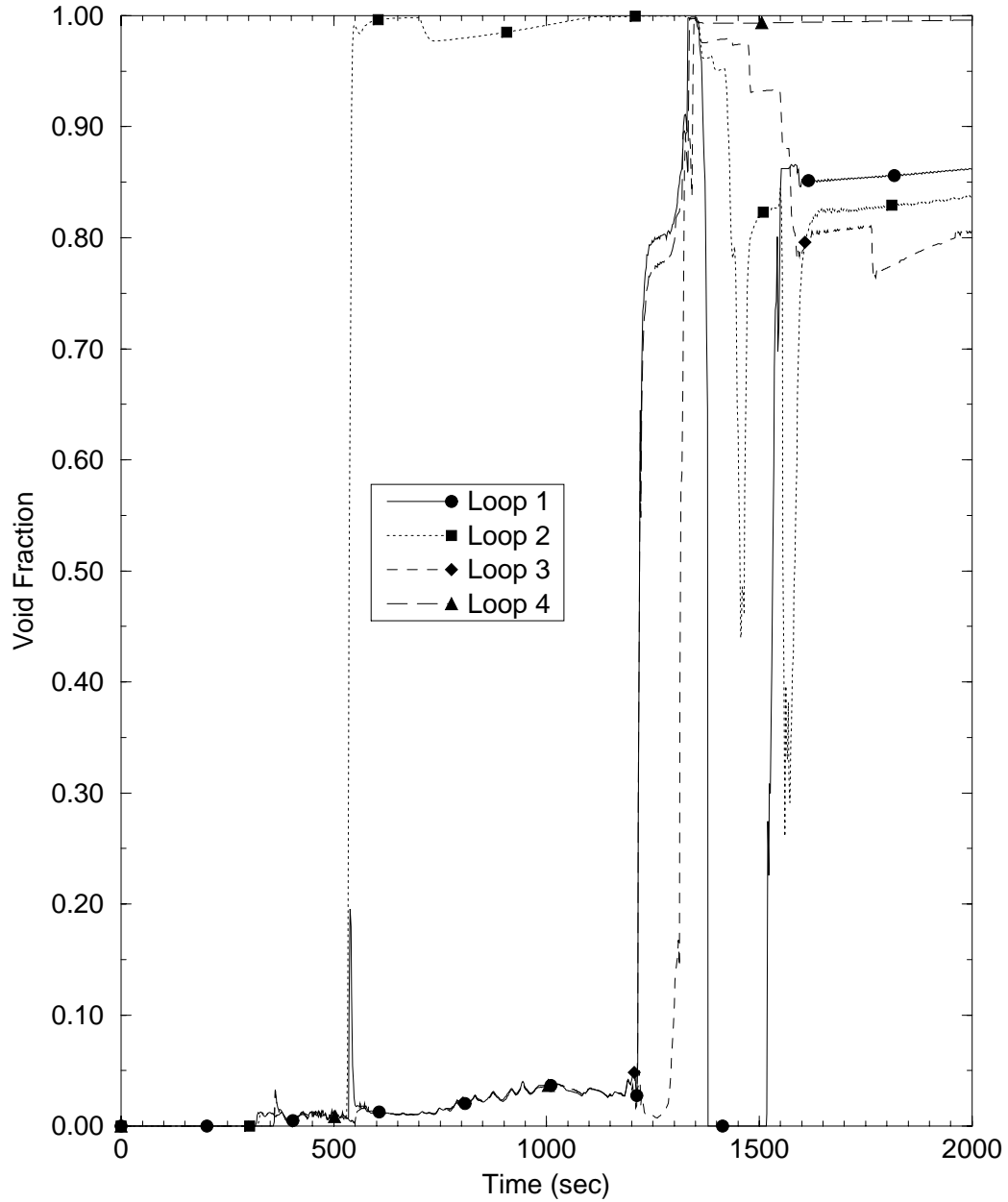
Figure C-10 Loop Seal Void Fraction for 4.0 Inch Break

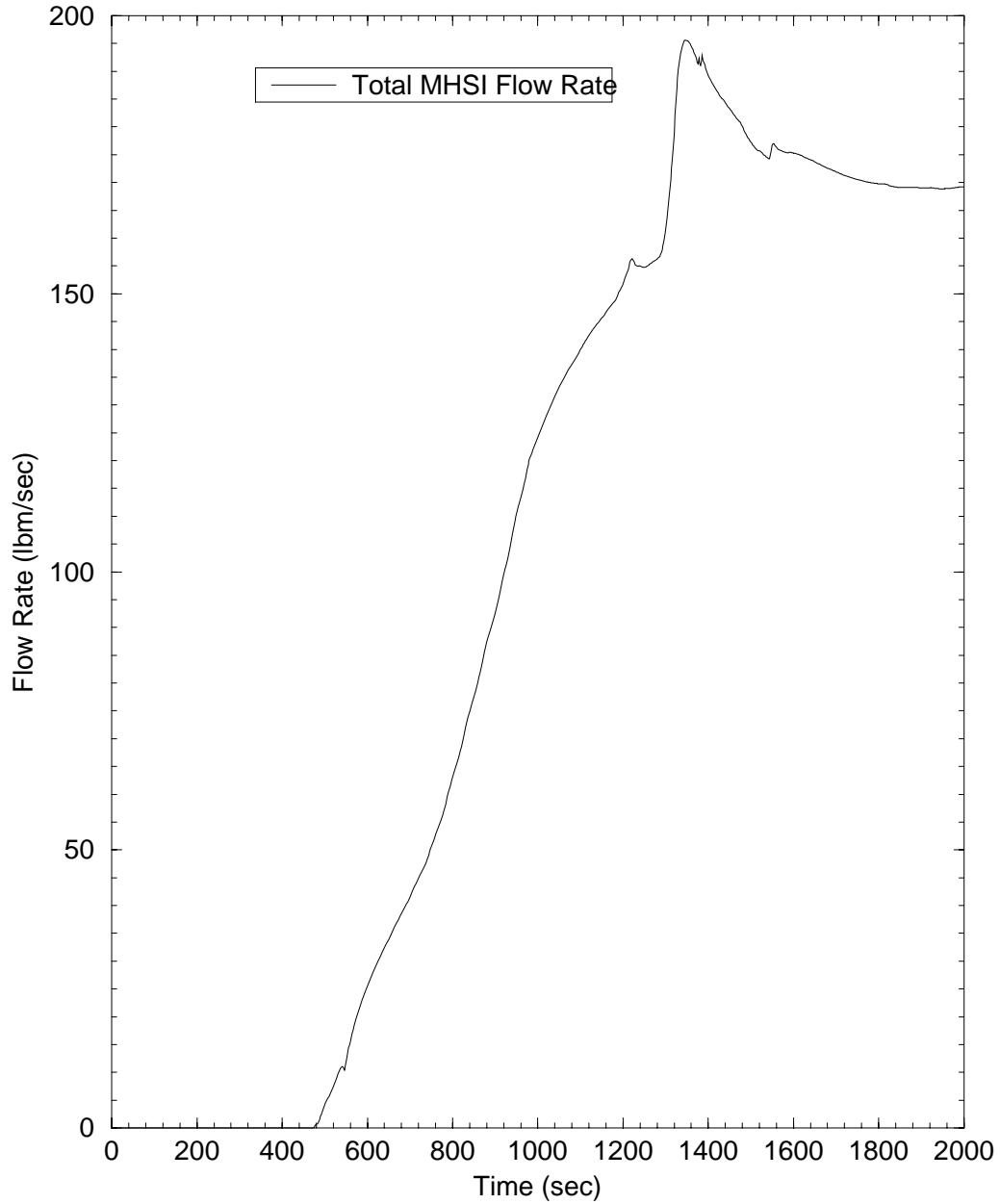
Figure C-11 Total MHSI Flow (Loops 3 and 4) for 4.0 Inch Break

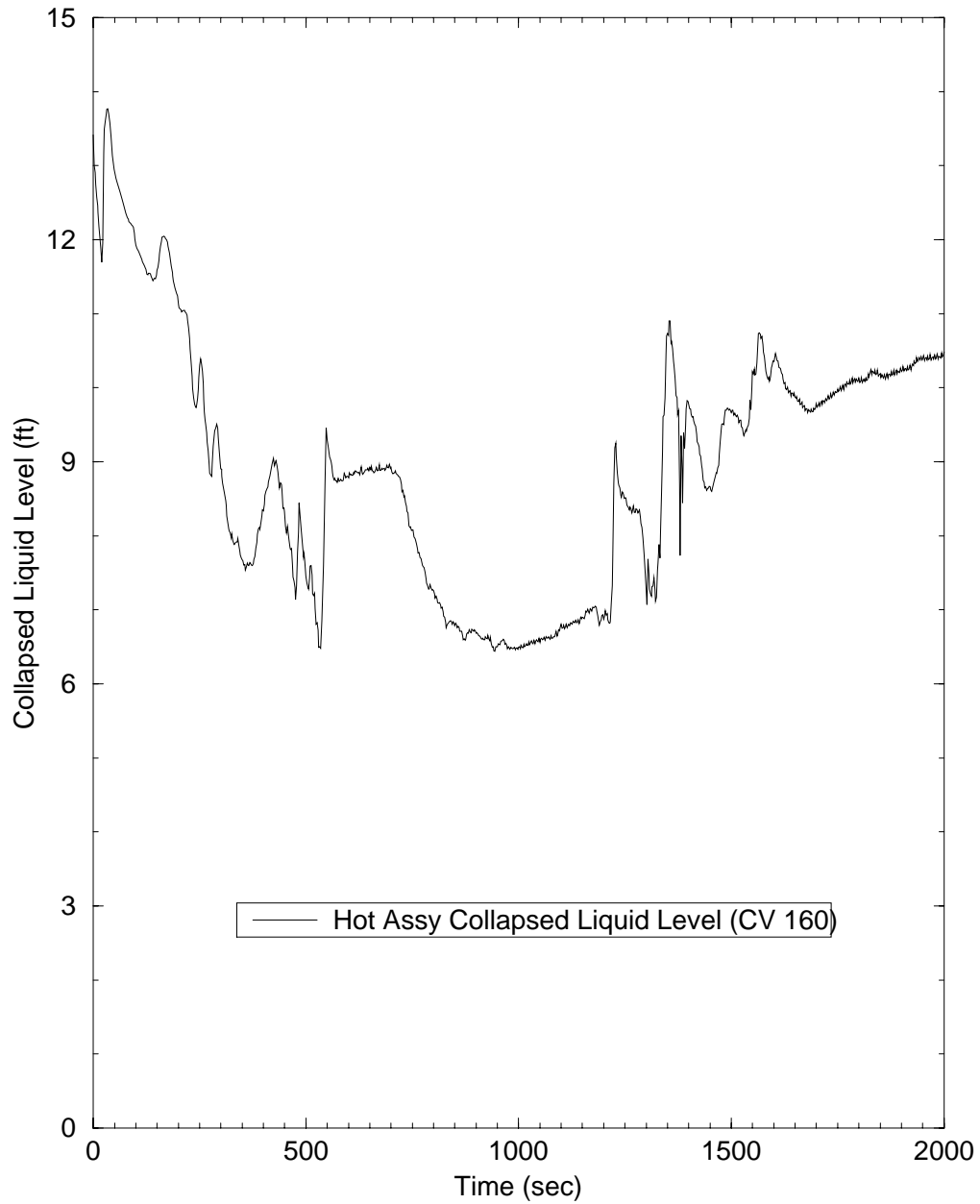
Figure C-12 Hot Assembly Collapsed Liquid Level for 4.0 Inch Break

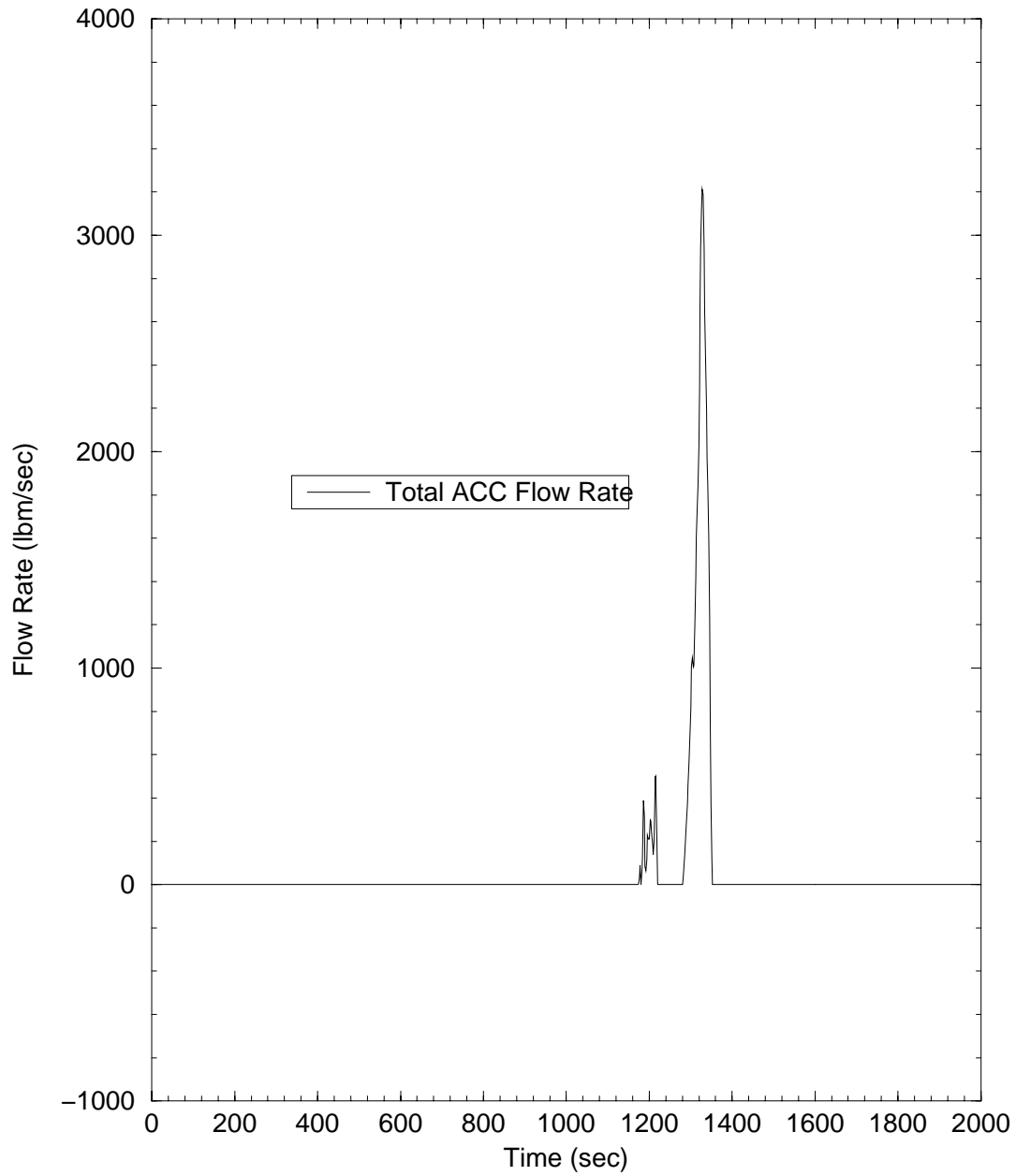
Figure C-13 Total Accumulator Flow for 4.0 Inch Break

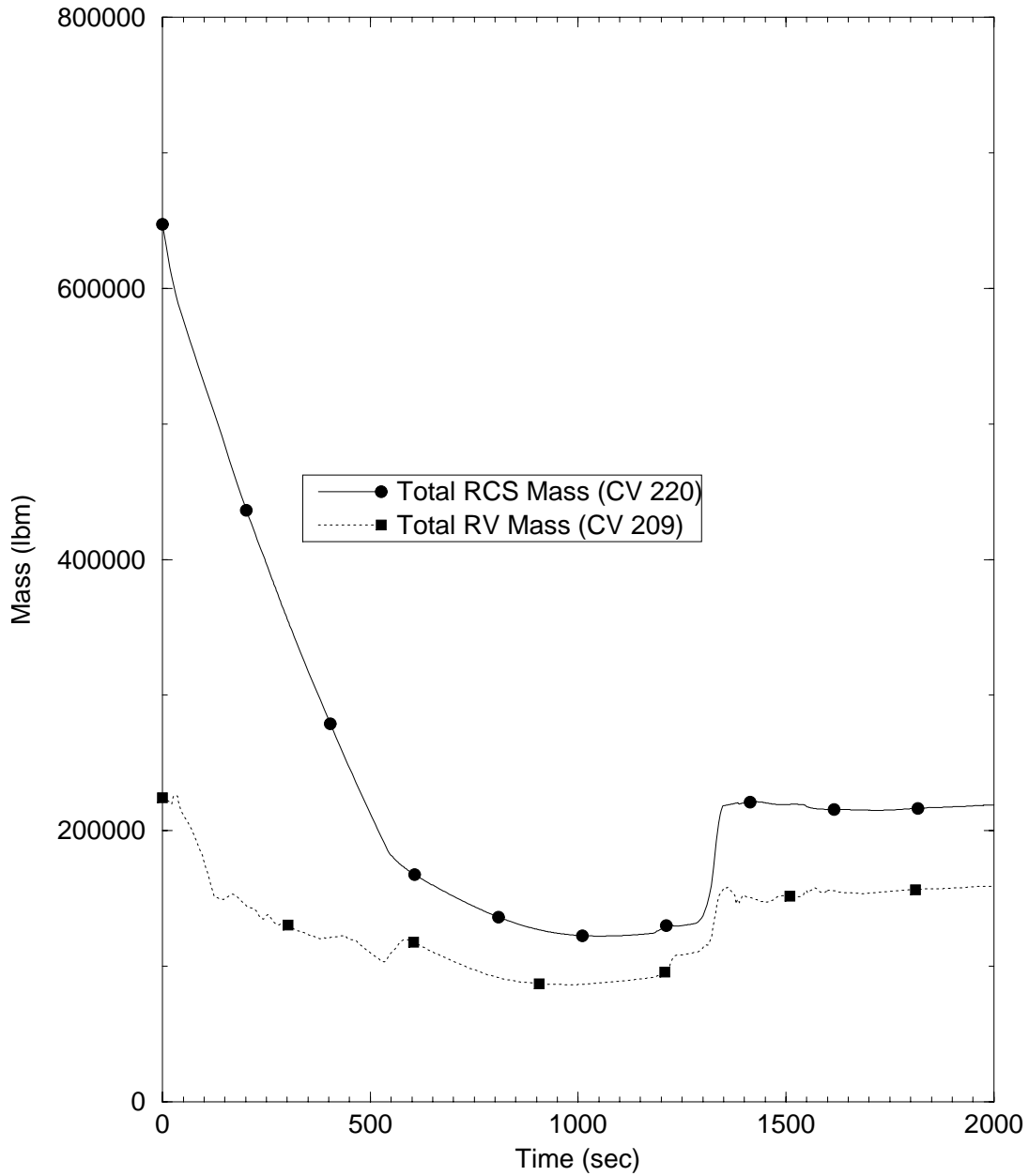
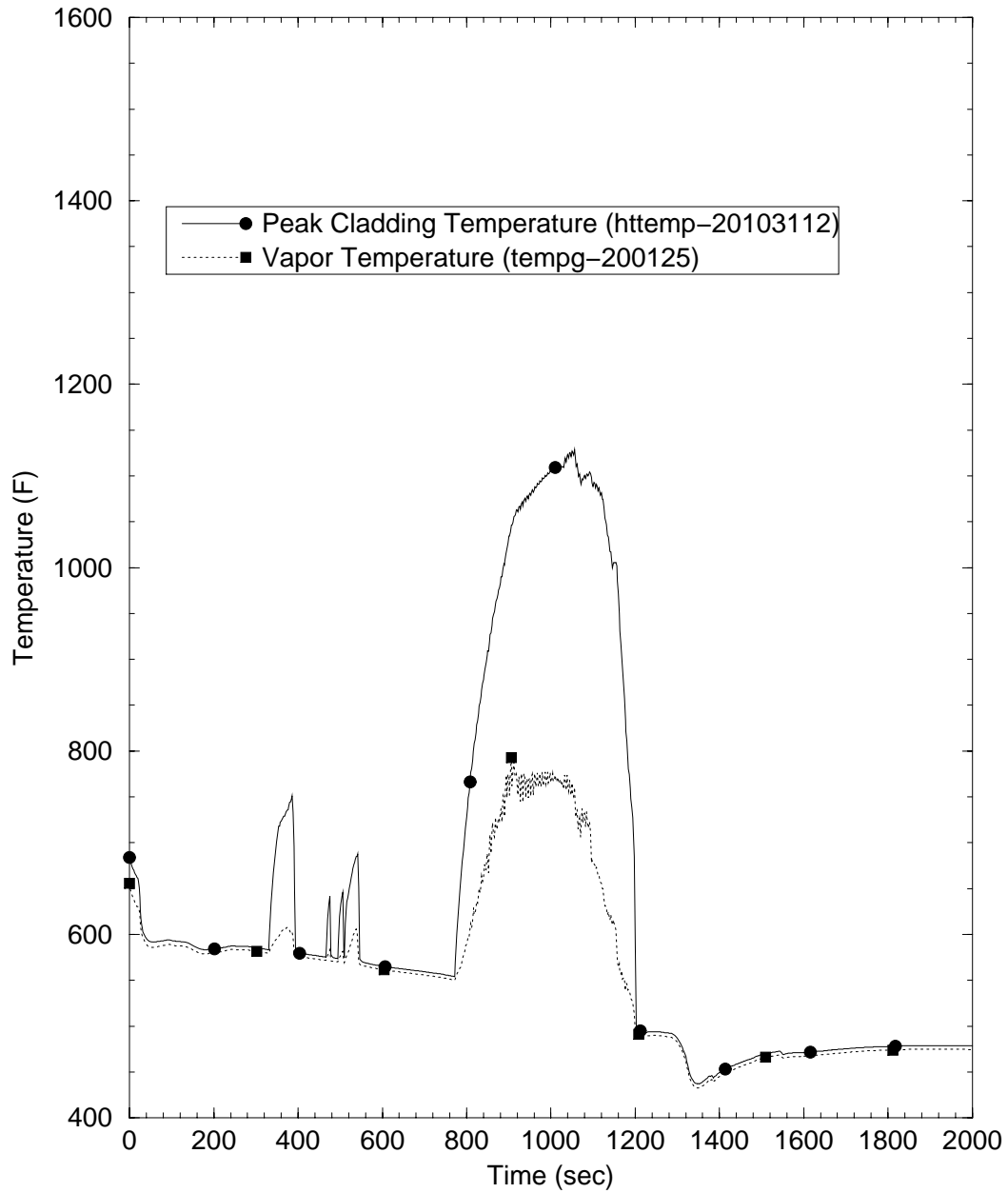
Figure C-14 Total RCS and RV Mass Inventories for a 4.0 Inch Break

Figure C-15 Vapor and Clad Temperature for Hot Node for 4.0 Inch Break

APPENDIX D

NON-LOCA SAMPLE CALCULATIONS

TABLE OF CONTENTS

	<u>Page</u>
D.1. Post-Scram MSLB.....	D-1
D.2. Loss of External Load/ Turbine Trip	D-4
D.3. Loss of Normal Feedwater	D-6
D.4. Loss of Coolant Flow.....	D-9
D.5. Uncontrolled RCCA Bank Withdrawal at Power	D-11
D.6. Steam Generator Tube Rupture.....	D-13
D.7. References.....	D-17

LIST OF TABLES

Table D.1-1 Sample Problem Initial Conditions	18
Table D.1-2 Post Scram MSLB Event Summary	19
Table D.2-1 Loss of Load/Turbine Trip (Primarily Overpressure Case) Event Summary	21
Table D.3-1 LONF Event Summary	22
Table D.4-1 LOCF Event Summary	23
Table D.5-1 UCBW at Power Event Summary	24
Table D.6-1 SGTR Event Summary	25
Table D.6-2 Integrated Break Flow and Steam Release to Atmosphere	27

LIST OF FIGURES

	<u>Page</u>
Figure D.1-1 Post Scram MSLB Break Flow Rates	D-28
Figure D.1-2 Post Scram MSLB Steam Generator Pressures	D-29
Figure D.1-3 Post Scram MSLB Main Steam Relief Train Flow Rates	D-30
Figure D.1-4 Post Scram MSLB Steam Generator Heat Transfer Rates	D-31
Figure D.1-5 Post Scram MSLB Feedwater Flow Rates	D-32
Figure D.1-6 Post Scram MSLB Steam Generator Secondary-Side Liquid Inventories	D-33
Figure D.1-7 Post Scram MSLB Core Inlet Temperatures	D-34
Figure D.1-8 Post Scram MSLB Pressurizer Pressure	D-35
Figure D.1-9 Post Scram MSLB Pressurizer Liquid Level	D-36
Figure D.1-10 Post Scram MSLB Reactivity	D-37
Figure D.1-11 Post Scram MSLB Reactor Power	D-38
Figure D.1-12 Post Scram MSLB Longer-Term Reactor Power	D-39
Figure D.2-1 LOEL/TT Steam Generator Pressures	D-40
Figure D.2-2 LOEL/TT RCS Temperatures	D-41
Figure D.2-3 LOEL/TT Pressurizer Pressure	D-42
Figure D.2-4 LOEL/TT Pressurizer Level	D-43
Figure D.2-5 LOEL/TT Reactor Power	D-44
Figure D.2-6 LOEL/TT Total Reactivity	D-45
Figure D.2-7 LOEL/TT RCS Loop Flow Rates	D-46
Figure D.2-8 LOEL/TT Pressure at Bottom of Reactor Vessel	D-47
Figure D.3-1 LONF (With Offsite Power) Reactor Power Level	D-48
Figure D.3-2 LONF (With Offsite Power) RCS Temperatures	D-49
Figure D.3-3 LONF (With Offsite Power) Pressurizer Pressure	D-50
Figure D.3-4 LONF (With Offsite Power) Pressurizer Liquid Level	D-51
Figure D.3-5 LONF (With Offsite Power) Steam Generator Pressure	D-52
Figure D.3-6 LONF (With Offsite Power) Steam Generator Inventory	D-53
Figure D.4-1 LOCF Reactor Power Level	D-54
Figure D.4-2 LOCF Pressurizer Pressure	D-55
Figure D.4-3 LOCF Reactivity	D-56
Figure D.4-4 LOCF Reactor Coolant System Flowrate	D-57
Figure D.5-1 UCBW Core Power	D-58
Figure D.5-2 UCBW Reactivity	D-59
Figure D.5-3 UCBW Average Fuel Rod Heat Flux	D-60
Figure D.5-4 UCBW RCS Temperatures	D-61
Figure D.5-5 UCBW Pressurizer Pressure	D-62
Figure D.5-6 UCBW Pressurizer Liquid Level	D-63
Figure D.5-7 UCBW Steam Generator One Pressure	D-64
Figure D.6-1 SGTR Reactor Power	D-65
Figure D.6-2 SGTR Pressurizer Pressure	D-66
Figure D.6-3 SGTR Pressurizer Liquid Level	D-67
Figure D.6-4 SGTR RCS Temperatures – Intact SG Loops	D-68

Codes and Methods Applicability Report
for the U.S. EPR

Figure D.6-5	SGTR RCS Temperatures – ruptured SG loop	D-69
Figure D.6-6	SGTR Steam Generator Pressure – intact SGs	D-70
Figure D.6-7	SGTR Steam Generator Pressure – ruptured SG	D-71
Figure D.6-8	SGTR Steam Generator Levels	D-72
Figure D.6-9	SGTR Steam Generator Mass – intact SG	D-73
Figure D.6-10	SGTR Steam Generator Mass – ruptured SG	D-74
Figure D.6-11	SGTR Active Core Mass Flow Rate	D-75
Figure D.6-12	SGTR MFW Flow Rates	D-76
Figure D.6-13	SGTR Break Flow Rate	D-77
Figure D.6-14	SGTR Integrated Break Flow	D-78
Figure D.6-15	SGTR Integrated MSRT Flows	D-79

Sample SRP Transients for U.S. EPR

A selected set of sample, SRP, non-LOCA transients has been analyzed to further demonstrate the adequacy of the S-RELAP5 methodology for application to the U.S. EPR. The nodalizations used in these sample problems are presented in Section 5 of this report. It should be noted that the four loops of the U.S. EPR are represented as individual loops in the model. The sample transients presented in the following sections include:

- Post-Scram MSLB
- Loss of Electrical Load / Turbine Trip
- Loss of Normal Feedwater
- Loss of Coolant Flow
- Uncontrolled RCCA Bank Withdrawal at Power
- Steam Generator Tube Rupture

These transients are the same cases presented in EMF-2310 (Reference D-1) to illustrate results for a standard PWR. Table D.1-1 provides a list of initial conditions for the sample problems. These conditions are biased to produce conservative results for each of the sample problems presented below.

Each sample transient section includes an event description, definition of events analyzed, analysis results, and plots of key parameters.

D.1. Post-Scram MSLB

Event Description

The Post-Scram MSLB selected for the sample problem is initiated by a postulated double-ended guillotine break in a main steam line upstream of the MSIV at EOC conditions. The system is assumed to be operating at full power conditions and offsite power remains available. After closure of the MSIVs on a High Main Steam Pressure Decrease signal, the transient becomes substantially asymmetric, with only the affected steam generator continuing to blow down. The release of high-energy steam through the break creates a power-cooling mismatch between heat generated in the core and

that removed in the steam generators. For the sector of the core that is associated with the affected steam generator, a rapid cooldown results. In conjunction with the negative moderator temperature coefficient (MTC), this cooldown causes an insertion of positive reactivity with a potential for a return to criticality and erosion of the margins to the fuel design limits.

Definition of Case Analyzed

The particular case analyzed is initiated by an inside-containment break at full-power conditions and has offsite power remaining available to operate the reactor coolant pumps. All four reactor coolant pumps have been assumed to remain operational throughout the transient so that forced flow conditions are maintained in the RCS. EOC conditions have been selected to maximize the magnitude of the negative MTC, thereby maximizing the positive reactivity insertion. Following reactor scram on the High Main Steam Pressure Decrease signal, all RCCAs have been assumed to be inserted except for the most reactive RCCA, which has been assumed to be stuck in the fully withdrawn position. Additional conservatism has been imposed by locating the stuck-out RCCA above the core sector being cooled with water from the affected loop.

The plant initial conditions have been biased in a conservative fashion to reflect limiting Technical Specification values and instrument uncertainties. To maximize cooling from the affected steam generator, it has been assumed that (1) the initial main feedwater delivery rate increases to match the increased main steam flow rate during the transient and continues until main feedwater is fully isolated following a High-High Main Steam Pressure Decrease low-load main feedwater isolation signal (conservatively not crediting high-load main feedwater isolation on the earlier High Main Steam Pressure Decrease signal) and (2) emergency feedwater delivery to the affected steam generator at an upper-bound flow rate is actuated when the transient is initiated. The availability of offsite power is responsible for the maintenance of forced flow conditions in the RCS and the enhancement of cooling in the affected loop.

The worst single-active-failure assumed in the analysis is the failure (fully open) of the main steam relief control valve associated with one of the unaffected steam generators

when the unaffected steam generators repressurize (following MSIV closure) sufficiently to actuate their main steam relief trains. *(Note that throughout this transient simulation RCS pressures remain well above the medium-head safety injection (MHSI) pump shutoff head, so postulating an active failure in a MHSI train would have no effect on the results.)*

Analysis Results

Table D.1-2 presents the sequence of events, and the responses of key system variables are given in Figure D.1-1 through Figure D.1-12.

Initially, the release of high-energy steam through the break causes an increase in the primary-to-secondary heat transfer rate for all four steam generators. Upon MSIV closure (on the High Main Steam Pressure Decrease signal), the cooldowns of the loops with the unaffected steam generators are arrested (until their main steam relief trains open), but the cooldown of the affected loop continues until the affected steam generator begins to dry out.

Shortly after the transient is initiated, the reactor is scrammed (on the High Main Steam Pressure Decrease signal). However, as the cooldown progresses, the shutdown worth is eroded by moderator and Doppler feedback (accentuated by the EOC conditions) until a return to criticality occurs. The increase in the reactor power above the decay heat level is terminated by negative Doppler and moderator feedback when the affected steam generator begins to dry out and the cooldown of the affected loop ends. The reactor power peaks at 19.4 percent of the rated power, with most of the power produced in the stuck-out RCCA region. The MDNBR for this condition was calculated to remain above the DNBR design limit. The peak linear heat rate is also predicted to remain below the FCM threshold.

Conclusion

The analysis demonstrates that application of the current NRC-approved methodology to the U.S. EPR (which is similar to conventional 4-loop plants designed by Westinghouse) provides a reasonable representation of this event scenario.

D.2. Loss of External Load/ Turbine Trip**Event Description**

This event is initiated by either an LOEL (Event 15.2.1) or a TT (Event 15.2.2). The major difference between the two events is the rate at which steam flow is reduced. Following a LOEL, a runback is initiated and the turbine throttle valves close at a moderately fast rate, but not instantaneously. In a turbine trip event, the turbine stop valves close almost instantly (typically within 0.1 sec). When sufficient margin exists, a transient scenario is constructed so that the safety analysis results bound the consequences of both LOEL and TT events as illustrated in this sample problem.

Upon either of these two conditions, the turbine stop valve is assumed to close rapidly (0.1 sec). The turbine bypass system also is assumed to be unavailable. These assumptions allow the analysis to bound the consequences of Loss of External Load (Event 15.2.1) or a Turbine Trip-Steam Atmospheric dump Unavailable (Event 15.2.2) and Closure of MSIVs – valve closure time is greater than 0.1 sec (Event 15.2.4).

The LOEL/TT event challenges the acceptance criteria for both primary and secondary system overpressure and DNBR. The event causes an increase in reactor coolant system temperature. The reactor coolant throughout the RCS expands causing an increase in the pressurizer pressure. The reactor coolant system is protected against overpressurization by three pressurizer safety valves (PSRVs). Pressure relief on the secondary side is by the steam line Main Steam Relief Train (MSRT) and Main Steam Safety Valves (MSSVs). Actuation of the primary and secondary side system safety valves limits the increase in reactor coolant temperature and pressure.

With a zero MTC, increasing reactor coolant system temperature has no effect on core power. The increase in primary side temperature reduces the margin-to-thermal limits and challenges the DNBR acceptance criterion.

Definition of Case Analyzed

The objectives in analyzing this event are to demonstrate that 1) the RCS pressure relief capacity is sufficient to limit the pressure to less than 110% of the design pressure, 2) the secondary side pressure relief capacity is capable of limiting the pressure to less than 110% of the design pressure, and 3) the MDNBR remains above the safety limit. For each of the above three objectives, a separate analysis is conducted with the plant parameters biased so as to maximize the challenge for the particular criterion being examined.

In this sample problem, the analysis is biased to challenge the RCS design pressure limit. The input parameters are biased to: 1) maximize the increase in reactor power during the transient (e.g., technical specification most positive value of MTC and maximum scram delay), 2) minimize the initial secondary pressure (e.g., maximum number of plugged SG tubes), and 3) minimize the RCS pressure relief capacity (e.g., upper-bound biases on initial pressurizer level and pressurizer safety valves (PSRVs) opening pressure). Pressurizer sprays are disabled. LOOP is assumed coincident with the Reactor Trip. The resulting loss of motive power to the RCPs exacerbates the RCS heatup during the short interval after the trip setpoint is reached until control rods have been inserted, reducing the RCS flow rate and primary/secondary heat transfer rate. This causes a rise in primary pressure. This approach provides for a conservative calculation of the peak RCS pressure during the transient.

Analysis Results

The sequence of events for this maximum RCS pressure case is given in Table D.2-1. The responses of key system parameters are depicted in Figures D.2-1 through D.2-8. The event is initiated with a ramped closure of the turbine stop valves in 0.1 seconds. The secondary side (see Figure D.2-1) pressurizes causing a decrease in the primary-to-secondary heat transfer. This, in turn, causes the RCS temperature to increase (see Figure D.2-2). The resulting in-surge into the pressurizer compresses the steam space and pressurizes the RCS (see Figures D.2-3 and D.2-4). The reactor scrams on high pressurizer pressure (see Figures D.2-5 and D.2-6), and the reactor coolant pumps

begin to coast down (see Figure D.2-7) due to the assumed loss of offsite power coincident with the reactor trip. The capacity of the pressurizer safety valves (PSRVs) is sufficient to limit maximum RCS pressure (bottom of the reactor vessel) to 2764 psia (see Figure D.2-8).

Conclusion

The maximum RCS pressure of 2764 psia remains below 110% of the design pressure (2803 psia). Therefore, the RCS overpressurization criterion for the LOEL and TT events is satisfied.

D.3. Loss of Normal Feedwater

Event Description

A LONF Flow transient is initiated by the termination of the MFW flow due to MFW pump failure or control valve malfunction. (The termination of MFW flow that results from a loss of power is considered in the Loss of Non-emergency AC Power event.)

The termination of MFW flow while the plant continues to operate at power will eventually result in reactor scram on low SG level, with long-term cooling subsequently provided by the EFWS.

This event is evaluated to confirm that the low SG level reactor trip setpoint, the low-low SG level EFW actuation setpoint, and the EFW flow capacity are adequate to provide for long-term decay heat removal. This event is also evaluated to confirm that the plant design and operating conditions preclude pressurizer overfill.

The loss of normal feedwater flow, while the plant continues to operate at power, causes the primary-to-secondary heat transfer rate to decrease. The resulting heatup of the reactor coolant causes a pressurizer surge due to the fluid expansion. Reactor coolant pressure increases and the pressurizer sprays actuate, contributing to further filling of the pressurizer. SG liquid levels, which have been steadily dropping since the termination of the MFW flow, soon reach the low SG level reactor trip setpoint. This initiates a reactor scram which ends the short-term heatup phase of the event. The

reactor trip and subsequent cooling of the reactor coolant act to reduce the fluid expansion and prevent pressurizer overfill.

The automatic turbine trip at reactor scram and the continuing primary-to-secondary transfer of the decaying core power and the RCP heat (for cases with offsite power available) cause SG pressures to rapidly increase. When SG pressures become high enough, the safety-grade MSRTs and/or the MSSVs serve to limit the increase in SG pressure. SG levels continue to drop and soon reach the low-low SG level EFW actuation setpoint. When the delivery of EFW begins, the rate of level decrease in the fed SGs slows. If EFW flow is sufficient to prevent dryout in the SGs then, as the decay heat rate diminishes, liquid levels in the SGs fed by EFW stabilize and begin to rise. Reactor coolant temperatures also stabilize and begin to decrease, marking the end of the challenge to the event acceptance criteria.

Definition of Case Analyzed

The objective of this analysis is to demonstrate the adequacy of the SG level setpoints and the EFW capacity to avoid the expulsion of liquid from the PSRVs and assure long-term cooling capability to a safe shutdown condition.

There are four potential acceptance criteria that could apply: 1) the DNB SAFDL, 2) the FCM SAFDL, 3) the pressure limit, and 4) the plant condition restriction (event must not generate a more serious plant condition without other faults occurring independently). For the short-term heatup phase, the MDNBR is bounded by the LOCF event, and for the long-term heat-up phase, the DNB SAFDL is not challenged, provided that the SGs receiving EFW flow retain liquid inventory (or the reactor coolant subcooling margin satisfies the plant-specific criterion). The FCM criterion is bounded by other Condition II events and is not credibly challenged by this event.

The peak primary and secondary pressures for this event are less than those of the LOEL/TT events provided that the pressurizer retains a steam “bubble” for pressure control, that is, the pressurizer does not overfill. Finally, the plant condition restriction is satisfied if the pressurizer does not become so full that liquid is expelled through the PSRVs (the pressurizer level remains below the PSRV inlet piping penetrations). In

summary, the acceptance criteria for this event reduce to the requirements that: 1) the pressurizer level must remain below the PSRV inlet piping penetrations, and 2) the fed SGs must not dry out (or the reactor coolant subcooling margin must satisfy the plant-specific criterion).

Consequently, the plant state and RPS setpoints are conservatively biased to maximize the potential for pressurizer overfill and SG dryout. Thus, a number of event specific analysis conservatisms are applied in addition to the more general ones that are routinely applied. To maximize heat generation in the reactor, the event is initiated from full power with EOC conditions that tend to maximize decay heat, all reactor trips except low SG level are disabled, the low SG level setpoint is biased to a minimum value (nominal minus uncertainty), and maximum scram delays are used. Also, the long-term cooling capability is more severely challenged for the case where offsite power is available (with heat from RCPs), and this is the sample calculation presented below.

The heat removal capacity of the secondary side is similarly degraded, primarily by complete loss of MFW to all SGs and minimum EFW flow. The limiting single failure of an active component is that of the loss of an EFW pump. Preventive maintenance of a second EFW train, combined with the loss of a train due to single failure would result in only two of four SGs being fed by EFW. Finally, to decrease margin to pressurizer overfill, the initial pressurizer level is biased high (nominal plus uncertainty and control deadband), and pressurizer sprays and PSRVs are modeled.

Analysis Results

The event is initiated by tripping all MFW pumps and the SSS pump for the SGs. The liquid levels of the SGs drop rapidly and at 56.4 seconds, a low SG level signal trips the reactor. Table D.3-1 presents the sequence of events, and the responses of key system variables are given in Figure D.3-1 through Figure D.3-6.

There is a large margin to pressurizer overfill. The maximum pressurizer level reached 78.9 percent of the span and the top of the span is approximately 3 feet below the PSRV inlet piping penetrations. The EFW flow capacity was sufficient to arrest the SG

level decrease and prevent dryout in the two fed SGs so that long-term cooling was assured.

Conclusion

The analysis demonstrates that application of the current NRC-approved methodology to the U.S. EPR (which is similar to conventional 4-loop plants designed by Westinghouse) provides a reasonable representation of the plant response in this event scenario.

D.4. Loss of Coolant Flow

Event Description

The LOCF transient is initiated by a disruption of the electrical power supplied to, or a mechanical failure in, one or more RCPs. These failures are assumed to cause a complete or partial loss of forced coolant flow. The complete LOCF with scram on low pump speed is the most limiting transient from the perspective of challenge to the DNB SAFDL. This scenario occurs when an under-frequency or under-voltage event causes the RCPs to trip without removing power from the control rod restraints. Furthermore, between the time when the RCPs trip and the time when their breakers trip, the RCPs act as generators and an electrical braking occurs, accelerating the coastdown.

The impact of losing one or more RCPs is a decrease in the active coolant flow rate in the reactor core and, consequently, an increase in core temperatures. The reactor trips on low pump speed. Prior to reactor trip, the combination of decreased flow and increased temperature poses a challenge to the DNB SAFDL. The FCM SAFDL is not challenged since there is no significant increase in core power. This event also produces an increase in system pressure due to increased temperatures and reduced heat transfer to the secondary side of the SGs, but it does not create a credible challenge to system pressure limits.

This event is terminated by reactor scram on the RCS low pump speed trip, and the purpose for analyzing this event is to verify that the RPS can respond fast enough to prevent violation of the DNB SAFDL.

Definition of Case Analyzed

The partial loss of coolant flow event is a less severe transient than the complete loss of coolant flow event. This sample problem simulates a complete loss of coolant flow event.

The issue being evaluated is the challenge to the DNB SAFDL. Therefore the plant state and trip points are biased so as to maximize this challenge. This event is analyzed from full power initial conditions and the core thermal margins are minimized. That is, the initial cold leg temperature is taken at its maximum value, the RCS flow rate at its Technical Specification minimum, and the core bypass flow rate at its maximum.

Similarly, the factors affecting the scram time are chosen to maximize the scram delay. The low pump speed trip setpoint is taken as its nominal value minus the uncertainty, while the trip signal delay and holding coil delay times are set to their maximum values. Further conservatisms are introduced by maximizing the reactor power through the selection of BOC conditions (Technical Specifications positive MTC) and biasing the Doppler coefficient.

Analysis Results

The overall response of the primary and secondary systems for this event is calculated by S-RELAP5. The transient is initiated by tripping all four RCPs. As the pumps coast down, the core flow is reduced causing the reactor to scram on low pump speed. The flow decrease causes reactor coolant temperatures to increase. The primary challenge to DNB is from the decreasing flow rate and increase in coolant temperatures. The sequence of events is given in Table D.4-1. Figures D.4-1 through D.4-4 show the response of key system parameters for the LOCF. The minimum DNBR is calculated to remain above the DNB SAFDL.

Conclusion

The results of the Loss Of Coolant Flow sample problem analysis demonstrate that application of the current NRC-approved S-RELAP5 methodology to the U.S. EPR (which is similar to conventional 4-loop plants designed by Westinghouse) provides a satisfactory representation of the plant response to a LOCF event.

D.5. Uncontrolled RCCA Bank Withdrawal at Power

Event Description

This event is initiated during power operation by an uncontrolled withdrawal of a control rod bank due either to a failure in the rod control system or to operator error. The positive reactivity addition causes a power transient that increases the core heat flux and challenges DNB margin. The DNB margin is further reduced by an increase in reactor coolant temperature that results from the power-cooling mismatch.

The RPS is designed to terminate this transient before the DNB limits are reached. The principal protective trips for this event are the Low DNBR trip, high neutron flux rate of change trip, and the High Core Power Level (HCPL) trip. The HCPL trip responds relatively slowly, due to its reliance on input from RCS loop temperature measurements to determine core power. The Low DNBR trip, which receives core power input directly from in-core power measurements, is expected to act more quickly and provide protection over a broad range of bank withdrawal conditions. The high neutron flux rate of change trip provides protection for relatively fast withdrawal rates where the other trips may not be as effective. For the sample problem provided below, protection is provided by the low DNBR trip.

Definition of Case Analyzed

This sample analysis evaluates the consequences of an uncontrolled control rod bank withdrawal from full power conditions. Control bank withdrawals at lower power levels, would be analyzed in actual plant calculations. A matrix of cases considering a range of reactivity insertion rates, from very slow (e.g., gradual boron dilution) to the maximum possible control bank withdrawal rate at maximum worth for two banks moving in normal sequence and overlap, and at BOC and EOC would also be calculated. A representative bank withdrawal rate, corresponding to 0.21 pcm/second, is analyzed for this sample analysis. This reactivity insertion is the same as utilized in the sample problem in the currently NRC-approved AREVA NP PWR SRP Chapter 15 non-LOCA event safety analysis methodology, Reference 5-1.



This sample analysis is performed for the minimum feedback case, at BOC conditions.

Analysis Results

The overall response of the primary and secondary systems for this event is calculated by S-RELAP5. The MDNBR for this event is calculated using the thermal-hydraulic conditions from the S-RELAP5 calculation as input to an approved core thermal performance code.

For this sample problem analysis, an uncontrolled control bank withdrawal transient was analyzed starting at full power conditions (102 percent of rated) with BOC kinetics and with an insertion rate of 0.21 pcm/ second. For this reactivity insertion a reactor trip occurred on low DNBR at 176 seconds.

Table D.5-1 presents a summary sequence of events. The transient responses of key parameters are presented in Figures D.5-1 through Figure D.5-7. As seen in Figure D.5-1, core power raises steadily until the reactor trip setpoint is reached, after which it falls rapidly. Figure D.5-2, the components of reactivity, shows that Doppler feedback slows the rate of reactivity insertion as core power increases. Figure D.5-4,

core fluid temperatures, shows that core temperatures increase with increasing core power until reactor scram. Figures D.5-5 and D.5-6 show pressurizer pressure and level, respectively. Pressurizer pressure increases as RCS temperature rises, forcing liquid into the pressurizer. Actuation of pressurizer spray at about 18 seconds slows the increase in pressure. Pressurizer level steadily increases until reactor scram, after which it drops rapidly as RCS temperatures fall. Figure D.5-7 shows steam generator pressure, which also rises with increasing RCS temperature. It increases more rapidly after reactor scram due to closure of the turbine flow control valve. The increase in steam generator pressure is limited by the action of the steam generator relief valves that open at 183.9 seconds.

Conclusion

The S-RELAP5 results reasonably represent the plant transient response. The DNB SAFDL for this event is protected by the low DNBR trip and the MDNBR remains above the limit. This indicates that no fuel failures due to DNB would occur and, therefore, that the acceptance criteria are met.

D.6. Steam Generator Tube Rupture

Event Description

The SGTR event selected for the sample problem is initiated by a postulated double-ended guillotine rupture of a single steam generator tube. Coolant from the RCS begins to escape through the break, driven by the pressure differential between the RCS and the affected SG secondary side, increasing the inventory and pressure in the SGs.

As the break flow begins to depressurize the RCS, the charging pumps activate in order to make-up the lost inventory. If the RCS inventory and pressure are stabilized via the charging pumps, no reactor trip will occur unless and until manual operator action is initiated to trip the plant. However, if the break flow exceeds the capacity of the pumps, RCS pressure and inventory will continue to decrease causing a reactor trip on a low RCS pressure signal (e.g., Low Pressurizer Pressure or Low DNB). Following the reactor trip, the turbine will trip and; in the case where offsite power is lost, the coolant

pumps will coast down and make-up flow will be temporarily interrupted until the charging pumps are loaded onto the emergency diesel power supply. If offsite power is available, a fast transfer to offsite power will keep the pumps running and the make-up flow available.

The loss of offsite power results in eventual loss of condenser vacuum and the steam dump valves are closed to protect the condenser. The continued mass and energy transfer between the primary and secondary side causes a rapid increase in SG pressure and discharge to the atmosphere via the MSRTs or MSSVs. If no credit is taken for loading of the charging pumps onto the emergency diesel power supply, break flow will exceed make-up flow capacity and RCS pressure will continue to decrease after the trip. As the RCS pressure continues to decrease, a low pressurizer pressure signal activates the SIS. The emergency diesels start and MHSI flow begins once RCS pressure falls below the MHSI shutoff head. If it is assumed that the charging pumps are loaded onto the emergency diesel power supply, a stable condition will be reached in which make-up flow compensates for leak flow through the break at a pressure above the low-pressure SIS activation setpoint.

Definition of Case Analyzed

The particular case analyzed for the sample problem is initiated by a postulated double-ended guillotine rupture of a single steam generator tube just above the tubesheet on the cold side of the tube bundle. The analysis was performed at BOC full power conditions. In order to maximize the primary to secondary ΔP and leakage flow across the break, CVCS charging flow is assumed at its maximum. No credit is taken for letdown flow or the interruption of flow following the loss of offsite power. A “nominal” scenario has been analyzed for the sample problem, in that no SAF is assumed other than the most reactive RCCA remains fully withdrawn after the reactor trip. The capacity of the MSRT associated with the affected SG is maximized while the capacities of the MSRTs associated with the unaffected SGs are minimized in order to maximize steam release from the affected SG. Similarly, the opening setpoint of the MSRT associated

with the affected SG is minimized while those of the intact SGs are maximized to maximize the steam release from the affected SG.

With maximum charging flow, RCS pressure does not drop below the low-pressure reactor trip signal within 30 minutes of the tube break. Therefore, it is assumed a manual reactor trip is initiated by the operator 30 minutes after break initiation in response to the continuing decrease in pressurizer level. All RCCAs are assumed to be inserted except for the most reactive RCCA, which is assumed to be stuck in the fully withdrawn position. Offsite power is assumed to be lost coincident with the reactor trip, causing a loss of power to the MFW pumps and RCPs. Following the loss of offsite power, natural circulation flow develops in the Reactor Coolant System (RCS) and decay heat is removed by steaming from the affected loop MSRT.

The operator is assumed to identify and isolate the ruptured steam generator 30 minutes after the reactor trip (1 hr. after break initiation) based on the higher level in the ruptured steam generator relative to the intact steam generators or main steamline activity. Operator actions at this time include:

- Initiation of affected loop MSIV closure.
- Isolation of the SG blowdown line from the ruptured SG and the EFW line to the ruptured steam generator.
- Initiation of the reset of the MSRT associated with the ruptured steam generator to a value higher than the MHSI shutoff head.
- Initiation of a Partial Cooldown. This function reduces the pressure setpoints of the MSRTs in the steam lines from the intact steam generators to a reduced value to implement a cooldown of the intact SGs at a 180°F/hr rate.

EFW flow to the intact SGs is automatically initiated a short while later by the low-low SG Level actuation signals. The operator is assumed to throttle EFW to maintain level when level returns to the normal water level in the unaffected SGs.

At the completion of the partial cooldown, the operator is assumed to throttle operation of the two CVCS charging pumps to minimize the continuing leak flow. Thereafter, the

operator is assumed to restore charging flow as necessary to maintain a minimum core exit subcooling of 25°F. The throttling of charging flow allows the RCS and ruptured pressure to equilibrate at a pressure slightly above the MHSI shutoff head.

The MHSI pumps are automatically actuated a short while after charging flow is throttled when RCS pressure decreases below the low-low pressure SIS actuation setpoint.

No further automatic or operator actions are assumed for the duration of this sample problem analysis, which extends to the point in time when a stable controlled condition is reached with the RCS and the affected SG pressures equilibrating at a pressure close to the MHSI pump shutoff head, thereby minimizing little leakage flow through the break.

The inputs and plant initial conditions assumed for the analysis are biased in a conservative fashion to reflect limiting values including instrument uncertainties.

Analysis Results

Table D.6-1 presents the sequence of events. Figures D.6-1 through D.6-15 present the responses of key system variables.

Initially, the release of RCS liquid through the break causes the pressurizer level and RCS pressure to drop slowly until the setpoint for the activation of a 2nd CVCS charging pump and letdown flow minimization (letdown not modeled) is reached. Level continues to drop slowly until a manual reactor trip is assumed 30 minutes after break initiation. Offsite power is assumed to be lost coincident with initiation of the reactor trip. This causes a loss of power to the RCPs and MFW pumps and the Main Steam Bypass system. Reactor trip is followed by a turbine/generator trip so the secondary side pressurizes. Inventory from both the RCS and the SGs is released by the opening of the MSRT in the ruptured SG (which has a biased low setpoint to maximize releases from the ruptured SG). The initially fully open MSRV modulates closed in 40 seconds since the relief capacity is more than adequate to rapidly bring SG pressure below the control setpoint. The MSRT on the line from the ruptured SG subsequently re-opens to provide decay heat removal until 1 hr after the break initiation when the operator is assumed to identify the ruptured SG, reset its MSRT setpoint to a higher value above the MHSI

pump shutoff head and initiate the partial cooldown gliding setpoint function for the intact SG MSRTs. The MSRT in the ruptured SG therefore closes while the SG MSRTs in the intact SGs open.

At the completion of the partial cooldown setpoint reduction the operator is assumed to throttle the CVCS charging flow to minimize the continuing leak flow. This causes RCS pressure to decrease. The MHSI pumps are automatically actuated when RCS pressure falls below the low-low pressure actuation setpoint. A stable controlled condition is reached when pressures in the RCS and the now isolated affected SG secondary side equilibrate near the MHSI pump shutoff head. This greatly reduces leak flow. The affected SG liquid volume is well below the total secondary side volume and water level remains below the steam outlet nozzle at that point in time.

The thermal-hydraulic code analysis of the SGTR event provides boundary conditions for the analysis of the radiological consequences. The key parameters affecting the radiological release are the break flow, flashing fraction and the steam release through the MSRTs and MSSVs from the affected SG to the atmosphere. The predicted total steam release from the ruptured SG and intact SGs, as well as integrated break flow and break mass flashed, is provided in Table D.6-2.

Conclusion

The SGTR sample problem analysis results demonstrate that application of the current NRC-approved S-RELAP5 methodology to the U.S. EPR (which is similar to conventional 4-loop plants designed by Westinghouse) provides a reasonable representation of the plant response to an SGTR event scenario.

D.7. References

- D-1 "SRP Chapter 15 Non-LOCA Methodology for Pressurized Water Reactors,"
AREVA/Framatome ANP Document EMF-2310(P)(A), Revision 1, June 2004.

Table D.1-1 Representative Initial Conditions

Parameter	Value
Initial reactor power	4500 MWt
Initial RCS loop flow rate	119,670 gpm/loop
Initial reactor vessel average temperature	596°F
Initial reactor vessel upper head temperature	596°F
Initial PZR pressure	2250 psia
Initial PZR liquid level	56% of span
Initial SG pressure	
No tube plugging	1131 psia
5% tube plugging	1108 psia
Initial SG secondary-side total fluid inventory	182,000 lb _m /SG
MFW temperature	446°F

Table D.1-2 Post-Scram MSLB Event Summary

Event	Time (s)
With plant operating at EOC full-power conditions, postulated double-ended guillotine break in MS line upstream of MSIV and inside containment occurs.	0.0
Affected SG EFW actuation is assumed.	0.0
Affected MS line pressure reaches High MS Pressure Decrease setpoint actuating reactor trip, turbine trip, and MS isolation.	0.0
Affected MS line pressure reaches High-High MS Pressure Decrease setpoint for isolating all MFW from affected SG.	0.0
Scram RCCAs are released, turbine is tripped, MFW heating is lost, and MSIVs begin to close.	0.9
Isolation of all MFW from affected SG is actuated.	0.9
Insertion of scram RCCAs begins.	1.2
MSIVs are fully closed.	5.9
Affected SG EFW delivery begins.	7.5
Unheated MFW reaches affected SG.	13.5
All affected SG MFW isolation valves are fully closed.	15.9
MS pressure for MS line 1 (unaffected) reaches MSRT opening setpoint.	~124
MS pressures for MS lines 2 and 3 (both unaffected) reach MSRTs opening setpoint.	~125
MSRIV for MS line 1 opens, with corresponding MSRV assumed to be failed in fully open position.	~127
MSRIVs for MS lines 2 and 3 open, and corresponding MSRVs begin to close (attempting to maintain pressures at setpoint).	~128
MSRVs for MS lines 2 and 3 reach fully closed positions.	~170
Unaffected SG 1 liquid level reaches Low-Low SG Level EFW actuation setpoint.	194
Unaffected SG 1 EFW delivery begins.	202

Event	Time (s)
Affected SG begins to dry out (as signified by sudden decrease in primary-to-secondary heat transfer rate, in conjunction with very low secondary-side liquid inventory).	~232
Affected core sector inlet temperature reaches minimum and then begins to increase.	~239
Reactor power reaches post-scam peak (19.4% of RTP) and then begins to decrease.	~239
PZR pressure reaches Low-Low PZR Pressure setpoint actuating MHSI and partial depressurization of unaffected SGs.	445
Credited MHSI pumps are running at full speed, but RCS pressures remain well above MHSI pump shutoff heads throughout transient simulation.	460
MS line 1 pressure reaches MSRT closing setpoint.	~599
Unaffected core sector inlet temperature reaches minimum and then begins to increase.	~605
Unaffected SG 1 MSRIV closes.	~605
Operator takes control of plant to bring it to safe shutdown condition.	1800

**Table D.2-1 Loss of Load/Turbine Trip (Primary System Overpressure Case)
Event Summary**

Event	Time (s)
Event Initiation – Turbine Trip	0.0
Turbine Stop Valve fully closed	0.1
Reactor Trip Setpoint reached on high Pressurizer pressure	6.8
Reactor Trip Signal Issued	7.7
LOOP occurs & RCPs begin to coast down; MFW pumps are tripped	7.7
Scram RCCA Insertion Begins	8.0
First PSRV Opens	9.2
Second PSRV Opens	10.5
RCS Peak Pressure (Bottom of Reactor Vessel)	11.0
Third PSRV opens	11.7
MSRTs open	13.0

Table D.3-1 LONF Event Summary

Event	Time (s)
Termination of feedwater flow to all SGs	0.0
Pressurizer Spray flow beings	1.6
SG water level reaches RPS trip setpoint	56.4
RPS trip signal on SG low water level	57.9
Turbine trip	57.9
Scam rod insertion begins	58.2
Peak post-scam RCS hot leg temperature	59.5
Maximum pressurizer pressure	61.7
Maximum pressurizer level	62.5
MSRT flow begins	64.6
EFWS signal on SG low-low water level	66.9
SG blowdown isolation signal, isolation valves begin to close	66.9
EFWS flow begins	81.9
SG blowdown flow isolation complete	96.9
Minimum SG liquid inventory per SG, SG-3,/SG-4 (fed by EFW)	104
SG liquid inventory < 100 lb _m , SG-1/SG-2 (not fed by EFW)	1380 1398
SG complete dryout, SG-1/SG-2	1796 1814

Table D.4-1 LOCF Event Summary

Event	Time (s)
RCPs Trip	0.0
Peak Power Occurs	0.0
RCP Reaches Low Speed Setpoint	1.18
Pressurizer Spray Actuates	1.85
MDNBR	3.7
Peak Pressurizer Pressure	5.6

Table D.5-1 UCBW at Power Event Summary

Slow CEA Bank Withdrawal Begins	0.0
Pressurizer Spray On	18
Reactor Trip Setpoint for low DNBR reached	176.0
Reactor Trip	176.8
Peak Core Power Minimum DNBR Occurs	176.8
SG MSSVs Open	183.9
End of Transient Calculation	200.0

Table D.6-1 SGTR Event Summary

Event	Time (sec)
Double-ended guillotine break at the tubesheet of a single U-tube in SG #4.	0
PZR level < setpoint for start of additional RCS charging pump.	122
Operator initiates a manual reactor trip, accompanied by coincident loss of offsite power	1800
Ruptured SG MSRIV fully open, steam relief through open MSRV	~1820
Ruptured SG MSRV modulates fully closed.	~1860
Ruptured SG MSRV modulates partly open (MS pressure > 1363 psia).	~1970
Operator identifies ruptured SG (ruptured SG level 22 %NR, intact SG levels off-scale low): <ul style="list-style-type: none"> • activates closure of affected loop MSIV, • resets ruptured SG MSRT setpoint to 1414 psia and intact SG MSRTs to Partial Cooldown gliding setpoints, • isolates the EFW line to the ruptured SG, • isolates SG blowdown from the ruptured SG 	3600
Unaffected SG MSRIVs fully open.	3603
Ruptured SG MSIVs fully closed	3605
Ruptured SG MSRT closed	3640
Ruptured SG MSRT re-opens (valve remains very slightly open until pressure drops below 1414 psia at ~ 10500 seconds)	3720

Event	Time (sec)
Low-low SG water level in unaffected SGs: EFWS to the unaffected SGs actuated. SG blowdown flow to unaffected SGs isolated.	~3820
Pressurizer level < low level heater cutoff	4632
MSRT gliding setpoint reaches 892 psia, Partial Cooldown complete, intact SG MSRTs begin modulating to maintain pressure.	4735
Operator throttles both CVCS charging pumps flow (core exit subcooling > 25°F).	~4735
PZR empties	~4920
PZR pressure reaches Low-Low PZR Pressure setpoint: MHSI pumps start.	5206
Credited MHSI pumps (4 out of 4) are running at full speed and ready to begin delivering borated water (no delay assumed to maximize break flow), but RCS cold leg pressures have not decreased to MHSI pump shutoff heads at which delivery can begin.	5206
Unaffected MS pressure < 892 psia, unaffected SG MSRTs close.	~5300
Unaffected SGs water levels return to NWL, operator throttles EFW to unaffected SGs to maintain levels.	~7100
Unaffected SGs MS pressure > 892 psia, MSRVs modulate open	~7520
RCS and ruptured SG pressures reach stable equilibrium minimal leak flow condition, with decay heat removed by unaffected SGs via MSRT with EFW make-up. Ruptured SG water level stable within NR band.	~10000

Table D.6-2 Integrated Break Flow and Steam Release to Atmosphere

Parameter	Value
Integrated break mass flow, lb _m	260,875
Integrated break mass flashed to steam, lb _m	1,157
Steam release from ruptured SG, lb _m	138,367
Steam release from intact SGs, lb _m	1,274,775

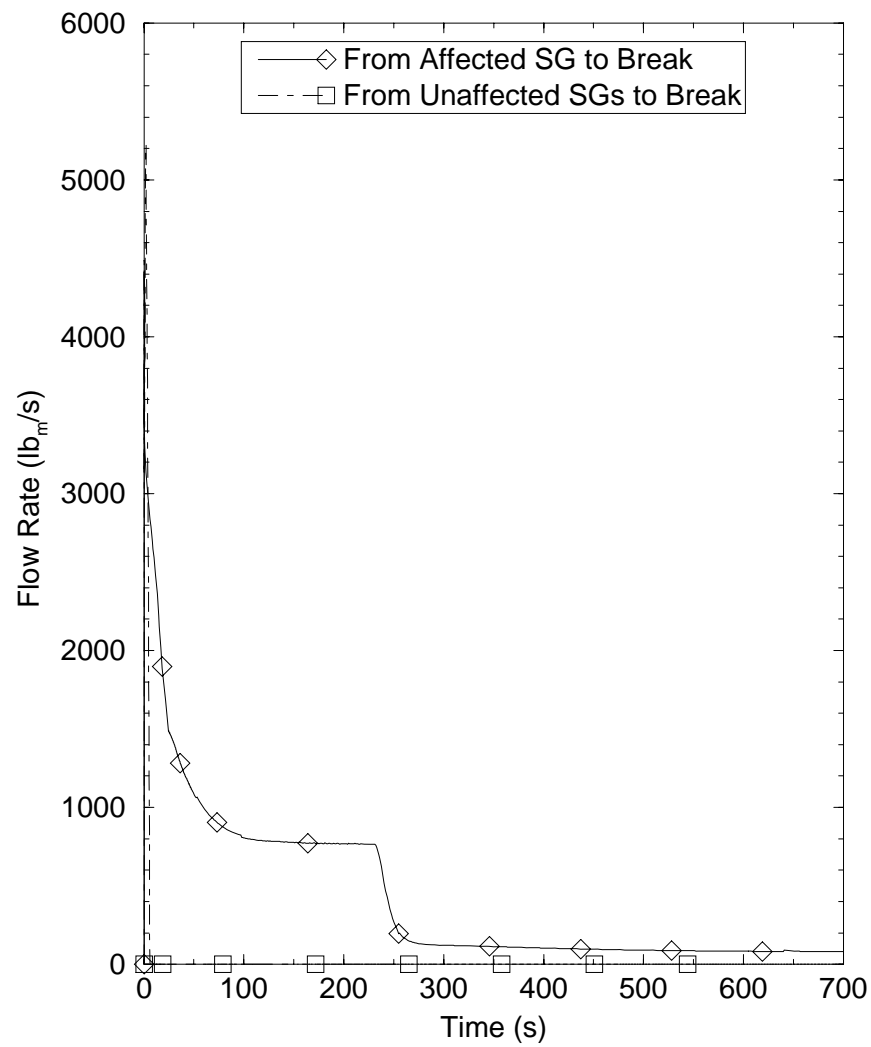
Figure D.1-1 Post-Scram MSLB Break Flow Rates

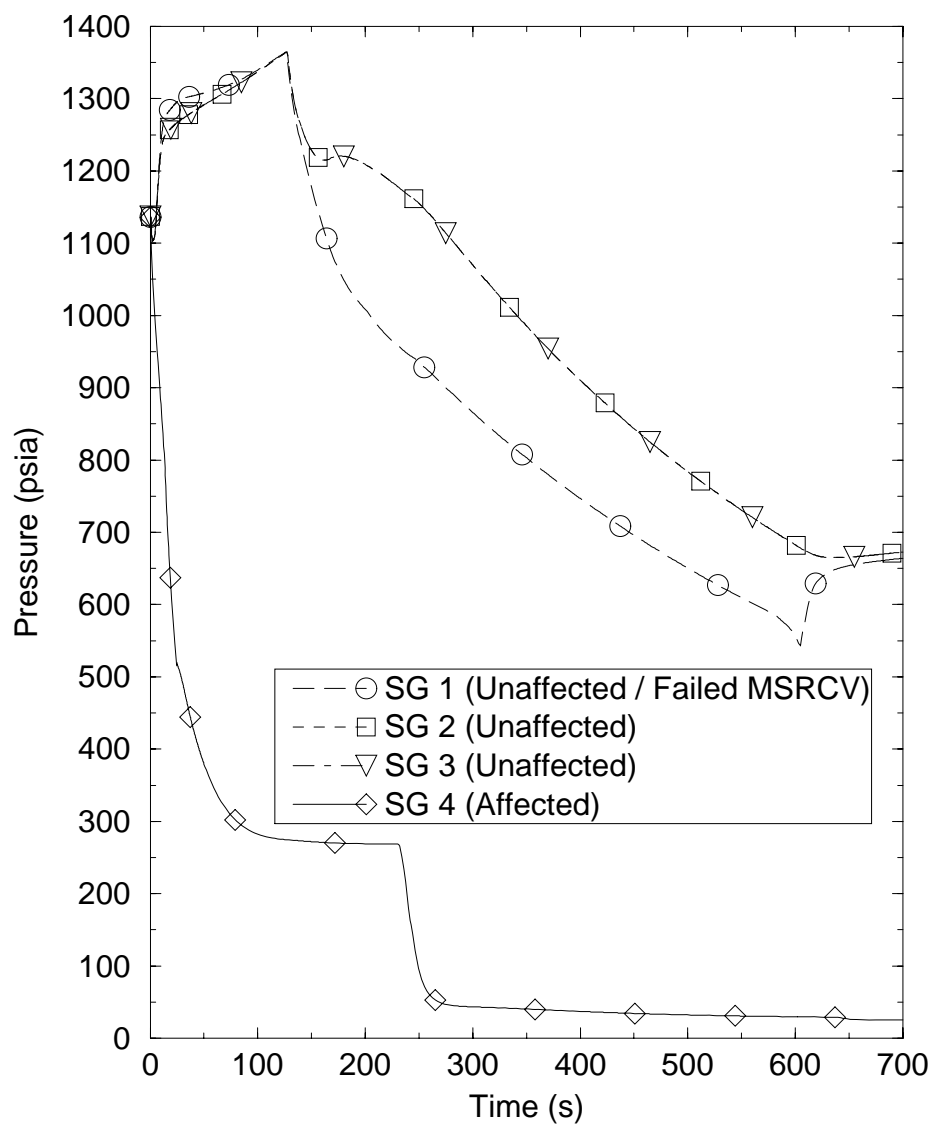
Figure D.1-2 Post-Scram MSLB Steam Generator Pressures

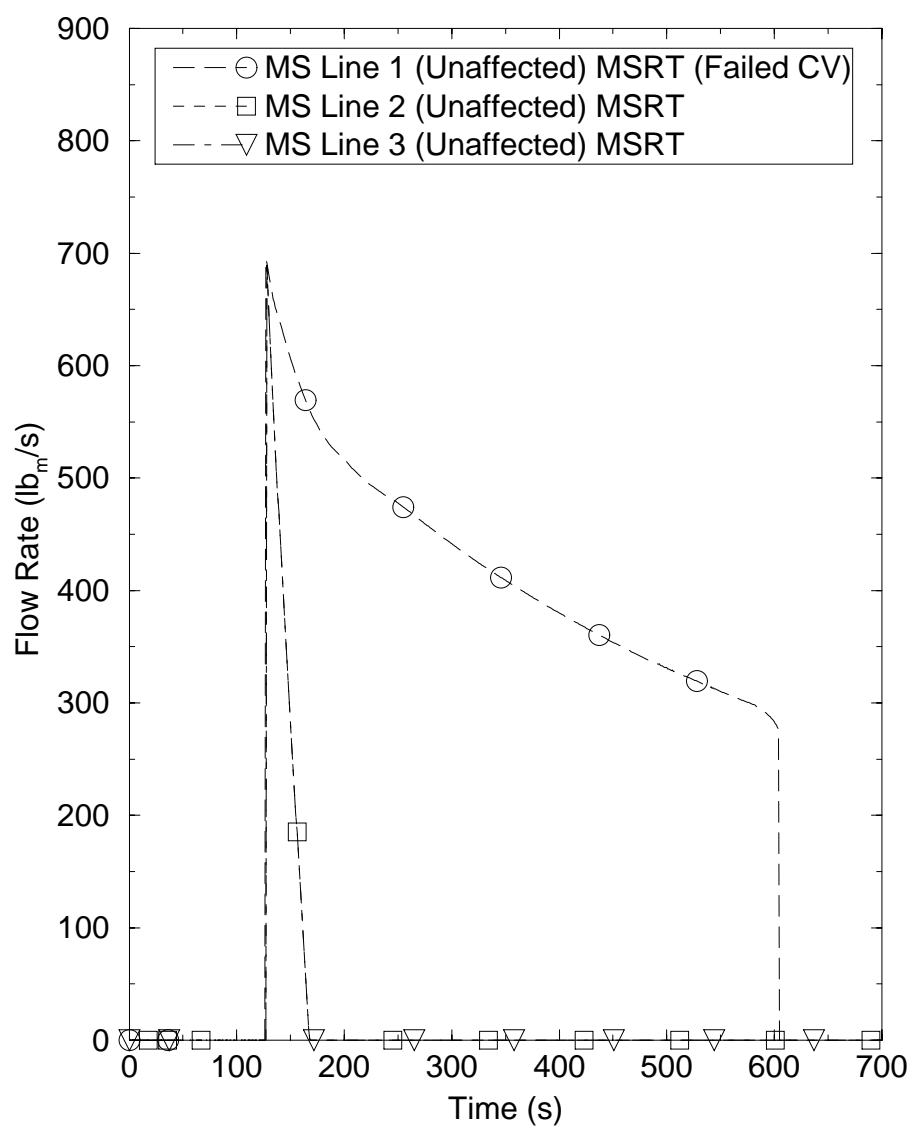
Figure D.1-3 Post-Scram MSLB Main Steam Relief Train Flow Rates

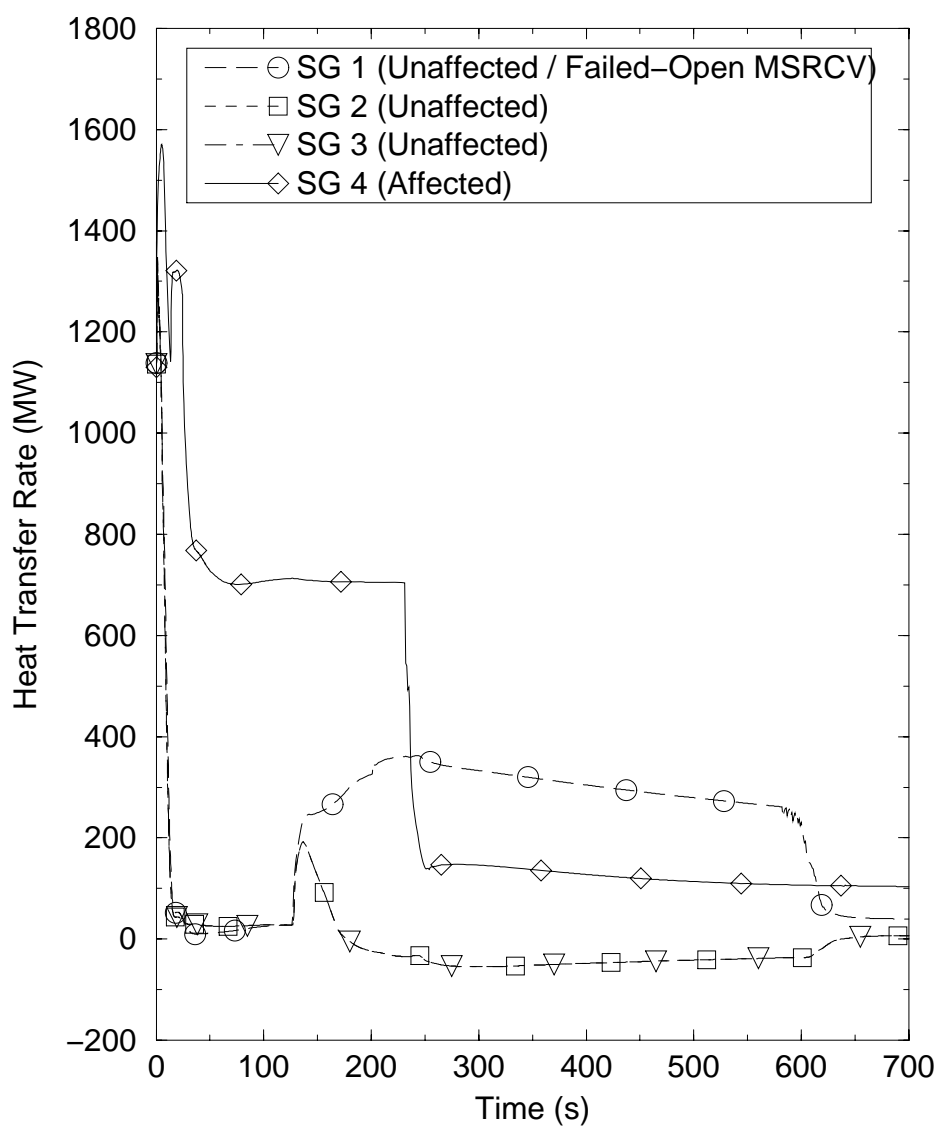
Figure D.1-4 Post-Scram MSLB Steam Generator Heat Transfer Rates

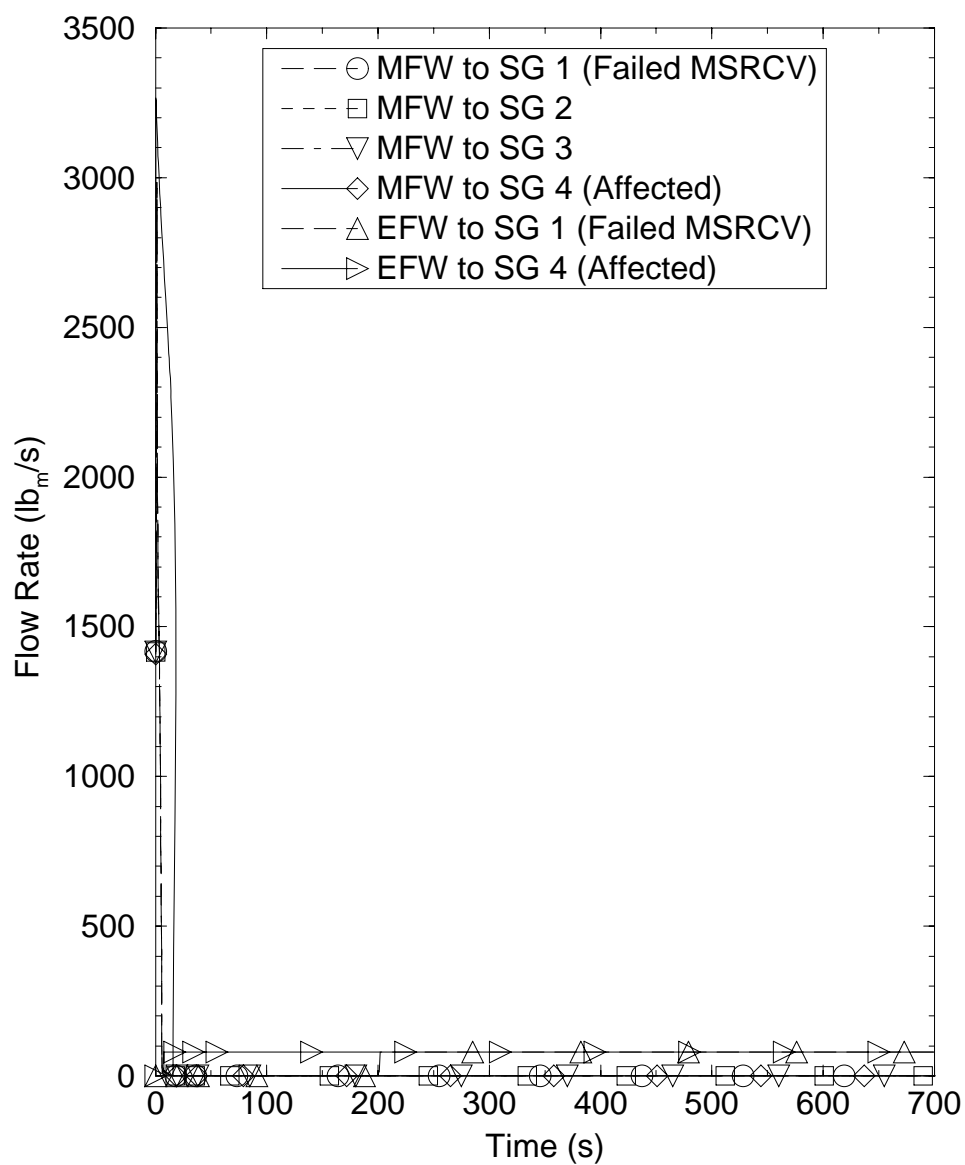
Figure D.1-5 Post-Scram MSLB Feedwater Flow Rates

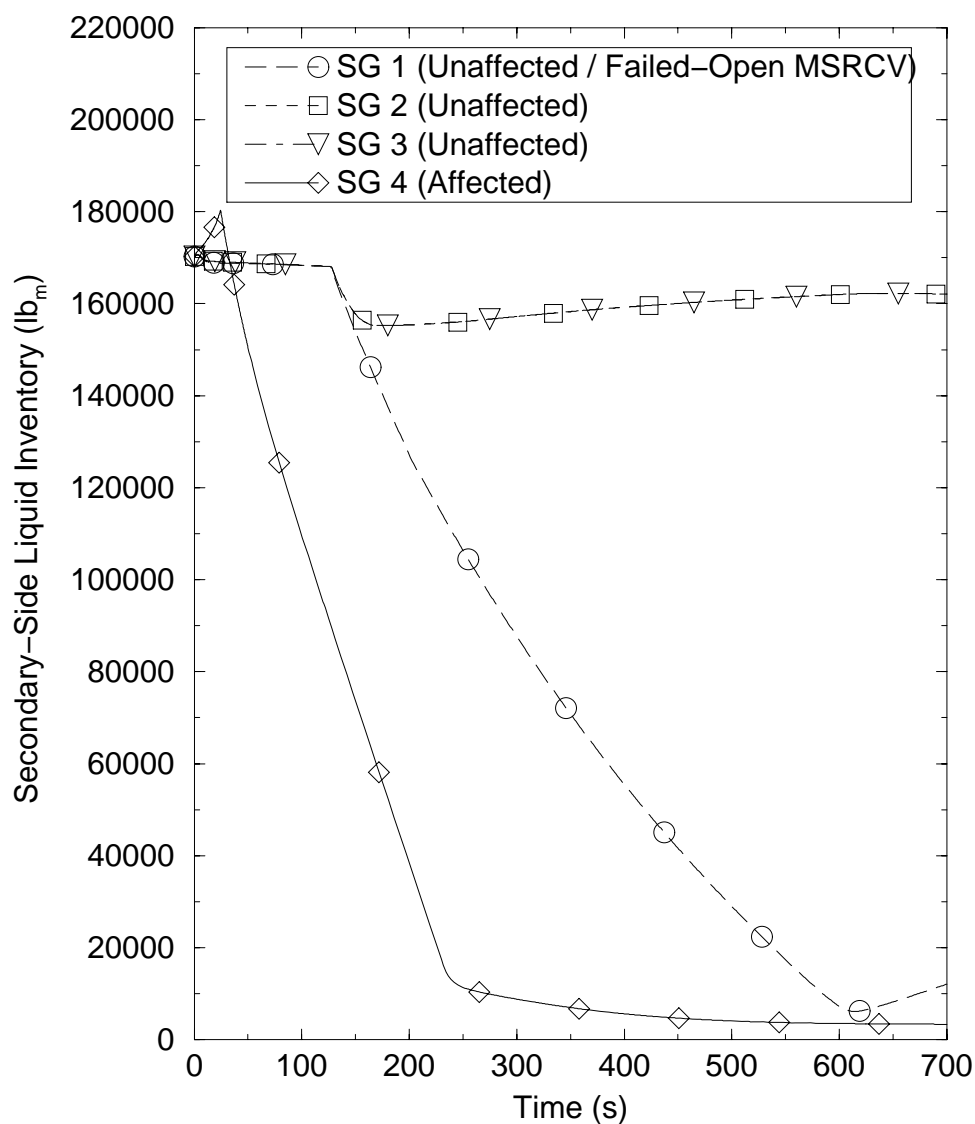
Figure D.1-6 Post-Scram MSLB Steam Generator Secondary-Side Liquid Inventories

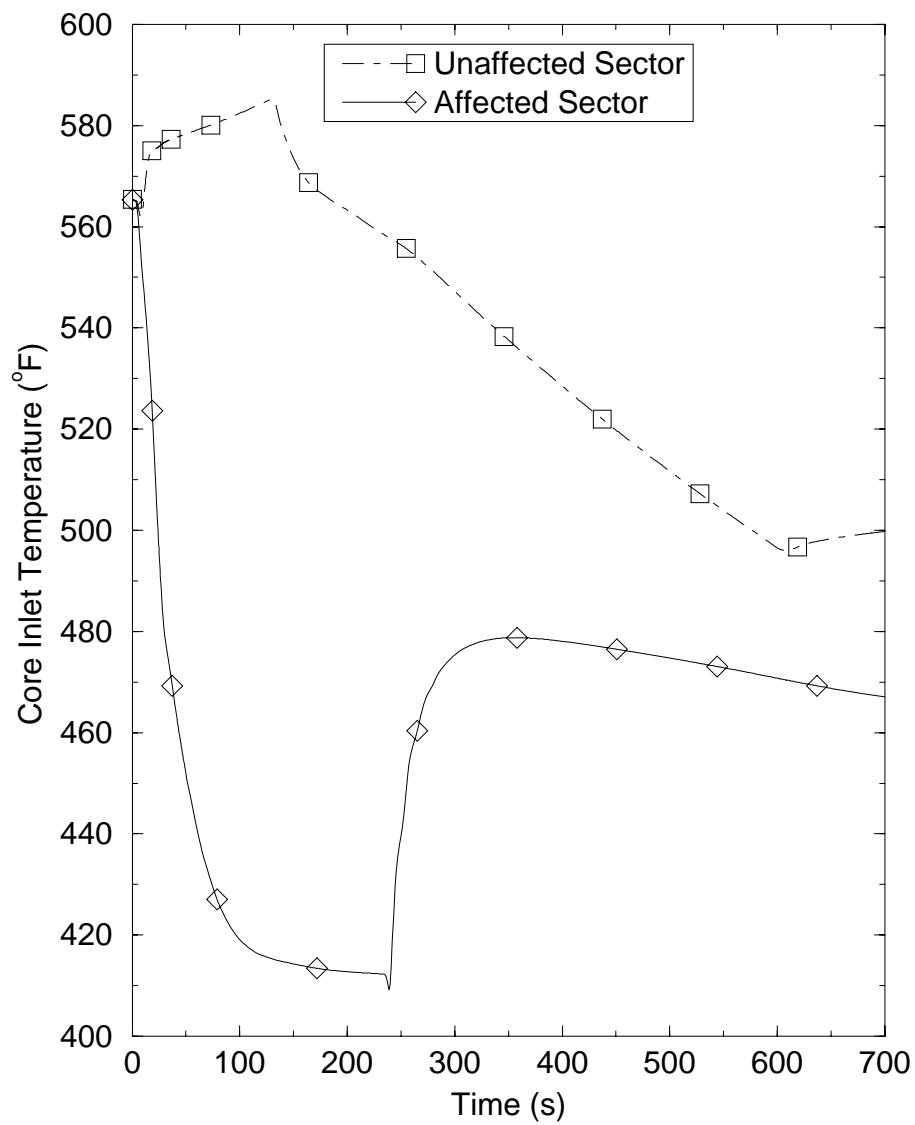
Figure D.1-7 Post-Scram MSLB Core Inlet Temperatures

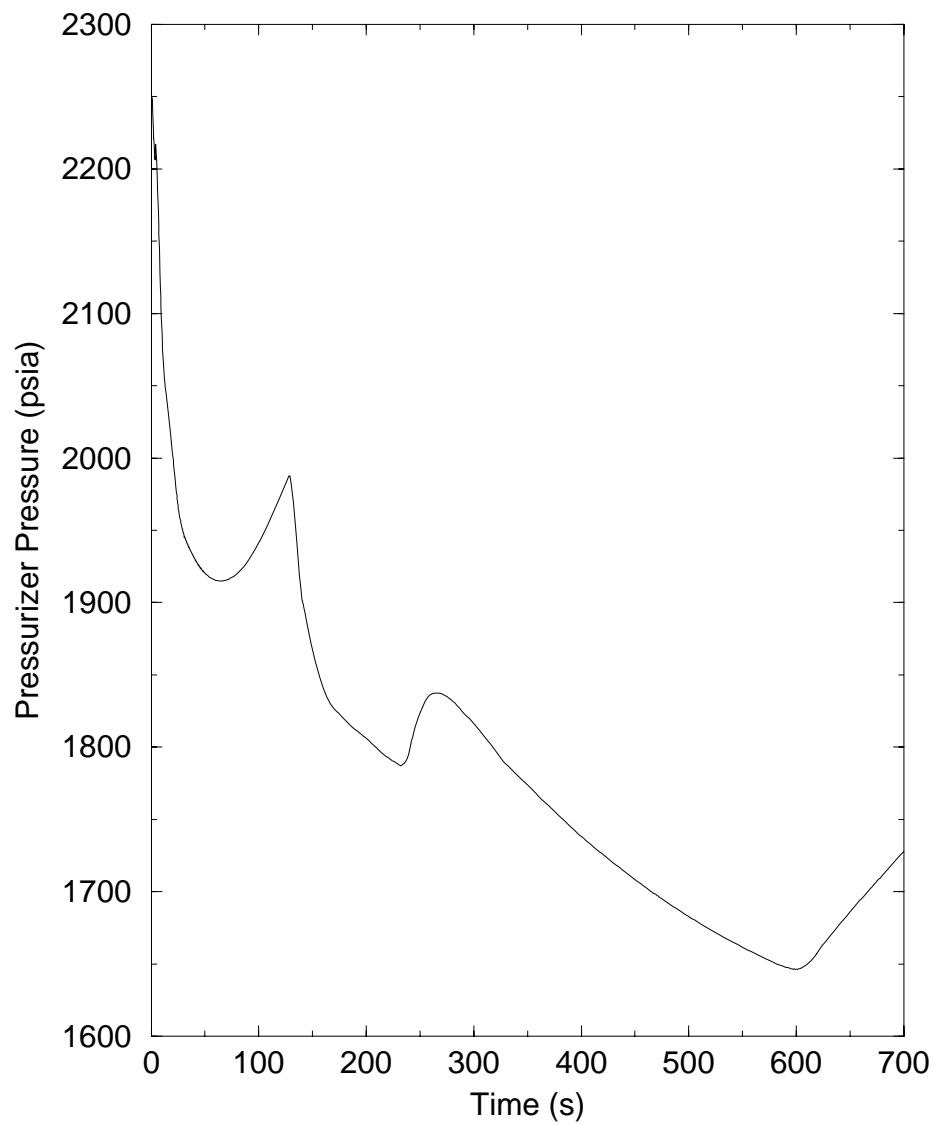
Figure D.1-8 Post-Scram MSLB Pressurizer Pressure

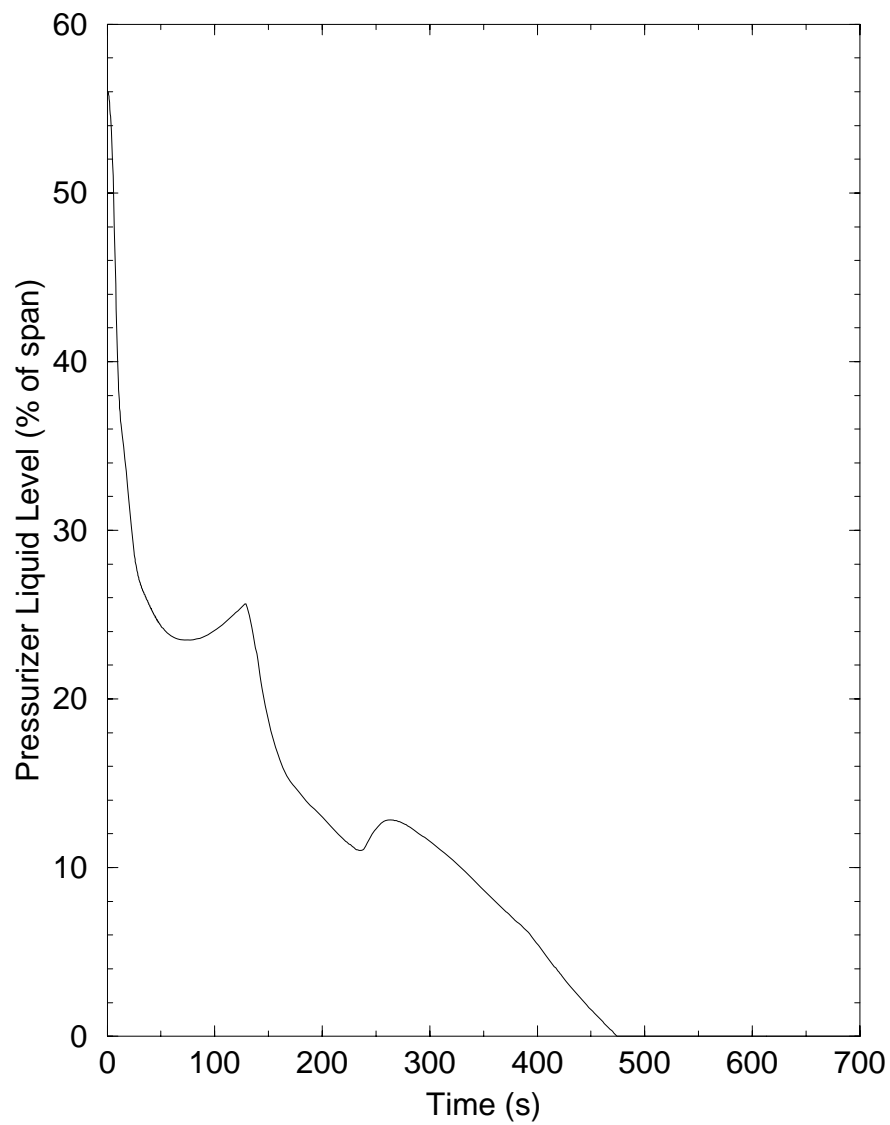
Figure D.1-9 Post-Scram MSLB Pressurizer Liquid Level

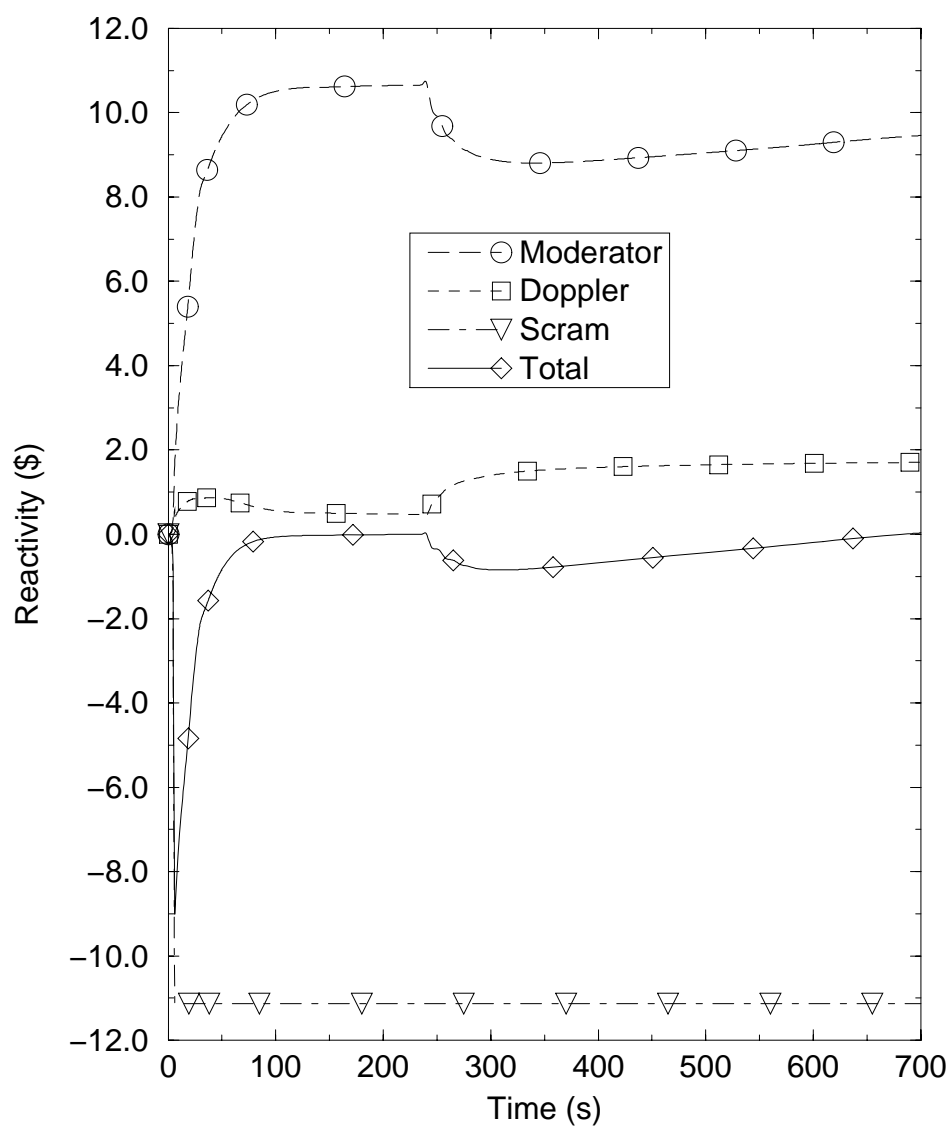
Figure D.1-10 Post-Scram MSLB Reactivity

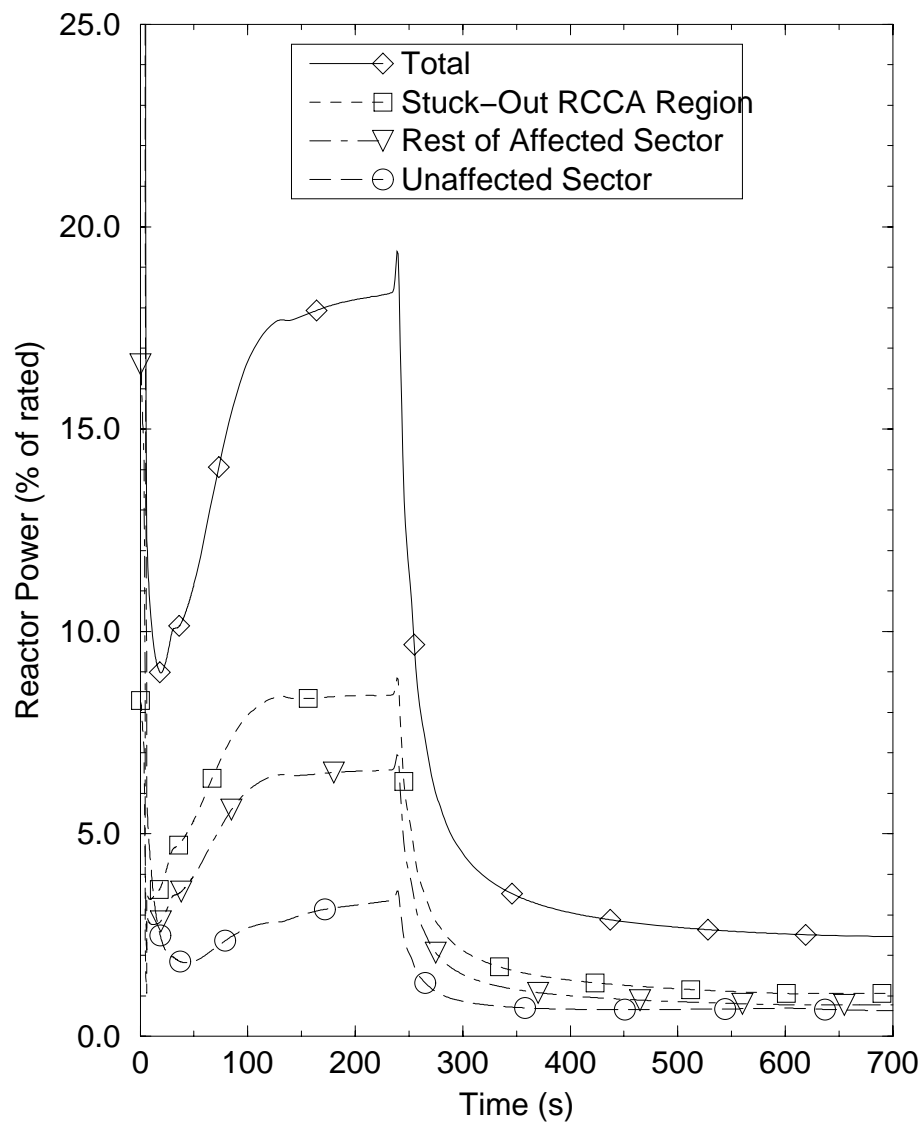
Figure D.1-11 Post-Scram MSLB Reactor Power

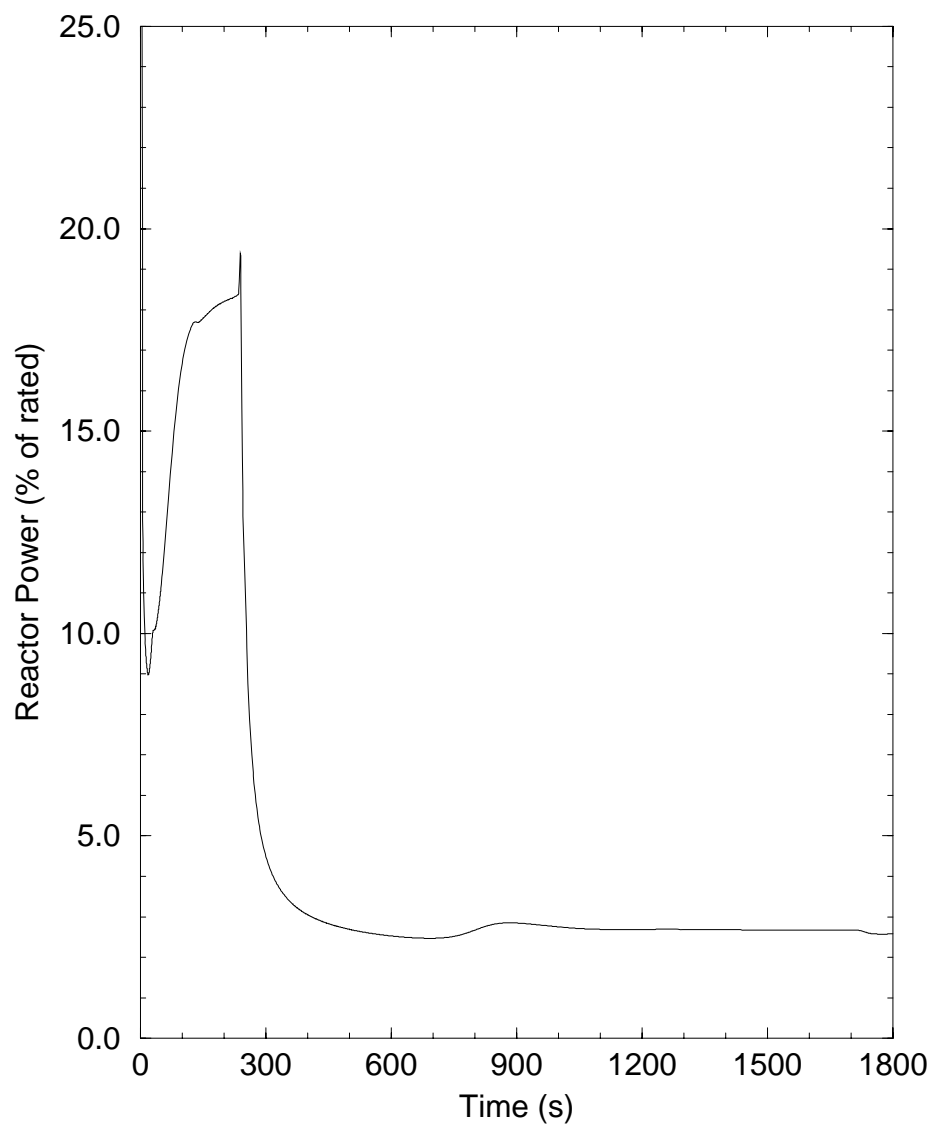
Figure D.1-12 Post-Scram MSLB Longer-Term Reactor Power

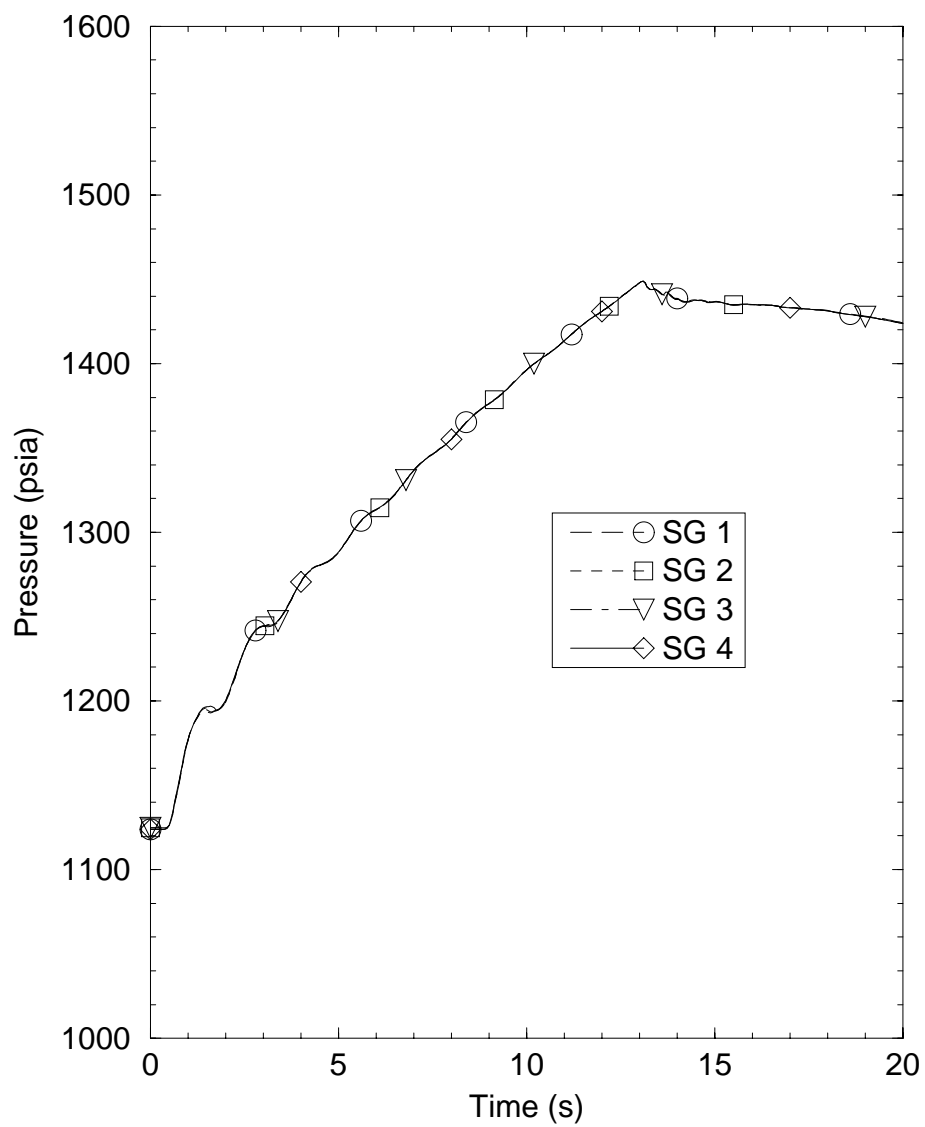
Figure D.2-1 LOEL/TT Steam Generator Pressures

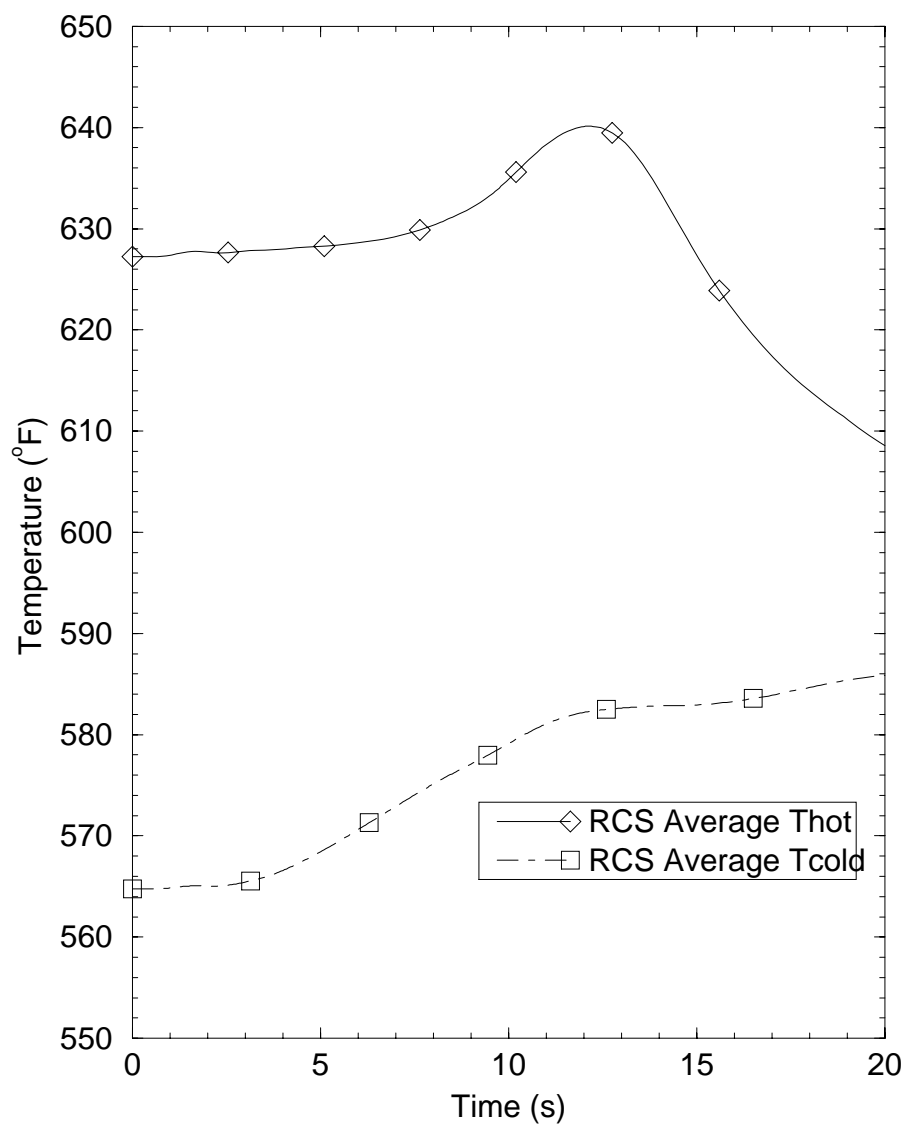
Figure D.2-2 LOEL/TT RCS Temperatures

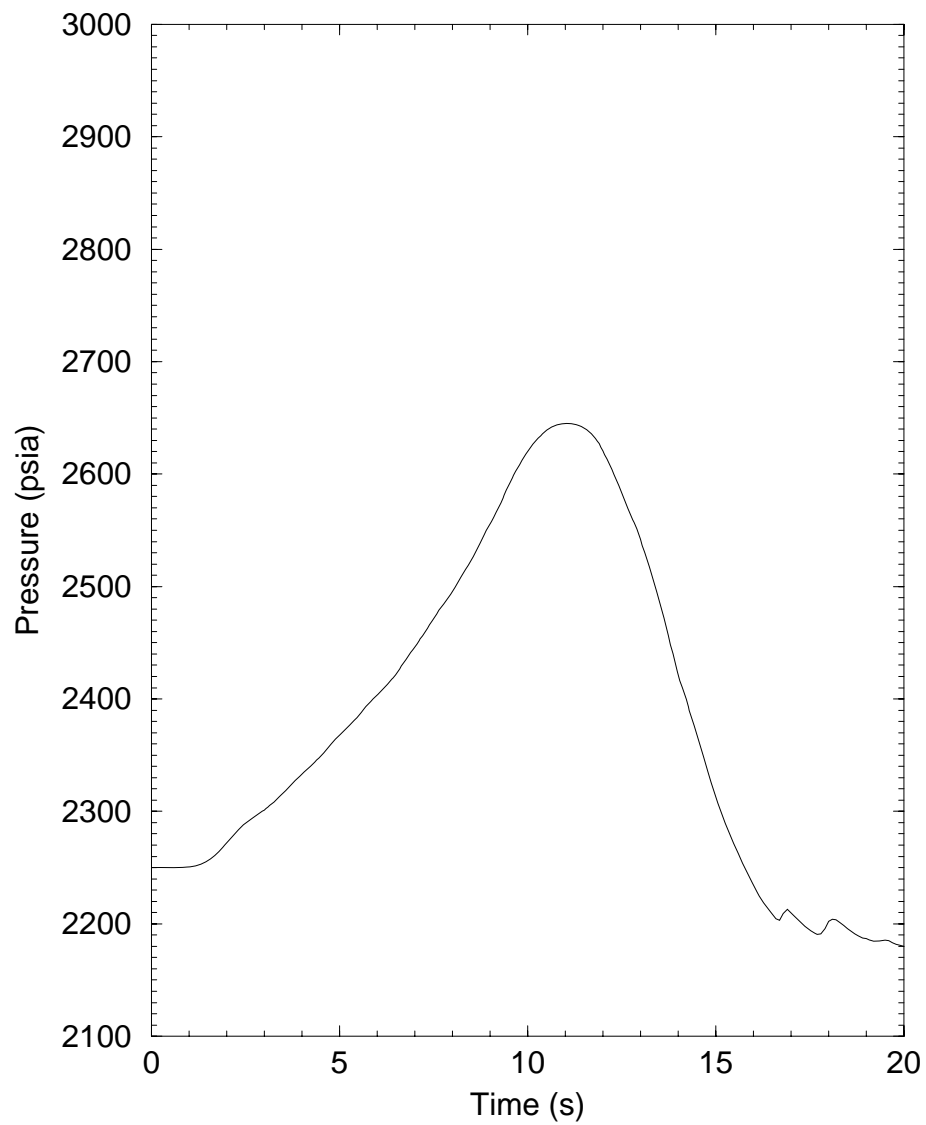
Figure D.2-3 LOEL/TT Pressurizer Pressure

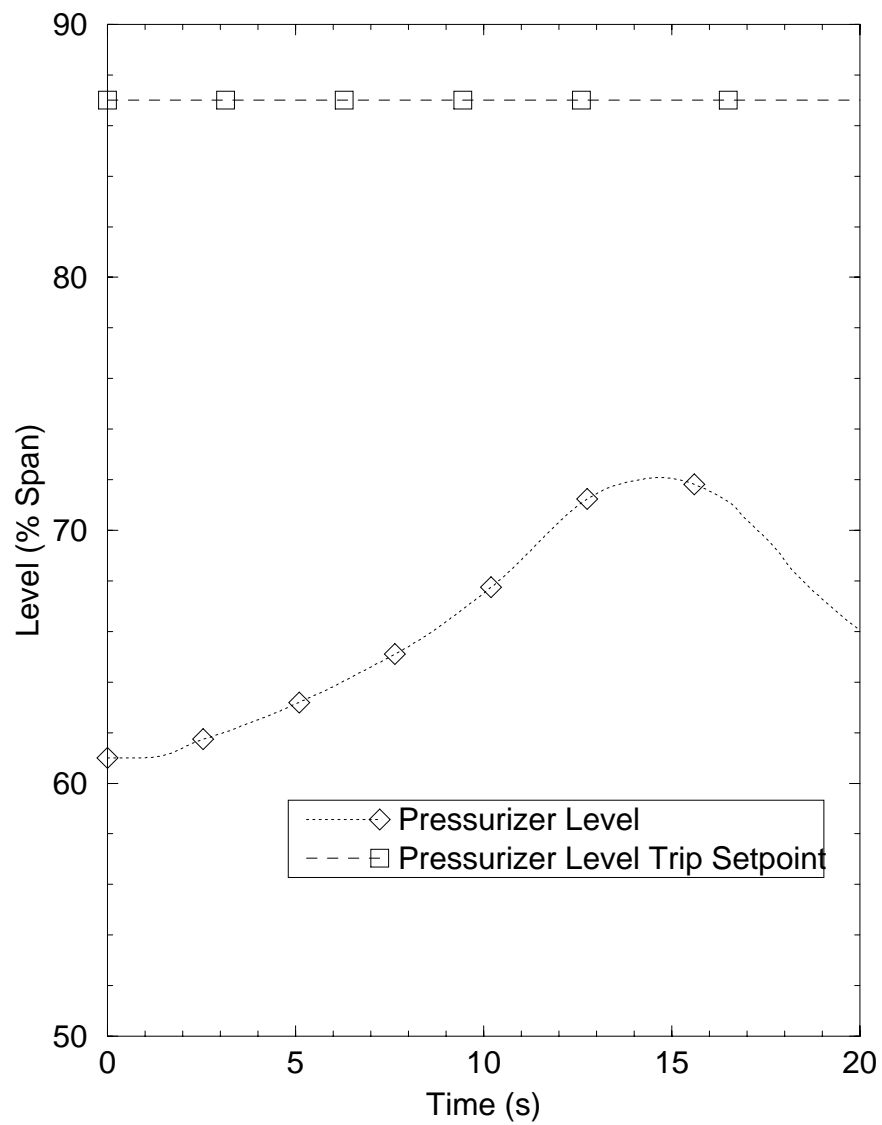
Figure D.2-4 LOEL/TT Pressurizer Level

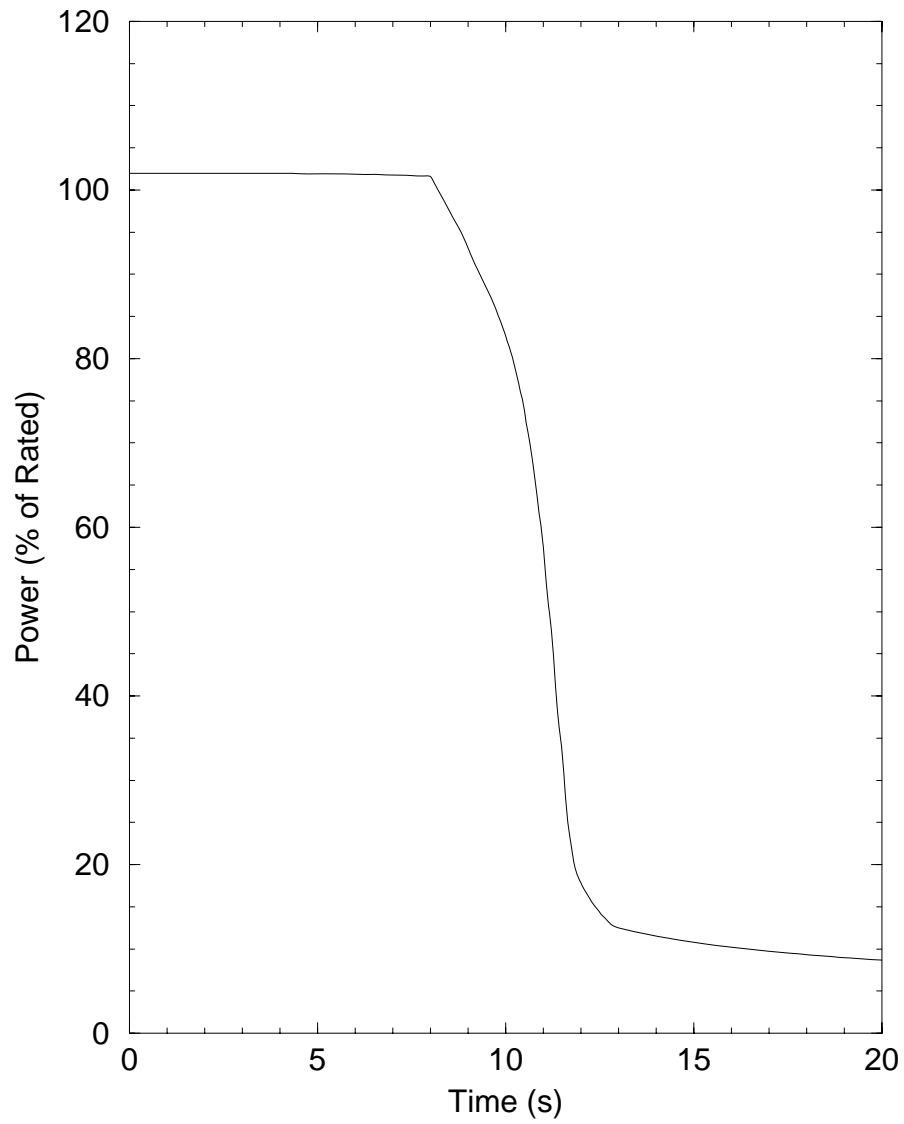
Figure D.2-5 LOEL/TT Reactor Power

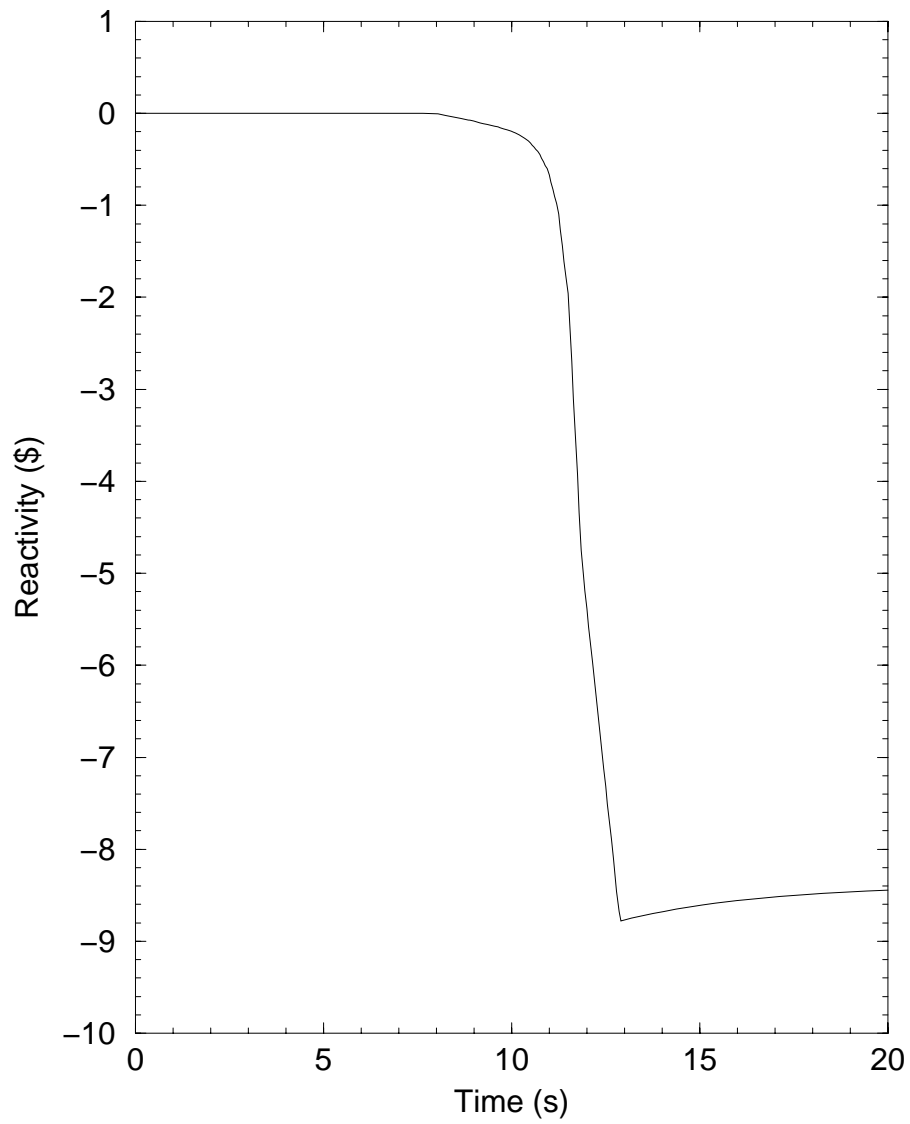
Figure D.2-6 LOEL/TT Total Reactivity

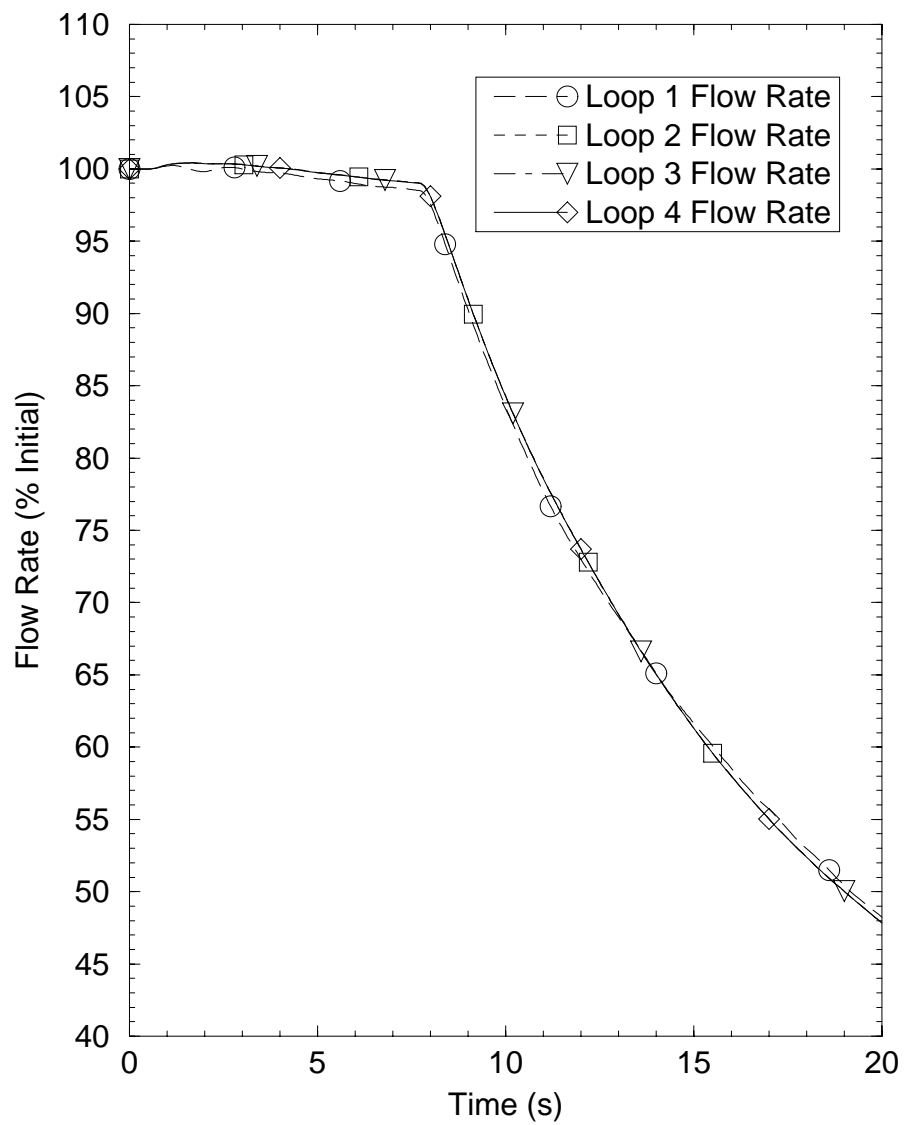
Figure D.2-7 LOEL/TT RCS Loop Flow Rates

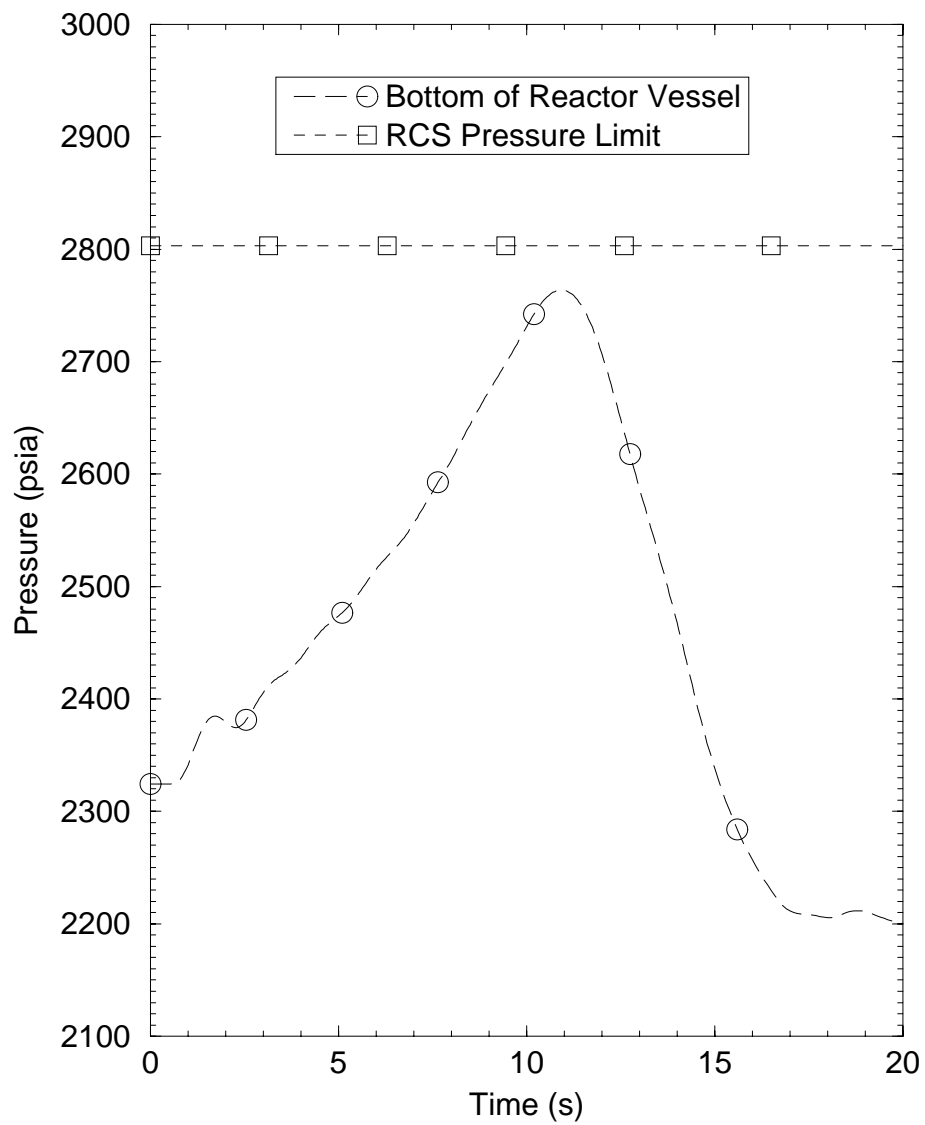
Figure D.2-8 LOEL/TT Pressure at Bottom of Reactor Vessel

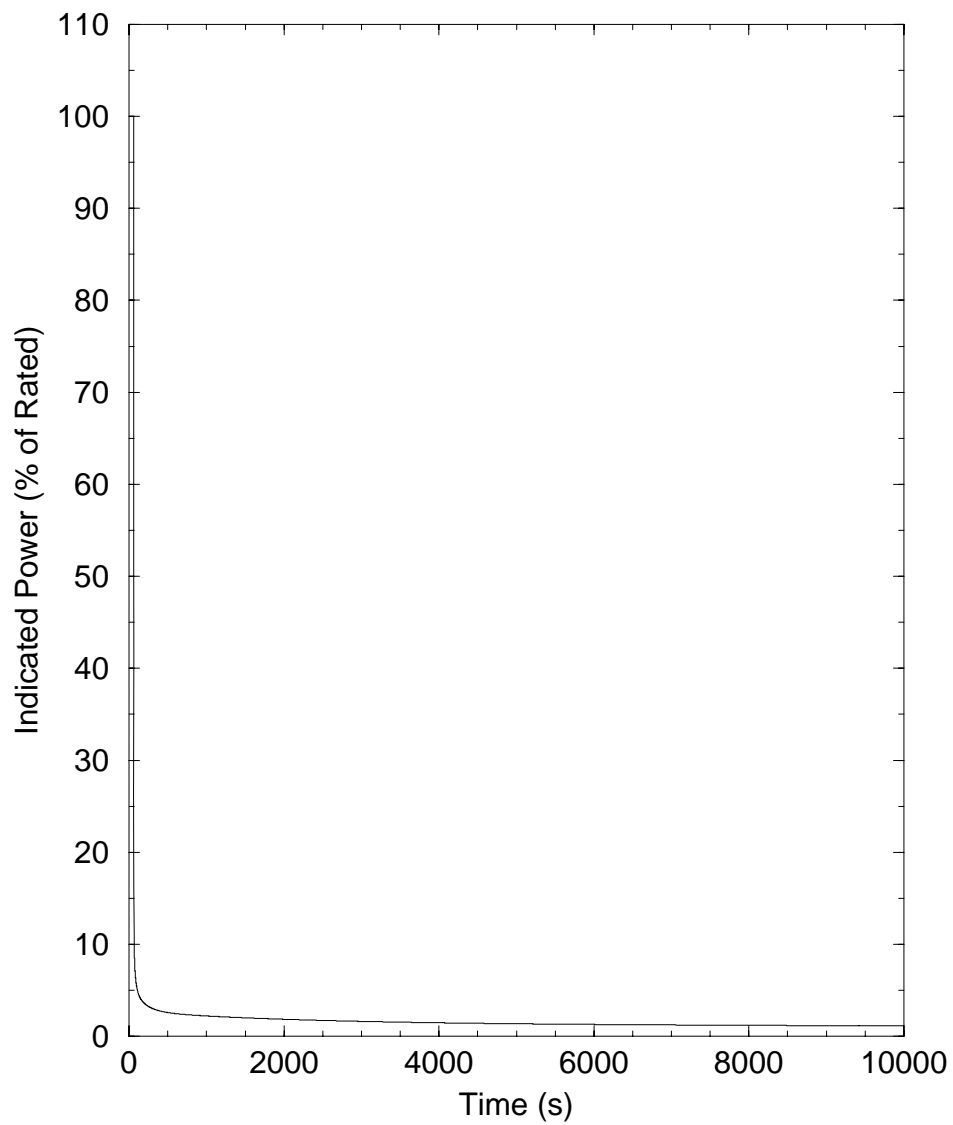
Figure D.3-1 LONF (With Offsite Power) Reactor Power Level

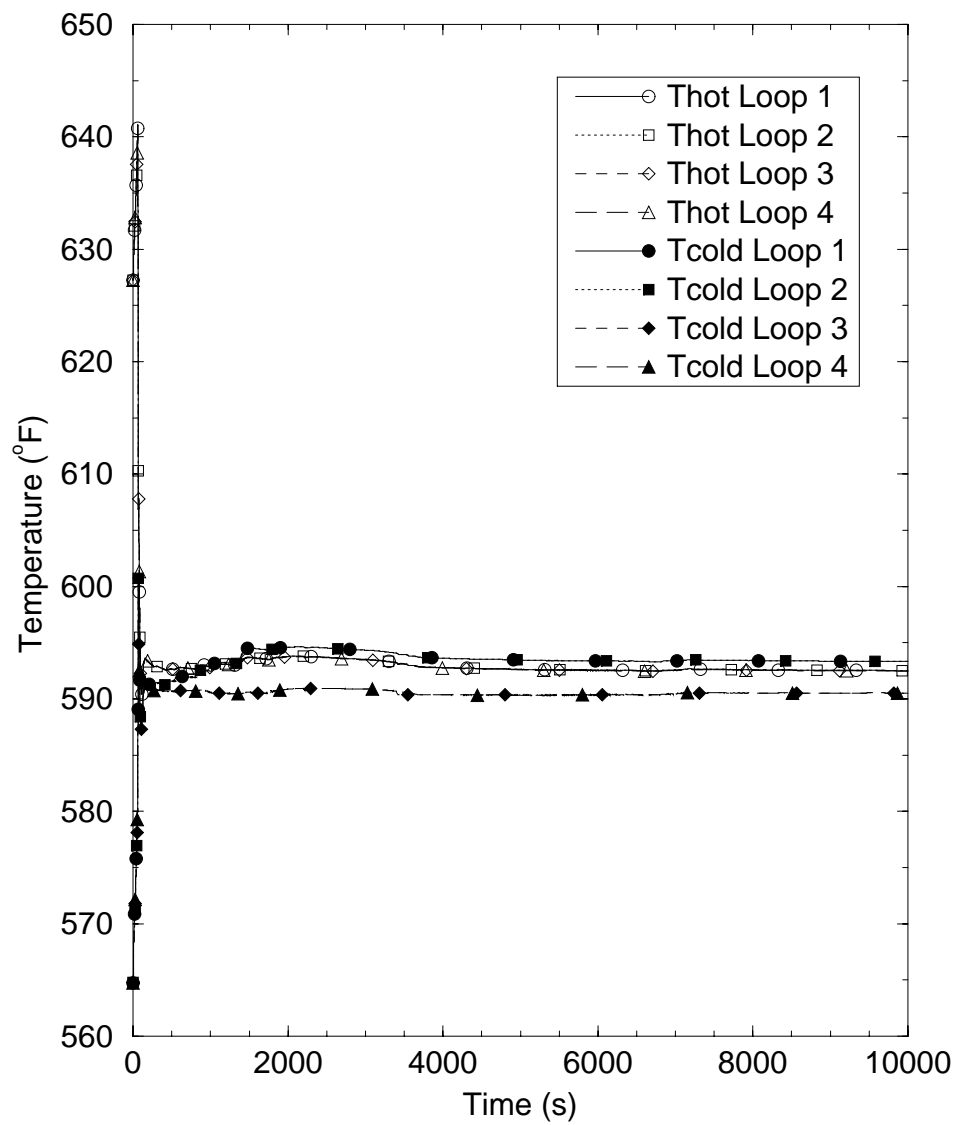
Figure D.3-2 LONF (With Offsite Power) RCS Temperatures

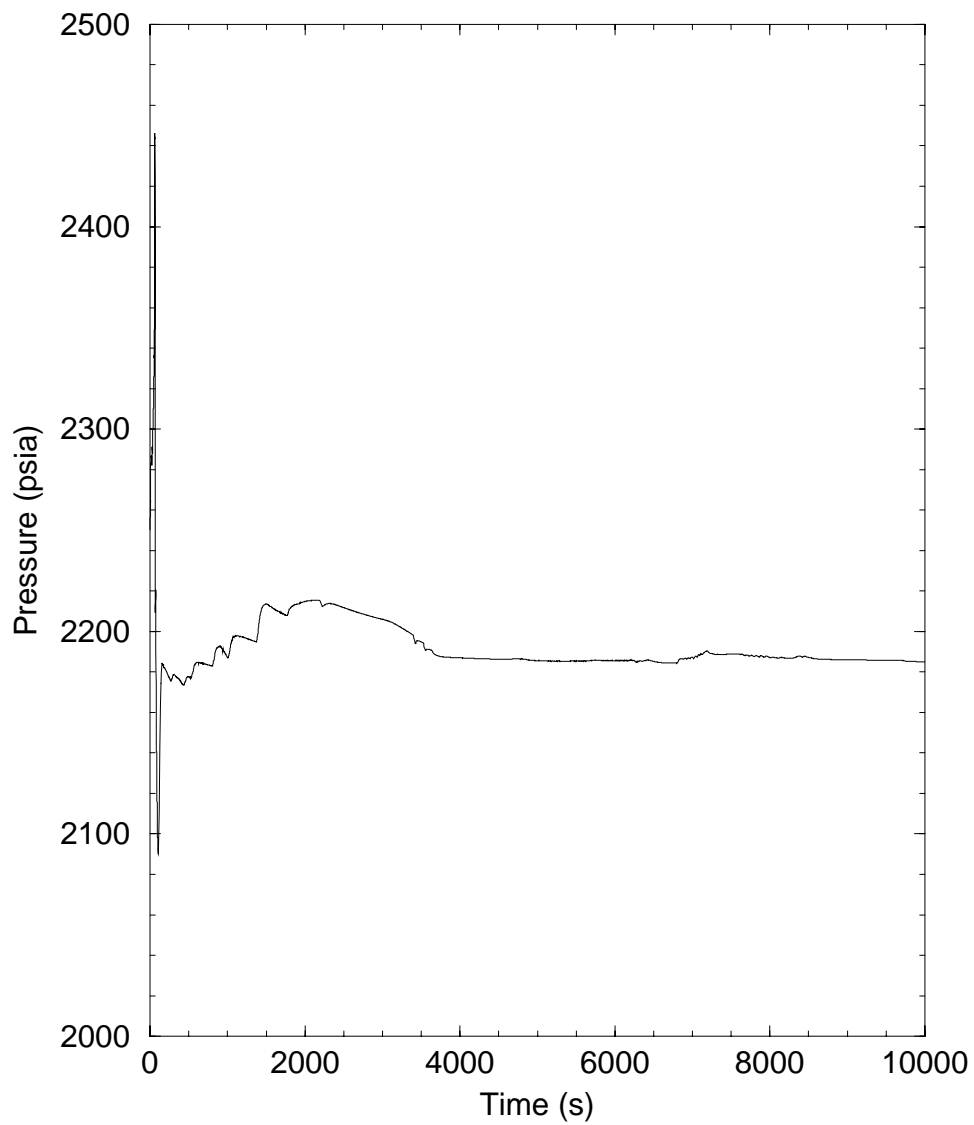
Figure D.3-3 LONF (With Offsite Power) Pressurizer Pressure

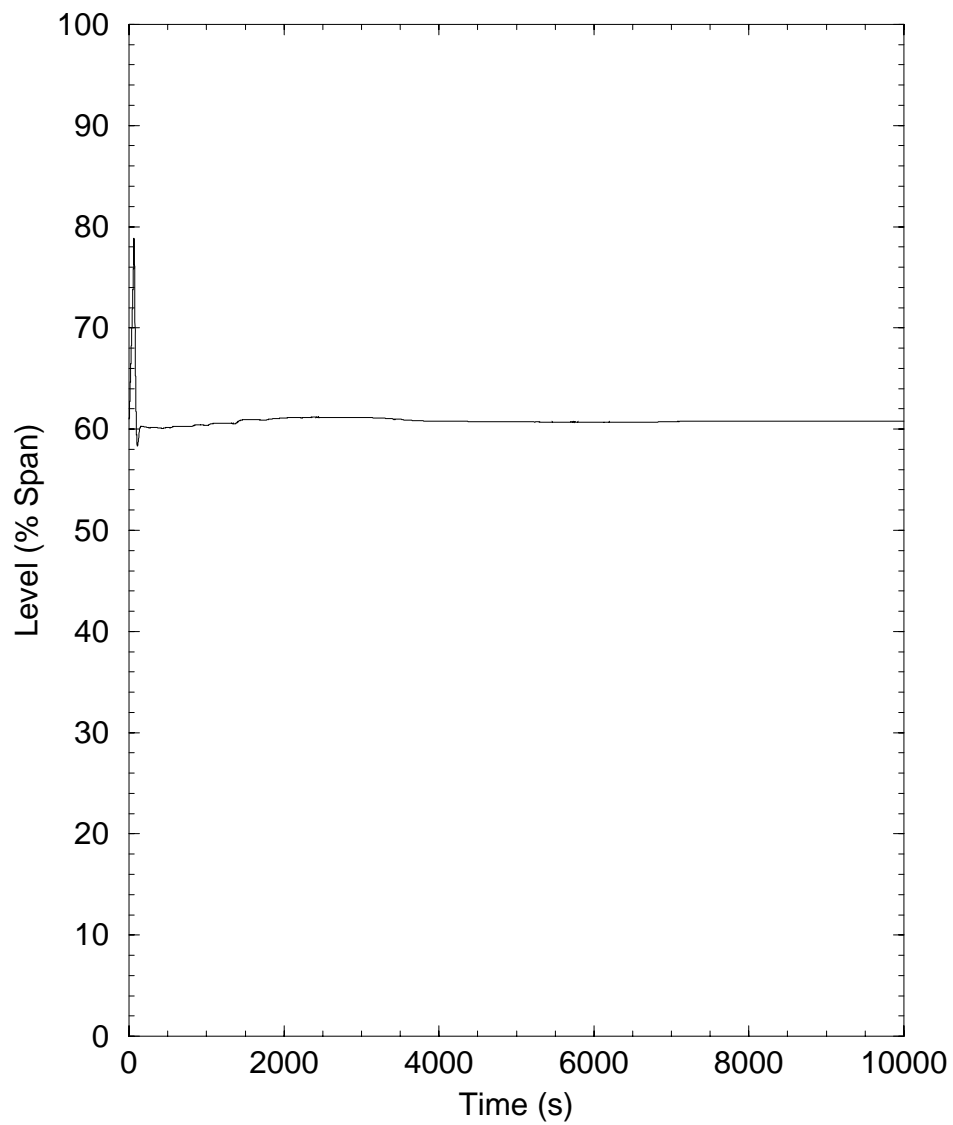
Figure D.3-4 LONF (With Offsite Power) Pressurizer Liquid Level

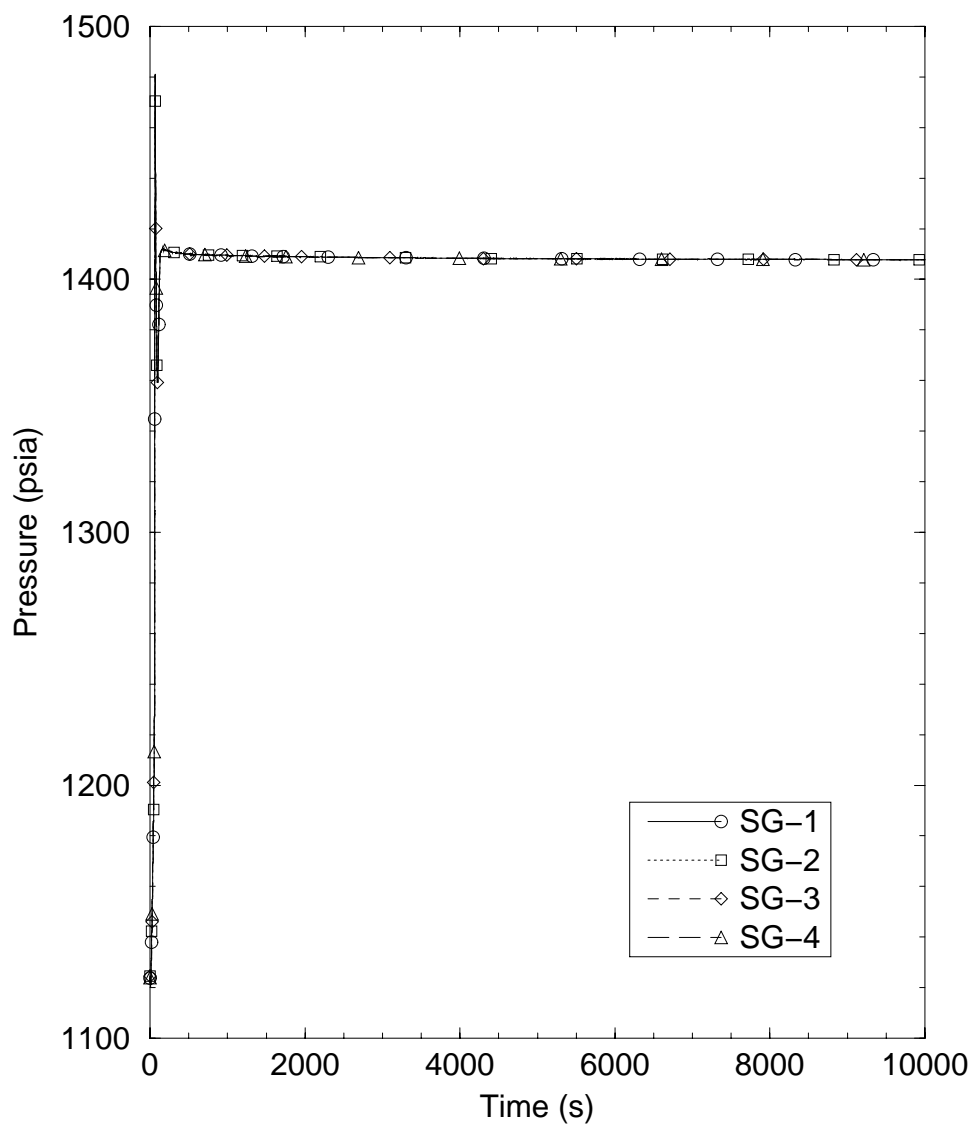
Figure D.3-5 LONF (With Offsite Power) Steam Generator Pressure

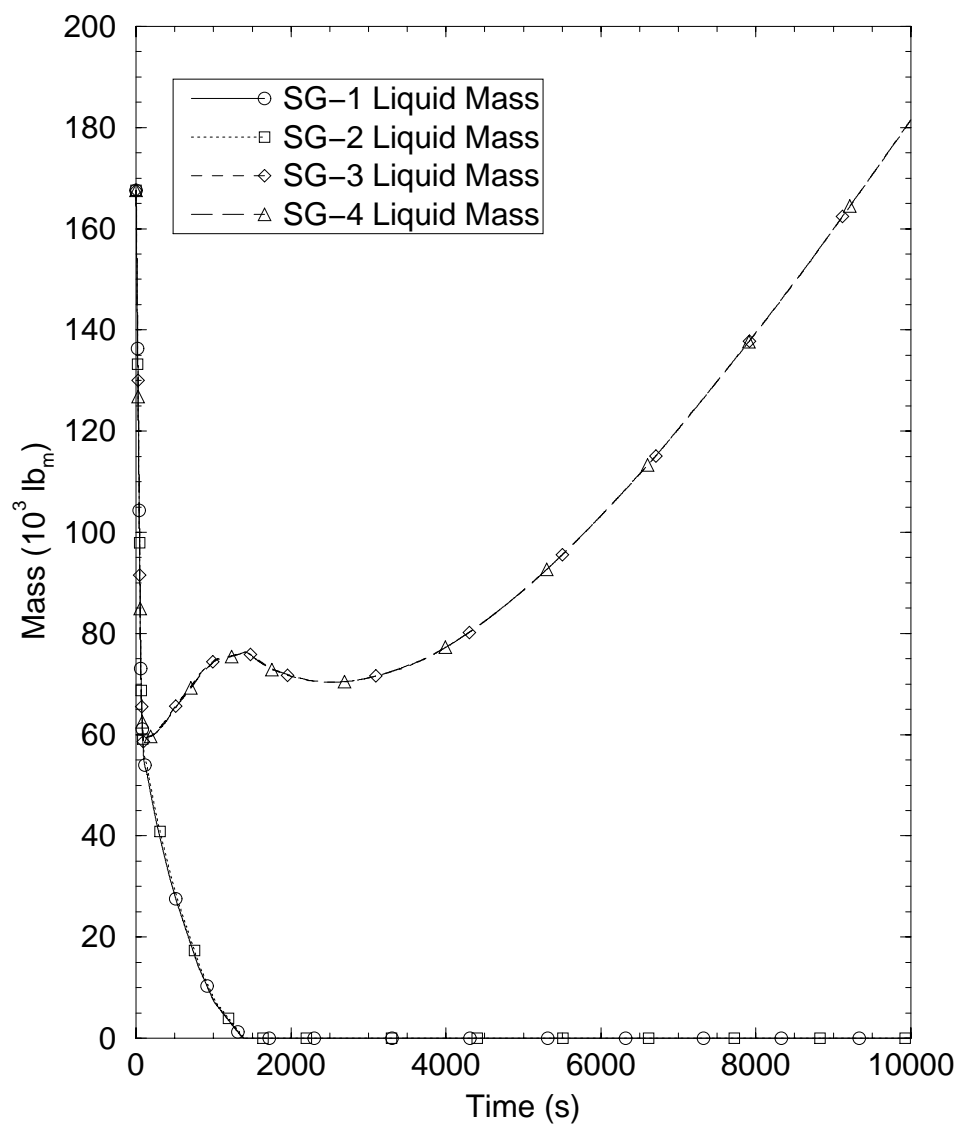
Figure D.3-6 LONF (With Offsite Power) Steam Generator Inventory

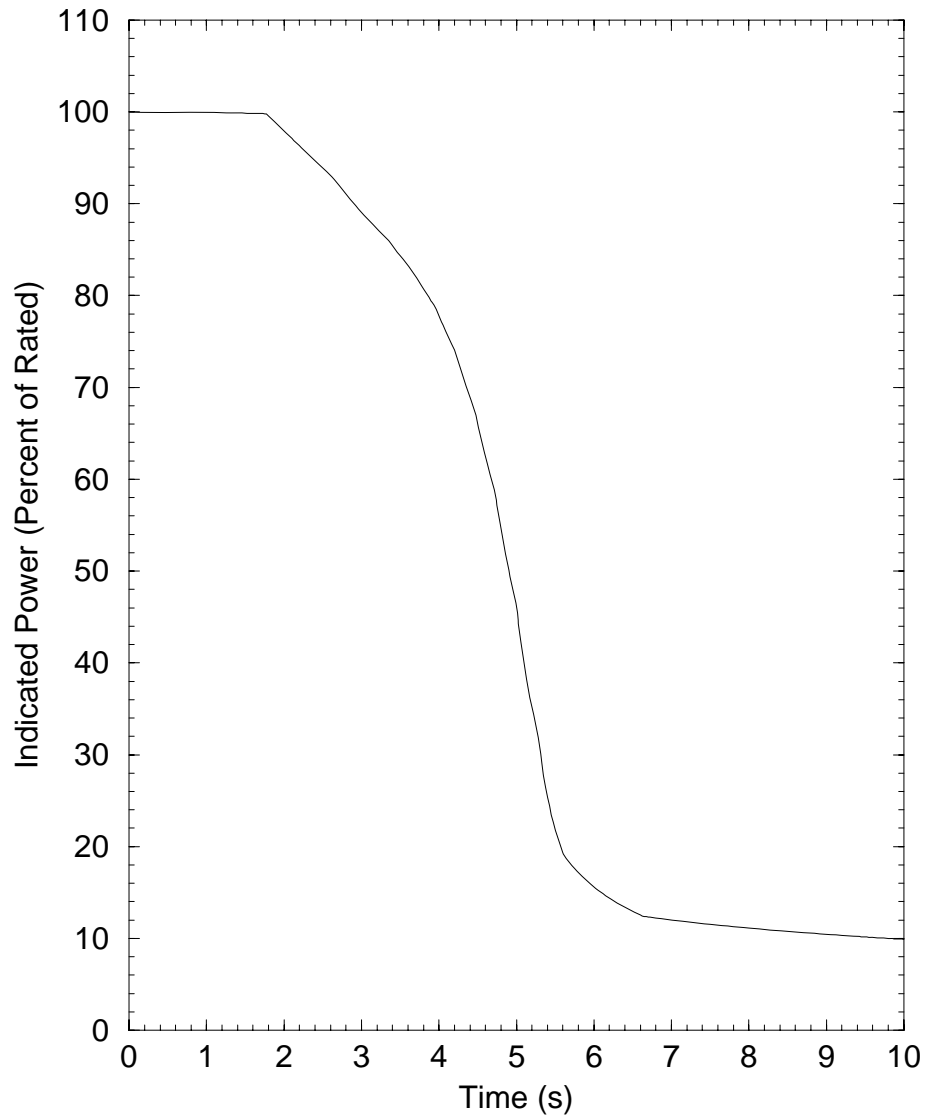
Figure D.4-1 LOCF Reactor Power Level

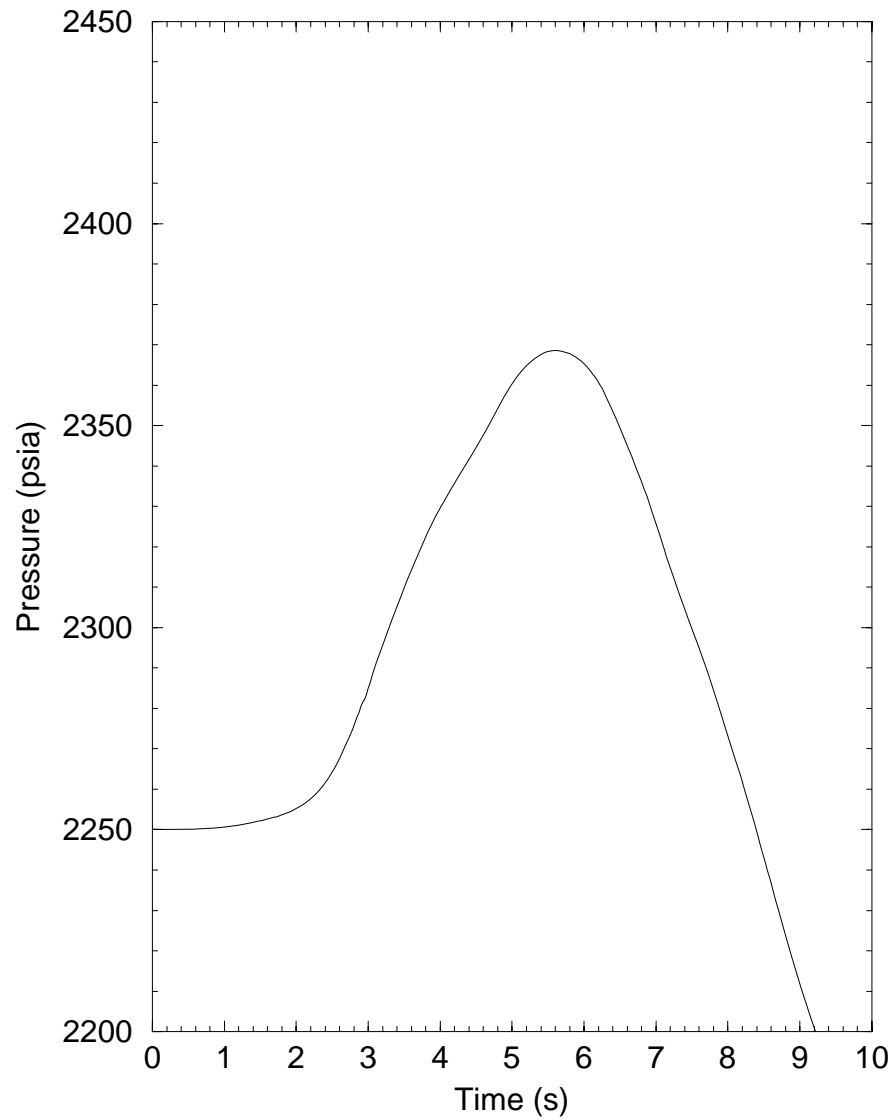
Figure D.4-2 LOCF Pressurizer Pressure

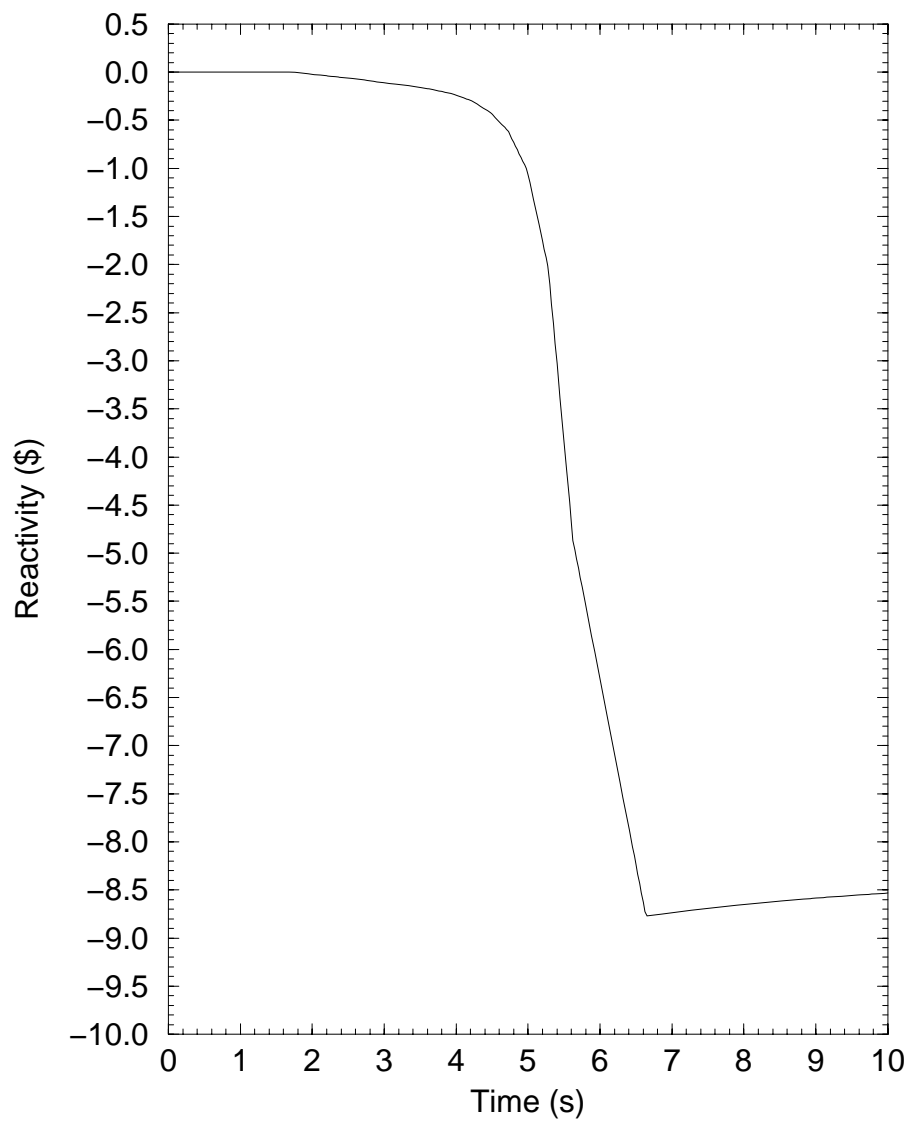
Figure D.4-3 LOCF Reactivity

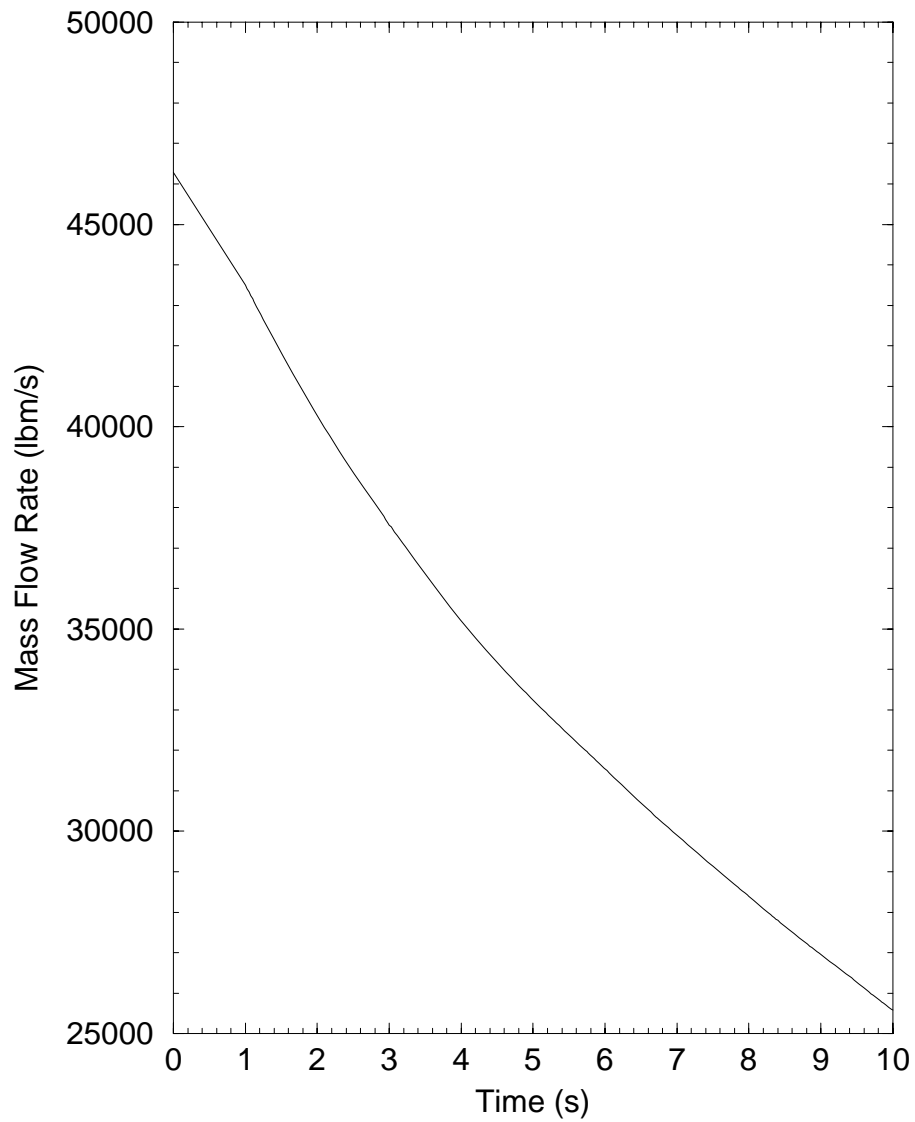
Figure D.4-4 LOCF Reactor Coolant System Flowrate

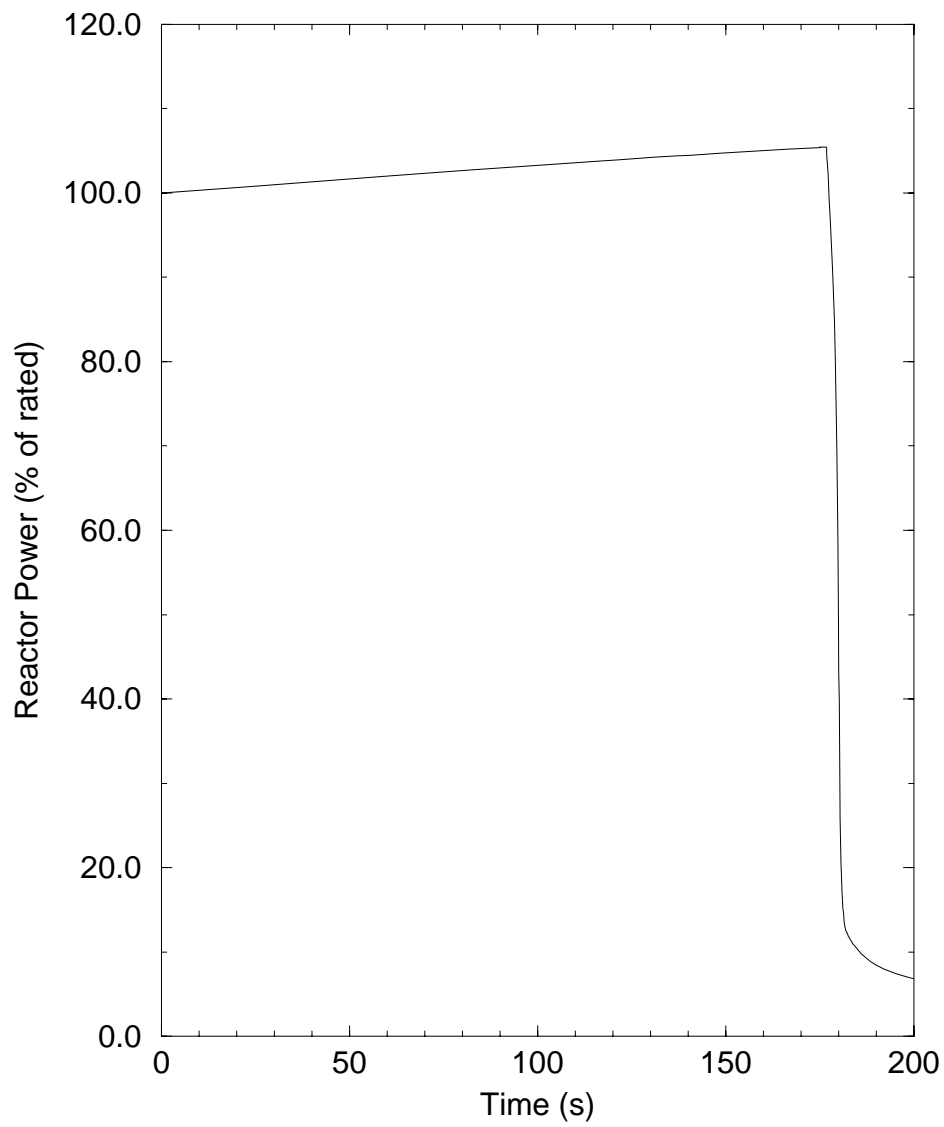
Figure D.5-1 UCBW Core Power

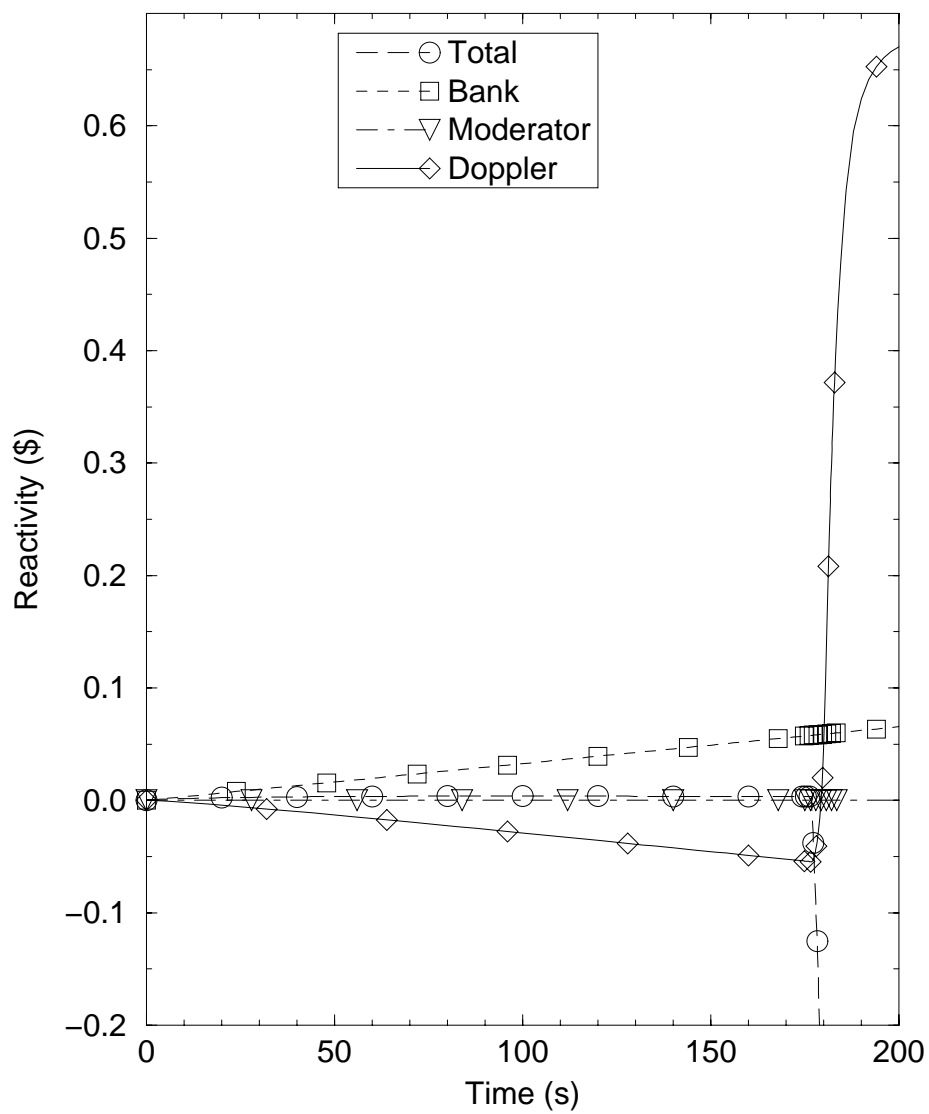
Figure D.5-2 UCBW Reactivity

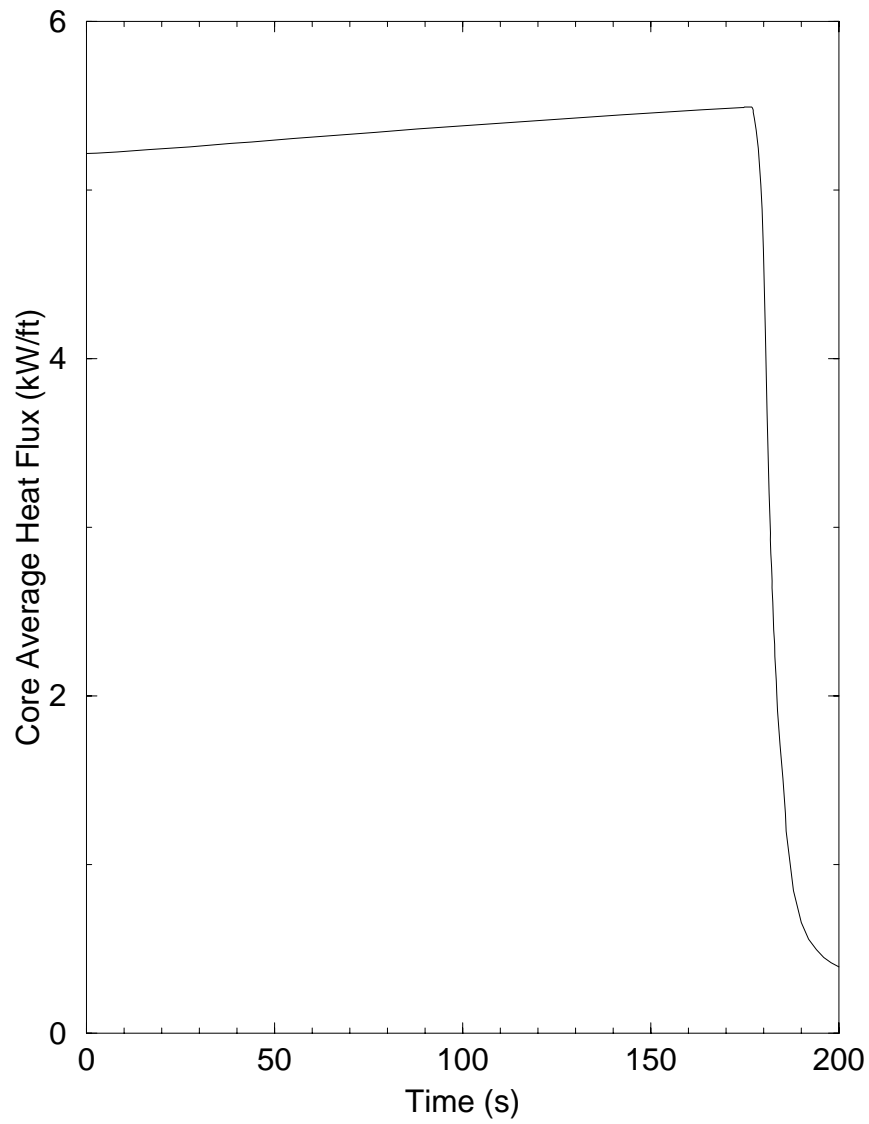
Figure D.5-3 UCBW Average Fuel Rod Heat Flux

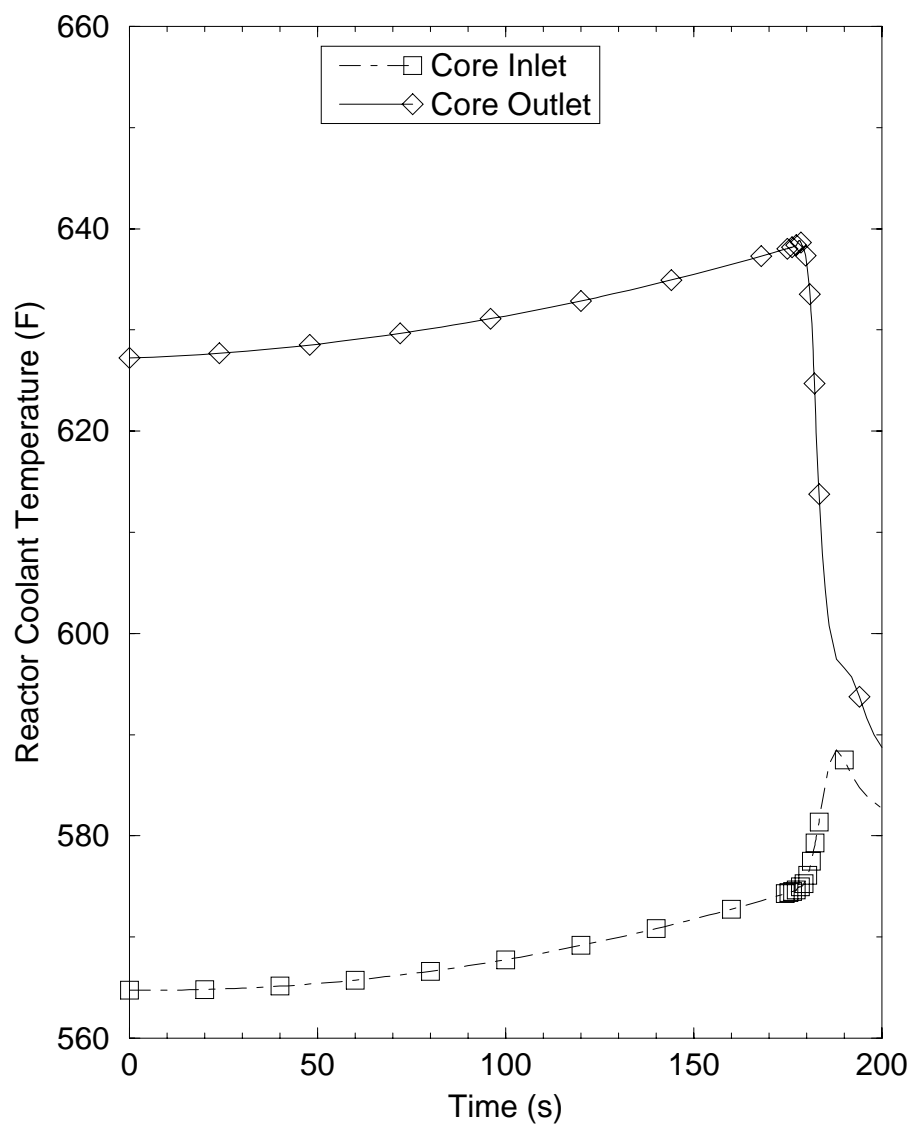
Figure D.5-4 UCBW RCS Temperatures

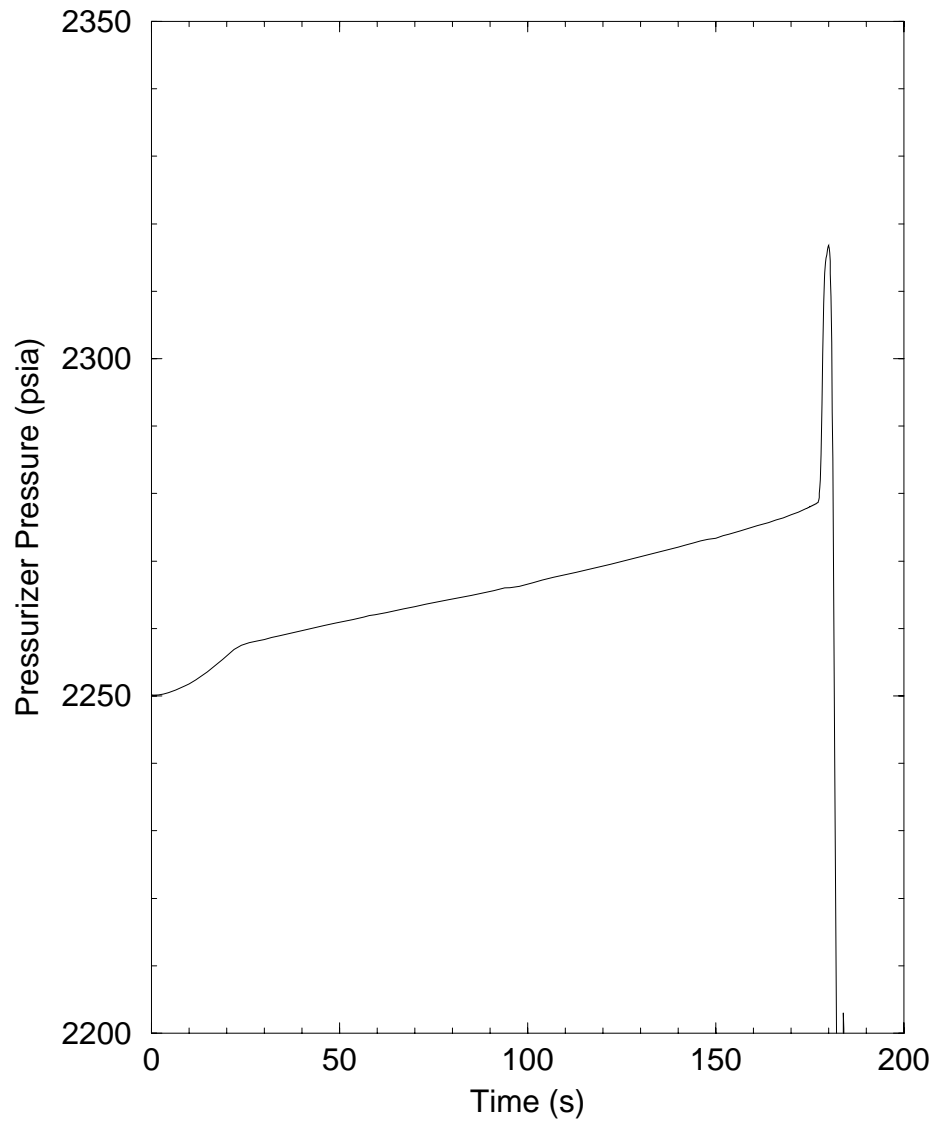
Figure D.5-5 UCBW Pressurizer Pressure

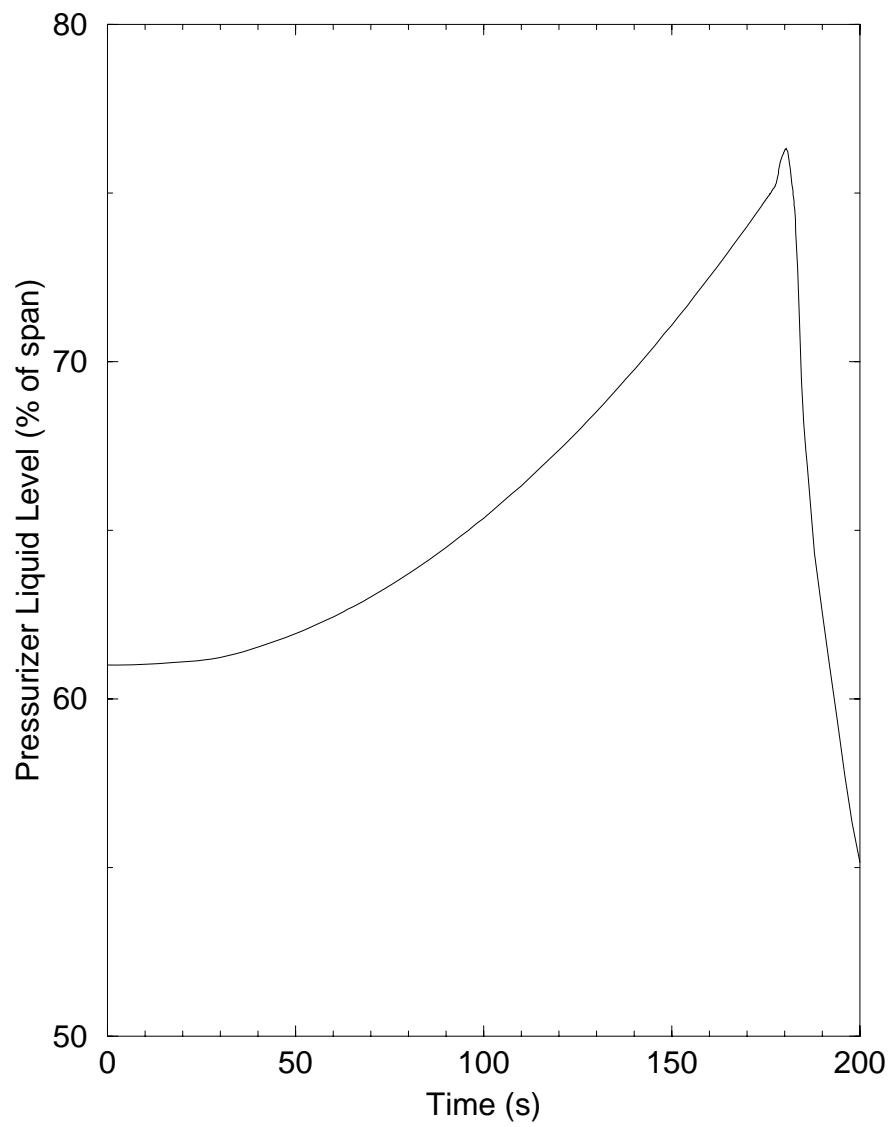
Figure D.5-6 UCBW Pressurizer Liquid Level

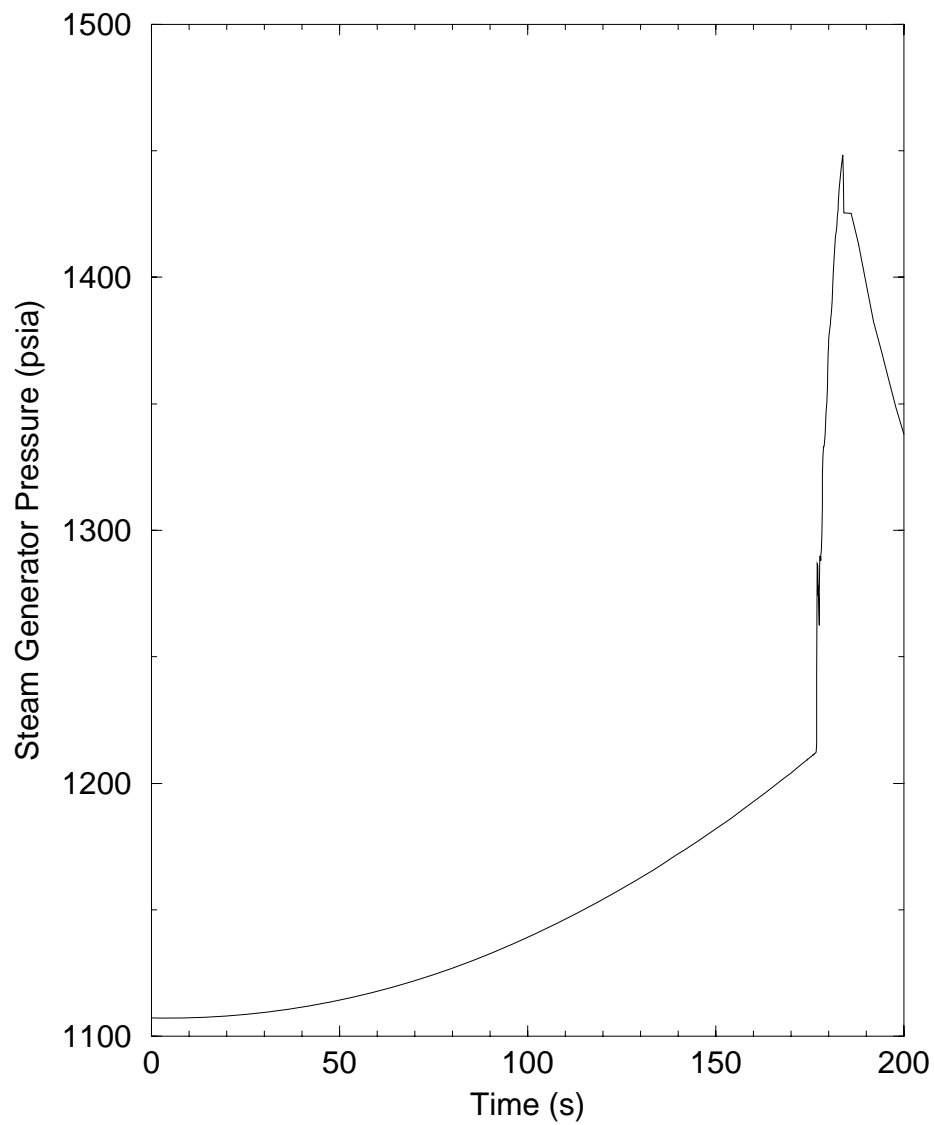
Figure D.5-7 UCBW Steam Generator One Pressure

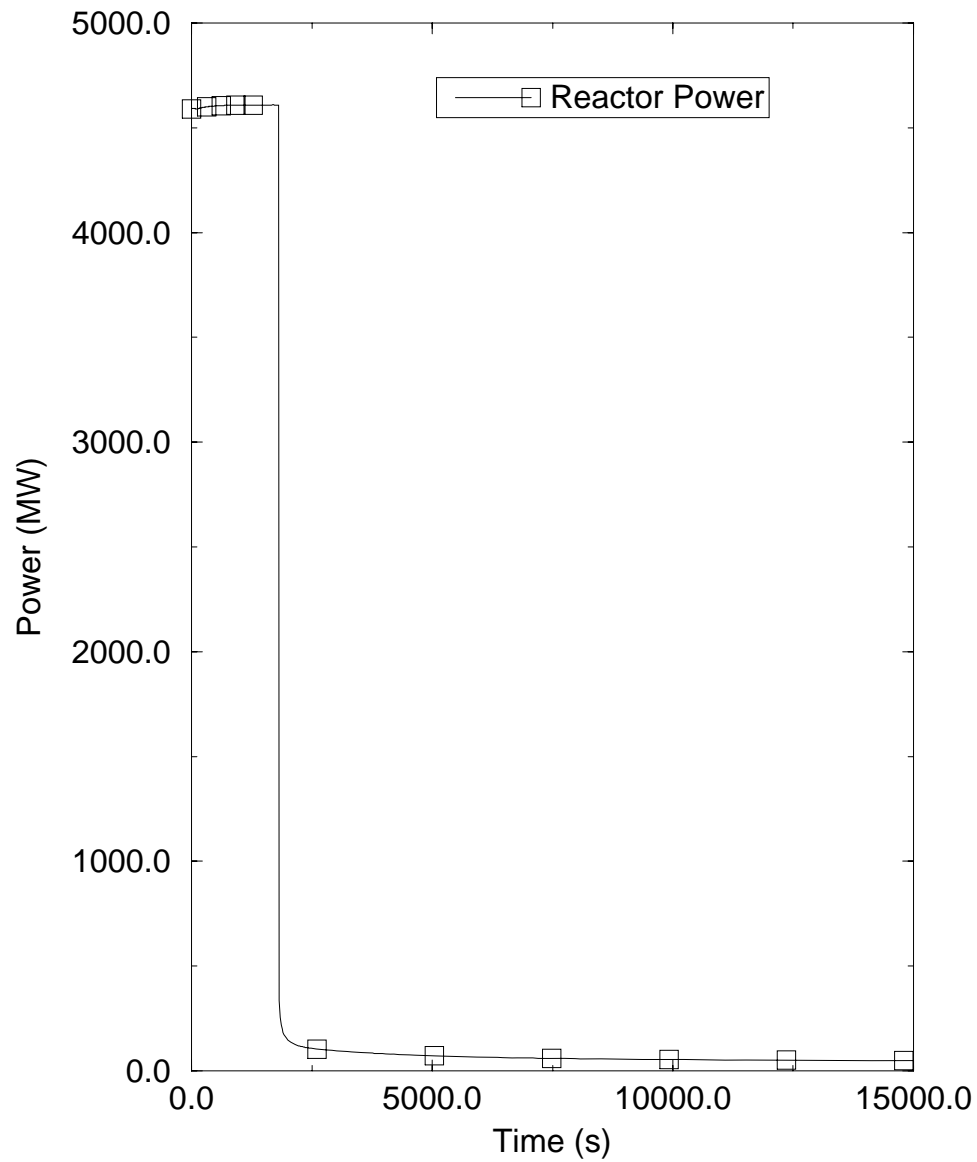
Figure D.6-1 SGTR Reactor Power

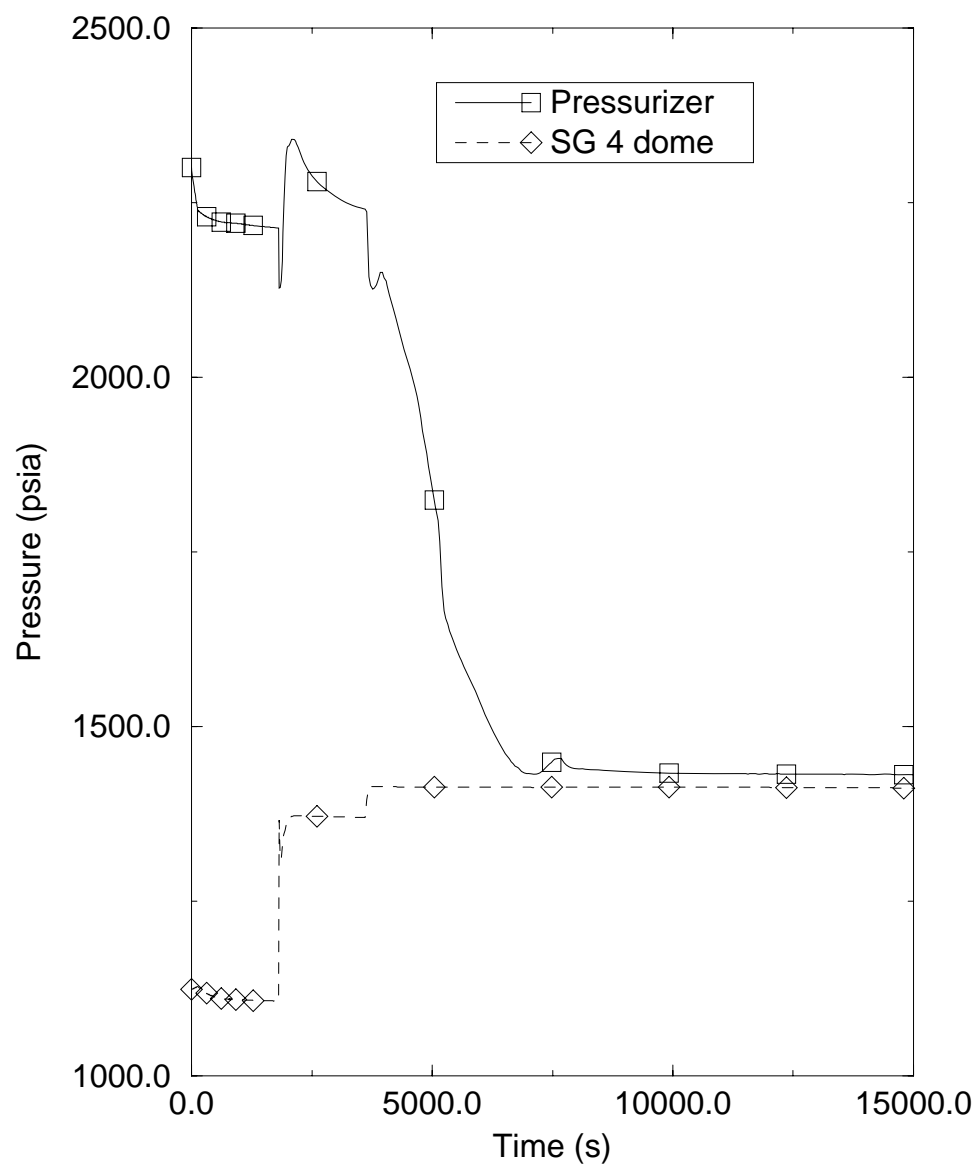
Figure D.6-2 SGTR Pressurizer Pressure

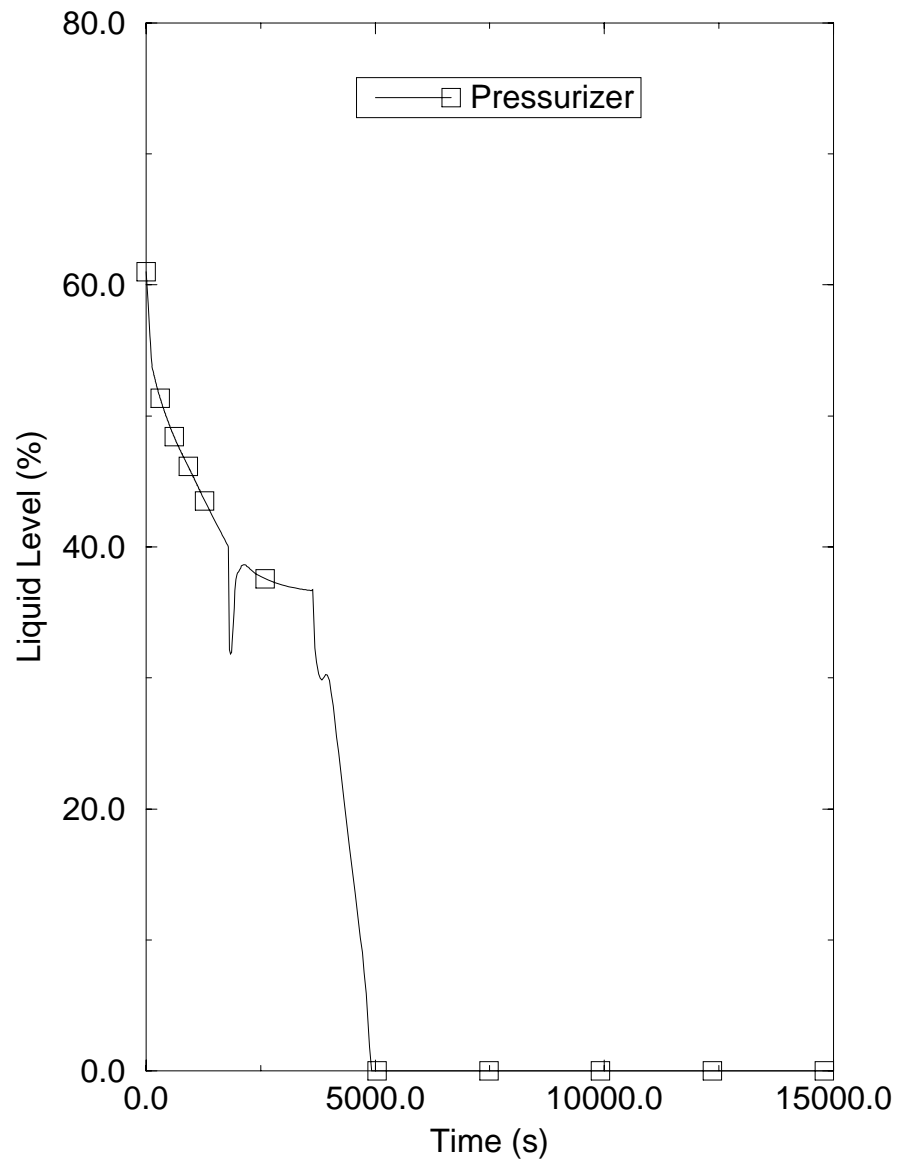
Figure D.6-3 SGTR Pressurizer Liquid Level

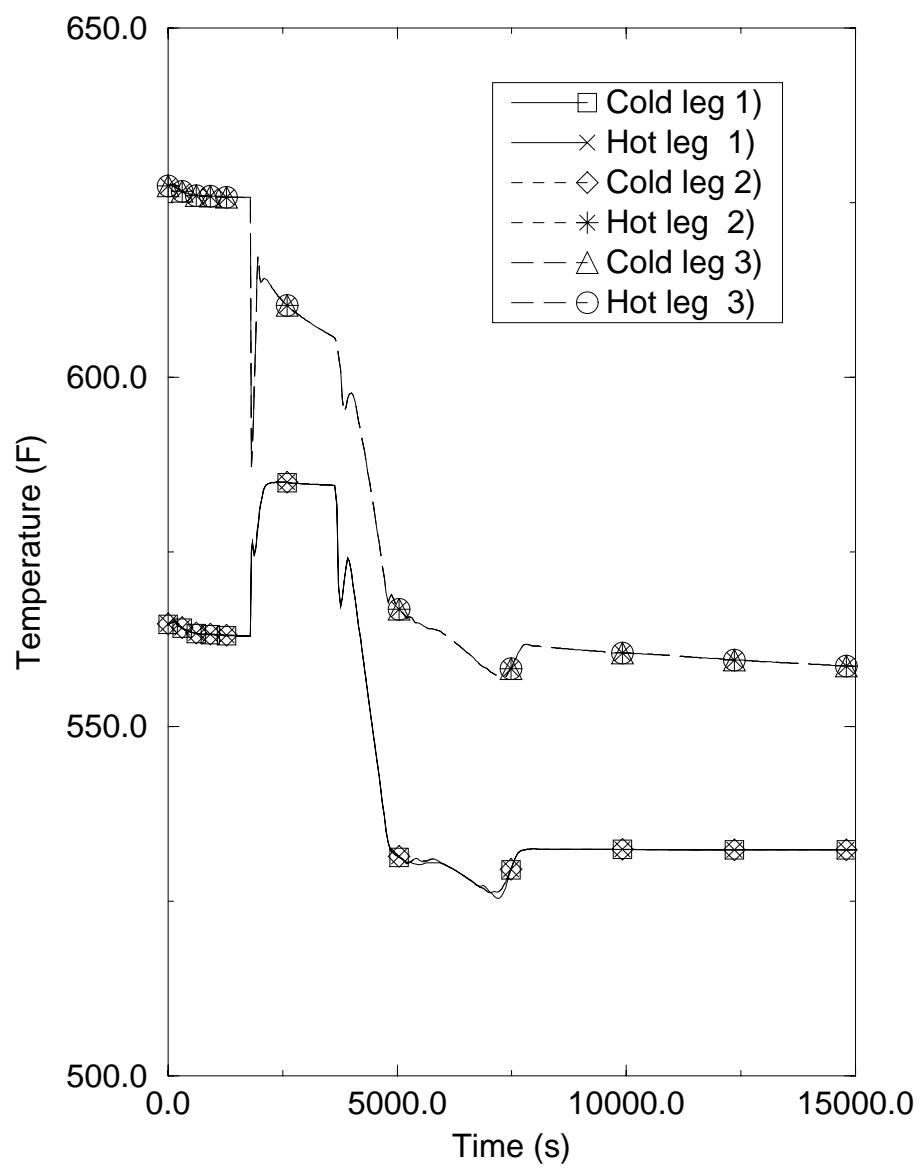
Figure D.6-4 SGTR RCS Temperatures – Intact SG Loops

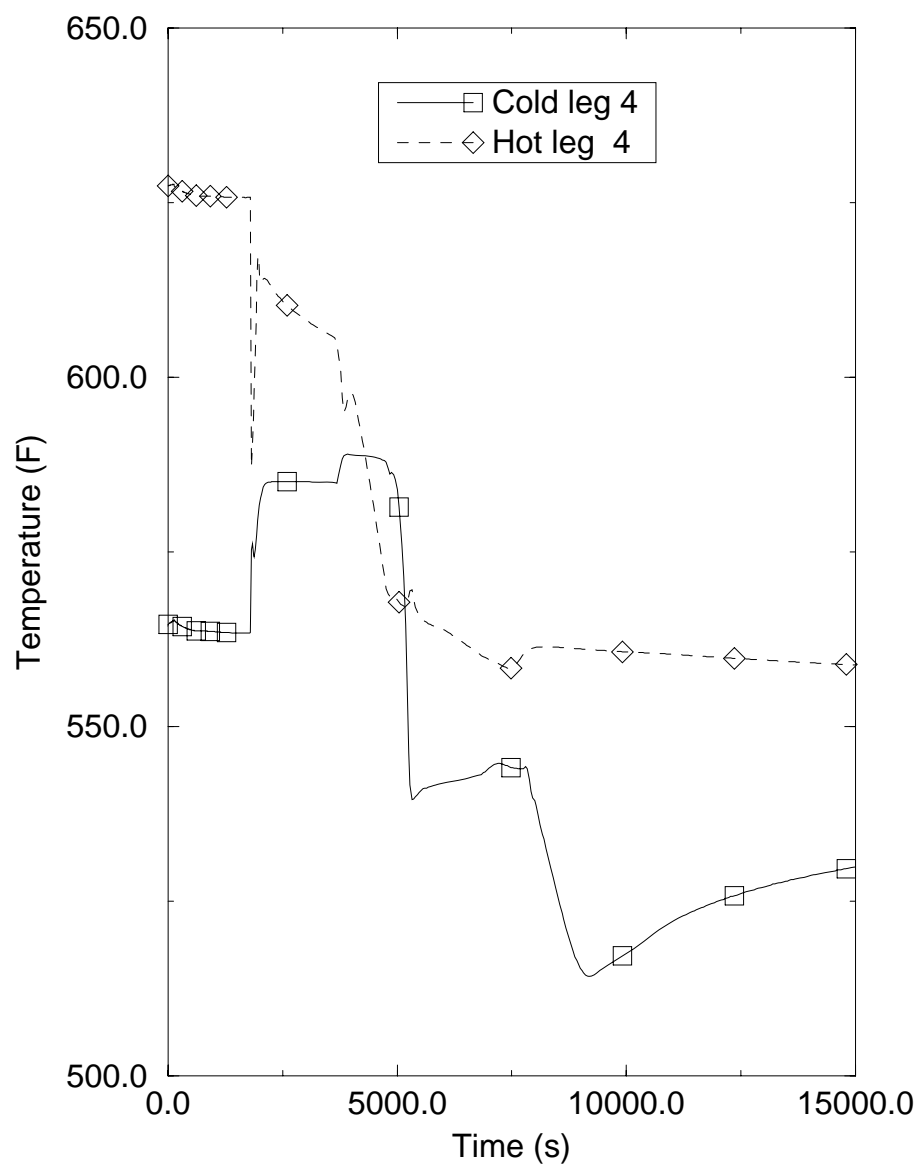
Figure D.6-5 SGTR RCS Temperatures – ruptured SG loop

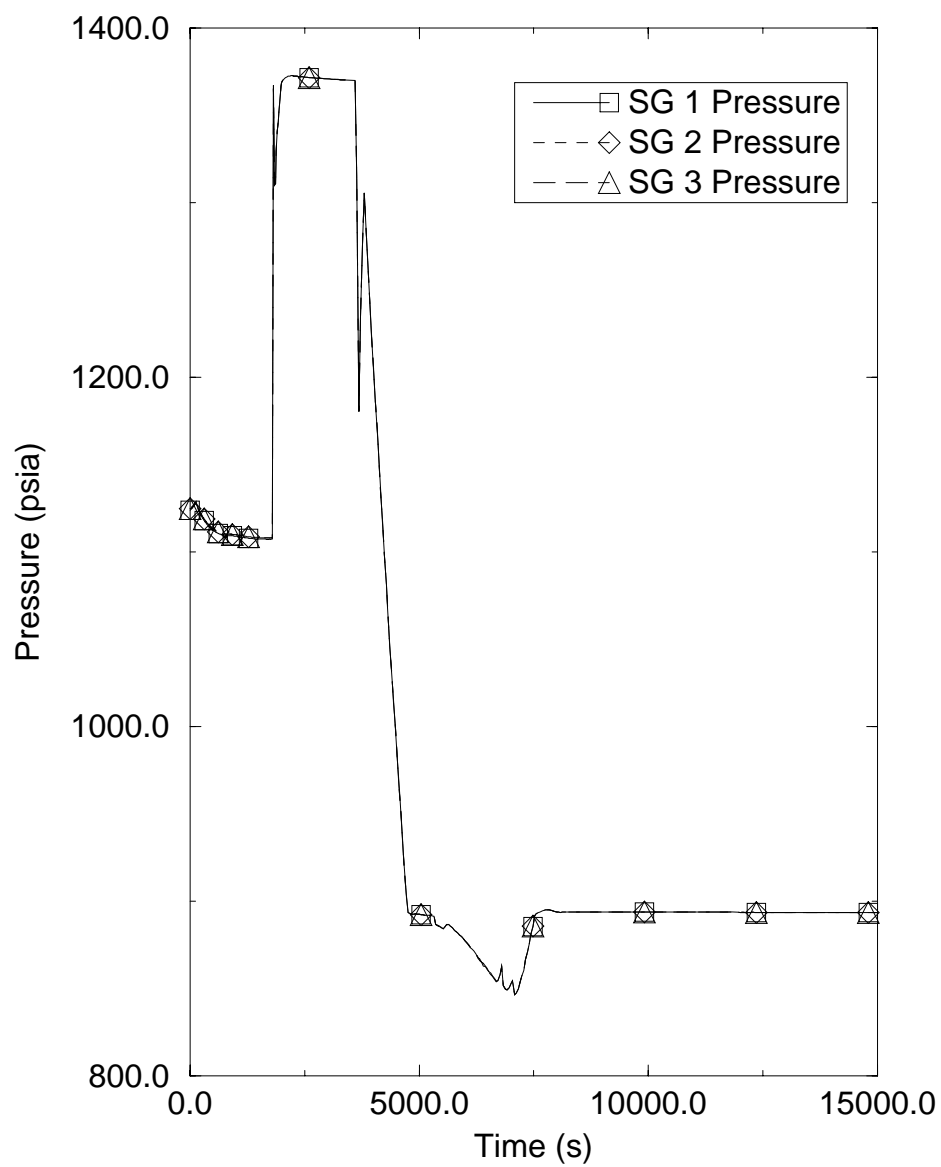
Figure D.6-6 SGTR Steam Generator Pressure – intact SGs

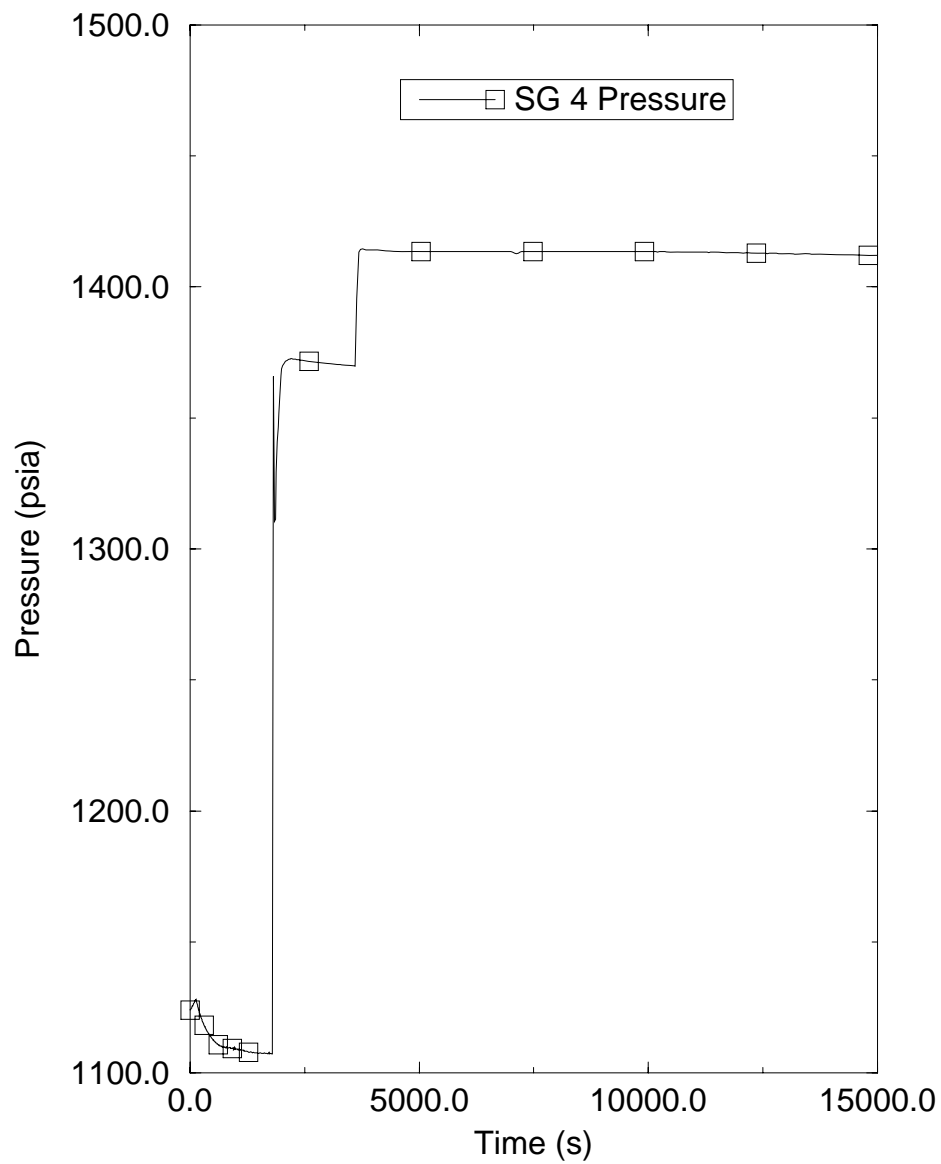
Figure D.6-7 SGTR Steam Generator Pressure – ruptured SG

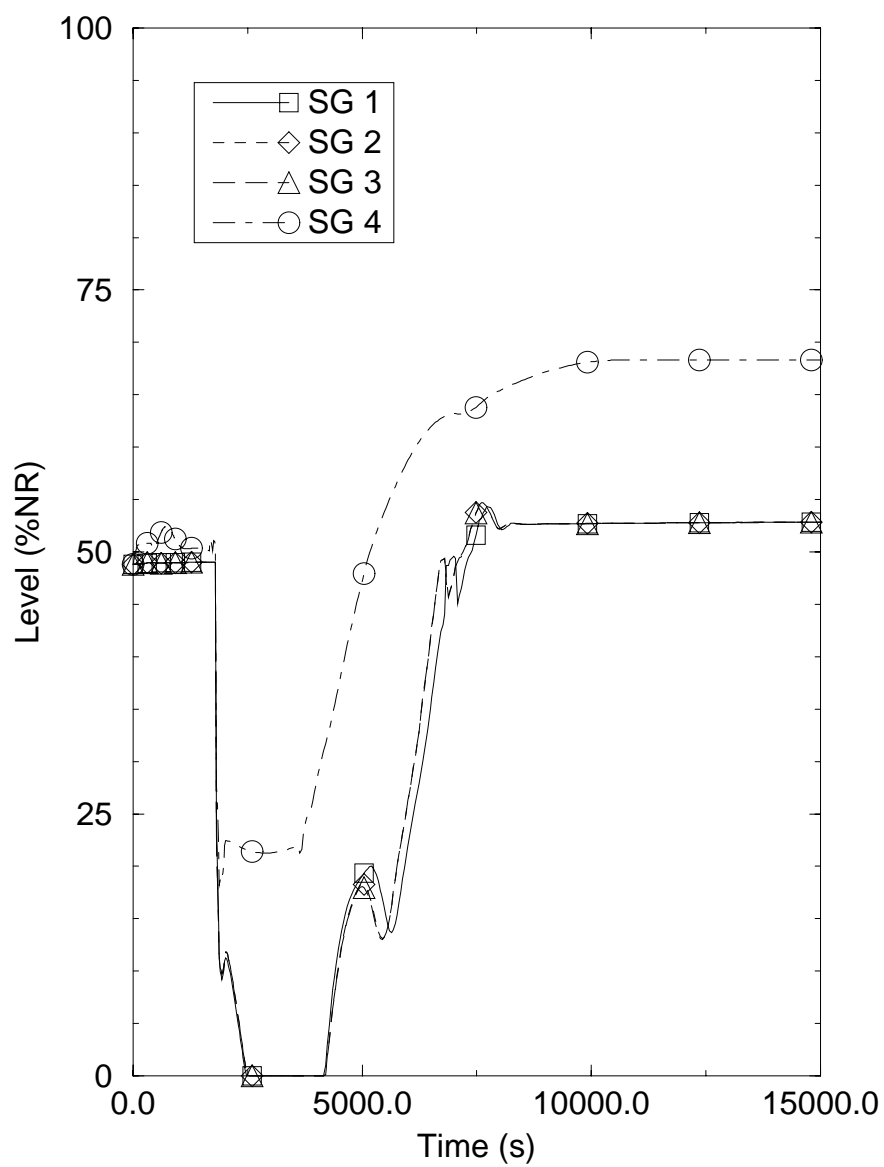
Figure D.6-8 SGTR Steam Generator Levels

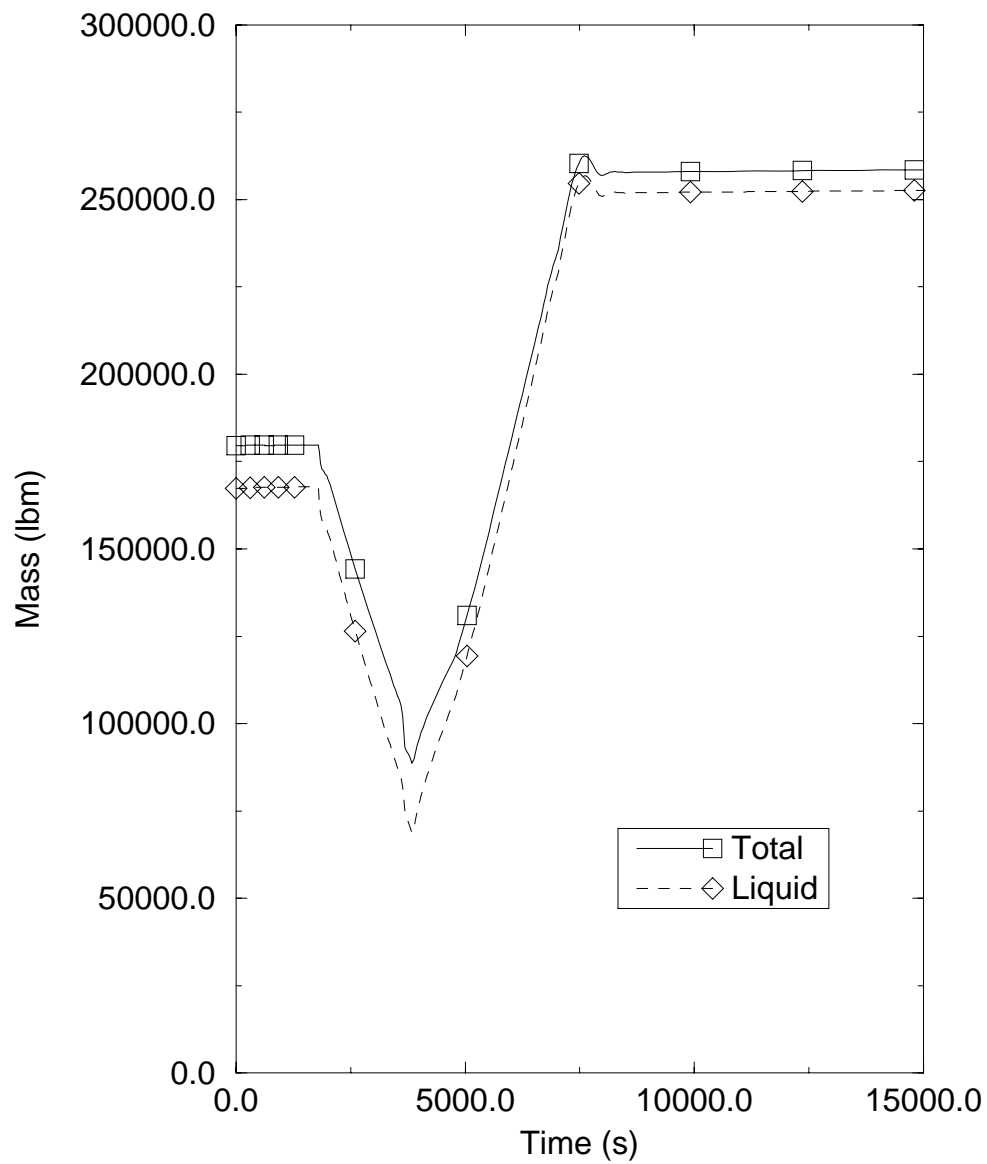
Figure D.6-9 SGTR Steam Generator Mass – intact SG

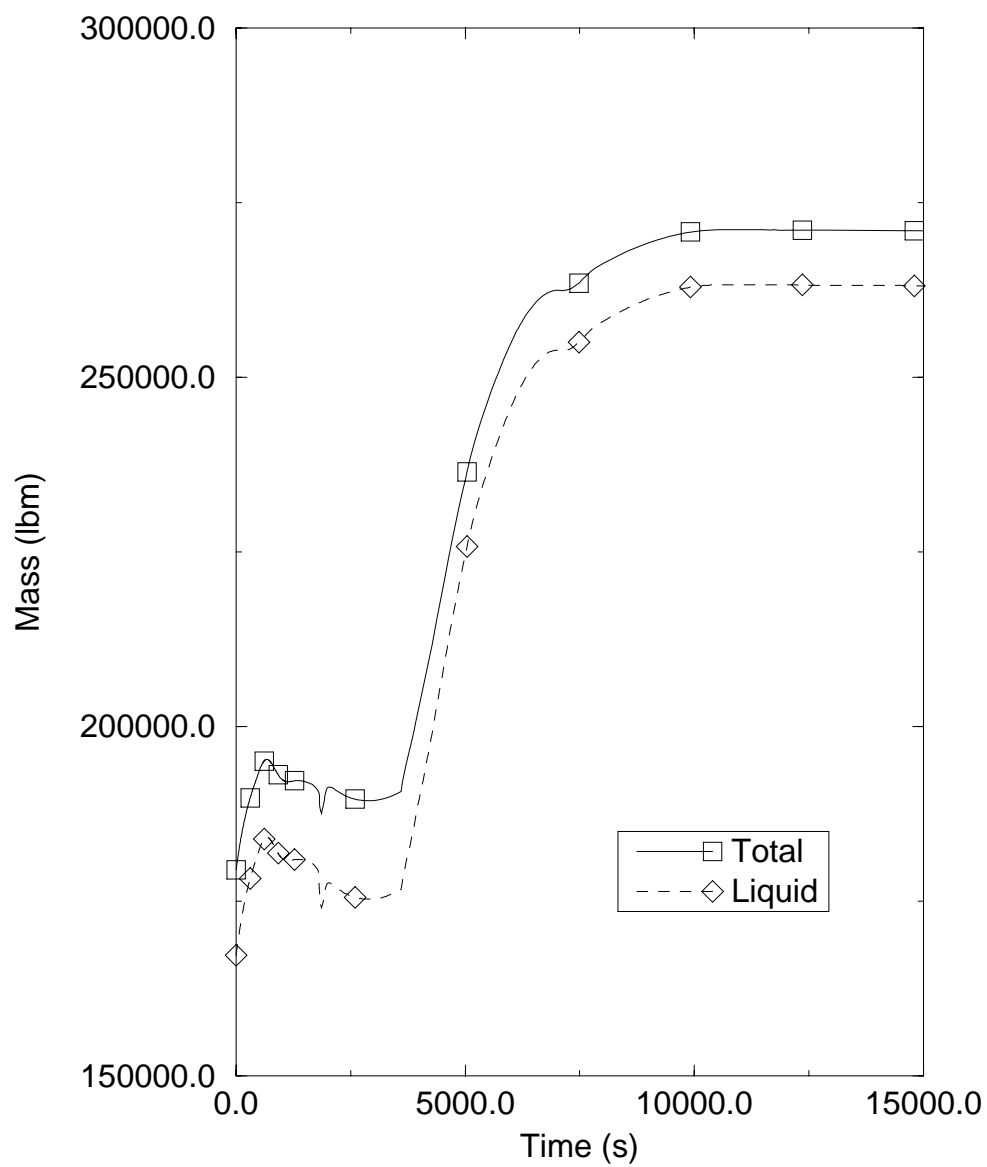
Figure D.6-10 SGTR Steam Generator Mass – ruptured SG

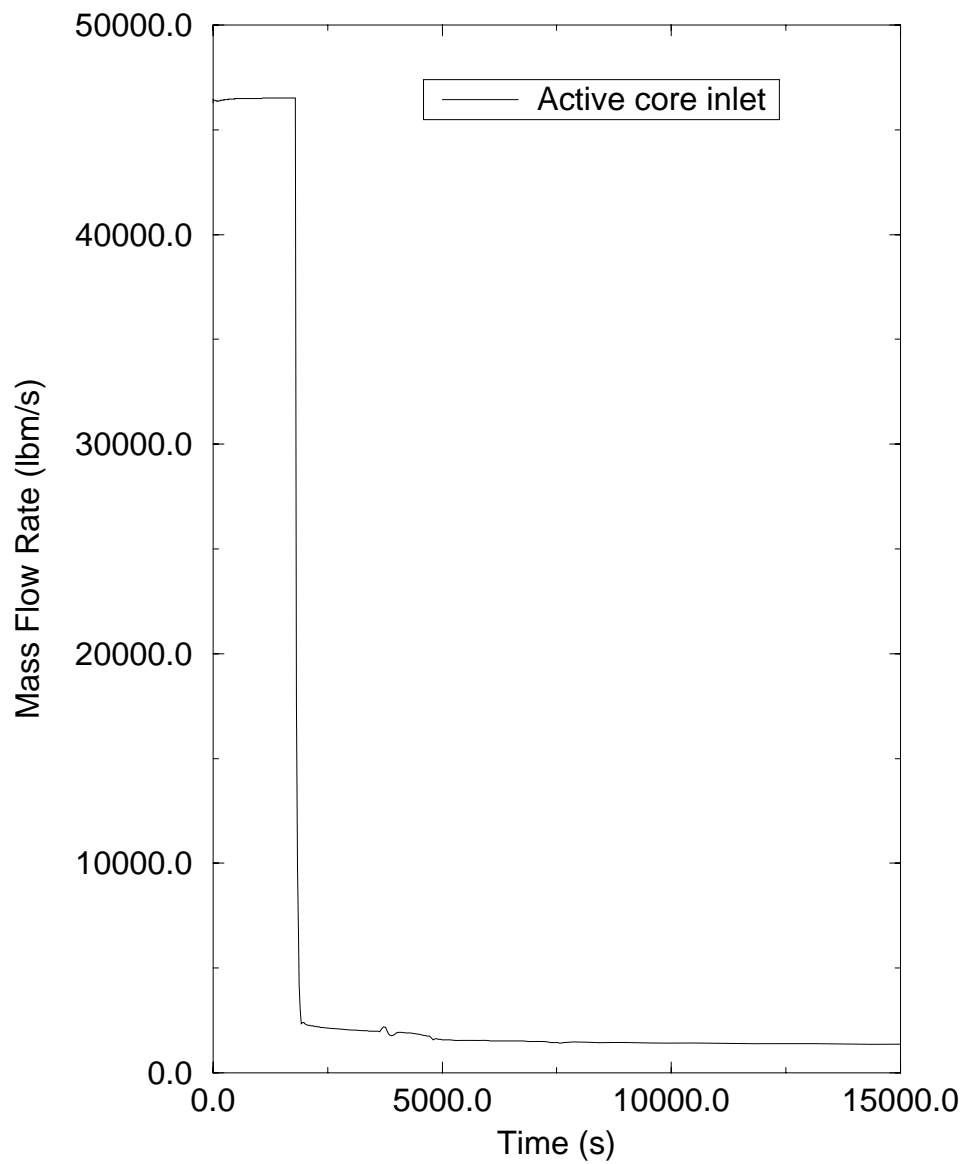
Figure D.6-11 SGTR Active Core Mass Flow Rate

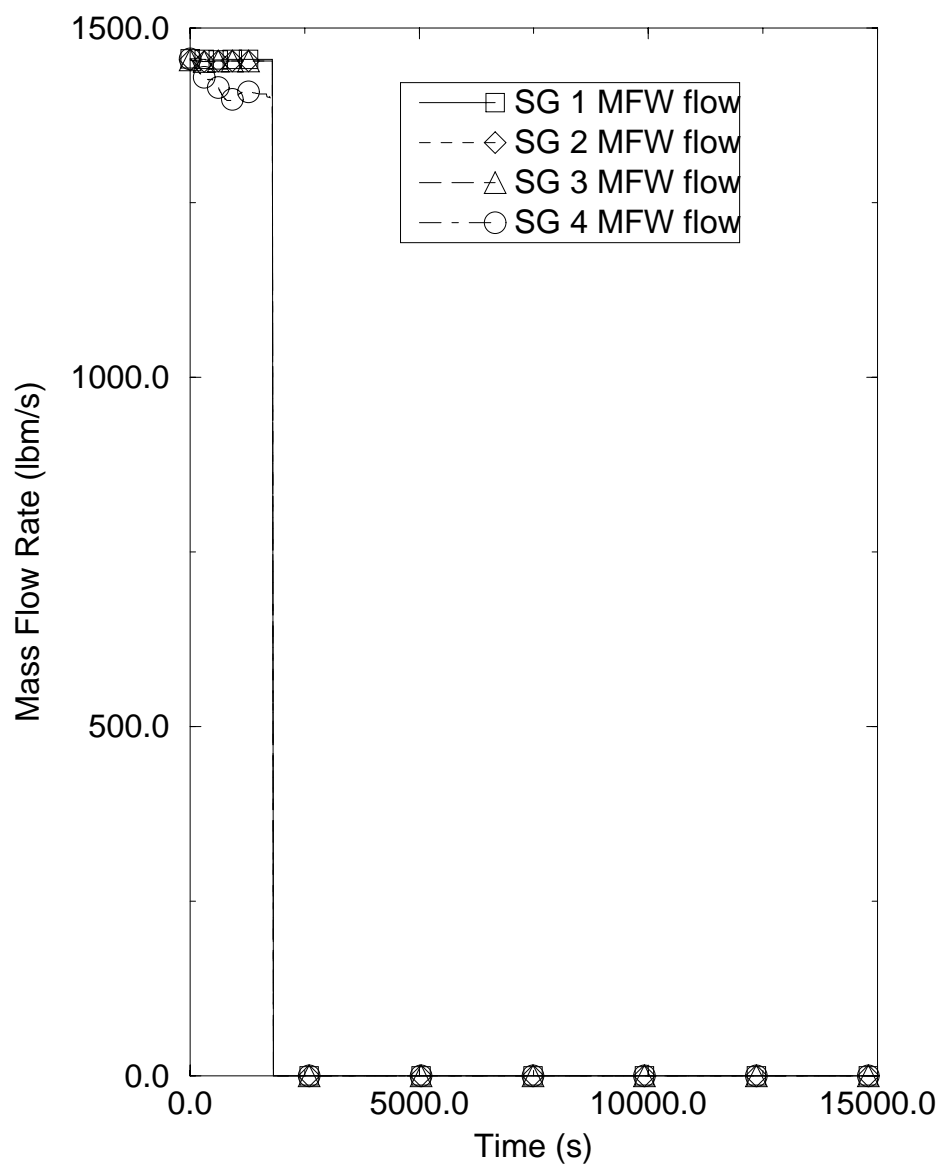
Figure D.6-12 SGTR MFW Flow Rates

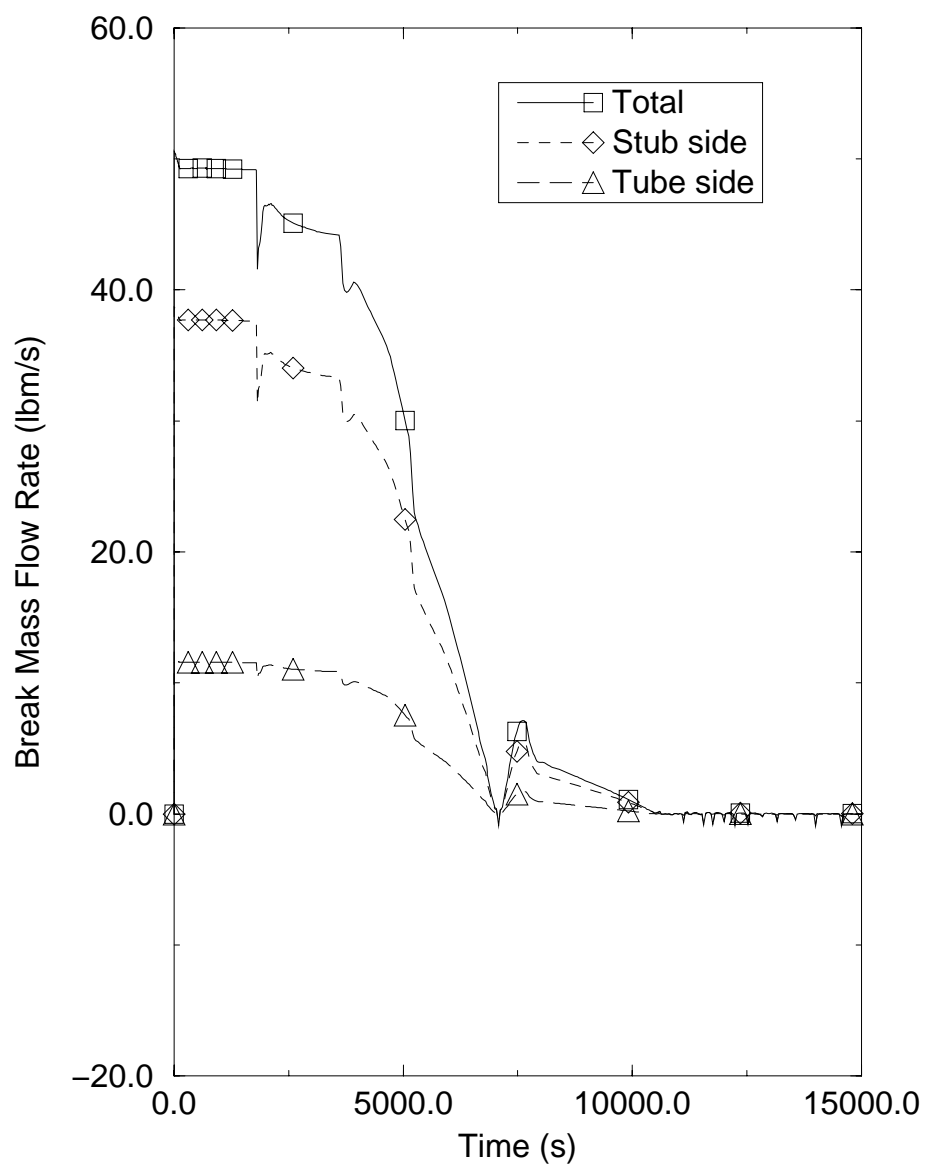
Figure D.6-13 SGTR Break Flow Rate

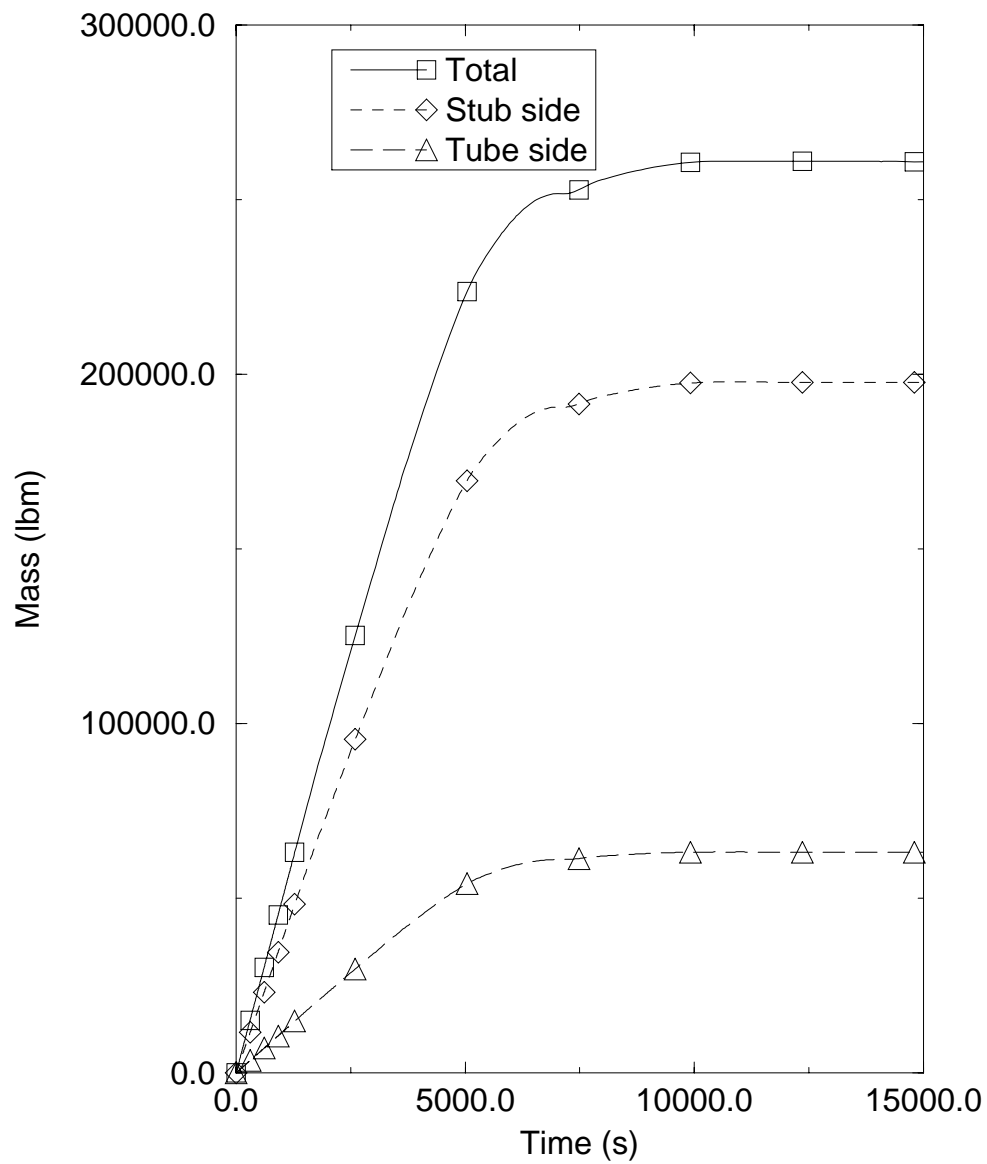
Figure D.6-14 SGTR Integrated Break Flow

Figure D.6-15 SGTR Integrated MSRT Flows